

Michael V. Sadovkii

**Selected Works
on Condensed
Matter Theory**

Volume 1

©M.V. Sadovskii, 2024

M.V. Sadovskii

**Selected Works on
Condensed Matter Theory**

Volume 1



Preface

These volumes presents selected papers of Michael V. Sadovskii on different aspects of condensed matter theory published by him from 1974 to 2024. From his total publication list of about 180 papers we have chosen only those which we consider conceptually most important. This choice is of rather subjective nature and is not related to any of currently popular metrics, like e.g. citation or Hirsch indices.

Selected reviews by M.V. Sadovskii were published in separate two – volume edition. All experimental papers as well as papers devoted to calculations of different properties of specific materials were just excluded from this edition.

All papers are published in original form without any editorial work or corrections of some minor misprints mainly of a technical nature.

At the end of this volume we present an extended list of the books, reviews and research papers by M.V. Sadovskii, which includes many of those dropped from this edition.

Contents:

1. L.N. Bulaevskii, M.V. Sadovskii. On the Influence of Crystal Lattice Disorder on Peierls Transition. *Sov. Phys. - Solid State* v. 16, No. 4, 743 (1974)
2. M.V. Sadovskii. A Model of a Disordered System (A Contribution to the Theory of "Liquid Semiconductors"). *Sov. Phys.-JETP* v. 39, No. 5, 845-850 (1974)
3. M.V. Sadovskii. Theory of Quasi-one-dimensional Systems Undergoing Peierls Transition. *Sov. Phys. - Solid State* v. 16, No. 9, 1632 (1974)
4. M.V. Sadovskii. Localization of Electrons in Disordered Systems. The Mobility Edge and Theory of Critical Phenomena. *Sov. Phys. - JETP* v. 43, No. 5, 1008-1010 (1976)
5. M.V. Sadovskii. Collective Excitations of Charge Density Waves in Quasi-one-dimensional Structures. *Sov. Phys. - Solid State* v. 19, No. 4, 607 (1977)
6. M.V. Sadovskii. Electron in a Random Field, Theory of Phase Transitions, and Finite-Action Nonlinear Solutions. *Sov. Phys. - Solid State* v. 21, No. 3, 435-439 (1979)
7. M.V. Sadovskii, Yu.N. Skryabin. Superconductivity in Spin-Glasses. *Phys. Stat. Sol. (b)* v. 95, No.1, 59-64 (1979)
8. M.V. Sadovskii. Exact Solution for the Density of Electronic States in a Model of a Disordered System. *Sov. Phys. - JETP* v. 50, No.5, 989-994 (1979)
9. M.V. Sadovskii. Electron Localization in the Random – Phase Model and in a Magnetic Field. *Sov. Phys. - JETP* v. 53, No. 3, 581-587 (1981)
10. M.V. Medvedev, M.V. Sadovskii. Localization of One-Particle Spin Excitations in a Ferromagnet with a Random Easy – Axis Anisotropy. *Sov. Phys. - Solid State* v. 23, No. 7, 1135-1137 (1981)
11. M.V. Medvedev, M.V. Sadovskii. Random Bond Ising Model in Self-Avoiding Walk Approximation. *Phys. Stat. Sol. (b)*, v. 109, 49-57 (1982)
12. M.V. Sadovskii. Localization Criterion in the Field Theory of an Electron in a Random Field. *Sov. Phys. JETP* v. 56, No.4, 816-822 (1982)
13. A.V. Myasnikov, M.V. Sadovskii. Self-Consistent Theory of Localization in Spaces with $2 < d < 4$ Dimensions. *Sov. Phys. - Solid State* v. 24, No. 12, 2033 (1982)
14. E.A. Kotov, M.V. Sadovskii. Self-Consistent Theory of Localization for the Anderson Model. *Zs. Phys.* v. 51, No.1, 17-23 (1983)
15. M.I. Katsnelson, M.V. Sadovskii. Density of States and Screening Near the Mobility Edge. *Sov. Phys. - JETP* v. 60, No.2, 300-306 (1984)
16. L.N. Bulaevskii, M.V. Sadovskii. *JETP Letters* v. 39, No. 11, 640-643 (1984)
17. L.N. Bulaevskii, M.V. Sadovskii. Anderson Localization and Superconductivity. *J. Low-Temp. Phys.* v. 59. No. 1/2, 89-113 (1985)

18. L.N. Bulaevskii, M.V. Sadovskii. Increase of Spatial Fluctuations in Superconductors Near the Anderson Transition. JETP Letters v. 43, No. 2, 99-103 (1986)
19. L.N. Bulaevskii, S.V. Panyukov, M.V. Sadovskii. Inhomogeneous Superconductivity in Disordered Metals. Sov.Phys. - JETP v. 65, No. 2, 380-388 (1987)
20. M.V. Sadovskii, A.A. Timofeev. The Two-Particle Green Function in a Model of a One-Dimensional Disordered System: An Exact Solution? J. Moscow Phys. Soc. v. 1, 391-406 (1991)
21. M.A. Erkabaev, M.V. Sadovskii. J. Moscow Phys. Soc. v. 2, 233-241 (1992)
22. E.Z. Kuchinskii, M.V. Sadovskii. M.A. Erkabaev. Superconductivity Suppression Close to the Metal - Insulator Transition in Strongly Disordered Systems. JETP v. 85, No. 1, 104-108 (1997)
23. A.I. Posazhennikova. M.V. Sadovskii. Ginzburg - Landau Expansion and the Slope of the Upper Critical Field in Superconductors with Anisotropic Normal Impurity Scattering . JETP v. 85, No. 6, 1162-1167 (1997)
24. E.Z. Kuchinskii, M.V. Sadovskii. Combinatorics of Feynman Diagrams for the Problems with Gaussian Random Field. JETP v. 86, No. 2, 367-374 (1998)
25. A.I. Posazhennikova, M.V. Sadovskii. Ginzburg – Landau Expansion in a Simple Model of a Superconductor with a Pseudogap. JETP v. 88, No. 2, 347-355 (1999)
26. E.Z. Kuchinskii, M.V. Sadovskii. Models of the Pseudogap State of Two - Dimensional Systems. JETP v. 88, No. 5, 968-979 (1999)
28. E.Z. Kuchinskii, M.V. Sadovskii. Superconductivity in a Simple Model of the Pseudogap State. JETP v. 90, No. 3, 535-543 (2000)
29. E.Z. Kuchinskii, M.V. Sadovskii. Superconductivity in the Pseudogap State due to Fluctuations of Short - Range Order. JETP v. 92, No. 3, 480-492 (2001)
30. E.Z. Kuchinskii, M.V. Sadovskii. Superconductivity in an Exactly Solvable Model of the Pseudogap State: Absence of Self - Averaging. JETP v. 94, No. 3, 654-769 (2002)

Effect of crystal lattice disorder on Peierls transitions

L. N. Bulaevskii and M. V. Sadovskii

P. N. Lebedev Institute of Physics,
Academy of Sciences of the USSR, Moscow
(Submitted November 30, 1973)
Fiz. Tverd. Tela, 16, 1159-1164 (April 1974)

The effect of disorder on Peierls structural transitions is considered for quasi-one-dimensional crystals of the $K_2Pt(CN)_4Br_{0.30} \cdot 3H_2O$ type and for salts based on TCNQ. The exactly solvable Lloyd disorder model and the "fragment" model are considered. It is shown that in both models disorder causes a strong suppression of the Peierls transition, and its effect is qualitatively similar to the effect of magnetic impurities on the superconducting transition. Possible experimental consequences are discussed.

The synthesis and study of physical properties of highly conducting quasi-one-dimensional crystals on bases of TCNQ salts¹ and of plane complexes of transition elements of the platinum group [the $K_2Pt(CN)_4Br_{0.33} \cdot 3H_2O$ type] raised the problem of applicability to those compounds of the Peierls argument on instability of one-dimensional electron systems with respect to a change in the lattice period. According to these concepts, a displacement by a wave vector $2k_F$ (k_F is the electron Fermi momentum) should appear at low temperatures in the original crystal lattice affected by the electron system, and below a temperature T_P the one-dimensional system must remain a dielectric, since a gap appears in the electron system at the Fermi surface. In $K_2Pt(CN)_4Br_{0.30} \cdot 3H_2O$ compounds diffuse x-ray scattering^{2,3} and inelastic neutron scattering⁴ indicate that the Peierls instability is indeed observed. According to the data of ref. 3 a static displacement of atoms (a sixfold increase of the period) occurs at a temperature below 77°K, and at higher temperatures this static distortion is preceded by softening of phonon frequencies with quasimomentum $\approx 2k_F$. Obviously, a Peierls period occurs also in the highly conducting TTF-TCNQ salt,⁵ while at the same time this transition has not been so far observed in magnetic data of other investigated TCNQ salts. Indeed, for a Peierls transition the paramagnetic susceptibility should fall with temperature lowered below T_P . Exactly such susceptibility behavior is observed⁶ in TTF-TCNQ, but not in other highly conducting TCNQ salts.⁷

It is clear that crystal lattice disorder has a large effect on the Peierls transition. Indeed, disorder washes out those features in the density of states of one-dimensional electron bands which lead to lattice instability in the displacements with gap formation at the Fermi surface. An internal instability, however, is inherent in all quasi-one-dimensional crystals, besides TTF-TCNQ. In platinum complexes halogen ions fill only part of the sites which they can occupy, and their site distribution is random. In the highly conducting TCNQ salts disorder is related to a random orientational distribution of asymmetric cations. Only for the TTF-TCNQ complex is the TTF cation totally symmetric and lattice disorder can be related only to structure defects.

In this paper we consider the effect of lattice disorder on the temperature and the order parameter of the Peierls transition. The calculations indicate that this effect is as strong as the effect of magnetic impurities on the superconducting transition. The results obtained below explain why the Peierls transition is not observed in all quasi-one-dimensional crystals. We also discuss new

properties added to this transition by lattice disorder.

1. INITIAL EQUATIONS AND DISORDER MODEL

We consider only the simplest example of a Peierls transition, one with a doubled period. Such a transition occurs if the original electron band is half full, and only in this case is a lattice change not accompanied by a redistribution of electron charge.⁸ For this ratio a transition with a doubled period is simplest, and to evaluate the transition temperature T_P in the static approximation it is necessary to know only the dependence of the electronic density of states on the displacement of the lattice atoms and the degree of lattice disorder. In doubling the displacement u_n of atom n we use

$$u_n = (-1)^n u. \quad (1)$$

For a half-filled band the free energy of the electrons and the lattice is expressed in terms of the parameter u as

$$F(u, T) = -T \int_{-\infty}^{\infty} dE \rho(u, E) \ln(1 + e^{E/T}) + \frac{1}{2} K u^2, \quad (2)$$

where K is the lattice elasticity coefficient with electrons localized at the sites,⁸ and $\rho(u, E)$ is the electronic density of states for displacement u . We consider below only disorder models leading to $\rho(u, E)$ symmetric with respect to the energy $E = 0$, i.e., $\rho(u, E) = \rho(u, -E)$. In this case the electronic chemical potential is $\mu = 0$. Below the Peierls transition temperature T_P the free energy is lowered at $u \neq 0$, and T_P is the temperature for which the equation

$$\left. \frac{\partial F(u, T)}{\partial u} \right|_{u=0} = 0. \quad (3)$$

has a nontrivial solution $u \neq 0$ for the first time.

The problem thus reduces to the determination of the electronic density of states $\rho(u, E)$ in a disordered lattice. The possibility of applying approximate methods in determining the density of states in a one-dimensional system seems doubtful; therefore we consider disorder models which allow accurate determination of the density of states. Such are the Lloyd⁹ and the "fragment"¹⁰ models.

2. THE LLOYD MODEL

In this model it is assumed that the electrons are described in the tight binding approximation by means of the Hamiltonian

$$H = \sum_{n, \sigma} \{ \varepsilon_n a_{n\sigma}^+ a_{n\sigma} + b_{n, n+1} (a_{n\sigma}^+ a_{n+1\sigma} + a_{n+1\sigma}^+ a_{n\sigma}) \}, \quad (4)$$

in which the transition parameter (the resonance integral) $b_{n, n+1}$ is not a random quantity, but the potentials ε_n are randomly distributed over the sites n . It is assumed that the distributions ε_n are independent for different sites, and are all described by a Lorentz distribution

$$P(\varepsilon) = \frac{1}{\pi} \frac{\varepsilon_1}{\varepsilon^2 + \varepsilon_1^2}. \quad (5)$$

Obviously, this model is qualitatively adequate for the platinum complexes, in which disorder in the Br or Cl ion positions leads to a random potential, acting on the conduction electrons of the chain. For the distribution (5) the density of states $\rho(E)$ in the disordered lattice ($\varepsilon_1 \neq 0$) is expressed in terms of the density of states $\rho_0(E)$ in an ideal lattice ($\varepsilon_1 = 0$) by the relation

$$\rho(E) = \frac{\varepsilon_1}{\pi} \int_{-\infty}^{\infty} dx \frac{\rho_0(x)}{(E-x)^2 + \varepsilon_1^2}. \quad (6)$$

In an ideal lattice with a doubled period the electron spectrum is of the form

$$\varepsilon(k) = \pm \sqrt{\Delta^2 + 4b^2 \cos^2 k}, \quad k = \frac{2\pi n}{N}, \quad n = 0, \pm 1, \pm 2, \dots, \pm \frac{N}{2}, \quad (7)$$

where N is the number of atoms in the system, $2b$ is the half-width of the original band (the band without doubling) $2b = b_{n, n-1} + b_{n, n+1}$ and $\Delta = |b_{n, n+1} - b_{n, n-1}|$; $\Delta/2b \ll 1$ (we consider only the case of small atomic displacements, i.e., $T_P \ll 2b$). The plus sign in (7) corresponds to the upper part of the band, and the minus sign to the lower. The density of states, proportional to the derivative $dk/d\varepsilon$, is infinite at the band edges ($k = 0, 2\pi$) for $N \rightarrow \infty$. This feature also causes the Peierls instability of the original ideal lattice.

We notice that in the Lloyd model the electronic free energy is infinite due to the slow decrease of the Lorentzian distribution function (5) for $\varepsilon \rightarrow \infty$; this divergence, however, is not crucial for us since the part of the electronic free energy which depends on the displacements u , i.e., $\partial E(u, T)/\partial u$, is finite. Physically the divergence in (2) for large E is removed if the ion energy is included in the same potential field ε_n .

We further choose for the transition parameter not the displacement u , but the quantity Δ proportional to it, which determines the gap in the electronic spectrum of an ideal lattice with the doubled period. We introduce also the dimensionless electron-lattice interaction constant g by means of the relation $Ku^2 = \Delta^2/\pi g^2 2b$. Taking into account the condition $\Delta/2b \ll 1$ for weak disorder $\varepsilon_1/2b \ll 1$, we obtain from (2), (3), (6), (7) for an infinite system the following equation for the transition temperature:

$$1 = g^2 \int_0^{2b} \frac{d\varepsilon}{V' \sqrt{1 - (\frac{\varepsilon}{2b})^2}} \frac{\varepsilon}{\varepsilon^2 + \varepsilon_1^2} \operatorname{th} \frac{\varepsilon}{2T}. \quad (8)$$

For an ideal lattice ($\varepsilon_1 = 0$) Eq. (8) differs from the BCS equation for the superconducting transition temper-

ature by the factor $[1 - (\varepsilon/2b)^2]^{-1/2}$ only. This factor describes the electronic density of states in the tight binding approximation, and its appearance in (8) is related to the fact that the whole electron band contributes to the Peierls instability, while in a superconductor the electron-phonon interaction differs from zero only in an energy interval of the order of the Debye frequency $\omega_D \ll 2b$ around the Fermi surface. In this narrow energy interval the density of states can be considered constant. The features of the density of states at the band edges, washed out by disorder, leads to the appearance in (8) of the factor $\varepsilon/(\varepsilon^2 + \varepsilon_1^2)$, regular for $\varepsilon \rightarrow 0$, which decreases the transition temperature T_P .

Equation (8) is easily transformed into the form

$$\ln \frac{T_{P0}}{T} = \psi\left(\frac{1}{2} + \frac{\varepsilon_1}{2\pi T}\right) - \psi\left(\frac{1}{2}\right); \quad T_{P0} = \frac{8\gamma b}{\pi} e^{-\frac{1}{\beta}}, \quad (9)$$

where $\ln \gamma = C$ is the Euler constant, and $\psi(x)$ is the digamma function. In (9) we see the full analogy between the effect of lattice disorder on the Peierls transition and the effect of magnetic impurities on the superconducting transition.¹¹ For increasing ε_1 the transition temperature T_P drops and the Peierls instability disappears when $\varepsilon_1 = \varepsilon_{1C} = \Delta_0/2$, where Δ_0 is the Peierls gap of an ideal crystal at $T = 0$, equal $\pi T_{P0}/\gamma$.

The dependence of the parameter Δ on the instability ε_1 is determined for $T = 0$ from the equation

$$\ln \frac{\Delta_0}{\varepsilon_1} = \frac{2}{\pi} \int_0^{\infty} dx \frac{\ln \left\{ 1 + \sqrt{\left(\frac{x\Delta}{\varepsilon_1}\right)^2 + 1} \right\}}{1 + x^2}. \quad (10)$$

For small disorder ($\varepsilon_1 \ll \Delta_0$) we obtain from (9), (10)

$$T_P = T_{P0} \left\{ 1 - \frac{\pi^2}{4\gamma} \frac{\varepsilon_1}{\Delta_0} \right\}; \quad \Delta = \Delta_0 \left\{ 1 - \frac{\varepsilon_1}{\Delta_0} \ln \frac{2e\Delta_0}{\varepsilon_1} \right\}, \quad (11)$$

and close to ε_{1C} , when the temperature T_P is low ($T_P \ll T_{P0}$),

$$T_P = \frac{T_{P0}}{4\gamma} \ln \frac{\Delta_0}{2\varepsilon_1}; \quad \frac{\Delta}{\varepsilon_1} \ln \frac{2e\varepsilon_1}{\Delta} = \frac{\pi}{4} \ln \frac{\Delta_0}{2\varepsilon_1}. \quad (12)$$

It is seen from (11) and (12) that in the Lloyd model the ratio Δ/T_P varies from π/γ (the BCS value) to zero for ε_1 varying from zero to ε_{1C} .

We notice that in a disordered system the Peierls transition does not cause a gap appearance in the electronic spectrum, since in this case the density of states remains nonzero in the energy interval from $-\Delta$ to Δ , although a pseudogap occurs in this region. Thus, in the center of the original band we have for $E = 0$

$$\rho(0) = \frac{\varepsilon_1}{b\Delta} < \rho_0(0) = \frac{1}{2b}.$$

3. THE "FRAGMENT" MODEL

The "fragment" model is realized if a quasi-one-dimensional crystal has structural defects or impurity atoms, through which conduction electrons with energies around the Fermi surface cannot pass (for example, closed-shell impurity molecules). In the Hamiltonian (4)

this situation corresponds to the case $\epsilon_n = 0$, but the resonant integral $b_{n, n+1}$ is a random quantity, vanishing for several neighboring atoms $n, n+1$, while having for other neighboring atoms the ideal lattice value. The linear system of atoms is then decomposed into a number of "fragments" and the Peierls transition in each of these fragments takes place independently at a temperature T_P depending on the number of atoms in the fragment. In a system of N atoms the electronic spectrum in the tight binding approximation is described, after doubling the period by Eq. (7). For finite N the discrete nature of the spectrum causes a weakening of the Peierls instability, and for decreasing N the transition temperature $T_P \rightarrow 0$.

For the density of states we have from (7)

$$\rho(E) = \sum_{n=-N/2}^{N/2} \delta\left(E \pm \sqrt{\Delta^2 + 4b^2 \cos^2 \frac{2\pi n}{N}}\right). \quad (13)$$

Further, let N be twice an odd number. The chemical potential is then $\mu = 0$, and this simplifies the calculations considerably (the final results are, obviously, independent of the choice of N). From (2), (3), and (11) we obtain the T dependence of Δ ,

$$1 = g^2 \sum_{n=-N/2}^{N/2} \text{th} \frac{\sqrt{\Delta^2 + 4b^2 \cos^2 \frac{2\pi n}{N}}}{2T} \frac{1}{\sqrt{\Delta^2 + 4b^2 \cos^2 \frac{2\pi n}{N}}}. \quad (14)$$

The Poisson summation equation allows to write (12) in the form

$$1 = g^2 \int_0^1 \frac{dx}{\sqrt{1-x^2}} \frac{\text{th} \left(\frac{1}{2T} \sqrt{\frac{\Delta^2}{4b^2} + x^2} \right)}{\sqrt{\frac{\Delta^2}{4b^2} + x^2}} \left(1 + 2 \sum_{n=1}^{\infty} \cos Nn \arccos x \right). \quad (15)$$

Using the condition $T_{P0} \ll 2b$ and choosing N as twice an odd number, we obtain from (15) an equation for the transition temperature:

$$\ln \frac{T_{P0}}{T} = 4 \sum_{n=1}^{\infty} \frac{1}{2n-1} \frac{1}{\frac{(2n-1)\pi T}{\epsilon_N} + 1}; \quad \epsilon_N = \frac{2b}{N}. \quad (16)$$

For the order parameter Δ at $T = 0$ we have

$$\ln \frac{\Delta}{\Delta_0} = 2 \sum_{n=1}^{\infty} (-1)^n K_0 \left(n \frac{\Delta}{\epsilon_N} \right), \quad (17)$$

where $K_0(x)$ is the modified Bessel function. From (16), (17) we obtain for large N (when $\epsilon_N \ll \Delta_0$)

$$T_P = T_{P0} \left(1 - e^{-\frac{\Delta_0}{\epsilon_N}} \right); \quad \Delta = \Delta_0 \left(1 - \sqrt{\frac{\pi \epsilon_N}{\Delta_0}} e^{-\frac{\Delta_0}{\epsilon_N}} \right), \quad (18)$$

and for small $T_P \ll T_{P0}$ we have

$$T = -\frac{6T_{P0}}{\pi} \ln \frac{T_{P0}}{\epsilon_N}; \quad \Delta = \frac{\pi T_{P0}}{\sqrt{\zeta(3)}} \sqrt{8 \ln \frac{T_{P0}}{\epsilon_N}}, \quad (19)$$

where $\zeta(x)$ is the Riemann function. A Peierls transition does not occur if $N < N_C = 2b/T_{P0}$. In this model the ratio Δ/T_P varies from π/γ to ∞ for N varying from ∞ to N_C .

4. DISCUSSION

The models considered by us differ in the nature of their instability. To compare their results and to compare, in particular, the Peierls transition criteria, we introduce a universal quantity for one-dimensional disordered systems, such as the electron localization length, which can be calculated if the density of states is known.¹² This quantity replaces in the one-dimensional case the mean free path and is essentially of similar nature. Clearly, in the "fragment" model the localization length l , expressed in interatomic distances, equals N . In the Lloyd model the localization length was calculated by Thouless,¹² and in the center of the original band at electron energies $E = 0$ and $\epsilon_1 \ll 2b$ it equals $2b/\epsilon_1$ (at the edge of the original band it is twice as large). Expressed in terms of the localization length l the parameters ϵ_1 and ϵ_N , characterizing disorder in the Lloyd and "fragment" models, coincide and equal $2b/l$. For the critical localization lengths in these models we obtain the very close values $(2\gamma/\pi)$ $(2b/T_{P0}) = 1.13$ $(2b/T_{P0})$ and $2b/T_{P0}$, respectively.

Thus, the criterion of Peierls transition appearance, expressed in terms of the localization length

$$l > l_c \approx \frac{2b}{T_{P0}}, \quad (20)$$

is, obviously, useful for any disorder. At the same time the ratio Δ/T_P can vary from π/γ to either side, depending on the nature of the disorder.

Applied to the platinum complexes, the results obtained allow us to assume that the smallness of the ratio $T_P/2b$ in $K_2Pt(CN)_4Br_{0.30} \cdot 3H_2O$ ($T_P \leq 77^\circ K$; $2b \sim 2$ eV) be related to disorder in their Br ions. We notice that a suppression of Peierls instability is also caused by electron transitions between chains, which destroy the symmetry condition of the electron spectrum

$$\epsilon(\mathbf{k}) - \mu = -\epsilon(\mathbf{k} + \mathbf{q}) + \mu \quad (21)$$

(\mathbf{q} is the wave vector of Peierls deformation), necessary for the occurrence of lattice instability^{13,14} in a three-dimensional crystal [in a one-dimensional system Eq. (21) is always satisfied at least for electrons around the Fermi surface for $\mathbf{q} = 2\mathbf{k}_F$]. If the resonance integral of interchain transitions leading to violation of (21) is denoted by b_1 , the transition temperature T_P is reduced¹⁴ by about b_1/T_{P0} . At room temperature the conductivity anisotropy¹⁵ in $K_2Pt(CN)_4Br_{0.30} \cdot 3H_2O$ exceeds 10^4 , and for this compound $b_1 \ll T_{P0}$.

An attempt has been made¹⁵ to explain the drop in conductivity in $K_2Pt(CN)_4Br_{0.30} \cdot 3H_2O$ by the appearance of a Peierls gap. As noted above, in a disordered system the gap is replaced by a "pseudogap," so that the appearance of an order parameter Δ does not, generally speaking, cause an exponential decrease of conductivity with temperature. The low-temperature conductivity is determined in this case by electron jumps over the energy levels inside the pseudogap. At the same time the electronic specific heat at low temperatures, proportional to the density of states at the Fermi surface, is strongly suppressed if the system undergoes a Peierls transition. Therefore, the small magnitude of electronic heat ca-

capacity in $K_2Pt(CN)_4Cl_{0.3} \cdot 3H_2O$ at low temperatures, measured by Greene and Little,¹⁶ can be explained by the occurrence of a Peierls transition in this crystal, as well as in $K_2Pt(CN)_4Br_{0.30} \cdot 3H_2O$.

According to the results of ref. 7, in highly conducting crystals on a TCNQ base with asymmetric cations the transition resonance integral is a random quantity and can acquire arbitrarily small values. In this case the localization length is small and the Peierls transition can indeed be totally suppressed.

¹I. F. Shchegalev, Phys. Status Solidi (a), 12, 9 (1972).

²R. Comes, M. Lambert, H. Launois, and H. Zeller, Phys. Rev., B8, 571 (1973).

³R. Comes, M. Lambert, and H. Zeller, Phys. Status Solidi (b), 58, 587 (1973).

⁴B. Renker, H. Ritschel, L. Pintschovins, W. Gläser, P. Brüesch, D. Kuse, and M. I. Rice, Phys. Rev. Lett., 30, 1144 (1973).

⁵L. B. Coleman, M. I. Cohen, D. J. Sandman, F. G. Yamagashi, A. F. Garito, and A. J. Heeger, Solid State Commun., 12, 1125 (1973).

⁶A. F. Garito and A. J. Heeger, Proc. Intern. Conf. on Magnetism, Moscow (1973).

⁷L. N. Bulaevskii, A. V. Zvorykina, Yu. S. Karimov, R. B. Lyubovskii, and I. F. Shchegalev, Zh. Eksp. Teor. Fiz., 62, 725 (1972) [Sov. Phys.-JETP, 36, 384 (1972)].

⁸S. Barišić, Phys. Rev., 5B, 932, 941 (1972).

⁹P. Lloyd, J. Phys. C 2, 1717 (1969).

¹⁰M. I. Rice and J. Bernasconi, J. Phys., 3, 55 (1973).

¹¹P. G. de Gennes, Superconductivity of Metals and Alloys, Benjamin (1966).

¹²D. I. Thouless, J. Phys. C 5, 77 (1972).

¹³A. M. Afanas'ev and Yu. Kagan, Zh. Eksp. Teor. Fiz., 43, 1456 (1962) [Sov. Phys.-JETP, 16, 1030 (1963)].

¹⁴Yu. V. Kopaev and R. Kh. Timerov, Zh. Eksp. Teor. Fiz., 63, 290 (1972) [Sov. Phys.-JETP, 36, 153 (1973)].

¹⁵H. R. Zeller, Solid State Problems [in German], Vol. XIII, 31, Viewag, Braunschweig (1973).

¹⁶R. I. Greene and W. A. Little, Phys. Rev. Lett., 29, 718 (1972).

A model of a disordered system (A contribution to the theory of "liquid semiconductors")

M. V. Sadovskii

P. N. Lebedev Physics Institute, USSR Academy of Sciences
(Submitted November 1, 1973)
Zh. Eksp. Teor. Fiz. 66, 1720-1733 (May 1974)

A model of the electronic properties of disordered systems of the "liquid-semiconductor" type is proposed. The one-electron Green's function is obtained and leads to a density of states with the characteristic "pseudo-gap" in the energy range corresponding to the forbidden band of the crystal. The dielectric properties, conductivity, and optical absorption are considered. Electron localization of the Bragg type is obtained, together with the analog of interband absorption in an ideal semiconductor. The dielectric properties of the model considered turn out to be intermediate between those of typical metals and insulators. It is noted that the results obtained can be applied to interpret the properties of quasi-one-dimensional systems (of the TTF-TCNQ type) near the Peierls structural transition point.

INTRODUCTION

In recent years interest has grown in both the theory and the experimental studies of the electronic properties of different disordered systems^[1]. In particular, great attention has been paid to the experimental study of melts of most of the known semiconductors (see the reviews^[2-4]). It has been found that semiconductors can be roughly divided into three groups, according to their kinetic properties in the liquid state.

The first contains substances of the type Ge, InSb and other $A_{III}B_{V}$, which, on transition to the liquid state, give melts with purely metallic properties. Evidently, this is connected with the fact that, in these substances, not only the long-range order but also the short-range order corresponding to the given crystal is destroyed on melting. The second group is formed by substances of the type PbTe, SnTe, PbSe, In_2Te_3 , Ga_2Te_3 , etc., which are typical semiconductors in the crystalline state. On melting, their electrical conductivity, in absolute magnitude and in the temperature dependence, has practically the same behavior as in the corresponding crystal. The sign of the thermoelectric power, as a rule, indicates p-type conductivity. In the Hall effect, however, they display typically metallic properties: the Hall constant is almost independent of temperature, its sign corresponds to n-type conductivity, and in absolute magnitude it is slightly greater than the value for a metal with two free electrons per atom. Thus, these substances, which are usually called "liquid semiconductors," form a group intermediate between typical metals and semiconductors. To all appearances, their properties can be considered in the framework of the nearly-free electron approximation, with allowance for strong scattering of the "Bragg" type in the energy range coinciding with the forbidden band of the corresponding crystal. Finally, the third group is formed by substances of the type GeS, SnS, etc., with very low electron mobility, which, evidently, must be treated in the approximation of tight binding of the electrons to the ions.

In this paper we propose a simple model that makes it possible to understand qualitatively the appearance of the distinctive type of "band structure" in the energy spectrum of substances of the second group, which appears in the form of a characteristic "pseudo-gap" (of the type assumed in the work of Mott and other authors^[1]) in the density of electron states. Also considered are the dielectric properties, high-frequency con-

ductivity and optical absorption. The "quasi-one-dimensional" character of the model permits us to hope that a considerable proportion of the results obtained below can be applied to describe the properties of one-dimensional systems (of the TTF-TCNQ type) near the Peierls structural transition point.

1. THE ONE-ELECTRON GREEN FUNCTION

We write the Hamiltonian of the interaction of an electron with the ions in the form

$$H_{int} = \frac{1}{N} \sum_{pq} \langle p+q | V | p \rangle a_{p+q}^+ a_p \rho_q, \quad (1.1)$$

where

$$\rho_q = \sum_i e^{-iqR_i}$$

is the Fourier component of the ion density (R_i are the positions of the ions and N is their total number), $\langle p+q | V | p \rangle$ is a matrix element of the (generally speaking, nonlocal) ionic pseudo-potential^[5], and a_p^+ and a_p are electron operators in second quantization.

We introduce the one-electron Green function in the Matsubara temperature technique:

$$G(p\tau) = -\langle T_\tau a_p(\tau) a_p^+(0) \rangle, \quad (1.2)$$

and also the Green function of the ion subsystem:

$$F(q\tau) = -\langle T_\tau \rho_q(\tau) \rho_q^+(0) \rangle. \quad (1.3)$$

For the Fourier transform of (1.3) we have the spectral representation^[6]

$$F(q\omega_m) = \int_{-\infty}^{\infty} d\omega' \frac{A(q\omega')}{i\omega_m - \omega'}, \quad (1.4)$$

where $\omega_m = 2\pi m T$ (T is the temperature),

$$A(q\omega) = Z^{-1} \sum_{mn} \exp \left[-\frac{E_n}{T} \right] |(\rho_q)_{mn}|^2 \left\{ 1 - \exp \left[-\frac{\omega_m}{T} \right] \right\} \delta(\omega - \omega_m),$$

$$\omega_m = E_m - E_n, \quad (\rho_q)_{mn} = \langle m | \rho_q | n \rangle, \quad Z = \sum_m \exp \left[-\frac{E_m}{T} \right], \quad (1.5)$$

and m and n label the exact level of the ion subsystem.

Next we introduce the dynamical form factor of the liquid^[7]

$$S(q\omega) = Z^{-1} \sum_{mn} |(\rho_q)_{mn}|^2 \exp \left[-\frac{E_n}{T} \right] \delta(\omega - \omega_m). \quad (1.6)$$

Comparing (1.5) and (1.6), we see that

$$A(\mathbf{q}\omega) = S(\mathbf{q}\omega) \{1 - e^{-\omega/T}\}. \quad (1.7)$$

The simplest contribution to the electron self-energy part has the form

$$\Sigma(\epsilon, \mathbf{p}) = \frac{T}{N^2} \sum_{\mathbf{q}} |\langle \mathbf{p} + \mathbf{q} | V | \mathbf{p} \rangle|^2 \sum_m F(\mathbf{q}\omega_m) \frac{1}{i\epsilon_n + i\omega_m - \xi_{\mathbf{p}+\mathbf{q}}}, \quad (1.8)$$

$$\epsilon_n = (2n+1)\pi T, \quad \xi_{\mathbf{p}} = p^2/2m - \mu.$$

We note that the characteristic energies of the ionic excitations (the frequencies at which $S(\mathbf{q}\omega)$ is nonzero) satisfy, in the liquid, the condition $\omega/T \ll 1$, whereas we are interested in the electron spectrum in a substantially wider range of energies $\gtrsim T$. This enables us to neglect the effect of the dynamics of the ion subsystem, i.e., to take into account only the terms with $m = n$ in (1.6):

$$S(\mathbf{q}\omega) \approx S(\mathbf{q})\delta(\omega), \quad (1.9)$$

$$S(\mathbf{q}) = \frac{1}{N} \int_{-\infty}^{\infty} d\omega S(\mathbf{q}\omega), \quad (1.10)$$

where $S(\mathbf{q})$ is the static structure factor of the liquid^[7]. Using (1.4)–(1.7) and (1.9) in (1.8), we obtain the static approximation

$$\Sigma(\epsilon, \mathbf{p}) \approx \frac{1}{N} \sum_{\mathbf{q}} |\langle \mathbf{p} + \mathbf{q} | V | \mathbf{p} \rangle|^2 S(\mathbf{q}) \frac{1}{i\epsilon_n - \xi_{\mathbf{p}+\mathbf{q}}}. \quad (1.11)$$

This approximation was used by Edwards in his well-known papers^[8]. The averaging he used, over all possible ion configurations, is contained implicitly in the definitions (1.5) and (1.6), in which averaging over the canonical ensemble of the liquid is performed.

The static structure factor $S(\mathbf{q})$ is determined experimentally from data on the elastic scattering of x-rays or neutrons. Its typical behavior in a liquid is represented in Fig. 1.

First we shall consider a one-dimensional model of a liquid. We shall model the structure factor by two narrow peaks at $q = \pm K$, this being the natural analog of Fig. 1 in the one-dimensional case. We shall assume that the Fermi level of the free electrons passes through the degeneracy points of their spectrum, at which Bragg gaps are formed in the case of an ideal periodic structure (see Fig. 2). We therefore take $2p_F = K$, where p_F is the Fermi momentum of the free electrons. The latter condition is typical for "liquid semiconductors"^[4], K being the analog of the reciprocal-lattice vector of the ideal crystal.

From (1.11) we have (L is the length of the system)

$$\Sigma(\epsilon, \mathbf{p}) = \frac{L}{N} \int \frac{dq}{2\pi} |\langle \mathbf{p} + \mathbf{q} | V | \mathbf{p} \rangle|^2 S(q) (i\epsilon_n - \xi_{\mathbf{p}+\mathbf{q}})^{-1} \approx \quad (1.12)$$

$$\approx A^2 \{i\epsilon_n - \xi_{\mathbf{p}-K}\}^{-1} + A^2 \{i\epsilon_n - \xi_{\mathbf{p}+K}\}^{-1}, \quad (1.13)$$

$$A^2 = \frac{L}{N} \int \frac{dq}{2\pi} |\langle \mathbf{p} + \mathbf{q} | V | \mathbf{p} \rangle|^2 S(q).$$

Here we have made use of the characteristic structure of $S(\mathbf{q})$, with two narrow peaks at $q = \pm K$.

It is not difficult to convince oneself^[9] that corrections for the finite width of the peaks are small if the conditions

$$\gamma = \frac{1}{R_c} \ll |p - p_F| \quad \text{or} \quad v_F \gamma \ll 2\pi T, \quad (1.14)$$

are fulfilled, where γ is the width of the peaks, v_F is the Fermi velocity of the free electrons, and the parameter R_c , defined in (1.14), in the one-dimensional case plays

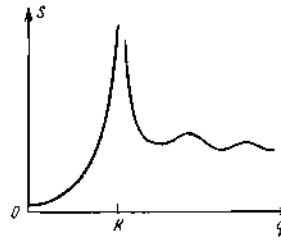


FIG. 1

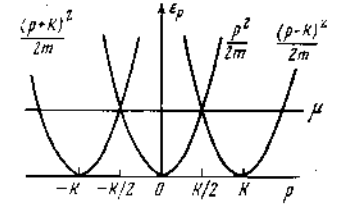


FIG. 2

the role of the correlation length of the short-range order.

From Fig. 2 the following symmetry properties of the free-electron spectrum in the one-dimensional case can be seen:

$$\xi_{\mathbf{p}-K} = -\xi_{\mathbf{p}} \quad \text{for } p \sim +K/2 \quad (1.15)$$

$$\xi_{\mathbf{p}+K} = -\xi_{\mathbf{p}} \quad \text{for } p \sim -K/2.$$

Then, considering the electron with $p \sim +K/2$ (the treatment of $p \sim -K/2$ is analogous), we may take into account only the first term in the right-hand side of (1.12):

$$\Sigma(\epsilon, \mathbf{p}) \approx A^2 G_0(\epsilon_n, -\xi_{\mathbf{p}}). \quad (1.16)$$

Thus, the use of the characteristic form of the liquid structure factor makes it possible to replace the real interaction $|\langle \mathbf{p} + \mathbf{q} | V | \mathbf{p} \rangle|^2 S(\mathbf{q})$ in the liquid by the model interaction $2\pi N L^{-1} A^2 \delta(\mathbf{q} - K)$. Then, the remaining perturbation

$$\bar{A}^2(q) = |\langle \mathbf{p} + \mathbf{q} | V | \mathbf{p} \rangle|^2 S(q) - 2\pi N L^{-1} A^2 \delta(q - K)$$

is unimportant, if the treatment is confined to the region specified by the conditions (1.14). It should be emphasized that the introduction of this model interaction does not imply the introduction of long-range crystalline order. The analysis is performed under the assumption of a microscopically homogeneous liquid, and the conditions (1.14) impose a restriction in the sense that the correlation length of the short-range order should be sufficiently large. The presence of long-range order entails the appearance of "anomalous" Green functions, which describe Umklapp processes^[10] and substantially alter the structure of the equations.

With the model interaction introduced above, we can now sum all the important diagrams. It is not difficult to see^[9] that, in each order of perturbation theory, diagrams with an alternating sequence of Green functions $\{i\epsilon_n - \xi_{\mathbf{p}}\}^{-1}$ and $\{i\epsilon_n + \xi_{\mathbf{p}}\}^{-1}$ (we are considering $p \sim K/2$) and an alternating sequence of vertices with incoming or outgoing interaction lines transferring momentum $\pm K$ give equal contributions (see Fig. 3). The general term in the expansion for the Green function then has the form

$$g_n(\epsilon, \mathbf{p}) = \frac{A^{2n} n!}{(i\epsilon_n - \xi_{\mathbf{p}})^n (i\epsilon_n + \xi_{\mathbf{p}})^n (i\epsilon_n - \xi_{\mathbf{p}})} = n! z^n(\epsilon; \xi_{\mathbf{p}}) G_0(\epsilon; \xi_{\mathbf{p}}), \quad (1.17)$$

where A^2 is defined by (1.13), n is the order of perturbation theory in A^2 , and $z(\epsilon; \xi_{\mathbf{p}}) = A^2 G_0(\epsilon; \xi_{\mathbf{p}}) G_0(\epsilon; -\xi_{\mathbf{p}})$.

The factor $n!$ arises from simple combinatorial considerations. In fact, there are $2n$ points to which interaction

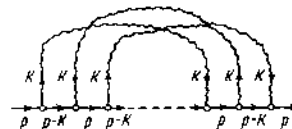


FIG. 3

lines are attached. Of these, n points have an outgoing line, which can enter the remaining n free vertices (corresponding to incoming lines) in any of $n!$ ways. We shall use the identity

$$\sum_{n=0}^{\infty} n! z^n = \sum_{n=0}^{\infty} \int_0^{\infty} d\xi e^{-\xi} (\xi z)^n = \int_0^{\infty} d\xi e^{-\xi} \frac{1}{1-\xi z}. \quad (1.18)$$

Then the one-electron Green function is

$$G(\epsilon, \mathbf{p}) = \sum_{n=0}^{\infty} g_n(\epsilon, \mathbf{p}) = \int_0^{\infty} d\xi e^{-\xi} \frac{i\epsilon_n + \xi_p}{(i\epsilon_n)^2 - \xi_p^2 - \xi A^2} = \langle G_{iA^2}(\epsilon, \mathbf{p}, \mathbf{p}) \rangle_t, \quad (1.19)$$

where

$$G_{iA^2}(\epsilon, \mathbf{p}, \mathbf{p}) = \frac{i\epsilon_n + \xi_p}{(i\epsilon_n)^2 - \xi_p^2 - A^2} \quad (1.20)$$

is the normal Green function of an ideal semiconductor with energy gap $2|A|$, and

$$\langle \dots \rangle_t = \int_0^{\infty} d\xi e^{-\xi} \dots$$

is a particular type of averaging over the "fluctuations" of the energy gap. Thus, the model considered for the disordered system is equivalent to an ensemble of ideal semiconductors, in the spectrum of which the energy gap takes random values, with a distribution of a special form.

Performing the analytic continuation to real frequencies in the usual way, we obtain the retarded (or advanced) Green function. The density of electron states can be found from the formula

$$N(\epsilon) = -\frac{N_0}{\pi} \int_{-\infty}^{\infty} d\xi_p \operatorname{Im} G^R(\epsilon, \xi_p), \quad (1.21)$$

where N_0 is the density of free-electron states. From (1.19) we have

$$\begin{aligned} \operatorname{Im} G^{R,A}(\epsilon, \xi_p) &= \mp \pi \int_0^{\infty} d\xi e^{-\xi} (\epsilon + \xi_p) \delta(\epsilon^2 - \xi_p^2 - \xi A^2) \\ &= \mp \frac{\pi}{A^2} (\epsilon + \xi_p) \theta(\epsilon^2 - \xi_p^2) e^{-(\epsilon^2 - \xi_p^2)/A^2} \end{aligned} \quad (1.22)$$

and the density of states is

$$\begin{aligned} \frac{N(\epsilon)}{N_0} &= \left| \frac{\epsilon}{A} \right| \int_0^{\epsilon^2/A^2} d\xi \frac{e^{-\xi}}{(\epsilon^2/A^2 - \xi)^{3/2}} = 2 \left| \frac{\epsilon}{A} \right| \exp\left[-\frac{\epsilon^2}{A^2}\right] \operatorname{Erfi}\left(\frac{\epsilon}{A}\right), \\ \operatorname{Erfi}(x) &= \int_0^x dx e^{x^2} \end{aligned} \quad (1.23)$$

is the error function of imaginary argument. The density of states (1.23) is represented graphically in Fig. 4.

We have thus obtained a "pseudo-gap," of the type proposed in the numerous papers of Mott and other authors in order to interpret the properties of "liquid semiconductors." The width of the pseudo-gap is equal in order of magnitude to the width of the forbidden band

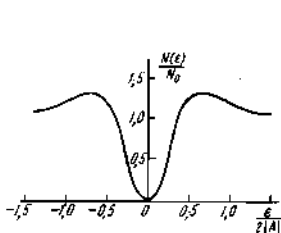


FIG. 4

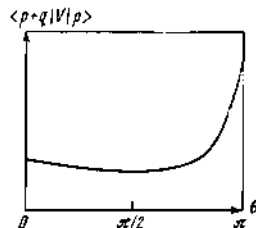


FIG. 5

of the corresponding crystal. The asymptotic behavior of (1.23) has the form

$$\frac{N(\epsilon)}{N_0} \rightarrow \begin{cases} 1 & \text{if } |\epsilon| \rightarrow \infty \\ 2\epsilon^2/A^2 \rightarrow 0 & \text{for } |\epsilon| \rightarrow 0. \end{cases} \quad (1.24)$$

We emphasize that the Green function (1.19) has no pole singularities in the vicinity of the "Fermi surface" and, in this sense, does not describe the spectrum of the elementary excitations in the region of energies corresponding to the pseudo-gap. The first of the conditions (1.14) indicates that the formulas obtained are inapplicable in the immediate vicinity $\epsilon \sim 0$ of the Fermi level. For $R_C \gtrsim 20a$, where a is the interatomic spacing, this limitation is extended to the region $|\xi_p| \lesssim 0.05 \epsilon_F$ (ϵ_F is the free-electron Fermi energy), which, for typical $|A| \sim (0.1-0.2)\epsilon_F$ amounts to approximately $(1/4)-(1/8)$ of the width of the pseudo-gap. The situation is improved with increasing R_C , but the vanishing of the density of states in the middle of the pseudo-gap raises doubts. Moreover, for "liquid semiconductors" the estimate $T \sim |A|$ is typical, so that the second condition (1.14) is already fulfilled when $R_C \gtrsim 10a$.

The generalization of the results obtained to the three-dimensional case encounters certain difficulties. In particular, if in (1.11) we make use of the usual local-pseudo-potential approximation, then, on integration over the polar angle between the vectors \mathbf{p} and \mathbf{q} , there arises a characteristic logarithmic expression for the self-energy part^[8, 11-13], which is considerably less singular than (1.12) in the energy region of interest and leads only to weak changes in the density of states as compared with the case of free electrons. It was pointed out by Ziman^[13] that, under certain assumptions concerning the higher correlation functions of the ions (in particular, the four-ion correlation function), contributions to the electron self-energy part that have a "one-dimensional" form of the type (1.12) can appear. Without denying this possibility, we should like to remark that these assumptions are too stringent, the more so because, at present, no theoretical or experimental methods exist that permit one to find the higher ionic correlators in the liquid. Incidentally, it turns out to be sufficient to impose only one condition on the ionic pseudo-potential (based essentially on its nonlocal nature) in order to obtain a result of the type (1.16) in the three-dimensional case. The matrix element $\langle \mathbf{p} + \mathbf{q} | V | \mathbf{p} \rangle$ of a nonlocal pseudo-potential depends not only on $|\mathbf{q}|$, but also, in the general case, on $|\mathbf{p}|$ and $|\mathbf{p} + \mathbf{q}|$, i.e., it depends also on the mutual orientation of the vectors \mathbf{p} and \mathbf{q} ^[5]. It then turns out that, in the region $|\mathbf{q}| \sim 2p_F$ of interest, the pseudo-potential corresponding to "almost-backward" scattering is considerably greater than for scattering through small angles^[5, 12].

A typical dependence of the matrix element $\langle \mathbf{p} + \mathbf{q} | V | \mathbf{p} \rangle$ ($|\mathbf{p}| \sim p_F$, $|\mathbf{q}| \approx 2p_F$) on the scattering angle is shown in Fig. 5. We shall assume that for the substances in which we are interested there is a sharply pronounced peak in the pseudo-potential in the region of scattering angles $\theta \sim \pi$. Then, from (1.11) we obtain (Ω_0 is the volume per atom)

$$\Sigma(\epsilon, \mathbf{p}) = \Omega_0 \int_0^{\infty} dq q^2 \frac{1}{4\pi^2} \int_{-1}^1 \frac{d \cos \theta |\langle \mathbf{p} + \mathbf{q} | V | \mathbf{p} \rangle|^2 S(\mathbf{q})}{i\epsilon_n - \xi_{|\mathbf{p} + \mathbf{q}|}} \approx A^2 (i\epsilon_n - \xi_{|\mathbf{p} + \mathbf{q}|})^{-1}, \quad (1.25)$$

and the problem reduces to a one-dimensional one.

Here,

$$A^2 = \Omega_0 \int_0^{\infty} dq q^2 \frac{1}{4\pi^2} \int_{-1}^1 d \cos \theta |\langle \mathbf{p} + \mathbf{q} | V | \mathbf{p} \rangle|^2 S(\mathbf{q}). \quad (1.26)$$

We assume that the conditions (1.14) are fulfilled and that the integration over $\cos \theta$ is effectively cut off in the interval

$$|\delta\theta|^2 \ll |p - p_F|/|p_F| \text{ or } |\delta\theta|^2 \ll 2\pi T/\epsilon_F \quad (1.27)$$

about $\theta \sim \pi$; this singles out a narrow cone, corresponding to the dominant role of the backward scattering. For $|p - p_F| \sim 0.05p_F$ we have $|\delta\theta| \lesssim 0.22$. Therefore, in the three-dimensional variant of our model the real interaction $|\langle \mathbf{p} + \mathbf{q} | V | \mathbf{p} \rangle|^2 S(\mathbf{q})$ is replaced by the model interaction

$$\frac{4\pi^2}{K^2 \Omega_0} A^2 \delta(q - K) \delta(\cos \theta + 1).$$

The remaining perturbation

$$\bar{A}^2(q, \theta) = |\langle \mathbf{p} + \mathbf{q} | V | \mathbf{p} \rangle|^2 S(\mathbf{q}) - \frac{4\pi^2}{K^2 \Omega_0} A^2 \delta(q - K) \delta(\cos \theta + 1)$$

leads to the appearance of the above-mentioned weak renormalizations of the density of states. It is not difficult to see that, in the three-dimensional case, in place of (1.15) we have

$$\xi_{|\mathbf{p} - \mathbf{K}|} = -\xi_{|\mathbf{p}|} \text{ for } |\mathbf{p}| \sim K/2. \quad (1.28)$$

The subsequent treatment coincides with (1.17)–(1.23), and all the formulas remain valid for the three-dimensional system too.

2. THE VERTEX PART, POLARIZATION OPERATOR AND DIELECTRIC FUNCTION

It is of interest to study, in the model under consideration, the properties of the vertex part describing the response of the system to an external electromagnetic perturbation. We have the following expression for the variation of the one-electron Green function on introduction of a weak external field^[6]:

$$\frac{\delta G(\epsilon \mathbf{p})}{\delta A_\mu(\mathbf{q}\omega)} = G(\epsilon \mathbf{p}) J^\mu(\epsilon \mathbf{p} \mathbf{e} + \omega \mathbf{p} + \mathbf{q}) G(\epsilon + \omega \mathbf{p} + \mathbf{q}), \quad (2.1)$$

where $\delta A_\mu(\mathbf{q}\omega) = \{\delta A_{\mathbf{q}\omega}^\mu; -\delta \varphi_{\mathbf{q}\omega}\}$ is the variation of the external field and $J^\mu(\epsilon \mathbf{p} \mathbf{e} + \omega \mathbf{p} + \mathbf{q})$ is the required vertex part. In this case we have for the free Green function:

$$\frac{\delta G_0(\epsilon \mathbf{p})}{\delta A_\mu(\mathbf{q}\omega)} = G_0(\epsilon \mathbf{p}) J_0^\mu(\epsilon \mathbf{p} \mathbf{e} + \omega \mathbf{p} + \mathbf{q}) G_0(\epsilon + \omega \mathbf{p} + \mathbf{q}), \quad (2.2)$$

where the free vertex

$$J_0^\mu(\epsilon \mathbf{p} \mathbf{e} + \omega \mathbf{p} + \mathbf{q}) = \begin{cases} -e\mathbf{p}/mc, & \mu = 1, 2, 3 \\ e, & \mu = 0 \end{cases} \quad (2.3)$$

In the model considered, the variational derivative (2.1) can be calculated directly. In fact, from (1.17)–(1.19) we have

$$\begin{aligned} \frac{\delta G(\epsilon \mathbf{p})}{\delta A_\mu(\mathbf{q}\omega)} &= \frac{\delta}{\delta A_\mu(\mathbf{q}\omega)} \left\{ \left\langle \sum_{n=0}^{\infty} [\zeta z(\epsilon \mathbf{p})]^n \right\rangle_c G_0(\epsilon \mathbf{p}) \right\} \\ &= \left\langle \sum_{n=1}^{\infty} \sum_{m=1}^{\infty} [\zeta z(\epsilon \mathbf{p})]^{n-1} \zeta \frac{\delta z(\epsilon \mathbf{p})}{\delta A_\mu(\mathbf{q}\omega)} [\zeta z(\epsilon + \omega \mathbf{p} + \mathbf{q})]^{m-1} \right. \\ &\quad \left. \times G_0(\epsilon + \omega \mathbf{p} + \mathbf{q}) + \sum_{n=1}^{\infty} [\zeta z(\epsilon \mathbf{p})]^n \frac{\delta G_0(\epsilon \mathbf{p})}{\delta A_\mu(\mathbf{q}\omega)} \right\rangle_c, \quad (2.4) \end{aligned}$$

since $\delta G(\epsilon \mathbf{p})/\delta A_\mu(\mathbf{q}\omega)$ is obtained from the set of diagrams of the type shown in Fig. 3 by inserting external-field lines into any of the electron lines in Fig. 3 (see Fig. 6a). In (2.4), m is the label of that block $z(\epsilon \mathbf{p})$ of Fig. 6a into which the external-field line enters. Using

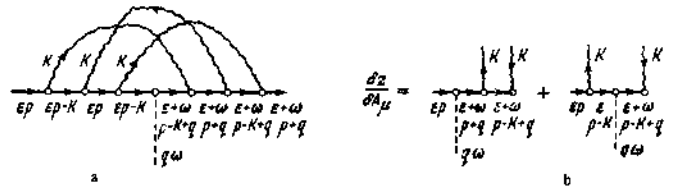


FIG. 6

(2.2), it is not difficult to convince oneself that (see Fig. 6b)

$$\begin{aligned} \frac{\delta z(\epsilon \mathbf{p})}{\delta A_\mu(\mathbf{q}\omega)} &= G_0(\epsilon \mathbf{p}) J_0^\mu(\epsilon \mathbf{p} \mathbf{e} + \omega \mathbf{p} + \mathbf{q}) z(\epsilon + \omega \mathbf{p} + \mathbf{q}) \\ &+ z(\epsilon \mathbf{p}) J_0^\mu(\epsilon \mathbf{p} - \mathbf{K} \mathbf{e} + \omega \mathbf{p} - \mathbf{K} + \mathbf{q}) G_0(\epsilon + \omega \mathbf{p} - \mathbf{K} + \mathbf{q}). \quad (2.5) \end{aligned}$$

Substituting (2.2) and (2.5) into (2.4), after certain transformations we obtain

$$\begin{aligned} \frac{\delta G(\epsilon \mathbf{p})}{\delta A_\mu(\mathbf{q}\omega)} &= J_0^\mu(\epsilon \mathbf{p} \mathbf{e} + \omega \mathbf{p} + \mathbf{q}) G_0(\epsilon \mathbf{p}) G_0(\epsilon + \omega \mathbf{p} + \mathbf{q}) \\ &\times \left\langle \sum_{n=0}^{\infty} \zeta^n z^n(\epsilon \mathbf{p}) \sum_{m=0}^{\infty} \zeta^m z^m(\epsilon + \omega \mathbf{p} + \mathbf{q}) \right\rangle_c, \quad (2.6) \end{aligned}$$

$$+ J_0^\mu(\epsilon \mathbf{p} - \mathbf{K} \mathbf{e} + \omega \mathbf{p} - \mathbf{K} + \mathbf{q}) \left\langle \frac{1}{\zeta A^2} \sum_{n=1}^{\infty} \zeta^n z^n(\epsilon \mathbf{p}) \sum_{m=1}^{\infty} \zeta^m z^m(\epsilon + \omega \mathbf{p} + \mathbf{q}) \right\rangle_c,$$

which reduces immediately to

$$\begin{aligned} \frac{\delta G(\epsilon \mathbf{p})}{\delta A_\mu(\mathbf{q}\omega)} &= J_0^\mu(\epsilon \mathbf{p} \mathbf{e} + \omega \mathbf{p} + \mathbf{q}) \langle G_{1A^2}(\epsilon \mathbf{p} \mathbf{p}) G_{1A^2}(\epsilon + \omega \mathbf{p} + \mathbf{q} \mathbf{p} + \mathbf{q}) \rangle_c \\ &+ J_0^\mu(\epsilon \mathbf{p} - \mathbf{K} \mathbf{e} + \omega \mathbf{p} - \mathbf{K} + \mathbf{q}) \langle G_{1A^2}(\epsilon \mathbf{p} \mathbf{p} - \mathbf{K}) G_{1A^2}(\epsilon + \omega \mathbf{p} - \mathbf{K} + \mathbf{q} \mathbf{p} + \mathbf{q}) \rangle_c, \quad (2.7) \end{aligned}$$

where $G_{1A^2}(\epsilon \mathbf{p} \mathbf{p})$ is defined in (1.20), while

$$G_{1A^2}(\epsilon \mathbf{p} \mathbf{p} - \mathbf{K}) = + \frac{A}{(i\epsilon_n)^2 - \xi_p^2 - A^2} \quad (2.8)$$

is the anomalous Green function of the ideal semiconductor, describing the elementary Umklapp process $\mathbf{p} - \mathbf{p} - \mathbf{K}$.

We see that, in the model considered, the electromagnetic response is described by the same formulas as in an ideal semiconductor of the excitonic-insulator type, but with a fluctuating energy gap. Finite expressions arise, associated with pair products of anomalous Green functions, while the average (of the type (1.19)) of (2.8) is absent, corresponding to the absence of long-range order in the system. The model interaction introduced above is the direct analog of the Bragg scattering in the ideal crystal and is responsible for the formation of the distinctive kind of band structure (the pseudo-gap) in the electron spectrum. However, like the scattering in the ideal crystal, it is insufficient for a correct description of the kinetics, for which we must take into account the dissipative scattering (the analog of defects and phonons in the crystal) associated with the discarded part of the real interaction.

We now turn to consider the dielectric properties of our system. Since the polarization operator is directly related to the scalar vertex, from (2.7) we have

$$\begin{aligned} \Pi(\mathbf{q}\omega_n) &= -2 \int_0^{\bar{T}} d\zeta e^{-\zeta T} \sum_{\mathbf{p}} \int \frac{d^3 p}{(2\pi)^3} \{ G_{1A^2}(\epsilon_n \mathbf{p} \mathbf{p}) G_{1A^2}(\epsilon_n + \omega_n \mathbf{p} + \mathbf{q} \mathbf{p} + \mathbf{q}) \\ &+ G_{1A^2}(\epsilon_n \mathbf{p} \mathbf{p} - \mathbf{K}) G_{1A^2}(\epsilon_n + \omega_n \mathbf{p} + \mathbf{q} \mathbf{p} - \mathbf{K} + \mathbf{q}) \} = \langle \Pi_{1A^2}(\mathbf{q}\omega_n) \rangle_c. \quad (2.9) \end{aligned}$$

Summing over the Matsubara frequencies in the standard manner and performing the analytic continuation $i\omega_m \rightarrow \omega + i\delta$, we obtain^[14]

$$\Pi_{A^2}(\mathbf{q}\omega) = -\frac{1}{2} \int \frac{d^3p}{(2\pi)^3} \frac{E_p E_{p+\mathbf{q}} + \xi_p \xi_{p+\mathbf{q}} + A^2}{E_p E_{p+\mathbf{q}}} (f(E_p) - f(E_{p+\mathbf{q}}))$$

$$\times \left\{ \frac{1}{E_p - E_{p+\mathbf{q}} + \omega + i\delta} + \frac{1}{E_p - E_{p+\mathbf{q}} - \omega - i\delta} \right\} + \frac{1}{2} \int \frac{d^3p}{(2\pi)^3} \frac{E_p E_{p+\mathbf{q}} - \xi_p \xi_{p+\mathbf{q}} - A^2}{E_p E_{p+\mathbf{q}}}$$

$$\times (1 - f(E_p) - f(E_{p+\mathbf{q}})) \left\{ \frac{1}{E_p + E_{p+\mathbf{q}} + \omega + i\delta} + \frac{1}{E_p + E_{p+\mathbf{q}} - \omega - i\delta} \right\} \quad (2.10)$$

i.e., the polarization operator of an ideal semiconductor. Here $E_p = (\xi_p^2 + A^2)^{1/2}$, $f(E_p) = \{\exp(E_p/T) + 1\}^{-1}$ is the Fermi distribution function.

As $A^2 \rightarrow 0$ the second term in (2.10) tends to zero, while the first gives the usual polarization operator of the electron gas. On the other hand, for $T \rightarrow 0$ but $A^2 \neq 0$, the first term in (2.10) vanishes, so that

$$\Pi_{A^2}(\mathbf{q}\omega) = \frac{1}{2} \int \frac{d^3p}{(2\pi)^3} \frac{E_p E_{p+\mathbf{q}} - \xi_p \xi_{p+\mathbf{q}} - A^2}{E_p E_{p+\mathbf{q}}} \quad (2.11)$$

$$\times \left\{ \frac{1}{E_p + E_{p+\mathbf{q}} + \omega + i\delta} + \frac{1}{E_p + E_{p+\mathbf{q}} - \omega - i\delta} \right\}.$$

The dielectric function is

$$\epsilon(\mathbf{q}\omega) = 1 + \frac{4\pi e^2}{q^2} \Pi(\mathbf{q}\omega) = \langle \epsilon_{iA^2}(\mathbf{q}\omega) \rangle_i, \quad (2.12)$$

where

$$\epsilon_{iA^2}(\mathbf{q}\omega) = 1 + \frac{4\pi e^2}{q^2} \Pi_{A^2}(\mathbf{q}\omega) \quad (2.13)$$

is the dielectric function of the ideal semiconductor.

We shall consider first the case $\omega = 0$. For $v_{FQ} \ll |A|$ we obtain from (2.11)

$$\Pi_{A^2}(\mathbf{q}0) = \frac{v_F^2 q^2}{18} \frac{m p_F}{\pi^2 A^2} = \frac{q^2}{4\pi e^2} \frac{v_F^2 \kappa^2}{18A^2}, \quad (2.14)$$

so that

$$\epsilon_{iA^2}(\mathbf{q}0) = 1 + v_F^2 \kappa^2 / 18A^2 = 1 + \omega_p^2 / 6A^2, \quad (2.15)$$

where $\kappa^2 = 4\pi p_F e^2 / \pi$ is the square of the inverse Debye screening length and $\omega_p^2 = 4\pi n e^2 / m$ is the square of the plasma frequency (n is the total electron density).

On the other hand, for $v_{FQ} \gg |A|$ it follows from (2.10)–(2.11) that

$$\Pi_{A^2}(\mathbf{q}0) = m p_F / \pi^2 = \kappa^2 / 4\pi e^2, \quad (2.16)$$

so that

$$\epsilon_{iA^2}(\mathbf{q}0) = 1 + \kappa^2 / q^2, \quad (2.17)$$

i.e., we have the usual Debye screening.

We shall use the simplest interpolation from (2.15) to (2.17):

$$\epsilon_{iA^2}(\mathbf{q}0) = 1 + \frac{\kappa^2}{q^2 + 18A^2 / v_F^2}. \quad (2.18)$$

Then for our model of a disordered system we obtain

$$\epsilon(\mathbf{q}0) = \int_0^{\infty} d\xi e^{-\xi} \epsilon_{iA^2}(\mathbf{q}0) = 1 - \frac{v_F^2 \kappa^2}{18A^2} \exp\left(\frac{v_F^2 q^2}{18A^2}\right) \text{Ei}\left(-\frac{v_F^2 q^2}{18A^2}\right), \quad (2.19)$$

where $\text{Ei}(-x)$ is the integral exponential function. For $v_{FQ} \gg |A|$ we use the asymptotic form

$$\text{Ei}(-x) \approx -e^{-x}/x$$

and obtain (2.17). For $v_{FQ} \ll |A|$ we use

$$\text{Ei}(-x) \approx \ln x,$$

so that

$$\epsilon(\mathbf{q}0) \approx 1 - \frac{v_F^2 \kappa^2}{18A^2} \ln \frac{v_F^2 q^2}{18A^2}. \quad (2.20)$$

Correspondingly, the effective Coulomb interaction takes the form

$$\Gamma(\mathbf{q}0) \approx 4\pi e^2 / q^2, \quad (2.21)$$

$$\epsilon^2 = e^2 / \left(1 - \frac{v_F^2 \kappa^2}{18A^2} \ln \frac{v_F^2 q^2}{18A^2}\right), \quad (2.22)$$

which formally resembles the well-known "zero-charge" situation in field theory. Behavior of the type (2.20)–(2.22) has been obtained recently in a treatment of the so-called zero-gap semiconductors^[15].

We turn to the analysis of the case $\omega \neq 0$, $v_{FQ} \ll |A|$. From (2.11) we have

$$\text{Re } \Pi_{A^2}(\mathbf{q}\omega) = \frac{v_F^2 q^2}{12} \frac{m p_F}{2\pi^2} \int_{-\infty}^{\infty} d\xi_p \frac{A^2}{(\xi_p^2 + A^2)^{3/2}} \frac{1}{\xi_p^2 + A^2 - \omega^2/4}, \quad (2.23)$$

$$\text{Im } \Pi_{A^2}(\mathbf{q}\omega) = \frac{v_F^2 q^2}{12} \frac{m p_F}{2\pi^2} \frac{\pi}{2} \int_{-\infty}^{\infty} d\xi_p \frac{A^2}{(\xi_p^2 + A^2)^{3/2}}$$

$$\times \left\{ \delta \left[\frac{\omega}{2} - (\xi_p^2 + A^2)^{1/2} \right] - \delta \left[\frac{\omega}{2} + (\xi_p^2 + A^2)^{1/2} \right] \right\}. \quad (2.24)$$

We first consider the real part of the dielectric function. From (2.23) we obtain

$$\text{Re } \epsilon_{iA^2}(\omega) = 1 + \frac{\pi}{2} \frac{n e^2}{m} \int_{-\infty}^{\infty} d\xi_p \frac{A^2}{(\xi_p^2 + A^2)^{3/2}} \frac{1}{\xi_p^2 + A^2 - \omega^2/4}. \quad (2.25)$$

For $\omega \rightarrow 0$ ($\omega \ll 2|A|$), (2.15) follows naturally from this. For $\omega \gg 2|A|$ we obtain the plasma limit:

$$\text{Re } \epsilon_{iA^2}(\omega) \approx 1 - \omega_p^2 / \omega^2. \quad (2.26)$$

We shall use the simplest approximation:

$$\text{Re } \epsilon_{iA^2}(\omega) = 1 + \frac{\omega_p^2}{6A^2} \theta\left(1 - \frac{\omega^2}{4A^2}\right) - \frac{\omega_p^2}{\omega^2} \theta\left(\frac{\omega^2}{4A^2} - 1\right). \quad (2.27)$$

Then, from (2.12),

$$\text{Re } \epsilon(\omega) = 1 - \frac{\omega_p^2}{6A^2} \text{Ei}\left(-\frac{\omega^2}{4A^2}\right) - \frac{\omega_p^2}{\omega^2} (1 - e^{-\omega^2/4A^2}). \quad (2.28)$$

From this, for $\omega \gg 2|A|$, the plasma limit (2.26) follows. For $\omega \ll 2|A|$ we obtain, analogously to (2.21),

$$\text{Re } \epsilon(\omega) \approx 1 - \frac{\omega_p^2}{6A^2} \ln \frac{\omega^2}{4A^2}. \quad (2.29)$$

We emphasize that the qualitative behavior of $\text{Re } \epsilon(\omega)$ turns out to be practically independent of the method of interpolation in the formulas of the type (2.19) and (2.27). We can combine (2.20) and (2.29) by writing a single expression, valid with logarithmic accuracy:

$$\text{Re } \epsilon(\mathbf{q}\omega) \approx 1 - \frac{\omega_p^2}{6A^2} \ln \frac{\max\{\omega^2; v_F^2 q^2\}}{4A^2}. \quad (2.30)$$

This result is valid only for $\omega \ll 2|A|$, $v_{FQ} \ll |A|$. The interpolation formula (2.28) describes the entire frequency interval. One can easily convince oneself that $\text{Re } \epsilon(\omega)$ given by (2.28) has no zeros other than the plasma zero, which arises in the limit $\omega \gg 2|A|$.

The behavior of the imaginary part of the dielectric function is of special interest, since it determines, in particular, the optical absorption in the system. The absorption is determined by the real part of the conductivity, which is related to $\text{Im } \epsilon(\omega)$ as follows:

$$\text{Re } \sigma(\omega) = \omega \text{Im } \epsilon(\omega) / 4\pi. \quad (2.31)$$

From (2.11) and (2.12) we obtain

$$\begin{aligned} \text{Im } \epsilon(\omega) &= \frac{\pi}{4} \frac{ne^2}{m} \int_0^{\infty} d\xi e^{-\xi} \int_{-\infty}^{\infty} d\xi_s \frac{\xi A^2}{(\xi_p^2 + \xi A^2)^2} \\ &\times \left\{ \delta \left[\frac{\omega}{2} - (\xi_p^2 + \xi A^2)^{1/2} \right] - \delta \left[\frac{\omega}{2} + (\xi_p^2 + \xi A^2)^{1/2} \right] \right\} \\ &= 2\pi^2 \frac{ne^2}{m} \frac{|A|}{\omega^2} \int_0^{\omega/2A} d\xi e^{-\xi} \frac{\xi}{(\omega^2/4A^2 - \xi)^{3/2}} \\ &= \pi \left(\frac{\omega_p}{\omega} \right)^2 \frac{|A|}{\omega} \exp \left\{ -\frac{\omega^2}{4A^2} \right\} \left\{ \frac{\omega^2}{4A^2} - \frac{d}{d\alpha} \right\} \text{Erfi } \alpha^{1/2} \frac{\omega}{2|A|} \Big|_{\alpha=1}. \end{aligned} \quad (2.32)$$

Correspondingly,

$$\text{Re } \sigma(\omega) = \pi \frac{ne^2}{m\omega} \frac{|A|}{\omega} \exp \left\{ -\frac{\omega^2}{4A^2} \right\} \left\{ \frac{\omega^2}{4A^2} - \frac{d}{d\alpha} \right\} \text{Erfi } \alpha^{1/2} \frac{\omega}{2|A|} \Big|_{\alpha=1}. \quad (2.33)$$

We have the following asymptotic behavior for $\omega \gg 2|A|$:

$$\text{Im } \epsilon(\omega) \approx \pi \left(\frac{\omega_p}{\omega} \right)^2 \left(\frac{A}{\omega} \right)^2, \quad (2.34)$$

$$\text{Re } \sigma(\omega) \approx \frac{ne^2}{m\omega} \pi \left(\frac{A}{\omega} \right)^2. \quad (2.35)$$

For $\omega \ll 2|A|$,

$$\text{Im } \epsilon(\omega) \approx \pi \omega_p^2 / 6A^2, \quad (2.36)$$

$$\text{Re } \sigma(\omega) \approx \frac{ne^2}{m} \pi \frac{\omega}{6A^2} \rightarrow 0 \quad \text{for } \omega \rightarrow 0. \quad (2.37)$$

The static conductivity in our approximation vanishes, indicating a particular type of Bragg electron-localization. Analogously, the static conductivity of the ideal semiconductor at $T = 0$ equals zero. We have obtained the analog of the usual interband absorption. In addition (2.36) shows that our model describes a substance intermediate between a metal and an insulator: in a metal $\text{Im } \epsilon(\omega) \propto 1/\omega$, and in an insulator $\text{Im } \epsilon(\omega) = 0$ for $\omega = 0$. In our case, $\text{Im } \epsilon(\omega)$ has a finite discontinuity at $\omega = 0$ ($\text{Im } \epsilon(\omega) = -\text{Im } \epsilon(-\omega)$).

It should be noted that, generally speaking, in view of the fact that the entire treatment is invalid (in the sense of the first of the conditions (1.14)) near the center of the pseudo-gap, when $\epsilon \sim \xi_p \sim 0$, our formulas are not valid in the region of low frequencies. Therefore, the calculation performed for the polarization operator is valid, clearly, only in the region of sufficiently high frequencies:

$$\omega \gg v_F \gamma = v_F / R_C, \quad (2.38)$$

where γ and R_C are defined in (1.14). For $R_C \geq 20a$, we are concerned with frequencies greater than or of the order of $(1/4) - (1/8)$ of the width of the pseudo-gap. The condition (2.38) has a clear meaning—in the characteristic time of variation of the external field the electron moves over a distance less than R_C . Naturally, allowance for the finite temperature will also change the asymptotic behavior of $\epsilon(q\omega)$ for small q and ω , because of the appearance of excited carriers in the "upper band".

In conclusion, we note that the model considered and all the results obtained above can be used in the analysis of the properties of one-dimensional systems (of the

TTF-TCNQ type) undergoing a Peierls structural transition, since the strong fluctuations of the order parameter in the one-dimensional case make such systems similar in a certain sense to "liquid semiconductors"^[16]. Inasmuch as R_C in this case can reach hundreds of interatomic spacings, and the temperatures are sufficiently low, the region of applicability of the theory is substantially broadened.

The author expresses his deep gratitude to L. V. Keldysh, E. G. Maksimov and D. I. Khomskif for numerous discussions and valuable comments.

¹N. F. Mott and E. A. Davis, *Electronic Processes in Noncrystalline Materials*, Oxford University Press, 1971; N. F. Mott, *Adv. Phys.* **16**, 49 (1967) (Russ. transl. Mir, M., 1969).

²R. S. Allgaier, *Phys. Rev.* **185**, 227 (1969); *Phys. Rev.* **B2**, 2257 (1970).

³A. R. Regel', A. A. Andreev, B. I. Kazandzhan, A. A. Lobanov, M. Mamadaliev, I. A. Smirnov and E. V. Shadrishchev, *Proc. Tenth Int. Conf. on the Physics of Semiconductors*, Cambridge, Massachusetts, 1970.

⁴V. A. Alekseev, A. A. Andreev and V. Ya. Prokhorenko, *Usp. Fiz. Nauk* **106**, 393 (1972) [*Sov. Phys.-Uspekhi* **15**, 139 (1972)].

⁵W. A. Harrison, *Pseudopotentials in the Theory of Metals*, Benjamin, N.Y., 1966 (Russ. transl., "Mir", M., 1968).

⁶A. A. Abrikosov, L. P. Gor'kov and I. E. Dzyaloshinskiĭ, *Metody kvantovoi teorii polya v statisticheskoi fizike (Quantum Field Theoretical Methods in Statistical Physics)*, Fizmatgiz, M., 1963 (English translation published by Pergamon Press, Oxford, 1965).

⁷D. Pines and P. Nozieres, *The Theory of Quantum Liquids*, Benjamin, N.Y., 1966 (Russ. transl., Mir, M., 1967).

⁸S. F. Edwards, *Phil. Mag.* **6**, 617 (1961); *Proc. Roy. Soc. A* **267**, 518 (1962).

⁹M. V. Sadovskii, *FIAN (Physics Institute of the Academy of Sciences) Preprint No. 63* (1973).

¹⁰N. N. Bogolyubov, *Kvazisrednie v zadachakh statisticheskoi mekhaniki (Quasi-averages in Problems in Statistical Mechanics)*, Preprint R-1451, Dubna (1963) (reprinted in *Izbrannye trudy (Selected Works)*, Vol. 3, Naukova Dumka, Kiev, 1971).

¹¹L. E. Ballentine, *Can. J. Phys.* **44**, 2533 (1966).

¹²R. W. Shaw and N. V. Smith, *Phys. Rev.* **178**, 985 (1969).

¹³J. M. Ziman, *J. Phys.* **C2**, 1704 (1969).

¹⁴A. N. Kozlov and L. A. Maksimov, *Zh. Eksp. Teor. Fiz.* **48**, 1184 (1965) [*Sov. Phys.-JETP* **21**, 790 (1965)].

¹⁵A. A. Abrikosov and S. D. Beneslavskii, *Zh. Eksp. Teor. Fiz.* **59**, 1280 (1970) [*Sov. Phys.-JETP* **32**, 699 (1971)].

¹⁶P. A. Lee, T. M. Rice and P. W. Anderson, *Phys. Rev. Lett.* **31**, 462 (1973).

Translated by P. J. Shepherd
177

Quasi-one-dimensional systems undergoing a Peierls transition

M. V. Sadovskii

P. N. Lebedev Physics Institute,
Academy of Sciences of the USSR, Moscow
(Submitted February 26, 1974)
Fiz. Tverd. Tela, 16, 2504-2511 (September 1974)

A model of a quasi-one-dimensional system undergoing a Peierls structural transition is analyzed on the basis of the Ginzburg-Landau one-dimensional model. The electronic-state density with a pseudogap is derived for a strictly one-dimensional system, in which there is no true transition. The pseudogap arises because of fluctuations in the short-range order corresponding to a Peierls lattice distortion. The dielectric properties of the system turn out to occupy an intermediate position between those of metals and dielectrics. An analysis is also made of the role of fluctuations below the temperature of the true transition, which is stabilized in a three-dimensional system. These fluctuations lead to the formation of a pseudogap in the state density, so that measurements of the electronic characteristics of the system cannot reveal the point at which the true transition occurs.

Quasi-one-dimensional systems having a metallic conductivity have recently been the object of considerable experimental work.^{1,2} Study of crystals based on TCNQ and platinum complexes [of the type $K_2Pt(CN)_4Br_{0.33}3H_2O$] has spurred interest in the familiar Peierls arguments regarding the instability of a one-dimensional metal with respect to a change in the lattice constant.³ According to x-ray structural^{4,5} and neutron-diffraction⁶ data, a Peierls transition actually occurs in the compound $K_2Pt(CN)_4Br_{0.33}3H_2O$, so that at temperatures $T \leq 80^\circ K$ the initial lattice constant is increased by a factor of 6, while at higher temperatures there is a pronounced softening of the frequency of phonons having a quasimomentum $\approx 2p_0$ (p_0 is the Fermi momentum of the electrons). It is also highly probable that a Peierls transition has been observed in the compound⁷ TFF-TCNQ, although as yet there is no direct evidence for a doubling of the lattice constant in this system.

Below we describe a model for systems of this type under conditions such that the correlation length for the fluctuations in the order parameter corresponding to the deformation of the lattice with the new lattice constant is much longer than the interatomic distance. We analyze the one-electron spectrum and the state density of the system. We then turn to the dielectric constant corresponding to the reaction to an electric field oriented parallel to the metallic chains, and we analyze the conductivity along the chains at high frequencies. The properties of this system turn out to occupy an intermediate position between typical metallic and typical semiconducting properties, implying that there are certain unique features in quasi-one-dimensional systems in which the fluctuations of the order parameter near a second-order phase transition are extremely important.

We begin from the Hamiltonian

$$H = \sum_p \xi_p a_p^\dagger a_p + \sum_q \omega_q b_q^\dagger b_q + \frac{1}{\sqrt{N}} \sum_{pq} g_q a_p^\dagger a_p (b_q + b_q^\dagger), \quad (1)$$

where ξ_p is the free-electron energy, reckoned from the Fermi level; ω_q is the phonon spectrum; g_p corresponds to the electron-phonon interaction; and a_p and b_p are the electron and phonon annihilation operators. Theory has already been worked out⁸⁻¹⁰ for a Peierls transition in the self-consistent-field approximation in a strictly one-dimensional system; it is also known¹¹ that fluctuations of the self-consistent field in a one-dimensional system are extremely important and rule out the possibility of phase

transitions altogether in a strictly one-dimensional system. Account of the three-dimensional nature of a real system can help stabilize the true transition (or suppress fluctuations). We are essentially adopting the Peierls-transition model proposed by Lee et al.,¹² which is based on the one-dimensional Ginzburg-Landau model, which has been analyzed in detail.¹³ Although there is no true transition according to this model, the correlation radius for short-range order becomes macroscopic at a certain temperature $T_p \approx 1/4 T_C$ (T_C is the transition temperature in the self-consistent-field approximation). We are interested in the temperature range $T \sim T_p$, in which this radius is quite large. If the true (three-dimensional) transition is stabilized at a certain temperature, i.e., if long-range order appears, the analysis must be modified. However, fluctuations are also important in the neighborhood of the true transition. The corresponding calculations are given in the Appendix.

Instead of the Ginzburg-Landau model we could adopt an interaction having a soft phonon mode near the transition point,¹⁴ but in this case we would have to use specific models for the soft mode, and the range of applicability of these models is unclear. For the problem under consideration here the Landau free energy is¹²

$$F(\psi_Q) = a(T, 2p_0) |\psi_Q|^2 + b(T, 2p_0) |\psi_Q|^4 + c(T, 2p_0) (Q - 2p_0)^2 |\psi_Q|^2, \quad (2)$$

where the order parameter $\psi_Q = g_Q \langle b_Q + b_{-Q}^\dagger \rangle$ is proportional to the Peierls lattice deformation. The expansion coefficients are

$$\left. \begin{aligned} a &= N_0 \frac{T - T_c}{T_c}, \quad T_c = \frac{2\gamma}{\pi} E_F \exp\left\{-\frac{\omega_{2p_0}}{g^2 N_0}\right\}, \\ b &= N_0 \left\{ b_0 + (b_1 - b_0) \frac{T}{T_c} \right\} \frac{1}{T_c^2}; \quad c = N_0 \xi_{\frac{1}{2}}(T); \\ \xi_{\frac{1}{2}}(T) &= \frac{7\zeta(3)}{16\pi^2 T^2}; \quad b_0 = \frac{1}{2} \frac{\gamma^2}{\pi^2}; \quad b_1 = \frac{7\zeta(3)}{16\pi^2}, \end{aligned} \right\} \quad (3)$$

where $\ln \gamma = C$ is the Euler constant, N_0 is the free-electron state density at the Fermi level, E_F is the Fermi energy, and v_F is the Fermi velocity. Account of the electron-band structure in the strong-coupling approximation alters the constants in (3) only slightly.¹⁵ In this model an electron is scattered in the static field of random fluctuations of the order parameter ψ_Q . The simplest eigenener-

gy part of the one-electron Green's function is ^{12,16} [$\epsilon_n = (2n + 1)\pi T$]

$$\Sigma(\epsilon_n, p) = \langle \psi^2 \rangle \int \frac{dQ}{2\pi} S(Q) \frac{1}{i\epsilon_n - \xi_{p+Q}}, \quad (4)$$

where $S(\beta)$ is the static structural factor for fluctuations of the order parameter, proportional to the Fourier transform of the two-point correlation function for the order parameter. For this model we have ^{12,13}

$$\frac{1}{2} S(Q) = \frac{\xi^{-1}(T)}{(Q - 2p_0)^2 + \xi^{-2}(T)} + \frac{\xi^{-1}(T)}{(Q + 2p_0)^2 + \xi^{-2}(T)}, \quad (5)$$

where $\xi(T)$ is the correlation length for fluctuations in the order parameter (the short-range correlation radius). At $T \approx 1/4 T_C$ the length $\xi(T)$ increases exponentially with decreasing temperature. ¹⁴ Now assuming an electron having $p \sim p_0$, we find

$$\Sigma(\epsilon_n, p) = \langle \psi^2 \rangle [i\epsilon_n + \xi_p + i\nu_p \xi^{-1}(T)]^{-1} \approx \Delta^2 (i\epsilon_n + \xi_p)^{-1}, \quad (6)$$

$$\Delta^2 = \langle \psi^2 \rangle, \quad (7)$$

where we have used $\xi_{p-2p_0} = -\xi_p$ for the one-dimensional system.

The approximate equality in (6) holds [the corrections for the finite width of the $S(Q)$ peak are small] under the conditions ¹⁷

$$\left. \begin{aligned} \xi(T) &\gg |p - p_0|^{-1}, \\ \nu_p \xi^{-1}(T) &\ll 2\pi T. \end{aligned} \right\} \quad (8)$$

The first condition in (8) imposes a restriction on our analysis in the immediate vicinity of the Fermi level $T \sim 1/4 T_C$, where $\xi(T)$ is large, the corresponding energy range is extremely narrow and of no particular interest. According to the data of ref. 5, we have ξ/a ($T = 300^\circ K$) $> 10^2$, where a is the Pt-Pt distance in the compound $K_2Pt(CN)_4Br_{0.33}H_2O$. Although the estimates of ref. 12 are less favorable, the values of $\xi(T)$ near the "transition" are undoubtedly very large and can reach hundreds of interatomic distances.

Using approximation (6) in the higher-order diagrams, we can sum all ¹¹ the important diagrams by the perturbation-theory method proposed in ref. 17. Scalapino et al. ¹³ analyzed the contribution of only the simplest diagram in (6), but the higher-order approximations are extremely important. Carrying out the summation, we find ¹⁷ the one-electron Green's function to be

$$G(\epsilon_n, p) = \int_0^\infty d\zeta e^{-\zeta} \frac{i\epsilon_n + \xi_p}{(i\epsilon_n)^2 - \xi_p^2 - \zeta \Delta^2} \equiv \langle G_{\zeta \Delta^2}(\epsilon_n, p, p) \rangle_\zeta, \quad (9)$$

where

$$G_{\zeta \Delta^2}(\epsilon_n, p, p) = \frac{i\epsilon_n + \xi_p}{(i\epsilon_n)^2 + \xi_p^2 - \Delta^2} \quad (10)$$

is the normal Green's function of an ideal Peierls insulator having an energy gap $|\Delta|$. It is easy to say that Eq. (9) is the Green's function of an electron in an external field $W \cos 2p_0 x$ whose amplitude "fluctuates" with a distribution $P\{W\} = |W|/\Delta^2 e^{-(W^2/\Delta^2)}$. The integral in (9) denotes an averaging over these fluctuations.

After the standard analytic continuation to the real frequencies, we find the electronic-state density to be

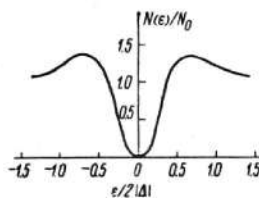


Fig. 1. Electronic density.

$$\frac{N(\epsilon)}{N_0} = \left| \frac{\epsilon}{\Delta} \right| \int_0^{\epsilon^2/\Delta^2} d\zeta \frac{e^{-\zeta}}{\sqrt{\frac{\epsilon^2}{\Delta^2} - \zeta}} = 2 \left| \frac{\epsilon}{\Delta} \right| e^{-\frac{\epsilon^2}{\Delta^2}} \text{Erfi} \left(\frac{\epsilon}{|\Delta|} \right), \quad (11)$$

where $\text{Erfi } x = \int_0^x dx' x'^2$. Figure 1 shows this state density, which contains a typical pseudogap having a width on the order of $|\Delta| \sim \langle \psi^2 \rangle^{1/2}$. The temperature dependence of $\langle \psi^2 \rangle$ was calculated in ref. 13; the asymptotic behavior is

$$\frac{N(\epsilon)}{N_0} \rightarrow 1 \text{ as } |\epsilon| \rightarrow \infty; \quad \frac{N(\epsilon)}{N_0} \approx 2 \frac{\epsilon^2}{\Delta^2} \rightarrow 0 \text{ as } |\epsilon| \rightarrow 0.$$

The vanishing of the state density in the middle of the pseudogap is nonphysical; our analysis is not valid in the immediate vicinity of the Fermi level because of restriction (8). Accordingly, in contrast with the situation in ref. 13, the summation of all the important diagrams leads to the existence of a pseudogap not only at $T \gtrsim 1/4 T_C$ but also at $T < 1/4 T_C$. A true gap does not arise even at low temperatures in the "dielectric" phase. ²⁾ As is shown in the Appendix, this result holds even in the case of a true phase transition (at $T \leq T_C$), so that, strictly speaking, measurements of the electronic characteristics of the system cannot reveal the transition point.

We turn now to the reaction of the system to a longitudinal electric field directed parallel to the metallic chains. A variation $\delta \varphi_{q\omega}$ (q is the wave vector along the chain and ω is the frequency of the external field) causes a variation in the one-electron Green's function:

$$\frac{\delta G(\epsilon, p)}{\delta \varphi_{q\omega}} = G(\epsilon, p) \Gamma(\epsilon, p, \epsilon + \omega, p + q) G(\epsilon + \omega, p + q), \quad (12)$$

where $\Gamma(\epsilon, p, \epsilon + \omega, p + q)$ is the corresponding vertex part. In this model the variational derivative in (12) can be calculated immediately; ¹⁷ we find

$$\begin{aligned} \frac{\delta G(\epsilon, p)}{\delta \varphi_{q\omega}} &= -e \langle G_{\zeta \Delta^2}(\epsilon, p, p) G_{\zeta \Delta^2}(\epsilon + \omega, p + q, p + q) \rangle_\zeta \\ &- e \langle G_{\zeta \Delta^2}(\epsilon, p, p - 2p_0) G_{\zeta \Delta^2}(\epsilon + \omega, p - 2p_0 + q, p + q) \rangle_\zeta, \end{aligned} \quad (13)$$

where e is the electronic charge, $G_{\Delta^2}(\epsilon, p, p)$ is given in (10), and

$$G_{\Delta^2}(\epsilon_n, p, p - 2p_0) = \frac{\Delta}{(i\epsilon_n)^2 - \xi_p^2 - \Delta^2} \quad (14)$$

is the anomalous Green's function of a Peierls dielectric, which describes the flipping $p \rightarrow p - 2p_0$. Accordingly, averages over binary products of anomalous Green's functions arise in the theory, while the anomalous functions themselves do not, in correspondence with the absence of long-range order in the system.

The polarization operator is ($\omega_m = 2\pi mT$)

$$\Pi(q\omega_m) = - \int_0^\infty d\zeta e^{-\zeta} 2T \sum_n N_0 \varphi \times$$

$$\begin{aligned} & \times \int_{-\infty}^{\infty} d\xi_p \{ G_{\zeta\Delta^2}(\xi_m, p, p) G_{\zeta\Delta^2}(\xi_n + \omega_m, p + q, p + q) \\ & + G_{\zeta\Delta^2}(\xi_m, p, p - 2p_0) G_{\zeta\Delta^2}(\xi_n + \omega_m, p + q, p - 2p_0 + q) \} \equiv \langle \Pi_{\zeta\Delta^2}(q, \omega_m) \rangle_{\zeta}, \end{aligned} \quad (15)$$

where $\Pi_{\Delta^2}(q, \omega_m)$ is the polarization operator of a Peierls dielectric, and ρ is the density of the metallic chains in a cross section of the sample (here we are interested in the response of a unit volume of the system). The analysis continues as in ref. 17. The dielectric constant along the metallic chains is

$$\epsilon(q, \omega) = 1 + \frac{4\pi e^2}{q^2} \Pi(q\omega) = \langle \epsilon_{\zeta\Delta^2}(q\omega) \rangle_{\zeta}, \quad (16)$$

where

$$\epsilon_{\Delta^2}(q\omega) = 1 + \frac{4\pi e^2}{q^2} \Pi_{\Delta^2}(q, \omega) \quad (17)$$

is the dielectric constant of a Peierls dielectric.

We consider first the case $\omega = 0$; then for this model we find¹⁷

$$\epsilon(q, 0) \approx 1 - \frac{v_F^2 \kappa^2}{6\Delta^2} \exp \frac{v_F^2 q^2}{6\Delta^2} \text{Ei} \left(-\frac{v_F^2 q^2}{6\Delta^2} \right), \quad (18)$$

where $\kappa^2 = 8\pi^2 N_0 \rho$ is the inverse square of the Debye screening radius, and $\text{Ei}(-x)$ is the integral exponential function. Hence, with $v_F q \gg |\Delta|$, we find $\epsilon(q, 0) \approx 1 + (\kappa^2/q^2)$. For $v_F q \ll |\Delta|$ we find

$$\epsilon(q, 0) \approx 1 - \frac{v_F^2 \kappa^2}{6\Delta^2} \ln \gamma \frac{v_F^2 q^2}{6\Delta^2}. \quad (19)$$

This $\epsilon(q, 0)$ behavior occupies an intermediate position between the behavior characteristic of metals and that characteristic of dielectrics.

Turning now to the case $\omega \neq 0$, $v_F q \ll |\Delta|$, we find¹⁷

$$\text{Re } \epsilon(\omega) \approx 1 - \frac{\omega_p^2}{6\Delta^2} \text{Ei} \left(-\frac{\omega^2}{4\Delta^2} \right) - \frac{\omega_p^2}{\omega^2} \left\{ 1 - e^{-\frac{\omega^2}{4\Delta^2}} \right\}, \quad (20)$$

where $\omega_p^2 = v_F^2 \kappa^2$ is the square of the plasma frequency.

In the case $\omega \gg 2|\Delta|$ we have $\text{Re } \epsilon(\omega) \approx 1 - (\omega_p^2/\omega^2)$; in the case $\omega \ll 2|\Delta|$ we have

$$\text{Re } \epsilon(\omega) \approx 1 - \frac{\omega_p^2}{6\Delta^2} \ln \gamma \frac{\omega^2}{4\Delta^2}. \quad (21)$$

Of particular interest is the behavior of the imaginary part of the dielectric constant, since it governs the absorption of electromagnetic energy in the system. The real part of the conductivity is

$$\text{Re } \sigma(\omega) = \frac{\omega}{4\pi} \text{Im } \epsilon(\omega). \quad (22)$$

By analogy with ref. 17 we have

$$\begin{aligned} \text{Im } \epsilon(\omega) &= \frac{\pi}{2} \omega_p^2 \frac{|\Delta|}{\omega^3} \int_0^{\frac{\omega^2}{4\Delta^2}} d\zeta e^{-\zeta} \frac{\zeta}{\sqrt{\frac{\omega^2}{4\Delta^2} - \zeta}} \\ &= \pi \omega_p^2 \frac{|\Delta|}{\omega^3} e^{-\frac{\omega^2}{4\Delta^2}} \left\{ \frac{\omega^2}{4\Delta^2} - \frac{d}{dx} \right\} \text{Erfi} \left(\sqrt{x} \frac{\omega}{2|\Delta|} \right) \Big|_{x=1}. \end{aligned} \quad (23)$$

Asymptotically we find

$$\left. \begin{aligned} \text{Im } \epsilon(\omega) &\approx \pi \left(\frac{\omega_p}{\omega} \right)^2 \left(\frac{\Delta}{\omega} \right)^2, \\ \text{Re } \sigma(\omega) &\approx \frac{1}{4} \left(\frac{\Delta}{\omega} \right)^2 \frac{\omega_p^2}{\omega} \end{aligned} \right\} \quad (24)$$

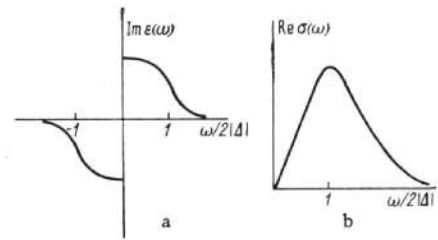


Fig. 2. Qualitative behavior of the imaginary part of the dielectric constant (a) and of the real part of the conductivity (b) as functions of the frequency of the external field.

for $\omega \gg 2|\Delta|$; for $\omega \ll 2|\Delta|$, we find

$$\left. \begin{aligned} \text{Im } \epsilon(\omega) &\approx \frac{\pi}{12} \frac{\omega_p^2}{\Delta^2}, \\ \text{Re } \sigma(\omega) &\approx \frac{1}{48} \left(\frac{\omega_p}{\Delta} \right)^2 \omega \rightarrow 0 \text{ for } \omega \rightarrow 0. \end{aligned} \right\} \quad (25)$$

Accordingly, the static conductivity vanishes in our approximation. Analogously, the static conductivity of a Peierls dielectric vanishes at zero temperature. Equation (23) describes a sort of interband absorption (Fig. 2), having a peak at $\omega \sim 2|\Delta|$. We also see that our model describes a substance whose properties are intermediate between those of metals and dielectrics: In a metal we would have $\text{Im } \epsilon(\omega) \sim 1/\omega$ as $\omega \rightarrow 0$, while in a dielectric we would have $\text{Im } \epsilon(\omega) = 0$ at $\omega = 0$. In our case the quantity $\text{Im } \epsilon(\omega)$ has a finite discontinuity at $\omega = 0$:

$$(\text{Im } \epsilon(\omega) = -\text{Im } \epsilon(-\omega)).$$

Strictly speaking, these equations do not hold at low frequencies, since the entire analysis breaks down near the Fermi level, according to the first condition in (8). Our calculation of the polarization operator holds only for

$$\omega \gg v_F \xi^{-1}(T). \quad (26)$$

This condition has a clear meaning: Over the scale time for a change in the external field an electron moves a distance shorter than $\xi(T)$.

A Peierls system thus apparently represents a substance whose properties occupy an intermediate position between those of metals and dielectrics. An experimental search for absorption peaks at frequencies corresponding to the width of the pseudogap would be very interesting. The possible anomalous behavior of $\epsilon(\omega)$ according to (21) and (25) at $\omega \ll 2|\Delta|$ emphasizes the importance of experiments in the rf range. No reliable experimental data are presently available.

In conclusion the author thanks L. V. Keldysh, L. N. Bulaevskii, and D. I. Khomskii for many discussions and comments.

APPENDIX

A phase transition cannot occur in a strictly one-dimensional system because of the disruptive influence of fluctuations.¹¹ In particular, the self-consistent-field approximation does not have a range of applicability because of the large width of the critical region, $\Delta T/T_C \sim 1$ (ref. 13). However, since real systems are three-dimensional in nature, fluctuations can be suppressed in some manner (e.g., the fluctuation amplitude can be limited by a long-range Coulomb interaction between electrons of neighbor

ing chains). Then a true phase transition is possible in the system at $T = T_C$. Apparently it is this case which occurs in $K_2Pt(CN)_4Br_{0.33}3H_2O$ (ref. 4), where the true (three-dimensional) transition stabilizes at $T_C \approx 80^\circ K$. Then, at $T < T_C$, a long-range order arises, and the system can be described satisfactorily in the self-consistent-field approximation. However, the fluctuations of the order parameter, even though suppressed, can turn out to be important even at $T < T_C$. In this case we have¹³

$$\psi_Q = \Delta + \delta\psi_Q, \quad (A.1)$$

where

$$\Delta = \left(-\frac{a}{2b}\right)^{1/2} = \begin{cases} \sqrt{\frac{8\pi^2 T_C}{7\zeta(3)}} \sqrt{T_C - T} & \text{at } T \leq T_C, \\ \frac{\pi}{T} T_C & \text{at } T = 0 \end{cases} \quad (A.2)$$

is the equilibrium value of the order parameter, and $\delta\psi_Q$ is its fluctuation. Here Δ plays the role of a coherent field, which transmits a momentum $2p_0$ and which leads to Bragg scattering of electrons by the boundaries of the new Brillouin zone, and $\delta\psi_Q$ is the random field. In the diagram technique we find two types of interaction lines: lines of the coherent field Δ , which transmit a momentum $2p_0$, and lines of the random field, which are associated with the correlator $\langle \delta\psi_Q \delta\psi_{-Q} \rangle = \langle \delta\psi^2 \rangle S(Q)$. Here $S(Q)$ is again given by (5) (ref. 13). The equations for $\langle \delta\psi^2 \rangle$ and $\xi(T)$ derived on the basis of the self-consistent-field approximation¹³ are now, generally speaking, inapplicable (because of the three-dimensional nature of the critical fluctuations), so that $\langle \delta\psi^2 \rangle$ and $\xi(T)$ are treated below as parameters of the theory. Near the transition point ($T \approx T_C$) the quantity $\xi(T)$ increases, so that we can again use an approximation like that in (6)-(8). Then the random-field lines also transmit a momentum $2p_0$. In the expansion of the one-electron Green's function a sequence of alternating Green's functions $\{i\epsilon_L - \xi_p\}^{-1}$ and $\{i\epsilon_L + \xi_p\}^{-1}$ dominates. In perturbation theory of order n there are $2n$ vertices, of which $2k$ are connected by random-field lines of the fluctuations, and with which factors $\delta\Delta^2 = \langle \delta\psi^2 \rangle$ are associated; at $2(n-k)$ vertices, single coherent-scattering lines arise, each of which is associated with a factor Δ . Then the expansion of the Green's function is

$$G(\epsilon_l, \xi_p) = \sum_{n=0}^{\infty} \sum_{k=0}^n B_n^k(\epsilon_l, \xi_p), \quad (A.3)$$

where

$$B_n^k = \quad (A.4)$$

$$|\Delta|^{2(n-k)} \left[\frac{n!}{k!(n-k)!} \right]^2 |\delta\Delta|^{2k} k! (i\epsilon_l - \xi_p)^{-n} (i\epsilon_l + \xi_p)^{-n} (i\epsilon_l - \xi_p)^{-1}.$$

Actually, an electronic line has $2k$ vertices, to which random-field lines are attached; of these vertices, k have an outgoing line, which goes to the remaining k vertices in any of $k!$ methods. Here $[n!/(k!(n-k)!)]^2$ is the number of arrangements of single coherent-field lines at any $2(n-k)$ vertices taken from the total of $2n$ vertices; the circumstance that the momentum $2p_0$ "enters" half of these vertices and "exits" from the other half is taken into account. We use the identity $(1+x)^n(1+y)^n =$

$$\sum_{k_1, k_2=0}^n x^{k_1} y^{k_2} C_n^{k_1} C_n^{k_2}, \text{ where we have set}$$

$$x = \zeta \frac{\delta\Delta}{\Delta} = |\zeta| e^{i\varphi} \frac{\delta\Delta}{\Delta}; \quad y = x^*;$$

$$\int_0^{2\pi} \frac{d\varphi}{2\pi} \left(1 + \zeta \frac{\delta\Delta}{\Delta}\right)^n \left(1 + \zeta^* \frac{\delta\Delta}{\Delta}\right)^n = \sum_{k=0}^n |C_n^k|^2 |\zeta|^{2k} \left(\frac{\delta\Delta}{\Delta}\right)^{2k}.$$

Using $\int_0^{2\pi} d|\zeta|^2 |\zeta|^{2k} e^{-|\zeta|^2} = k!$, we find

$$G(\epsilon_l, \xi_p) = \int_0^{\infty} d|\zeta|^2 e^{-|\zeta|^2} \times \int_0^{2\pi} \frac{d\varphi}{2\pi} \frac{i\epsilon_l + \xi_p}{(i\epsilon_l)^2 - \xi_p^2 - \Delta^2 \left[1 + |\zeta|^2 \left(\frac{\delta\Delta}{\Delta}\right)^2 + 2|\zeta| \frac{\delta\Delta}{\Delta} \cos \varphi\right]} = \frac{1}{\pi} \int d^2\zeta e^{-|\zeta|^2} \frac{i\epsilon_l + \xi_p}{(i\epsilon_l)^2 - \xi_p^2 - \Delta^2 \left|1 + \zeta \frac{\delta\Delta}{\Delta}\right|^2}, \quad (A.5)$$

where

$$\int d^2\zeta \dots \equiv \int d \operatorname{Re} \zeta d \operatorname{Im} \zeta \dots = \int_0^{\infty} d|\zeta| |\zeta| \int_0^{2\pi} d\varphi \dots$$

We have obtained a normal Green's function with a gap which "fluctuates" around Δ as given by Eqs. (A.2). The equation for the anomalous Green's function is obvious. As $\Delta \rightarrow 0$, Eq. (A.5) converts into Eq. (9), and in the case $\delta\Delta \rightarrow 0$ we find (10), i.e., an ideal Peierls dielectric. Accordingly, the analysis above is valid for the case $T \approx T_C$. Obviously, even in the case $T < T_C$ the fluctuations are extremely important. For the state density we have

$$\frac{N(\epsilon)}{N_0} = \frac{|\epsilon|}{\pi} \int d^2\zeta e^{-|\zeta|^2} \frac{\Theta \left[\epsilon^2 - \Delta^2 \left|1 + \zeta \frac{\delta\Delta}{\Delta}\right|^2 \right]}{\sqrt{\epsilon^2 - \Delta^2 \left|1 + \zeta \frac{\delta\Delta}{\Delta}\right|^2}}. \quad (A.6)$$

Omitting the lengthy details, we state that as $\delta\Delta \rightarrow 0$ (i.e., as $T \rightarrow 0$) we would have

$$\frac{N(\epsilon)}{N_0} \rightarrow \begin{cases} \frac{|\epsilon|}{\sqrt{\epsilon^2 - \Delta^2}} & \text{for } |\epsilon| > \Delta, \\ 0 & \text{for } |\epsilon| < \Delta, \end{cases} \quad (A.7)$$

i.e., we find an ideal dielectric with a gap 2Δ . When $\delta\Delta$ is finite we always have $N(\epsilon)/N_0 \neq 0$ for $|\epsilon| < \Delta$.

For example, as $|\epsilon| \rightarrow 0$ we would have

$$\frac{N(\epsilon)}{N_0} \approx \frac{2}{\sqrt{\pi}} \frac{|\epsilon|}{|\delta\Delta|} \cdot 1.68 \left\{ 1 - \operatorname{Erfc} \left(\frac{1}{2} \left| \frac{\Delta}{\delta\Delta} \right| \right) \right\}, \quad (A.8)$$

where $\operatorname{Erfc} x = 2/\sqrt{\pi} \int_0^x dx e^{-x^2}$. With $|\epsilon| = \Delta$ we find

$$N(|\epsilon| = \Delta)/N_0 \approx \sqrt{\Delta/|\delta\Delta|}.$$

Accordingly, we again find a state density having a pseudogap. In the case $|\delta\Delta| \ll \Delta$ the state density in the energy gap is of course small, but this is not generally true in the case $T < T_C$. We see that fluctuations of the order parameter are extremely important even in the case of a true phase transition. Near the transition, the state density has a pseudogap at both $T \approx T_C$ and $T < T_C$. In this sense the transition point is not defined and cannot be determined from measurements of electronic characteristics of the system. In terms of their effects, the fluctuations turn out to be analogous to an internal disorder of the system, analyzed in ref. 18: They suppress the true transi-

tion and "smear" its effects on the electronic properties.

Note added in proof. D. B. Tanner recently reported [Phys. Rev. Lett., 32, 1303 (1974)] experimental data on IR absorption in TTF = TCNQ at 65 and 320°K. The results are qualitatively analogous to Fig. 2b, with $\text{Re } \sigma$ ($\omega = 2 |\Delta|$) $\approx 5 \cdot 10^2 - 10^3 \Omega^{-1} \cdot \text{cm}^{-1}$. Extrapolating (25) to $\omega = 2 |\Delta|$ and using the experimental values $2 |\Delta| = 0.14$ eV, and $\omega_p = 1.2$ eV, we find $\text{Re } \sigma$ ($\omega = 2 |\Delta|$) $\approx 8 \cdot 10 \Omega^{-1} \cdot \text{cm}^{-1}$.

¹⁾We assume that all the higher-order correlators for the order parameter can be factored into binary correlators; this procedure is equivalent to taking only Gaussian fluctuations into account.

²⁾Account of non-Gaussian fluctuations could hardly have a qualitative effect on this result. The gap can appear only in the presence of a true long-range order.

¹⁾I. F. Shchegolev, Phys. Status Solidi (a), 12, 9 (1972).

²⁾H. R. Zeller, Festkörperprobleme, 13, 31 (1973).

³⁾R. Peierls, Quantum Theory of Solids, Oxford Univ. Press, London (1955).

⁴⁾R. Comes, M. Lambert, and H. R. Zeller, Phys. Status Solidi (b), 58, 587 (1973).

⁵⁾R. Comes, M. Lambert, H. Launois, and H. R. Zeller, Phys. Rev., B8, 571 (1973).

⁶⁾B. Renker, H. Rietschel, L. Pintschovius, W. Gläser, P. Brüesch, D. Kuse, and M. J. Rice, Phys. Rev. Lett., 30, 1144 (1973).

⁷⁾L. B. Coleman, M. J. Cohen, D. J. Sandman, F. G. Yamagishi, A. F. Garito, and A. J. Heeger, Solid State Commun., 12, 1125 (1973).

⁸⁾H. Fröhlich, Proc. R. Soc. A., 223, 296 (1954).

⁹⁾C. G. Kuper, Proc. R. Soc. A., 227, 214 (1955).

¹⁰⁾M. J. Rice and S. Strässler, Solid State Commun., 13, 125, 1931 (1973).

¹¹⁾P. C. Hohenberg, Phys. Rev., 158, 383 (1967).

¹²⁾P. A. Lee, T. M. Rice, and P. W. Anderson, Phys. Rev. Lett., 31, 462 (1973).

¹³⁾D. J. Scalapino, M. Sears, and R. Ferrel, Phys. Rev., B6, 3409 (1972).

¹⁴⁾M. J. Rice and S. Strässler, Solid State Commun., 13, 1389 (1973).

¹⁵⁾D. Allender, J. Bray, and J. Bardeen, Phys. Rev., B9, 119 (1974).

¹⁶⁾S. F. Edwards, Phil. Mag., 6, 617 (1961).

¹⁷⁾M. V. Sadovskii, Zh. Eksp. Teor. Fiz., 66, 1720 (1974).

¹⁸⁾L. N. Bulaeviskii and M. V. Sadovskii, Fiz. Tverd. Tela, 16, 1159 (1974) [Sov. Phys. - Solid State, 16, 773 (1974)].

Localization of electrons in disordered systems. The mobility edge and theory of critical phenomena

M. V. Sadovskii

Metal Physics Institute, Urals Scientific Center, Academy of Sciences of the USSR
(Submitted December 3, 1975)
Zh. Eksp. Teor. Fiz. 70, 1936-1940 (May 1976)

It is shown that the most probable spatial behavior of the one-electron Green function in the region of localized states near the mobility edge in the Anderson model coincides with the spatial behavior of the correlation function in the critical region of a second-order phase transition with a zero-component order parameter.

PACS numbers: 71.50.+t

Ideas about the localization of electrons in a random field lie at the basis of the modern theory of disordered systems.^[1] The most highly developed scheme for treating the problem of localization is the well-known Anderson model^[2-4] describing an electron propagating in a regular lattice with random energy levels at the different sites. Most of the papers on the Anderson model are devoted to proving the localization of electron states when the ratio of the parameter W describing the spread of levels to the amplitude V of an electron transition from site to site is sufficiently large, to determining the critical ratio W_c/V , and also to determining the mobility edges E_c , i. e., the critical electron energies separating the regions of localized and delocalized states in the band.^[1,2,4] It is of great interest to study the character of the electron states near the mobility edge, since the corresponding characteris-

tics essentially determine the kinetics and other electronic properties of disordered systems.^[5] Attempts in this direction have been undertaken in papers by Anderson, Edwards, and Freed.^[3,6,7]

There exist a number of obvious analogies between the problem of the localization of an electron near the mobility edge and the problem of describing the critical phenomena near a second-order phase-transition point. For example, as the electron energy approaches the mobility edge in the region of localized states the localization length of the electron wavefunction diverges, just as the correlation length of fluctuations at a phase-transition point diverges. This prompts the thought that the spatial behavior of electron states near the mobility edge can be described by the (scaling) dependences that are characteristic for the phase-transition problem.

with critical indices determined only by the dimensionality of space and of the corresponding order parameter.^[8]

In the present paper, using the method of Anderson,^[3] we show that the most probable spatial behavior of the one-electron Green function at the mobility edge coincides with the spatial behavior of the correlation function for the problem of critical phenomena with a zero-component order parameter.^[9,10]

The Hamiltonian of the Anderson model has the form^[2,3]

$$H = \sum_j E_j a_j^\dagger a_j + \sum_{ij} V_{ij} a_i^\dagger a_j. \quad (1)$$

Here, a_i^\dagger and a_i are the electron creation and annihilation operators at the lattice site i , and E_j are the random energy levels at the sites, distributed in accordance with the law

$$P(E_j) = \begin{cases} 1/W, & |E_j| < 1/2 W \\ 0, & |E_j| > 1/2 W \end{cases}. \quad (2)$$

The transition amplitude V_{ij} from site to site is assumed to be nonzero, and equal to a constant V , for transitions between nearest neighbors only.

The character of the electron states is determined by the one-electron Green function

$$G_{ij}(E) = \langle \mathbf{R}_i | \frac{1}{E-H} | \mathbf{R}_j \rangle, \quad (3)$$

which is the transition amplitude from the site at the point \mathbf{R}_j to the site at the point \mathbf{R}_i for an electron with energy E . A renormalized perturbation-theory series in V is constructed for this Green function. As Anderson has shown,^[2] the localization problem reduces to investigating the convergence of this series, where, in view of the random character of the quantities E_j , the convergence is understood in the sense of convergence with a certain probability.^[2,4] In the region of localized states the series converges with probability unity, and the condition for convergence determines the critical ratio W_c/V or the position of the localization edge in the band.

The most probable behavior of the Green function can be represented in the form^[2,3]

$$G_{ij}(E)|_{E=0} \sim \sum_{N=0}^{\infty} Z_N(\mathbf{R}_i - \mathbf{R}_j) \left(\frac{2eV}{W} \right)^N \Psi^N \left(\frac{V}{W}, K \right), \quad (4)$$

where $Z_N(\mathbf{R}_i - \mathbf{R}_j)$ is the number of paths of N steps, without intersections, linking site j with site i , and Ψ is a slowly varying (logarithmic) function of the ratio V/W and of the so-called connectivity constant K of the lattice.^[2] For simplicity we consider below an Anderson transition in the center of the band (at $E=0$). In the general case, in (4) we must replace $2V/W$ by $2V\rho(E)$, where $\rho(E)$ is the density of electron states.^[3] The critical bandwidth W_c corresponding to the threshold of localization is determined by the equation^[2]

$$1 = \frac{2eV}{W_c} K \Psi \left(\frac{V}{W_c}, K \right). \quad (5)$$

For $E \neq 0$ a condition of the type (5) was discussed in^[1,4].

Thus, the spatial behavior of the Green function is entirely determined by the statistics of nonintersecting paths, through the function $Z_N(\mathbf{R}_i - \mathbf{R}_j)$. Anderson^[3] and Thouless^[11] used a $Z_N(\mathbf{R})$ obtained as the result of machine experiments. We shall make use of the analytic theory of de Gennes and des Cloizeaux.^[10] Using Wilson's ϵ -expansion method,^[6] de Gennes and des Cloizeaux considered the statistics of random walks without intersections and showed that the function $Z_N(\mathbf{R})$ of interest to us is determined, in a space of d dimensions, by the inverse Laplace transform

$$Z_N(\mathbf{R}) = \int_{c-i\infty}^{c+i\infty} \frac{ds}{2\pi i} e^{N s} G_U(s, \mathbf{R}) \quad (6)$$

of the unrenormalized Green function $G_U(s, \mathbf{R})$ of a Euclidian field theory (Landau-Ginzburg phase-transition theory) with Lagrangian of the form

$$\mathcal{L}(\Phi) = \frac{1}{2} \sum_{j=1}^n \{ (\nabla \Phi_j)^2 + m_0^2 \Phi_j^2 \} + \frac{1}{8} g_0 \left(\sum_{j=1}^n \Phi_j^2 \right)^2, \quad (7)$$

where n is the number of components of the field Φ and is equal to zero in the problem under consideration. (The condition $n=0$ eliminates the "superfluous" diagrams with loops, which are absent in the nonintersecting random-walk problem.) The dimensionless parameter s is related to the unrenormalized mass: $s = m_0^2 a^2$, where a is a characteristic length of the order of the lattice constant. The phase transition corresponds^[6] to the vanishing of the renormalized mass m of the field theory (7) as $s \rightarrow s_c$:

$$m \sim a^{-1} (s - s_c)^{-\nu}, \quad (8)$$

where ν is the critical index of the correlation length.

In (6) we must take $c > s_c$. The parameter s_c is related to the connectivity of the lattice^[9,10,12]:

$$K = \exp(s_c). \quad (9)$$

Using (6) and (3), we obtain

$$\begin{aligned} G_{ij} &\sim \sum_{N=0}^{\infty} \int_{c-i\infty}^{c+i\infty} \frac{ds}{2\pi i} \exp\{N(s-s_c)\} G_U(s, \mathbf{R}_i - \mathbf{R}_j) \left(\frac{2eV}{W} K \right)^N \Psi^N \left(\frac{V}{W}, K \right) \\ &\approx \int_{c-i\infty}^{c+i\infty} \frac{ds}{2\pi i} G_U(s, \mathbf{R}_i - \mathbf{R}_j) \sum_{N=0}^{\infty} \exp\left\{ N(s-s_c) + N \ln \frac{W_c}{W} \right\} \\ &= G_U \left(\ln \frac{W}{W_c} + s_c; \mathbf{R}_i - \mathbf{R}_j \right) \end{aligned} \quad (10)$$

which is the main result, showing that the most probable spatial behavior of the one-electron Green function of the Anderson model in the region of localized states near the mobility edge ($W \gtrsim W_c$) coincides with the behavior of the correlation function of the phase-transition theory (7) with $n=0$, and $W = W_c$ corresponds to the transition point.

For $W \gtrsim W_c$ the Green function falls off exponentially with distance^[8]:

$$G_{ij} \sim \exp \left\{ - \frac{|\mathbf{R}|}{R_{loc}} \right\}; \quad |\mathbf{R}| = |\mathbf{R}_i - \mathbf{R}_j| \gg R_{loc}, \quad (11)$$

where

$$R_{loc} \sim m^{-1} \sim a \left| \frac{W - W_c}{W_c} \right|^{-\nu} \quad (12)$$

plays the role of the localization length. Analogously, for $E \neq 0$, but for $E \approx E_c$,

$$R_{loc} \sim a \left| \frac{E - E_c}{E_c} \right|^{-\nu}$$

In the framework of the Wilson ϵ -expansion ($d = 4 - \epsilon$) for $n = 0$, we have

$$\nu \approx \frac{1}{2} \left\{ 1 + \frac{\epsilon}{8} + \frac{15}{256} \epsilon^2 + \dots \right\} \approx 0.592 \quad \text{for } \epsilon = 1, \quad (13)$$

in excellent agreement with Anderson's result $\nu = 0.6$,^[3] obtained from a machine analysis of the statistics of nonintersecting paths.

For $W = W_c$ we have

$$G_{ij} \sim |\mathbf{R}|^{-(d-2+\eta)}, \quad (14)$$

where

$$\eta \approx \frac{\epsilon^2}{64} \left\{ 1 + \frac{17}{16} \epsilon \right\} \approx 0.032 \quad \text{for } \epsilon = 1. \quad (15)$$

The small value of the critical index η implies that the localization assumed by Thouless^[11] (who evidently used unreliable numerical values, obtained in the machine analysis, for the critical indices in the pre-exponential factor in $Z_N(\mathbf{R})$), with a power-law decay of the wavefunctions, is impossible in the given model. In the analog of formula (14) in^[11], the exponent is equal to $17/9$, which falls in the region of possible values (from $\frac{3}{2}$ to $\frac{5}{2}$, according to Thouless) of the localization exponent. In our case, $d - 2 + \eta \approx 1.032$ for $d = 3$.

Naturally, the asymptotic formulas (11) and (14) given above can also be obtained by direct use of the asymptotic formulas for $Z_N(\mathbf{R})$ obtained by des Cloizeaux.^[10]

The analysis carried out is inapplicable in the one-dimensional case, since in the model under consideration, with nearest-neighbor interaction, Anderson's renormalized series for the electron Green function contains only two terms, corresponding to the two possible nonintersecting paths.^[13] The question of localization reduces to an investigation of the convergence of a certain continued fraction, and the statistics of nonintersecting paths do not play a special role. Therefore, a one-dimensional model of a phase transition, of the Landau-Ginzburg type, evidently has no direct relation

to the problem of the localization of electrons in a one-dimensional disordered system. The same conclusion is obtained from other arguments in a recent paper by Thouless.^[14]

In conclusion, we emphasize that the most probable electron Green function near the mobility edge was considered above. In papers by Edwards^[6] and Freed^[7] an analogy has been noted between the problem of nonintersecting random walks and the problem of calculating the one-electron Green function averaged over random configurations of impurities. Starting from this analogy, it is not difficult to convince oneself that the diagrammatic series of Edwards for this Green function,^[15] in the Gaussian approximation for the statistics of the impurities, is generated by the diagrammatic series for $G_U(s)$ of the problem (7) with $n = 0$, after the appropriate analytic continuation in the parameters of the Lagrangian (see also the paper^[14]). The important point here, however, is that the sign of the interaction constant g_0 changes, so that the correspondence with the theory of phase transitions is evidently lost. Physically, this is connected with the fact that random walks without intersections are equivalent to the thermodynamics of a polymer chain with repulsion between the links, whereas the thermodynamics of an electron in a system of impurities is equivalent to the thermodynamics of a polymer with attraction.^[6] The question of the possibility of applying Wilson's ϵ -expansion in this problem remains open.

The author expresses his deep gratitude to L. V. Keldysh and Yu. A. Izyumov for discussion of a wide range of questions associated with this work.

¹D. J. Thouless, Phys. Rep. 13C, 93 (1974).

²P. W. Anderson, Phys. Rev. 109, 1492 (1958).

³P. W. Anderson, Proc. Nat. Acad. Sci. U.S.A. 69, 1097 (1972).

⁴E. N. Economou and W. H. Cohen, Phys. Rev. B5, 2931 (1972).

⁵N. F. Mott and E. A. Davis, Electronic Processes in Non-crystalline Materials, Oxford University Press, 1971.

⁶S. F. Edwards, J. Noncryst. Solids 4, 417 (1970); R. A. Abram and S. F. Edwards, J. Phys. C5, 1183, 1196 (1972).

⁷K. F. Freed, Phys. Rev. B5, 4802 (1972).

⁸K. G. Wilson and J. Kogut, Phys. Rep. 12C, 75 (1974).

⁹P. G. de Gennes, Phys. Lett. 38A, 339 (1972).

¹⁰J. des Cloizeaux, Phys. Rev. A10, 1665 (1974).

¹¹B. J. Last and D. J. Thouless, J. Phys. C7, 699 (1974).

¹²V. K. S. Shante and S. Kirkpatrick, Adv. Phys. 20, 325 (1971).

¹³D. J. Thouless, J. Phys. C8, 1803 (1975).

¹⁴S. F. Edwards, Phil. Mag. 3, 1020 (1958).

Translated by P. J. Shepherd

Collective excitation of charge-density waves in quasi-one-dimensional structures

M. V. Sadovskii

Institute of Metal Physics, Urals Scientific Center, USSR Academy of Sciences, Sverdlovsk

(Submitted July 5, 1976; resubmitted October 28, 1976)

Fiz. Tverd. Tela (Leningrad) 19, 1044-1053 (April 1977)

Oscillations of the phase of the order parameter are considered in quasi-one-dimensional systems that undergo a Peierls structural transition. Their spectrum is calculated with allowance for the effects of the Coulomb interaction of the charge-density wave (CDW) on different chains and within a single chain. It is shown that the interaction of the CDW with charged impurities leads to pinning of the wave. Nonlinear excitations of CDW of the soliton type are considered. CDW interaction on neighboring chains leads to a binding of solitons and antisolitons into pairs that play the role of defects in the CDW structure.

PACS numbers: 64.70. - p

Recent years have seen an increased interest in the study of the properties of quasi-one-dimensional systems, particularly systems that undergo a Peierls structural transition.¹ This interest is stimulated by the experimental observation of a Peierls transition in compounds of the type $K_2Pt(CN)_4Br_{0.3} \cdot 3H_2O(KCP)$ (Refs. 2-4) and TTF-TCNQ (Refs. 5 and 6), and also the possibility of observing anomalous conductivity connected with displacement of the charge-density wave (CDW) that occurs in the transition.⁷⁻⁹ This latter property of such systems turns out to be closely connected with collective excitations of CDW (Refs. 9 and 10) which are being actively studied experimentally.¹¹⁻¹²

The present paper is devoted to a consideration of

the spectrum of the collective excitations of CDW in the low-temperature region, on the basis of a generalized semiphenomenological model proposed in Refs. 13 and 14. The model is generalized from the pure one-dimensional case to include the quasi-one-dimensional case, and the influence of the impurities and of commensurability effects is investigated. The possible existence of new modes of the collective-excitation spectrum of the soliton type in a purely one-dimensional model is considered, with a qualitative allowance for three-dimensional and Coulomb effects.

The model is quite general, and the main results may be applicable to CDW that are not of the Peierls type.

1. FORMULATION OF THE MODEL AND EXCITATION SPECTRUM IN THE LINEAR APPROXIMATION

We consider a quasi-one-dimensional system at temperatures much lower than the Peierls-transition point [$T_p \sim 120$ K for KCP (Ref. 4), $T_p = 54$ K for TTF-TCNQ (Ref. 6)]. In each chain there exists a nonzero order parameter of the CDW,

$$\text{Re } \Psi(x) = \text{Re} \{ \Delta \exp [i(Qx + \Phi)] \}, \quad (1)$$

where Δ is the amplitude of the order parameter and is connected with the gap in the spectrum of the single-electron excitations of the Peierls phase¹; Φ is the phase shift of the order parameter and determines the position of the CDW relative to the immobile coordinate system⁹; $Q = 2p_F$, where p_F is the Fermi momentum of the electrons and is connected with their linear density by the relation $p_F = (\pi/2)n$.

The collective excitations of the CDW correspond to the fact that in (1) the amplitude and phase $\Delta(x,t)$ and $\Phi(x,t)$ become coordinate and time functions that are different from the equilibrium values Δ and Φ . We consider henceforth only excitations of the phase shift of the order parameter,¹⁴ which can be regarded in first-order approximation independently of the amplitude oscillations,⁹ at least at sufficiently low temperatures $T \ll T_p$. This question was considered in greater detail by Brazovskii and Dayaloshinskii.¹⁰ It will be assumed that $\Phi(x,t)$ is a sufficiently smooth function of the coordinate and of the time.

From the form of (1) it is easily seen^{9,14} that the dependence of the CDW phase on the time means displacement of the wave along the chain with velocity

$$v_1 = -\frac{1}{Q} \frac{\partial \Phi}{\partial t}. \quad (2)$$

Analogously, the presence of a spatial gradient of the phase means local variation of the Fermi momentum of the electrons

$$\delta p_F = \frac{1}{2} \frac{\partial \Phi}{\partial x}; \quad (3)$$

and then the excitation of $\Phi(x,t)$ corresponds to a linear energy density

$$E = \frac{n_s}{2m} (\delta p_F)^2 + \frac{1}{2} m^* n_s v_1^2 = \frac{n_s m^*}{Q^2} \left\{ \frac{1}{2} \left(\frac{\partial \Phi}{\partial t} \right)^2 + \frac{s^2}{2} \left(\frac{\partial \Phi}{\partial x} \right)^2 \right\}, \quad (4)$$

where n_s is the linear density of the electrons that move together with the CDW; m^* is the effective mass connected with the motion of the CDW (Refs. 13 and 14); m is the effective mass of the electron in the chain

$$s^2 = \frac{p_F^2}{mm^*}. \quad (5)$$

The phenomenological parameters n_s and m^* can be determined from the microscopic theory and depend on the concrete model whereby the CDW is produced. In the simplest theory of Peierls transitions at $T \ll T_p$ we have^{9,13,14}

$$\left. \begin{aligned} n_s &\approx n, \\ \frac{m^*}{m} &= 1 + \frac{4\Delta^2}{\lambda\omega_Q^2} \approx \frac{4\Delta^2}{\lambda\omega_Q^2}, \end{aligned} \right\} \quad (6)$$

where n is the total linear density of the electrons in the chain, Δ is the gap in the electron spectrum at $T = 0$, ω_Q^2 is the characteristic frequency of the "bare" phonon ($\omega_Q \sim \theta_D$ is the Debye temperature), and λ is the dimensionless constant of the electron-phonon interaction. Usually $m^* \gg m$, for example $m^* \approx 10^3 m$ for KCP (Refs. 11 and 13).

It follows from Refs. 1 and 4 that the effective Lagrangian of a CDW on an isolated chain is

$$\mathcal{L}_0 = nm^* \frac{1}{Q^2} \left\{ \frac{1}{2} \left(\frac{\partial \Phi}{\partial t} \right)^2 - \frac{1}{2} s^2 \left(\frac{\partial \Phi}{\partial x} \right)^2 \right\}. \quad (7)$$

The derivation of such a Lagrangian from the microscopic theory is given in Ref. 10. This leads to the standard wave equation

$$\frac{\partial^2 \Phi}{\partial t^2} - s^2 \frac{\partial^2 \Phi}{\partial x^2} = 0, \quad (8)$$

which coincides, when account is taken of (2) and (3), with the hydrodynamic equation of motion¹⁴

$$nm \frac{\partial v_x}{\partial t} = -n \frac{m}{m^*} \nabla \mu, \quad (9)$$

where μ is the chemical potential (Fermi energy) of the electrons, and the factor m/m^* determines the fraction of the CDW mass carried by the electrons. The spectrum of the CDW phase oscillations under the foregoing assumptions takes the form

$$\omega^2 = s^2 q^2. \quad (10)$$

which corresponds to the Goldstone mode of Lee, Rice, and Anderson, corresponding to the Fröhlich "superconductivity" in the considered model.⁹

Our purpose is to consider the role of various interactions that are not taken into account by the zero-order Lagrangian (7). These include primarily the interaction of the CDW on various chains in a quasi-one-dimensional systems, the role of Coulomb effects in one chain, and interactions with charged impurities.

The Peierls CDW corresponds to modulation of the density of an electron charge along the chain, in the form⁹

$$\rho(x) = ne \frac{\Delta}{\lambda E_F} \cos(Qx + \Phi), \quad (11)$$

so that this chain produces around itself an electrostatic field with a potential

$$\varphi(r_{\perp}, x) = 2ne \frac{\Delta}{\lambda E_F} \cos(Qx + \Phi) K_0(Qr_{\perp}). \quad (12)$$

where e is the electron charge, E_F is the Fermi energy of the chain, r_{\perp} is the radial distance from the chain, and $K_0(x)$ is a modified Bessel function. Accordingly, in a system of chains forming a regular lattice in a plane orthogonal to the chains, with a lattice constant $r_{\perp} = b$, an elec-

trostatic interaction energy is produced (per unit length of the system)

$$U = nm^* \frac{1}{Q^2} \sum_n \sum_{\langle m \rangle} \omega_c^2 \cos(\Phi_n - \Phi_m), \quad (13)$$

$$\omega_c^2 = \omega_p^2 \left(\frac{\omega_p}{4E_F} \right)^2 \frac{(Qr_\perp)^2}{2\pi\lambda\epsilon_\perp} K_0(Qr_\perp) |r_\perp|^{-2}, \quad (14)$$

where \mathbf{n} and \mathbf{m} determine the positions of the chains in the plane lattice, ω_p is the plasma frequency of the electrons, and ϵ_\perp is the dielectric constant of the system in a direction transverse to the chains. It suffices to take into account in (13) the nearest-neighbor interaction, since $K_0(Qr_\perp)$ is exponentially small when $Qr_\perp \gg 1$. The interaction (13), in particular, causes the CDW on the neighboring chains to be conveniently aligned in such a way that their phases differ by π , as is indeed observed experimentally in KCP (Ref. 4).

The Lagrangian of the system now takes the form¹⁾

$$\mathcal{L} = nm^* \frac{1}{Q^2} \sum_n \frac{1}{2} \left\{ \left(\frac{\partial \Phi_n}{\partial t} \right)^2 - s^2 \left(\frac{\partial \Phi_n}{\partial x} \right)^2 \right\} - \sum_n \sum_{\langle m \rangle} \omega_c^2 (1 + \cos(\Phi_n - \Phi_m)). \quad (15)$$

We consider a linearized variant of the theory, corresponding to $\Phi_n \ll 1$, $\Phi_m \approx \pi$, so that (15) goes over into

$$\mathcal{L} \approx nm^* \frac{1}{Q^2} \left\{ \sum_n \frac{1}{2} \left[\left(\frac{\partial \Phi_n}{\partial t} \right)^2 - s^2 \left(\frac{\partial \Phi_n}{\partial x} \right)^2 - 2\omega_c^2 \Phi_n^2 \right] + \omega_c^2 \sum_n \sum_{\langle m \rangle} \Phi_n \Phi_m \right\}, \quad (16)$$

where all the Φ_n , Φ_m now denote small deviations from the equilibrium values. The corresponding equations of motion take the form

$$\frac{\partial^2 \Phi_n}{\partial t^2} - s^2 \frac{\partial^2 \Phi_n}{\partial x^2} - 4\omega_c^2 \Phi_n = \omega_c^2 \sum_{\langle m \rangle} \Phi_m. \quad (17)$$

We seek the solution in the form

$$\Phi_n(xt) = \sum_{q_\perp} \Phi_{q_\perp} e^{i(qx + q_\perp n - \omega t)} \quad (18)$$

and obtain the spectrum

$$\omega^2 = s^2 q^2 + 2\omega_c^2 (2 - \cos q_\perp b - \cos q_\perp^* b), \quad (19)$$

where the lattice of chain is assumed for simplicity to be quadratic (b is the lattice constant). For $q_\perp = 0$ we have again the acoustic spectrum (10). Thus, the interaction of the chains does not lead to pinning of the CDW.

We now take into account the Coulomb effect in an individual chain. The phase gradient, according to (3) and according to the connection between the Fermi momentum and the electron density, signifies local variation of the charge density

$$v_p = \frac{e}{\pi} \frac{\partial \Phi}{\partial x}, \quad (20)$$

which produces a corresponding electric field in the chain. To take this circumstance into account it is necessary to

solve in place of (17) a coupled system of equations of motion

$$\frac{\partial^2 \Phi_n}{\partial t^2} - s^2 \frac{\partial^2 \Phi_n}{\partial x^2} + 4\omega_c^2 \Phi_n = \omega_c^2 \sum_{\langle m \rangle} \Phi_m + \frac{\pi n e}{m^* \epsilon_b} \frac{\partial \varphi_n}{\partial x}, \quad (21)$$

which take into account the action of the electric field with potential φ_n , defined by a differential-difference Poisson equation

$$-\frac{\partial^2 \varphi_n}{\partial x^2} - \frac{1}{b^2} \sum_{i=y, x} [\varphi_{n+b_i} - 2\varphi_n + \varphi_{n-b_i}] = 4e \frac{\partial \Phi_n}{\partial x} \sum_{\kappa_\perp} e^{i\kappa_\perp n}. \quad (22)$$

The last term in (21) corresponds to replacement of the chemical potential in (9) by the electrochemical potential. Here ϵ_b is the dielectric constant due to electron transitions through the Peierls gap

$$\epsilon_b = 1 + \frac{\omega_p^2}{\Omega \Delta^2}. \quad (23)$$

In (22), κ_\perp are the reciprocal-lattice vectors of the chains. We seek the solution for $\Phi_n(xt)\varphi_n(xt)$ in the form (18) and in analogous form for $\varphi_n(xt)$. Solving the corresponding secular equation, we obtain the spectrum of the excitations

$$\omega^2 = s^2 q^2 + \frac{\omega_p^2}{\epsilon_b} \frac{q^2}{q^2 + \frac{2}{b^2} [2 - \cos q_\perp^* b - \cos q_\perp b]} + 2\omega_c^2 [2 - \cos q_\perp^* b - \cos q_\perp b], \quad (24)$$

where $\omega_p^{*2} = 4\pi n e^2 / m^*$. The Coulomb effects lead to a finite frequency $\omega_p^{*2} / \epsilon_b \approx (3/2)\lambda \omega_Q^2$ of the phase oscillations at $q_\perp = 0$; at $q_\perp b \ll 1$ we have

$$\omega^2 = \frac{\omega_p^{*2}}{\epsilon_b} \cos^2 \theta + s^2 q^2 + \omega_c^2 b^2 q^2, \quad (25)$$

where $\text{tg } \theta = q_\perp / q$. For $q_\perp = (\pi/b, \pi/b)$ we have

$$\omega^2 = 8\omega_c^2 + \left\{ s^2 + \frac{1}{8} b^2 \frac{\omega_p^{*2}}{\epsilon_b} \right\} q^2. \quad (26)$$

The spectrum (24) constitutes a natural generalization of the results of Refs. 9 and 14 to the case of quasi-one-dimensional systems. The displacement of the atoms in the n -th chain following excitation of small oscillations of the order-parameter phase shift is proportional to

$$u_n \sim \exp \left\{ iQx + i \frac{\pi}{b} n + i \Phi_{q_\perp} e^{i(qx + i q_\perp n - \omega t)} \right\} \approx e^{iQx + i \frac{\pi}{b} n} + i \Phi_{q_\perp} e^{i(q+Q)x + i \left(\frac{\pi}{b} + q_\perp \right) n - i\omega t}. \quad (27)$$

Thus, the phase oscillations with wave vector $\mathbf{q} = (q, q_\perp)$ correspond to excitation of phonons with wave vector $(Q + q, \pi/b + q_\perp^y, \pi/b + q_\perp^z)$, so that the study of the phonon spectrum at the point $(Q, \pi/b, \pi/b)$ corresponds to a study of phase oscillations with $\mathbf{q} = (0, 0, 0)$. As seen

from (27), these oscillations correspond to antiparallel displacements of the atoms in the neighboring chains.¹⁵ Analogously, the phonon spectrum at the point $(Q, 0, 0)$ is connected with the phase oscillations with $q = (0, \pi/b, \pi/b)$ corresponding to parallel displacements in the neighboring chains.

Low-frequency optical phonons were observed in Ref. 12 in KCP at the points $(Q, \pi/b, \pi/b)$ and $(Q, 0, 0)$, which can tentatively be interpreted as connected with oscillations of the order-parameter phase shift. The weak dispersion of these phonons is explained by the gap-like character of their spectrum (an unjustified comparison with the acoustic spectrum (10) was made in Ref. 12). At the same time, the equality of the phonon frequencies observed at the points $(Q, \pi/b, \pi/b)$ and $(Q, 0, 0)$ remains unexplained. We emphasize that the absence of total three-dimensional ordering in KCP (Ref. 4), which is apparently due to disorder effects, can lead to a discernible change of the results obtained above, which are valid, strictly speaking, only for a system consisting of one-dimensional chains of the same type, without the internal disorder inherent in systems of the KCP type.

2. EFFECT OF IMPURITIES ON THE CDW EXCITATION SPECTRUM

Lee, Rice, and Anderson⁹ have advanced arguments favoring the assumption that the interaction of CDW with charged impurities converts the acoustic-type phase-oscillation spectrum (10) into a spectrum with a gap, meaning a pinning of the CDW on the impurities and elimination of the Frohlich "superconductivity." At the same time, it was stated in Ref. 16 that the interaction of CDW with random impurities does not lead to pinning. There is as yet no calculation of the spectrum of the phase oscillations of the CDW with allowance for the interaction with the impurities in any concrete model. We present below such a calculation in the considered semiphenomenological theory.

We consider a system of charges disposed in random fashion along a chain with CDW, at a distance r_{\perp} from the chain. Such a situation is apparently realized in KCP, where the acceptor atoms (of the Br type) are randomly arranged in the system along Pt chains.¹ The impurity charge density

$$\rho(x) = \sum_j e\delta(x - x_j), \quad (28)$$

where x_j are the impurity coordinates, interacts with the CDW potential (12), so that the interaction energy per unit length of the system is

$$U_{\text{imp}} = nm^* \frac{1}{Q^2} \omega_{\text{imp}}^2 \frac{1}{N} \sum_j \{\cos(Qx_j + \Phi)\}, \quad (29)$$

where

$$\omega_{\text{imp}}^2 = \frac{\omega_p^2}{4\pi\lambda\nu e_{\perp}} \left(\frac{\Delta}{E_F}\right) (Qr_{\perp})^2 K_0(Qr_{\perp}), \quad (30)$$

N is the number of atoms in the chain and ν is the number of conduction electrons per atom.

We consider again the linearized theory ($\Phi \ll 1$). The Lagrangian of the system takes the form

$$\mathcal{L} = nm^* \frac{1}{Q^2} \left\{ \frac{1}{2} \left(\frac{\partial\Phi}{\partial t}\right)^2 - \frac{s^2}{2} \left(\frac{\partial\Phi}{\partial x}\right)^2 + \omega_{\text{imp}}^2 \frac{1}{N} \sum_j \sin Qx_j \Phi + \omega_{\text{imp}}^2 \frac{1}{N} \sum_j \cos Qx_j \Phi^2 \right\}. \quad (31)$$

The equations of motion are given by

$$\frac{\partial^2\Phi}{\partial t^2} - s^2 \frac{\partial^2\Phi}{\partial x^2} = \omega_{\text{imp}}^2 \frac{1}{N} \sum_j \sin Qx_j + \omega_{\text{imp}}^2 \frac{1}{N} \sum_j \cos Qx_j \Phi. \quad (32)$$

In a system with impurities

$$\Phi = \Phi(xt; (x_j)) \quad (33)$$

is the functional of the impurity positions. On the other hand, the phase shift, as a component of the order parameter, is a thermodynamic quantity and must be averaged over the ensemble of random impurity configurations. Averaging (32), we obtain

$$\left(\frac{\partial^2}{\partial t^2} - s^2 \frac{\partial^2}{\partial x^2}\right) \langle \Phi \rangle = \omega_{\text{imp}}^2 \left\langle \frac{1}{N} \sum_j \cos Qx_j \Phi \right\rangle. \quad (34)$$

This gives rise in natural fashion to a chain of equations expressed in terms of the Fourier components in the form

$$(-\omega^2 + s^2 q^2) \langle \Phi_{q\omega} \rangle = \omega_{\text{imp}}^2 \left\langle \frac{1}{N} \sum_j \cos Qx_j \Phi \right\rangle_{q\omega}, \quad (35)$$

$$\begin{aligned} & (-\omega^2 + s^2 q^2) \left\langle \frac{1}{N} \sum_j \cos Qx_j \Phi \right\rangle_{q\omega} \\ &= \omega_{\text{imp}}^2 \left\langle \frac{1}{N^2} \sum_j \sin Qx_j \sum_i \cos Qx_i \right\rangle \delta(\omega) \delta(q) \\ &+ \omega_{\text{imp}}^2 \left\langle \frac{1}{N^2} \sum_j \cos Qx_j \sum_i \cos Qx_i \Phi \right\rangle_{q\omega}. \end{aligned} \quad (36)$$

Carrying out in (36) a very simple decoupling in the impurity correlators, we obtain (at $\omega \neq 0, q \neq 0$)

$$\left\{ -\omega^2 + s^2 q^2 + \frac{\omega_{\text{imp}}^4}{\omega^2 - s^2 q^2} \frac{1}{2} S(Q) \right\} \langle \Phi_{q\omega} \rangle = 0, \quad (37)$$

where

$$S(Q) = \frac{1}{N^2} \left\langle \sum_{ij} e^{iQ(x_i - x_j)} \right\rangle \quad (38)$$

is the structure factor of the impurity positions. From (37) follows the phase-oscillation spectrum

$$\omega^2 = \left\{ \frac{1}{2} S(Q) \right\}^{1/2} \omega_{\text{imp}}^2 + s^2 q^2. \quad (39)$$

For random impurities $S(Q)$ is equal to the impurity

concentration c_{imp} . Thus, the impurities lead to pinning of the CDW, the gap in the spectrum being

$$\omega_T^2 = \left\{ \frac{1}{2} c_{\text{imp}} \right\}^{1/2} \omega_{\text{imp}}^2 \quad (40)$$

The foregoing analysis is valid for sufficiently low impurity concentrations, which do not influence substantially the Peierls transition itself¹⁷ and which allow the decoupling carried out above. The allowance for the quasi-one-dimensionality and for the Coulomb effects is in the same manner as above; leaving out the calculations, we indicate that as the result the gap ω_T^2 is simply added to the right-hand side of expression (19) or (25). The gap in the spectrum is different from zero at arbitrary q and q_{\perp} .² It is possible that the equality of the phonon frequencies at the points $(Q, \pi/b, \pi/b)$ and $(Q, 0, 0)$, which was observed in Ref. 12, is due to the dominant role of the impurities in the formation of the gap.

3. EFFECTS OF COMMENSURABILITY AND NONLINEAR EXCITATIONS

The existence of a Goldstone mode with a spectrum (10) is directly connected with degeneracy of the CDW with respect to the phase Φ . This degeneracy of the CDW having a period that is commensurate with the period of the original chain. In the commensurate case $Q = 2\pi m \cdot (Ma)^{-1}$, where a is the period of the initial chain, and $m < M$ are integers. The CDW energy then acquires a commensurability term^{18,14,9}

$$U_{\text{comm}} \sim \Delta^M \cos M\Phi. \quad (41)$$

The proper Lagrangian of one chain takes the form

$$\mathcal{L} = \mathcal{L}_0 + nm^* \frac{1}{Q^2} \frac{\omega_T^2}{M^2} (\cos M\Phi - 1), \quad (42)$$

where^{9,14}

$$\omega_T^2 \sim \lambda M^2 \omega_Q^2 \left(\frac{\Delta}{E_F} \right)^{M-2}. \quad (43)$$

In the linear approximation we can confine ourselves to expansion of $\cos M\Phi$ up to quadratic terms, and obtain the spectrum of the phase oscillations in the form⁹

$$\omega^2 = \omega_T^2 + s^2 q^2. \quad (44)$$

Thus, the commensurability effects lead to a pinning of the CDW.

The nonlinear Lagrangian (42) leads to an equation of motion of the sine-Gordon type

$$\frac{\partial^2 \Phi}{\partial t^2} - s^2 \frac{\partial^2 \Phi}{\partial x^2} = - \frac{\omega_T^2}{M^2} \sin M\Phi, \quad (45)$$

for which an extensive spectrum of classical and quantum solutions has been obtained.¹⁹ In addition to the branch corresponding to the linear oscillations of Φ near zero (44), it is possible to excite in the system an arbitrary

number of soliton-antisoliton pairs moving with velocity $v < s$

$$\Phi_{\text{sol}}(xt) = \frac{4}{M} \text{arctg} \left\{ \exp \left(\frac{\omega_T}{s} \frac{x - v/st}{1 - \frac{v^2}{s^2}} \right) \right\}, \quad (46)$$

$$\Phi_{\text{antisol}}(xt) = -\Phi_{\text{sol}}(xt). \quad (47)$$

The energy of the soliton is expressed by the standard "relativistic" formula

$$E_{\text{sol}} = \frac{M_{\text{sol}} s^2}{\left(1 - \frac{v^2}{s^2}\right)^{1/2}} = \sqrt{\Delta_{\text{sol}}^2 + s^2 p^2}, \quad (48)$$

where the mass M_{sol} ($\Delta_{\text{sol}} = M_{\text{sol}} s^2$, p is the soliton momentum), in the quasiclassical (WKB) approximation (Refs. 18 and 19)³, using the parameters of our model, is equal to

$$M_{\text{sol}} = nm^* \frac{1}{Q^2} \frac{8\omega_T}{\gamma s} = \frac{4}{\pi} \frac{\omega_T}{s p_F} m^* \frac{1}{\gamma}, \quad (49)$$

where γ is the renormalized coupling constant, equal in the present model to

$$\gamma = \frac{M^2}{1 - \frac{8\pi}{M^2}}. \quad (50)$$

In classical soliton theory we have $\gamma = M^2$. The possible existence of soliton excitations in CDW of the Peierls type was considered in the classical approximation in a recent paper.²⁸ The form of the soliton solution as a function of x (at $v = 0$) is shown in Fig. 1. In a region having linear dimensions of the order of

$$\xi_{\text{sol}} \approx \frac{s}{\omega_T} \quad (51)$$

(the soliton dimensions) the gradient of the phase differs effectively from zero, i.e., in accordance with (20), there is an excess charge density

$$\delta \rho_{\text{sol}} = \frac{2}{M} \frac{e}{\pi} \frac{\omega_T}{s} \text{ch}^{-1} \frac{\omega_T}{s} x; \quad (52)$$

from which it is clear that the soliton carries an electric charge

$$Q_{\text{sol}} = \frac{4}{M} e. \quad (53)$$

Antisoliton carry a charge of opposite sign. The motion of the solitons produces a current density [see (3)]

$$j_{\text{sol}}(xt) = - \frac{ne}{Q} \Phi_{\text{sol}}(xt) = \delta \rho_{\text{sol}}(x) v. \quad (54)$$

Solitons and antisolitons can be produced only in pairs and are subject to Fermi statistics.²¹

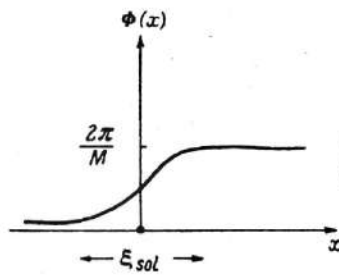


FIG. 1. Change of phase in the region of the soliton solution.

It is easily seen that the considered model is equivalent to a simple generalization of a one-dimensional dislocation after Frenkel' and Kontorova^{22,23}, dealing with the motion of a chain of "atoms" and mass m^* in a periodic field of a "substrate" produced by the commensurability effects. In this sense, solitons constitute "dislocations" in the CDW lattice.

In addition to solitons, the model under consideration admits of spectrum branches corresponding to bound soliton-antisoliton states, which have not been considered in Ref. 20. Such a "doublet" solution of (45) in the rest system ($v = 0$) takes the form^{18,19}

$$\Phi_d(xt) = \frac{4}{M} \operatorname{arctg} \left\{ \epsilon \frac{\sin\left(\frac{2\pi}{\tau} t\right)}{\operatorname{ch}\left(\epsilon \frac{2\pi}{\tau} x\right)} \right\}, \quad (55)$$

where

$$\epsilon = \left[\left(\frac{\tau \omega_T}{2\pi} \right)^2 - 1 \right]^{1/2}, \quad \tau = \frac{2\pi}{\omega_T \cos \frac{N\gamma}{16}}. \quad (56)$$

Here $N = 1, 2, \dots, < 8\pi/\gamma$ (Ref. 19) number the stable (in quantum theory) branches of the doublet spectrum. Their masses (gaps in the spectrum) are given in the WKB approximation by¹⁹

$$M_N = nm^* \frac{1}{Q^2} \frac{16\omega_T}{\gamma s} \sin\left(\frac{N\gamma}{16}\right) = \frac{8}{\pi} \frac{\omega_T}{s p_F} m^* \frac{1}{\gamma} \sin\left(\frac{N\gamma}{16}\right). \quad (57)$$

Taking into account the form of γ (52) and the fact that only $M \geq 3$ is meaningful in the considered model (Ref. 9),⁴⁾ we verify that $N = 1$ for $M = 3$, and for $M > 3$ the doublet solutions are unstable.

The doublet solution is shown graphically in Fig. 2. It is obvious that the total charge carried by the doublet is equal to zero, i.e., their motion does not contribute to the constant current. However, a doublet has a dipole moment that oscillates with frequency $2\pi/\tau$, and this could manifest itself in principle in the dielectric constant.

We note that in Ref. 24 an attempt was made to construct doublet-like solutions of an equation of the type (45). However, the approximate formations obtained there have nothing in common with the exact solutions (55) and are apparently unstable. In addition, it is erroneously stated in Ref. 24 that such solutions contribute to the dc conductivity.⁵⁾

We consider now the degree to which the obtained

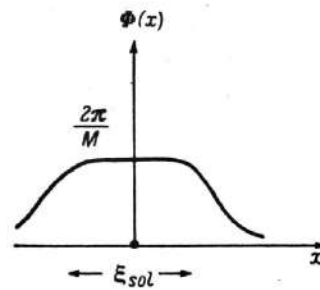


FIG. 2. Change of phase in the region of the bound soliton-antisoliton state.

purely one-dimensional solutions are preserved when account is taken of the Coulomb effects in a single chain, as well as of chain-interaction effects.

The formation of a soliton is not profitable from the point of view of Coulomb effects, since it involves an energy loss $Q_{\text{sol}}^2 / \xi_{\text{sol}} \epsilon_b$. This energy shortage is immaterial if it is smaller than $M_{\text{sol}} s^2$, which leads to the condition $e^2 m / \hbar p_F \ll (1/16) \epsilon_b$, which can be readily satisfied. To take into account the interaction of CDW of neighboring chains it is necessary to consider systems of coupled nonlinear equations.

We present a simple qualitative analysis. The production of a soliton-antisoliton pair on one of the chains leads to a loss of chain-interaction energy [see (13)]

$$U_{\perp} \sim nm^* \frac{\omega_c^2}{Q^2} \xi \left\{ \cos \pi \left(1 - \frac{2}{M} \right) + 1 \right\}, \quad (58)$$

where ξ is the soliton-antisoliton distance. The influence of this loss on the soliton mass is immaterial if $2M_{\text{sol}} s^2 \gg U_{\perp}$, leading to the requirement

$$\xi \ll \frac{16}{M^2} \left(\frac{\omega_T}{\omega_c} \right)^2 \xi_{\text{sol}}, \quad (59)$$

i.e., the soliton and the antisoliton must be close enough. At the same time it is necessary to have $\xi \gg \xi_{\text{sol}}$, for only then can we speak of "individual" solitons. In view of the smallness of ω_T (43) relative to the parameter $(\Delta/E_F) M^{-2} \ll 1$, this condition is difficult to satisfy for the known systems of the type KCP or TTF-TCNQ. At the same time, ω_c decreases exponentially with the increasing distance between the chains (14) in such a way that the situation becomes more favorable in a system of sufficiently separated chains. Owing to (58), the solitons and antisolitons are attracted with a force $\sim nm(\omega_c^2/Q^2)$, and, strictly speaking, are always bound. Let us estimate the minimum dimension of a bound soliton-antisoliton state in the potential well (58)

$$\frac{1}{M_{\text{sol}} \xi_b^2} \sim nm^* \frac{\omega_c^2}{Q^2} \xi_b,$$

i.e.,

$$\frac{\xi_b}{\xi_{\text{sol}}} \sim M^{2/5} \left(\frac{\omega_T}{\omega_c} \right)^{2/5} \left(\frac{m}{m^*} \right)^{1/5}. \quad (60)$$

Here, too, it is necessary to stipulate $\xi_b > \xi_{\text{sol}}$, which

can be readily satisfied. Thus, solutions of the soliton type are not profitable from the point of view of interaction between the chains and can hardly be realized in known systems.⁶⁾ In addition, even under conditions when one can speak of the existence of solitons in individual chains, they are bound into soliton-antisoliton pairs and make no contribution to the conductivity in weak fields,⁷⁾ in contradiction to the statements made in Ref. 21.

We note in conclusion that the loss of energy of the type (58) disappears in a situation corresponding to formation of solitons on all chains in a sample cross section perpendicular to the chains. It can be proved rigorously, however, that such soliton "planes" are not profitable from the point of view of Coulomb effects. For lack of space, this question is not considered here.

In conclusion, the author is grateful to L. N. Bulaevskii for numerous discussions and critical remarks.

¹⁾A constant has been added here to make the ground state correspond to $\varphi=0$, thereby fixing the energy origin.

²⁾Since the phase oscillations are in fact three-dimensional, questions concerning the specific character of the action of impurities in a strictly one-dimensional system are not raised.

³⁾It appears that the WKB mass values used here are exact.¹⁹

⁴⁾At $M=2$, the phase oscillations of CDW coincide with the amplitude oscillations, which are not considered here.

⁵⁾In Ref. 24, and in fact also in Ref. 20, they considered an interaction Lagrangian of the type (42) with $M=1$. We do not know of any physical mechanisms that lead to such an interaction. It appears that a nonlinear interaction between the chains does not lead to formation of soliton solutions, since it does not ensure pinning of the CDW.

⁶⁾We note, however, that the binding energies of soliton-antisoliton pairs decrease exponentially with increasing distance between chains.

⁷⁾A sufficiently strong field $E \sim 2 \cdot 3(N/\pi)(e/\tau^2)\omega_c^2/\lambda\omega_Q$ will break the soliton-antisoliton pair and their contribution to the conductivity becomes in principle possible. The magnitude of this field also decreases exponentially with increasing distance between chains.

¹⁾L. N. Bulaevskii, Usp. Fiz. Nauk **115**, 263 (1975) [Sov. Phys. Usp. **18**, 131 (1975)].

- ²⁾R. Comes, N. Lambert, H. Launois, and H. R. Zeller, Phys. Rev. B **8**, 571 (1973).
- ³⁾B. Renker, H. Rietschel, L. Pintschovius, W. Glaser, P. Bruesch, D. Kuse, and M. J. Rice, Phys. Rev. Lett. **30**, 1144 (1973).
- ⁴⁾B. Renker, L. Pintschovius, W. Glaser, H. Rietschel, R. Comes, L. Liebart, and W. Drexel, Phys. Rev. Lett. **32**, 836 (1974).
- ⁵⁾F. Denoyer, R. Comes, A. Garito, and A. J. Heeger, Phys. Rev. Lett. **35**, 445 (1975).
- ⁶⁾R. Comes, S. Shapiro, G. Shirane, A. F. Garito, and A. J. Heeger, Phys. Rev. Lett. **35**, 1518 (1975).
- ⁷⁾H. Frohlich, Proc. R. Soc. Lond. Ser. A **223**, 296 (1954).
- ⁸⁾D. Allender, J. Bray, and J. Bardeen, Phys. Rev. B **9**, 119 (1974).
- ⁹⁾P. A. Lee, T. M. Rice, and P. W. Anderson, Solid State Commun. **14**, 703 (1974).
- ¹⁰⁾S. A. Brazovskii and I. E. Dzyaloshinskii, Zh. Eksp. Teor. Fiz. **71**, 2338 (1976) [Sov. Phys. JETP **44** (1976)].
- ¹¹⁾D. Tanner, C. Jacobsen, A. Garito, and A. J. Heeger, Phys. Rev. B **13**, 3381 (1976); P. Bruesch, S. Strassler, and H. R. Zeller, Phys. Rev. B **12**, 219 (1975).
- ¹²⁾R. Comes, B. Renker, L. Pintschovius, R. Currat, W. Glaser, and G. Schneider, Phys. Status Solidi B **71**, 171 (1975).
- ¹³⁾M. J. Rice, S. Strassler, and W. Schneider, One Dimensional Conductors, ed. H. G. Schuster, Springer Verlag, 1975, p. 282.
- ¹⁴⁾T. M. Rice, Solid State Commun. **17**, 1055 (1975).
- ¹⁵⁾P. Bruesch and H. R. Zeller, Solid State Commun. **14**, 1037 (1974).
- ¹⁶⁾J. B. Sokoloff, Solid State Commun. **16**, 375 (1975).
- ¹⁷⁾L. N. Bulaevskii and M. V. Sadovskii, Fiz. Tverd. Tela (Leningrad) **16**, 1159 (1974) [Sov. Phys. Solid State **16**, 773 (1974)].
- ¹⁸⁾I. E. Dzyaloshinskii, Collective Properties of the Physical Systems (Nobel Symposium 24), ed. B. Lundquist and S. Lundquist, Academic Press, New York, 1974, p. 143.
- ¹⁹⁾R. Dashen, B. Hasslacher, and A. Neveu, Phys. Rev. D **11**, 3424 (1975); R. Rajaraman, Phys. Rep. **21**, 227 (1975).
- ²⁰⁾M. J. Rice, A. Bishop, J. Krumhansl, and S. Trullinger, Phys. Rev. Lett. **36**, 432 (1976).
- ²¹⁾S. Mandelstam, Phys. Rev. D **11**, 3026 (1975).
- ²²⁾Ya. I. Frenkel' and T. A. Kontorova, Zh. Eksp. Teor. Fiz. **8**, 89, 1340, 1349 (1938).
- ²³⁾Ya. I. Frenkel', Introduction to the Theory of Metals [in Russian], Nauka, 1973.
- ²⁴⁾L. Pietronero, S. Strassler, and G. Toombs, Phys. Rev. B **12**, 5213 (1975).

Translated by J. George Adashko

Erratum: Collective excitation of charge-density waves in quasi-one-dimensional structures [Sov. Phys. Solid State 19, 607-613 (April 1977)]

M. V. Sadovskii

Institute of Metal Physics, Ural Scientific Center, Academy of Sciences of the USSR, Sverdlovsk
Fiz. Tverd. Tela (Leningrad) **19**, 3708 (December 1977)

PACS numbers: 99.10.+g, 64.70.-p

The author has made an error in Eqs. (21) and (22) in this article. The correct forms of these equations are

$$\frac{\partial^2 \Phi_{\mathbf{n}}}{\partial t^2} - s^2 \frac{\partial^2 \Phi_{\mathbf{n}}}{\partial x^2} + 4\omega_c^2 \Phi_{\mathbf{n}} = \omega_c^2 \sum_{\langle \mathbf{m} \rangle} \Phi_{\mathbf{m}} + \frac{\pi n e}{m^*} \frac{\partial \varphi_{\mathbf{n}}}{\partial x}, \quad (21)$$

$$-s_b^2 \frac{\partial^2 \varphi_{\mathbf{n}}}{\partial x^2} - \frac{1}{b^2} \varepsilon_{\perp} \sum_{i=y,z} [\varphi_{\mathbf{n}+b_i} - 2\varphi_{\mathbf{n}} + \varphi_{\mathbf{n}-b_i}] = 4e \frac{\partial \Phi_{\mathbf{n}}}{\partial x} \sum_{\mathbf{x}_1} e^{i\mathbf{x}_1 \cdot \mathbf{n}}. \quad (22)$$

Equation (24) then becomes

$$\omega^2 = s^2 q^2 + \frac{\omega_p^2}{\varepsilon_b} \frac{q^2}{q^2 + \frac{2\varepsilon_{\perp}}{b^2 \varepsilon_b} [2 - \cos q_1^2 b - \cos q_2^2 b]} + 2\omega_c^2 [2 - \cos q_1^2 b - \cos q_2^2 b]. \quad (24)$$

Equation (25) is then valid only for $\varepsilon_{\perp} = \varepsilon_b$.

Translated by A. Tybulewicz

Electron in a random field, theory of phase transitions, and finite-action nonlinear solutions

M. V. Sadovskii

Institute of Metal Physics, Ural Scientific Center of the Academy of Sciences of the USSR, Sverdlovsk

(Submitted September 25, 1978)

Fiz. Tverd. Tela (Leningrad) 21, 743-751 (March 1979)

It is shown that the profile of an electron density-of-states tail in a Gaussian random field is given by the solution of finite-action nonlinear equations for a zero-component scalar field. Ideas of the phase transition theory and the dispersion equation for the coupling constant are used to calculate the preexponential factor in the expression for the density-of-states tail. The applicability of a scaling theory at the mobility edge is discussed.

PACS numbers: 71.25.Mg

1. Ideas of the modern theory of critical phenomena⁷ have been used¹⁻⁶ to describe the behavior of electron states near the mobility threshold of disordered systems. A formal correspondence between the problem of an electron in a random field and a phase transition with a zero-component order parameter (Euclidean theory of a zero-component scalar field)^{8,9} has been used in most papers devoted to this subject (with the exception of Refs. 1 and 3). However, it was pointed out in Refs. 1, 2, 4-6 that the aforementioned correspondence is incomplete since the coupling constant in the corresponding field theory has the "incorrect" sign. Consequently, the standard theory of critical phenomena⁷ cannot be applied and the incorrect sign of the coupling parameter indicates that perturbation theory fails in the range of energies of interest.^{2,4} The neighborhood of the mobility edge, where the perturbation theory fails, is analogous to the "Ginzburg" critical region in the theory of critical phenomena.²

It is our aim to extend Ref. 2 and study in detail the region of localized states (region of negative energies). The present approach is a development of the method proposed by Langer¹⁰ and Zittartz and Langer.¹¹ It will be shown that the profile of a tail in the electron density of states in a random field is governed by the classical solutions of the field theory studied in Refs. 2, 4, and 5 that are characterized by a finite action.^{12,13} We also propose a new method of calculation of the preexponential factor in the density-of-states tail which is based on a dispersion equation for the coupling constant.^{14,15} Our approach is analogous to the theory of critical phenomena. Finally, we shall discuss the validity of scaling at the mobility edge.

2. We shall consider an electron in the field of a random distribution of point scatterers and calculate the Fourier transform $G(E)$ of the one-electron Green's function averaged over all the configurations of scatterers. In the limit $\rho \rightarrow \infty$, $V \rightarrow 0$, $\rho V^2 \rightarrow \text{const}$, where ρ is the density and V is the scattering potential, the problem under study is equivalent to the motion of an electron in a Gaussian random field with a "white noise" correlation function.^{2,11} It was shown in Ref. 2 that such a Green's function can be identified with the Green's function of a scalar field theory with the following Lagrangian (m is the electron mass and E its energy):

$$\mathcal{L} = \frac{1}{2} \sum_{j=1}^n \left\{ \frac{1}{2m} (\nabla \Phi_j)^2 - E \Phi_j^2 \right\} - \frac{1}{8} g V^2 \left(\sum_{j=1}^n \Phi_j^2 \right)^2, \quad (1)$$

where n is the number of components of the field Φ (n should be set equal to zero after all the calculations have been carried out), which eliminates the "superfluous" diagrams with loops that do not appear in the problem of an electron in a random field.^{2,8,9} We have studied² the range of energies $E > 0$, where the standard perturbation theory is applicable (the parquet approximation). The region $E < 0$ (the region of localized states) was discussed in Ref. 2 only qualitatively.¹ It is our aim to study in detail the region $E < 0$.

The main difficulty of the aforementioned theory is due to negative sign of the coupling constant in Eq. (1), which leads to an instability of the ground state in such a field theory and to a failure of the perturbation theory to describe the electron energies^{2,4}

$$E \ll E_{so} = \frac{1}{2ma^2} \left(\frac{u}{4-d} \right)^{\frac{2}{4-d}}, \quad (2)$$

where

$$u = \frac{m^2 a^{4-d}}{2\pi^2} g V^2, \quad (3)$$

is the dimensionless coupling constant, a is a distance related to the cutoff of divergent integrals (the shortest distance in our problem which is related to the difference between the random field correction function and the correlation function of white noise), and d is the dimensionality of the space considered.

A physically correct approach to such a problem was proposed by Langer,¹⁰ who showed that all the correlation functions should be calculated by an analytic continuation with respect to the coupling constant and exhibit a cut along the negative real axis in the complex plane of the values of the coupling constant. Any correlation function (Green's function) of such a theory can be represented as the following dispersion relation for the coupling constant^{14,15} (g is an arbitrary coupling constant):

$$G(z) = \frac{1}{\pi} \int_{-\infty}^0 dz' \frac{\Delta(z')}{z' - z}, \quad (4)$$

and

$$\Delta(g) = \frac{1}{2i} [G(g + i\epsilon) - G(g - i\epsilon)] = \text{Im} G(g) \quad (5)$$

is a discontinuity over the cut (nonzero for $g < 0$) which can be obtained from the nonlinear solutions of the classical field theory equation (1) with a finite action.¹²⁻¹⁵ We shall always assume that $G(g)$ is the one-particle Green's function.

3. The action of the field theory defined by Eq. (1) is given by

$$S[\Phi] = \int d^d r \mathcal{L}(r) \quad (6)$$

and the Green's function is given by the following functional integral:

$$G(r-r'|g) = -Z^{-1} \frac{1}{n} \sum_{j=1}^n \int (\delta\Phi(r)) \Phi_j(r) \Phi_j(r') \exp\{-S[\Phi]\}, \quad (7)$$

where

$$Z = \int (\delta\Phi(r)) \exp\{-S[\Phi]\}. \quad (8)$$

The minus sign in Eq. (7) is chosen to yield the correct zeroth-order electron Green's function.

The minimization $\delta S[\Phi] = 0$ yields the following classical field equations:

$$\frac{1}{2m} \Delta\Phi_j = -E\Phi_j - \frac{1}{2} \rho V^2 \Phi_j \left(\sum_{j=1}^n \Phi_j^2 \right), \quad (9)$$

We shall seek the solution of the field equations in the form^{12,13}

$$\Phi_j(r) = \Phi_0(r) u_j, \quad (10)$$

where u is a unit vector ($u^2 = 1$) in the "isospin" space of the theory [O(n) symmetric] considered. Restricting ourselves to the class of spherically symmetric solutions (Refs. 16-18), we obtain from Eq. (9) the following result:

$$\frac{1}{2m} \left\{ \frac{d^2\Phi_0}{dr^2} + \frac{d-1}{r} \frac{d\Phi_0}{dr} \right\} = -E\Phi_0 - \frac{1}{2} \rho V^2 \Phi_0^3. \quad (11)$$

Equation (11) has a trivial solution $\Phi_0 = 0$. We shall consider nontrivial solutions of Eq. (11) with a finite action [i.e., such that the integral in Eq. (6) converges]. For $d = 1$, it is possible to obtain an exact solution of Eq. (11) (see Ref. 10). Using the results of Refs. 18 and 19, we can show that the required solution appropriate to the problem under study exists only for $d < 4$. We shall discuss the solutions qualitatively following the method of Ref. 20 (see also Ref. 17).

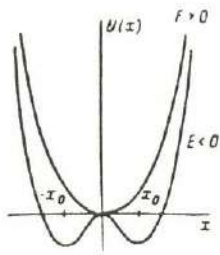


FIG. 1. "Potential energy" corresponding to the equation of motion (13).

We shall introduce new variables

$$\begin{aligned} \Phi_0(r) &= \left(\frac{2|E|}{\rho V^2} \right)^{1/2} x(t), \\ r &= (2m|E|)^{-1/2} t. \end{aligned} \quad (12)$$

Equation (11) then assumes the following dimensionless form:

$$\frac{d^2x}{dt^2} + \frac{d-1}{t} \frac{dx}{dt} = \pm x - x^3, \quad (13)$$

where the upper sign corresponds to $E < 0$ and the lower sign to $E > 0$.

We can now use an obvious mechanical analogy, i.e., Eq. (13) is an equation of motion for a particle with unit mass in the following potential (Fig. 1):

$$U(x) = \mp \frac{x^2}{2} + \frac{x^4}{4}. \quad (14)$$

The particle in question moves subject to a friction force depending on time as $\sim 1/t$. By considering the "energy"

$$\mathcal{E} = \frac{1}{2} \left(\frac{dx}{dt} \right)^2 + U(x), \quad (15)$$

we can easily demonstrate the dissipative nature of the motion. Using Eq. (13), we obtain

$$\frac{d\mathcal{E}}{dt} = - \left(\frac{dx}{dt} \right)^2 \frac{d-1}{t} < 0; \quad d > 1. \quad (16)$$

The qualitative behavior of the motion is shown in Fig. 2. The motion in question satisfies the following initial conditions:

$$\left. \begin{aligned} x|_{t=0} &= \text{const}, \\ \frac{dx}{dt} \Big|_{t=0} &= 0. \end{aligned} \right\} \quad (17)$$

For $t \gg 1$, we can linearize Eq. (13) near the extrema of $U(x)$, i.e., near the points $x = 0$, $x = \pm x_0 = \pm 1$ to obtain the asymptotic behavior of the solution defined by Eq. (13). It is quite clear that the solutions of type 2 and 3 shown in Fig. 2 are of no interest since the corresponding action integral defined by Eq. (6) diverges [the field defined by Eq. (12) tends to a constant at infinity]. The asymptotic behavior ($t \gg 1$) of the solution of type 4 in Fig. 2 ($E > 0$) is given by

$$x(t) \approx \frac{\text{const}}{t^{\frac{d-1}{2}}} J_{\frac{d-1}{2}}(t); \quad t \gg 1, \quad (18)$$

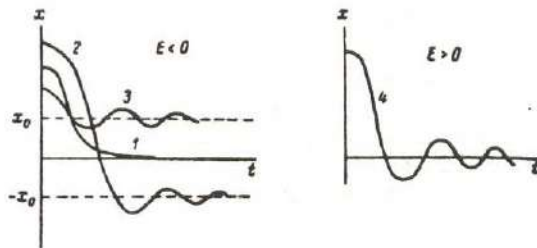


FIG. 2. Qualitative behavior of the solutions of Eq. (13).

[$J_{\frac{d}{2}-1}(t)$ are the Bessel functions] and the integral defined by Eq. (6) also diverges as a function of the upper limit for $d \geq 2$. Therefore, we are left with a unique solution of type 1 shown in Fig. 2 ($E < 0$). The fact that the solution is unique follows from physical considerations. In fact, there is a single point on the curve $U(x)$ which has the property that a particle starting its motion from this point terminates its motion at the point $x = 0$. The asymptotic behavior of the aforementioned unique solution ($t \gg 1$) is given by

$$x(t) \approx \frac{\text{const}}{t^{\frac{d}{2}-1}} K_{\frac{d}{2}-1}(t) \approx \frac{\text{const}}{t^{\frac{d-1}{2}}} \exp(-t); \quad t \gg 1. \quad (19)$$

[$K_{\frac{d}{2}-1}(t)$ is the modified Bessel function] and the corresponding action integral defined by Eq. (6) converges.

Using Eq. (12), we obtain

$$S[\Phi_0] = \int d^d r \mathcal{L}(r | \Phi_0(r)) = A_d \frac{m^{-d/2}}{\rho V^2} |E|^{2-d/2}. \quad (20)$$

The constant A_d , which depends on the dimensionality, is determined by dimensionless integrals of $x(t)$. The calculation of A_d requires numerical integration of the equation of motion (13) supplemented by the initial conditions (17).

4. The functional integral in Eq. (7) can be evaluated by the steepest descent method near the classical solutions with a finite action defined by Eq. (12) (see Refs. 10, 12-15). For $E > 0$, only the trivial solution $\Phi_0 = 0$ exists and the steepest descent method yields the standard perturbation theory,^{10,15} which was used in Ref. 2. For $E < 0$, there is a nontrivial solution with a finite action defined by Eqs. (12), (17), and (19). The field $\Phi(\mathbf{r})$ can be expanded near $\Phi_0(\mathbf{r})$ as follows:

$$\Phi(\mathbf{r}) = \Phi_0(\mathbf{r} - \mathbf{R}_0) + \varphi(\mathbf{r}). \quad (21)$$

It is then possible to perform all the calculations in the lowest order of a perturbation theory with respect to $\varphi(\mathbf{r})$. All the correlation functions will contain a factor $\exp(-S[\Phi_0])$ which is nonanalytic in the coupling constant and also a preexponential factor which is obtained in the evaluation of the Gaussian integral in the variable $\varphi(\mathbf{r})$. The problems related to the negative sign of the coupling constant, to the arbitrary choice of the location of the solution $\Phi_0(\mathbf{r} - \mathbf{R}_0)$ in space (arbitrary choice of \mathbf{R}_0), and to the arbitrary orientation of the vector \mathbf{u} in the isotopic space introduced in Eq. (10) [0(n) symmetry] require special discussion. All the required calculations are analogous to the calculations of Refs. 10, 12-15, 17. The imaginary part of the one-electron Green's function is given by

$$\text{Im } G(E, \mathbf{p} | -\rho V^2) = C(|E|, \mathbf{p}) \exp\left\{-\frac{A(E)}{\rho V^2}\right\} \frac{\theta(-\rho V^2)}{(\rho V^2)^{\frac{d+1}{2}}}, \quad (22)$$

where $C(|E|, \mathbf{p})$ is a function of E and \mathbf{p} which is independent of the coupling constant ρV^2 ,

$$A(E) = A_d m^{-d/2} |E|^{2-d/2}. \quad (23)$$

the theta function in Eq. (22) indicates that the imaginary part of the Green's function is nonzero only for negative values of the coupling constant in the field theory with the Lagrangian defined by Eq. (1). The power of the coupling constant in the preexponential factor in Eq. (22) can be easily understood. The translation invariance (arbitrary choice of \mathbf{R}_0) yields a factor^{15,17} $(\rho V^2)^{-d/2}$ (there are d translation "zero" modes); an additional factor $(\rho V^2)^{-\frac{n-1}{2}}$ is related to arbitrary orientation of the vector \mathbf{u} ($n-1$ rotational "zero" modes); and the factor $(\rho V^2)^{-\nu/2}$ is related to the product of ν fields which appears in the definition of the $\nu/2$ -th Green's function¹⁵ (in the case considered, $\nu = 2$). These results are independent of the actual form of the classical solutions $\Phi_0(\mathbf{r} - \mathbf{R}_0)$ (see Refs. 15, 17); the type of solution determines $C(|E|, \mathbf{p})$.

The Green's function can be calculated from $\text{Im } G(E, \mathbf{p} | -\rho V^2)$ (i.e., from the discontinuity across the cut in the complex coupling constant plane) via the dispersion integral (4).

$$G(E, \mathbf{p} | g) = \frac{1}{\pi} C(|E|, \mathbf{p}) \int_{-\infty}^0 dx \frac{\exp\left\{\frac{A(E)}{g}\right\}}{(x-g)(-x)^{\frac{d+1}{2}}}, \quad (24)$$

where g is an arbitrary coupling constant for an electron in a random field $g = -\rho V^2$. The integral in Eq. (24) can be easily evaluated:

$$G(E, \mathbf{p} | g) = -\frac{1}{\pi} C(|E|, \mathbf{p}) g^{-\frac{d+1}{2}} \exp\left\{\frac{A(E)}{g}\right\} \Gamma\left(\frac{d+1}{2}\right) \Gamma\left(\frac{1-d}{2}\right) \frac{A(E)}{g}, \quad (25)$$

where $\Gamma(\alpha, x) = \int_x^\infty dt e^{-t} t^{\alpha-1}$ is the incomplete gamma function.

The Green's function of an electron in a random field represents the analytic continuation of Eq. (25) from the region $g > 0$ to negative values $g = -\rho V^2$ (see Ref. 21).

It follows from Eq. (22) that our preexponential factor in the tail of the density of states is correct.^{11,22,23} The preexponential factor is completely determined by the classical solutions of the field theory defined by Eq. (1) with a finite action. The main advantage of our method is that it yields automatically correct results and does not introduce the additional assumptions employed in Refs. 11, 22, and 23 such as the assumption that the first level of the fluctuation well is dominant. Different treatments of the energy ranges $E > 0$ and $E < 0$ are also introduced automatically since the classical solutions with a finite action exist only for $E < 0$. Nonanalytic dependences on the coupling constant also arise quite naturally in the present method (breakdown of the standard perturbation theory).

The condition of validity of our results can be formulated as $S[\Phi_0] \gg 1$, i.e., our results hold when the method of steepest descent used in the evaluation of the functional integral in Eq. (7) is justified. In other words, the following condition should be satisfied:

$$\frac{A(E)}{\rho V^2} = \frac{A_d}{2\pi^2} \frac{1}{4-d} \left(\frac{|E|}{\rho V^2}\right)^{2-d/2} \gg 1,$$

i.e.,

$$|E| \gg E_{sc} \quad (25a)$$

which reduces to the condition obtained in Ref. 2. The condition of validity of the "perturbation theory" near the classical solution with a finite action defined by Eq. (21) is the same as the criterion of validity of the standard perturbation theory in the energy range $E > 0$. It was noted in Ref. 2 that an interval of width $2E_{sc}$ about $E = 0$ is an analog of the "Ginzburg" critical region in the theory of critical phenomena. However, in contrast to the theory of critical phenomena, perturbation theory, when applied to the case considered, fails even for space of dimensionality $d = 4 - \epsilon$.

5. The preexponential factor $C(|E|, p)$ in Eq. (22) can be evaluated provided the classical solutions with a finite action are known explicitly. For $d > 1$, such solutions can be obtained only numerically. We shall now develop a method of calculation of the preexponential factor based on the analogy with the theory of phase transitions, which makes it possible to avoid numerical calculations.

For $g > 0$, the Green's function defined by Eq. (25) corresponds to the correlation function of a stable field theory (the theory of second-order phase transitions). Far from the critical region, the aforementioned correlation function is well known,⁷ i.e., the correlation function is given by the standard Ornstein-Zernike expression. For $|E| \gg E_{sc}$, we obtain

$$G(Ep | g > 0) \approx - \frac{1}{|E| + \frac{p^2}{2m}} \quad (26)$$

On the other hand, using the asymptotic expression^{23,24} for the incomplete gamma function, we find that Eq. (25) yields ($|E| \gg E_{sc}$; $E < 0$)

$$G(Ep | g > 0) \approx - \frac{1}{\pi} \Gamma\left(\frac{d+1}{2}\right) [A(E)]^{-\frac{d+1}{2}} C(|E|, p) \quad (27)$$

Comparing Eqs. (26) and (27), we obtain

$$C(|E|, p) \approx \frac{\pi A_d^{\frac{d+1}{2}}}{\Gamma\left(\frac{d+1}{2}\right) m} \frac{|E|^{(d+1)\left(1-\frac{d}{2}\right)}}{|E| + \frac{p^2}{2m}}, \quad (28)$$

$|E| \gg E_{sc}$.

The imaginary part of the electron Green's function is then given by ($|E| \gg E_{sc}$)

$$\text{Im } G(Ep | -pV^2) \approx \pm \frac{\pi A_d^{\frac{d+1}{2}}}{\Gamma\left(\frac{d+1}{2}\right)} \frac{|E|^{(d+1)\left(1-\frac{d}{2}\right)}}{|E| + \frac{p^2}{2m}} \frac{1}{\left(m^{\frac{d}{2}} p V^2\right)^{\frac{d+1}{2}}} \exp\left\{-\frac{A(E)}{pV^2}\right\} \quad (29)$$

We can now calculate the density of electron states in the tail region including the preexponential factor. We find that ($|E| \gg E_{sc}$; $E < 0$)

$$N(E) = - \frac{1}{\pi} \int \frac{d^d p}{(2\pi)^d} \text{Im } G^R(Ep | -pV^2)$$

$$\approx K_d \frac{A_d^{\frac{d+1}{2}}}{\Gamma\left(\frac{d+1}{2}\right)} \frac{|E|^{(d+1)\left(1-\frac{d}{2}\right)}}{\left(m^{\frac{d}{2}} p V^2\right)^{\frac{d+1}{2}}} \exp\left\{-\frac{A(E)}{pV^2}\right\} \int_0^{1/a} d p p^{d-1} \frac{1}{|E| + \frac{p^2}{2m}} \quad (30)$$

where $K_d = 2^{-(d-1)} \pi^{-\frac{d}{2}} \frac{1}{\Gamma\left(\frac{d}{2}\right)}$. For $d = 1$, we can take the limit $a \rightarrow 0$ and Eq. (30) yields

$$N(E) = K_1 \frac{\pi A_1}{\sqrt{2}} \frac{|E|}{pV^2} \exp\left\{-A_1 \frac{|E|^{1/2}}{m^{1/2} p V^2}\right\} \quad (31)$$

It follows from Ref. 11 that $A_1 = 4\sqrt{2}/3$ [Eq. (11) for $d = 1$ can be solved exactly] and Eq. (31) reduces to the exact result of Refs. 25 and 11 with an accuracy up to the factor $3/\pi$. For $d \geq 2$, the divergent integral in Eq. (30) is cut off at a momentum $\sim 1/a$, the cut-off momentum being related to the reciprocal of the range of the correlation function of random fields. Our calculations are valid for energies $|E| \ll E_0 = 1/2ma^2$. For $|E| \gg E_0$, the tail of the density of states is governed by the quasiclassical approximation.²⁵⁻²⁸ For $d = 2$, Eq. (30) yields ($E_{sc} \ll |E| \ll E_0$)

$$N(E) \approx \text{const} \frac{|E|^{1/2}}{m^{1/2} (pV^2)^{1/2}} \ln \frac{E_0}{|E|} \exp\left\{-A_2 \frac{|E|}{m p V^2}\right\} \quad (32)$$

for $d = 3$, we obtain

$$N(E) \approx \text{const} \frac{|E| E_0^{1/2}}{m^{1/2} (pV^2)^2} \exp\left\{-A_3 \frac{|E|^{1/2}}{m^{1/2} p V^2}\right\} \quad (33)$$

For $2 < d < 4$, the tail in the density of states is given by

$$N(E) \approx K_d \left(\frac{A_d}{2\pi^2 (4-d)}\right)^{\frac{d+1}{2}} \frac{2m}{\Gamma\left(\frac{d+1}{2}\right)} \frac{(2mE_0)^{\frac{d-2}{2}}}{(d-2)} \times \left(\frac{|E|}{E_{sc}}\right)^{(d+1)\left(1-\frac{d}{2}\right)} \exp\left\{-A_d \frac{m^{-\frac{d}{2}}}{p V^2} |E|^{\frac{d-2}{2}}\right\} \quad (34)$$

We believe that the aforementioned expressions yield (with an accuracy up to a constant factor) exact expressions for the preexponential factor of the density of states in the energy range considered.

6. The energy range $|E| \ll E_{sc}$ lies outside the region of validity of our theory. It follows from the theory of critical phenomena that, for $g > 0$ and for energies $|E| \ll E_{sc}$, the correlation function obeys the standard scaling

$$G(Ep | g > 0) \approx C |E|^{-\gamma} D(p^2 \xi^2); \quad \xi \sim |E|^{-\nu} \quad (35)$$

Here, γ and ν are the critical indices of the susceptibility and correlation length ξ , $D(x)$ is a universal (independent of the details of the interaction) function, and C is a non-universal factor. Since it is well known that the discontinuity across the cut in the dispersion relation (4) [$\Delta(z)$ in Eq. (4) is unique for arbitrary g] is universal, this seems to indicate that the Green's function should exhibit an analogous universal behavior for $|E| \ll E_{sc}$ irrespective of the sign of g . Applying formally Eq. (25) to the region $|E| \ll E_{sc}$ and using $\Gamma(\alpha, x) \rightarrow \Gamma(\alpha)$ for $x \rightarrow 0$ ($\alpha \neq 0, -1, -2, \dots$), and also $A(E) \rightarrow 0$ for $E \rightarrow 0$ and $\Gamma(1/2 +$

$d/2) \Gamma(1/2 - d/2) = \pi / \cos(\pi d/2)$, we obtain

$$G(Ep|g > 0) \approx -\frac{1}{\cos \frac{\pi d}{2}} \frac{d+1}{2} C(|E|, p); |E| \ll E_{sc}, \quad (36)$$

where $d \neq 1, 3$ but the values $d = 2$ and $d = 4 - \epsilon$ are admissible. Comparing Eqs. (35) and (36), we obtain

$$C(|E|, p) \sim |E|^{-\gamma} D(p^2 \xi^2), \quad (37)$$

Equation (22) then yields

$$\text{Im} G(Ep| - \rho V^2) \approx B |E|^{-\gamma} D(p^2 \xi^2), \quad (38)$$

where B is a (nonuniversal) constant (independent of E and p). It must be understood that Eqs. (36)-(38) represent an extrapolation of Eq. (25) beyond its range of validity. However, mere assumption that the discontinuity across the cut in the dispersion equation (4) can be factorized leads to a result similar to that defined by Eq. (38), i.e.,

$$\Delta(Ep|x) = \text{Im} G(Ep|x) \approx C(|E|, p) / (x) \quad (39)$$

for $|E| \ll E_{sc}$. Such a factorization holds when Eq. (25) is applied formally to the region $|E| \ll E_{sc}$ and implies the scaling defined by Eq. (37) irrespective of the sign of g . Unfortunately, we are unable to prove Eq. (39). However, if we assume the validity of Eq. (39), we find that Eq. (35) yields Eqs. (37) and (38) and the density of states for $|E| \ll E_{sc}$ is given by

$$N(E) \approx -\frac{B}{\pi} |E|^{-\gamma} \int \frac{d^d p}{(2\pi)^d} D(p^2 \xi^2) = D(\text{const} + |E|^{1-\alpha}), \quad (40)$$

where α is the specific-heat critical index. For $d = 4 - \epsilon$ and $n = 0$, we obtain

$$\alpha \approx \frac{\epsilon}{4} + O(\epsilon^2), \quad (41)$$

where D is a constant (independent of E). As a result, we obtain

$$\frac{dN(E)}{dE} \sim |E|^{-\alpha}; |E| \rightarrow 0. \quad (42)$$

The density of states in the limit $|E| \rightarrow 0$ exhibits a kink and its derivative diverges as the specific heat in the theory of critical phenomena.

Consequently, assuming the factorization defined by Eq. (39), we obtain a scaling at the mobility edge which holds for the average electron Green's function in a random field. If this is the case, the well-known discrepancy between the Anderson result that considers the "most probable" electron Green's function¹ and the standard ap-

proach due to Edwards based on the average Green's function disappears. An alternative approach is to treat the neighborhood of the mobility edge as an analog of the transition region in the Kondo problem, where the Anderson and Edwards treatments are complementary.²

The author is grateful to L. V. Keldysh for his discussions and interest in the present work and to D. V. Shirkov for making available a preprint of Ref. 15.

¹Equation (26) of Ref. 2 contains an error and the resulting equation (27), which states that the effective interaction reaches a constant value for large negative energies, is incorrect.

¹M. V. Sadovskii, Zh. Eksp. Teor. Fiz. **70**, 1936 (1976) [Sov. Phys. JETP **43**, 1008 (1976)].

²M. V. Sadovskii, Fiz. Tverd. Tela (Leningrad) **19**, 2334 (1977) [Sov. Phys. Solid State **19**, 1366 (1977)].

³F. J. Wegner, Z. Phys. B **25**, 327 (1976).

⁴S. F. Edwards, M. B. Green, and G. Srinivasan, Philos. Mag. **35**, 1421 (1977).

⁵A. Nitzan, K. F. Freed, and M. H. Cohen, Phys. Rev. B **15**, 4476 (1977).

⁶A. Aharony and Y. Imry, J. Phys. C **10**, L487 (1977).

⁷K. G. Wilson and J. Kogut, Phys. Rep. C **12**, 75 (1974).

⁸P. G. de Gennes, Phys. Lett. A **38**, 339 (1972).

⁹J. des Cloizeaux, Phys. Rev. A **10**, 1665 (1974).

¹⁰J. S. Langer, Ann. Phys. (N.Y.) **41**, 108 (1967).

¹¹J. Zittartz and J. S. Langer, Phys. Rev. **148**, 741 (1966).

¹²L. N. Lipatov, Zh. Eksp. Teor. Fiz. **72**, 411 (1977) [Sov. Phys. JETP **45**, 216 (1977)].

¹³E. Brezin, J. C. Le Guillou, and J. Zinn-Justin, Phys. Rev. D **15**, 1544 (1977).

¹⁴E. B. Bogomolny, Phys. Lett. B **67**, 193 (1977).

¹⁵B. D. Dorfel, D. I. Kazakov, and D. V. Shirkov, Preprint No. E2-10720, Joint Institute for Nuclear Research, Dubna (1977).

¹⁶S. Coleman, Phys. Rev. D **15**, 2929 (1977).

¹⁷C. G. Callan, Jr., and S. Coleman, Phys. Rev. D **16**, 1762 (1977).

¹⁸S. Coleman, V. Glaser, and M. Martin, Preprint No. TH2364, CERN, Geneva (1977).

¹⁹V. G. Makhankov, Phys. Lett. A **61**, 431 (1977).

²⁰R. Finkelstein, R. Le Levier, and M. Ruderman, Phys. Rev. **83**, 326 (1951).

²¹D. J. Thouless, J. Phys. C **8**, 1803 (1975).

²²I. M. Lifshits, Zh. Eksp. Teor. Fiz. **53**, 743 (1967) [Sov. Phys. JETP **26**, 462 (1968)].

²³I. M. Lifshits, S. A. Gredeskul, and L. A. Pastur, Fiz. Nizk. Temp. **2**, 1093 (1976) [Sov. J. Low Temp. Phys. **2**, 533 (1976)].

²⁴A. Erdelyi et al. (ed.), Higher Transcendental Functions (California Institute of Technology, H. Bateman MS Project), Vol. 1, McGraw-Hill, New York (1953); Vol. 2, McGraw-Hill, New York (1953); Vol. 3, McGraw-Hill, New York (1953).

²⁵B. I. Halperin, Phys. Rev. **139**, A104 (1965).

²⁶L. V. Keldysh, Author's Abstract of Thesis for Candidate's Degree [In Russian], P. N. Lebedev Physics Institute, Academy of Sciences of the USSR, Moscow (1965).

²⁷A. L. Éfros, Zh. Eksp. Teor. Fiz. **59**, 880 (1970) [Sov. Phys. JETP **32**, 479 (1971)].

²⁸M. Saitoh and S. F. Edwards, J. Phys. C **7**, 3937 (1974).

Translated by D. Mathon

phys. stat. sol. (b) **95**, 59 (1979)

Subject classification: 14.2; 18.2; 21

*Institute for Metal Physics, Academy of Sciences of the USSR,
Ural Scientific Centre, Sverdlovsk¹⁾*

Superconductivity in Spin-Glasses

By

M. V. SADOVSKII and YU. N. SKRYABIN

It is shown that spin glass ordering does not affect the superconductivity as a result of total compensation of the paramagnetic effect and the effect of spin-flip scattering freezing out in a spin-glass phase.

Показано, что упорядочение спинов при переходе в состояние спинового стекла не оказывает влияния на сверхпроводимость, что является следствием взаимной компенсации парамагнитного эффекта и эффекта вымораживания процессов рассеяния с переворотом спина.

1. Introduction

Recently there has been a considerable growth of the literature on the coexistence of superconductivity and magnetic ordering [1, 2], due to the experimental discovery of such phenomena in some rare-earth compounds with regular positions of magnetic atoms [3 to 5]. Likewise it has been known for a long time that there is some experimental-evidence of such a coexistence in dilute alloys of transition metals in a superconducting matrix [1]. In such systems the type of magnetic ordering is unknown in most cases. In the theory of dilute alloys of magnetic impurities the concept of the spin-glass phase is preferred now due to the long-range and oscillating behaviour of the indirect exchange interaction via the conduction electrons [6, 7]. There is good experimental evidence for the coexistence of superconductivity and spin-glass ordering in $Gd_xTh_{1-x}Ru_2$ [8] and $Gd_xCe_{1-x}Ru_2$ [8], as well as some evidence for it in the amorphous alloy of $La_{80}Au_{20}$ with Gd impurities [9].

The influence of magnetic impurities upon superconductivity was first considered by Abrikosov and Gorkov [10]. Gorkov and Rusinov have considered a possibility of coexistence of superconductivity and ferromagnetism in such a system [11]. In the present paper we will attempt to analyze the influence of spin-glass ordering upon superconductivity.

2. General Formalism

To describe superconductivity in a system with some kind of magnetic ordering it is convenient to use a four-dimensional matrix formalism, defining the electron operators in spinor form [1, 2]:

$$\hat{\Psi}(\mathbf{r}) = \begin{pmatrix} \psi_{\uparrow}(\mathbf{r}) \\ \psi_{\downarrow}(\mathbf{r}) \\ \psi_{\uparrow}^{\dagger}(\mathbf{r}) \\ \psi_{\downarrow}^{\dagger}(\mathbf{r}) \end{pmatrix}; \quad \hat{\Psi}^{\dagger}(\mathbf{r}) = (\psi_{\uparrow}^{\dagger}(\mathbf{r}) \ \psi_{\downarrow}^{\dagger}(\mathbf{r}) \ \psi_{\uparrow}(\mathbf{r}) \ \psi_{\downarrow}(\mathbf{r})), \quad (1)$$

where $\psi_{\uparrow}(\mathbf{r})$ is the ordinary electron destruction operator with spin directed upwards and so on.

¹⁾ Sverdlovsk 620 170, USSR.

The zero-order Hamiltonian for a superconducting system takes the form

$$\mathcal{H}_0 = \int d\mathbf{r} \hat{\Psi}^\dagger(\mathbf{r}) \hat{h}_0(\mathbf{r}) \hat{\Psi}(\mathbf{r}), \quad (2)$$

where

$$\hat{h}_0(\mathbf{r}) = \begin{pmatrix} \hat{H}_0(\mathbf{r}) & \hat{\Delta}(\mathbf{r}) \\ \hat{\Delta}^\dagger(\mathbf{r}) & -\hat{H}_0^\dagger(\mathbf{r}) \end{pmatrix} = H_0(\mathbf{r}) \sigma_0 \tau_3 + \Delta_1 \sigma_2 \tau_2 + \Delta_2 \sigma_2 \tau_1. \quad (3)$$

$H_0(\mathbf{r})$ is the free-electron Hamiltonian, σ_i and τ_i are two independent sets of Pauli matrices, direct product of which can be used to represent any 4×4 matrix, $\Delta_1 = \text{Re } \Delta$, $\Delta_2 = \text{Im } \Delta$, where Δ is the gap function of superconductivity theory.

The electron interaction with magnetic atoms can be described by the ordinary s-d exchange model and the interaction Hamiltonian in the four-dimensional matrix formalism takes the form [1]

$$\mathcal{H}_{\text{int}} = \frac{1}{2} \int d\mathbf{r} \hat{\Psi}^\dagger(\mathbf{r}) V(\mathbf{r}) \hat{\Psi}(\mathbf{r}), \quad (4)$$

where

$$\hat{V}(\mathbf{r}) = \sum_i J(\mathbf{r} - \mathbf{R}_i) \boldsymbol{\alpha} \cdot \mathbf{S}_i, \quad (5)$$

$$\boldsymbol{\alpha}_\mu = \begin{pmatrix} \sigma_\mu & 0 \\ 0 & -\sigma_\mu^{\text{tr}} \end{pmatrix}. \quad (6)$$

$\frac{1}{2}\sigma$ is the electron spin operator, $J(\mathbf{r} - \mathbf{R}_i)$ is the s-d exchange integral, \mathbf{S}_i is the spin of the magnetic atom at the site \mathbf{R}_i .

To consider superconductivity with any kind of magnetic ordering it is useful to isolate the mean-field effects. The Hamiltonian of electron interaction with a mean magnetic field, following from (5) is

$$\mathcal{H}_{\text{int}}^{\text{MF}} = \frac{1}{2} \int d\mathbf{r} \hat{\Psi}^\dagger(\mathbf{r}) \mathbf{H}(\mathbf{r}) \boldsymbol{\alpha} \hat{\Psi}(\mathbf{r}), \quad (7)$$

where

$$\mathbf{H}(\mathbf{r}) \boldsymbol{\alpha} = \begin{pmatrix} \mathbf{H}(\mathbf{r}) \boldsymbol{\sigma} & 0 \\ 0 & -\mathbf{H}(\mathbf{r}) \boldsymbol{\sigma}^{\text{tr}} \end{pmatrix} = H^\nu \boldsymbol{\alpha}_\nu, \quad (8)$$

$$\mathbf{H}(\mathbf{r}) = \sum_i J(\mathbf{r} - \mathbf{R}_i) \langle \mathbf{S}_i \rangle \quad (9)$$

is the mean magnetic field at the point \mathbf{r} , $\langle \mathbf{S}_i \rangle$ the thermodynamic average of the impurity spin. The mean field $\mathbf{H}(\mathbf{r})$ leads to the paramagnetic effect suppressing superconductivity.

We must also consider a perturbation (fluctuations) over the mean-field:

$$\tilde{\mathcal{H}}_{\text{int}} = \mathcal{H}_{\text{int}} - \mathcal{H}_{\text{int}}^{\text{MF}} = \int d\mathbf{r} \hat{\Psi}^\dagger(\mathbf{r}) \sum_i J(\mathbf{r} - \mathbf{R}_i) \boldsymbol{\alpha} (\mathbf{S}_i - \langle \mathbf{S}_i \rangle) \hat{\Psi}(\mathbf{r}). \quad (10)$$

The perturbation theory over \mathcal{H}_{int} produces the Green's function

$$D_{ij}^{\mu\nu}(\tau, \tau') = - \langle T_\tau (S_i^\mu(\tau) - \langle S_i^\mu \rangle) (S_j^\nu(\tau') - \langle S_j^\nu \rangle) \rangle, \quad (11)$$

where τ is the Matsubara "time".

3. Spin-Glass Ordering and Superconductivity

At present there is no complete spin-glass theory even in the mean field approximation. The most popular Edwards-Anderson model of spin-glass behaviour [12, 13] is based on the so-called replica method and the limit of replica number $n \rightarrow 0$ and faces some basic difficulties (such as negative entropy) [7]. Some other models were proposed not using the replica method [14 to 16]. All of these models try to describe the spin-glass phase via the order-parameter $q = \langle \langle \mathbf{S}_i \rangle^2 \rangle_c$ [12], where $\langle \dots \rangle_c$ denotes the configurational averaging, and lead to a practically equivalent behaviour of physical quantities, though not in complete agreement with the experiment [6]. There is even some doubt in the existence of the spin-glass transition itself [17].

Our aim is to consider the influence of the Edwards-Anderson order-parameter upon superconductivity. The main results will be in fact independent of any specific model of spin-glass in the mean-field approximation. Thus we consider the simplest model of [14], which leads to the same main results as the Edwards-Anderson model, but is free from the unphysical artefacts of the replica method.

In the Medvedev-Zaborov model and analogous models of [15, 16] it is supposed that the chaotic orientations of impurity spins lead to a random magnetic mean field at every site $\mathbf{h}_i = \mathbf{h}(\mathbf{R}_i)$. The distribution function of this field can be shown to be Gaussian [14]:

$$P(\mathbf{h}_i) = \left(\frac{2}{3} \pi A q\right)^{-3/2} \exp\left(-\frac{|\mathbf{h}_i|^2}{\frac{2}{3} A q}\right), \quad (12)$$

where q is the Edwards-Anderson order-parameter defined by

$$q = \int_0^\infty d\mathbf{h} P(\mathbf{h}) b_S^2\left(\frac{\mathbf{h}}{T}\right), \quad (13)$$

where

$$P(\mathbf{h}) = 4\pi h^2 \left(\frac{2}{3} \pi q A\right)^{-3/2} \exp\left(-\frac{h^2}{\frac{2}{3} q A}\right) \quad (14)$$

is the distribution function for the absolute value of the mean field, $b_S(x)$ is the Brillouin function,

$$A = \frac{c}{v_0 v_a} \int d\mathbf{R} I^2(\mathbf{R}) \equiv cI^2, \quad (15)$$

where $I(\mathbf{R})$ is the indirect exchange integral (for example of the RKKY type), c the concentration of magnetic atoms, v_0 the volume per one such an atom, T the absolute temperature. The integration in (15) goes over the whole volume of the system except the volume v_0 around the origin.

The solution of (13) for $q(T)$ leads to dependences similar to that of the Edwards-Anderson theory, $q(T) \neq 0$ for $T < T_f$, where T_f is the spin-glass "freezing" temperature:

$$T_f = \frac{1}{3} S(S+1) A^{1/2} = \frac{1}{3} S(S+1) c^{1/2} I^{1/2}, \quad (16)$$

where S is the magnitude of the impurity spin.

The distribution of molecular fields is factorized over the sites:

$$P(\mathbf{h}_i) = \prod_i P(\mathbf{h}_i) \quad (17)$$

and there is no short-range magnetic order:

$$\langle \mathbf{h}_i \mathbf{h}_j \rangle_c = q A \delta_{ij}. \quad (18)$$

Following the methods of [14] it is easy to show that the mean magnetic field $\mathbf{H}(\mathbf{r})$ acting upon a conduction electron is also Gaussian:

$$\mathcal{P}(\mathbf{H}(\mathbf{r})) = \left(\frac{2}{3} \pi q \mathcal{A}\right)^{-3/2} \exp\left\{-\frac{|\mathbf{H}(\mathbf{r})|^2}{\frac{2}{3} q \mathcal{A}}\right\}, \quad (19)$$

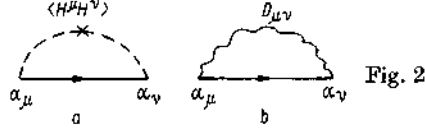
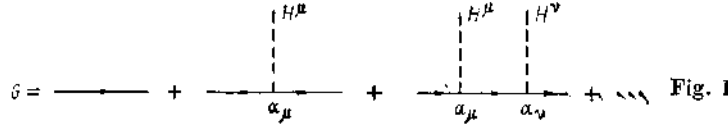
$$\mathcal{P}\{\mathbf{H}(\mathbf{r})\} = \prod_{\mathbf{r}} \mathcal{P}(\mathbf{H}(\mathbf{r})), \quad (20)$$

$$\langle \mathbf{H}(\mathbf{r}) \mathbf{H}(\mathbf{r}') \rangle_c = q \mathcal{A} \delta(\mathbf{r} - \mathbf{r}'), \quad (21)$$

where

$$\mathcal{A} = \frac{c}{v_0} \int d\mathbf{R} J^2(\mathbf{R}) \equiv cJ^2 \quad (22)$$

and $q(T)$ is defined by (13).



Now we have to consider the superconductivity of electrons under the influence of the random magnetic field $\mathbf{H}(\mathbf{r})$ distributed according to (19) to (21). The interaction given by (7) can be analyzed by perturbation theory, which leads to the summation of graphs for the electrons Green's function shown in Figure 1.

Here the continuous line represents the matrix Green's function defined by the equation of motion

$$\left\{ -\frac{\partial}{\partial \tau} \alpha_0 \tau_0 - \hat{h}_0(\mathbf{r}) \right\} g_0(\mathbf{r}\tau, \mathbf{r}'\tau') = \delta(\mathbf{r} - \mathbf{r}') \delta(\tau - \tau'). \quad (23)$$

The dashed line describes the interaction with the random field $\mathbf{H}(\mathbf{r})$. Averaging over (19), (20) we obtain that the second graph in Fig. 1 is equal to zero, while the third one gives the ordinary electron self-energy in the random field (see Fig. 2a). It is equal to

$$\begin{aligned} \Sigma_{\text{MF}}(\mathbf{r} - \mathbf{r}', \tau - \tau') &= \int \{ \delta \mathbf{H}(\mathbf{r}) \} \mathcal{P}\{ \mathbf{H}(\mathbf{r}) \} H^\mu(\mathbf{r}) H^\nu(\mathbf{r}') \alpha_\mu g_0(\mathbf{r}\tau, \mathbf{r}'\tau') \alpha_\nu = \\ &= \langle \sum_{ij} J(\mathbf{r} - \mathbf{R}_i) J(\mathbf{r}' - \mathbf{R}_j) \langle S_i^\mu \rangle \langle S_j^\nu \rangle \rangle_c \alpha_\mu g_0(\mathbf{r}\tau; \mathbf{r}'\tau') \alpha_\nu \end{aligned} \quad (24)$$

or, using (21),

$$\Sigma_{\text{MF}}(\mathbf{r} - \mathbf{r}', \tau - \tau') = \frac{1}{3} \mathcal{A}q \delta(\mathbf{r} - \mathbf{r}') \alpha_\mu g_0(\mathbf{r}\tau, \mathbf{r}'\tau') \alpha_\mu \quad (25)$$

or, in the momentum representation,

$$\Sigma_{\text{MF}}(\mathbf{p}\varepsilon_n) = \mathcal{A}q N_0 \frac{1}{3} \int d\varepsilon_p \alpha_\mu g_0(\mathbf{p}\varepsilon_n) \alpha_\mu, \quad (26)$$

where N_0 is the free-electron density of states at the Fermi level. Equation (26) coincides with the appropriate expression of the Abrikosov-Gorkov theory [1, 10] with the substitution of the ordinary spin-flip scattering rate by $\Gamma_{\text{sf}}' = 2\pi \mathcal{A}q(T) N_0 = 2\pi c J^2 q(T) N_0$. Thus the paramagnetic effect (random molecular field) in spin-glasses influences the superconductivity in the same way as magnetic impurities in the Abrikosov-Gorkov theory.

Consider now the rest of the interaction given by the Hamiltonian (10). The simplest self-energy corresponding to this interaction is shown in Fig. 2b:

$$\tilde{\Sigma}(\mathbf{r}\tau, \mathbf{r}'\tau') = - \sum_{ij} J(\mathbf{r} - \mathbf{R}_i) J(\mathbf{r}' - \mathbf{R}_j) D_{ij}^{\mu\nu}(\tau, \tau') \alpha_\mu g_0(\mathbf{r}\tau, \mathbf{r}'\tau') \alpha_\nu. \quad (27)$$

We use now the static approximation for $D_{ij}^{\mu\nu}(\tau, \tau')$,

$$D_{ij}^{\mu\nu}(\tau, \tau') \rightarrow - \langle S_i^\mu S_j^\nu \rangle + \langle S_i^\mu \rangle \langle S_j^\nu \rangle. \quad (28)$$

Then

$$\begin{aligned} \Sigma(\mathbf{r}\tau, \mathbf{r}'\tau') &= \sum_{ij} J(\mathbf{r} - \mathbf{R}_i) J(\mathbf{r}' - \mathbf{R}_j) \langle S_i^\mu S_j^\nu \rangle \alpha_\mu g_0(\mathbf{r}\tau, \mathbf{r}'\tau') \alpha_\nu - \\ &- H^\mu(\mathbf{r}) H^\nu(\mathbf{r}') \alpha_\mu g_0(\mathbf{r}\tau, \mathbf{r}'\tau') \alpha_\nu. \end{aligned} \quad (29)$$

After the configurational averaging we get

$$\begin{aligned} \tilde{\Sigma}(\mathbf{r} - \mathbf{r}', \tau - \tau') &= \langle \sum_{ij} J(\mathbf{r} - \mathbf{R}_i) J(\mathbf{r}' - \mathbf{R}_j) \langle S_i^\mu S_j^\nu \rangle \rangle_c \alpha_\mu g_0(\mathbf{r}\tau, \mathbf{r}'\tau') \alpha_\nu - \\ &- \frac{1}{3} \mathcal{A}q \delta(\mathbf{r} - \mathbf{r}') \alpha_\mu g_0(\mathbf{r}\tau, \mathbf{r}'\tau') \alpha_\nu. \end{aligned} \quad (30)$$

In the following we use the standard assumption of the spin-glass theory [7, 13], corresponding to the absence of short-range magnetic order:

$$\langle\langle S_i^x S_j^x \rangle\rangle_c \approx \delta_{\mu\nu} \delta_{ij} \frac{1}{2} S(S+1). \quad (31)$$

Then the total electron self-energy is equal to

$$\begin{aligned} \Sigma(\mathbf{r} - \mathbf{r}', \tau - \tau') &= \Sigma_{\text{MF}}(\mathbf{r} - \mathbf{r}', \tau - \tau') + \tilde{\Sigma}(\mathbf{r} - \mathbf{r}', \tau - \tau') \approx \\ &\approx \langle \sum_i J(\mathbf{r} - \mathbf{R}_i) J(\mathbf{r}' - \mathbf{R}_i) \rangle_c \frac{1}{2} S(S+1) \alpha_\mu g_0(\mathbf{r}\tau, \mathbf{r}'\tau') \alpha_\nu \approx \\ &\approx \frac{1}{2} cJ^2 S(S+1) \alpha_\mu g_0(\mathbf{r}\tau, \mathbf{r}'\tau') \alpha_\mu \delta(\mathbf{r} - \mathbf{r}'), \end{aligned} \quad (32)$$

where the last equality is valid for the point-like s-d exchange. In the momentum representation

$$\Sigma(\mathbf{p}\varepsilon_n) = \frac{\Gamma_{\text{sf}}}{2\pi} \frac{1}{3} \int d\xi_p \alpha_\mu g_0(\mathbf{p}\varepsilon_n) \alpha_\mu, \quad (33)$$

where

$$\Gamma_{\text{sf}} = 2\pi cJ^2 S(S+1) N_0 \quad (34)$$

is the standard electron spin-flip scattering rate (in Born approximation) coincides with the well-known result of the Abrikosov-Gorkov theory. In the sum of (25) and (30) the contributions dependent on the Edwards-Anderson order-parameter have cancelled each other completely. The physical meaning of such a cancellation is absolutely clear. We have seen that the paramagnetic effect in spin-glasses is equivalent to the spin-flip scattering rate $\Gamma_{\text{sf}} = 2\pi cJ^2 q(T) N_0$. At the same time the "freezing" of spins during the spin-glass transition "freezes" out the ordinary mechanism of spin-flip scattering in such a way that the corresponding scattering rate becomes equal to $\Gamma_{\text{sf}}' = \Gamma_{\text{sf}} - 2\pi cJ^2 q(T) N_0 \approx S(S+1) - \langle\langle S \rangle^2 \rangle_c$. Both effects just compensate each other $\Gamma_{\text{sf}} = \Gamma_{\text{sf}} + \Gamma_{\text{sf}}'$. Superconductivity in the system of magnetic impurities is determined by the dependences of the Abrikosov-Gorkov theory despite the spin-glass ordering.

4. Discussion

The cancellation of the Edwards-Anderson order parameter demonstrated for the simplest graphs of Fig. 2 persists for all diagrams in higher orders of perturbation theory. This is quite obvious for diagrams without crossing interaction lines and also can be demonstrated directly for diagrams with crossing lines. This cancellation follows from the fact that the configurational average of the random molecular field is equal to zero and the Abrikosov-Gorkov behaviour is due to equation (31) holding both in paramagnetic and spin-glass phases. Note that we neglect the quantum nature of impurity spins which allows us to use the standard diagram technique.

Spin dynamics can be neglected [1] if the characteristic frequencies of spin motion in the spin-glass phase $\Omega_{\text{SG}} \ll T_c \sim \Delta_0$ where T_c is the temperature of superconducting transition, and Δ_0 the superconductivity gap for $T = 0$. Ω_{SG} can be a characteristic frequency of a spin wave or the typical inverse time of change of the Edwards-Anderson order parameter when on the average it is equal to zero due to the slow relaxation processes [17]. Spin-glass dynamics can lead to a change in superconducting behavior in comparison with the Abrikosov-Gorkov theory. For example it is well known, that electron-electron interaction due to the exchange of spin-waves is repulsive, thus lowering the superconducting T_c .

Under the specific conditions [14] the system considered can undergo a transition not to a spin-glass phase but to that of a random ferromagnet (with a non-zero spontaneous magnetic moment). This leads to a change of the distribution function

of the random molecular fields, particularly the average of the second graph in Fig. 1 as well as all graphs of odd power in the random field become non-zero. Then there is no compensation of the paramagnetic effect and spin-flip scattering freezing out, as in the case of ordinary ferromagnets [1, 2]. It is possible that such a situation was realized in the experiments with $Gd_xLa_{1-x}Ru_2$ [18], where two superconducting transition temperatures (re-entrant superconductivity) have been found for some concentrations of Gd.

Finally, note that we have neglected the influence of the superconducting transition upon a spin-glass transition. The appropriate analysis seems difficult due to the present status of spin-glass theory. The oscillating behaviour of the indirect exchange interaction via the conduction electrons remains in the superconducting phase and in fact this interaction is almost the same as in normal metals up to distances of the order of the superconducting coherence length [19]. This interaction is effectively cut off at distances of the order of the electron mean-free path, thus in the case of mean-free paths shorter than the superconducting coherence length the effective interaction of impurity spins is unchanged in a superconducting phase. In general, the interaction parameter (15) determining the spin-glass transition is apparently almost the same as in the case of a normal metal.

Acknowledgements

The authors are greatly indebted to Dr. M. V. Medvedev for numerous discussions on the theory of spin-glasses. We are also grateful to Prof. Yu. A. Izyumov for his interest in this work.

References

- [1] S. V. VONSOVSKII and YU. A. IZYUMOV, Superconductivity of transition metals, their alloys and compounds, Nauka, Moscow 1977.
- [2] YU. A. IZYUMOV and YU. N. SKRYABIN, *phys. stat. sol. (b)* **61**, 9 (1974).
- [3] W. A. FERTIG, D. C. JOHNSTON, L. E. DELONG, R. W. MCCALLUM, M. B. MAPLE, and B. T. MATTHIAS, *Phys. Rev. Letters* **38**, 987 (1977).
- [4] D. E. MONCTON, D. B. MCWHAN, J. ECKERT, G. SHIRANE, and W. THOMLINSON, *Phys. Rev. Letters* **39**, 1164 (1977).
- [5] D. E. MONCTON, G. SHIRANE, W. THOMLINSON, M. ISHIKAWA, and O. FISHER, *Phys. Rev. Letters* **41**, 1133 (1978).
- [6] J. A. MYDOSH, *Amorphous Magnetism II*, Ed. R. A. LEVY and R. HASEGAWA, Plenum Press, New York-London 1977 (p. 73).
- [7] K. H. FISHER, *Physica* **86-88B+C**, 813 (1977); P. W. ANDERSON, *Amorphous Magnetism II*, Ed. R. A. LEVY and R. HASEGAWA, Plenum Press, New York 1977 (p. 1).
- [8] D. DAVIDOV, K. BABERSCHKE, J. A. MYDOSH, and G. J. NIENWENHUYNS, *J. Phys. F* **7**, L47 (1977).
- [9] S. J. POON and J. DURAND, *Solid State Commun.* **21**, 999 (1977).
- [10] A. A. ABRIKOSOV and L. P. GORKOV, *Zh. eksper. teor. Fiz.* **39**, 1781 (1960); **42**, 1088 (1962).
- [11] L. P. GORKOV and A. I. RUSINOV, *Zh. eksper. teor. Fiz.* **46**, 1363 (1964).
- [12] S. F. EDWARDS and P. W. ANDERSON, *J. Phys. F* **5**, 965 (1975).
- [13] K. H. FISCHER, *Phys. Rev. Letters* **34**, 1438 (1975).
- [14] M. V. MEDVEDEV and A. V. ZABOROV, *phys. stat. sol. (b)* **79**, 379 (1977); *Fiz. Metallov i Metallovedenie* **43**, 924 (1977).
- [15] M. KLEIN, *Phys. Rev. B* **14**, 5008 (1976).
- [16] T. PLEPKA, *J. Phys. F* **6**, L327 (1976).
- [17] A. J. BRAY, M. A. MOORE, and P. REED, *J. Phys. C* **11**, 1187 (1978).
- [18] T. E. JONES, J. F. KWAK, E. P. CHOCK, and P. M. CHAIRIN, *Solid State Commun.* **27**, 209 (1978).
- [19] P. W. ANDERSON and H. SUHL, *Phys. Rev.* **116**, 898 (1959).

(Received May 3, 1979)

Exact solution for the density of electronic states in a model of a disordered system

M. V. Sadovskii

Institute of the Physics of Metals, Ural Scientific Center, Academy of Sciences of the USSR
(Submitted 24 May 1979)
Zh. Eksp. Teor. Fiz. 77, 2070-2080 (November 1979)

A one-dimensional system of electrons is considered, in a Gaussian random field with a correlator whose form (in the momentum representation) is a Lorentzian with its center at $Q = 2p_F$. This can be considered as a Gaussian model of the Peierls transition in the fluctuation region. An exact summation of all Feynman diagrams is carried out, and a representation of the averaged one-electron Green's function as a continued fraction is obtained. A density of states with a characteristic pseudogap is found. It is shown that when the correlation range of the short-range order is decreased there is a gradual filling in of the pseudogap and a transition to a "metallic" state.

PACS numbers: 71.20. + c, 71.30. + h, 71.25.Cx

INTRODUCTION

There is a limited number of models of the electronic structure of one-dimensional disordered systems that admit of exact solution.¹ Interest in such models is due both to the general problem of studying the electronic properties of disordered systems and to questions of the physics of quasi-one-dimensional systems, the majority of which display some sort or other of properties associated with their disorder. In the last few years several important new results have been obtained, casting considerable light on the situation of an electron in a one-dimensional random field.²⁻⁴ This work is also mostly characterized by the use of specific methods of solution, specially adapted to the solution of one-dimensional problems, and as a rule not capable of further generalization because they are so cumbersome. Only in a very few cases is it possible to obtain an exact solution of a problem about the electron in a one-dimensional random field by means of standard methods of present-day many-particle theory.⁵

One model of this sort was proposed some time ago by the present writer (see Ref. 6). In the framework of this model it could be shown now the scattering of the electron by a random field with a definite type of short-range order leads to the formation of a peculiar "band structure" of the energy spectrum, which appears in the form of a characteristic pseudogap in the density of electronic states, in the absence of any sort of long-range order. It was also possible to consider high-frequency conductivity and optical absorption in terms of the pseudogap. This model was used to describe the fluctuation region of quasi-one-dimensional systems that undergo a Peierls transition,⁷ with the result that the predictions of this model are in good quantitative agreement with optical experiments on KCP and TTF-TCNQ,⁸ at least at sufficiently high temperatures.

A form of this model was considered in Ref. 9 as an extension⁷ to the fluctuation region of a commensurate Peierls transition. The exact solution^{6,7} was obtained in the limit of large range of the close-order correlation, and qualitative criteria were indicated for the applicability of this treatment for a finite correlation

length. In the present paper an exact solution for the one-electron Green's function is obtained in the form of a continued fraction, and also for the density of electron states, for arbitrary values of the correlation length for short-range order; this permits us to trace a smooth transition to the "metallic" state (pseudogap filled in) as the correlation length is decreased and to justify the qualitative criteria given earlier⁷ for the use of the asymptotic form for large correlation lengths.

1. FORMULATION OF THE MODEL AND ANALYSIS OF THE FEYNMAN DIAGRAMS

We consider an electron in a Gaussian random field $\Delta(x)$ with the correlation function

$$\langle \Delta(x)\Delta(x') \rangle = \Delta^2 \exp[-|x-x'|/\xi] \cos 2p_F(x-x'), \quad (1)$$

where Δ^2 gives the mean square fluctuation of the field, ξ is the correlation length (close-order correlation range), and p_F in the Fermi momentum of the electrons. This is precisely the correlator that is obtained for the fluctuations of the order parameter in the one-dimensional Ginzburg-Landau model for the Peierls transition,¹⁰ and therefore we shall speak of it in concrete terms as a Peierls system in the fluctuation region.

It must be noted that our assumption that the random field $\Delta(x)$ is Gaussian obviously does not apply to real Peierls systems, at least for sufficiently low temperatures $T \ll T_{p0}$, where T_{p0} is the temperature of the Peierls transition in the self-consistent field approximation.¹¹ We are considering the Gaussian model of a Peierls system [with the exact correlator (1)] because it admits of an exact solution, derived below, and also because it is evidently not so very far from reality in the region $T \sim T_{p0}$.

The correlation length will be regarded as a parameter of the theory, just as the quantity Δ^2 is. Finding them requires a complete microscopic theory of the Peierls transition. The model under consideration can also be derived in a certain variant of the static approximation of the dynamic theory of the Peierls transition,^{6,9} (the assumption that there is a clearly expressed

central peak in the dynamic structure factor of the lattice which is undergoing the Peierls transition). The model can also have a bearing on the properties of liquid semiconductors.⁶

The Fourier transform of (1) (the static structure factor) is of the form

$$S(Q) = 2\Delta^2 \left\{ \frac{\kappa}{(Q-2p_F)^2 + \kappa^2} + \frac{\kappa}{(Q+2p_F)^2 + \kappa^2} \right\}, \quad (2)$$

where $\kappa = \xi^{-1}$. The simplest proper-energy part of the one-electron Green's function is given by (p is the momentum of the electron)

$$\Sigma(\epsilon, p) = \Delta^2 \int \frac{dQ}{2\pi} S(Q) \frac{1}{i\epsilon_n - \xi_p + Q}, \quad (3)$$

and is shown graphically in Fig. 1, a, where the wavy line corresponds to the formula (2) and the solid line is the free Green's function of the electron. Here ξ_p is the energy of free electrons, measured from the Fermi level, and $\epsilon_n = (2n+1)\pi T$.

We shall deal in the most detail with the case of all-most free electrons:

$$\xi_p = p^2/2m - \mu \approx v_F (|p| - p_F), \quad (4)$$

where m is the mass of the electron, v_F is the Fermi velocity, and μ is the chemical potential. Furthermore $2p_F$ is in general considered to be incommensurable with the period of the initial lattice.

Besides this, we shall consider the selected⁹ case of the spectrum in the strong coupling approximation

$$\xi_p = -W \cos pa, \quad (5)$$

where a is the initial lattice period, setting $2p_F = \pi/a$, which corresponds to a half-filled band with doubled period, i.e., to the case of limiting commensurability, when the Peierls order parameter becomes real.

From Eqs. (2) and (3) we get (we shall consider the initial momentum of the electron $p_0 = p_F$)

$$\Sigma(\epsilon, p) = \Delta^2 (i\epsilon_n + \xi_p + iv_F \kappa)^{-1} = \Delta^2 G_0(\epsilon_n, -\xi_p - iv_F \kappa), \quad (6)$$

where we have used the fact that for a one-dimensional system $\xi_{p-2p_F} = -\xi_p$. The expression (6), which corresponds to the simplest diagram, Fig. 1, a, was taken as the basis of the analysis conducted in the paper of Lee, Rice, and Anderson.¹⁰ In Refs. 6 and 7 all diagrams of the Gaussian model of the Peierls transition were summed in the asymptotic case $\kappa = 0$, which, as can be seen from Eq. (6), is justified when the inequality

$$v_F \kappa = v_F \xi^{-1} \ll \xi_p; 2\pi T \quad (7)$$

is satisfied. This imposes a limitation on the description of the immediate neighborhood of the Fermi level.

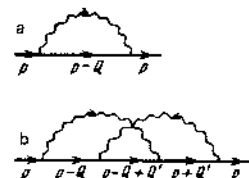


FIG. 1.

Our problem is now to sum all of the graphs of the Gaussian model for finite κ .

As was stated earlier,⁷ in each order of perturbation theory the contribution of one order is given by diagrams with a sequence of successive vertices with incoming or outgoing interaction lines transmitting a momentum $Q \sim 2p_F$. Diagrams of the type of Fig. 1, b are small of the order of the parameter ξ_p/ϵ_F (ϵ_F is the Fermi energy), and can be dropped. Therefore in order $2n$ ($2n$ is the number of vertices) we need include only $n!$ diagrams. Figure 2 shows all essential diagrams of sixth order. Let us consider the contribution of the diagram 2, d. After elementary calculations we find that the quantity corresponding to Fig. 2, d is

$$\Delta^6 \frac{1}{i\epsilon_n - \xi_p} \frac{1}{i\epsilon_n + \xi_p + iv_F \kappa} \frac{1}{i\epsilon_n - \xi_p + 2iv_F \kappa} \frac{1}{i\epsilon_n + \xi_p + 3iv_F \kappa} \times \frac{1}{i\epsilon_n - \xi_p + 2iv_F \kappa} \frac{1}{i\epsilon_n + \xi_p + iv_F \kappa} \frac{1}{i\epsilon_n - \xi_p}.$$

The contributions for the other diagrams of Fig. 2 are entirely analogous; the numbers over the electron lines in Fig. 2 indicate how many times $iv_F \kappa$ occurs in the corresponding denominator. We note that the contribution of the "crossed" diagram Fig. 2, d is equal to that of the diagram without crossing of the interaction lines, Fig. 2, e. We emphasize that the simplicity of the expressions for the contributions of the various diagrams is due to the choice of the structure factor $S(Q)$ in the Lorentzian form (2).

In eighth order there are in all $4! = 24$ essential diagrams; all of the irreducible diagrams are shown in Fig. 3. The corresponding contributions are easily found and are analogous in form, and the use of the numbers over the electron lines is as in Fig. 3. Furthermore, again there are quite a number of equalities among the diagrams: $a = b = c = d$; $e = f = g = h$; $i = j$; $k = l$.

The general rules for writing out the expression corresponding to an arbitrary diagram are now clear. The contribution of any diagram is determined by the arrangement of the initial and final vertices (in Fig. 3 they are marked with the letters I and F). In each electron line following a vertex of type I a term $iv_F \kappa$ is added in the denominator, and in an electron line fol-

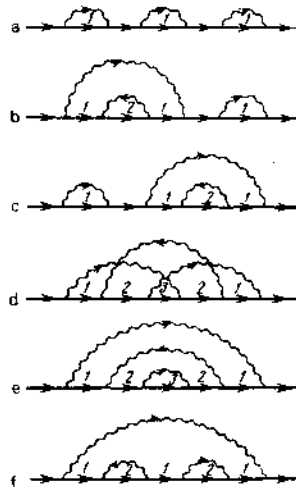


FIG. 2.

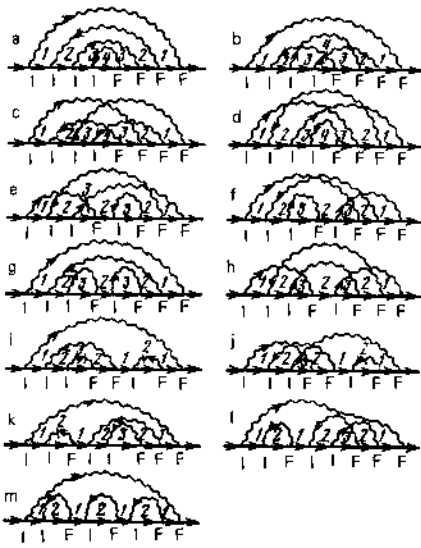


FIG. 3.

lowing a vertex of type F, such a term is subtracted. In this connection, the sense (direction) of the interaction lines is immaterial.

These rules hold also for the treatment of the problem with spectrum (5) in the strong-coupling approximation for the half-filled band. Here, however, we must include also diagrams of the type of Fig. 1, b, in which the interaction lines do not have to be arranged in succession according to the directions of motion of the transferred momentum, since with the spectrum (5) the points $p, p + 2p_F$, and $p - 2p_F$ are equivalent (with $2p_F = \pi/a$),⁹ i.e., all possible diagrams. Then in order $2n$ there are in all $(2n - 1)!! = (2n - 1)! / 2^{n-1} (n - 1)!$ diagrams, and also the contribution of each interaction line is multiplied by 2.⁹ The rule about the appearance of terms $iv_{F\kappa}$ in denominators of Green's functions is the same as before.

We then follow a method proposed (for a different problem) by Elyutin.¹³ From the foregoing it is easy to see that the contribution of any diagram is determined by the arrangement of initial and final vertices. Furthermore any diagram with intersecting interaction lines can be uniquely represented by a diagram without any intersections, since any diagram with intersections is equivalent to some diagram without any. The recipe for the construction of the corresponding diagram without intersections (for a given arrangement of I and F vertices) is: Counting from the left, the first final vertex must be connected with an interaction line to the nearest initial vertex on its left, and so on for the remaining vertices not so far connected with interaction lines. Thus, for example, the diagrams of Fig. 3, b, c, d reduce to the form of Fig. 3, a, the diagrams Fig. 3, e, f reduce to the form of Fig. 3, g, and so on. For a fixed distribution of initial vertices in a problem with the electron spectrum (4) the final vertices can be chosen only from points of opposite parity, but for a problem with the spectrum (5) the final vertices can be chosen also from points of the same parity as the initial ones. The numbers put with the electron lines in Figs. 2 and 3 can be transferred to the vertices, by

assigning to a vertex the number of terms $iv_{F\kappa}$ in the denominator corresponding to the line proceeding after that vertex. The general rule is¹³: To an initial vertex is assigned the number $N_n = N_{n-1} + 1$, where N_{n-1} is the number assigned to the nearest vertex on the left. To a final vertex is assigned the number $N_n - 1$. Also $N_0 = 0$, and n is the order number of a vertex.

Let us introduce

$$v(k) = \begin{cases} (k+1)/2 & k=2m+1 \\ k/2 & k=2m \end{cases} \quad (8)$$

for a problem with the spectrum (4) and

$$v(k) = k \quad (9)$$

for a problem with the spectrum (5). Then it can be verified that the number of irreducible self-energy diagrams which are equal to a given diagram without intersections of interaction lines is equal to the product of the quantities $v(N_n)$ for all initial vertices of that diagram.¹³ Accordingly, we can conduct all further arguments in terms of diagrams without intersections of interaction lines by applying to all initial vertices the appropriate factors $v(N_n)$.

2. THE ONE-ELECTRON GREEN'S FUNCTION

Any diagram for an irreducible proper-energy part, when restructured according to the rules that have been formulated here, contains an all-surrounding interaction line, i.e., reduces to the form shown in Fig. 4, a. This enables us to derive recurrence formulas for determining a proper-energy part, which are the basis of Elyutin's method.¹³ By the definition of a proper-energy part, we have the Dyson equation for the Green's function:

$$G^{-1}(\epsilon_n, \xi_p) = G_0^{-1}(\epsilon_n, \xi_p) - \Sigma_1(\epsilon_n, \xi_p), \quad (10)$$

where (see Fig. 4, a)

$$\Sigma_1(\epsilon_n, \xi_p) = \frac{\Delta^2}{(i\epsilon_n + \xi_p + iv_{F\kappa})^2} \Xi_1(\epsilon_n, \xi_p) = \Delta^2 G_0^{-2}(\epsilon_n, -\xi_p - iv_{F\kappa}) \Xi_1(\epsilon_n, \xi_p), \quad (11)$$

and for $\Xi_1(\epsilon_n, \xi_p)$ we have the expansion of Fig. 4, b in terms of diagrams without intersections of interaction lines, with the factors $v(N_n)$ applied to their vertices. This expansion can be expressed in the standard way in terms of the corresponding irreducible graphs:

$$\Xi_1(\epsilon_n, \xi_p) = G_0^{-2}(\epsilon_n, -\xi_p - iv_{F\kappa}) \{G_0^{-1}(\epsilon_n, -\xi_p - iv_{F\kappa}) - \Sigma_2(\epsilon_n, \xi_p)\}, \quad (12)$$

where $\Sigma_2(\epsilon_n, \xi_p)$ can be expressed as a sum of the ir-

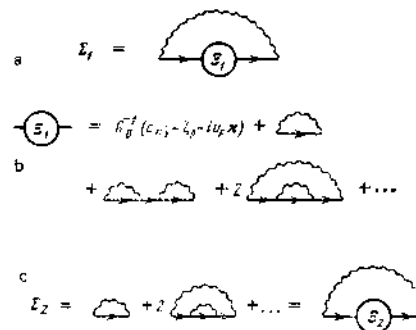


FIG. 4.

reducible graphs of Fig. 4, c:

$$\Sigma_1(\varepsilon_n, \xi_p) = \Delta^2 G_0^2(\varepsilon_n, \xi_p - 2i\nu_F \kappa) \Sigma_1(\varepsilon_n, \xi_p), \quad (13)$$

$$\Sigma_2(\varepsilon_n, \xi_p) = G_0^{-1}(\varepsilon_n, \xi_p - 2i\nu_F \kappa) \{G_0^{-1}(\varepsilon_n, \xi_p - 2i\nu_F \kappa) - \Sigma_1(\varepsilon_n, \xi_p)\} \quad (14)$$

and so on. We have finally:

$$\Sigma_k(\varepsilon_n, \xi_p) = \Delta^2 G_0^2(\varepsilon_n, (-1)^k \xi_p - ik\nu_F \kappa) v(k) \Sigma_k(\varepsilon_n, \xi_p), \quad (15)$$

$$\Sigma_k(\varepsilon_n, \xi_p) = G_0^{-1}(\varepsilon_n, (-1)^k \xi_p - ik\nu_F \kappa) \{G_0^{-1}(\varepsilon_n, (-1)^k \xi_p - ik\nu_F \kappa) - \Sigma_{k+1}(\varepsilon_n, \xi_p)\}, \quad (16)$$

$$\Sigma_k(\varepsilon_n, \xi_p) = \frac{\Delta^2 v(k)}{G_0^{-1}(\varepsilon_n, (-1)^k \xi_p - ik\nu_F \kappa) - \Sigma_{k+1}(\varepsilon_n, \xi_p)}. \quad (17)$$

This is the fundamental recurrence formula. The Green's function is accordingly expressible in the form of a continued fraction:

$$\begin{aligned} & \frac{G(\varepsilon_n, \xi_p)}{1} \\ & \frac{1}{i\varepsilon_n - \xi_p - \frac{\Delta^2}{i\varepsilon_n + \xi_p + i\nu_F \kappa - \frac{\Delta^2}{i\varepsilon_n - \xi_p + 2i\nu_F \kappa - \frac{2\Delta^2}{i\varepsilon_n + \xi_p + 3i\nu_F \kappa - \dots}}} \\ & = \left[0; \frac{1}{i\varepsilon_n - \xi_p}, \frac{-\Delta^2}{i\varepsilon_n + \xi_p + i\nu_F \kappa}, \dots, \frac{-\Delta^2 v(k)}{i\varepsilon_n - (-1)^k \xi_p + ik\nu_F \kappa}, \dots \right]. \end{aligned} \quad (18)$$

For $\kappa = 0$ we can use the well known representation of the incomplete Γ function as a continued fraction¹⁴:

$$\Gamma(\alpha, z) = \int_z^\infty dt e^{-t} t^{\alpha-1} = \frac{z^\alpha e^{-z}}{z + \frac{1-\alpha}{1 + \frac{1}{z + \frac{1-2\alpha}{1 + \dots}}}} \quad (19)$$

and also the relation $\Gamma(0, x) = -Ei(-x)$ to verify that

$$\begin{aligned} G(\varepsilon_n, \xi_p) &= \frac{e + \xi_p}{\Delta^2} \exp\left(-\frac{e^2 - \xi_p^2}{\Delta^2}\right) Ei\left(\frac{e^2 - \xi_p^2}{\Delta^2}\right) \\ &= \int_0^\infty d\xi e^{-\xi} \frac{e + \xi_p}{e^2 - \xi_p^2 - \xi^2 \Delta^2} = \int_0^\infty dW P_\kappa(W) \frac{e + \xi_p}{e^2 - \xi_p^2 - W^2}, \end{aligned} \quad (20)$$

where the usual analytic continuation $i\varepsilon_n - \varepsilon \pm i\delta$ is to be understood. Here

$$P_\kappa(W) = \frac{2W}{\Delta^2} \exp\left(-\frac{W^2}{\Delta^2}\right) \quad (21)$$

is the Rayleigh distribution¹⁵ which describes the uniform fluctuations of a semiconducting slit over all space. The Rayleigh distribution arises because in this case we have to do with a complex Gaussian field of fluctuations.¹⁵ Accordingly, for $\kappa = 0$ we get the result of Ref. 6. In the general case ($\kappa \neq 0$) we cannot put the expression (18) in any closed form, but the continued-fraction representation is convenient for numerical computation.

For the problem with the spectrum (5) and $2p_F = \pi/a$ (limiting commensurable case, doubled period) we get in a similar way the recurrence relation (17) with $v(k)$ given by Eq. (9), so that

$$\begin{aligned} & \frac{G(\varepsilon_n, \xi_p)}{1} \\ & \frac{1}{i\varepsilon_n - \xi_p - \frac{\Delta^2}{i\varepsilon_n + \xi_p + i\nu_F \kappa - \frac{2\Delta^2}{i\varepsilon_n - \xi_p + 2i\nu_F \kappa - \frac{2 \cdot 2\Delta^2}{i\varepsilon_n + \xi_p + 3i\nu_F \kappa - \dots}}} \\ & = \left[0; \frac{1}{i\varepsilon_n - \xi_p}, \frac{-2\Delta^2}{i\varepsilon_n + \xi_p + i\nu_F \kappa}, \dots, \frac{-k \cdot 2\Delta^2}{i\varepsilon_n - (-1)^k \xi_p + ik\nu_F \kappa}, \dots \right]. \end{aligned} \quad (22)$$

Here Δ^2 has a coefficient 2 owing to the necessity of including the two directions of interaction lines, as explained earlier.

For $\kappa = 0$ we can again use Eq. (19), and after simple calculations we get

$$\begin{aligned} G(\varepsilon_n, \xi_p) &= -\frac{1}{2\Delta} \left(\frac{\xi_p + e}{\xi_p - e}\right)^{1/2} \exp\left(-\frac{e^2 - \xi_p^2}{4\Delta^2}\right) \Gamma\left(\frac{1}{2}, -\frac{e^2 - \xi_p^2}{4\Delta^2}\right) \\ &= \frac{1}{\pi^{1/2}} \int_0^\infty d\xi \exp\left(-\frac{\xi^2}{4}\right) \frac{e + \xi_p}{e^2 - \xi_p^2 - \xi^2 \Delta^2} = \int_{-\infty}^\infty dW P_0(W) \frac{e + \xi_p}{e^2 - \xi_p^2 - W^2}, \end{aligned} \quad (23)$$

where

$$P_0(W) = \frac{1}{2\pi^{1/2} \Delta} \exp\left(-\frac{W^2}{4\Delta^2}\right), \quad (24)$$

which agrees with the result obtained in Ref. 9. The appearance of the Gaussian distribution here is due to the fact that in this case we are dealing with a real Gaussian field of fluctuations. In the general case, $\kappa \neq 0$, we are also obliged to use the continued-fraction representation (22) for the Green's function.

3. THE DENSITY OF STATES

Let us proceed to the calculation of the density of electron states corresponding to the Green's functions (17) and (22). For the problem with the spectrum (4) (incommensurable transition) we have

$$\begin{aligned} \frac{N(e)}{N_0} &= -\frac{1}{\pi} \int_{-\infty}^\infty d\xi_p \operatorname{Im} G^A(\varepsilon, \xi_p) \\ &= -\frac{1}{\pi} \int_{-\infty}^\infty d\xi_p \frac{\operatorname{Im} \Sigma_1(\varepsilon, \xi_p)}{[e - \xi_p - \operatorname{Re} \Sigma_1(\varepsilon, \xi_p)]^2 + \operatorname{Im}^2 \Sigma_1(\varepsilon, \xi_p)}, \end{aligned} \quad (25)$$

where N_0 is the density of states of free electrons at the Fermi level. From the fundamental recurrence relation (17) we have:

$$\begin{aligned} \operatorname{Re} \Sigma_k(\varepsilon, \xi_p) &= \frac{\Delta^2 v(k) [e - (-1)^k \xi_p - \operatorname{Re} \Sigma_{k+1}(\varepsilon, \xi_p)]}{[e - (-1)^k \xi_p - \operatorname{Re} \Sigma_{k+1}(\varepsilon, \xi_p)]^2 + [\kappa \nu_F \kappa - \operatorname{Im} \Sigma_{k+1}(\varepsilon, \xi_p)]^2}, \\ \operatorname{Im} \Sigma_k(\varepsilon, \xi_p) &= \frac{-\Delta^2 v(k) [\kappa \nu_F \kappa - \operatorname{Im} \Sigma_{k+1}(\varepsilon, \xi_p)]}{[e - (-1)^k \xi_p - \operatorname{Re} \Sigma_{k+1}(\varepsilon, \xi_p)]^2 + [\kappa \nu_F \kappa - \operatorname{Im} \Sigma_{k+1}(\varepsilon, \xi_p)]^2}. \end{aligned} \quad (26)$$

Calculations of the density of states were made with a BESM-6 computer; the convergence of the iteration procedure (26) was found to be very good. The results are shown in Fig. 5, where the different curves of the density of states correspond to different values of the dimensionless parameter $\Gamma = v_F \kappa / \Delta = v_F \xi^{-1} / \Delta$. The curve with $\Gamma = 0$ corresponds to the case in which the density of states can be found analytically.⁷ It can be seen that as the correlation length ξ decreases there is a gradual filling up of the pseudogap, i.e., a transition to a "metallic" state. For $v_F \xi^{-1} \ll \Delta$ the approximation $\kappa = 0$ works very well everywhere except in the range

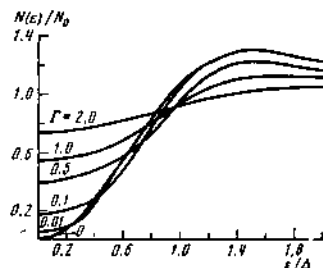


FIG. 5.

of energies $\sim v_F \xi^{-1}$ around the Fermi level, which confirms the qualitative conclusions of previous papers.^{6,7} For large values $\Gamma \gg 2$ the difference between the results of Lee, Rice, and Anderson,¹⁰ based on the use of only the one diagram of Fig. 1, a, and those of the present calculation done by including all graphs becomes inappreciable. The main difference appears for small Γ , when the approach of Ref. 10 predicts a transition to a density of states of the BCS type for $\Gamma \rightarrow 0$.

Figure 6 shows the dependence of the density of states on the Fermi level (which governs, for example, the Pauli paramagnetic susceptibility) as a function of Γ . Curve 1 is our result, and curve 2 is the result of Ref. 10 (adjusted to our notation). It can be seen that the filling in of the pseudogap occurs more rapidly in our model; for $\Gamma < 1.5$ curve 1 can be approximated with the formula $N(0)/N_0 \approx (0.541 \pm 0.013)\Gamma^{1/2}$.

In attempts to compare our results with experiments on the Peierls transition in KCP or TTF-TCNQ it must be kept in mind that we have neglected all nongaussian fluctuations, which may be important for $T \ll T_{p0}$.¹¹ This Gaussian model can be applied for $T \lesssim T_{p0}$, or for KCP and TTF-TCNQ for $T \approx 200$ K at any rate. From neutron diffraction and x-ray data it follows^{16,17} that at these temperatures in KCP $\xi > 10^2 a$ (a is the lattice constant), i.e., $\Gamma \propto \epsilon_F a / \Delta \xi < 0.1$, which may explain the good agreement of the results obtained in Refs. 6 and 7 for the optical absorption by the pseudogap with experiments on KCP (Ref. 18, see also Ref. 8). There is no generally accepted theory of the correlation length for the Peierls transition. The experimental data do not contradict the results of Blunck,¹⁹ which indicate that $\xi(300 \text{ K}) \approx 10^2 a$, $\xi(200 \text{ K}) \approx 10^3 a$, i.e., $\Gamma(300 \text{ K}) \leq 0.1$, $\Gamma(200 \text{ K}) \leq 0.01$. The nongaussian character of the fluctuations for $T \ll T_{p0}$ evidently leads to a more sharply expressed pseudogap in the density of states,¹¹ which can also be seen in the optical experiment.¹⁸ We note, however, that in the range of temperatures when a sharper gap is observed experimentally, even a three-dimensional ordering effects are already important.

For the extreme case of commensurability [the spectrum (5)] we have

$$\frac{N(\epsilon, W)}{N_0} = \frac{1}{\pi} \int_{-W}^W \frac{d\xi_p}{(1 - \xi_p^2/W^2)^{1/2}} \frac{\text{Im} \Sigma_1(\epsilon \xi_p)}{[\epsilon - \xi_p - \text{Re} \Sigma_1(\epsilon \xi_p)]^2 + \text{Im}^2 \Sigma_1(\epsilon \xi_p)} \quad (27)$$

The iteration procedure is given by the formulas (26) with the substitution $k \rightarrow 2k$. Figure 7 shows the results of calculations of the density of states for the case $W = \infty$ (infinitely broad band) which is most simply

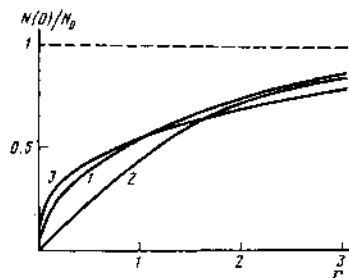


FIG. 6.

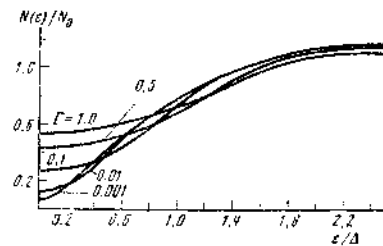


FIG. 7.

compared with the free electron case which we have considered. For finite values of W there is a characteristic peak of the density of states at $\epsilon = W$,⁹ owing to the smearing out of the singularity at the edge of the band of the one-dimensional metal. Furthermore, in the case $W \gg \Delta$ the form of the density of states for $\epsilon \lesssim \Delta$ is practically not different from that obtained in the limit $W \rightarrow \infty$, and this is precisely the region of most interest to us. Again it can be seen that as ξ decreases there is a smooth transition to a metallic state. The density of states at the Fermi level as a function of Γ is shown for this problem as curve 3 in Fig. 6.

Again it is easy to trace the transition to the case 0, for which the problem can be solved analytically⁹; this approximation works well when the inequalities (7) are satisfied. For $\Gamma < 3$ curve 3 is approximated by the formula $(0.546 \pm 0.016)\Gamma^{1/2}$. There is a curious coincidence in the values of the constants in the expressions for the density of states at the Fermi level as function of the parameter Γ in the two different problems. In the case now being considered (commensurable) the pseudogap in the density of states is less sharply expressed, and it is filled in much more rapidly as ξ decreases, than in the incommensurable case previously considered, and the criterion for the applicability of the approximation $\Gamma = 0$ is more strictly quantitative in this case, although qualitatively it is again expressed by the inequalities (7).

In conclusion the writer expresses his deep gratitude to B. M. Letfulov for carrying out the numerical calculations. He is also grateful to S. A. Brazovskii and L. V. Keldysh for discussions and for their interest in this work.

¹B. I. Halperin, Adv. Chem. Phys. 13, 123 (1968).

²V. L. Berezinskii, Zh. Eksp. Teor. Fiz. 65, 1251 (1973) [Sov. Phys. JETP 38, 620 (1974)].

³A. A. Abrikosov and I. A. Ryzhkin, Adv. Phys. 27, 147 (1978).

⁴A. A. Ovchinnikov and N. S. Erikhman, Zh. Eksp. Teor. Fiz. 73, 650 (1977) [Sov. Phys. JETP 46, 340 (1977)].

⁵A. A. Abrikosov, L. P. Gor'kov, and I. E. Dzyaloshinskii, Metody kvantovoi teorii polya v statisticheskoi fizike (Methods of quantum field theory in statistical physics), Fizmatgiz, 1963. English transl., New York, Prentice-Hall, 1963.

⁶M. V. Sadovskii, Zh. Eksp. Teor. Fiz. 66, 1720 (1974) [Sov. Phys. JETP 39, 845 (1974)].

⁷M. V. Sadovskii, Fiz. Tverd. Tela 16, 2504 (1974) [Sov. Phys. Solid State 16, 1632 (1975)].

⁸W. Wonneberger, J. Phys. C 10, 1073 (1977).

⁹W. Wonneberger and R. Lautenschlager, J. Phys. C 9, 2865 (1976).

¹⁰P. A. Lee, T. M. Rice, and P. W. Anderson, Phys. Rev. Lett. 31, 462 (1973).

¹¹S. A. Brazovskii and I. E. Dzyaloshinskii, Zh. Eksp. Teor.

- Flz. 71, 2338 (1976) [Sov. Phys. JETP 44, 1233 (1976)].
- ¹²M. V. Sadovskii, Preprint FIAN (Fiz. Inst. Akad. Nauk) No. 63, 1973.
- ¹³P. V. Elyutin, Opt. Spektrosk. 43, 542 (1977) [Opt. Spectrosc. (USSR) 43, 318 (1977)].
- ¹⁴Bateman Manuscript Project, A. Erdelyi, Ed., Higher Transcendental functions, Vol. 2, New York, McGraw-Hill, 1953.
- ¹⁵S. M. Rytov, Vvedenie v statisticheskuyu radiofiziku (Introduction to Radio Physics), Nauka, 1966.

- ¹⁶R. Comès, M. Lambert, H. Launois, and H. R. Zeller, Phys. Rev. B8, 571 (1973).
- ¹⁷J. W. Lynn, M. Izumi, G. Shirane, S. A. Werner, and R. B. Saillant, Phys. Rev. B12, 219 (1975).
- ¹⁸P. Bruesch, S. Strassler, and H. R. Zeller, Phys. Rev. B12, 1154 (1975).
- ¹⁹M. Blunck, Phys. Lett. 62A, 237 (1978); Z. Phys. B31, 1 (1978).

Translated by W. H. Furry

Electron localization in the random-phase model and in a magnetic field

M. V. Sadovskii

Institute of Metal Physics, Ural Scientific Center, USSR Academy of Sciences

(Submitted 7 July 1980)

Zh. Eksp. Teor. Fiz. 80, 1135-1148 (March 1981)

Electron localization with disorder in the phases of the transport integrals is considered in the Anderson model. It is shown with the aid of Anderson's method that a disorder of this type leads in the general case to an effective decrease of the lattice connectivity constant, and contributes to the localization. Total localization of the band on account of the phase disorder alone, however, is impossible. The influence of an external magnetic field and the positions of the mobility edge is considered (neglecting the spin effects). It is shown that the result of the action of the magnetic field is determined by the distribution function of the areas of the self-avoiding walks on the lattice. In the general case, the magnetic field contributes to the localization, and its action is similar to the effect of random phases of the transport integrals. The results are valid in the region of sufficiently strong fields, in which the effects connected with the Langer-Neal diagrams are suppressed.

PACS numbers: 71.50. + t

INTRODUCTION

Interest in the localization of electrons in disordered systems has increased lately.¹⁻³ This is due both to the importance of this phenomenon to the theory of disordered systems, and to the reports of new experiments in which the localization manifests itself in unusual manner.³ At the same time, the level of the theoretical understanding of the localization is still too low; this is manifest, in particular, in the fact that the roles of different external fields (primarily magnetic) and of different types of disorder have not yet been investigated. Until recently most papers were devoted to the study of localization in the Anderson model^{4,5} with diagonal (site) disorder of the electron in the lattice. What was mainly discussed was the critical disorder that leads to complete localization of all states in a band. Only recently has serious interest been evinced in the role of off-diagonal disorder (transport integrals), and this led immediately to conclusions concerning the unusual role of this disorder in the phenomenon considered, especially to the conclusion that complete localization in a band on account of only a disorder of this type is impossible.⁶ Finally, a paper by Abrahams *et al.*⁷ increased sharply the interest in the critical behavior at the mobility edge and in the interesting predictions made concerning localization in two-dimensional systems⁷⁻¹⁰ (see the review³).

In this paper we consider the localization phenomenon in a specific model of off-diagonal disorder (the random-phase model), whose interesting distinguishing feature is the presence of local gauge invariance. Generalization of the results obtained with this model make it possible to examine the effect of an external magnetic field in the positions of the mobility edges in terms of its influence on the orbital motion (neglecting spin effects). The analysis is carried out within the framework of Anderson's standard approach.⁴⁻⁶ The relation between our results and those obtained within the framework of another approach^{9,10} will be discussed in the Conclusion.

1. LOCAL GAUGE INVARIANCE IN THE ANDERSON MODEL

We consider the Hamiltonian of the Anderson model

$$H = \sum_{\langle ij \rangle} J_{ij} a_i^\dagger a_j + \sum_i E_i a_i^\dagger a_i, \quad (1)$$

where a_i^\dagger and a_i are the electron creation and annihilation operators on the i -th and j -th lattice sites. The energies E_i at the sites are assumed to be random, and their distribution is specified in the usual form

$$P(E_i) = \prod_i P(E_i), \quad (2)$$

$$P(E_i) = \begin{cases} W^{-1}, & |E_i| < W \\ 0, & |E_i| > W \end{cases}$$

The transport integrals J_{ij} , which are assumed to differ from zero only between nearest neighbors, also take on random values.

We consider a specific disorder model, in which the random quantity is the phase rather than the modulus of the transport integral, as considered by Antoniou and Economou.⁶ We thus assume (the random-phase model)

$$J_{ij} = J \exp(i\Phi_{ij}) = JU_{ij}, \quad (3)$$

$$J_{ij} = J_{ji}, \quad \Phi_{ij} = -\Phi_{ji}$$

where Φ_{ij} is a random quantity whose distribution in the lattice is assumed to be factorizable in the bonds:

$$P(\Phi_{ij}) = \prod_{\langle ij \rangle} P(\Phi_{ij}), \quad (4)$$

and we consider for $P(\Phi_{ij})$ different cases:

$$P(\Phi_{ij}) = \frac{1}{(2\pi)^{1/2}} \exp\left\{-\frac{\Phi_{ij}^2}{2\Phi^2}\right\}, \quad (5)$$

$$P(\Phi_{ij}) = \begin{cases} \Phi^{-1}, & |\Phi_{ij}| < \Phi \\ 0, & |\Phi_{ij}| > \Phi \end{cases} \quad (6)$$

$$P(\Phi_{ij}) = c\delta(\Phi_{ij} - \pi) + (1-c)\delta(\Phi_{ij}), \quad 0 < c < 1, \quad (7)$$

etc. Case (7) corresponds to random introduction (with density c) of "antiferromagnetic" bonds:

$$J_{ij} = JA_{ij}, \quad (8)$$

$$P(A_{ij}) = \begin{cases} c & A_{ij} = -1 \\ 1-c & A_{ij} = +1 \end{cases} \quad (9)$$

It is easily seen that the Anderson Hamiltonian (1) has local gauge symmetry. It is invariant to a transformation of the type

$$(G): a_i \rightarrow \exp(i\Phi_i) a_i, \quad a_j \rightarrow \exp(-i\Phi_j) a_j, \quad (10)$$

$$J_{ij} \rightarrow \exp(-i\Phi_i) J_{ij} \exp(i\Phi_j).$$

This is the analog of the local gauge transformation in the Yang-Mills theory on a lattice, a transformation actively used of late in the theory of random spin systems (spin glasses).^{11,12} This invariance is known to lead to a number of nontrivial conclusions for magnetic systems,^{11,12} some of which can be directly crossed over also to the model considered. In particular, if in (3)

$$\Phi_i = \alpha_i + \alpha_j, \quad (11)$$

where α_i and α_j are random quantities, then this disorder is trivial and can be eliminated by a suitable local gauge transformation. This crosses over to the case (8) if $A_{ij} = c_i c_j$, where $c_i = \pm 1$ in random fashion (the analog of the Mattis model in spin-glass theory). Interest attaches to the nontrivial (gauge-invariant) disorder determined^{11,12} by distribution of the frustrations on the considered lattice. The definition of the frustration¹¹ (or of the frustration angle¹²) can be formulated in the considered electronic model in complete analogy with the definitions in the theory of random spin systems. The frustration distributions investigated in spin lattices^{12,13} can turn out to be useful also in localization theory.

Proceeding to consideration of the electron Green's function in the Anderson lattice, we note that the single-electron Green's function

$$G_{ij}(E) = \langle i | \frac{1}{E-H} | j \rangle = \langle 0 | a_i \frac{1}{E-H} a_j^\dagger | 0 \rangle \quad (12)$$

is not gauge-invariant:

$$(G): G_{ij}(E) \rightarrow G_{ij}(E) \exp[i(\Phi_i - \Phi_j)]. \quad (13)$$

The only gauge invariant element in this function is $G_{ii}(E)$, which is diagonal in the sites and is customarily used in the study of localization in the standard Anderson approach.⁴⁻⁶ It is obvious from the foregoing that in the random-phase model the averaged single-electron Green's function is diagonal in the site indices:

$$\langle G_{ij}(E) \rangle = G(E) \delta_{ij}, \quad (14)$$

a reflection of the vanishing of the gauge-noninvariant off-diagonal elements upon averaging over the gauge-invariant distribution of the frustrations. It is therefore meaningless to use (14) for the investigation of the localization. For the averaged two-particle Green's function we have

$$\langle G_{ij}(E) G_{kl}(E') \rangle \sim \delta_{ij} \delta_{kl}; \quad \delta_{ik} \delta_{jl}; \quad \delta_{il} \delta_{jk}. \quad (15)$$

A similar situation (in another model) was dealt with in Refs. 14 and 15.

We can introduce the gauge-invariant electron Green's functions

$$\mathcal{G}_{ij}^\pm(E) = \langle 0 | a_i \frac{1}{E-H} \prod_{\Gamma} U_{ki} a_j^\dagger | 0 \rangle, \quad (16)$$

where $\prod_{\Gamma} U_{ki}$ determines the product of the elements

U_{ki} from (3) [or A_{ki} from (9)] along an arbitrary walk Γ that connects the sites i and j of the lattice. Expression (16) is obviously gauge invariant, and (14) does not hold for it. Correlators of the type (16) are therefore capable of containing definite information on the localization, but they have an explicit dependence on the walk Γ , and their behavior after the averaging has not been investigated.

At the same time, as noted above, Anderson's standard approach⁴⁻⁶ is perfectly suited for the analysis of problems of this type, in view of the local gauge invariance of $G_{ii}(E)$.

2. LOCALIZATION IN THE RANDOM PHASE MODEL

Following Anderson's method, we investigate the convergence of the renormalized perturbation-theory series for the self-energy part $\Delta_i(E)$ that enters in the matrix element, diagonal in the sites, of the non-averaged Green's function:

$$G_{ii}(E) = \frac{1}{E - E_i - \Delta_i(E)}; \quad (17)$$

$$\Delta_i(E) = \sum_{k \neq i} J_{ik} \frac{1}{E - E_k - \Delta_k(E)} J_{ki} \quad (18)$$

$$+ \sum_{k_1, k_2 \neq i, k} J_{ik_1} \frac{1}{E - E_{k_1} - \Delta_{k_1}(E)} J_{k_1 k_2} \frac{1}{E - E_{k_2} - \Delta_{k_2}(E)} J_{k_2 k} + \dots,$$

where $\Delta_k^{ij \dots}(E)$ is determined by a series such as (18), but corresponding to the Hamiltonian (1), in which we put $E_i = E_j = E_k = \dots = \infty$.⁵ We have excluded from (18) the repeated indices of the sites, i.e., in $(N+1)$ -st order in J_{ij} , the summation proceeds along a self-avoiding walk Γ_N consisting of N steps on the lattice, starting with the i -th site and returning to the i -th site [Fig. 1(a)]. Multiple scattering processes [Fig. 1(b)] with return are implicitly taken into account here by introducing $\Delta_k^{ij \dots}(E)$ in the denominators of (18),^{4,5} and it is this which allows us to consider self-avoiding walks on the lattice. The representation (8) is exact. An electron of energy E is localized if the series $\Delta_i(E)$ converges in the sense of convergence with respect to probability.^{4,5}

To investigate the convergence of the series (18), we consider the modulus of the term of $(N+1)$ -st order in J_{ij} :

$$\left| \Delta_i^{(N)}(E) \right| = \left| \sum_{\Gamma_N} T_{\Gamma_N}(E) \right|, \quad (19)$$

where \sum denotes summation over self-avoiding walks consisting of N steps starting and ending at the site i , and $T_{\Gamma_N}(E)$ is the contribution of one such walk. According to Economou and Cohen,⁵ it can be shown that

$$\left| \Delta_i^{(N)}(E) \right| \approx L^N(E) \quad (20)$$

$$= \left| \sum_{\Gamma_N} J \exp(i\Phi_{i_1}) G_{i_1}^+(E) J \exp(i\Phi_{i_2}) G_{i_2}^+(E) \dots J \exp(i\Phi_{i_N}) \right|,$$

$$\ln G_{i_1}^{(N)}(E) = \left\langle \ln \left| \frac{1}{E - E_{i_1} - \Delta_{i_1}^{(N)}(E)} \right| \right\rangle, \quad (21)$$

where the angle brackets denote averaging over the diagonal disorder (2). The quantity $L^N(E)$ is obviously gauge-invariant, since the walks Γ_N on the lattice are closed. Then $L(E) < 1$ is the condition for the convergence of the series (18) (Ref. 5) and can be regarded as

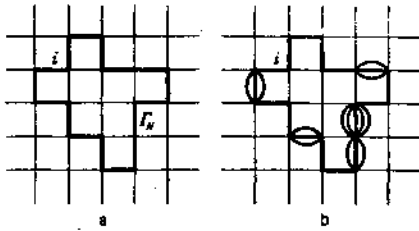


FIG. 1.

a criterion of the localization. The delocalized states correspond to the condition $L(E) > 1$.

Expression (21) is too complicated for actual calculations, owing to the need for taking the contribution $\Delta_k^{i_1 \dots i_N}(E)$ into account. There are several ways of getting around this difficulty,⁴⁻⁶ but we shall use the simplest one—we neglect completely the contributions of these quantities^{5,16}:

$$G_k^{i_1 \dots i_N}(E) \approx \exp\{-N \langle \ln |E - E_k| \rangle\}. \quad (22)$$

This approximation facilitates all the calculations, and its result for the positions of the mobility edges and for the critical disorder do not differ greatly from those of the more accurate analysis.^{4,5,17} It is therefore usually assumed that a more consistent account of $\Delta_k^{i_1 \dots i_N}(E)$ in (21) leads simply to a quantitative refinement of the localization condition⁵ (see, however, the discussion in the Conclusion).

We then have

$$L^N(E) \approx J^{N+1} \left| \sum_{r_N} \exp(i\Phi_{r_N}) \right| \exp\{-N \langle \ln |E - E_k| \rangle\}, \quad (23)$$

where

$$\Phi_{r_N} = \Phi_0 + \Phi_1 + \dots + \Phi_N \quad (24)$$

is the phase advance along the walk Γ_N . Equation (24) has only N terms, \sum_{r_N} contains $\sim K^N$ terms, where K is the so-called lattice connectivity constant¹⁸:

$$\ln K = \lim_{N \rightarrow \infty} \frac{1}{N} \ln Z_N,$$

where Z_N is the total number of self-avoiding walks of N steps.

We consider now

$$X_N = \sum_{r_N} \exp(i\Phi_{r_N}). \quad (25)$$

If all the phase shifts in (24) are zero (or fixed), then obviously $|X_N| \sim K^N$ and we obtain correspondingly the usual answer^{5,16}

$$L^N(E) \approx J^{N+1} K^N \exp\{-N \langle \ln |E - E_k| \rangle\}, \quad (26)$$

$$L(E) \approx \alpha K \exp \mathcal{F}(E, W/J), \quad (27)$$

$$\mathcal{F}\left(E, \frac{W}{J}\right) = \frac{1}{W} \int_{-W/2}^{W/2} dE_k \ln \left| \frac{J}{E - E_k} \right|$$

$$= 1 - \frac{1}{2} \left\{ \left(1 + \frac{2E}{W}\right) \ln \left| \frac{W}{2J} + \frac{E}{J} \right| + \left(1 - \frac{2E}{W}\right) \ln \left| \frac{W}{2J} - \frac{E}{J} \right| \right\}.$$

Here $\alpha = Z/K$ (Z is the number of nearest neighbors) is a correction factor⁵ that makes it possible to describe correctly the limit of the regular lattice. The condition $L(0) = 1$ then yields for the critical disorder need for complete localization

$$(W/J)_c = 2eZ. \quad (28)$$

In the random phase model, $|X_N|$ is the length of the walk on a plane as a result of random K^N steps of unit length. The most substantial effect is reached for fully random phases, when Φ_{ij} have a distribution (6), with $\Phi = 2\pi n$ ($n = 1, 2, \dots$). We are then dealing with Brownian motion on a plane, and $|X_N|$ has the Rayleigh distribution^{19,20}

$$P(|X_N|) \approx \frac{2|X_N|}{K^N} \exp\left\{-\frac{|X_N|^2}{K^N}\right\}, \quad (29)$$

$$\langle |X_N|^2 \rangle = K^N. \quad (30)$$

The most probable value is $|X_N| \sim \langle |X_N|^2 \rangle^{1/2} \sim K^{N/2}$. Then

$$L^N(E) \approx J^{N+1} K^{N/2} \exp\{-N \langle \ln |E - E_k| \rangle\}, \quad (31)$$

$$L(E) \approx \alpha K^{3/2} \exp \mathcal{F}(E, W/J).$$

The stochastization of the phases leads thus to a decrease of the effective connectivity constant of the lattice. The condition for complete localization when the phases are completely random takes then the form

$$(W/J)_c^{\text{RPM}} = 2\alpha K^{3/2} = 2eZK^{-1/2}. \quad (32)$$

It is obvious that

$$(W/J)_c^{\text{RPM}} < (W/J)_c,$$

i.e., the localization condition is less stringent.

In the absence of diagonal disorder, $E_k = E_0$ for all k . Then, if nondiagonal disorder is also absent, we have⁵

$$L(E) = \alpha K \frac{J}{|E - E_0|} - Z \frac{J}{|E - E_0|}, \quad (33)$$

and when the phases are completely randomized

$$L(E) = \alpha K^{3/2} \frac{J}{|E - E_0|} = \frac{Z}{K^{1/2}} \frac{J}{|E - E_0|}. \quad (34)$$

Then at $L(E) > 1$ we obtain the width of the band of extended states in the model of completely random phases:

$$B_{\text{ext}}^{\text{RPM}} = K^{-1/2} B, \quad (35)$$

where $B = 2ZJ$ is the usual width of the band in the regular case.

Thus, in the absence of diagonal disorder complete localization in the entire band is impossible, and a region of extended states, of widths $B_{\text{ext}}^{\text{RPM}}$, always remains around the center of the band. Table I shows the values of K and $K^{-1/2}$ for different lattices.¹⁸ It is seen that the phase disorder can localize in all cases approximately $\frac{1}{2}$ to $\frac{2}{3}$ of the initial band.

In the general case, obviously, $K^{N/2} \leq |X_N| \leq K^N$. The problem of calculating the statistical distribution of sums of the type (25) was investigated in detail in connection with various problems of statistical radio engineering.¹⁹⁻²² This distribution is relatively easy to obtain when the distribution of the Φ_{r_N} is such that the central limit theorem is satisfied.^{21,22} In particular,

$$P(|X_N|) = \frac{|X_N| e^{-s}}{(s_1 s_2)^{1/2}} \sum_{m=0}^{\infty} (-1)^m e_m J_m(P) I_{2m}((Q^2 + R^2)^{1/2}) \times \cos \left[2m \arctg \frac{R}{Q} \right] \quad (36)$$

TABLE I.

Lattice	z	κ	$\kappa^{-1/2}$	$\ln \kappa$
Triangular	6	4.1515	0.4908	1.4235
Quadratic	4	2.6390	0.5156	0.9704
Diamond	4	2.878	0.5896	1.0571
PC	6	4.6826	0.4624	1.5438
BCC	8	6.5288	0.3914	1.8762
FCC	12	10.035	0.3157	2.3061

the so-called Nakagami distribution.²² Here $I_m(x)$ is a modified Bessel function of order m , $\epsilon_0 = 1$, and $\epsilon_m = 2$ at $m \neq 0$,

$$S = \frac{s_1 + s_2}{4s_1s_2} |X_N|^2 + \frac{\alpha^2}{2s_1} + \frac{\beta^2}{2s_2},$$

$$P = \frac{s_1 - s_2}{4s_1s_2} |X_N|^2, \quad Q = |X_N| \frac{\alpha}{s_1}, \quad R = |X_N| \frac{\beta}{s_2};$$

$$\alpha = \sum_{\Gamma_N} \int d\Phi_{\Gamma_N} P(\Phi_{\Gamma_N}) \cos \Phi_{\Gamma_N} = \sum_{\Gamma_N} \alpha_{\Gamma_N}, \quad (37)$$

$$\beta = \sum_{\Gamma_N} \int d\Phi_{\Gamma_N} P(\Phi_{\Gamma_N}) \sin \Phi_{\Gamma_N} = \sum_{\Gamma_N} \beta_{\Gamma_N},$$

$$s_1 = \sum_{\Gamma_N} \int d\Phi_{\Gamma_N} P(\Phi_{\Gamma_N}) \cos^2 \Phi_{\Gamma_N} = \sum_{\Gamma_N} \alpha_{\Gamma_N}^2,$$

$$s_2 = \sum_{\Gamma_N} \int d\Phi_{\Gamma_N} P(\Phi_{\Gamma_N}) \sin^2 \Phi_{\Gamma_N} = \sum_{\Gamma_N} \beta_{\Gamma_N}^2, \quad (38)$$

where $P(\Phi_{\Gamma_N})$ is the distribution function of Φ_{Γ_N} . It is easily seen here that^{21,22}

$$\langle |X_N|^2 \rangle = s_1 + s_2 + \alpha^2 + \beta^2, \quad (39)$$

i.e., it is determined completely by the mean values α and β and by the variances s_1 and s_2 from (38). The Rayleigh distribution (29) is obtained from (36) at $\alpha = \beta = 0$ and $s_1 = s_2 = K^N/2$.

We consider now several examples. We begin with the Gaussian case (5). It is then easily seen that

$$P(\Phi_{\Gamma_N}) = \frac{1}{(2\pi)^{1/2} \Phi_N} \exp\left\{-\frac{\Phi_{\Gamma_N}^2}{2\Phi_N^2}\right\}, \quad (40)$$

$$\Phi_N^2 = \langle \Phi_{\Gamma_N}^2 \rangle + \langle \Phi_{\Gamma_N}^4 \rangle + \dots + \langle \Phi_{\Gamma_N}^{2N} \rangle = N\Phi^2. \quad (41)$$

From (38) and (39) we easily obtain

$$\langle |X_N|^2 \rangle = K^{2N} \exp(-N\Phi^2) + K^N (1 - \exp(-N\Phi^2)). \quad (42)$$

In the general case we get from (23)

$$L(E) \approx \alpha \mathcal{K} \exp \mathcal{F}(E, W/I), \quad (43)$$

where the effective connectivity constant \mathcal{K} is defined as

$$\mathcal{K} = \lim_{N \rightarrow \infty} \langle |X_N|^2 \rangle^{1/2N}. \quad (44)$$

For the case (40)–(42) it is correspondingly easy to show that

$$\mathcal{K} = \begin{cases} K \exp(-\Phi^2/2), & \Phi^2 < \ln K \\ K^{1/2}, & \Phi^2 > \ln K \end{cases} \quad (45)$$

The "effective connectivity" of the lattice as a function of the phase disorder is shown in Fig. 2. \mathcal{K} first increases with increasing Φ^2 , and at $\Phi^2 > \ln K$ the phases become completely randomized and \mathcal{K} takes the asymptotic form $K^{1/2}$.

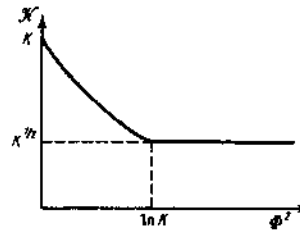


FIG. 2.

We consider now the case of the distribution (6) with $\Phi \neq 2\pi n$ ($n = 1, 2, \dots$). Then, obviously,

$$P(\Phi_{\Gamma_N}) = \begin{cases} 1/N\Phi, & |\Phi_{\Gamma_N}| < N\Phi \\ 0, & |\Phi_{\Gamma_N}| > N\Phi \end{cases} \quad (46)$$

We then obtain

$$\mathcal{K} = \lim_{N \rightarrow \infty} \left\{ K^{2N} \frac{\sin^2 N\Phi}{(N\Phi)^2} + K^N \left(1 - \frac{\sin^2 N\Phi}{(N\Phi)^2} \right) \right\}^{1/2N} = K. \quad (47)$$

Thus, in this case there is not even partial randomization of the phases. A nondiagonal disorder of this type does not influence the localization. It is seen from (47) that at $\Phi = \pi n$ ($N = 1, 2, \dots$) we return to the full stochastization considered above.

The cases (7)–(9) can be treated similarly. Let n be the number of negative bonds along a given walk Γ_N . The probability of realization of such a bond distribution is given by the binomial distribution

$$P_N(n_{\Gamma_N}) = C_N^{n_{\Gamma_N}} c^{n_{\Gamma_N}} (1-c)^{N-n_{\Gamma_N}}. \quad (48)$$

Using the limiting behavior of (48) as $N \rightarrow \infty$ and the fact that in this case $\Phi_{\Gamma_N} = \pm n_{\Gamma_N} \pi$, we obtain directly

$$P(\Phi_{\Gamma_N}) = \frac{1}{2} [2\pi^2 N c (1-c)]^{-1/2} \{ \exp[-(\Phi_{\Gamma_N} - c\pi N)^2 / 2Nc(1-c)\pi^2] + \exp[-(\Phi_{\Gamma_N} + c\pi N)^2 / 2Nc(1-c)\pi^2] \}. \quad (49)$$

The appearance of two terms in (49) is due to the fact that the walk Γ_N can follow two circuit directions, and the phase advance is $\pm n_{\Gamma_N} \pi$ by virtue of $\Phi_{ij} = -\Phi_{ji}$ (3). From (49) we get

$$K = \begin{cases} K \exp[-c(1-c)\pi^2/2], & c < c_1^*, \quad c > c_2^* = (1-c_1^*), \\ K^{1/2}, & c_1^* < c < c_2^*, \end{cases} \quad (50)$$

where $c_{1,2}^*$ is obtained by solving the equation $c(1-c)\pi^2 = \ln K$.

Thus, the inclusion of a sufficient number of antiferromagnetic bonds (with $c > c_1^*$) leads to complete stochastization of the phases and brings \mathcal{K} to the level $K^{1/2}$. The values of $c_{1,2}^*$ for different lattices are given in Table II. We note that the critical concentrations obtained in this manner are very close to the critical antiferromagnetic-bond concentrations at which ferromagnetism vanishes in the corresponding Ising lattices.^{23,24}

TABLE II.

Lattice	Triangular	Quadratic	Diamond	PC	BCC	FCC
c_1^*	0.1748	0.1106	0.1220	0.1941	0.2445	0.3722
c_2^*	0.8252	0.8894	0.8780	0.8059	0.7455	0.6278

3. LOCALIZATION IN A MAGNETIC FIELD

Application of a constant external magnetic field \mathbf{H} adds, as is well known, an additional phase factor in the transport integral J_{ij} (the Peierls factor)^{25,26}

$$J_{ij} = \exp(-i\Phi_{ij})J_{ij},$$

$$\Phi_{ij} = \frac{1}{2} \frac{e}{\hbar c} \mathbf{H}[\mathbf{R}_i \times \mathbf{R}_j], \quad (51)$$

where \mathbf{R}_i is the radius vector that determines the position of the i -th site in the lattice. The main property of these factors is²⁶ that the sum along a closed walk Γ_N on the lattice is gauge-invariant and is equal to the flux of the magnetic field \mathbf{H} through the area S_{Γ_N} enclosed by the contour Γ_N measured in units of the magnetic-flux quantum $\Phi_0 = \hbar c/e$:

$$\Phi_{\Gamma_N} = \Phi_{ij} + \Phi_{jk} + \dots + \Phi_{ni} = \Phi_0^{-1} \mathbf{H} S_{\Gamma_N}. \quad (52)$$

The result (51) is valid in not too strong fields, for which one can neglect the deformation of the atomic wave functions in the magnetic field (this changes also the modulus J_{ij}).

We see now that the influence of the magnetic field on the localization is similar to the influence, considered above, of the random phases J_{ij} . It is determined completely by the statistics of the area S_{Γ_N} of the self-avoiding walks on the lattice. To my knowledge, the problem of the distribution of the areas of the self-avoiding paths has not been considered before. It appears that reliable results can be obtained here only by computer simulation. Nonetheless, regardless of the statistics of S_{Γ_N} , it is clear from the foregoing that the appearance of the phase factors Φ_{Γ_N} (52) in (23) can only improve the convergence of the Anderson series (or at least have no effect on it), and decrease effectively the connectivity constant of the lattice. Therefore, neglecting spin effects (their influence on the hopping conductivity was considered recently by Fukuyama and Yosida²⁷), the magnetic field can only promote localization in this approximation. We present below a simple qualitative analysis aimed at revealing the principal relations and estimating the scale of the phenomena.

It is known from the scaling theory of self-avoiding walks^{28,29} that the mean squared dimension of Φ_{Γ_N} is

$$\langle R^2 \rangle \sim N^2 a^2, \quad (53)$$

where a is the lattice constant and ν is the critical exponent of the correlation length. For a qualitative treatment we can therefore assume

$$\langle |S_{\Gamma_N}| \rangle \sim \pi \langle R^2 \rangle \sim \pi a^2 N^{2\nu} \quad (54)$$

as an estimate of the average area of Γ_N .

In the two-dimensional case, with the magnetic field perpendicular to the plane of the system, it is clear that the values of Φ_{Γ_N} (52) are distributed about

$$\pm \mathcal{F}_0 = \pm H \langle |S_{\Gamma_N}| \rangle \sim \pi N^{2\nu} H a^2.$$

(The two signs are again connected with the two possible circuit directions of Φ_{Γ_N}). The distribution function $P(\Phi_{\Gamma_N})$ can then be simulated by two Gaussian peaks:

$$P(\Phi_{\Gamma_N}) = \frac{1}{2\sqrt{2\pi\sigma_N}} \left\{ \exp\left[-\frac{(\Phi_{\Gamma_N} - \mathcal{F}_0)^2}{2\sigma_N^2}\right] + \exp\left[-\frac{(\Phi_{\Gamma_N} + \mathcal{F}_0)^2}{2\sigma_N^2}\right] \right\}, \quad (55)$$

where

$$\sigma_N^2 \sim f(N) H^2 a^4 / \Phi_0^2 \quad (56)$$

is the variance of this distribution. It is difficult at present to draw any definite conclusions concerning the behavior of $f(N)$, other than it apparently increases like a certain power of N . In addition, we assume that the distributions of the areas (i.e., and of Φ_{Γ_N}) of the different Γ_N are independent, an assumption that is of course rather doubtful when the statistics of self-avoiding walks is considered.

From the foregoing analysis of the random-phase model we then obtain directly for the effective connectivity constant in a magnetic field the expression

$$\mathcal{K} = \lim_{N \rightarrow \infty} \left\{ K^{2N} e^{-\sigma_N^2 \cos^2 \mathcal{F}_0} + K^N [1 - e^{-\sigma_N^2 \cos^2 \mathcal{F}_0}]^{1/2N} \right\} \\ = \begin{cases} K; & \sigma_N^2 \sim N^{1-\nu} H^2 a^4 / \Phi_0^2, \\ K^0; & \sigma_N^2 \sim N^{1+\nu} H^2 a^4 / \Phi_0^2, \quad \delta > 0. \end{cases} \quad (57)$$

Only in the case $\sigma_N^2 \sim N H^2 a^4 / \Phi_0^2$ do we obtain

$$\mathcal{K} = \begin{cases} K \exp(-\text{const } H^2 a^4 / \Phi_0^2); & \text{const } H^2 a^4 / \Phi_0^2 < \ln K \\ K^0; & \text{const } H^2 a^4 / \Phi_0^2 > \ln K \end{cases} \quad (58)$$

i.e., a behavior of the type shown in Fig. 2. At $H a^2 \sim \Phi_0$, the phases are thus completely randomized. The behavior (57a), i.e., the absence of an influence of the field on the localization, is also perfectly feasible. The case (57b) has low probability.

We note that in the case (58) the effect saturates in fields $H a^2 \sim \Phi_0$, i.e., $H \sim 10^6$ G at $a \sim 3$ Å. In the limit $H a^2 \ll \Phi_0$ it follows from (58) that

$$L(E) \approx \alpha K \left\{ 1 - \text{const} \frac{H^2 a^4}{\Phi_0^2} \right\} \exp \mathcal{F} \left(E, \frac{W}{J} \right), \quad (59)$$

i.e., the mobility thresholds are shifted inside the band in proportion to the square of the field.

In the three-dimensional case we again assume factorization of the distribution function \mathcal{S}_{Γ_N} with respect to various Γ_N . In addition we assume also complete randomization of the orientations of \mathcal{S}_{Γ_N} in space, so that

$$P(S_{\Gamma_N}) = P(S_{\Gamma_N}^x) P(S_{\Gamma_N}^y) P(S_{\Gamma_N}^z). \quad (60)$$

Simulating each of the factors in (60) by a simple Gaussian distribution (with zero mean value), we obtain for the distribution function of the flux through the contour Γ_N

$$P(\Phi_{\Gamma_N}) = \frac{1}{(2\pi)^{3/2} \sigma_N} \exp\left(-\frac{\Phi_{\Gamma_N}^2}{2\sigma_N^2}\right), \quad (61)$$

where for σ_N we again assume a behavior of the type (56). In the three-dimensional case we then obtain the results (57)–(59).

Another possible approximation for $P(\Phi_{\Gamma_N})$ is obtained if the variance of \mathcal{S}_{Γ_N} is neglected. It can then be assumed that all the Γ_N have a fixed area of the order of (54), but the directions of S_{Γ_N} are random in space. We obtain readily

$$P(\Phi_{\Gamma_N}) = \begin{cases} \Phi_0/2H \langle |S_{\Gamma_N}| \rangle; & |\Phi_{\Gamma_N}| < H \langle |S_{\Gamma_N}| \rangle \\ 0; & |\Phi_{\Gamma_N}| > H \langle |S_{\Gamma_N}| \rangle \end{cases} \quad (62)$$

and for the effective connectivity we get a result of the type of (47), i.e., the magnetic field does not affect the localization. It seems to me that the most probable is a behavior of the type (58), (59), but the final solution of the problem depends on the behavior of the variance σ_N (56).

CONCLUSION

In conclusion, we discuss the relation between the results above and the deductions of the scaling theory of localization^{3,7} and the predictions concerning the influence of the magnetic field.^{9,10} It was shown in Ref. 7 that in two-dimensional systems an arbitrarily small disorder suffices for complete localization of all the states in a band. Although this conclusion met with certain objections (see the review³), it is confirmed by simple perturbation-theory calculations in the limit of weak disorder,^{8,9} when $l \gg a$, where l is the mean free path due to elastic scattering. Analogous calculations^{9,10} have demonstrated the strong influence of a magnetic field on two-dimensional localization, viz., a negative magnetoresistance sets in, i.e., the field destroys the localization. These results raise the question of the physical meaning of the two dimensional mobility edges obtained in Anderson's standard approach,^{4,5} as well as of the meaning of the conclusion arrived at above, that the magnetic field can only promote localization (or, in the extreme case, have no influence on it).

We note first that despite the complete localization, two-dimensional thresholds retain according to Ref. 7 a certain definite physical meaning of the threshold energies that separate the quasimetallic energy region in two-dimensional systems from the dielectric region. When the Fermi energy passes through these threshold, a rather abrupt transition should take from quasimetallic to hopping conductivity.³ The localization effects in the "quasimetallic" region are connected^{7,8} with the singular behavior of a special class of perturbation-theory diagrams (the Langer-Neal graphs,³⁰). In the standard Anderson approach^{4,5} the analog of such processes are apparently multiple scattering with return [Fig. 1(b)], which contribute to the self-energy parts $\Delta_s^{j1 \dots jn}(E)$. Neglect of such contribution or insufficient allowance for them in the usual approach^{4,5} does not lead to weak (logarithmic) effects of complete localization in the quasimetallic region of a two-dimensional system.

At the same time, the contribution of the Langer-Neal graphs is quite sensitive to the magnetic field (and also to scattering by magnetic impurities),^{9,10} A rather weak field suffices to exclude such scattering processes, i.e., to destroy the localization in the quasimetallic region, and it is this which leads^{9,10} to the effect of negative magnetoresistance. However, even if the Langer-Neal processes are completely neglected, the ordinary Anderson localization, which sets in at $l \sim a$, is possible when the disorder increases in the system. In a two-dimensional zone of a system located in a magnetic field, at sufficiently strong disorder (and

field), there exist ordinary mobility edges, whose behavior was in fact considered above.

It is clear from the foregoing that the results of Refs. 9 and 10 and of the present study pertain to different ranges of magnetic-field variation. In particular, if the critical-field estimates of Refs. 9-10 are rewritten in our notation, we find that the negative-magnetoresistance effect saturates ($\sim \ln H$) in fields $H a^2 / \Phi_0 \sim (a/l)^2$ at $T=0$, or in fields $H a^2 / \Phi_0 \sim a^2 / l_{in}$ at $T \neq 0$, where l_{in} is the mean free path for inelastic-scattering processes. By virtue of the condition $a \ll l \ll l_{in}$ ($T=0$) used in Refs. 9 and 10, it is seen that $H a^2 \ll \Phi_0$. Typical values of the critical field in Refs. 9 and 10 are of the order of 10-100 G. At the same time, the effects discussed above have a characteristic scale $H a^2 \approx \Phi_0$ and saturate at $H a^2 \sim \Phi_0$, i.e., they refer to fields $H \sim 10^4 - 10^6$ G, where they should lead to positive magnetoresistance [this can occur earlier in the case of the behavior (57b)]. We note that positive-magnetoresistance effects are implicitly contained in Refs. 9 and 10 via the magnetic-field dependence of the classical diffusion coefficient.

In conclusion, the author is deeply grateful to M. V. Medvedev and D. E. Khmel'nitskii for valuable discussions, and B. I. Shklovskii for interest in the work.

¹D. J. Thouless, Phys. Reports 13, 94 (1974).

²A. L. Éfros, Usp. Fiz. Nauk 126, 41 (1978) [Sov. Phys. Usp. 21, 756 (1978)].

³M. V. Sadovskii, Usp. Fiz. Nauk 133, 223 (1981) [Sov. Phys. Usp. 24, 96 (1981)].

⁴P. W. Anderson, Phys. Rev. 109, 1492 (1958).

⁵E. N. Economou and M. H. Cohen, Phys. Rev. B5, 2932 (1972).

⁶P. D. Antoniou and E. N. Economou, Phys. Rev. B16, 3768 (1977).

⁷E. Abrahams, P. W. Anderson, D. C. Licciardello, and T. V. Ramakrishnan, Phys. Rev. Lett. 42, 673 (1979).

⁸L. P. Gor'kov, A. I. Larkin, and D. E. Khmel'nitskii, Pis'ma Zh. Eksp. Teor. Fiz. 30, 248 (1979) [JETP Lett. 30, 228 (1979)].

⁹B. L. Altshuler, D. E. Khmel'nitskii, D. E. Larkin, and P. A. Lee, Phys. Rev. B22, 4142 (1980).

¹⁰S. Hikami, A. I. Larkin, and Y. Nagaoka, Prog. Theor. Phys. 63, 707 (1980).

¹¹G. Toulouse, Comm. Phys. 2, 115 (1977).

¹²E. Fradkin, B. Huberman, and S. H. Shenker, Phys. Rev. B18, 4789 (1978).

¹³H. G. Shuster, Zs. Phys. B35, 163 (1979).

¹⁴F. J. Wegner, Phys. Rev. B19, 783 (1979).

¹⁵R. Opperman and F. J. Wegner, Z. Phys. B34, 327 (1979).

¹⁶J. M. Ziman, J. Phys. C2, 1230 (1969).

¹⁷D. C. Licciardello and E. N. Economou, Phys. Rev. B11, 3697 (1975).

¹⁸V. K. Shante and S. Kirkpatrick, Adv. Phys. 20, 325 (1971).

¹⁹B. R. Levin, Teoreticheskie osnovy statisticheskoi radio-tekhnikii (Theoretical Principles of Statistical Radiophysics) Sovetskoe radio, 1969.

²⁰S. M. Rytov, Vvedenie statisticheskuyu radiofiziku (Introduction to Statistical Radiophysics), part 1, Nauka, 1976.

²¹P. Beckmann, J. Res. NBS 66D (Radio Propagation), 231 (1962).

²²P. Beckmann, J. Res. NBS 68D (Radio Science), 927 (1964).

²³S. Kirkpatrick, Phys. Rev. B16, 4630 (1977).

- ²⁴M. V. Medvedev, *Phys. Stat. Sol. (b)* **86**, 109 (1979).
²⁵R. Peierls, *Zs. Phys.* **80**, 467 (1933).
²⁶L. Friedmann, *Phil. Mag.* **38**, 467 (1978).
²⁷H. Fukuyama and K. Yosida, *J. Phys. Soc. Japan* **46**, 103 (1979).

- ²⁸P. G. de Gennes, *Phys. Lett.* **38A**, 339 (1972).
²⁹J. des Clizeaux, *Phys. Rev. A* **10**, 1665 (1976).
³⁰J. S. Langer and T. Neal, *Phys. Rev. Lett.* **16**, 984 (1966).

Translated by J. G. Adashko

Localization of one-particle spin excitations in a ferromagnet with a random easy-axis anisotropy

M. V. Medvedev and M. V. Sadovskii

Institute of Metal Physics, Ural Scientific Center of the Academy of Sciences of the USSR, Sverdlovsk

(Submitted December 17, 1980)

Fiz. Tverd. Tela (Leningrad) 23, 1943-1947 (July 1981)

Spin wave excitations in a ferromagnet with a random easy-axis anisotropy are studied. It is shown that anomalous damping of magnons near the edge of the spin wave band takes place and this damping is attributed to the localization of magnons. It is shown that the problem of localization of magnons is equivalent to the localization of electrons in the Anderson model with a diagonal disorder. The position of the mobility edge is calculated.

PACS numbers: 75.30.Ds, 75.30.Gw

1. The effect of fluctuations of the uniaxial anisotropy parameter on the spectrum of spin waves of an amorphous ferromagnet was studied in Ref. 1 on the basis of the phenomenological Landau-Lifshitz equation. It was suggested in Ref. 1 that the spin wave spectroscopy methods could be used to detect the resulting modification in the dispersion law of spin waves and thus estimate the fluctuations in the anisotropy parameter at different sites and determine their spatial correlation. It is of interest to investigate this problem within a lattice model of an amorphous ferromagnet and compare the spin wave spectrum calculated by a perturbation theory method with the results on the position of the mobility edge of spin wave excitations (in the spirit of the Anderson theory of localization of electrons²).

We shall, therefore, consider a model of a uniaxial Heisenberg ferromagnet in which only the anisotropy parameter $K(n) \geq 0$ characterizing an easy-axis anisotropy is a random quantity and all the other parameters are regular

$$H = -\frac{1}{2}J \sum_{n=1}^N \sum_{\lambda=1}^Z S_n S_{n+\lambda} - \sum_{n=1}^N K(n) (S_n^z)^2. \quad (1)$$

Here, $J > 0$; Z is the number of nearest neighbors, and we assume that the uniaxial properties of a crystal manifest themselves only by a uniaxial single-ion anisotropy but do not influence the lattice parameters or the exchange interaction. It follows that the magnetic lattice can be well approximated by a cubic lattice. The condition $K(n) \geq 0$ indicates that the ordering of all the spins in the ground state $|\Psi_0\rangle$ is ferromagnetic and the energy of the ground state is given by

$$E_0 = -\frac{1}{2}JNZS^2 - S^2 \sum_n K(n).$$

We shall now write the Schrödinger equation for a state $|\Psi_1\rangle$ corresponding to a single spin deviation (the

total z component of the spin moment of the crystal is given by $S_{\text{sum}}^z = NS - 1$)

$$H |\Psi_1\rangle = E_1 |\Psi_1\rangle. \quad (2)$$

The wave function $|\Psi_1\rangle$ can be expanded in terms of the basis of one-particle spin deviations localized at the lattice sites

$$|\Psi_1\rangle = \sum_{n=1}^N c_n |n\rangle; \quad |n\rangle = (2S)^{-1/2} S_n^- |\Psi_0\rangle. \quad (3)$$

As a result, we obtain either homogeneous equations for the coefficients

$$(E - JSZ - (2S - 1)K(n))c_n + JS \sum_{\lambda=1}^Z c_{n+\lambda} = 0 \quad (4)$$

or inhomogeneous equations for the corresponding Green's function

$$(E - JSZ - (2S - 1)K(n))G_{np} + JS \sum_{\lambda=1}^Z G_{n+\lambda,p} = \delta_{np} \quad (5)$$

(the energy $E = E_1 - E_0$ is measured from the ground state energy). Here, $G_{np}(E + i0^+)$ is the Fourier transform of the retarded Green's function

$$G_{np}(t) = -i\theta(t)(2S)^{-1} \langle \Psi_0 | S_n^+(t) S_p^-(0) | \Psi_0 \rangle.$$

We can calculate the self-energy corrections to the spectrum of spin waves $\epsilon_{\mathbf{q}}^0$ in the mean-field approximation

$$\epsilon_{\mathbf{q}}^0 = (2S - 1)K(n) + JS \left(Z - \sum_{\lambda} e^{i\mathbf{q}\cdot\mathbf{a}\lambda} \right) \quad (6)$$

using the Edwards-Jones method,³ which yields the following dispersion law in the Born approximation:

$$\epsilon_{\mathbf{q}} \approx (2S - 1)K \left[1 - \left(\frac{2S - 1}{2S} \right) \frac{D(K)}{KJ} \zeta \right] + JSa^2q^2 \left[1 - \left(\frac{2S - 1}{2S} \right)^2 \frac{D(K)}{J^2} \zeta \right]. \quad (7)$$

The damping of spin waves is given by

$$\Gamma_q \approx (2S-1)^2 D\{K\} \pi g_0(\epsilon_q^0) \approx (2S-1)^2 \frac{D\{K\}}{\pi J S} a q \quad (8)$$

in the long-wavelength limit $a q \ll 1$ (a is the lattice parameter and g_0 is the spin wave density of states in a crystal in the mean-field approximation).

We have used in the derivation of Eqs. (7) and (8) the assumption that the fluctuations of the anisotropy parameter at different lattice sites are statistically independent, i.e., that the averaging over the disorder is performed as follows:

$$\overline{K(n)K(n)} = \overline{K^2(n)} = \overline{K^2} + (K')^2 \equiv D\{K\} + (K')^2, \quad (9)$$

where $D\{K\}$ is the dispersion of the anisotropy parameter. The approximation which neglects all spatial correlations of the fluctuations of the anisotropy is not necessary but it is convenient for our comparison with the theory of localization. The numerical coefficients ζ and η in Eq. (7) are given by

$$\zeta = \frac{1}{N} \sum_q \frac{2}{Z - \sum_{\mathbf{q}'} e^{i\mathbf{q}\cdot\mathbf{q}'}} \approx 0.51 \text{ for simple lattice,}$$

$$\eta = \lim_{a \rightarrow 0^+} \frac{1}{N} \sum_q \frac{4}{(Z - 2a - \sum_{\mathbf{q}'} e^{i\mathbf{q}\cdot\mathbf{q}'})^2} \approx 0.05 \text{ for cubic lattice.}^4$$

Since the ratio $(2S-1)/2S$ is of the order of unity, the requirement that corrections to the mean-field theory should be small assumes the form $D\{K\}/\bar{K}J \ll 1$ and $D\{K\}\eta/J^2 \ll 1$. It can be seen that the fluctuations of the anisotropy parameter reduce the gap in the spin wave spectrum and the spin wave stiffness. It should be noted that the gap in the spin wave spectrum is defined as $\epsilon_{\mathbf{q}=0}$ rather than the actual gap in the density of states of single-particle spin excitations corresponding to the lowest Lifshitz boundary of the one-particle spectrum for $\epsilon_{\min} = (2S-1)\min\{K(n)\}$. The density of states of one-particle excitations increases rapidly at energies $\sim \epsilon_{\mathbf{q}=0}$.

The most interesting physical result which can be deduced from Eqs. (7) and (8) can be formulated as follows. The dispersion curve near $\epsilon_{\mathbf{q}=0}$ is not well defined due to damping $\Gamma_{\mathbf{q}} \sim a q$ and the change in the excitation energy near the gap is given by $\epsilon_{\mathbf{q}} - \epsilon_{\mathbf{q}=0} \sim a^2 q^2$. It follows that the dispersion curve of spin waves in the long-wavelength limit is well defined only if the condition

$$\frac{\Gamma_{\mathbf{q}}}{\epsilon_{\mathbf{q}} - \epsilon_{\mathbf{q}=0}} \approx \frac{1}{\pi} \left(\frac{2S-1}{2S} \right)^2 \frac{D\{K\}}{J^2} \frac{1}{a q} \ll 1 \quad (10)$$

is satisfied, i.e., for $D\{K\}/J^2 \ll a q \ll 1$. It appears that this important result was first noted by Korenblit and Shender⁵ for an asperomagnet with a random distribution of the easy-magnetization axes.

It should be noted that the Goldstone gapless mode does not appear in our model. The existence of such a mode is due to continuous degeneracy of the ground state which does not occur in systems with an easy-axis anisotropy. However, the situation is quite different for systems with an easy-plane anisotropy [$K(n) < 0$ in Eq. (1)] where the ground state is invariant with respect to rotations in the plane of the easy magnetization.

2. Since there is a region in which the perturbation theory breaks down near the energies corresponding to the

bottom of the spin wave band calculated in the mean field approximation, spin wave excitations can become localized near the bottom of the band.

Introducing the notation

$$\epsilon_n \equiv (2S-1)K(n) + JSZ, \quad V \equiv JS, \quad (11)$$

we can see that Eqs. (4) and (5) demonstrate that the present model is equivalent to the Anderson model with diagonal disorder.^{2,6,7} The quantity ϵ_n plays the role of a random electron energy at the n -th site and V is the amplitude of the electron hopping between sites. Consequently, we can apply to our model the criteria developed for the mobility edge of electrons. We shall not require a great numerical accuracy in the calculation of the mobility edge and restrict ourselves to a qualitative analysis. Consequently, we can use the Ziman criterion of localization of excitations⁸

$$Z \exp \left\{ \ln \left| \frac{JS}{E - JSZ - (2S-1)K(n)} \right| \right\} \ll 1, \quad (12)$$

We shall consider a uniform distribution of the anisotropy parameter in the interval

$$K - \frac{W}{2} < K(n) < K + \frac{W}{2}, \quad W \leq 2K. \quad (13)$$

Performing the averaging in Eq. (12), we find that the one-particle spin excitations become localized provided the condition

$$Z e \frac{1}{|x^2 - y^2|^{1/2}} \left| \frac{x-y}{x+y} \right|^{x/y} \ll 1 \quad (14)$$

is satisfied, where $x = [E - JSZ - (2S-1)\bar{K}]/JS$ is the dimensionless energy and $y = (2S-1)W/2JS$ is the dimensionless scatter of the random values of the anisotropy parameter.

The equality in Eq. (14) yields an equation for the calculation of the mobility edge of spin excitations. Since Eq. (14) is invariant under the substitution $x \rightarrow -x$, it follows that the mobility edges are symmetrically localized with respect to the point $x = 0$ [or with respect to $E = (2S-1)K + JSZ$, which represents the center of the spin wave band in the mean field approximation]. Setting $x = 0$, we find the following condition for the scatter in the anisotropy which is required for the localization in the whole band:

$$\frac{2(2S-1)K}{2JS} > \frac{(2S-1)W}{2JS} > Z e. \quad (15)$$

However, the case when the dispersion $D\{K\} = W^2/12$ is small compared with $\bar{K}J$ and J^2 is more interesting. Equation (14) yields $x = \pm Z$ for $y \rightarrow 0$. For $y/x \approx y/Z \ll 1$, we then obtain

$$|x| \approx Z \left[1 + \frac{1}{6} \left(\frac{y}{Z} \right)^2 \right] \quad (16)$$

which has the following solution:

$$x \approx \pm Z \left[1 + \frac{1}{6} \left(\frac{y}{Z} \right)^2 \right]. \quad (17)$$

The lowest value of the mobility edge ϵ_{loc} is then given by

$$\begin{aligned} \frac{\epsilon_{loc}}{2JS} &= \frac{(2S-1)K}{2JS} \left[1 - \frac{1}{Z} \left(\frac{2S-1}{2S} \right) \frac{D(K)}{KJ} \right] \\ &= \frac{\epsilon_{q=0}}{2JS} + \left(\frac{2S-1}{2S} \right)^2 \left(\zeta - \frac{1}{Z} \right) \frac{D(K)}{J^2}, \end{aligned} \quad (18)$$

where we have used, for comparison, the energy of the gap $\epsilon_{q=0}$ given by Eq. (7) and $\zeta = 1/Z \approx 0.34$ for a simple cubic lattice.

The method of Ref. 9 yields analogous results with a different numerical factor

$$\begin{aligned} \frac{\epsilon_{loc}}{2JS} &= \frac{(2S-1)K}{2JS} \left[1 - \frac{2}{K_c} \left(\frac{2S-1}{2S} \right) \frac{D(K)}{KJ} \right] \\ &= \frac{\epsilon_{q=0}}{2JS} + \left(\frac{2S-1}{2S} \right)^2 \left(\zeta - \frac{2}{K_c} \right) \frac{D(K)}{J^2}, \end{aligned} \quad (19)$$

where K_c is the lattice connectivity constant¹⁰ and $\zeta = 2/K_c \approx 0.08$ for a simple cubic lattice.

We find that, when the dispersion of the anisotropy $D\{K\}/J^2 \ll 1$ is small compared with the exchange interaction, the region in which the spin waves are not well defined extends approximately up to energies $\sim D^2\{K\}/J$ from the bottom of the spin wave band of the unperturbed "average" crystal, and the lowest value of the mobility edge lies at a distance $\sim D\{K\}/J$ below the gap in the spin wave spectrum of the unperturbed crystal (however, it lies above the gap $\epsilon_{q=0}$ calculated in the perturbation theory). An estimate based on the Ziman theory⁸ yields a somewhat higher position of the mobility edge than the estimate due to Abou-Chacra and Thouless.⁹

It follows that fluctuations of the anisotropy parameter of a crystal with an easy-axis anisotropy lead to a rapid increase in the damping near the bottom of the spin wave band and to a localization of magnons in the region of anomalous damping. Unfortunately, the region in question cannot be studied by the resonance method because of a sharp increase in the damping (for example, by the spin wave resonance). However, we may assume that the existence of localized spin excitations should manifest itself in the transport effects (for example, it should influence the magnitude of the magnon contribution to the thermal conductivity, etc.).

The appearance of a region of anomalous damping $\Gamma_{\mathbf{q}} \sim \alpha q$ near the bottom of the spin wave band is typical of disordered magnetic materials with an easy-axis anisotropy and, in particular, it manifests itself in asperomagnets with randomly oriented axes of the easy magnetization⁵ and in ferromagnets with a regular easy-axis anisotropy but with a random distribution of exchange integrals of different signs.¹¹ Consequently, the relationship between the anomalous behavior of the damping of magnons and their localization which was demonstrated in the present problem indicates that the localization of magnons near the bottom of the one-particle spin excitations should occur in all such cases. Such localization should be most important for the thermodynamic and transport properties of magnetic materials. For disordered magnetic materials with an isotropic exchange interaction or with an easy-plane anisotropy, spin excitations should become localized in the upper part of the energy band. This was recently demonstrated for an isotropic Heisenberg spin glass (Ref. 12). It appears that the problem of localization of magnons near the bottom of the energy band requires separate discussion for each model system because of the possible appearance of a low-lying impurity band of local spin excitations with their polarization opposite to the polarization of the spin excitations of the matrix of the unperturbed magnetic crystal.

¹V. A. Ignatchenko and R. S. Iskhakov, Zh. Eksp. Teor. Fiz. **72**, 1005 (1977) [Sov. Phys. JETP **45**, 526 (1977)].

²P. W. Anderson, Phys. Rev. **109**, 1492 (1958).

³S. F. Edwards and R. C. Jones, J. Phys. C **4**, 2109 (1971).

⁴J. Oitmaa, Solid State Commun. **9**, 745 (1971).

⁵I. Ya. Korenblit and E. F. Shender, J. Phys. F **9**, 2245 (1979).

⁶E. N. Economou and M. H. Cohen, Phys. Rev. B **5**, 2931 (1972).

⁷D. J. Thouless, Phys. Rep. (Phys. Lett. C) **13**, 93 (1974).

⁸J. M. Ziman, J. Phys. C **2**, 1230 (1969).

⁹R. Abou-Chacra and D. J. Thouless, J. Phys. C **7**, 65 (1974).

¹⁰V. K. S. Shante and S. Kirkpatrick, Adv. Phys. **20**, 325 (1971).

¹¹M. V. Medvedev, Phys. Status Solidi B **88**, 117 (1978).

¹²R. Bhargava and D. Kumar, Phys. Rev. B **19**, 2764 (1979).

Translated by D. Mathon

phys. stat. sol. (b) 109, 49 (1982)

Subject classification: 18.1; 18.2; 18.4

*Institute for Metal Physics, Academy of Sciences of the USSR,
Ural Scientific Centre, Sverdlovsk¹⁾*

Random Bond Ising Model in Self-Avoiding Walk Approximation

By

M. V. MEDVEDEV and M. V. SADOVSKII

Free energy of random bond Ising model is analysed by high-temperature expansion in self-avoiding walk approximation. Conditions of instability of the paramagnetic state are determined through the convergence criterion of the random high-temperature series. Critical concentrations for the loss of the long-range magnetic order are determined for different 2d and 3d lattices.

Методами высокотемпературных разложений в приближении путей без пересечений исследуется свободная энергия модели Изинга со случайными обменными связями. Из определения порогов сходимости случайных высокотемпературных рядов найдены условия неустойчивости парамагнитного состояния. Для различных двумерных и трехмерных решеток определены критические концентрации, при которых происходит разрушение дальнего магнитного порядка.

1. Introduction

In recent years there has been considerable interest in the properties of disordered magnetic systems [1], and in particular the random bond Ising model was actively studied [2 to 10]. We have the situation in mind of the Ising lattice with antiferromagnetic bonds distributed with concentration c , and ferromagnetic bonds — with concentration $1 - c$. In this model the important concept of frustration has been formulated for the first time [2, 5, 7, 9]. One of the basic (and not yet completely solved) problems in this model is the structure of its phase diagram [3 to 6, 8 to 10] and, especially, the value of the critical concentration c_1^* of the antiferromagnetic bonds, at which ferromagnetism in the system disappears. These problems have been analysed by different methods, from numerical simulation [3 to 5] and renormalization group [4, 8] to relatively simple variants of molecular-field approximation for disordered systems [6, 10].

In this paper these problems are studied by a simple method based upon the convergence criterion of the high-temperature expansion for the Ising model in the self-avoiding walk approximation, used previously for regular systems by Domb [11]. Our approach is based in part on the previous work by one of the authors [12], where the convergence of a similar random series had been considered related to the problem of electron localization in disordered systems. The main attractive feature of our method is its simplicity, as well as the similarity of the obtained results, to those of more refined approaches. This leads us to believe in a rather high accuracy of these results. At the same time we are able to analyse some of more general cases than those considered before by different authors.

¹⁾ S. Kovalevskii str. 18, GSP-170, Sverdlovsk 620219, USSR.

2. High-Temperature Expansion for the Free Energy in the Self-Avoiding Walk Approximation

Consider an Ising lattice described by the Hamiltonian

$$H = - \sum_{\langle ij \rangle} J_{ij} \sigma_i \sigma_j, \quad (1)$$

where the exchange interaction J_{ij} of the nearest neighbours takes random values, $\sigma_i = \pm 1$ is an Ising spin. The distribution function of exchange interactions is factorized over the bonds on the lattice,

$$\mathcal{P}\{J_{ij}\} = \prod_{\langle ij \rangle} P(J_{ij}), \quad (2)$$

where

$$P(J_{ij}) = c \delta(J_{ij} - J_B) + (1 - c) \delta(J_{ij} - J_A). \quad (3)$$

Here $J_A > 0$ is the "ferromagnetic" exchange integral, $J_B < 0$ is the "antiferromagnetic" exchange integral, $0 \leq c \leq 1$ is the concentration of antiferromagnetic bonds.

The partition function of the system can be represented as usual in the following form [13]:

$$\begin{aligned} Z\{\beta\} &= \sum_{\{\sigma\}} [\exp \sum_{\langle ij \rangle} K_{ij} \sigma_i \sigma_j] = \\ &= \sum_{\{\sigma\}} [\prod_{\langle ij \rangle} (\cosh K_{ij}) (1 + w_{ij} \sigma_i \sigma_j)], \end{aligned} \quad (4)$$

where $w_{ij} = \tanh K_{ij}$, $K_{ij} = \beta J_{ij}$, $\beta = 1/T$, T is the temperature. High-temperature expansion is the expansion in powers of w_{ij} . The coefficient of the N -th power of w_{ij} consists of all possible products of N pairs of $\sigma_i \sigma_j$. Because of $\sum_{\{\sigma\}} \sigma_i = 0$; $\sum_{\{\sigma\}} \sigma_i^2 = \sum_{\{\sigma\}} 1 = 1$, this coefficient can be represented by a closed polygon on the lattice [13] (Fig. 1). Every bond on the graph represents a factor $\tanh K_{ij}$ and each bond appears only once. At each vertex of the graph only an even number of bonds can meet.

The expansion of $Z\{\beta\}$ consists of all possible polygons (including unconnected ones) constructed on the lattice by these rules. In the lowest orders in N most of these graphs are just self-avoiding walks (SAW) on the lattice. (Cf. Fig. 1 a to c for $N = 8$.)

The logarithm of the partition sum (4),

$$\ln Z\{\beta\} = \sum_{\langle ij \rangle} \ln \cosh K_{ij} + \ln \sum_{\{\sigma\}} \prod_{\langle ij \rangle} (1 + w_{ij} \sigma_i \sigma_j), \quad (5)$$

can also be expressed as an expansion in powers of w_{ij} [11]. This expansion consists only of connected graphs, which can be represented by the closed paths on the lattice, starting and ending in the given lattice site. However, in this case the graphs are not

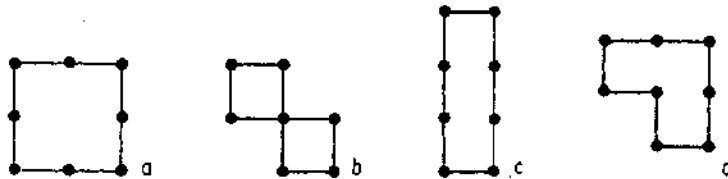


Fig. 1. Examples of graphs in the expansion of $Z\{\beta\}$ for $N = 8$

so simple as in the case of the partition function. In particular, every bond can appear several times, though again only an even number of bonds can meet at each vertex. This graphs can be classified over the so-called cyclomatic number $C = l - p + 1$ [11], where l is the number of the lines in the graph (multiple bonds are calculated as one), p is the number of vertices. The class corresponding to $C = 1$ consists of graphs topologically equivalent to the closed SAW's (which can be traced several times, however). Examples of such graphs are given in Fig. 2 a to c. In Fig. 2d we show the graph with $C = 2$ (the so-called θ -topology [11]). Our approximation neglects all the graphs with $C > 1$, thus we take into account only the graphs topologically equivalent to the closed SAW's.

Then we get

$$\begin{aligned} \ln \bar{Z}(\beta) &= \ln Z(\beta) - \sum_{\langle ij \rangle} \ln \cosh K_{ij} = \\ &= \sum_N \sum_i \sum_{\Gamma_N^i} \frac{1}{N} w_{ij} w_{jk} \dots w_{ii} - \\ &\quad - \frac{1}{2} \sum_N \sum_i \sum_{\Gamma_{N/2}^i} \frac{2}{N} w_{ij}^2 w_{jk}^2 \dots w_{ii}^2 + \frac{1}{3} \sum_N \sum_i \sum_{\Gamma_{N/3}^i} \frac{3}{N} w_{ij}^3 w_{jk}^3 \dots w_{ii}^3 + \dots \end{aligned} \quad (6)$$

Here the products of w_{ij} , w_{ij}^2 , ... etc, are taken along all possible SAW's Γ_N^i of N steps, $\Gamma_{N/2}^i$ of $N/2$ steps (but with two bonds on each step) etc., starting and ending in the i -th site. The structure of the expansion (6) is clear from (5) and the expansion of $\ln(1+x) = x - 1/2x^2 + 1/3x^3 - 1/4x^4 + \dots$. The extra combinatorial factors $1/N$ for the contribution of Γ_N^i , $2/N$ for the contribution of $\Gamma_{N/2}^i$, etc. are due to the fact that the initial vertex i of Γ_N^i can be chosen arbitrarily among N vertices of Γ_N^i , among $N/2$ vertices for $\Gamma_{N/2}^i$, etc.

The instability of the paramagnetic phase is determined by the convergence criterion of the high-temperature expansion (6) [11, 13]. In the regular case $w_{ij} = w_{jk} = \dots = w = \tanh \beta J$ and the problem reduces to the convergence criterion of the series [11],

$$\ln \bar{Z}(\beta) \approx \sum_N a_N w^N, \quad (7)$$

where

$$a_N = p(N) - \frac{1}{2} p(N/2) + \frac{1}{3} p(N/3) + \dots, \quad (8)$$

$$p(N) = \frac{1}{N} U_N,$$

and U_N is the number of the closed SAW's of N steps on the lattice, associated with the given site. It is known [11, 14] that for $N \gg 1$ $U_N \approx N^{-h} \mu^N$ ($h > 0$), where μ is

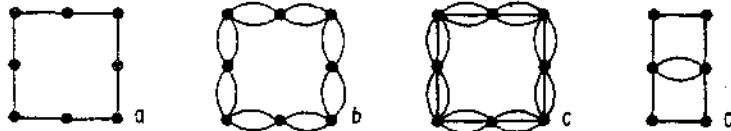


Fig. 2. Examples of graphs in the expansion of $\ln Z(\beta)$

the so-called connectivity constant of the lattice. Then it is obvious that for $N \gg 1$ only the first term in (8) is relevant (because of $\mu > \mu^{1/2} > \mu^{1/3} \dots$) and the series in (7) diverges if $\mu w = \mu \tanh \beta J \geq 1$. The equality determines the critical temperature [11]. The error of the SAW-approximation in regular case is $\approx 3\%$ for the 3d lattices, and $\approx 10\%$ for the 2d lattices [11].

3. Convergence Criterion of the Random High-Temperature Series

In a disordered system the high-temperature expansion (6) is a random series and its convergence must be treated statistically. It is generally accepted [1] that this expansion must be averaged over (2) and (3) and considered as representing the observable free-energy of the system. However, first of all we shall consider the convergence of the series (6) in the sense of convergence in probability, as it is done in localization theory [15, 16]. Our analysis will be similar to that used in [12].

First of all let us consider qualitatively the case of $J_A = -J_B$ and $c = 1/2$ in (3). Now only the terms with odd powers of w_{ij} on the bonds in (6) are random (in sign!). Consider the first series in (6). In the N -th order in w_{ij} it consists of terms $\sim \mu^N$, corresponding to the number of SAW's F_N^+ , and the sign of each of them is absolutely random for $c = 1/2$ (positive and negative bonds are equally probable). Then from the obvious analogy with the one-dimensional Brownian motion it is clear, that the modulus of this term for $N \gg 1$ is of the order of $\mu^{N/2} w^N$, where $w = \tanh \beta J_A = \tanh \beta |J_B|$. The limit of convergence of the series is then determined by $\mu^{1/2} w = 1$, and this coincides by the way with the limit of convergence of the second (non-random) series in (6): there are terms $\sim \mu^{N/2}$, each contributing a factor of w^N . Only the first two terms in (6) are relevant due to $\mu > \mu^{1/2} > \mu^{1/3}$, etc. Note, that the average of the first term in (6) is exactly equal to zero for $c = 1/2$, $J_A = |J_B|$, and the convergence of the averaged high-temperature series is determined by the second term in (6). We shall demonstrate that this is the general property of the high-temperature series for the random bond Ising model. The possibility of a singularity in the high-temperature expansion for this model at $\mu^{1/2} w = 1$ for $c = 1/2$, $J_A = -J_B$ was first noted by Domb [17] (see, however, [19]).

Consider now the general case of distribution (2) and (3). Let us analyse the modulus of the N -th order term in the first series in (6). Obviously we have

$$|\ln \bar{Z}^{(N)}(\beta)| = \left| \sum_{F_N} w_A^{n_{F_N}} (-w_B)^{n_{F_N}} \right| = w_A^N \left| \sum_{F_N} (-a)^{n_{F_N}} \right| \equiv w_A^N |X_N|, \quad (9)$$

where n_{F_N} is the number of negative bonds on the path F_N , $a = w_B/w_A$, $w_A = \tanh \beta J_A$, $w_B = \tanh \beta |J_B|$. The probability of n_{F_N} is given by the binomial distribution

$$P_N(n_{F_N}) = \frac{N!}{n_{F_N}!(N - n_{F_N})!} c^{n_{F_N}} (1 - c)^{N - n_{F_N}}. \quad (10)$$

Then it is easy to find

$$\begin{aligned} \langle (-a)^{n_{F_N}} \rangle &= (1 - c - ca)^N, \\ \langle (-a)^{2n_{F_N}} \rangle &= (1 - c + ca^2)^N \end{aligned} \quad (11)$$

and the dispersion of an isolated term in (9) is equal to

$$\langle (-a)^{2n_{F_N}} \rangle - \langle (-a)^{n_{F_N}} \rangle^2 = (1 - c + ca^2)^N - (1 - c - ca)^{2N}. \quad (12)$$

Let us estimate the most probable value of $|X_N|$ by $\langle X_N^2 \rangle^{1/2}$. The dispersion of the sum of independent random variables equals the sum of dispersions of isolated terms in the sum. Thus, supposing independence (for $N \gg 1$) of terms $\sim \mu^N$ in X_N we get

$$\langle X_N^2 \rangle - \langle X_N \rangle^2 \approx \mu^N [(1 - c + ca^2)^N - (1 - c - ca)^{2N}]. \quad (13)$$

Use now

$$\langle X_N \rangle \approx \mu^N \langle (-a)^{n_{FN}} \rangle = \mu^N (1 - c - ca)^N \quad (14)$$

to get

$$\langle X_N^2 \rangle \approx \mu^{2N} [(1 - c + ca^2)^N - (1 - c - ca)^{2N}] + \mu^{2N} (1 - c - ca)^{2N}. \quad (15)$$

Independence of contributions from the different paths Γ_N is crucial for our analysis. Obviously some of $\sim \mu^N$ paths have some parts in common. We suppose, that this leads to correlations negligible in the limit of $N \rightarrow \infty$.

The convergence condition for the first series in (6) is given now by

$$w_A \lim_{N \rightarrow \infty} \langle X_N^2 \rangle^{1/2N} < 1 \quad (16)$$

and the critical temperature is determined by the equation

$$w_A \lim_{N \rightarrow \infty} \left\{ \mu^{2N} \left(1 - c - c \frac{w_B}{w_A} \right)^{2N} + \mu^N \left[\left(1 - c + c \frac{w_B^2}{w_A^2} \right)^N - \left(1 - c - c \frac{w_B}{w_A} \right)^{2N} \right] \right\}^{1/2N} = 1. \quad (17)$$

In particular, for $a = w_B/w_A = 1$, i.e. $|J_B| = J_A = J$, we have

$$w \lim_{N \rightarrow \infty} \{ \mu^{2N} (1 - 2c)^{2N} + \mu^N [1 - (1 - 2c)^{2N}] \}^{1/2N} = 1. \quad (18)$$

From (18) we get

$$\mu^{1/2} w = 1 \quad (19)$$

or $c_1^* < c < c_2^*$ and

$$\mu w |1 - 2c| = 1 \quad (20)$$

for $c < c_1^*$, $c > c_2^*$, where the critical concentrations $c_{1,2}^*$ are determined by the equation $\mu(1 - 2c)^2 = 1$ and are

$$c_{1,2}^* = \frac{1}{2} \mp \frac{1}{2\sqrt{\mu}}. \quad (21)$$

Table 1

lattice	square	honeycomb	s.c.	b.c.c.
$\bar{\mu}$	2.6390	1.8484	4.6826	6.5283
μ	2.4142	1.7321	4.5840	6.4032
c_1^*	0.1782	0.1201	0.2665	0.3024
c_2^*	0.8218	0.8799	0.7335	0.6976

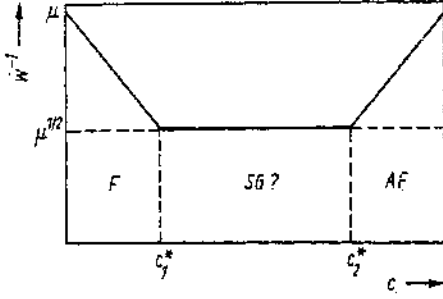


Fig. 3. Phase diagram for the case of $J_A = |J_B|$. F ferromagnetic region, AF antiferromagnetic region, SG spin-glass region (?)

Note, that the result (19) simply means that in the concentration interval $c_1^* < c < c_2^*$ all terms $\approx \mu^N$ in X_N are random in sign (with equal probability!).

For the numerical estimates we use the constant μ which is not the connectivity constant of the lattice, as it should be done in the SAW approximation [11, 14], but instead we use an "Ising constant" μ , which determines the exact critical temperature for the regular case by the relation $\mu w = 1$ [11]. This assures the matching with the regular case for $c = 0;1$, and we hope that such an approximation takes into account qualitatively the role of graphs with cyclomatic number $C > 1$, neglected above. As was noted before (it can be seen also from Table 1, where $\bar{\mu}$ denotes now the connectivity constant), this leads to a rather small change of the results, diminishing slightly the critical temperature. Critical concentrations $c_{1,2}^*$ determined for different lattices are given in Table 1. We assume, that these concentrations correspond to the loss of the long-range ferromagnetic and antiferromagnetic order in the system. The phase diagram is shown in Fig. 3.

In the general case of $w_A \neq w_B$ we obtain from (17)

$$\mu^{1/2} \{(1-c)w_A^2 + cw_B^2\}^{1/2} = 1 \quad (22)$$

for $c_1^* < c < c_2^*$, and

$$\mu \{(1-c)w_A - cw_B\} = 1 \quad (23)$$

for $c < c_1^*$ and $c > c_2^*$, where the critical concentrations $c_{1,2}^*$ are determined by the roots of the equation

$$1 - c + c \frac{w_B^2}{w_A^2} = \mu \left(1 - c - c \frac{w_B}{w_A} \right)^2. \quad (24)$$

In Table 2 we give critical concentrations $c_{1,2}^*$ for different lattices and ratios w_A/w_B . In Fig. 4 the phase diagram of the system for $w_A \neq w_B$ is shown.

Consider finally the case of $w_B \rightarrow 0$, $w_A \neq 0$, i.e. the percolation limit. In this case we obtain from (17)

$$\mu(1-c)w_A = 1 \quad (25)$$

for $c < c^*$, where

$$c^* = 1 - \mu^{-1} \equiv 1 - \tilde{c}^*. \quad (26)$$

For $c > c^*$ the critical temperature is zero, thus $\tilde{c}^* = 1/\mu$ is the critical concentration of the percolation transition, i.e. the critical concentration of the ferromagnetic bonds for the appearance of the long-range ferromagnetic order. In Table 3 we give the values of \tilde{c}^* for the different lattices according to (26), as well as the exact critical

Table 2

lattice		square	honeycomb	s.c.	b.c.c.
$w_B/w_A = 1.5$	c_1^*	0.1234	0.0810	0.1920	0.2214
	c_2^*	0.7595	0.8344	0.6517	0.6098
$w_B/w_A = 2.0$	c_1^*	0.0912	0.0587	0.1465	0.1713
	c_2^*	0.7135	0.8004	0.5928	0.5476
$w_B/w_A = 2.5$	c_1^*	0.0705	0.0446	0.1163	0.1375
	c_2^*	0.6785	0.7743	0.5485	0.5008
$w_B/w_A = 3.0$	c_1^*	0.0562	0.0350	0.0950	0.1135
	c_2^*	0.6508	0.7536	0.5138	0.4646

concentrations for the bond percolation [14]. From these results one may estimate the accuracy of our approach, but one must also remember that classical percolation is relevant for $T = 0$, i.e. strictly speaking it cannot be analysed on the basis of high-temperature expansions.

Our results up to now were obtained from the convergence in probability criterion for the first series in (6) (which consists of terms of random signs). Now we show that the same results follow also from the analysis of the convergence of the series for the average of $\ln \tilde{Z}(\beta)$,

$$\begin{aligned} \langle \ln \tilde{Z}(\beta) \rangle &= \sum_N \sum_i \sum_{\Gamma_N^i} \frac{1}{N} \langle w_{ij} w_{jk} \dots w_{li} \rangle_{\Gamma_N^i} - \\ &\quad - \frac{1}{2} \sum_N \sum_i \sum_{\Gamma_{N/2}^i} \frac{2}{N} \langle w_{ij}^2 w_{jk}^2 \dots w_{li}^2 \rangle_{\Gamma_{N/2}^i} + \dots \end{aligned} \quad (27)$$

The averaging can be performed directly with the help of (10). Analogously to (11) we get

$$\langle w_{ij} w_{jk} \dots w_{li} \rangle_{\Gamma_N^i} = w_A^N \left(1 - c - c \frac{w_B}{w_A} \right)^{N/2}, \quad (28)$$

$$\langle w_{ij}^2 w_{jk}^2 \dots w_{li}^2 \rangle_{\Gamma_{N/2}^i} = w_A^N \left(1 - c + c \frac{w_B^2}{w_A^2} \right)^{N/2}.$$

Then the limit of convergence for the first series in (27) is

$$\mu |(1 - c) w_A - c w_B| = 1 \quad (29)$$

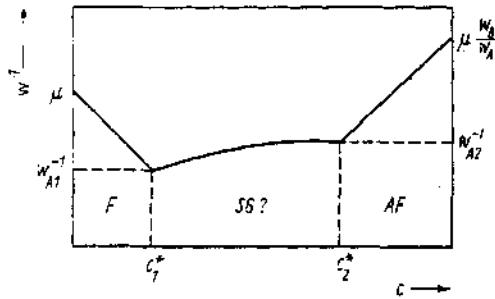


Fig. 4. Phase diagram for the case of $J_A < |J_B|$. Notations are the same as in Fig. 3. $1/w_{A1,2} = (1/2) [\sqrt{4\mu a + (1 - a^2)} \pm (1 - a)]$; $a = w_B/w_A$

Table 3

lattice	square	honeycomb	s.c.	b.c.c.
$\tilde{z}^* = 1/\mu$	0.4142	0.5773	0.2181	0.1561
c^* [14]	0.5000	0.6527	0.2470	0.1780

and for the second series it is given by

$$\mu^{1/2}\{(1-c)w_A^2 + cw_B^2\} = 1. \quad (30)$$

These coincide with (23) and (22), respectively. The convergence of the whole series for $\langle \ln \bar{Z}(\beta) \rangle$ is determined by (29) for $c < c_1^*$, $c > c_2^*$, and by (30) for $c_1^* < c < c_2^*$, where $c_{1,2}^*$ are determined from the condition of equivalence of (29) and (30), which coincides with (24). It is easy to see that the neglected terms of (27) (with triple and other multiple bonds) are irrelevant, because the corresponding series converge if (29) and (30) are satisfied.

Thus the convergence criterion for the averaged high-temperature expansion leads to exactly the same results as the convergence in the probability criterion. During the averaging we were not using the assumption of statistical independence of different paths Γ_N (for $N \gg 1$), and the result obtained confirms the use of this assumption in the analysis of the convergence in probability. The equivalence of both approaches is based in fact on the following theorem [19]: a random series (with independent terms) converges with probability equal to unity, if both the averaged series converge, and the series the terms of which are equal to the dispersions of the terms of the initial series.

4. Discussion

Consider now the physical meaning of the results obtained. Our analysis of the convergence in probability allows one to give a very simple interpretation of these results in terms of distribution of frustrations. It is well known [2, 5, 7, 9] that the model under consideration possesses a local gauge invariance and the statistical mechanics of the model should be expressed in terms of gauge invariant quantities. In our approach this is assured by the closed character of the paths Γ_N^i on the lattice. Consider for simplicity the case of $J_A = |J_B|$ on the square lattice. Then the product of w_{ij} 's along the path Γ_N^i (in the first series in (6)) is equal to

$$w_{ij}w_{jk} \dots w_{li} = w^N \operatorname{sgn} J_{ij}J_{jk} \dots J_{li} = w^N \prod_p \Phi_p, \quad (31)$$

where [2, 7]

$$\Phi_p = \operatorname{sgn} J_{ij}J_{jk}J_{kl}J_{li} \quad (32)$$

is the product of J_{ij} 's around the elementary plaquette ($\Phi_p = \pm 1$). The product of Φ_p 's in (31) is taken over all the plaquettes inside the contour of Γ_N^i . Thus, its sign is positive or negative depending on whether there is an even or odd number of frustrated ($\Phi_p = -1$) plaquettes inside Γ_N^i . As was noted above, for high enough concentration of negative (positive) bonds, greater than $c_1^*(c_2^*)$, the value of $\prod_p \Phi_p$ in (31) is equal to ± 1 with the same probability. This means that in the concentration interval $c_1^* < c < c_2^*$ an odd or an even number of frustrated plaquettes belong to the interior of an arbitrary SAW Γ_N^i ($N \gg 1$) with the same probability. It is natural to assume that in such a situation there is no long-range ferromagnetic or antiferromagnetic order,

which leads to the interpretation of $c_{1,2}^*$ given above. In the previous considerations [2, 5, 7, 9] different aspects of frustration distributions with the variance of c had been discussed, but the interpretation of the instability of long-range order based upon a stochastic parity of frustrated plaquettes inside a closed SAW on the lattice has not been, apparently, given before.

On the basis of our results it seems possible to assume the existence of a spin-glass state in the concentration region $c_1^* < c < c_2^*$, but in fact our approximations are too crude to solve this problem. The SAW-approximation has a tendency to overestimate the critical temperature of the phase transition [11], and also the role of neglected graphs is not very clear in this region (cf. [18]). Our method is based upon the high-temperature expansion and is inapplicable for the discussion of the nature of condensed phases (below the phase-transition line in Fig. 3, 4).

The critical concentrations $c_{1,2}^*$ found above are in good agreement with the results of other authors [3 to 6, 8]. Note, however, that in most of these papers only the case of $J_A = J_B$ was considered for the simplest lattices. Our results coincide with the results of molecular field approximation for the critical temperatures [6] if we replace there the number of nearest neighbours z by the connectivity constant μ and the ratio J/T by $\tanh J/T$, which is typical also for the regular Ising model [11]. However, our results are obtained without any assumptions about the nature of condensed phases, such as an introduction of the Edwards-Anderson order parameter. Note, that the critical concentrations determined above are related to the line of the instability of the paramagnetic state (see Fig. 3, 4), they are naturally different from the similar concentrations for $T = 0$ [6], which cannot be found from the high-temperature expansion. We hope that the accuracy of our results is approximately the same as for the SAW approximation in the regular case [11].

Acknowledgement

The authors are grateful to Prof. Yu. A. Izyumov for his interest in this work.

References

- [1] A. BLANDIN, *J. Physique* **39**, C6-1499 (1978).
- [2] G. TOULOUSE, *Commun. Phys.* **2**, 115 (1977).
- [3] J. VANNINEMUS and G. TOULOUSE, *J. Phys. C* **10**, 537 (1977).
- [4] C. JAYAPRAKASH, J. CHALUPA, and M. WORTIS, *Phys. Rev. B* **15**, 1495 (1977).
- [5] S. KIRKPATRICK, *Phys. Rev. B* **16**, 4630 (1977).
- [6] M. V. MEDVEDEV, *phys. stat. sol. (b)* **86**, 109 (1978).
- [7] E. FRADKIN, B. A. HUBERMAN, and S. H. SHENKER, *Phys. Rev. B* **18**, 4789 (1978).
- [8] G. GRINSTEIN, C. JAYAPRAKASH, and M. WORTIS, *Phys. Rev. B* **19**, 260 (1979).
- [9] H. G. SCHUSTER, *Z. Phys. B* **35**, 163 (1979).
- [10] L. TURBAN and P. GUILMIN, *J. Physique, Lettres* **41**, L-145 (1980).
- [11] C. DOMB, *J. Phys. C* **3**, 258 (1970).
- [12] M. V. SADOVSKII, *Zh. eksper. teor. Fiz.* **80**, 1135 (1981).
- [13] M. E. FISHER, in: *Lectures in Theoretical Physics, Vol. VIIc*, Univ. Colorado Press, Boulder (Colorado) 1965.
- [14] V. K. S. SHANTE and S. KIRKPATRICK, *Adv. Phys.* **20**, 325 (1971).
- [15] P. W. ANDERSON, *Phys. Rev.* **109**, 1492 (1958).
- [16] E. N. ECONOMOU and M. H. COHEN, *Phys. Rev. B* **5**, 2931 (1972).
- [17] C. DOMB, *J. Phys. A* **9**, L17 (1976).
- [18] R. J. CHERRY and C. DOMB, *J. Phys. A* **11**, L5 (1978).
- [19] YU. V. PROKHOROV and YU. A. ROZANOV, *Teoriya Veroyatnostej (Theory of Probability)*, Chap. 5, Sec. 3, Nauka Moskva 1973 (in Russian).

(Received April 20, 1981)

Localization criterion in the field theory of an electron in a random field

M. V. Sadovskii

Institute of the Physics of Metals, Ural Scientific Center, Academy of Sciences of the USSR

(Submitted 2 April 1982)

Zh. Eksp. Teor. Fiz. 83, 1418–1429 (October 1982)

This paper is devoted to a study of the general localization criterion in the field theory of an electron in a random field. We show the equivalence of the Economou-Cohen and the Berezinskiĭ-Gor'kov localization criteria. The general localization criterion is formulated as the requirement of the existence of a pole contribution in the two-particle Green function with a factorizable residue (in momentum space). We search for a solution of this kind on the basis of a study of the homogeneous Bethe-Salpeter equation and in the framework of the instanton approach. We show that the Bethe-Salpeter equation determines the point where the "normal" (metallic) phase becomes unstable. The instanton approach describes the energy region corresponding to the localized phase. In both approaches the critical energy for which the transition occurs (mobility threshold) falls in the "Ginzburg critical region" which goes substantially beyond the framework of the approximations used. Both approaches follow naturally from an effective action formalism, but they reflect different mechanisms for the instability of the normal phase.

PACS numbers: 11.10.St

1. INTRODUCTION

The obvious analogy which exists between the phenomenon of the localization of electrons in disordered systems (Anderson transition) and the usual phase transitions has led to many attempts to construct a field theory for an electron in a random field (see the review¹ and Refs. 2 to 5). The results of these papers are rather contradictory and the general picture of the transition is still not at all clear. In particular, this is true of the problem of the possibility of describing the localization on the basis of some kind of order-parameter representation.

The problem of how the localization manifests itself in the basic quantities with which the theory operates, such as the Green function, has also not been studied sufficiently. This makes the final solution of the problem much more difficult. It is, for example, clear that the problem of the realization of the localization effect itself is, in general, different from the problem of the behavior of the conductivity near the mobility threshold, the solution of which may turn out to be much more complex. The present paper is devoted to an analysis of the general criterion for localization and to some attempts to look for the corresponding solutions from the basic equations of the theory of an electron in a random field.

2. EQUIVALENCE OF ECONOMOU-COHEN AND BEREZINSKIĬ-GOR'KOV LOCALIZATION CRITERIA

We consider noninteracting electrons moving in the field of impurities which are randomly distributed (in a d -dimensional space). Following Berezinskiĭ and Gor'kov⁶ we define the spectral density:

$$\langle\langle \rho_E(\mathbf{r}) \rho_{E+\omega}(\mathbf{r}') \rangle\rangle = \frac{1}{N(E)} \left\langle \sum_{\mathbf{v}} \varphi_{\mathbf{v}}(\mathbf{r}) \varphi_{\mathbf{v}'}(\mathbf{r}) \varphi_{\mathbf{v}'}^*(\mathbf{r}') \varphi_{\mathbf{v}}(\mathbf{r}') \right. \\ \left. \times \delta(E - \varepsilon_{\mathbf{v}}) \delta(E + \omega - \varepsilon_{\mathbf{v}'}) \right\rangle, \quad (1)$$

$$N(E) = \left\langle \sum_{\mathbf{v}} \varphi_{\mathbf{v}}(\mathbf{r}) \varphi_{\mathbf{v}'}^*(\mathbf{r}) \delta(E - \varepsilon_{\mathbf{v}}) \right\rangle \quad (2)$$

is the electron density of states averaged over the configurations of the random potential: $\varphi_{\mathbf{v}}(\mathbf{r})$ and $\varepsilon_{\mathbf{v}}$ are the exact wavefunctions and energy levels of the electron in the field of the impurities, \mathbf{v} is a set of quantum numbers characterizing these states, E is the energy of the electron, and ω is an arbitrary frequency.

According to the localization criterion proposed in Ref. 6 there arises in the range of energies E corresponding to localized states a contribution which has a δ -shape:

$$\langle\langle \rho_E(\mathbf{r}) \rho_{E+\omega}(\mathbf{r}') \rangle\rangle = A_E(\mathbf{r} - \mathbf{r}') \delta(\omega) + \rho_{\mathbf{r}}^E(\mathbf{r} - \mathbf{r}', \omega), \quad (3)$$

or, in the momentum representation,

$$\langle\langle \rho_E \rho_{E+\omega} \rangle\rangle_{\mathbf{q}} = A_E(\mathbf{q}) \delta(\omega) + \rho_{\mathbf{r}}^E(\mathbf{q}, \omega). \quad (4)$$

The second term in (3) or (4) is regular in ω . In the region of delocalized states $A_E(\mathbf{r} - \mathbf{r}') = A_E(\mathbf{q}) = 0$.

As the quantities $A_E(\mathbf{q})$ or $A_E(\mathbf{r} - \mathbf{r}')$ signal the appearance of localized states it is useful to change to their definition in the standard formalism (Green functions). Introducing retarded and advanced averaged Green functions for the electron

$$G^{R,A}(\mathbf{r}\mathbf{r}'E) = \sum_{\mathbf{v}} (\varphi_{\mathbf{v}}(\mathbf{r}) \varphi_{\mathbf{v}'}^*(\mathbf{r}') / (E - \varepsilon_{\mathbf{v}} \pm i\delta)) \quad (5)$$

and using the definition (1) we get immediately

$$\langle\langle \rho_E(\mathbf{r}) \rho_{E+\omega}(\mathbf{r}') \rangle\rangle = \frac{1}{\pi^2 N(E)} \langle \text{Im } G^{R,A}(\mathbf{r}\mathbf{r}'E + \omega) \text{Im } G^{R,A}(\mathbf{r}'\mathbf{r}E) \rangle \\ = \frac{1}{2\pi^2 N(E)} \text{Re} \{ \langle G^R(\mathbf{r}\mathbf{r}'E + \omega) G^A(\mathbf{r}'\mathbf{r}E) \rangle \\ - \langle G^{R,A}(\mathbf{r}\mathbf{r}'E + \omega) G^{R,A}(\mathbf{r}'\mathbf{r}E) \rangle \}, \quad (6)$$

or, in momentum space,

$$\langle\langle \rho_E \rho_{E+\omega} \rangle\rangle_{\mathbf{q}} = \frac{1}{\pi N(E)} \text{Im} \{ \phi^{RA}(E\omega\mathbf{q}) - \phi^{RR}(E\omega\mathbf{q}) \}, \quad (7)$$

where, for simplicity, we have introduced the notation⁷

$$\phi^{RA}(E\omega\mathbf{q}) = -\frac{1}{2\pi i} \sum_{pp'} \langle G^R(\mathbf{p}_+, \mathbf{p}_+ + E + \omega) G^A(\mathbf{p}_-, \mathbf{p}_- - E) \rangle, \quad (8)$$

where $\mathbf{p}_{\pm} = \mathbf{p} \pm \mathbf{q}/2$. The quantities $\phi^{RR}(E\omega\mathbf{q})$ or $\phi^{AA}(E\omega\mathbf{q})$ are defined similarly. One sees easily^{7,8} that as $\mathbf{q} \rightarrow 0$, $\omega \rightarrow 0$ the quantities ϕ^{RR} and ϕ^{AA} behave regularly. It is clear that the singular contribution to (4) corresponding to the appearance of localized states can arise only from the first term in (8). One sees easily that

$$\begin{aligned} A_E(\mathbf{q}) &= \lim_{\delta \rightarrow 0} \frac{1}{N(E)} \delta \text{Im} \phi^{RA}(E\omega + i\delta\mathbf{q})|_{\omega=0} \\ &= \frac{1}{2\pi N(E)} \lim_{\delta \rightarrow 0} \delta \sum_{pp'} \text{Re} \langle G^R(\mathbf{p}_+, \mathbf{p}_+ + E + i\delta) G^A(\mathbf{p}_-, \mathbf{p}_- - E - i\delta) \rangle, \end{aligned} \quad (9)$$

or, in the coordinate representation,

$$A_E(\mathbf{r} - \mathbf{r}') = \frac{1}{2\pi N(E)} \lim_{\delta \rightarrow 0} \delta \langle |G(\mathbf{r}\mathbf{r}'E + i\delta)|^2 \rangle. \quad (10)$$

It is useful to introduce the quantity

$$\begin{aligned} A_E &= A_E(\mathbf{r} - \mathbf{r}')|_{\mathbf{r}=\mathbf{r}'} = \int \frac{d^d\mathbf{q}}{(2\pi)^d} A_E(\mathbf{q}) \\ &= \frac{1}{2\pi N(E)} \lim_{\delta \rightarrow 0} \delta \langle |G(\mathbf{r}\mathbf{r}'E + i\delta)|^2 \rangle|_{\mathbf{r}=\mathbf{r}'}, \end{aligned} \quad (11)$$

which is proportional to the averaged probability that an electron returns to the initial point in coordinate space after infinite time.⁹ Hence it is clear that the general Berezinskii-Gor'kov localization criterion⁶ is equivalent to the generalized Economou-Cohen localization criterion.⁹

3. LOCALIZATION FROM THE BETHE-SALPETER EQUATION

We consider the two-particle Green function

$$\phi_{pp'}(E\mathbf{q}\omega) = -\frac{1}{2\pi i} \langle G^R(\mathbf{p}_+, \mathbf{p}_+ + E + \omega) G^A(\mathbf{p}_-, \mathbf{p}_- - E) \rangle. \quad (12)$$

It is well known that in the framework of perturbation theory it is determined by the Bethe-Salpeter integral equation^{7,8}

$$\begin{aligned} \phi_{pp'}(E\mathbf{q}\omega) &= G^R(E + \omega, \mathbf{p}_+) G^A(E, \mathbf{p}_-) \left\{ -\frac{1}{2\pi i} \delta(\mathbf{p} - \mathbf{p}') \right. \\ &\quad \left. + \sum_{p''} U_{pp''}^E(\mathbf{q}\omega) \phi_{p''p'}(E\mathbf{q}\omega) \right\}, \end{aligned} \quad (13)$$

where $G^{R,A}(E\mathbf{p})$ is the complete averaged retarded (advanced) single-electron Green function, while the irreducible vertex part $U_{pp'}^E(\mathbf{q}\omega)$ is determined by the sum of all graphs which cannot be cut along two lines—an advanced and a retarded one (see Fig. 1, where the dashed line indicates the “interaction” ρV^2 , where ρ is the density of the impurities and V the Fourier transform of the potential of a single impurity, which for the sake of simplicity we assume to be a point impurity).

We consider the problem of whether the solution of Eq. (13) can lead to a two-particle Green function containing singularities corresponding to localization. Starting from

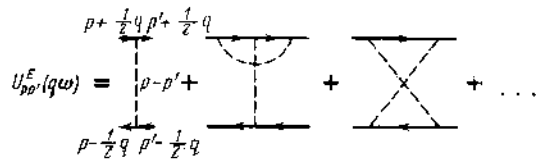


FIG. 1.

the results of the preceding section we assume that in the range of energies E where there exist localized states in the system, $\tilde{\phi}_{pp'}(E\mathbf{q}\omega)$ has the form with a pole

$$\phi_{pp'}(E\mathbf{q}\omega) = -\frac{\psi_{\mathbf{p}'}^{\mathbf{q}}(E) \psi_{\mathbf{p}}^{-\mathbf{q}}(E)}{\omega + i\delta} + \tilde{\phi}_{pp'}(E\mathbf{q}\omega), \quad (14)$$

where $\tilde{\phi}_{pp'}(E\mathbf{q}\omega)$ is the regular part while the factorization of the residue at the pole (in momentum space) is assumed by analogy with the problem of bound states. We give a certain justification for this assumption in that follows.

From (8) and (13) we get at once

$$\phi^{RA}(E\mathbf{q}\omega) = -\frac{\chi_{\mathbf{q}}(E) \chi_{-\mathbf{q}}(E)}{\omega + i\delta} + \sum_{pp'} \tilde{\phi}_{pp'}(E\mathbf{q}\omega), \quad (15)$$

$$\chi_{\mathbf{q}}(E) = \sum_{\mathbf{p}} \psi_{\mathbf{p}}^{\mathbf{q}}(E). \quad (16)$$

It then follows from (9) that

$$A_E(\mathbf{q}) = \frac{1}{N(E)} \chi_{\mathbf{q}}(E) \chi_{-\mathbf{q}}(E). \quad (17)$$

One sees easily that $\chi_{\pm\mathbf{q}}(E) = \chi_{\pm\mathbf{q}}(E)$. From the general property that⁶ $A_E(\mathbf{q} = 0) = 1$ there follows the normalization condition $\chi_{\mathbf{q}}(E) = N^{1/2}(E)$. For the return probability A_E [Eq. (11)] we get

$$A_E = \frac{1}{N(E)} \sum_{\mathbf{q}} \chi_{\mathbf{q}}(E) \chi_{-\mathbf{q}}(E). \quad (18)$$

The basic advantage of the localization criterion (14) formulated here is that when we substitute (14) into (13) the pole term dominates (as $\omega \rightarrow 0$) and we get the homogeneous Bethe-Salpeter equation for $\psi_{\mathbf{p}}^{\mathbf{q}}(E)$:

$$\psi_{\mathbf{p}}^{\mathbf{q}}(E) = G^R(E, \mathbf{p}_+) G^A(E, \mathbf{p}_-) \sum_{\mathbf{p}'} U_{pp'}^E(\mathbf{q}\omega=0) \psi_{\mathbf{p}'}^{\mathbf{q}}(E). \quad (19)$$

It appears that a study of such an equation is appreciably simpler than the solution of the general Eq. (13). Localization would correspond to the appearance of a nontrivial solution $\psi_{\mathbf{p}}^{\mathbf{q}}(E) \neq 0$ of Eq. (19) which would remain nonvanishing in the whole energy range $E < E_c$ where E_c is the mobility threshold. However, it may turn out (and we show in what follows that this is, apparently, the case) that Eq. (19) only gives the threshold E_c itself but does not describe the region $E < E_c$. We assume therefore that Eq. (19) gives a relatively simple method for finding the instability threshold of the “normal” (metallic) state.

It is obvious that an analysis of Eq. (19) in its general form is impossible. It is clear after the appearance of Refs. 10, 11 that at least in the “quasi-metallic” range of two-dimensional systems localization effects are connected with the contribution of the “maximally interesting” graphs for $U_{pp'}^E(\mathbf{q}\omega)$ (Fig. 2):

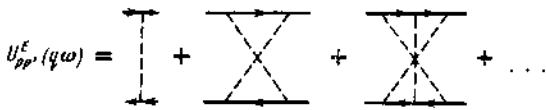


FIG. 2.

$$U_{pp'}^E(q, \omega) = 2\gamma(E)\rho V^2 / (D_0^E(p+p')^2 - i\omega), \quad (20)$$

where $D_0^E = E/md\gamma(E)$ is the classical diffusion coefficient, $\gamma(E)$ is the classical diffusion coefficient, $\gamma(E) = \pi\rho V^2 N(E)$.

In the metallic range Eq. (19) then takes the form

$$\begin{aligned} & \left[E - \frac{1}{2m} \left(\mathbf{p} + \frac{1}{2} \mathbf{q} \right)^2 + i\gamma(E) \right] \\ & \times \left[E - \frac{1}{2m} \left(\mathbf{p} - \frac{1}{2} \mathbf{q} \right)^2 - i\gamma(E) \right] \psi_{pp'}^q(E) \\ & = \lambda(E) \int \frac{d^d \mathbf{p}'}{(2\pi)^d (\mathbf{p} + \mathbf{p}')^2}, \end{aligned} \quad (21)$$

where $\lambda(E) = 2dm\gamma^2(E)\rho V^2/E$. After changing to dimensionless variables $\mathbf{p} \rightarrow \mathbf{p}/(2mE)^{1/2}$ we write Eq. (19) in the symmetrized form

$$\bar{\psi}_{-p}^q(E) = \lambda_\varepsilon \int d^d \mathbf{p}' K_q^E(\mathbf{p}, \mathbf{p}') \bar{\psi}_{p'}^q(E), \quad (22)$$

where

$$\bar{\psi}_{-p}^q(E) = R_q^{-1/2}(\mathbf{p}) \psi_{-p}^q(E),$$

$$R_q(\mathbf{p}) = [1 - (\mathbf{p} - 1/2 \mathbf{q})^2 + i\gamma/E]^{-1} [1 - (\mathbf{p} + 1/2 \mathbf{q})^2 - i\gamma/E]^{-1},$$

$$\lambda_\varepsilon = 4(2\pi)^d m^2 (2mE)^{d/2-3} \lambda(E), \quad (23)$$

while

$$K_q^E(\mathbf{p}, \mathbf{p}') = R_q^{1/2}(\mathbf{p}) R_q^{1/2}(-\mathbf{p}') \frac{1}{|\mathbf{p} - \mathbf{p}'|^2} \quad (24)$$

is a positive-type¹² symmetric (Hermitian) kernel satisfying the inequality

$$K_q^E(\mathbf{p}, \mathbf{p}') < E^2/\gamma^2 |\mathbf{p} - \mathbf{p}'|^2. \quad (25)$$

Hence it is clear that for $2 < d < 4$ the equation considered is an integral equation with a kernel with a weak singularity¹² and certainly possesses a finite (or denumerable) eigenvalue spectrum lying on a section of the real axis with a length determined by the norm of the integral operator. From Enz's theorem¹² it follows that the first eigenvalue of this kernel is positive and simple while the corresponding eigenfunction is everywhere positive definite. Using the boundedness of the integral operator one checks easily that the equation considered does not have any trivial solutions when

$$\lambda_\varepsilon < \left\{ \frac{2\pi^{d/2}}{\Gamma(d/2)} \frac{1}{d-2} \frac{E^2}{\gamma^2} \right\}^{-1}, \quad (26)$$

i.e., when

$$E > \left(\frac{A_d}{d-2} \right)^{2/(4-d)} E_{sc}, \quad (27)$$

where $A_d = 2^{1-d/2} \pi^{-d/2} d/\Gamma(d/2)$ and where we have introduced the characteristic energy

$$E_{sc} = m^{d/(4-d)} (\rho V^2)^{2/(4-d)}. \quad (28)$$

Hence it is clear that for $d = 3$ the corresponding threshold energy falls in the "strong coupling" region $E_{sc} = m^3(\rho V^2)^2$, where the selection we made of diagrams is, generally speaking, invalid^{1,13} and one needs to take all diagrams of the perturbation theory into account. As $d \rightarrow 2$ the range of energies for which there is no solution "takes off" to infinity which means that in that case the mobility threshold $E_c \rightarrow \infty$. In our opinion this result is a rather exact proof of the ideas of a total localization when $d = 2$ (Ref. 10). At the same time one sees easily that inequality (27) gives the analogue of the "Ginzburg critical region"^{1,13} in which higher orders of the perturbation theory are important. Therefore, as $d \rightarrow 2$ simple perturbation theory becomes inapplicable for all energies.

4. LOCALIZATION AND INSTANTONS

In view of the fact that when we describe the region of the localized states itself the approach given above, which is based upon the homogeneous Bethe-Salpeter equation, is, apparently, insufficient, we turn to an alternative approach which enables us to obtain a two-particle Green function of the form (14) in the whole energy range. It is well known^{1,14,15} that the localization phenomenon is closely connected with the appearance (in the appropriate energy range) of nonlinear solutions with a finite action (instantons) of the classical equations of an effective field theory which is associated with the problem of an electron in a random field.¹ We consider in detail the contribution of such solutions to the two-particle Green function.

To evaluate the two-particle electron Green function in a random field we can introduce¹ the following effective Lagrangian:

$$\begin{aligned} \mathcal{L}(\mathbf{r}) = & \frac{1}{2} \sum_{j=1}^n \left\{ \frac{1}{2m} (\nabla \phi_j)^2 - (E + \omega + i\delta) \phi_j^2 \right\} \\ & + \frac{1}{2} \sum_{i=1}^m \left\{ \frac{1}{2m} (\nabla \varphi_i)^2 - (E - i\delta) \varphi_i^2 \right\} \\ & - \frac{1}{8} \rho V^2 \left\{ \left(\sum_{j=1}^n \phi_j^2 \right)^2 + \left(\sum_{i=1}^m \varphi_i^2 \right)^2 + 2 \sum_{j=1}^n \sum_{i=1}^m \phi_j^2 \varphi_i^2 \right\}, \end{aligned} \quad (29)$$

where at the end of the calculations one understands that one must take the limit $n \rightarrow 0, m \rightarrow 0$. Using the qualitative analysis of the classical field equations following from a Lagrangian^{14,15} one can check that when $E < 0, E + \omega > 0$ these equations have a spherically symmetric instanton solution of the form

$$\varphi_{ci}(\mathbf{r}) = \varphi_{ci}(r) e_i, \quad \phi_{ci}(\mathbf{r}) = 0, \quad (30)$$

$$\varphi_{ci}(r) = \left(\frac{2|E|}{\rho V^2} \right)^{1/2} \chi_{ci}(t), \quad r = (2m|E|)^{-1/2} t, \quad (31)$$

where $\chi_{ci}(t) \propto t^{1-d/2} \exp(-t)$ when $t \ll 1, \chi_{ci}'(0) = 0$. In (30) e_i is the unit (m -component) isotopic vector of the field φ .

Considering in the corresponding functional integral contribution connected with the Gaussian fluctuations around classical solution (30) we get

$$\langle G^R(\mathbf{r}\mathbf{r}'; E+\omega+i\delta) G^A(\mathbf{r}'\mathbf{r}; E-i\delta) \rangle \sim \exp\{-S[\varphi_{cl}]\} \\ \times J_L^{d/2}[\varphi_{cl}] J_T^{(m-1)/2}[\varphi_{cl}] \int d^d\mathbf{R}_0 \int d\mathbf{e} \varphi_{cl}(\mathbf{r}'-\mathbf{R}_0) \\ \times \varphi_{cl}(\mathbf{r}-\mathbf{R}_0) \int D\phi \int \tilde{D}\varphi_j(\mathbf{r}) \phi_j(\mathbf{r}') \exp\{-S_0[\phi, \varphi]\}, \quad (32)$$

where $S[\varphi_{cl}] \propto m^{-d/2} |E|^{2d/2} / \rho V^2$ is the classical action on the instanton,

$$J_L[\varphi_{cl}] = \int d^d\mathbf{r} (\nabla \varphi_{cl})^2 \sim m^{-d/2} |E|^{(d-1)/2} / \rho V^2, \\ J_T[\varphi_{cl}] = \int d^d\mathbf{r} \varphi_{cl}^2(\mathbf{r}) \sim m^{-d/2} |E|^{(2-d)/2} / \rho V^2 \quad (33)$$

is the Jacobian of the change to integration over the collective variables \mathbf{R}_0 (center of the instanton) and \mathbf{e} (direction in isotopic space), $S_0[\phi, \varphi]$ is the action describing the Gaussian fluctuations in the vicinity of the instanton solution (φ denotes now the deviation from φ_{cl})

$$S_0[\phi, \varphi] = \int d^d\mathbf{r} (\mathcal{L}_0(\phi) + \mathcal{L}_0(\varphi)), \quad (34)$$

$$\mathcal{L}_0(\varphi) = \sum_i \varphi_i (M_T + i\delta) (\delta_{ij} - e_i e_j) \varphi_j + \sum_j \varphi_j (M_L + i\delta) e_i e_j \varphi_i, \quad (35)$$

$$\mathcal{L}_0(\phi) = \sum_{ij} \phi_i (M_T - \omega - i\delta) \delta_{ij} \phi_j, \quad (36)$$

where

$$M_L = -\frac{1}{2m} \nabla^2 - E - \frac{3}{2} \rho V^2 \varphi_{cl}^2, \\ M_T = -\frac{1}{2m} \nabla^2 - E - \frac{1}{2} \rho V^2 \varphi_{cl}^2. \quad (37)$$

The tilde above the symbol for the functional integration over φ indicates that the zero eigenvalues of the operators M_L and M_T (the "zero modes") which are taken into account through the integration over the collective variables \mathbf{R}_0 and \mathbf{e} must be excluded.

Introducing the eigenfunctions and eigenvalues

$$M_L \Psi_k^L = \lambda_k^L \Psi_k^L, \quad M_T \Psi_k^T = \lambda_k^T \Psi_k^T, \quad (38)$$

we get easily

$$\int D\phi \phi_j(\mathbf{r}) \phi_j(\mathbf{r}') \exp\{-S_0[\phi, \varphi]\} \\ \sim \sum_k \frac{\Psi_k^T(\mathbf{r}-\mathbf{R}_0) \Psi_k^T(\mathbf{r}'-\mathbf{R}_0)}{(\lambda_k^T - \omega - i\delta)^{1+n/2}} \xrightarrow{n \rightarrow 0} \frac{\Psi_0^T(\mathbf{r}-\mathbf{R}_0) \Psi_0^T(\mathbf{r}'-\mathbf{R}_0)}{\omega + i\delta} \\ + \sum_{k \neq 0} \dots \quad (39)$$

where the normalized eigenfunction of the lowest level of the operator M_T ($\lambda_0^T = 0$, the "rotational" zero mode^{14,15}) has the form

$$\Psi_0^T(\mathbf{r}-\mathbf{R}_0) = J_T^{-1/4}[\varphi_{cl}] \varphi_{cl}(\mathbf{r}-\mathbf{R}_0). \quad (40)$$

As a result we get the singular contribution to the two-particle Green function:

$$\langle G^R(\mathbf{r}\mathbf{r}'; E+\omega+i\delta) G^A(\mathbf{r}'\mathbf{r}; E-i\delta) \rangle \\ \sim \frac{i}{\omega+i\delta} \exp\{-S[\varphi_{cl}]\} J_L^{d/2}[\varphi_{cl}] \\ \times J_T^{1/2}[\varphi_{cl}] (|\text{Det}' M_L|)^{-1/2} (\text{Det}' M_T)^{1/2} \\ \times \int d^d\mathbf{R}_0 \varphi_{cl}^2(\mathbf{r}-\mathbf{R}_0) \varphi_{cl}^2(\mathbf{r}'-\mathbf{R}_0). \quad (41)$$

Here $\text{Det}' M_L$ and $\text{Det}' M_T$ do not contain contributions from the zero eigenvalues of the operators M_L and M_T . Cardy¹⁴ was the first to give an expression equivalent to (41) (for $\omega = 0$). Taking into account the sketchy nature of that paper we decided to perform rather detailed calculations. We note that the singular contribution turns out to be connected with the existence of a "zero" rotational mode, i.e., in fact with the symmetry of the system. One may thus expect that this contribution does not vanish even when we take into corrections to the Gaussian approximation.

Taking now the explicit form of the density of states into account which in the energy range considered is determined by a similar instanton contribution^{14,15} we get at once from (10), (11), and (41)

$$A_E(\mathbf{r}-\mathbf{r}') \sim \int d^d\mathbf{R}_0 \varphi_{cl}^2(\mathbf{r}-\mathbf{R}_0) \varphi_{cl}^2(\mathbf{r}'-\mathbf{R}_0) \left[\int d^d\mathbf{r} \varphi_{cl}^2(\mathbf{r}) \right]^{-1}, \quad (42)$$

which is valid up to dimensionless constants. For the return probability we get from this: $A_E \propto |E|^{d/2}$.

Changing to the momentum representation by using

$$\chi_{\mathbf{q}} = \int d^d\mathbf{r} e^{-i\mathbf{q}\mathbf{r}} \varphi_{cl}^2(\mathbf{r}), \quad (43)$$

we get

$$A_E(\mathbf{q}) \sim \tilde{\chi}_{\mathbf{q}} \tilde{\chi}_{-\mathbf{q}}, \quad (44)$$

which reproduces (17). Introducing the Fourier transform of the instanton

$$\varphi_{\mathbf{q}}^{cl} = \int d^d\mathbf{r} e^{-i\mathbf{q}\mathbf{r}} \varphi_{cl}(\mathbf{r}), \quad (45)$$

we see that

$$\tilde{\chi}_{\mathbf{q}} = \int \frac{d^d\mathbf{p}}{(2\pi)^d} \varphi_{\mathbf{p}}^{cl} \varphi_{\mathbf{q}-\mathbf{p}}^{cl}, \quad (46)$$

and comparing this with (16) we get

$$\psi_{\mathbf{p}}^{\mathbf{q}}(E) \sim \varphi_{\mathbf{p}}^{cl}(E) \varphi_{\mathbf{q}-\mathbf{p}}^{cl}(E). \quad (47)$$

The consideration given her is thus in fact a validation, in the framework of the instanton approach, of the above in (14), assumed form of the singular contribution to the two-particle Green function corresponding to localization. The residue in the pole is then expressed in terms of instantons. The region of applicability of the instanton approach is roughly determined by the condition^{14,15} $S[\varphi_{cl}] \gg 1$ which leads to the requirement $|E| \gg E_{sc}$ where E_{sc} is defined in (28) (the necessary refinements will be given in what follows).

5. EFFECTIVE-ACTION FORMALISM

There arises the problem of the relation between the two approaches discussed above for finding the singular part of

the two-particle Green function. We show below that both description methods naturally arise as a manifestation of, in general, different instabilities of the system in the framework of the effective action formalism for the component fields.¹⁶ For the system considered of the fields \varnothing and φ the effective action is¹⁶ a functional Γ of the "classical" (average) values of the fields \varnothing_{cl} and φ_{cl} and of the corresponding Green functions which satisfies the variational principle:

$$\frac{\delta\Gamma}{\delta\varnothing_{cl}(\mathbf{r})} = 0, \quad \frac{\delta\Gamma}{\delta\varphi_{cl}(\mathbf{r})} = 0, \quad \frac{\delta\Gamma}{\delta\hat{G}(\mathbf{r}, \mathbf{r}')} = 0. \quad (48)$$

$$\hat{G}_0^{-1}(\mathbf{r}\mathbf{r}') = \begin{bmatrix} \left\{ -\frac{1}{2m}\nabla^2 - (E + \omega + i\delta) \right\} \delta_{ij} & 0 \\ 0 & \left\{ -\frac{1}{2m}\nabla^2 - (E - i\delta) \right\} \delta_{ij} \end{bmatrix} \times \delta(\mathbf{r} - \mathbf{r}'). \quad (52)$$

According to Ref. 16 with an obvious generalization to the case of two fields we have

$$\Gamma(\Phi_{cl}, \hat{G}) = S(\Phi_{cl}) - \frac{1}{2} \text{Tr} \ln \hat{G}^{-1} - \frac{1}{2} \text{Tr} \{ \hat{G}^{-1} \hat{G} - 1 \} + \mathcal{F}(\Phi_{cl}, \hat{G}), \quad (53)$$

where Tr and ln are understood in the functional sense,¹⁶ i.e., in particular Tr includes all necessary integrations while $\ln \hat{G} = \ln \text{Det} \hat{G}$, \hat{G}^{-1} is the reciprocal of the Green function matrix in the classical field:

$$\hat{G}^{-1}(\mathbf{r}, \mathbf{r}') = \begin{bmatrix} a & b \\ c & d \end{bmatrix} \delta(\mathbf{r} - \mathbf{r}'), \quad (54)$$

where

$$a = \left\{ -\frac{1}{2m}\nabla^2 - (E + \omega + i\delta) - \frac{1}{2}\rho V^2(\phi_{cl}^2 + \varphi_{cl}^2) \right\} \times \delta_{ij} - \rho V^2 \phi_{cl,i} \phi_{cl,j},$$

$$b = -\rho V^2 \phi_{cl,i} \varphi_{cl,j}, \quad c = -\rho V^2 \varphi_{cl,i} \phi_{cl,j},$$

$$d = \left\{ -\frac{1}{2m}\nabla^2 - (E - i\delta) - \frac{1}{2}\rho V^2(\phi_{cl}^2 + \varphi_{cl}^2) \right\} \times \delta_{ij} - \rho V^2 \varphi_{cl,i} \varphi_{cl,j};$$

$$\phi_{cl}^2 = \sum_{j=1}^n \phi_{cl,j}^2, \quad \varphi_{cl}^2 = \sum_{i=1}^m \varphi_{cl,i}^2.$$

The functional $\mathcal{F}(\Phi_{cl}, \hat{G})$ satisfies the conditions

$$\delta\mathcal{F}/\delta\hat{G} = \frac{1}{2}\hat{\Sigma} \quad (55)$$

such that the equation

$$\delta\Gamma/\delta\hat{G} = \frac{1}{2}\hat{G}^{-1} - \frac{1}{2}\hat{G}^{-1}\hat{\Sigma} + \frac{1}{2}\hat{\Sigma} = 0 \quad (56)$$

is simply the Dyson equation while the matrix $\hat{\Sigma}$ consists of the irreducible self-energy parts with dressed internal lines. One can get the formal scheme for calculation $\mathcal{F}(\Phi_{cl}, \hat{G})$ easily by an appropriate generalization of the prescriptions of Ref. 16.

It is convenient to use a matrix notation

$$\Phi = \begin{pmatrix} \varnothing \\ \varphi \end{pmatrix}, \quad \Phi^+ = (\varnothing, \varphi). \quad (49)$$

$$\hat{G} = \begin{bmatrix} G_{\varnothing\varnothing} & G_{\varnothing\varphi} \\ G_{\varphi\varnothing} & G_{\varphi\varphi} \end{bmatrix}, \quad G_{\varnothing\varphi} = G_{\varphi\varnothing}. \quad (50)$$

The Lagrangian (29) can be rewritten in compact form:

$$\mathcal{L}(\mathbf{r}) = \frac{1}{2} \text{Sp} \int d^4\mathbf{r}' \Phi^+ \hat{G}_0^{-1} \Phi - \frac{1}{8\rho} V^2 (\text{Sp} \Phi^+ \Phi)^2. \quad (51)$$

We first consider the "normal" phase in which $\varnothing_{cl} = \varphi_{cl} = 0$ and only the Green functions $G_{\varnothing\varnothing}$ and $G_{\varphi\varphi}$ are nonvanishing. In that case (53) simplifies

$$\Gamma(\hat{G}) = \mathcal{F}(\hat{G}) - \frac{1}{2} \text{Tr} \ln \hat{G}^{-1} - \frac{1}{2} \text{Tr} \{ \hat{G}_0^{-1} \hat{G} - 1 \}. \quad (57)$$

The matrix (54) reduces to (52). A stable system must satisfy the condition $\delta^2\Gamma > 0$ for any variations in Φ_{cl} and \hat{G} . We consider the stability against arbitrary variations of the Green functions in the "normal" phase. We show graphically in Fig. 3 examples of variations of the self-energy parts when the Green functions are varied. Hence one finds, in particular, easily that

$$\frac{\delta^2\Gamma}{\delta G_{\varphi\varphi} \delta G_{\varphi\varphi}} = \frac{1}{2} \frac{\delta G_{\varphi\varphi}^{-1}}{\delta G_{\varphi\varphi}} + \frac{1}{2} \frac{\delta \Sigma_{\varphi\varphi}}{\delta G_{\varphi\varphi}} = -\frac{1}{2} G_{\varphi\varphi}^{-1} G_{\varphi\varphi}^{-1} + \frac{1}{2} U_{\varphi\varphi\varphi\varphi}, \quad (58)$$

etc., where $U_{\varnothing\varphi\varnothing\varphi}$ is the irreducible vertex part in appropriate two-particle channel. The problem of the instability of the system with respect to variations $\delta G_{\varnothing\varphi}$ is of interest to us. In a stable system

$$\text{Tr} \delta G_{\varnothing\varphi} \frac{\delta^2\Gamma}{\delta G_{\varnothing\varphi} \delta G_{\varphi\varphi}} \delta G_{\varphi\varphi} \geq 0. \quad (59)$$

Using $\delta G_{\varnothing\varphi} = G_{\varnothing\varnothing} \psi_{\varnothing\varphi} G_{\varphi\varphi}$ (see Fig. 3) in (59) and (58) we see that the stability threshold of the "normal" phase is given by

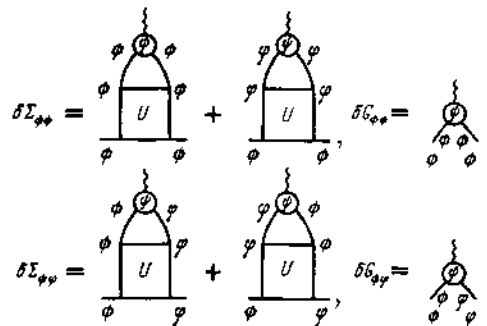


FIG. 3.

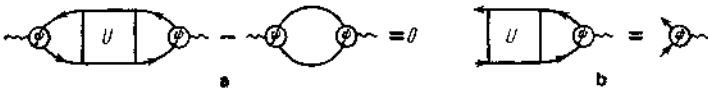


FIG. 4.

the condition

$$\text{Tr } G_{\psi\psi} G_{\phi\phi} U_{\phi\psi\psi} G_{\phi\psi\psi} G_{\psi\psi} - \text{Tr } G_{\psi\psi} G_{\phi\phi} \psi_{\phi\psi} G_{\psi\psi} = 0, \quad (60)$$

which is graphically represented in Fig. 4a. It is fairly obvious that when there appears a nontrivial solution of the homogeneous Bethe-Salpeter Eq. (19) the stability of the system is violated (Fig. 4b).

The analysis given here shows that the appearance of a nontrivial solution of Eq. (19) gives in the general case the

$$G^{-1}(\mathbf{r}\mathbf{r}') = \begin{bmatrix} (M_T - \omega - i\delta) \delta_{ij} & 0 \\ 0 & (M_L + i\delta) e_i e_j + (M_T + i\delta) (\delta_{ij} - e_i e_j) \end{bmatrix} \delta(\mathbf{r} - \mathbf{r}'), \quad (61)$$

and the simplest approximation for $\Gamma(\Phi_{cl}, \hat{G})$ reduces to neglecting in (53) the contribution $\mathcal{F}(\Phi_{cl}, \hat{G})$. In that case (53) gives

$$\begin{aligned} \Gamma(\varphi_{cl}) &= S(\varphi_{cl}) - 1/2 \text{Tr} \ln \tilde{G}_{\phi\psi}^{-1} - 1/2 \text{Tr} \ln \tilde{G}_{\psi\psi}^{-1} \\ &= S(\varphi_{cl}) + \Gamma_1(\varphi_{cl}), \end{aligned} \quad (62)$$

and the equation $\delta\Gamma/\delta\varphi_{cl} = 0$ reduces to

$$-\frac{1}{2m} \nabla^2 \varphi_{cl} - E \varphi_{cl} - \frac{1}{2} \rho V^2 \varphi_{cl}^3 + \frac{\delta\Gamma_1(\varphi_{cl})}{\delta\varphi_{cl}} = 0, \quad (63)$$

which is the generalized equation for instantons leading to the solution (30). Here $\Gamma_1(\varphi_{cl})$ is the result of summing the single-loop corrections to the classical action. Considering in it the term of first order in $\rho V^2 \varphi_{cl}^2$ we get

$$\begin{aligned} \Gamma_1^{(1)}(\varphi_{cl}) &= -\frac{1}{2} \rho V^2 \int d^d \mathbf{r} \varphi_{cl}^2(\mathbf{r}) \int \frac{d^d \mathbf{p}}{(2\pi)^d} \frac{1}{\mathbf{p}^2/2m - E} \\ &= -\frac{1}{2} \delta E \int d^d \mathbf{r} \varphi_{cl}^2(\mathbf{r}), \end{aligned} \quad (64)$$

where δE gives the single-loop "mass" renormalization in the original Lagrangian. Taking for E the already renormalized "mass" we shall assume that the "critical point" corresponds to $E \rightarrow 0$ so that in terms of the "bare mass"

$$E_0 = E - \delta E \xrightarrow{E \rightarrow 0} E_{0c} = -\rho V^2 \int \frac{d^d \mathbf{p}}{(2\pi)^d} \frac{1}{\mathbf{p}^2/2m} = -\rho V^2 2m S_d \frac{p_0^{d-2}}{d-2}, \quad (65)$$

which determines the (in the single-loop approximation) shifted band edge. Here p_0 is the cut-off momentum, $S_d = 2^{-(d-1)} \pi^{-d/2} / \Gamma(d/2)$. Our definition of the shifted band edge differs from the one assumed in Ref. 17. For E we get the equation

$$\begin{aligned} E = E_0 + \delta E = E_0 - E_{0c} - \rho V^2 \\ \times \left[\int \frac{d^d \mathbf{p}}{(2\pi)^d} \frac{1}{\mathbf{p}^2/2m - E} - \int \frac{d^d \mathbf{p}}{(2\pi)^d} \frac{1}{\mathbf{p}^2/2m} \right] \\ = E - E_{0c} + \rho V^2 \pi m S_d (-2mE)^{d/2-1} \left\{ \sin \pi \left(\frac{d}{2} - 1 \right) \right\}^{-1}, \\ 2 < d < 4. \end{aligned} \quad (66)$$

threshold for the stability of the "normal" phase where we are talking about stability with respect to variations $\delta G_{\phi\psi}$. An expansion of the functional $\Gamma(G)$ from (57) in powers of $\delta G_{\phi\psi} \propto \psi_{\phi\psi}$ gives in principle a method to consider the corresponding "condensed" phase while in that case $\psi_{\phi\psi}$ plays the role of the order parameter.

The first two Eqs. (48) are in fact a generalization of the classical field equations following from the Lagrangian (29), (51). The case when they acquire nontrivial solutions of the kind (30) is important for us. The matrix (54) then reduces to

The "Ginzburg criterion" follows¹⁸ from the requirement that the simplest formula $E \approx E_0 - E_{0c}$ be valid which means the equation for the renormalized electron "mass" energy reckoned from the shifted band edge. This is just the meaning of the variable E in that paper and in Refs. 1, 14, 15. It is clear that the equation is satisfied when

$$|E| \gg \left(\frac{B_d}{|\sin(\pi d/2)|} \right)^{2/(4-d)} E_{sc}, \quad 2 < d < 4, \quad (67)$$

where $B_d = 2^{-d/2} \pi^{1-d/2} / \Gamma(d/2)$ while E_{sc} is defined in (28). This inequality which determines the condition for the applicability of our approximation is equivalent, in particular, to the inequality (27) obtained earlier. In the negative energy range it delimits the region beyond which the instanton approach is valid.

From the effective action formalism there follows thus in a natural manner both the instability of the "normal" (metallic) phase which is connected with the appearance of a nontrivial solution of the homogeneous Bethe-Salpeter Eq. (19) and the instability of that phase connected with the appearance of instanton solutions. In the framework of the approximations used these two instabilities remain independent which may, in principle, indicate the existence of two kinds of electron localization. At the same time it is clear that the complete solution of the problem of the relation between the two instabilities requires one to go beyond the framework of the approximations used and to penetrate really the "strong coupling" region. The effective action formalism gives, at least in principle, a convenient apparatus for a joint consideration of these instabilities.

¹M. V. Sadovskii, Usp. Fiz. Nauk **133**, 233 (1981) [Sov. Phys. Usp. **24**, 96 (1981)].

²K. B. Efetov, A. I. Larkin, and D. E. Khmel'nitskii, Zh. Eksp. Teor. Fiz. **79**, 1120 (1980) [Sov. Phys. JETP **52**, 568 (1980)].

³A. J. McKane and M. Stone, Ann. Phys. (N. Y.) **131**, 36 (1981).

⁴G. Parisi, J. Phys. **A14**, 735 (1981).

⁵A. B. Harris and T. C. Lubensky, Phys. Rev. **B23**, 2640 (1981).

⁶V. L. Berezinskii and L. P. Gor'kov, Zh. Eksp. Teor. Fiz. **77**, 2498 (1979)

- [Sov. Phys. JETP **50**, 1209 (1979)].
- ⁷D. Vollhardt and P. Wölfle, Phys. Rev. **B22**, 4666 (1980).
- ⁸S. V. Maleev and B. P. Toperverg, Zh. Eksp. Teor. Fiz. **69**, 1440 (1975) [Sov. Phys. JETP **42**, 734 (1975)].
- ⁹E. N. Economou and M. H. Cohen, Phys. Rev. **B5**, 2931 (1972).
- ¹⁰E. Abrahams, P. W. Anderson, D. C. Licciardello, and T. V. Ramakrishnan, Phys. Rev. Lett. **42**, 673 (1979).
- ¹¹L. P. Gor'kov, A. I. Larkin, and D. E. Khmel'nitskiĭ, Pis'ma Zh. Eksp. Teor. Fiz. **30**, 248 (1979) [JETP Lett. **30**, 228 (1979)].
- ¹²V. S. Vladimirov, *Uravneniya matematicheskoi fiziki* (Equations of Mathematical Physics) Moscow, Nauka, 1967.
- ¹³M. V. Sadovskii, Fiz. Tverd. Tela (Leningrad) **19**, 2334 (1977) [Sov. Phys. Solid State **19**, 1366 (1977)].
- ¹⁴J. L. Cardy, J. Phys. **C11**, L321 (1978).
- ¹⁵M. V. Sadovskii, Fiz. Tverd. Tela (Leningrad) **21**, 743 (1979) [Sov. Phys. Solid State **21**, 435 (1979)].
- ¹⁶J. M. Cornwall, R. Jackiw, and E. Tomnoulis, Phys. Rev. **D10**, 2428 (1974).
- ¹⁷E. Brezin and G. Parisi, J. Phys. **C13**, L307 (1980).
- ¹⁸D. J. Amit, J. Phys. **C7**, 3369 (1974).

Translated by D. ter Haar

Self-consistent theory of localization in $2 \leq d < 4$ dimensions

A. V. Myasnikov and M. V. Sadovskii

Institute of Metal Physics, Ural Scientific Center of the Academy of Sciences of the USSR, Sverdlovsk

(Submitted June 29, 1982)

Fiz. Tverd. Tela (Leningrad) **24**, 3569-3574 (December 1982)

The self-consistent theory of electron localization in disordered systems proposed by Vollhardt and Wölfle [Phys. Rev. B **22**, 4666 (1980)] is generalized to $2 \leq d < 4$ dimensions. The mobility edge position is determined and the critical behavior of various physical quantities in the vicinity of the mobility edge is discussed. It is shown that the description of the vicinity of the mobility edge in a self-consistent theory is outside the range of validity of perturbation theory and, therefore, the results obtained by perturbation theory are only qualitative. The case of $d \geq 4$ is briefly discussed and the frequency dependence of the electrical conductivity for $d = 2$ is also considered.

PACS numbers: 71.55.Jv, 71.10. + x

1. It is well known that there are fundamental difficulties in the consistent description of localization of electrons in disordered systems.¹ In particular, it has not been possible to describe the localization effect itself within the standard formalism based on averaged Green functions. The only exception is the one-dimensional case. In higher dimensions, it has been necessary to resort to nonstandard methods based on the original Anderson paper.² However, it is practically impossible to calculate various physical quantities within the Anderson method.¹ We believe that the recent self-consistent approach to the localization theory developed in Ref. 3 represents an important step toward the solution of the localization problem. The main advantage of this method is its simplicity and standard formulation which make it possible to generalize such a theory to include new scattering mechanisms and the effects of applied fields (see, for example, Refs. 4 and 5). Reference 3 is mainly concerned with the two-dimensional case which is of particular interest in the context of the present theory.¹ The approach of Ref. 3 is particularly suitable in the two-dimensional case since it is based on the summation of a

special class of diagrams^{3,6,7} which dominate the perturbation series for $d = 2$. However, the aforementioned method can be easily generalized to dimensions $d > 2$. It will be shown that such a generalization yields reasonable and qualitatively correct results for all the principal physical quantities of interest near the mobility edge. The position of the mobility edge is also obtained within such theory. After the completion of the present work, Ref. 8 appeared and some of our results are quoted in Ref. 8 (without derivation and discussion). Our aim is to address ourselves to a number of questions which have not been answered satisfactorily in Refs. 3-5 and 8. In particular, we shall demonstrate explicitly that the description of the mobility edge $2 < d < 4$ in dimensions, obtained in the self-consistent theory of localization, is outside the range of validity of the self-consistent theory. We shall also discuss some special features of conduction in two-dimensional systems. The behavior of the theory for $d \geq 4$ is also briefly discussed.

2. The self-consistent theory of Ref. 3 is based on the two-electron Green function averaged over the dis-

$$\varphi_E^{RA}(\omega, \mathbf{q}) = -\frac{1}{2\pi i} \sum_{\mathbf{p}, \mathbf{p}'} \langle G^R(\mathbf{p}_+, \mathbf{p}'_+; E + \omega) G^A(\mathbf{p}'_-, \mathbf{p}_-; E) \rangle, \quad (1)$$

where G_R and G_A are the one-electron Green functions before averaging; E is the electron energy (Fermi energy); ω is the frequency; $\mathbf{p}_\pm = \mathbf{p} \pm (1/2)\mathbf{q}$; and the angular brackets indicate averaging over impurities. The quantity $\varphi_E^{RA}(\omega, \mathbf{q})$ determines the density-density response function and, therefore, the conductivity of the system.

The function $\varphi_E^{RA}(\omega, \mathbf{q})$ can be obtained as the solution of an approximate "transport equation" in the following form (m is the electron mass):

$$\varphi_E^{RA}(\omega, \mathbf{q}) = -N(E) \frac{\omega + M_E(\mathbf{q}, \omega)}{\omega^2 + \omega M_E(\mathbf{q}, \omega) - \frac{2E}{md} q^2}, \quad (2)$$

where $M_E(\mathbf{q}, \omega)$ is the so-called "relaxation kernel."³ In general, the relaxation kernel is determined by the sum of diagrams for the irreducible vertex part in the two-particle (R-A) channel and $N(E)$ is the one-electron density of states.

By considering a self-consistent generalization of the summation of Langer-Neal^{6,7} diagrams which yields the dominant contribution for $d = 2$, Vollhardt and Wölfle³ derived the following self-consistent equation for $M_E(\mathbf{q} = 0, \omega)$:

$$M_E(0, \omega) = \frac{i}{\tau} - 2\rho V^2 \sum_{|\mathbf{k}| < k_0} \frac{1}{\omega - \tau M_E(0, \omega) - \frac{D_0 k^2}{\tau}}, \quad (3)$$

where $1/\tau = 2\pi\rho V^2 N(E)$ is the Born rate of the scattering electrons from impurities which are assumed to be randomly distributed in space with a concentration ρ ; V is the Fourier transform of the impurity potential which is assumed to be completely localized; and $D_0 = 2E\tau/md$ is the classical diffusion coefficient. The choice of the cutoff momentum k_0 in Eq. (3) is discussed below.

The frequency-dependent electrical conductivity of the system is given by³

$$\sigma_E(\omega) = \frac{ne^2}{m} \frac{i}{\omega + M_E(0, \omega)}. \quad (4)$$

It can be seen that $\text{Re } M_E(0, \omega = 0) = 0$ holds in the metallic region.

In the energy range corresponding to localized states, we obtain $\sigma_E(\omega \rightarrow 0) \rightarrow 0$ and the quantity

$$A_E(\mathbf{q}) = \frac{1}{2\pi N(E)} \lim_{\delta \rightarrow 0} \sum_{\mathbf{p}, \mathbf{p}'} \langle G^R(\mathbf{p}_+, \mathbf{p}'_+; E + i\delta) G^A(\mathbf{p}'_-, \mathbf{p}_-; E - i\delta) \rangle = -\frac{1}{N(E)} \lim_{\omega \rightarrow 0} \omega \varphi_E^{RA}(\omega, \mathbf{q}) = \lim_{\omega \rightarrow 0} \frac{\omega M_E(\mathbf{q}, \omega)}{\omega M_E(\mathbf{q}, \omega) - \frac{2E}{md} q^2} \quad (5)$$

which determines the "localization probability" becomes nonzero.^{4,9} For $q \rightarrow 0$, we obtain¹⁰

$$A_E(\mathbf{q}) \approx 1 - q^2 R_{loc}^2(E), \quad (6)$$

where the localization radius $R_{loc}(E)$ is given by

$$R_{loc}^2(E) = \frac{2E}{md\omega_0^2(E)}; \quad \omega_0^2 = -\lim_{\omega \rightarrow 0} \omega M_E(0, \omega) > 0. \quad (7)$$

It follows that the localization is related in the present formalism to the divergence of the relaxation kernel $M_E(0, \omega)$ for $\omega \rightarrow 0$ (see Ref. 3).

The self-consistent equation (3) was studied in Ref. 3 only for $d = 2$. However, it can be easily generalized to arbitrary dimensions d . It is clear that the corresponding results can describe localization only qualitatively since Eq. (3) is based completely on the summation of Langer-Neal diagrams which are important only for $d = 2$. Nevertheless, such calculations are interesting since they yield a simple description of localization in arbitrary dimension and, undoubtedly, describe correctly some features of the localization. The validity of such calculations will be discussed later.

3. Introducing in Eq. (3) a dimensionless integration variable, we can write this equation in the following form which is more suitable for our further calculations:

$$M_E(\omega) = \frac{i}{\tau} + d\lambda x_0^{d-2} M_E(\omega) \int_0^1 dy y^{d-1} \frac{1}{y^2 - \frac{M_E(\omega) \omega d}{4(x_0 E)^2}}, \quad (8)$$

$$\lambda = \frac{1}{2\pi\tau E} = \left(\frac{m}{2\pi}\right)^{\frac{d}{2}} \frac{E^{\frac{d}{2}-2}}{\Gamma\left(\frac{d}{2}\right)} \rho V^2, \quad (9)$$

where λ is a dimensionless coupling constant and $x_0 = k_0/\sqrt{2mE}$. Careful examination of the equations of Ref. 3 [prior to the introduction of $M_E(\mathbf{q}, \omega)$ in Eq. (27) of Ref. 3] indicates that $k_0 \sim p_F \sim \sqrt{2mE}$ (p_F is the Fermi momentum). Such a choice of the cutoff momentum was used in Ref. 3 although the authors of Ref. 3 do not discuss in detail their choice of k_0 (see Ref. 8, where the momentum k_0 in Ref. 4 was chosen differently). We believe that the choice of the cutoff momentum $k_0 \sim p_F \sim \sqrt{2mE}$ is unique and very important for the subsequent estimates. For such a choice, it is clear that $x_0 = \text{const} \sim 1$.

Setting $\omega = 0$ in Eq. (8) and considering the metallic regime $\text{Re } M_E(0, \omega = 0) = 0$, we find that

$$\frac{i}{M_E} = \tau \left(1 - \frac{d}{d-2} \lambda x_0^{d-2}\right). \quad (10)$$

Equations (4) and (13) yield

$$\sigma_E(\omega = 0) = \frac{ne^2}{m} \tau \left\{1 - \left(\frac{E_c}{E}\right)^{\frac{4-d}{2}}\right\}; \quad 2 < d < 4, \quad (11)$$

where

$$E_c = \left\{ \frac{d}{d-2} \frac{x_0^{d-2}}{2\Gamma\left(\frac{d}{2}\right)} (2\pi)^{\frac{d}{2}} \right\}^{\frac{2}{4-d}} E_c. \quad (12)$$

$$E_{sc} = m^{\frac{d}{4-d}} (\rho V^2)^{\frac{2}{4-d}}. \quad (13)$$

It can be seen that E_c plays the role of a mobility edge

$$\sigma_E \approx \frac{ne^2}{m} \tau \left(\frac{4-d}{2}\right) \left(\frac{E-E_c}{E_c}\right); \quad 2 < d < 4 \quad (14)$$

for $E \gg E_c$. Our result (12) is practically identical with the estimate of E_c obtained by another method in Ref. 9. For $d = 3$, the mobility edge E_c lies in the "strong cou-

pling" region $E_{SC} = m^3(\rho V^2)^2$ where the set of diagrams used in the calculation of this quantity is no longer dominant^{1,9} and all the diagrams of perturbation theory should be included. In fact, it follows from Eq. (9) that the condition $E \gg E_{SC}$ is equivalent to the requirement $\lambda \ll 1$, i.e., it represents the simplest condition of validity of perturbation theory. For $d \rightarrow 2$, we obtain $E_c \rightarrow \infty$, which corresponds to the currently accepted view that there is complete localization in two dimensions.^{1,3,9} Moreover, as shown in Ref. 9, it is more important that Eq. (12) defines essentially the dimensions of the "Ginzburg critical region"^{1,9} where higher orders of perturbation theory are important since the geometric factor $(d-2)/(d-4)$ appears in the theory. It follows that, in spite of the fact that the inequality $E_c \gg E_{SC}$ ($\lambda \ll 1$) is satisfied, the mobility edge defined by Eq. (12) falls even for $d \rightarrow 2$ in an energy range where perturbation theory (and the corresponding choice of diagrams used in the present self-consistent theory) is not valid. Nevertheless, it is reasonable to assume that Eq. (12) yields a correct order-of-magnitude estimate of the mobility edge. At the same time, the result (14) implying that the conductivity tends to zero linearly in the limit $E \rightarrow E_c$ cannot be regarded as proved.

We shall now discuss the region of localized states ($E < E_c$). We shall set [see Eq. (7)] $\text{Im} M_E(0, \omega) = 0$ and $\text{Re} M_E(0, \omega) = -\omega_0^2/\omega_0$ and multiply Eq. (8) by ω , which yields in the limit $\omega \rightarrow 0$ the following equation for ω_0^2 :

$$1 = d\lambda x_0^{d-2} \int_0^1 dy \frac{y^{d-1}}{y^2+z}; \quad z = \frac{d\omega_0^2}{4(x_0 E)^2}. \quad (15)$$

The integral in Eq. (15) can be expressed in terms of the hypergeometric function and Eq. (15) then assumes the form

$$1 = \lambda x_0^{d-2} \frac{1}{z} {}_2F_1\left(1, \frac{d}{2}; 1 + \frac{d}{2}; -\frac{1}{z}\right). \quad (16)$$

When the mobility edge is approached from below ($E \rightarrow E_c$), we can expand Eq. (16) in powers of z (small ω_0^2). Simple transformations yield

$$\omega_0^2 = \frac{4}{d} \left\{ \Gamma\left(\frac{d}{2}\right) \Gamma\left(\frac{4-d}{2}\right) \right\}^{-\frac{2}{d-2}} x_0^2 E^2 \left\{ 1 - \left(\frac{E}{E_c}\right)^{\frac{4-d}{2}} \right\}^{\frac{2}{d-2}}; \quad 2 < d < 4. \quad (17)$$

It follows from Eq. (7) that the localization radius is given by

$$R_{loc}(E) = \frac{1}{x_0 \sqrt{2mE}} \left\{ \Gamma\left(\frac{d}{2}\right) \Gamma\left(\frac{4-d}{2}\right) \right\}^{\frac{1}{d-2}} \left\{ 1 - \left(\frac{E}{E_c}\right)^{\frac{4-d}{2}} \right\}^{-\frac{1}{d-2}} \sim \left(\frac{E_c - E}{E_c}\right)^{-\nu}, \quad (18)$$

$E \leq E_c; \quad 2 < d < 4,$

where the critical index of the localization radius is

$$\nu = \frac{1}{d-2}. \quad (19)$$

Equations (19) and (14) indicate that Wegner's scaling relation $s = (d-2)\nu$ is satisfied for the critical conductivity index.¹ The corresponding values of the critical indices describing the behavior of physical quantities near the mobility edge agree with the results obtained in the principal approximation in the $\varepsilon = d-2$ expansion

obtained by the field-theoretic method based on nonlinear σ models (see, for example, Refs. 11-13) and also on the basis of the ε expansion in the qualitative scaling theory.¹⁴ We believe that these results should not be taken too seriously since they were obtained by extrapolations outside the range of validity of perturbation theory and are based on an inconsistent self-consistency procedure. Nevertheless, the self-consistent theory of localization of Ref. 3 is a powerful method since it yields quite simple results that are equivalent to the results obtained by more complex methods.¹¹⁻¹³

4. We shall now discuss the results of the present self-consistent theory for $d \geq 4$. It follows from Eq. (10) that

$$z_E = \begin{cases} \frac{ne^2}{m} \tau \left[1 - \left(\frac{E}{E_c}\right)^{\frac{d-4}{2}} \right] \approx \frac{ne^2}{m} \tau \left(\frac{d-4}{2}\right) \left(\frac{E_c - E}{E_c}\right); & d > 4, \\ \frac{ne^2}{m} \tau \left[1 - \left(\frac{m}{2\pi}\right)^2 x_0^2 V^2 \right]; & d = 4. \end{cases} \quad (20)$$

The solution defined by Eq. (20) for $d > 4$ is clearly not physical since the region of localized states and the metallic region are interchanged. For $d = 4$, we obtain metal conduction and $m^2\rho V^2$ is the dimensionless coupling constant of the four-dimensional theory of Ref. 15. Our treatment is clearly meaningful for $m^2\rho V^2 \ll 1$. [It follows from Eq. (15) that $\omega_0^2 < 0$]. This result also follows since the quantity E_{SC} defined by Eq. (13) tends to zero for $d = 4$ (from below) for $m^2\rho V^2 \ll 1$. The interchange of the metallic region and of the region of localized states for $d > 4$ is a natural consequence of the following fact noted already in Refs. 15 and 16: the perturbation expansion in the present theory is in powers of the parameter $(E/E_{SC})^{(4-d)/2}$ and such an expansion for $d < 4$ diverges in the limit $E \rightarrow 0$; for $d > 4$, it diverges for $E \rightarrow \infty$. No physical behavior of the model for $d > 4$ indicates that a model based on a point interaction (correlation of a random potential of "white noise" type) is not adequate for $d > 4$ (see Ref. 17). The situation changes completely if we assume that the cutoff parameter k_0 in Eq. (3) is determined by the range of the potential (pair correlation function of random potential) rather than by the Fermi momentum i.e., by R_{int} , which implies $k_0 \sim R_{int}^{-1} \ll p_F$ (long-range interactions). For $d < 4$, we obtain the same results as before but the mobility edge is now given by

$$E_c = \frac{d}{d-2} \left(\frac{m}{2\pi}\right)^{d/2} \frac{E_c^{d/2-1}}{\Gamma\left(\frac{d}{2}\right)} \rho V^2; \quad E_0 = \frac{k_0^2}{2m}. \quad (21)$$

For $d \geq 4$, we obtain

$$z \approx \frac{ne^2}{m} \tau \frac{E - E_c}{E_c}, \quad E \gg E_c, \quad (22)$$

$$\omega_0^2 \approx \frac{4}{d} \frac{d-4}{d-2} \left(1 - \frac{E}{E_c}\right). \quad (23)$$

It follows that the critical index of the localization radius is $\nu = 1/2$ for $d > 4$. In this sense, we can regard $d = 4$ as the upper bound on the dimension of space in which localization effect can occur.¹ However, we would like to point out that a choice of k_0 independent of p_F does not follow from the model under study which is applicable to $d < 4$. This important factor has not been discussed in Ref. 8.

5. Finally, we shall quote (in more detail than in Ref. 3) our results on the frequency dependence of the conductivity in the self-consistent theory applying to $d = 2$. A somewhat lengthy but straightforward analysis of Eq. (3) for $d = 2$ indicates that there are several frequency intervals with different behavior of the conductivity. At very low frequencies $\omega \ll (1/\lambda)e^{-1/\lambda}(1/\tau)$, we obtain

$$\sigma_E(\omega) \approx \frac{ne^2}{m} \frac{1}{\tau \lambda} \frac{e^{2/\lambda}}{4(x_0 E)^4} \omega^2, \quad (24)$$

i.e., we obtain insulating behavior.³ At somewhat higher frequencies

$$\sigma_E(\omega) \approx \frac{ne^2}{m} \frac{e^{1/\lambda}}{2(x_0 E)^2} \omega, \quad (25)$$

"Quasimetallic" behavior with logarithmic corrections first derived in Ref. 7 is obtained at frequencies satisfying $(1/\lambda^2)e^{-1/\lambda}(1/\tau) \ll \omega \ll (\lambda^2/\tau)$, i.e.,

$$\sigma_E(\omega) \approx \frac{ne^2}{m} \tau \left(1 - \lambda \ln \frac{1}{\omega \tau}\right). \quad (26)$$

Finally, for $\lambda^2/\tau \ll \omega \ll 1/\tau$, the self-consistent theory yields

$$\sigma_E(\omega) \approx \frac{ne^2}{m} \tau \left(1 - \frac{\tilde{E}_c}{E}\right), \quad (27)$$

where

$$\tilde{E}_c \approx \frac{m}{\pi} \tau V^2 \ln \frac{x_0}{2}. \quad (28)$$

The last result is especially interesting since the conduc-

tivity in this frequency range is essentially constant (dependent of ω) and corresponds to metallic conduct with the mobility edge \tilde{E}_c defined by Eq. (28). It is possible that this result explains the well-known discrepancy between various numerical approaches to the calculation of the two-dimensional conductivity¹: logarithmic corrections and insulating behavior manifest themselves at extremely low frequencies and, at the same time, is an interval of frequencies (since λ is small) in which the system is characterized by a finite mobility edge.

¹M. V. Sadovskii, Usp. Fiz. Nauk **133**, 223 (1981) [Sov. Phys. Usp. (1981)].

²P. W. Anderson, Phys. Rev. **109**, 1492 (1958).

³D. Vollhardt and P. Wölfle, Phys. Rev. B **22**, 4666 (1980).

⁴D. Yoshioka, Y. Ono, and H. Fukuyama, J. Phys. Soc. Jpn. **50**, 34 (1981).

⁵D. Yoshioka, J. Phys. Soc. Jpn. **51**, 716 (1982).

⁶J. S. Langer and T. Neal, Phys. Rev. Lett. **16**, 984 (1966).

⁷L. P. Gor'kov, A. I. Larkin, and D. E. Khmel'nitskii, Pis'ma Zh. Eksp. Teor. Fiz. **30**, 248 (1979) [JETP Lett. **30**, 228 (1979)].

⁸D. Vollhardt and P. Wölfle, Phys. Rev. Lett. **48**, 699 (1982).

⁹M. V. Sadovskii, Zh. Eksp. Teor. Fiz. **83**, 1418 (1982).

¹⁰V. L. Berezinskii and L. P. Gor'kov, Zh. Eksp. Teor. Fiz. **77**, 24 (1979) [Sov. Phys. JETP **50**, 1209 (1979)].

¹¹F. Wegner, Z. Phys. B **35**, 207 (1979).

¹²A. J. McKane and M. Stone, Ann. Phys. (N.Y.) **131**, 36 (1981).

¹³S. Hikami, Phys. Rev. B **24**, 2671 (1981).

¹⁴B. Shapiro and E. Abrahams, Phys. Rev. B **24**, 4025 (1981).

¹⁵M. V. Sadovskii, Fiz. Tverd. Tela (Leningrad) **19**, 2334 (1977) [Solid State **19**, 1366 (1977)].

¹⁶S. F. Edwards, M. B. Green, and G. Srinivasan, Philos. Mag. **35**, 14 (1977).

¹⁷D. J. Thouless, J. Phys. C **9**, L603 (1976).

Translated by D. Mathon

Self-Consistent Theory of Localization for the Anderson Model

E.A. Kotov

Complex Research Institute, Far-Eastern Scientific Research Center,
USSR Academy of Sciences, Blagovestschensk, USSR

M.V. Sadovskii*

Universität Ulm, Federal Republic of Germany

Received January 25, 1983

The self-consistent theory of electron localization in a random system in the form proposed by Vollhardt and Wölfle is generalized for the analysis of localization in the Anderson model. We derive the general equations appropriate for the system with rather general form of the electronic spectrum. Explicit calculations are restricted to the lattices of cubic symmetry and use the effective mass approximation to obtain the final results. Anderson's critical ratio for the localization of all the electronic states in the tight-binding band is evaluated and found to be in surprisingly good agreement with the results of numerical analysis of localization in the Anderson model.

1. Introduction

The phenomenon of electron localization in disordered systems, which is actively studied in recent years [1], usually is described within the framework of the well-known Anderson model [2, 3]. In most of the papers published up to now, either quite non-traditional methods, originating from the classic paper by Anderson [2], or numerical analysis were used. But the few attempts to derive localization via more or less standard formalism of the modern many-particle theory, involving the averaged Green functions, were mostly unsuccessful. Because of this situation we believe, that the development of the so-called self-consistent theory of localization, in the form proposed by Vollhardt and Wölfle [4], deserves a great attention. This approach allows to get rather reasonable description of localization of electronic states in a two-dimensional system ($d=2$), and also at least qualitatively describes the Anderson transition for $d>2$ [5, 6], in close correspondence with the scaling picture of this transition, proposed in the famous paper by Abrahams, Anderson, Licciardello and Ramakrishnan [7]. In papers [4-6] the model of electrons scattered by the randomly distributed point-like scatterers was considered. Thus, due to the existence of rather large number of

references, devoted to the study of localization in the Anderson model (cf. the reviews [1, 8]), it seems to be interesting to generalize the self-consistent theory for the description of localization in this model. The first attempt of this kind was undertaken by Prelovšek [9], in the framework of self-consistent approach proposed by Götze [10]. In this paper we shall concentrate on the study of localization in the Anderson model within the theory of Vollhardt and Wölfle [4].

2. General Equations

The Hamiltonian of the Anderson model in a regular lattice has the form:

$$H = \sum_j E_j a_j^+ a_j + \sum_{ij} V_{ij} a_i^+ a_j \quad (1)$$

where a_j and a_j^+ are the usual destruction and creation operators of the electron at a site j . The energy levels E_j are considered to be independently distributed on different sites of the lattice. The distribution at the given site is usually defined as [2]:

$$P(E_j) = \begin{cases} \frac{1}{W}; & |E_j| < \frac{1}{2}W \\ 0; & |E_j| > \frac{1}{2}W \end{cases} \quad (2)$$

* Permanent address: Institute for Metal Physics, Ural Scientific Research Center, USSR Academy of Sciences, Sverdlovsk, 620219, USSR

corresponding to the homogeneous distribution of energies in the energy interval of the width W . But in the main part of this work we shall assume the Gaussian distribution

$$P(E_j) = \frac{1}{\sqrt{2\pi} \tilde{W}} \exp\left\{-\frac{E_j^2}{2\tilde{W}^2}\right\} \quad (3)$$

which considerably simplifies the corresponding diagram technique. The transfer integral V_{ij} is assumed to be different from zero and equal to a constant V only for the transitions between the sites which are nearest neighbours in the lattice.

After the Fourier transformation (1) can be written as:

$$H = \sum_{\mathbf{p}} \varepsilon(\mathbf{p}) a_{\mathbf{p}}^+ a_{\mathbf{p}} + \sum_{\mathbf{p}\mathbf{q}} U_{\mathbf{q}} a_{\mathbf{p}+\mathbf{q}}^+ a_{\mathbf{p}} \quad (4)$$

where

$$\varepsilon(\mathbf{p}) = V \sum_{\mathbf{h}} e^{i\mathbf{p}\mathbf{h}} \quad (5)$$

is the standard electronic spectrum in a tight-binding approximation [11], and the vector $\mathbf{h}_{ij} = \mathbf{R}_i - \mathbf{R}_j$ defines the positions of the neighboring sites in the lattice (the summation in (5) is assumed over the nearest neighbours). The Gaussian random field $U_{\mathbf{q}}$, entering the second term in (4) (N - is the number of sites in lattice):

$$U_{\mathbf{q}} = \frac{1}{N} \sum_j E_j e^{i\mathbf{q}\mathbf{R}_j} \quad (6)$$

has in the momentum space the correlation function of the following form:

$$\langle U_{\mathbf{q}} U_{\mathbf{q}'} \rangle = \frac{\tilde{W}^2}{N} \delta_{\mathbf{q}, -\mathbf{q}'} = \tilde{W}^2 \Omega_0 \delta_{\mathbf{q}, -\mathbf{q}'} \quad (7)$$

corresponding to the assumed form of correlation of energy levels E_j in the lattice:

$$\langle E_i E_j \rangle = \tilde{W}^2 \delta_{ij}. \quad (8)$$

In (7) Ω_0 is just the volume per single site of the lattice. In the following we are considering the lattices of cubic symmetry and put the total volume of the system equal to unity, which gives $1/N = \Omega_0$ (the volume of primitive cell of the crystal). The higher-order correlation functions in case of the Gaussian random field are factorizable in terms of the pair correlators (7), (8), so that the form of diagram technique for the calculation of the averaged Green functions, corresponding to the Hamiltonian (4), is quite obvious [12].

The derivation of the main equations of the self-consistent theory follows the main steps of [4]. The

only complication is connected with the necessity to take rather general form of the electronic spectrum (5) into account. The formalism is based upon the Bethe-Salpeter equation for the averaged two-particle Green function $\phi_{\mathbf{p}\mathbf{p}'}^{RA}(E\omega\mathbf{q})$, which is used to define the function

$$\begin{aligned} \phi_E(\omega\mathbf{q}) &\equiv \sum_{\mathbf{p}\mathbf{p}'} \phi_{\mathbf{p}\mathbf{p}'}^{RA}(E\omega\mathbf{q}) \\ &= -\frac{1}{2\pi i} \sum_{\mathbf{p}\mathbf{p}'} \langle G^R(\mathbf{p}_+, \mathbf{p}'_+, E+\omega) G^A(\mathbf{p}'_-, \mathbf{p}_-, E) \rangle \\ \mathbf{p}_{\pm} &= \mathbf{p} \pm \frac{1}{2}\mathbf{q}. \end{aligned} \quad (9)$$

The Bethe-Salpeter equation takes the form (for small q)

$$\begin{aligned} \{\omega - \mathbf{q} \cdot \mathbf{v}_{\mathbf{p}} - \Sigma_{\mathbf{p}_+}^R(E+\omega) + \Sigma_{\mathbf{p}_-}^A(E)\} \phi_{\mathbf{p}\mathbf{p}'}^{RA}(E\omega\mathbf{q}) \\ = \Delta G_{\mathbf{p}} \left\{ \frac{1}{2\pi i} \delta_{\mathbf{p}\mathbf{p}'} - \sum_{\mathbf{p}''} U_{\mathbf{p}\mathbf{p}''}^E(\mathbf{q}\omega) \phi_{\mathbf{p}''\mathbf{p}'}^{RA}(E\omega\mathbf{q}) \right\} \end{aligned} \quad (10)$$

where $\mathbf{v}_{\mathbf{p}} = \partial\varepsilon(\mathbf{p})/\partial\mathbf{p}$ is the group velocity of the electron, and

$$\Delta G_{\mathbf{p}} \equiv G^R(E+\omega, \mathbf{p}_+) - G^A(E, \mathbf{p}_-) \quad (11)$$

while the averaged one-electron Green functions are taken in the standard form:

$$G^{R,A}(E\mathbf{p}) = \frac{1}{E - \varepsilon(\mathbf{p}) - \Sigma_{\mathbf{p}}^{R,A}(E)} \approx \frac{1}{E - \varepsilon(\mathbf{p}) \pm i\gamma(E)} \quad (12)$$

where the last expression in (12) is obtained through the ordinary summation of simplest diagrams [12] (without intersecting interaction lines) and

$$\gamma(E) = \pi \tilde{W}^2 \Omega_0 N(E) \quad (13)$$

is just the scattering rate of the electron on the random levels and $N(E)$ - is the one-electron density of states. In Eq. (10) $U_{\mathbf{p}\mathbf{p}'}^E(\mathbf{q}\omega)$ is the irreducible (in two-particle $R-A$ channel) vertex.

Summing both sides of (10) over \mathbf{p} and \mathbf{p}' and using the Ward identity derived in [4], we get the equation for $\phi_E(\omega\mathbf{q})$:

$$\omega \phi_E(\omega\mathbf{q}) - q \phi_j^E(\omega\mathbf{q}) = -N(E) \quad (14)$$

where we have introduced the function:

$$\phi_j^E(\omega\mathbf{q}) = \sum_{\mathbf{p}\mathbf{p}'} (\mathbf{v}_{\mathbf{p}} \cdot \hat{\mathbf{q}}) \phi_{\mathbf{p}\mathbf{p}'}^{RA}(E\omega\mathbf{q}) \quad (15)$$

where $\hat{\mathbf{q}}$ is the unit vector in the direction of \mathbf{q} . To obtain the equation for $\phi_j^E(\omega\mathbf{q})$ we multiply (10) by $\mathbf{v}_{\mathbf{p}} \cdot \hat{\mathbf{q}}$ and sum again over \mathbf{p} and \mathbf{p}' . Then to "close up" the system of equations in terms of the functions $\phi_E(\omega\mathbf{q})$ and $\phi_j^E(\omega\mathbf{q})$ we use the following approxi-

mate relation:^{*}

$$\sum_{\mathbf{p}} \phi_{\mathbf{p}\mathbf{p}'}^{RA}(E\omega\mathbf{q}) \simeq -[2\pi iN(E)]^{-1} \Delta G_{\mathbf{p}} \cdot \sum_{\mathbf{p}'} \left\{ 1 + \frac{(\mathbf{v}_{\mathbf{p}} \cdot \hat{\mathbf{q}})(\mathbf{v}_{\mathbf{p}'} \cdot \hat{\mathbf{q}})}{v_E^2(\hat{\mathbf{q}})} \right\} \phi_{\mathbf{p}\mathbf{p}'}^{RA}(E\omega\mathbf{q}) \quad (16)$$

where

$$v_E^2(\hat{\mathbf{q}}) = -\frac{1}{2\pi iN(E)} \sum_{\mathbf{p}} (\mathbf{v}_{\mathbf{p}} \cdot \hat{\mathbf{q}})^2 \Delta G_{\mathbf{p}} \quad (17)$$

is just the "averaged in the vicinity of the isoenergetic surface $\varepsilon(\mathbf{p})=E$ " square of the projection of the velocity $\mathbf{v}_{\mathbf{p}}$ on the direction of $\hat{\mathbf{q}}$. In the lattices of cubic symmetry (which are the only lattices considered below), due to the isotropy of their physical properties we have:

$$v_E^2(\hat{\mathbf{q}}) \equiv \frac{1}{d} v_E^2 = -\frac{1}{2\pi iN(E)d} \sum_{\mathbf{p}} v_{\mathbf{p}}^2 \Delta G_{\mathbf{p}} \approx \frac{1}{N(E)d} \sum_{\mathbf{p}} v_{\mathbf{p}}^2 \delta(E - \varepsilon(\mathbf{p})) \quad (18)$$

where the last equality is approximately valid in the limit of small disorder.

Then for $\phi_j^E(\omega\mathbf{q})$ we get the following equation:

$$\{\omega + M_E(\mathbf{q}\omega)\} \phi_j^E(\omega\mathbf{q}) - \frac{1}{d} v_E^2 q^2 \phi_E(\omega\mathbf{q}) = 0 \quad (19)$$

where the so called "relaxation kernel" $M_E(\mathbf{q}\omega)$ takes the form:

$$M_E(\mathbf{q}\omega) = \frac{1}{2\pi iN(E)v_E^2} \sum_{\mathbf{p}} v_{\mathbf{p}}^2 \Delta G_{\mathbf{p}} \cdot [\Sigma_{\mathbf{p}_+}^R(E+\omega) - \Sigma_{\mathbf{p}_-}^A(E)] - \frac{d}{2\pi iN(E)v_E^2} \sum_{\mathbf{p}\mathbf{p}'} (\mathbf{v}_{\mathbf{p}} \cdot \hat{\mathbf{q}}) \Delta G_{\mathbf{p}} U_{\mathbf{p}\mathbf{p}'}^E(\mathbf{q}\omega) \Delta G_{\mathbf{p}'} (\mathbf{v}_{\mathbf{p}'} \cdot \hat{\mathbf{q}}) \approx 2i\gamma(E) - \frac{d}{2\pi iN(E)v_E^2} \sum_{\mathbf{p}\mathbf{p}'} (\mathbf{v}_{\mathbf{p}} \cdot \hat{\mathbf{q}}) \Delta G_{\mathbf{p}} U_{\mathbf{p}\mathbf{p}'}^E(\mathbf{q}\omega) \cdot \Delta G_{\mathbf{p}'} (\mathbf{v}_{\mathbf{p}'} \cdot \hat{\mathbf{q}}) \quad (20)$$

where the last equality is valid in the limit of small \mathbf{q} and ω , taking (12) into account.

Solving the system of (14) and (19) we obtain:

$$\phi_E(\omega\mathbf{q}) = -N(E) \frac{\omega + M_E(\mathbf{q}\omega)}{\omega^2 + \omega M_E(\mathbf{q}\omega) - \frac{1}{d} v_E^2 q^2} \quad (21)$$

so that the corresponding density-density response function (cf. Ref. 4) is given by:

* This relation is the natural generalization of (25) in [4] for the case of electrons with the arbitrary spectrum $\varepsilon(\mathbf{p})$

$$\chi_E(\mathbf{q}\omega) = \omega \phi_E(\omega\mathbf{q}) + N(E) = \frac{\frac{1}{d} N(E) v_E^2 q^2}{\omega^2 + \omega M_E(\mathbf{q}\omega) - \frac{1}{d} v_E^2 q^2} \quad (22)$$

Neglecting the ω^2 term in the denominator of (22) we can rewrite $\chi_E(\mathbf{q}\omega)$ in the form:

$$\chi_E(\mathbf{q}\omega) = N(E) \frac{iD_E(\mathbf{q}\omega) q^2}{\omega + iD_E(\mathbf{q}\omega) q^2} \quad (23)$$

where we have introduced the generalized diffusion coefficient:

$$D_E(\mathbf{q}\omega) = \frac{i}{d} \frac{v_E^2}{M_E(\mathbf{q}\omega)} \quad (24)$$

The electrical conductivity is given by (cf. Ref. 4):

$$\sigma_E(\omega) = e^2 \lim_{q \rightarrow 0} \left(-\frac{i\omega}{q^2} \right) \chi_E(\mathbf{q}\omega) = \frac{e^2}{d} N(E) v_E^2 \frac{i}{\omega + M_E(0\omega)} \quad (25)$$

The localization is signalled by the appearance (in the corresponding energy range) of the finite limit for the following expression [3, 6, 13]:

$$A_E(\mathbf{q}) = \frac{1}{2\pi N(E)} \lim_{\delta \rightarrow 0} \sum_{\mathbf{p}\mathbf{p}'} \langle G^R(\mathbf{p}_+ \mathbf{p}'_+ E + i\delta) G^A(\mathbf{p}'_- \mathbf{p}_- E - i\delta) \rangle = -\frac{1}{N(E)} \lim_{\omega \rightarrow 0} \omega \phi_E(\omega\mathbf{q}) = \lim_{\omega \rightarrow 0} \left\{ 1 - \frac{v_E^2 q^2}{d M_E(\mathbf{q}\omega) \omega} \right\}^{-1} \quad (26)$$

For $q \rightarrow 0$ we have [14]:

$$A_E(\mathbf{q}) \approx 1 - q^2 R_{\text{loc}}^2(E) \quad (27)$$

where the localization length is defined by:

$$R_{\text{loc}}^2(E) = \frac{v_E^2}{d \omega_0^2(E)}; \quad \omega_0^2(E) = -\lim_{\omega \rightarrow 0} \omega M_E(0\omega) > 0. \quad (28)$$

It can be seen, that in this formalism the localization phenomenon is connected to the divergence of the "relaxation kernel" $M_E(0\omega)$ for $\omega \rightarrow 0$, which leads to the appearance of the non-zero limit for $\omega_0^2 > 0$ in (28).

In the self-consistent theory of Vollhardt and Wölfle the irreducible kernel $U_{\mathbf{p}\mathbf{p}'}^E(q\omega)$ is taken as a sum of the so called Langer-Neal (or maximally crossed) diagrams [15], which for the model under consid-

ration reduces to:

$$U_{\mathbf{p}\mathbf{p}'}^E(\mathbf{q}\omega) \simeq \frac{2\gamma(E)\tilde{W}^2\Omega_0}{-i\omega + D_0^E(\mathbf{p}+\mathbf{p}')^2} \quad (29)$$

where $D_0^E = \frac{1}{d} \frac{v_E^2}{\gamma(E)}$ is the classical diffusion coefficient, and we assume that $|\mathbf{p}+\mathbf{p}'|$ is small with respect to the characteristic sizes of the Fermi surface. The main idea of the self-consistent approach of the Ref. 4 was the substitution of D_0^E in (29) by the "renormalized" diffusion coefficient defined according to (24). Then Eq. (20) defines the self-consistent equation for $M_E(0\omega)$, which after some transformations can be written as:

$$M_E(0\omega) = \frac{i}{\tau} - 2\tilde{W}^2\Omega_0\theta_E \sum_{\mathbf{k}} \frac{1}{\omega - k^2 D_0^E/M_E(0\omega)\tau} \quad (30)$$

where

$$\theta_E = \frac{2\tilde{W}^2\Omega_0}{v_E^2} \sum_{\mathbf{p}} v_{\mathbf{p}}^2 [\text{Im} G_{\mathbf{p}}(E)]^2 \quad (31)$$

and we have denoted $2\gamma(E) = 1/\tau$. Equation (30) generalizes (42) of [4] for the case of general electronic spectrum $\varepsilon(\mathbf{p})$ in the lattices of cubic symmetry. It is not difficult to write the similar expressions for the lattices of some general symmetry, when the dependence on the direction of the vector \mathbf{q} appears explicitly (cf. (16), (17)).

For $\omega=0$ we get from (25) and (30):

$$\begin{aligned} \sigma_E(0) &= \frac{e^2}{d} N(E) v_E^2 \frac{i}{M_E(00)} \\ &= \frac{e^2}{d} N(E) v_E^2 \tau \left\{ 1 - \frac{2d\tilde{W}^2\Omega_0}{v_E^2} \theta_E \sum_{\mathbf{k}} \frac{1}{k^2} \right\} \end{aligned} \quad (32)$$

defining mobility edge by the relation $\sigma_{E_c}(0) = 0$ we get the equation determining its position E_c :

$$1 = \frac{2d\tilde{W}^2\Omega_0}{v_{E_c}^2} \theta_{E_c} \sum_{\mathbf{k}} \frac{1}{k^2}. \quad (33)$$

In the energy range corresponding to localized states we have [4, 6]: $\lim_{\omega \rightarrow 0} \omega \text{Im} M_E(0\omega) = 0$, $\text{Re} M_E(0\omega) = -\omega_0^2(E)/\omega$, so that from (28) and (30) we can easily find the following equation for $\omega_0^2(E)$:

$$1 = 2\tilde{W}^2\Omega_0\theta_E \sum_{\mathbf{k}} \frac{1}{\omega_0^2(E) + \frac{1}{d} v_E^2 k^2}. \quad (34)$$

For $\omega_0^2(E = E_c) = 0$ it obviously reduces to (33). Remembering that the expression (29) is valid for rather small values of $|\mathbf{p}+\mathbf{p}'|$, we see that the sum-

mation over \mathbf{k} in (30), (32)–(34) should be restricted to the values of \mathbf{k} lying inside of some isoenergetic surface in the momentum space with the characteristic dimensions of the order of "doubled" Fermi surface. In fact it follows automatically from (20), because of two factors of $\Delta G_{\mathbf{p}}$ and $\Delta G_{\mathbf{p}'}$ under the sum over \mathbf{p} and \mathbf{p}' in it, because these factors are rather sharply peaked in the vicinity of the Fermi surface.

3. The Effective Mass Approximation

The above relations are rather general and are valid for the arbitrary electronic spectrum $\varepsilon(\mathbf{p})$, with the only limitation to the lattices of cubic symmetry, which allows not to deal with the anisotropy of physical properties. The actual calculations will be performed with the use of the effective mass approximation, which allows to evaluate all the integrals in momentum space by elementary means. Near the "left" band-edge we have from (5):

$$\varepsilon(\mathbf{p}) \approx -ZV + \frac{\mathbf{p}^2}{2m^*} \quad (35)$$

where Z is the number of nearest neighbours, and the effective mass can be easily evaluated from the known expressions [11] for the electronic tight-binding spectra to be $m^* = 1/2Va^2$ for SC, BCC and FCC lattices (a - is the lattice constant). Using (35) it is shown by direct calculation that θ_E defined in (31) is equal to unity in this approximation. We choose the upper cut-off for the momentum space integration in (30), (32)–(34) equal to $k_0 = x_0 p_F$, where $p_F = \sqrt{2m^* \varepsilon}$ ($\varepsilon = E + ZV$ is the energy distance from the band edge) is the Fermi momentum, $x_0 \simeq 1 \div 2$ (cf. the discussion of the cut-off in Ref. 6). Then, evaluating the integral in (32) for the d -dimensional space we obtain:

$$\begin{aligned} \sigma_E(0) &= \frac{e^2}{d} N(\varepsilon) v_F^2 \tau \left\{ 1 - \frac{d}{d-2} \lambda x_0^{d-2} \right\} \\ &= \frac{e^2}{2\pi d} \frac{v_F^2}{\tilde{W}^2\Omega_0} \left\{ 1 - \frac{d}{d-2} \lambda x_0^{d-2} \right\}; \quad 2 < d < 4 \end{aligned}$$

where

$$\lambda = \frac{1}{2\pi \varepsilon \tau} = \left(\frac{m^*}{2\pi} \right)^{d/2} \frac{\tilde{W}^2\Omega_0}{\Gamma(d/2)} \varepsilon^{\frac{d-4}{2}} \quad (37)$$

is the dimensionless "coupling constant" of this theory [6], $v_F = p_F/m^*$.

Similarly from (33) we get:

$$\left(\frac{\tilde{W}}{V} \right)^2 = \frac{d-2}{d} \Gamma\left(\frac{d}{2}\right) \left(\frac{m^*}{2\pi} \right)^{-\frac{d}{2}} \frac{x_0^{2-d}}{V^2\Omega_0} \varepsilon^{\frac{4-d}{2}}. \quad (38)$$

For the fixed disorder W/V this equation defines $\varepsilon = \varepsilon_c$ - the position of the mobility edge inside the band. For the fixed ε (Fermi energy!) (38) defines the critical ratio $(W/V)_c$, sufficient to localize all the electronic states on the Fermi surface. For the half-filled band $\varepsilon = ZV$ (i.e. $E=0$, corresponding to the standard problem of the localization of the whole band in the Anderson model [2, 3]), and we get:

$$\left(\frac{\tilde{W}}{V}\right)_c^2 = \frac{d-2}{d} \Gamma\left(\frac{d}{2}\right) \left(\frac{m^*V}{2\pi}\right)^{-\frac{d}{2}} \frac{x_0^{2-d}}{\Omega_0} Z^{\frac{4-d}{2}}. \quad (39)$$

For $\tilde{W}/V < (\tilde{W}/V)_c$ we obtain the following expression for the mobility edge

$$\varepsilon_c = \left\{ \frac{d}{d-2} \frac{x_0^{d-2}}{\Gamma(d/2)} (2\pi)^{-\frac{d}{2}} \right\}^{\frac{2}{4-d}} E_{sc} \quad (40)$$

where

$$E_{sc} = (m^*)^{\frac{d}{4-d}} (\Omega_0)^{\frac{2}{4-d}} V^{\frac{4}{4-d}} \left(\frac{\tilde{W}}{V}\right)^{\frac{4}{4-d}} \sim V \left(\frac{\tilde{W}}{V}\right)^{\frac{4}{4-d}} \quad (41)$$

is the energy defining the strong-coupling region [1, 6, 13] for the problem under consideration. When the Fermi energy lowers in the band below this energy, we get $\lambda \sim 1$, and the perturbation theory clearly breaks down.

While comparing our result with the literature on the Anderson model it should be taken into account, that our parameter \tilde{W}^2 is just the dispersion of the Gaussian distribution (3). For the homogeneous law (2) dispersion is equal to $W^2/12$. Thus, for the "Anderson's critical ratio" we obtain*: $(W/V)_c^2 = 12(\tilde{W}/V)_c^2$. In Table 1 we give the numerical values of the critical disorder for the localization of the whole band calculated from (39) for the different three-dimensional cubic lattices, for two different values of the dimensionless cut-off. Despite the obvious crudeness of the theory we get the amazingly good correspondence of these values with the results of numerical calculation for the SC lattice: $(W/V)_c \approx 15$ [16], $(W/V)_c = 19 \pm 0.5$ [17], $(W/V)_c = 16 \pm 0.5$ [18], for the "Anderson's type of disorder", and also with the results of the most accurate analysis of localization within the Anderson approach given by Licciardello and Economou: $(W/V)_c \approx 14.5$ [19]. Also quite reasonable is the agreement with the only known to us result of numerical analysis of

* It is certain, that such a procedure gives only the approximate description of the Anderson's type of disorder (2), because we actually neglect all the perturbation theory diagrams connected with the higher-order cumulants of the random field E_j , which are clearly not equal to zero for the distribution law (2)

Table 1. Critical disorder, corresponding to the localization of the whole band for the Gaussian distribution of energy levels $(\tilde{W}/V)_c$ and for the Anderson's type of distribution of levels $(W/V)_c$, for the lattices of cubic symmetry

Lattice	Z	Ω_0	$(\tilde{W}/V)_c$	$(\tilde{W}/V)_c$	$(W/V)_c$	$(W/V)_c$
			$x_0=1$	$x_0=2$	$x_0=1$	$x_0=2$
SC	6	a^3	5.67	4.01	19.67	13.91
BCC	8	$a^3/2$	8.63	6.10	29.88	21.13
FCC	12	$a^3/4$	13.50	9.55	46.78	33.08

the Gaussian disorder: $(\tilde{W}/V)_c \approx 7$ [20]. We are not aware of any numerical calculations for the BCC and FCC lattices.

In the following we quote only the results for the d -dimensional hypercubic lattices. In particular, for the static conductivity in the half-filled band case we get from (36) ($2 < d < 4$):

$$\sigma = \sigma_{mm} \frac{(\tilde{W}/V) - (\tilde{W}/V)_c}{(\tilde{W}/V)_c}; \quad \left(\frac{\tilde{W}}{V}\right)^2 \lesssim \left(\frac{W}{V}\right)_c^2 = \frac{d-2}{d} \Gamma\left(\frac{d}{2}\right) \frac{x_0^{2-d}}{2^{\frac{d}{2}}} Z^{\frac{4-d}{2}} \quad (42)$$

where we have introduced:

$$\sigma_{mm} = \frac{4Z}{\pi d} \frac{e^2}{a^{d-2}} \left(\frac{V}{\tilde{W}}\right)_c^2 \quad (43)$$

which practically coincides with the Mott's "minimal metallic conductivity" [20]. For $d=3$ and the Anderson's type of disorder we get:

$$\sigma_{mm} \approx 0.013 \frac{e^2}{\hbar a} \approx 10^2 \Omega^{-1} \text{ cm}^{-1} \quad \text{for } a \approx 3A^0.$$

It is curious to note that for $d \rightarrow 2$ $\sigma_{mm} \sim \frac{e^2}{a^{d-2}} \frac{1}{d-2} \rightarrow \infty$, because of $(W/V)_c \rightarrow 0$ (39), which reflects the crossover to the complete localization of the band by the infinitesimal disorder in the two-dimensional system [1, 4-7].

Similarly, for the vicinity of some mobility edge inside the band we obtain:

$$\sigma = \sigma_0 \frac{4-d}{2} \left(\frac{\varepsilon - \varepsilon_c}{\varepsilon_c}\right); \quad \varepsilon \gtrsim \varepsilon_c \quad (44)$$

where

$$\sigma_0 = \frac{e^2 v_F^2}{d} N(\varepsilon) \tau = \frac{n e^2}{m^*} \tau \quad (45)$$

is the ordinary Drude-like conductivity of a metal (n - is the total electron density). This result coincides with that obtained in Ref. 6.

Let us now consider the results, following from (34), limiting ourselves only to the case of the half-filled band and $(\tilde{W}/V) \gtrsim (\tilde{W}/V)_c$, which corresponds to the

localized phase*. In dimensionless variables this equation takes the form (use also (35)):

$$1 = d \lambda x_0^{d-2} \int_0^1 dy \frac{y^{d-1}}{y^2 + Z^2}; \quad Z_E^2 = \frac{d \omega_0^2(E)}{2m^* \varepsilon v_F^2 x_0^2}. \quad (46)$$

All the calculations are similar to that done in Ref. 6, so that using $\varepsilon = ZV$, $m^* = (2Va^2)^{-1}$ and $v_F^2 = 4ZVa^2$, we obtain: ($2 < d < 4$)

$$\begin{aligned} \omega_0^2(\varepsilon = ZV) &= \frac{4}{d} \left\{ \frac{d}{d-2} \Gamma\left(\frac{d}{2}\right) \Gamma\left(2 - \frac{d}{2}\right) \right\}^{-\frac{2}{d-2}} Z^2 V^2 x_0^2 \\ &\cdot \left\{ 1 - \frac{(\tilde{W}/V)_c^2}{(\tilde{W}/V)^2} \right\}^{\frac{2}{d-2}} \\ &\approx \frac{4}{d} \left\{ \frac{d}{d-2} \Gamma\left(\frac{d}{2}\right) \Gamma\left(2 - \frac{d}{2}\right) \right\}^{-\frac{2}{d-2}} \\ &\cdot Z^2 V^2 x_0^2 \left\{ 2 \frac{(\tilde{W}/V) - (\tilde{W}/V)_c}{(\tilde{W}/V)_c} \right\}^{\frac{2}{d-2}}. \end{aligned} \quad (47)$$

From (28) and (47) we get the following expression for the localization length in the center of the band:

$$R_{\text{loc}}(\varepsilon = ZV) \approx a \left\{ 2 \frac{(\tilde{W}/V) - (\tilde{W}/V)_c}{(\tilde{W}/V)_c} \right\}^{-\frac{1}{d-2}} \quad (48)$$

so that the critical exponent for the localization length in the self-consistent theory is:

$$\nu = \frac{1}{d-2} \quad (49)$$

also for the Anderson transition in the center of the band (Cf. Refs. 5, 6). From (49) and (42) it is seen that Wegner's scaling law $s = (d-2)\nu$ for the conductivity exponent is also satisfied.

Thus, the critical behaviour at the mobility edge in the self-consistent approach to the Anderson model is the same, as in the model of free electrons, scattered by the random impurities [6]. Also valid are all the remarks concerning the inapplicability of perturbation theory in the vicinity of the mobility edge made in Ref. 6. Thus, the results obtained may give at best only the qualitative description of the Anderson transition (this is especially so for the critical exponents).

Finally, let us briefly analyze the two-dimensional case, when there is a total localization of the band, even for small disorder [1, 4-7]. Dealing again only with the localization in the middle of the band ($\varepsilon = ZV$) and solving the (46), we find:

* For $\varepsilon \geq \varepsilon_c$, i.e. in the vicinity of some mobility edge inside the band (34) essentially gives the same results, as obtained in [6], because of effective mass approximation (35)

$$\omega_0^2(\varepsilon = ZV) = 2Z^2 V^2 x_0^2 \exp \left\{ -2Z \left(\frac{V}{\tilde{W}} \right)^2 \right\} \quad (50)$$

so that for the localization length in the center of the band of a square ($Z=4$) lattice we get:

$$\begin{aligned} R_{\text{loc}}(\varepsilon = ZV) &= aV \sqrt{2Z} \omega_0^{-1}(\varepsilon = ZV) \\ &= \frac{a}{2x_0} \exp \left\{ 4 \left(\frac{V}{\tilde{W}} \right)^2 \right\}. \end{aligned} \quad (51)$$

De-Broglie wave length for the electron in this case is $\sim a/2$ and from (51) it is clearly seen, that R_{loc} grows exponentially, starting with the value of $a/2$ with \tilde{W}/V diminishing from $(\tilde{W}/V)_c^2 = 4/\ln x_0$, which gives $(\tilde{W}/V)_c \simeq 2.40$ for $x_0 = 2$. Note, that the value of $(\tilde{W}/V)_c$ defined in this way is rather sensitive to the change of x_0 in the interval $1 \leq x_0 \leq 2$. It is probable, that such a behaviour "explains" the results of most numerical calculations, giving for $d=2$ the finite value of Anderson's critical ratio $(W/V)_c \simeq 6$ [16, 22-24] for the square Anderson lattice (Cf. the similar behaviour of the frequency dependent conductivity, discussed in [6], and giving a kind of a "quasitransition" at a finite "mobility edge").

The authors appreciate the useful discussions with A.V. Myasnikov at the initial stages of this work. One of the authors (M.V.S.) expresses his deep gratitude to Prof. W. Wonneberger for the hospitality, extended to him during his stay at the University of Ulm, where this paper has been completed.

Appendix

The above discussion is slightly imprecise. The reason for this is that the parameter E in the second equality in (12) is, in fact, a "renormalized" energy, which includes $\text{Re} \Sigma^{R,A}(E)$, defined in the simplest approximation, taking into account the diagrams with no intersecting interaction lines [12]. This leads to the shift of the band edge, due to the interaction with random field. We have:

$$\Sigma^{R,A}(E_0) = \tilde{W}^2 \Omega_0 \int \frac{d^d \mathbf{p}}{(2\pi)^d} \frac{1}{E_0 - \Sigma^{R,A}(E_0) - \varepsilon(\mathbf{p})} \quad (52)$$

where E_0 denotes the "bare" energy. Defining:

$$E(E_0) = E_0 - \text{Re} \Sigma^{R,A}(E_0)$$

we can rewrite (52) in the form:

$$\begin{aligned} E_0 - E(E_0) + i \text{Im} \Sigma^{R,A}(E_0) &= \tilde{W}^2 \Omega_0 \int \frac{d^d \mathbf{p}}{(2\pi)^d} \frac{1}{E(E_0) - \varepsilon(\mathbf{p}) - i \text{Im} \Sigma^{R,A}(E_0)}. \end{aligned} \quad (53)$$

In terms of the "bare" energy the band edge E_{0c} is defined from the obvious condition of the vanishing density of states:

$$N(E_0) = \mp \frac{1}{\pi} \int \frac{d^d \mathbf{p}}{(2\pi)^d} \text{Im} G^{R,A}(E_0, \mathbf{p}) \xrightarrow{E_0 \rightarrow E_{0c}} 0$$

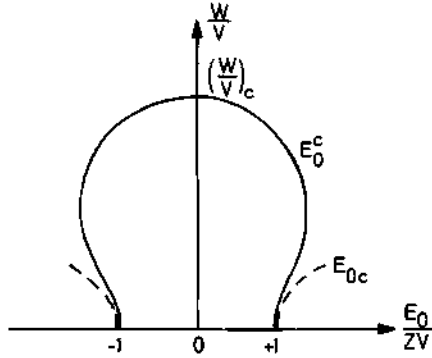


Fig. 1. "Mobility edge trajectory". Broken line shows the position of the band edge

which for our model is equivalent to the condition:

$$E(E_0) \xrightarrow{E_0 \rightarrow E_{0c}} -ZV; \quad \text{Im} \Sigma^{R,A}(E=E_{0c}) \equiv 0. \quad (54)$$

We consider here the "left" edge of the band. Then, from (53) and (54) we obtain the equation defining E_{0c} :

$$E_{0c} = -ZV - \tilde{W}^2 \Omega_0 \int \frac{d^d \mathbf{p}}{(2\pi)^d} \frac{1}{ZV + \varepsilon(\mathbf{p})}. \quad (55)$$

Analogous treatment for the free-electron case was given in [13]. In the simplest approximation (35) we get:

$$\begin{aligned} E_{0c} &= -ZV - \tilde{W}^2 \Omega_0 \int \frac{d^d \mathbf{p}}{(2\pi)^d} \frac{1}{\mathbf{p}^2/2m^*} \\ &= -ZV - \tilde{W}^2 \Omega_0 S_d \frac{2m^* p_0^{d-2}}{d-2} = -ZV - \frac{\tilde{W}^2 S_d}{V} \frac{1}{d-2}. \end{aligned} \quad (56)$$

where we have introduced the upper cut-off $p_0 = 1/a$, and the last equality in (56) is written for hypercubic lattice, so that $\Omega_0 = a^d$, $m^* = (2Va^2)^{-1}$ and $S_d = 2^{-(d-1)} \pi^{d/2} / \Gamma(d/2)$.

Remember now, that the parameter ε , entering (38) is actually the distance from the physical band edge: $\varepsilon = E_0 - E_{0c}$. Then, from (38) and (40) we obtain the equation, defining the mobility edge position E_0^c in terms of the "bare" energy. For hypercubic lattice we get:

$$E_0^c - E_{0c} = \left\{ \frac{d}{d-2} \frac{x_0^{d-2}}{\Gamma(d/2)} (4\pi)^{-\frac{d}{2}} \right\}^{\frac{2}{4-d}} V \left(\frac{\tilde{W}}{V} \right)^{\frac{4}{4-d}} \quad (57)$$

and for $d=3$, using (56) we find:

$$\frac{E_0^c}{ZV} = -1 - \frac{1}{2\pi^2 Z} \left(\frac{\tilde{W}}{V} \right)^2 + \left(\frac{3x_0^2}{4\pi^2} \right)^2 \frac{1}{Z} \left(\frac{\tilde{W}}{V} \right)^4 \quad (58)$$

defining the "mobility edge trajectory", shown in Fig. 1 (the picture is just the same near the "right" band edge), which is similar to that obtained in the Anderson's approach to localization [3, 22]. If we let $E_0^c = 0$ in (58), we get a biquadratic equation, determining the critical ratio $(\tilde{W}/V)_c$ for the complete localization of the band, taking the shift of the band

edge into account. The elementary solution, for $x_0 = 2$ and $Z=6$ (sc lattice) gives $(\tilde{W}/V)_c \simeq 4.15$. Comparing this with the corresponding value in Table 1 shows that the influence of the shift of the band edge is rather small, which justifies the simple approach, used in the main part of this paper.

References

1. Sadovskii, M.V.: Usp. Fiz. Nauk **133**, 223 (1981) (Sov. Phys. Usp. **24**, 96 (1981))
2. Anderson, P.W.: Phys. Rev. **109**, 1492 (1958)
3. Economou, E.N., Cohen, M.H.: Phys. Rev. **B5**, 2931 (1972)
4. Vollhardt, D., Wölfle, P.: Phys. Rev. **B22**, 4666 (1980)
5. Vollhardt, D., Wölfle, P.: Phys. Rev. Lett. **48**, 699 (1982)
6. Myasnikov, A.V., Sadovskii, M.V.: Fiz. Tverd. Tela. **24**, 3569 (1982)
7. Abrahams, E., Anderson, P.W., Licciardello, D.C., Ramakrishnan, T.V.: Phys. Rev. Lett. **42**, 673 (1979)
8. Thouless, D.J.: Phys. Rep. **13**, 93 (1974)
9. Prelovšek, P.: Phys. Rev. **B23**, 1304 (1981)
10. Götze, W.: J. Phys. **C12**, 1279 (1979)
11. Anselm, A.I.: Vvedeniye v Fiziku Poluprovodnikov (Introduction to the Physics of Semiconductors). Chap. IV (in Russian). Moscow: "Nauka" 1978
12. Edwards, S.F.: Philos. Mag. **8**, 1020 (1958)
13. Sadovskii, M.V.: Zh. Eksp. Theor. Fiz. **83**, 1418 (1982)
14. Berezinskii, V.L., Gorkov, L.P.: Zh. Eksp. Theor. Fiz. **77**, 2498 (1978)
15. Langer, J.S., Neal, T.: Phys. Rev. Lett. **16**, 984 (1966)
16. Kramer, B., Mac Kinnon, A., Weaire, D.: Phys. Rev. **B23**, 6357 (1981)
17. Pichard, J., Sarma, G.: J. Phys. **C14**, L127, L617 (1981)
18. Mac Kinnon, A., Kramer, B.: Phys. Rev. Lett. **47**, 1546 (1981)
19. Licciardello, D.C., Economou, E.N.: Phys. Rev. **B11**, 3697 (1975)
20. Domany, E., Sarker, S.: Phys. Rev. **B23**, 6018 (1981)
21. Mott, N.F., Davis, E.A.: Electronic processes in non-crystalline materials. Oxford: Clarendon Press 1979
22. Licciardello, D.C., Thouless, D.J.: Phys. Rev. Lett. **35**, 1475 (1975)
23. Stein, J., Krey, U.: Z. Phys. B - Condensed Matter **34**, 287 (1979)
24. Lee, P.A.: Phys. Rev. Lett. **42**, 1492 (1979)

E.A. Kotov
Complex Research Institute
Far-Eastern Scientific
Research Center
USSR Academy of Sciences
Blagovestschensk, Amur obl.
USSR

M.V. Sadovskii
Institute for Metal Physics
Ural Scientific Research Center
USSR Academy of Sciences
Sverdlovsk, 620219
USSR

Note Added in Proof

We should like to add two important references which recently became known to us. The comprehensive survey of self-consistent diagrammatic theory of localization is given by Wölfle, P., Vollhardt, D.: Anderson localization. In: Springer Series in Solid State Sciences. Nagaoka, Y., Fukuyama, H. (eds.), Vol. 39, p. 26. Berlin, Heidelberg, New York: Springer-Verlag 1982. Localization in Anderson model within the self-consistent approach was also treated by Götze, W.: In: Recent developments in condensed matter. Devreese, J.T. (ed.), Vol. 1, p. 133. New York, London: Plenum Press 1981.

Density of states and screening near the mobility threshold

M. I. Katsnel'son and M. V. Sadovskii

Institute of Metal Physics, Ural Scientific Center, USSR Academy of Sciences

(Submitted 21 June 1983; resubmitted 22 March 1984)

Zh. Eksp. Teor. Fiz. **87**, 523–536 (August 1984)

The Hartree-Fock corrections to the density of states and to the thermodynamic quantities near the mobility threshold, necessitated by the interaction between the electrons, are calculated within the framework of the formalism of exact eigenfunctions. Principal attention is paid to the region of localized states. The "localization" corrections directly connected with the electron-return probability are found. Using a self-consistent localization theory, the known results of Aronov and Al'tshuler are generalized to include the case of an insulator. The localization contribution to the polarization operator, corresponding to a non-ergodic behavior of the system and leading to a difference between the isothermal and adiabatic responses, is considered. It is shown that the static isothermal dielectric constant has a metallic behavior and corresponds to a finite screening radius also in the dielectric "phase," whereas both the high-frequency and the adiabatic responses are described by expressions that are typical for dielectrics.

1. INTRODUCTION

In the theoretical study of electron localization in disordered systems, which is attracting so much attention of late, interelectron-interaction effects are usually disregarded.¹ Yet it is known that an important role is played by these effects both in metals with small impurity density,^{2,3} and for electrons in strongly localized states.^{4,5} In a number of recent approaches^{6–11} to metal-insulator transitions in disordered systems attempts are made to take the influence of interelectron interaction into account. All these studies deal only with the metallic (or quasimetallic in the case of two-dimensional systems) "phase" in the vicinity of the Anderson (or Mott) transition, and the insulator phase is disregarded. The role of interelectron interactions for localized electrons was considered, besides the already mentioned Refs. 4 and 5, only in various attempts to develop a theory for Fermi glasses.^{12,13} All these studies demonstrate the important, if not decisive, role of correlations in the description of metal-insulator transitions in disordered systems. At the same time, the results of these studies are highly contradictory and the problem is still far from completely solved. There is even no clear answer to such a fundamental question as the possible existence of localization itself in systems with interaction. The situation is aggravated by the known difficulties¹ that arise in the theoretical description of the Anderson transition even in the one-electron application.

This being the situation, it makes sense to analyze first the case of weak interaction for strong disorder, as an attempt to determine which physical processes are particularly strongly influenced by the correlation. The present paper is devoted to the first-order perturbation-theory corrections to the density of states and to certain other characteristics of the system in the vicinity of the Anderson transition; principal attention will be paid to the region of localized state. In this sense, an attempt is made here to extend and generalize the known results of Aronov and Al'tshuler² for the metallic phase to include also the insulator state. We shall employ mainly the method proposed in Ref. 14 to derive the main

results of Ref. 2. We shall regard the Anderson single-electron problem as solved, and for many actual calculations we shall use the self-consistent localization theory in the variant proposed by Vollhardt and Wölfle,¹ which comprises apparently a qualitatively correct interpolation analysis scheme that permits a description of the entire region of the transition from a metallic into a localized phase.^{16–18}

2. GENERAL RELATIONS

Regarding the single-electron problem as solved, we introduce a complete orthonormalized system of exact wave functions $\varphi_\nu(\mathbf{r})$ and the corresponding eigenvalues of the electron energy in the random field of a disordered system. These functions and energies can correspond to both localized and delocalized states. We consider the single-electron causal Green's function in the representation of these exact eigenfunctions, particularly its diagonal matrix element

$$G_{\nu\nu}(\varepsilon) = \langle \nu | (\varepsilon - H + i\delta \operatorname{sign} \varepsilon)^{-1} | \nu \rangle, \quad (1)$$

where H is the total Hamiltonian that takes the interelectron interaction into account and ε is the energy reckoned from the Fermi level. The influence of the interaction is taken into account by introducing a corresponding self-energy part $\Sigma_\nu(\varepsilon)$ (Refs. 12–14).

$$G_{\nu\nu}(\varepsilon) = [\varepsilon - \varepsilon_\nu - \Sigma_\nu(\varepsilon)]^{-1}, \quad \Sigma_\nu(\varepsilon) = \Delta_\nu(\varepsilon) + i\Gamma_\nu(\varepsilon) \operatorname{sign} \varepsilon. \quad (2)$$

Following the standard procedure^{14,19} we introduced the renormalized energy $\tilde{\varepsilon}_\nu$ as the solution of the equation

$$\tilde{\varepsilon}_\nu - \varepsilon_\nu - \Delta_\nu(\tilde{\varepsilon}_\nu) = 0, \quad (3)$$

and represent (2) at $\varepsilon \approx \tilde{\varepsilon}_\nu$ in the form

$$G_{\nu\nu}(\varepsilon) = Z_\nu [\varepsilon - \tilde{\varepsilon}_\nu + i\gamma_\nu \operatorname{sign} \varepsilon]^{-1}, \quad (4)$$

where

$$Z_\nu = \left[1 - \frac{\partial \Delta_\nu(\varepsilon)}{\partial \varepsilon} \right]_{\varepsilon = \tilde{\varepsilon}_\nu}^{-1}, \quad \gamma_\nu = Z_\nu \Gamma_\nu(\varepsilon = \tilde{\varepsilon}_\nu). \quad (5)$$

We introduce 14 the self-energy part $\tilde{\Sigma}_E(\varepsilon)$ averaged over some equal-energy surface $E = \varepsilon_\nu$ and over the configuration of the disordered-system random field that defines

the single-electron problem:

$$\Sigma_E(\varepsilon) = \bar{\Delta}_E(\varepsilon) + i\Gamma_E(\varepsilon) = N_0^{-1}(E) \left\langle \sum_{\nu} \delta(E - \varepsilon_{\nu}) \Sigma_{\nu}(\varepsilon) \right\rangle, \quad (6)$$

where the angle brackets denote the aforementioned configuration averaging and $N_0(E)$ is the single-electron (averaged) density of states.

We shall be interested in the single-electron density of states with account taken of the interaction; we define this state in the usual fashion

$$N(E) = -\pi^{-1} \left\langle \sum_{\nu} \text{Im} G_{\nu\nu}^R(E) \right\rangle. \quad (7)$$

Assuming the corrections for the interaction to be small, $\gamma_{\nu} \ll \varepsilon_{\nu} \sim \bar{\varepsilon}_{\nu}$, it is easy to verify that in first-order approximation

$$\frac{\delta N(E)}{N_0(E)} = \frac{N(E) - N_0(E)}{N_0(E)} \approx -\frac{\partial \bar{\Delta}_E(\bar{\varepsilon}_{\nu})}{\partial E} + \frac{\partial \bar{\Delta}_E(\bar{\varepsilon}_{\nu})}{\partial \bar{\varepsilon}_{\nu}}. \quad (8)$$

For reasons explained below we shall call the quantity

$$\frac{\delta \bar{N}(E)}{N_0(E)} = -\frac{\partial \bar{\Delta}_E(\bar{\varepsilon}_{\nu})}{\partial E} \quad (9)$$

the correction to the thermodynamic density of states. This density of states was first introduced in Ref. 14 (see also Ref. 8).

3. CORRECTIONS FOR INTERACTION: CONTRIBUTION FROM LOCALIZATION

We shall consider hereafter a model problem in which the interelectron interaction is described by a static repelling potential with a finite effective radius:

$$H_{int} = \frac{1}{2} \int dx \int dx' \times \sum_{\mu\nu\mu'\nu'} \varphi_{\mu}^*(\mathbf{r}') \varphi_{\nu}^*(\mathbf{r}) v(\mathbf{r}-\mathbf{r}') \varphi_{\mu'}(\mathbf{r}) \varphi_{\nu'}(\mathbf{r}') a_{\mu}^+ a_{\nu}^+ a_{\mu'} a_{\nu'}. \quad (10)$$

An examination of the Hartree and Fock diagrams (Fig. 1) yields then

$$\Sigma_{\mu}^H = \int dx \int dx' v(\mathbf{r}-\mathbf{r}') \sum_{\nu} f_{\nu} \varphi_{\mu}^*(\mathbf{r}') \varphi_{\nu}^*(\mathbf{r}) \varphi_{\nu}(\mathbf{r}) \varphi_{\mu}(\mathbf{r}'),$$

$$\Sigma_{\mu}^F = - \int dx \int dx' v(\mathbf{r}-\mathbf{r}') \sum_{\nu} f_{\nu} \varphi_{\mu}^*(\mathbf{r}') \varphi_{\nu}^*(\mathbf{r}) \varphi_{\mu}(\mathbf{r}) \varphi_{\nu}(\mathbf{r}'), \quad (11)$$

where $f_{\nu} = f(\varepsilon_{\nu})$ is the Fermi distribution function. We have accordingly from the definition (6)

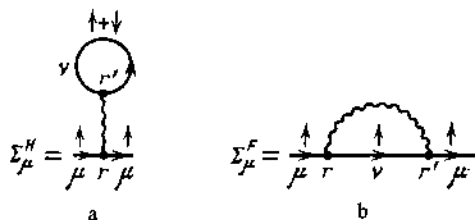


FIG. 1.

$$\Sigma_E^{H,F} = \int_{-\infty}^{\infty} d\omega f(E+\omega) \int dx \int dx' v(\mathbf{r}-\mathbf{r}') \langle \rho_E(\mathbf{r}) \rho_{E+\omega}(\mathbf{r}') \rangle^{H,F}, \quad (12)$$

where we have introduced the following spectral densities:

$$\langle \rho_E(\mathbf{r}) \rho_{E+\omega}(\mathbf{r}') \rangle^H = \frac{1}{N_0(E)} \left\langle \sum_{\mu\nu} \delta(E - \varepsilon_{\mu}) \delta(E + \omega - \varepsilon_{\nu}) \times \varphi_{\mu}^*(\mathbf{r}') \varphi_{\mu}(\mathbf{r}') \varphi_{\nu}^*(\mathbf{r}) \varphi_{\nu}(\mathbf{r}) \right\rangle, \quad (13a)$$

$$\langle \rho_E(\mathbf{r}) \rho_{E+\omega}(\mathbf{r}') \rangle^F = \frac{1}{N_0(E)} \left\langle \sum_{\mu\nu} \delta(E - \varepsilon_{\mu}) \delta(E + \omega - \varepsilon_{\nu}) \times \varphi_{\mu}^*(\mathbf{r}') \varphi_{\mu}(\mathbf{r}) \varphi_{\nu}^*(\mathbf{r}) \varphi_{\nu}(\mathbf{r}') \right\rangle. \quad (13b)$$

The spectral density (13b) was first considered by Berzinskii and Gor'kov²⁰ in connection with a general localization criterion formulated in it. The gist of this criterion is that at energies $E < E_c$ (where E_c is the mobility threshold), i.e., in the region of the localized states, these spectral densities acquire a contribution that is a δ function of ω :

$$\langle \langle \rho_E(\mathbf{r}) \rho_{E+\omega}(\mathbf{r}') \rangle \rangle^H = A_E(\mathbf{r}-\mathbf{r}') \delta(\omega) + \rho_E^H(\omega, \mathbf{r}-\mathbf{r}'), \quad (14a)$$

$$\langle \langle \rho_E(\mathbf{r}) \rho_{E+\omega}(\mathbf{r}') \rangle \rangle^F = A_E(\mathbf{r}-\mathbf{r}') \delta(\omega) + \rho_E^F(\omega, \mathbf{r}-\mathbf{r}'), \quad (14b)$$

where the quantity

$$A_E(\mathbf{r}-\mathbf{r}') = \frac{1}{N_0(E)} \left\langle \sum_{\mu} \delta(E - \varepsilon_{\mu}) |\varphi_{\mu}(\mathbf{r})|^2 |\varphi_{\mu}(\mathbf{r}')|^2 \right\rangle \neq 0, \quad E < E_c. \quad (15)$$

is connected²¹ with the probability of the electron returning to the initial point, so that the Berzinskii-Gor'kov localization criterion is equivalent to the known Economou-Cohen criterion.²² The validity of (14a) can be verified directly by repeating the arguments of Ref. 20.

Substituting (14) in (12) we obtain the following contributions to $\bar{\Sigma}_E$, which is due to the onset of localized states in the system:

$$\Sigma_E^{H,F} = \bar{\Delta}_E^{H,F} = \pm f(E) \int dx \int dx' v(\mathbf{r}-\mathbf{r}') A_E(\mathbf{r}-\mathbf{r}') = \pm f(E) \int \frac{d^d \mathbf{q}}{(2\pi)^d} v(-\mathbf{q}) A_E(\mathbf{q}), \quad (16)$$

where we have transformed in the last equation to the Fourier representation (d is the dimensionality of space). For a point interaction $v(\mathbf{r}-\mathbf{r}') = v_0 \delta(\mathbf{r}-\mathbf{r}')$ we have

$$\Sigma_E^{H,F} = \pm f(E) v_0 \int \frac{d^d \mathbf{q}}{(2\pi)^d} A_E(\mathbf{q}) = \pm f(E) v_0 A_E, \quad (17)$$

where A_E is proportional²¹ to the total probability of the electron returning to the initial point after an infinite time. We note that for a point interaction, by virtue of a property obvious from (13)

$$\langle \langle \rho_E(\mathbf{r}) \rho_{E'}(\mathbf{r}') \rangle \rangle^H = \langle \langle \rho_E(\mathbf{r}) \rho_{E'}(\mathbf{r}') \rangle \rangle^F \quad (18)$$

the "regular" contributions to $\bar{\Sigma}_E^H$ and $\bar{\Sigma}_E^F$ due to $\rho_E^{H,F}$ in (14) are equal (and of opposite sign).

For zero-spin fermions, the Hartree and the Fock contributions (17) cancel each other. It can be easily seen from (16) this cancellation does not depend on the interaction radius. When the spin is taken into account the Hartree contri-

bution acquires an "extra" factor 2 connected with the summation over the spin in the electron loop of Fig. 1a. This results in a nonzero localization contribution:

$$\tilde{\Sigma}_E^{H+F} = \tilde{\Delta}_E^{H+F} = f(E) v_0 A_E. \quad (19)$$

We write down for the sake of argument the equations for the point interaction. We recognize that the main energy dependence in (19) is determined by a Fermi function that varies strongly near the Fermi energy E_F . The quantity A_E at $E \approx E_F$ can be regarded as a constant (a smooth function of E). This assumption can, generally speaking, turn out to be correct near the mobility threshold, when A_E vanishes. The corresponding "critical exponent" is not known exactly, but it can be concluded from the available estimates²¹ that $\partial A_E / \partial E \rightarrow 0$ also as $E \rightarrow E_c$. We then obtain from (9) and (19)

$$\left(\frac{\delta N(E)}{N_0(E)} \right)_{loc} = - \frac{\partial}{\partial E} \tilde{\Delta}_E^{H+F} \approx v_0 A_{E_F} \left(- \frac{\partial f(E)}{\partial E} \right). \quad (20)$$

The singular (localization) contribution (20) is cancelled in the total density of states defined in (7) by the second term of (8):

$$\begin{aligned} \frac{\partial}{\partial \varepsilon_\nu} \tilde{\Delta}_E^{H+F} &= \frac{1}{N_0(E)} \left\langle \sum_\nu \frac{\partial \tilde{\Delta}_E^{H+F}(\varepsilon_\nu)}{\partial \varepsilon_\nu} \delta(E - \varepsilon_\nu) \right\rangle \\ &= \frac{1}{N_0(E)} \left\langle \sum_\nu \int \int dr' \right. \\ &\quad \left. \chi v(\mathbf{r}-\mathbf{r}') \frac{\partial f_\nu}{\partial \varepsilon_\nu} \delta(E - \varepsilon_\nu) |\varphi_\nu(\mathbf{r})|^2 |\varphi_\nu(\mathbf{r}')|^2 \right\rangle = v_0 A_{E_F} \frac{\partial f(E)}{\partial E}. \end{aligned} \quad (21)$$

We shall see nevertheless that the thermodynamic density of states (9) governs the behavior of a number of thermodynamic quantities, and retains the localization contribution (20).

To understand better the physical meaning of the localization contribution to $\tilde{\Sigma}_E^{H+F}$, we note that in fact we are dealing here with allowance for the interaction of electrons that are in one and the same quantum state ν . It can be seen that in the case of diagrams *a* and *b* of Fig. 1 the contributions from the interaction of electrons with equal spin projections (shown by arrows in Fig. 1) cancel out completely, and $\tilde{\Delta}_E^{H+F}$ is determined by the interaction of two electrons with opposite spins, which are in a state ν , i.e., by an effective interaction of the Hubbard type:

$$H_{eff} = \frac{1}{2} \sum_\nu \int \int dr' \int dr v(\mathbf{r}-\mathbf{r}') |\varphi_\nu(\mathbf{r})|^2 |\varphi_\nu(\mathbf{r}')|^2 n_{\nu\sigma} n_{\nu-\sigma}, \quad (22)$$

where $n_{\nu\sigma}$ is the operator of the number of electrons in a state ν and with a spin σ . Using the simplest estimate of A_E (Ref. 21) we have ($E_F < E_c$)

$$\tilde{\Delta}_E^{H+F} \approx \begin{cases} v_0 R_{loc}^{-d}(E), & E < E_F \\ 0, & E > E_F \end{cases}, \quad (23)$$

where $R_{loc}(E)$ is the localization radius of the electronic states with energy E . Comparing the results with Mott's known qualitative reasoning,²³ we see that $\tilde{\Delta}_E^{H+F}$ coincides with the width of the narrow band of "singly occupied" electronic states produced below the Fermi level in the localization region.



FIG. 2.

Considering the Hartree-Fock corrections to the thermodynamic potential, which are determined by the plots of Fig. 2, we obtain by direct calculation

$$\langle \delta \Omega_{H,F} \rangle = \int_{-\infty}^{\infty} dE f(E) N_0(E) \tilde{\Sigma}_E^{H+F}. \quad (24)$$

After integrating by parts we have

$$\delta \Omega = \langle \delta \Omega_H \rangle + \langle \delta \Omega_F \rangle = T \int_{-\infty}^{\infty} dE N_0(E) \left(\frac{\partial}{\partial E} \tilde{\Sigma}_E^{H+F} \right) \ln(1 + e^{-E/T}). \quad (25)$$

Comparison of (25) and of the known expression for the thermodynamic potential of free fermions:

$$\Omega = -T \int_{-\infty}^{\infty} dE N(E) \ln(1 + e^{-E/T}) \quad (26)$$

explains the use of the term "thermodynamic density of states" in connection with the definition (9). The singular (localization) part of the thermodynamic potential is given by

$$\begin{aligned} \delta \Omega_{loc} &= \int dr \int dr' v(\mathbf{r}-\mathbf{r}') \int A_E(\mathbf{r}-\mathbf{r}') N_0(E) f^2(E) dE \\ &= \int dE \int \frac{d^d \mathbf{q}}{(2\pi)^d} v(-\mathbf{q}) A_E(\mathbf{q}) N_0(E) f^2(E). \end{aligned} \quad (27)$$

The corresponding contributions to the entropy and to the heat capacity are

$$S_{loc} = - \frac{\partial \delta \Omega_{loc}}{\partial T} = - \int_{-\infty}^{\infty} dE N_0(E) \frac{\partial f^2(E)}{\partial T} v_0 A_E \xrightarrow{T \rightarrow 0} v_0 N_0(E_F) A_{E_F}, \quad (28)$$

$$C_{loc} = T \frac{\partial S_{loc}}{\partial T} \approx - \frac{\pi^2}{3} T v_0 \frac{\partial}{\partial E_F} \{ N_0(E_F) A_{E_F} \}; \quad (29)$$

C_{loc} is connected with a small ($\sim \partial A_E / \partial E$) correction to the thermodynamic potential. The corresponding correction to the density of states in (20) was neglected. The localization correction to the correlation contribution to the compressibility is also small:

$$\begin{aligned} \delta \kappa_{loc} &= - \frac{\partial^2}{\partial \mu^2} \delta \Omega_{loc} = - v_0 \int_{-\infty}^{\infty} dE A_E N_0(E) \frac{\partial^2}{\partial \mu^2} f^2(E) \\ &= v_0 \frac{\partial}{\partial E_F} \{ N_0(E_F) A_{E_F} \}. \end{aligned} \quad (30)$$

Thus, the singular contribution (20) to the thermodynamic density of states does not lead to any contradiction whatever with the third law of thermodynamics. The finite contribution to the entropy as $T \rightarrow 0$ (28) is obviously due to the existence of "free" spins in the Mott strip.

4. REGULAR CONTRIBUTIONS

Up to now our analysis was quite general. We must now assume a certain specific one-electron model for the Ander-

son transition. We are principally interested in the contributions made to the density of states by the "regular" terms in the spectral densities (14). We confine ourselves only to the Fock contribution to (12) since, as noted in Refs. 3, 14, and 24, the Hartree contribution is small in terms of the parameter

$$F = \int d\Omega v \left(q = 2p_F \sin \frac{\theta}{2} \right) / \int d\Omega v(0), \quad (31)$$

where p_F is the Fermi momentum and the integration is over a solid angle on the Fermi surface. It is easily seen that $F < 1$ if the interaction potential decreases over a length exceeding the reciprocal Fermi momentum. It can be verified²⁵ that the estimate (31) remains in force also for the regular contribution to (12) in the localized phase. For a point interaction, as is clear from (18), the Hartree contribution is double (when the spin is taken into account) the Fock contribution, so that the results that follow must simply be taken with the sign reversed.

As shown in Ref. 21, the connection between the Fourier transform of the spectral density (14b) and the two-particle Green's function of the one-electron problem is

$$\langle \rho_E \rho_{E+\omega} \rangle_{\mathbf{q}}^F = \frac{1}{\pi N_0(E)} \text{Im} \{ \Phi^{RA}(E\omega\mathbf{q}) - \Phi^{RR}(E\omega\mathbf{q}) \}, \quad (32)$$

where

$$\Phi^{RA(R)}(E\omega\mathbf{q}) = -\frac{1}{2\pi i} \sum_{\mathbf{p}\mathbf{p}'} \langle G^R(\mathbf{p}_+\mathbf{p}_+'E+\omega) G^{A(R)}(\mathbf{p}_-\mathbf{p}_-'E) \rangle, \quad (33)$$

$$\mathbf{p}_\pm = \mathbf{p} \pm \frac{\mathbf{q}}{2}.$$

A similar representation can also be written for (14a). At small ω and \mathbf{q} , the function $\Phi^{RR}(E\omega\mathbf{q})$, in contrast to $\Phi^{RA}(E\omega\mathbf{q})$, is regular.¹⁵ We shall therefore neglect its contribution to the spectral density and assume it does not lead to a substantial renormalization of the density of states. As the one-electron model of the Anderson transition we employ the self-consistent localization theory in the form proposed by Vollhardt and Wölfle.¹⁵⁻¹⁸ In this theory

$$\Phi^{RA}(E_F\omega\mathbf{q}) = -N_0(E_F) [\omega + M_{E_F}(\mathbf{q}\omega)] [\omega^2 + \omega M_{E_F}(\mathbf{q}\omega) - 2E_F q^2/dm]^{-1}, \quad (34)$$

and the relaxation kernel M is determined as $q \rightarrow 0$ by the following self-consistent equation

$$M_{E_F}(\omega) = \frac{i}{\tau_0} \left\{ 1 + \frac{1}{\pi N_0(E_F)} \int \frac{d^d\mathbf{q}}{(2\pi)^d} [-i\omega + D_{E_F}(\omega)q^2]^{-1} \right\}, \quad (35)$$

where

$$D_{E_F}(\omega) = \frac{2E_F}{dm} \frac{i}{M_{E_F}(\omega)} \quad (36)$$

is a generalized diffusion coefficient, τ_0 is the Born free-path time, and m is the electron mass. The solution of (35) is

$$M_{E_F}(\omega) = \frac{i}{\tau_{E_F}} - \frac{\omega_0^2(E_F)}{\omega}, \quad (37)$$

where

$$\omega_0^2(E_F) = -\lim_{\omega \rightarrow 0} \omega M_{E_F}(\omega) > 0$$

for $E_F < E_c$, i.e., below the mobility threshold whose location is defined by the equation $\omega_0^2(E_c) = 0$. From (32) and

(34) we easily obtain

$$\langle \rho_E \rho_{E+\omega} \rangle_{\mathbf{q}}^F = \frac{1}{\pi} \frac{D_{E_F} q^2}{\omega^2 + (D_{E_F} q^2)^2}, \quad E_F > E_c, \quad (38)$$

$$\langle \rho_E \rho_{E+\omega} \rangle_{\mathbf{q}}^F = A_{E_F}(q) \delta(\omega) + \frac{1}{\pi} \frac{D_{E_F} q^2}{\omega^2 + [\omega_0^2(E_F) \tau_{E_F} + D_{E_F} q^2]^2},$$

$E_F < E_c$,

where

$$A_{E_F}(q) = \frac{\omega_0^2(E_F) \tau_{E_F}}{\omega_0^2(E_F) \tau_{E_F} + D_{E_F} q^2} = (1 + R_{loc}^2(E_F) q^2)^{-1}, \quad (39)$$

where $R_{loc}^2(E_F) = 2E_F/dm\omega_0^2$ is the square of the localization radius and $D_{E_F} = (2E_F/dm)\tau_{E_F}$ is the renormalized diffusion coefficient. From (12) and (38) we obtain for the regular contribution $\tilde{\Sigma}_E^F$ at $T=0$:

$$\tilde{\Sigma}_E^F = -\frac{1}{\pi} \int_{-\infty}^0 dE' \int \frac{d^d\mathbf{q}}{(2\pi)^d} v(\mathbf{q}) \times \frac{D_{E_F} q^2}{(E' - E)^2 + [\omega_0^2(E_F) \tau_{E_F} + D_{E_F} q^2]^2}. \quad (40)$$

For the correction to the density of states we obtain correspondingly

$$\frac{\delta N(E)}{N_0(E_F)} = -\frac{\partial}{\partial E} \tilde{\Sigma}_E^F = -\frac{1}{\pi} \int \frac{d^d\mathbf{q}}{(2\pi)^d} v(\mathbf{q}) \frac{D_{E_F} q^2}{E^2 + [\omega_0^2(E_F) \tau_{E_F} + D_{E_F} q^2]^2}. \quad (41)$$

Assuming now for simplicity the point-interaction model and recalling that up to now the energy E was reckoned from the Fermi energy E_F , we get for $2 < d < 4$

$$\frac{\delta N(E)}{N_0(E_F)} \approx \frac{v_0}{\pi} \frac{S_d}{d-2} D_{E_F}^{-d/2} = |E - E_F|^{(d-2)/2} \bar{E}^{(d-2)/2},$$

$$|E - E_F| \gg \omega_0^2(E_F) \tau_{E_F}, \quad (42)$$

$$\frac{\delta N(E)}{N_0(E_F)} \approx \frac{v_0}{\pi} \frac{S_d}{d-2} D_{E_F}^{-d/2} = \omega_0^{d-2}(E_F) \tau_{E_F}^{(d-2)/2} \bar{E}^{(d-2)/2},$$

$$|E - E_F| \ll \omega_0^2(E_F) \tau_{E_F},$$

where $S_d = [2^{d-1} \pi^{d/2} \Gamma(d/2)]^{-1}$. The characteristic energy E is connected here with the choice of the cutoff parameter on the upper limit of the integral with respect to q in (41). This cutoff is necessary because the "diffusion" approximation is not valid for the integrand and at large momenta. In accord with the consideration of the analogous cutoff in the integral of (35), which was carried out in Refs. 15 and 17, we choose a cutoff parameter equal to the Fermi momentum, so that

$$E = D_{E_F} p_F^2. \quad (43)$$

An alternative is the choice of a cutoff parameter equal to the reciprocal l^{-1} of the Born mean free path,¹⁶ but near the mobility threshold we have $l^{-1} \sim p_F$, so that the two choices are equivalent. According to Lee's scaling reasoning,⁸ near the mobility threshold, when $R_{loc}(E_F) \gg l$, p_F^{-1} , the cutoff parameter is proportional to R_{loc}^{-1} and $\bar{E} \sim \omega_0^2(E_F) \tau_{E_F}$. This

choice, however, contradicts the self-consistent localization theory on which our calculations are based. In fact, use of cutoff at momenta on the order of p_F or l^{-1} in the basic self-consistency equation (35) yields the usual results¹⁵⁻¹⁷ that agree with the scaling picture of the Anderson transition.^{15,16} On the other hand, using in (35) cutoff in the sense of Ref. 8 does not lead to equations in closed form. It must be emphasized, however, that in the self-consistent theory we still have the unsolved problem of determining the q dependence of the parameters $\omega_0^2(E_F)$ and D_{E_F} or τ_{E_F} at large q , since Eq. (35) is derived in the limit as $q \rightarrow 0$.

The estimate (50) is valid if the following condition

$$|E - E_F|, \omega_0^2(E_F)\tau_{E_F} \ll \bar{E} \quad (44)$$

is satisfied. For the special case $d = 2$ we obtain in place of (42)

$$\frac{\delta N(E)}{N_0(E_F)} = \frac{v_0}{4\pi^2 D_{E_F}} \begin{cases} \ln \frac{|E - E_F|}{E}, & |E - E_F| \gg \omega_0^2(E_F)\tau_{E_F}, \\ \ln \frac{\omega_0^2(E_F)\tau_{E_F}}{E}, & |E - E_F| \ll \omega_0^2(E_F)\tau_{E_F}. \end{cases} \quad (45)$$

At $\omega_0^2(E_F) = 0$, i.e., in the metallic phase, Eqs. (42) and (44) agree with the usual results of Aronov and Al'tshuler.^{2,3} It can be seen that at $|E - E_F| \gg \omega_0^2(E_F)\tau_{E_F}$ the metallic-phase kink in the density of the states at the Fermi level become smoothed out and is replaced by a smooth minimum. This conclusion, as can be easily verified, remains in force regardless of the cutoff used in the integral (41). A diagrammatic analysis in Ref. 25 has shown that (42) yields the main correction to the density of states everywhere except in an exponentially small vicinity of the Fermi surface, where an additional nonzero logarithmic contribution appears in the dielectric state.

We present actual relations that are obtained in the self-consistent localization theory. At $2 < d < 4$ and $E_F \lesssim E_c$ the solution of Eq. (35) produces in the dielectric phase (we omit some inessential constants)¹⁷

$$\omega_0^2(E_F) \sim E_F^2 \left[1 - \left(\frac{E_F}{E_c} \right)^{(4-d)/2} \right] \sim E_F^2 \left| \frac{E_F - E_c}{E_c} \right|^{2/(d-2)}, \quad (46)$$

$$R_{loc}(E_F) \sim p_F^{-1} \left[1 - \left(\frac{E_F}{E_c} \right)^{(4-d)/2} \right]^{-\nu} \sim p_F^{-1} \left| \frac{E_F - E_c}{E_c} \right|^{-\nu}, \quad (47)$$

$$\frac{\tau_{E_F}}{\tau_0} \sim \frac{d\lambda}{4-d} \left[\frac{d\omega_0^2(E_F)}{4E_F^2} \right]^{(d-2)/2} \sim \frac{d\lambda}{4-d} [p_F R_{loc}(E)]^{2-d} \sim \lambda \left| \frac{E_F - E_c}{E_c} \right|^{(d-2)\nu}, \quad (48)$$

where $\lambda = (2\pi E_F \tau_0)^{-1}$ is the dimensionless constant of perturbation theory in scattering by a disorder, and $\nu = (d-2)^{-1}$ is the critical exponent of the localization radius. The mobility threshold in the model of point scatterers randomly distributed in space at a density ρ and with a scattering amplitude V (Ref. 17) is

$$E_c \sim \left[\frac{d}{d-2} (2\pi)^{-d/2} \Gamma \left(\frac{d}{2} \right) \right]^{2/(4-d)} E_{sc},$$

$$E_{sc} = m^{d/(4-d)} (\rho V^2)^{2/(4-d)}. \quad (49)$$

Where E_{sc} is the "strong-coupling" energy.^{1,2} At $E_F \sim E_{sc}$ we have $\lambda \sim 1$, and perturbation theory no longer holds. From (46)–(48) at $E_F \lesssim E_c$ we have

$$\omega_0^2(E_F)\tau_{E_F} \sim \frac{\lambda}{4-d} \frac{E_F}{[p_F R_{loc}(E_F)]^d} \sim \frac{\lambda E_F}{4-d} \left| \frac{E_F - E_c}{E_c} \right|^{d\nu}, \quad (50)$$

$$D_{E_F} \sim \frac{1}{4-d} \frac{1}{m} [p_F R_{loc}(E_F)]^{2-d} \sim \frac{1}{m} \left| \frac{E_F - E_c}{E_c} \right|^{(d-2)\nu}, \quad (51)$$

$$E \sim E_F [p_F R_{loc}(E_F)]^{2-d} \sim E_F \left| \frac{E_F - E_c}{E_c} \right|^{(d-2)\nu}. \quad (52)$$

It can be seen that satisfaction of the condition (44) entails no difficulty. For the correction to the density of states on the Fermi level ($|E - E_F| \ll \omega_0^2(E_F)\tau_{E_F}$) we obtain from (42) and (50)–(52) as $E_F \rightarrow E_c$

$$\frac{\delta N(E_F)}{N_0(E_F)} \sim \frac{4-d}{d-2} v_0 m^{d/2} E_F^{d/2-1} \{1 - [p_F R_{loc}(E_F)]^{d-2}\} \sim -v_0 N_0(E_F) \left| \frac{E_F - E_c}{E_c} \right|^{-(d-2)\nu} \quad (53)$$

The divergence of the correction as $E_F \rightarrow E_c$, which follows from the last equality in (53) (a similar divergence occurs also in the metallic phase) indicates that our analysis cannot be used in the immediate vicinity of the mobility threshold. Our estimates are meaningful so long as $|\delta N(E)/N_0| \ll 1$. The divergence becomes logarithmic if the cutoff in (41) is in accord with the scheme of Ref. 8, in analogy with the corresponding result obtained there for the metallic region.

The corrections obtained above to the density of states can be found from the following qualitative arguments. Consider the interaction between an electron in a state ν with energy E , on the one hand, and an electron in a state with energy E_F , on the other. The relative correction to its wave function is then in first-order perturbation theory

$$\frac{\delta \varphi_\nu}{\varphi_\nu} \sim \int_0^\infty dt H_{in,\nu}(t), \quad (54)$$

where $t = 0$ is the instant when the interaction is turned on. After a time t the electron diffuses within the confines of the volume $(D_{E_F} t)^{d/2}$. We estimate the matrix element of the interaction for short-range repulsion at $v_0 (D_{E_F} t)^{-d/2}$. Then

$$\frac{\delta \varphi_\nu}{\varphi_\nu} \sim v_0 \int_{t_{min}}^{t_{max}} dt (D_{E_F} t)^{-d/2} \sim v_0 D_{E_F}^{-d/2} \{t_{min}^{1-d/2} - t_{max}^{1-d/2}\}. \quad (55)$$

It is natural to determine t_{min} here from the condition for the applicability of the diffusion approximation: $\{D_{E_F} t_{min}\}^{1/2} \sim p_F^{-1}$, i.e., $t_{min} \sim (D_{E_F} p_F^2)^{-1} \sim \bar{E}^{-1}$. The time t_{max} is determined by two factors. First, the matrix element of the interaction vanishes at times $t > |E - E_F|$ because of the of the temporal oscillations of the wave functions. Second, in the region of the localized states the interaction electrons cannot move apart by more than $R_{loc}(E_F)$, and the diffusion approximation is valid so long as

$t \lesssim R_{loc}^2(E_F) D_{E_F} \sim (\omega_0^2 \tau_{E_F})^{-1}$. Therefore $t_{max} \sim \min \{|E - E_F|^{-1}, (\omega_0^2 \tau_{E_F})^{-1}\}$. Then, assuming that $\delta N(E)/N_0 \sim \delta \varphi_v / \varphi_v$, we obtain directly (42). Of course, these estimates are only purely explanatory.

The results provide a simple explanation of the analysis of Aronov and Al'tshuler^{2,3} on the dielectric side of the Anderson transition. The approximations used do not contain a Coulomb gap,^{4,5} primarily because of the short-range character of the interaction, and also perhaps because the model is crude and is based only on allowance for Hartree-Fock corrections.

5. POLARIZATION OPERATOR

We consider in this section, from a general viewpoint, how the localization affects the behavior of the polarization operator, i.e., actually the question of the character of the screening of the electric field in a Fermi glass.

Using again the representation of exact eigenfunctions of the one-electron problem, we have for the Fourier transform of the polarization operator of non-interacting electrons

$$\begin{aligned} \Pi(\mathbf{q}\omega) &= \left\langle \sum_{\substack{\mu\nu \\ \mathbf{p}\mathbf{p}'} } \frac{f_\mu - f_\nu}{\epsilon_\mu - \epsilon_\nu + \omega + i\delta \operatorname{sign} \omega} \right. \\ &\quad \times \varphi_\nu(\mathbf{p}_+) \varphi_\nu^*(\mathbf{p}_+') \varphi_\mu(\mathbf{p}_-') \varphi_\mu^*(\mathbf{p}_-') \left. \right\rangle \\ &= \int_{-\infty}^{\infty} dE \int_{-\infty}^{\infty} d\Omega \frac{f(E) - f(E+\Omega)}{\Omega + \omega + i\delta \operatorname{sign} \omega} N_0(E) \langle \rho_{\mathbf{E}\mathbf{E}+\mathbf{q}} \rangle_{\mathbf{q}}^T \end{aligned} \quad (56)$$

in the zero-temperature formalism and

$$\Pi(\mathbf{q}\omega_m) = \int_{-\infty}^{\infty} dE \int_{-\infty}^{\infty} d\Omega \frac{f(E) - f(E+\Omega)}{\Omega + i\omega} N_0(E) \langle \rho_{\mathbf{E}\mathbf{E}+\mathbf{q}} \rangle_{\mathbf{q}}^P \quad (57)$$

in the Matsubara technique ($\omega_m = 2\pi mT$). Substituting the singular part of (14b) in (56), we obtain

$$\Pi_{loc}(\mathbf{q}\omega) = 0,$$

and a nonzero contribution comes only from the regular part of (14b):

$$\begin{aligned} \Pi(\mathbf{q}\omega) &= \Pi_{reg}(\mathbf{q}\omega) \\ &= \int_{-\infty}^{\infty} dE \int_{-\infty}^{\infty} d\Omega \frac{f(E) - f(E+\Omega)}{\Omega + \omega + i\delta \operatorname{sign} \omega} N_0(E) \rho_{\mathbf{E}\mathbf{E}}^P(\mathbf{q}\Omega). \end{aligned} \quad (58)$$

The situation in the Matsubara technique is different:

$$\begin{aligned} \Pi_{loc}(\mathbf{q}\omega_m \neq 0) &= 0, \\ \Pi_{loc}(\mathbf{q}\omega_m = 0) &= \int_{-\infty}^{\infty} dE \left(-\frac{\partial f(E)}{\partial E} \right) N_0(E) A_{\mathbf{E}}(\mathbf{q}) \\ &= N_0(E_F) A_{\mathbf{E}_F}(\mathbf{q}), \end{aligned} \quad (59)$$

so that

$$\begin{aligned} \Pi(\mathbf{q}\omega_m) &= \frac{\delta m_0}{T} \int_{-\infty}^{\infty} dE f(E) [1 - f(E)] N_0(E) A_{\mathbf{E}}(\mathbf{q}) \\ &+ \int_{-\infty}^{\infty} dE \int_{-\infty}^{\infty} d\Omega \frac{f(E) - f(E+\Omega)}{\Omega + i\omega_m} N_0(E) \rho_{\mathbf{E}\mathbf{E}}^P(\mathbf{q}\Omega). \end{aligned} \quad (60)$$

Taking into account the explicit form of the regular part of the spectral density, which arises in the self-consistent theory (38), we can obtain

$$\Pi(\mathbf{q}\omega) = \Pi_{reg}(\mathbf{q}\omega) = N_0(E_F) \frac{D_{E_F} q^2}{D_{E_F} q^2 + \omega_0^2(E_F) \tau_{E_F} - i\omega} \quad (61)$$

In the metallic phase $\omega_0^2(E_F) = 0$, and (61) reduces to the known expression for the polarization operator of a "dirty" metal,^{2,3,7} in the localization region, recognizing that $\omega_0^2(E_F) \tau_{E_F} = D_{E_F} R_{loc}^{-2}$ we

$$\Pi_{reg}(\mathbf{q}0) = N_0(E_F) q^2 [q^2 + R_{loc}^{-2}(E_F)]^{-1}. \quad (62)$$

Analogous calculations yield for the Matsubara polarization operator

$$\begin{aligned} \Pi(\mathbf{q}\omega_m) &= N_0(E_F) \left\{ A_{E_F}(q) \delta_{m0} + \frac{D_{E_F}(\omega_m) q^2}{\omega_m + D_{E_F}(\omega_m) q^2} \theta(\omega_m) \right. \\ &\quad \left. + \frac{D_{E_F}(-\omega_m) q^2}{-\omega_m + D_{E_F}(-\omega_m) q^2} \theta(-\omega_m) \right\}, \quad (63) \\ \theta(\omega_m) &= \begin{cases} 1, & m \geq 0 \\ 0, & m < 0 \end{cases} \end{aligned}$$

where the generalized diffusion coefficient is

$$D_{E_F}(\omega_m) = \frac{2E_F}{dm} \frac{i}{M_{E_F}(\omega_m)}, \quad M_{E_F}(\omega_m) = \frac{i}{\tau_{E_F}} - \frac{\omega_0^2(E_F)}{i\omega_m}. \quad (64)$$

The difference obtained in the behavior of the polarization operator at $T = 0$ and in the Matsubara technique, a difference that manifests itself only at zero frequency (screening of the static field), is the consequence of the known difference between the static adiabatic and static isothermal responses in systems with non-ergodic behavior.^{26,27} The latter leads to the appearance of a δ -function anomaly of the spectral density at zero frequency, which in our case is a consequence of the Anderson localization—of a typically non-ergodic phenomenon. The Matsubara response "senses" the nonergodicity manifestation,²⁷ whereas the response determined by the commutator Green's functions is insensitive to it. The polarization operator is connected with the electronic compressibility. For the static isothermal compressibility we have (cf. Ref. 27)

$$\kappa^T(q0) = \Pi(\mathbf{q}\omega_m = 0), \quad (65)$$

whereas the adiabatic compressibility is

$$\kappa^A(q0) = \Pi_{reg}(q\omega \rightarrow 0). \quad (66)$$

We get then from (58) and (59)

$$\kappa^T(q0) - \kappa^A(q0) = N_0(E_F) A_{E_F}(q) = N_0(E_F) [1 + q^2 R_{loc}^2(E_F)]^{-1}. \quad (67)$$

The fact that $A_{E_F}(q)$ determines the difference between the isothermal and adiabatic compressibilities was first noted in Refs. 28 and 29. This difference, naturally, appears only in the static response. From (59)–(62) we obtain for the static isothermal polarization operator

$$\begin{aligned} \Pi^T(q0) &= \Pi(q\omega_m = 0) = \Pi_{loc}(q0) + \Pi_{reg}(q0) \\ &= N_0(E_F) \left[\frac{1}{1 + q^2 R_{loc}^2(E_F)} + \frac{q^2}{q^2 + R_{loc}^{-2}(E_F)} \right] = N_0(E_F). \end{aligned} \quad (68)$$

Accordingly, for the static adiabatic dielectric constant we have

$$\varepsilon^A(q \rightarrow 0) = 1 + \frac{4\pi e^2}{q^2} \Pi_{reg}(q0) \\ = \begin{cases} 1 + \kappa_D^2/q^2, & q \gg R_{loc}^{-1}(E_F), \\ 1 + \kappa_D^2 R_{loc}^2(E_F), & q \leq R_{loc}^{-1}(E_F), \end{cases} \quad (69)$$

where $\kappa_D^2 = 4\pi e^2 N_0(E_F)$, whereas the static isothermal dielectric constant is

$$\varepsilon^T(q0) = 1 + \frac{4\pi e^2}{q^2} \Pi^T(q0) = 1 + \frac{\kappa_D^2}{q^2}. \quad (70)$$

It is precisely the latter dielectric constant that agrees with a real experiment on the screening of a static external field.³⁰ It can be seen from (70) that the Fermi-glass screens a static field.¹¹ This fact was first noted qualitatively in Refs. 30 and 31. At any arbitrarily low temperature the hopping conduction over the localized states aligns the electrons in an Anderson dielectric in a way that ensures complete screening. The characteristic times are obviously determined here by the frequency $\omega^* \sim D_{hop} q^2$, where D_{hop} is the coefficient of diffusion due to the hopping conduction, and $q \sim 1/L$, where the length L is determined by the characteristic scale of the external-field inhomogeneities in the given experiment^{30,31} (e.g., by the distance between the capacitor electrodes). It is precisely in the sense of the condition $\omega < \omega^*$ that one must understand the static character of the field (and of the response) in the formalism described above (in which hopping conduction is not taken explicitly into account).

The divergence of the dielectric constant, observed in the approach to the metal-insulator transition in the known experiments on *P*-doped Si (Ref. 32) is probably due to the divergence of the localization radius $R_{loc}(E_F \rightarrow E_c)$ in (69). It would be quite interesting to attempt a measurement of the dielectric constant of this system in a static field.

The authors thank D. I. Khomskii and M. I. Auslender for a discussion of a number of processes touched upon in this paper.

¹¹In the employed formalism it is possible also to demonstrate directly that the corrections to $\Pi(q_0)$, which lead to singularities such as (42) in the density of states, are mutually cancelled out by the interaction. This agrees fully with the important circumstance noted in Refs. 8 and 9, viz., the

screening radius is determined not by the density of state but by the quantity $\partial N / \partial \mu = \Pi(q \rightarrow 0, 0)$, where N is the total density of the electrons. This was not taken into account in Ref. 6.

- ¹M. V. Sadovskii, Usp. Fiz. Nauk **133**, 223 (1981) [Sov. Phys. Usp **24**, 96 (1981)].
- ²B. L. Alshuler and A. G. Aronov, Zh. Eksp. Teor. Fiz. **77**, 2028 (1979) [Sov. Phys. JETP **50**, 968 (1979)].
- ³B. L. Alshuler, A. G. Aronov, D. E. Khmel'nitskii, and A. I. Larkin, in: Quantum Theory of Solids, I. M. Lifshitz, ed., Mir, 1980, p. 130 [orig. in English].
- ⁴A. L. Efros and B. I. Shklovskii, J. Phys. **C8**, L49 (1975).
- ⁵B. I. Shklovskii and A. L. Efros, Elektronnyye svoystva legirovannykh poluprovodnikov (Electronic Properties of Doped Semiconductors), Nauka, 1979.
- ⁶W. L. McMillan, Phys. Rev. **B24**, 1739 (1981).
- ⁷Y. Imry, Y. Gefen, and D. J. Bergmann, Phys. Rev. **B26**, 3436 (1982).
- ⁸P. A. Lee, Phys. Rev. **B26**, 5882 (1982).
- ⁹A. M. Finkel'shtein, Zh. Eksp. Teor. Fiz. **84**, 168 (1983) [Sov. Phys. JETP **57**, 97 (1983)].
- ¹⁰G. S. Grest and P. A. Lee, Phys. Rev. Lett. **50**, 693 (1983).
- ¹¹R. Z. Oppermann, Z. Phys. **B49**, 273 (1983).
- ¹²R. Freedman and J. A. Hertz, Phys. Rev. **B15**, 2384 (1977).
- ¹³L. Fleishman and P. W. Anderson, Phys. Rev. **B21**, 2366 (1980).
- ¹⁴E. Abrahams, P. W. Anderson, P. A. Lee, and T. Ramakrishnan, Phys. Rev. **B24**, 6783 (1981).
- ¹⁵D. Vollhardt and P. Wölfle, Phys. Rev. **B22**, 4666 (1980).
- ¹⁶P. Wölfle and D. Vollhardt, in: Anderson Localization (Y. Nagaoka and H. Fukuyama, eds.), Springer, 1982, p. 26.
- ¹⁷A. V. Myasnikov and M. V. Sadovskii, Fiz. Tverd. Tela (Leningrad) **24**, 3569 (1982) [Sov. Phys. Solid State **24**, 2033 (1982)].
- ¹⁸E. A. Kotov and M. V. Sadovskii, Z. Phys. **B51**, 17 (1983).
- ¹⁹A. B. Migdal, Teoriya konechnykh fermi-sistem i svoystva atomnykh yader (Theory of Finite Fermi Systems and Properties of Atomic Nuclei), Nauka, 1965.
- ²⁰V. L. Berezinskii and L. P. Gor'kov, Zh. Eksp. Teor. Fiz. **77**, 2498 (1979) [Sov. Phys. JETP **50**, 1209 (1979)].
- ²¹M. V. Sadovskii, Zh. Eksp. Teor. Fiz. **83**, 1418 (1982) [Sov. Phys. JETP **56**, 816 (1982)].
- ²²E. N. Economou and M. H. Cohen, Phys. Rev. **B5**, 2931 (1972).
- ²³N. F. Mott, Phil. Mag. **24**, 935 (1971).
- ²⁴P. A. Lee, in Ref. 16, p. 78.
- ²⁵M. I. Katsnel'son and M. V. Sadovskii, Fiz. Tverd. Tela (Leningrad) **25**, 3372 (1983) [Sov. Phys. Solid State **25**, 1942 (1983)].
- ²⁶R. J. Kubo, J. Phys. Soc. Japan **12**, 570 (1957).
- ²⁷P. C. Kwok and T. D. Schulz, J. Phys. **C2**, 1196 (1969).
- ²⁸W. Gotze, Phil. Mag. **B43**, 219 (1981).
- ²⁹P. Prelovsek, Phys. Rev. **B23**, 194 (1981).
- ³⁰J. Jackle, Phil. Mag. **B45**, 313 (1982).
- ³¹T. M. Rice, in: Disordered Systems and Localization, Lecture Notes in Physics, Vol. 149, p. 220, Springer, 1981.
- ³²H. F. Hess, K. de Konde, T. F. Rosenbaum, and G. A. Thomas, Phys. Rev. **B25**, 5578 (1982).

Translated by J. G. Adashko

Localization and superconductivity

L. N. Bulaevskii and M. V. Sadovskii

P. N. Lebedev Physics Institute, Academy of Sciences of the USSR, Moscow

(Submitted 26 April 1984)

Pis'ma Zh. Eksp. Teor. Fiz. **39**, No. 11, 524–527 (10 June 1984)

A system in a state of Anderson localization in its normal state can go superconducting below the critical temperature T_c . The Ginzburg-Landau coefficients are derived for the superconducting transition in the region of Anderson localization. The behavior of the upper critical magnetic field H_{c2} as a function of the degree of disorder is studied in the metallic and insulating regions.

The introduction of a sufficient amount of disorder in a metallic system gives rise to a localization of electronic states near the Fermi level, i.e., to an Anderson transition.^{1,2} On the other hand, the attraction of electrons near the Fermi level gives rise to a superconducting ground state at low temperatures. We might ask about the relationship between these two types of transitions, which lead to fundamentally different ground states. This question is also of applied importance in connection with research on the superconductivity of highly amorphous metals and compounds bombarded by fast neutrons.

The effect of localization on superconductivity has recently been the subject of an extensive discussion in the literature.^{3–5} In the present letter we show that a three-dimensional system in the state of an Anderson insulator in its normal state can go superconducting below a certain critical superconducting transition temperature T_c .

Assuming that there is an effective attraction of electrons at the Fermi surface, we use the Bardeen-Cooper-Schrieffer theory to calculate the coefficients of the Ginzburg-Landau functional:

$$F = A |\Delta|^2 + \frac{1}{2} B |\Delta|^4 + C \left| \left(\frac{\partial}{\partial \mathbf{r}} - \frac{2ie}{\hbar c} A \right) \Delta \right|^2. \quad (1)$$

The coefficients A , B , and C are determined by the Matsubara two-particle Green's function of the system of electrons in the normal state. This function $\phi(\mathbf{q}\omega_m)$, which determines the kinetic properties of the normal state and the transition to localization, can be found in the self-consistent theory of localization.^{6–8} As the degree of disorder increases (with a decrease in the "seed" electron mean free path l), the mobility threshold E_c approaches the Fermi level E_F and crosses it. At this point the conductivity vanishes, and the system goes into the insulating region ($E_F < E_c$). Near the transition point ($E_F \approx E_c$) we have

$$\phi(\mathbf{q}\omega_m) = - \frac{N(E_F)}{i|\omega_m| + iD_0(|\omega_m|\tau)^{1/3}q^2}; \quad \omega_m = 2\pi mT, \quad (2)$$

where

$$D_0 = \frac{1}{3} v_F l, \quad \tau = l/v_F.$$

According to the BCS model, the coefficients A and B , remain independent of the degree of disorder (the Anderson theorem) as long as there is a sufficiently large number of states near the Fermi level in an energy layer on the order of T_c in the localization region. We are thus primarily interested in the coefficient C , which describes the superconducting response of the system. For an ordinary dirty superconductor, C is proportional to the conductivity of the system, σ . This conductivity vanishes at $E_F = E_c$, and the question of the value of C near the Anderson transition and in the localization region is less trivial. Using the relation

$$C = i\pi T \sum_{\epsilon_n} \frac{\partial^2}{\partial \mathbf{q}^2} \phi(\mathbf{q}, 2\epsilon_n) \Big|_{\mathbf{q}=\mathbf{0}}; \quad \epsilon_n = (2n+1)\pi T \quad (3)$$

we find the following results for the square of the correlation length:

$$\xi^2(T) = \xi_0 l \frac{\sigma}{\sigma_0} \left(1 - \frac{T}{T_c}\right)^{-1}; \quad R_l \ll (\xi_0 l^2)^{1/3}, \quad E_c < E_F.$$

$$\xi^2(T) = (\xi_0 l^2)^{1/3} \left(1 - \frac{T}{T_c}\right)^{-1}; \quad R_l > (\xi_0 l^2)^{1/3}, \quad E_c \approx E_F. \quad (4)$$

$$\xi_0 = 1.18 \hbar v_F / T_c,$$

where $R_l = k_F^{-1} |1 - E_F/E_c|^{-1}$ is the correlation length of the Anderson transition, $\sigma = \sigma_c (k_F R_l)^{-1}$ is the static conductivity of the metal near the transition, σ_0 is the Drude conductivity of a dirty superconductor, and $\sigma_c = l^2 k_F / \pi^2 \hbar$ is the minimal metallic conductivity in the Mott sense [$\sigma_c \approx 250$ S/cm with $k_F \approx (3 \text{ \AA})^{-1}$], which determines the scale of the conductivity at the metal-insulator transition. In the insulating region, R_l determines the localization radius.

We see that the superconducting response is also preserved in the localization region. It disappears only upon a violation of the inequality $R_l > (\xi_0 l^2)^{1/3}$, i.e., only for highly localized states, for which the discrete spacing of the levels in a region on the order of R_l in size is important.

We calculated the behavior of the upper critical magnetic field $H_{c2}(T)$, ignoring the effect of the magnetic field on the Anderson transition. This approximation is justified near T_c . The relationship among σ , the derivative $(dH_{c2}/dT)_{T_c}$, and the state density at the Fermi surface is

$$k = - \frac{\sigma}{8e\hbar N(E_F)} \left(\frac{dH_{c2}}{dT} \right)_{T_c} \approx \begin{cases} 1; & \sigma \gg \sigma^* \\ \sigma & \\ \frac{\sigma}{16l^2 [N(E_F)T_c]^{1/3}}; & \sigma \ll \sigma^*, \end{cases} \quad (5a)$$

$$(5b)$$

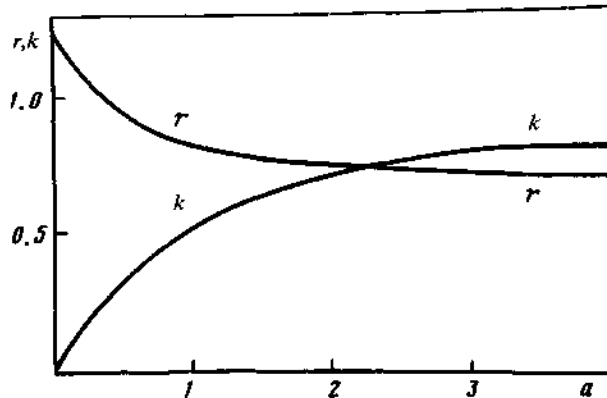


FIG. 1.

where $\sigma^* \approx \sigma_c (k_F \xi_0)^{-1/3}$ is a measure of the effect of localization on the superconductivity. This quantity is approximately equal to the minimal metallic conductivity. We see from (5) that relation (5a), which is familiar relation in the theory of dirty superconductors, is violated as we approach the Anderson transition. Figure 1 shows the complete dependence of the coefficient k on the parameter

$$a = 1.23 \frac{\sigma}{\sigma^*} \left[1 + \frac{\sigma}{\sigma^*} (k_F \xi_0)^{-1/3} \right]^{-1}.$$

Also shown here is the dependence $r(a) = -H_{c2}(0)/T_c (dH_{c2}/dT)_{T_c}$. As the degree of disorder increases, this coefficient increases from the value 0.69, characteristic of ordinary dirty superconductors, to 1.24. The positive curvature on the $H_{c2}(T)$ curve gives way to a negative curvature.

We know from the work of Anderson, Muttalib, and Ramakrishnan⁴ that as a system approaches the localization threshold, the critical temperature T_c falls off because of an intensification of the effective Coulomb repulsion of electrons (the attenuation of the diffusion of electrons opposes their dispersal). Our calculations show that in systems with low values of E_F (on the order of 1000 K) and a rather high initial temperature T_c (on the order of 10–15 K in the absence of disorder) the localization region can be reached while a significant value of T_c is retained.

A behavior of σ and $(dH_{c2}/dT)_{T_c}$, which agrees with (5) and Fig. 1, has been observed in some real systems: the bombarded ternary chalcogenides SnMo_5S_6 (Ref. 9) and $\text{Pb}_{1-x}\text{U}_x\text{Mo}_6\text{S}_8$ (Ref. 10). Measurements⁹ of the coefficient γ in the specific heat show that the state density $N(E_F)$ is essentially independent of the degree of disorder. We might note that compounds of both types are convenient for arranging the Anderson transition, because the values of E_F in these compounds lie near a band edge and because of the comparatively high temperatures, $T_c \approx 10$ –15 K. The pronounced disordering which results from bombardment causes T_c to decrease to 1 K in these materials, causes the residual resistance to increase to values $> 10^{-3} \Omega \text{ cm}$, and leads to a negative coefficient of the resistance which is significant in magnitude over the entire temperature range studied. These results strongly indicate that these compounds, when subjected to neutron bombardment, are in fact near an Anderson transition while retaining superconducting properties.

We wish to thank O. V. Dolgov, E. G. Maksimov, V. N. Flerov, D. E. Khmel'nitskiĭ, and D. I. Khomskiĭ for useful discussions. We also thank N. E. Alekseevskiĭ, V. E. Arkhipov, and B. N. Goshitskiĭ for information on experiments on bombarded superconductors.

¹P. W. Anderson, *Phys. Rev.* **109**, 1492 (1958).

²M. V. Sadovskii, *Usp. Fiz. Nauk* **133**, 223 (1981) [*Sov. Phys. Usp.* **24**, 96 (1981)].

³Y. Imry and M. Strongin, *Phys. Rev. B* **24**, 6353 (1981).

⁴P. W. Anderson, K. A. Muttalib, and T. V. Ramakrishnan, *Phys. Rev. B* **28**, 117 (1983).

⁵L. Coffey, K. A. Muttalib, and K. Levin, *Phys. Rev. Lett.* **52**, 783 (1984).

⁶W. Götze, *J. Phys. C* **12**, 1251 (1979).

⁷D. Vollhardt and P. Wölffe, *Anderson Localization* (ed. Y. Nagaoka and H. Fukuyama), Springer Series in Solid Sciences, Vol. 39, Springer-Verlag, New York, 1982, p. 26.

⁸A. V. Myasnikov and M. V. Sadovskii, *Fiz. Tverd. Tela (Leningrad)* **24**, 3569 (1982) [*Sov. Phys. Solid State* **24**, 2033 (1982)].

⁹S. A. Davydov, V. E. Arkhipov, V. I. Voronin, and B. N. Goshitskiĭ, *Fiz. Met. Metalloved.* **55**, 931 (1983).

¹⁰N. E. Alekseevskiĭ, A. V. Mitin, V. N. Samosyuk, and V. I. Firsov, *Zh. Eksp. Teor. Fiz.* **85**, 1092 (1983) [*Sov. Phys. JETP* **58**, (3) (1983)].

Translated by Dave Parsons

Edited by S. J. Amoretty

Anderson Localization and Superconductivity

L. N. Bulaevskii

P. N. Lebedev Physical Institute, USSR Academy of Sciences, Moscow, USSR

M. V. Sadovskii

Institute for Metal Physics, Ural Scientific Centre, USSR Academy of Sciences, Sverdlovsk, USSR

(Received July 3, 1984; revised October 11, 1984)

The possibility of superconductivity is considered for a strongly disordered metal approaching the Anderson transition. A microscopic derivation of the coefficients of the Ginzburg-Landau expansion is given for a system in the vicinity of the mobility edge. The localization transition is described within the framework of the self-consistent theory of localization. The superconducting response persists in the localization region. The appropriate change in the behavior of the upper critical field H_{c2} is considered for the localization region. The Coulomb repulsion grows as the Fermi level approaches the mobility edge, leading to a degradation of the superconducting T_c . However, under rather rigid conditions superconductivity is possible both at the mobility edge and in a narrow region below the mobility edge, i.e., in an Anderson insulator. Finally, experimental data for superconducting molybdenum sulfides irradiated by fast neutrons are discussed.

1. INTRODUCTION

The concept of localization forms the basis of the modern theory of electrons in strongly disordered systems.^{1,2} Sufficiently strong disorder introduced into an ideal metallic system leads to the localization of electronic states in the vicinity of the Fermi level (Anderson transition).³ The electronic density of states at the Fermi level remains finite, but because of spatial localization of the electronic wave functions, dc electrical conductivity at zero temperature is impossible, i.e., the system becomes an insulator. At the same time if there exists an attraction of electrons in the vicinity of the Fermi level, the metallic system becomes superconducting at low temperatures.⁴ So the problem arises of the interplay of these two types of transitions, leading to essentially different ground states of the system (insulator versus superconductor). This question is also important from an

experimental point of view due to a strong dependence of the superconducting properties of some compounds on the degree of the structural disorder, which can be changed greatly by fast neutron irradiation.

The influence of localization on superconductivity has been dealt with in a number of recent theoretical papers.⁵⁻¹³ Attention was paid particularly to the study of localization corrections in two-dimensional superconductors.⁶⁻¹⁰ However, the possibility of superconductivity in the vicinity of a real Anderson transition was not studied. In this paper we address the problem of superconductivity in a three-dimensional metal undergoing an Anderson transition. From the experimental point of view we consider a rather exotic situation. In fact in most metals the Anderson transition is not realized even for the fully amorphous state. This is due to the rather high values of the typical Fermi energy E_F . Possible candidates are metals with low values of E_F (semimetals, narrow-band conductors) and also quasi-one-dimensional and quasi-two-dimensional conductors.

In the first part of the paper we treat the problem in the framework of the BCS model,⁴ which assumes the existence of an attractive interaction between electrons near the Fermi level. For this model a statement can be proved (Anderson theorem)¹⁴ that claims the unimportant influence of structural disorder on the superconducting transition temperature T_c . The arguments used in this proof are, in fact, independent of whether the electronic states are localized or not.^{6,8,11} However a question arises about the physical meaning of T_c in the localization region, as to whether below this temperature the system still has the Meissner response to an external magnetic field and can sustain a persistent current. This problem can be solved by the derivation of the Ginzburg-Landau (GL) equations for the system in the vicinity of the Anderson transition. We shall demonstrate that superconductivity persists for $T < T_c$, i.e., an Anderson insulator-superconductor transition is possible. On the basis of the GL equations, we study the behavior of the upper critical field H_{c2} in the region of the Anderson transition.

To justify the applicability of the BCS model we must show that the electron-phonon mechanism of electron-electron attraction may dominate over Coulomb repulsion even in the localization region. In a recent paper Anderson *et al.*¹² demonstrate that the diffusive nature of electron motion in a disordered system leads to the growth of an effective repulsion of electrons forming Cooper pairs and to the appropriate suppression of T_c with disorder. We shall show, however, that under rather rigid conditions the value of T_c remains finite both at the mobility edge and in some narrow region below the mobility edge (Anderson insulator), although it is the growth of the Coulomb repulsion that leads to the destruction of superconductivity in the insulator phase at some critical disorder.

Finally, we discuss some experiments on superconductors irradiated by fast neutrons, which give some evidence on the possible realization of our theoretical estimates in real systems.

2. GINZBURG-LANDAU EQUATIONS

2.1. General Relations

Consider the electrons in a disordered system, assuming the existence of an effective electron-electron attraction g , in an energy region of the order of $2\omega_D$ around the Fermi level (ω_D is the Debye frequency). To study the problem of superconductivity in such a system we must not only discuss the value of T_c , but also consider the response to an external vector potential \mathbf{A} .

In the general case, the study of response functions for a superconducting system with localized one-electron states presents a rather difficult problem. However, near T_c the problem simplifies, and in fact we must only show that the free energy density for our system can be represented by the standard GL form^{15,16}

$$F = F_n + A|\Delta|^2 + \frac{1}{2}B|\Delta|^4 + C \left| \left(\frac{\partial}{\partial \mathbf{r}} - \frac{2ie}{\hbar c} \mathbf{A} \right) \Delta \right|^2 \quad (1)$$

where F_n is the free energy density for the normal state and Δ is the superconducting order parameter. Now the problem reduces to the microscopic derivation of the coefficients A , B , and C in (1), taking into account the possibility of electron localization in the disordered system, thus generalizing the results of Gorkov^{15,16} for "dirty" superconductors. In the following we use the system of units $\hbar = 1$, restoring the value of \hbar only in some final expressions.

Within the BCS model the coefficients A and B in fact do not change in comparison with the ordinary theory of "dirty" superconductors, even as we approach the mobility edge, so long as the Anderson theorem can be applied. Below we shall determine the appropriate conditions. Less trivial is the behavior of the coefficients C , which in fact determines the superconducting response. In the limit of ordinary "dirty" superconductors it is proportional to the diffusion coefficient of electrons, i.e., to the conductivity at $T=0$. As we approach the mobility edge this conductivity goes to zero. However, we shall show that in the region of the Anderson transition C remains finite even in the region of localized states.

To determine the coefficients of the GL expansion it is sufficient to study the two-particle Green's functions for the normal system.¹⁵ We introduce two-particle Matsubara Green's functions for electrons in the normal

system in the momentum representation¹⁷⁻¹⁹:

$$\begin{aligned}\psi(\mathbf{q}\omega_m \varepsilon_n) &= -\frac{1}{2\pi i} \int \frac{d^3\mathbf{p}}{(2\pi)^3} \int \frac{d^3\mathbf{p}'}{(2\pi)^3} \\ &\quad \times \langle G(\mathbf{p}_+, \mathbf{p}'_+ - \varepsilon_n + \omega_m) G(-\mathbf{p}'_- - \mathbf{p}_- - \varepsilon_n) \rangle \\ \phi(\mathbf{q}\omega_m \varepsilon_n) &= -\frac{1}{2\pi i} \int \frac{d^3\mathbf{p}}{(2\pi)^3} \int \frac{d^3\mathbf{p}'}{(2\pi)^3} \\ &\quad \times \langle G(\mathbf{p}_+, \mathbf{p}'_+ - \varepsilon_n + \omega_m) G(\mathbf{p}'_- \mathbf{p}_- - \varepsilon_n) \rangle\end{aligned}\quad (2)$$

where the angular brackets denote averaging over the random configurations of the disordered system, $\mathbf{p}_\pm = \mathbf{p} \pm \frac{1}{2}\mathbf{q}$, $\varepsilon_n = (2n+1)\pi T$, and $\omega_m = 2\pi mT$. Graphically these functions are represented (for $\omega_m = 2\varepsilon_n$) in Fig. 1, where shaded blocks denote the exact vertex parts in the standard impurity diagram technique.

Then for the coefficients A , B , and C we get^{9,15,16}

$$A = \frac{1}{g} + 2\pi i T \sum_{\varepsilon_n} \psi(\mathbf{q}=0, \omega_m = 2\varepsilon_n) \quad (3)$$

$$C = i\pi T \sum_{\varepsilon_n} \frac{\partial^2}{\partial q^2} \psi(\mathbf{q}\omega_m = 2\varepsilon_n)|_{q=0} \quad (4)$$

We see that the superconducting properties are determined by the function ψ describing the propagation of two electrons. At the same time the function ϕ describes the kinetic properties of the normal state and the localization transition. In the case of time-reversal invariance, i.e., in the absence of external magnetic field and magnetic impurities, we have^{18,19}

$$\psi(\mathbf{q}\omega_m) = \phi(\mathbf{q}\omega_m) \quad (5)$$

and our problem reduces to the calculation of $\phi(\mathbf{q}\omega_m)$.

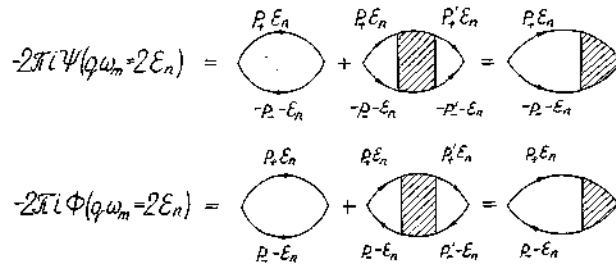


Fig. 1. Diagrammatic representation for ψ and ϕ . Shaded blocks denote the exact vertexes of the impurity diagram technique. There is no summation over ε_n in the loops.

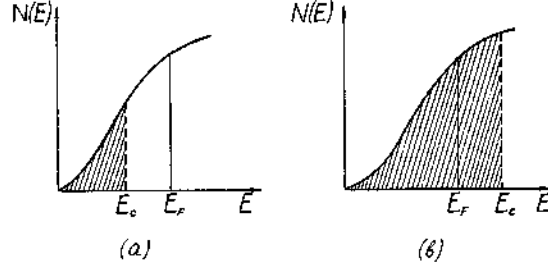


Fig. 2. Anderson transition showing the density of states in the conduction band. States with $E < E_c$ are localized. (a) Metallic phase ($E_F > E_c$); (b) insulator phase ($E_F < E_c$).

For a disordered system the electronic states of the conduction band are localized near the band edge up to an energy E_c (the mobility edge). As the disorder grows, the value of E_c moves upward and can pass the Fermi level E_F (see Fig. 2). Thus we have an Anderson transition. As a one-electron model of this transition we take Götze's self-consistent theory of localization in the form proposed by Vollhardt and Wölfle.¹⁷⁻²¹ The main attraction of this theory is the practical possibility of performing calculations for the whole range of parameters of the system, from "good" metal to Anderson insulator. For small \mathbf{q} and ω_m we have

$$\phi(\mathbf{q}\omega_m) = -\frac{N(E_F)}{i|\omega_m| + i\tilde{D}(|\omega_m|)q^2} \quad (6)$$

where the generalized diffusion coefficient at the Fermi level $\tilde{D}(\omega_m)$ is determined by the self-consistency equation^{17,18}

$$\frac{D_0}{\tilde{D}(\omega_m)} = 1 - \frac{i}{\pi N^2(E_F)} \int \frac{d^3\mathbf{q}}{(2\pi)^3} \phi(\mathbf{q}\omega_m) \quad (7)$$

Here $N(E_F)$ is the electronic density of states at the Fermi level in a disordered system, $D_0 = \frac{1}{3}v_F^2\tau$ is the "bare" diffusion coefficient, τ is the mean free time in the Born approximation, and v_F is the Fermi velocity. For a model of pointlike random scatterers with scattering amplitude V and spatial density ρ we have $1/\tau = 2\pi\rho V^2 N(E_F)$. In the following the "bare" mean free time τ and the appropriate mean free path $l = v_F\tau$ will characterize the degree of disorder. In the localization region these parameters obviously do not have the same simple meaning, which is clear in the metallic state.

For the three-dimensional case (7) reduces to^{18,21}

$$\frac{\tilde{D}(\omega_m)}{D_0} = 1 - \frac{\lambda}{\lambda_c} - \frac{\pi}{2} \frac{\lambda}{\lambda_c} \left[\frac{D_0}{\tilde{D}(\omega_m)} \omega_m \tau \right]^{1/2} \quad (8)$$

where $\lambda = (2\pi E_F \tau)^{-1}$ and λ_c is the value of λ for $E_F = E_c$. The solution of (8) can be written approximately as

$$\tilde{D}(\omega_m) \approx \text{Max} \left[D \frac{\omega_m}{\omega_m + 3D\omega_0^2/v_F^2}; D_0(\omega_m \tau)^{1/3} \right] \quad (9)$$

where

$$D = D_0(k_F R_l)^{-1} \quad (10)$$

is the renormalized diffusion coefficient, while the characteristic frequency ω_0 is

$$\omega_0^2 = \begin{cases} \frac{1}{3} v_F^2 R_l^{-2}; & E_F < E_c \quad (\text{insulator}) \\ 0; & E_F \geq E_c \quad (\text{metal}) \end{cases} \quad (11)$$

Here R_l is the correlation length for the Anderson transition.^{1,18,20} For E_F near E_c we have

$$R_l = \frac{1}{k_F} \left| 1 - \frac{\lambda}{\lambda_c} \right|^{-\nu} \approx \frac{1}{k_F} \left| \frac{E_F - E_c}{E_c} \right|^{-\nu} \quad (12)$$

where ν is the critical exponent. In the self-consistent theory, for the three-dimensional case $\nu = 1$; however, experimentally the value may differ. The frequency ω_0 is in many respects similar to an order parameter in the usual theory of phase transitions. It becomes nonzero in the localized phase and determines the insulator nature of the electromagnetic response, e.g., the dielectric function.^{17-20,31} In principle it is a measurable characteristic of the localized phase and gives information on R_l [see (11)] in the insulator region in the same manner as σ defines it in the metal region (see below).

The position of the mobility edge in the conduction band for free electrons in the model of pointlike scatterers is determined by the estimate²⁰

$$E_c = \frac{9}{2\pi^4} m^3 (\rho V^2)^2 = \frac{9}{4\pi^2} E_F (E_F \tau)^{-2} \Big|_{E_F = E_c} \quad (13)$$

At the mobility edge ($E_F = E_c$) we have $E_F \tau = 3/2\pi$ or $k_F l = 3/\pi$. With the growth of disorder, i.e., of the value of ρV^2 , τ diminishes and R_l grows in the metallic region ($E_F > E_c$), while the renormalized diffusion coefficient (and conductivity) drops to zero at the transition at $E_F = E_c$ where $R_l = \infty$. With further growth of disorder we enter the localization region, where R_l determines the localization length of an electron. Here R_l drops as E_F moves deep into the localization region, while ω_0 grows, similarly to the growth of an order parameter in the condensed phase in the theory of phase transitions.

Note that the equations of the self-consistent theory of localization are derived with the essential use of perturbation theory over the parameter $(E_F\tau)^{-1}$. Actually, as we have seen above, this parameter is not small at the mobility edge, and the self-consistent theory in fact has no controllable small parameter.²⁰

For the metallic phase ($E_F \geq E_c$) the experimentally measurable static conductivity σ is determined by the renormalized diffusion coefficient and can be expressed as

$$\sigma = 2e^2 DN(E_F) = \sigma_0/k_F R_l = \sigma_0 - \sigma_c \quad (14)$$

where $\sigma_0 = 2e^2 D_0 N(E_F)$ is the usual Drude conductivity and σ_c is its value at the mobility edge ($E_F = E_c$): $\sigma_c = e^2 k_F / \pi^3 \hbar$. The last equality in (14) is valid for $\nu = 1$. We shall use this relation following from the self-consistent theory to simplify the analysis, although, as we have already stressed, the experimental value of ν may be quite different and for $\sigma_0 \approx \sigma_c$ the relation (14) is replaced by

$$\sigma \approx \sigma_c \left(\frac{\sigma_0 - \sigma_c}{\sigma_c} \right)^\nu$$

In most experiments on the strongly disordered metals the typical scale for σ_0 is determined by the Ioffe-Regel limit²²; the mean free path is of the order of a few interatomic distances and $\sigma \approx \sigma_0 \approx 10^3 \Omega^{-1} \text{cm}^{-1}$.^{*} However, near the Anderson transition the value of σ_0 drops to σ_c , which is obviously of the order of the minimum metallic conductivity due to Mott and Davis²³: $\sigma_c \approx (2-5) \times 10^2 \Omega^{-1} \text{cm}^{-1}$. This is a characteristic conductivity scale for the continuous Anderson transition.¹ Using (14), we can, in principle, relate σ_0 to the experimental value of the conductivity σ : $\sigma_0 = \sigma_c + \sigma$. However, the value of σ_c should be considered as an obvious fitting parameter, to be determined from experimental dependences.

An obvious limitation of our theory is the explicit neglect of the effect of the electron-electron interaction upon the metal-insulator transition in the disordered system. We assume the validity of the picture of the Anderson transition³ as described in the one-electron approximation. However, it is known^{31,32} that the electron interaction has an important effect in the vicinity of this transition. Within the framework of the BSC model where the only interelectron interaction is an attraction in the vicinity of the Fermi level,

^{*}The Ioffe-Regel conductivity region is characterized by a very low negative temperature coefficient of resistivity and strictly speaking cannot be described by the usual Boltzmann-Drude theory. In most of this paper we are concerned with still lower values of the conductivity, of the order of σ_c , typical of the vicinity of the Anderson transition. However, it is possible that the actual behavior of the system in the Ioffe-Regel region is intimately connected to localization.

described by the pairing constant g , we are free to assume the weakness of this interaction, i.e., $gN(E_F) \ll 1$, and neglect its influence upon the pair propagator $\phi(q, \omega_m)$ completely. In a real system we apparently have to consider electron-phonon and Coulomb interactions and disorder on an equal footing (see below). Unfortunately, there is no complete theory of the metal-insulator transition in disordered systems.

Thus we limit ourselves to the study of the coexistence of localization and superconductivity in the framework of the BCS model in the weak coupling limit.

2.2. Coefficients of the GL Expansion

The details of the calculations leading to the final expressions for the GL coefficients A , B , and C are given in Appendix A. Here we quote only the results. The coefficients A and B , determining the transition temperature and the order parameter near T_c in complete accordance with the Anderson theorem, are described by the usual expressions for "dirty" superconductors^{15,16}:

$$\begin{aligned} A &= N(E_F) \ln \frac{T}{T_c} \approx N(E_F) \frac{T - T_c}{T_c} \\ B &= \frac{7\zeta(3)}{8\pi^2 T_c^2} N(E_F); \quad T_c = 1.13\omega_D e^{-1/\lambda} \end{aligned} \quad (15)$$

where $\lambda = gN(E_F)$. These expressions depend on disorder only through $N(E_F)$, but they are valid even below the mobility edge ($E_F < E_c$), i.e., in an Anderson insulator.

Significant changes occur in the coefficient C of the gradient term of the GL expansion. Using (4)-(6) and (9), we find

$$C \approx \begin{cases} \frac{\pi}{8T_c} N(E_F) D; & R_l < (\xi_0 l^2)^{1/3}; E_F > E_c \\ N(E_F) \left(\frac{D_0 l}{T_c} \right)^{2/3} \approx N(E_F) (\xi_0 l^2)^{2/3}; & R_l > (\xi_0 l^2)^{1/3}; E_F \approx E_c \\ N(E_F) R_l^2 \ln \frac{1.78 D}{\pi T_c R_l^2}; & R_l < (\xi_0 l^2)^{1/3}; E_F < E_c \end{cases} \quad (16)$$

where $\xi_0 = 0.18 v_F / T_c$ is the superconducting coherence length. In the metallic region, as the Fermi energy E_F approaches the mobility edge E_c , the characteristic length R_l grows and the coefficient C diminishes as the renormalized diffusion coefficient D from (10) and is proportional to the metallic conductivity (14). However, in the vicinity of the mobility edge,

as $\sigma \rightarrow 0$, C diminishes more slowly and remains finite even for $E_F < E_c$ (Anderson insulator). With further lowering of E_F deep into the localization region, C is determined by the localization length R_b , which diminishes as E_F moves apart from E_c .

Our analysis of the insulator region ($E_F < E_c$) is limited to the range of sufficiently large R_b such that⁵

$$[N(E_F)R_b^3]^{-1} \ll T_c \quad (17)$$

This is the condition of a large number of discrete energy levels within a sphere of radius R_b in the energy interval T_c , which is the necessary condition for Cooper pairing of localized electrons. It is easy to see that (17) reduces to

$$R_b \gg [N(E_F)T_c]^{-1/3} \sim (\xi_0/k_F^2)^{1/3} \sim (\xi_0 l^2)^{1/3}; \quad E_F < E_c \quad (18)$$

Thus the final asymptotics in (16) in fact has no region of applicability, and within the BCS model the condition of superconductivity in the insulator phase is given by (17) and (18). The meaning of these results is that the electron motion within a localization region of size R_b is sufficient to produce coherent Cooper pairs.

For the superconducting correlation length $\xi(T)$ and the London penetration length λ_L we obtain, using (1) and (14)–(16) (cf. Ref. 16)

$$\xi^2(T) \approx \left(\frac{T_c - T}{T_c}\right)^{-1} \begin{cases} \xi_0 l \frac{\sigma}{\sigma + \sigma_c}; & \sigma > \sigma^* (E_F > E_c) \\ (\xi_0 l^2)^{2/3}; & \sigma < \sigma^* (E_F \cong E_c) \end{cases} \quad (19)$$

$$\lambda_L^{-2} = 32\pi e^2 c^{-2} N(E_F) \Delta^2 \xi^2(T) (1 - T/T_c)$$

From (19) we can see that both $\xi^2(T)$ and λ_L^{-2} initially drop proportionally to σ , while the disorder grows, but already in the metallic region, for $R_b \gg (\xi_0 l^2)^{1/3}$, these quantities diminish more slowly than the conductivity. This change of behavior starts for

$$\sigma \approx \sigma^* \approx \sigma_c (k_F \xi_0)^{-1/3} \quad (20)$$

which is the key quantity for the effect of localization on the superconducting coherence length. For typical values of $\xi_0 \sim 100l$ and $l \sim k_F^{-1}$ we have $\sigma^* \approx 10^2 \Omega^{-1} \text{ cm}^{-1}$, i.e., the value of σ^* is smaller in general than the minimal metallic conductivity. However, it is again better to understand it as a parameter to be determined from experiments, showing the transition to a behavior different from the predictions of the usual theory of “dirty” superconductors.

For the insulator phase the values of $\xi^2(T)$ and λ_L^{-2} remain finite, although they diminish further with l . The critical current for a thin supercon-

ducting plate is proportional to $\lambda_L^{-2}/\xi(T)$,¹⁶ and remains finite after σ becomes zero.

Finally, we note that our results give evidence of localization destruction for electrons forming Cooper pairs. However, the character of the wave functions and kinetic properties for one-particle excitations below T_c are at present unknown.

2.3. The Upper Critical Field

Direct information about $\xi^2(T)$ can be obtained through measurements of the upper critical field H_{c2} ,¹⁶

$$H_{c2} = \phi_0/2\pi\xi^2(T); \quad \phi_0 = \pi\hbar/e \quad (21)$$

Using (19), we obtain a relation connecting σ , $(dH_{c2}/dT)_{T_c}$, and the value of $N(E_F)$, which can be determined through independent measurements of the electronic specific heat:

$$-\frac{\sigma}{N(E_F)}\left(\frac{dH_{c2}}{dT}\right)_{T_c} \approx \begin{cases} \frac{8e^2}{\pi^2\hbar}\phi_0; & \sigma > \sigma^* \\ \frac{\phi_0}{2\pi} \frac{\sigma}{[N(E_F)T_c]^{1/3}}; & \sigma < \sigma^* \end{cases} \quad (22a)$$

$$(22b)$$

On the rhs of (22a) only fundamental constants appear, and this relation is often used for the interpretation of measurements on irradiated superconductors.^{24,25} Using this relation, we can find values of $N(E_F)$ for different degrees of disorder from the measured values of $(dH_{c2}/dT)_{T_c}$ and conductivity σ . However, near the metal-insulator transition, when $\sigma \leq \sigma^*$, this relation is already invalid and the described method of interpretation of measurements of $(dH_{c2}/dT)_{T_c}$ simulates a fall of $N(E_F)$ with σ according to (22b). In real systems this behavior was observed in Refs. 24 and 25 and we stress the importance of independent experiments to determine $N(E_F)$. According to preliminary data obtained by the authors of Ref. 24 via specific heat measurements, the value of $N(E_F)$ remains practically unchanged with the growth of disorder.

Here it is appropriate to note that our derivation of the coefficient C essentially used time-reversal invariance, as expressed by (5), which is correct in the absence of external magnetic field (and magnetic impurities). So our results are formally correct in the limit of an infinitesimal external field, which is sufficient for the demonstration of the superconducting (Meissner) response and for the determination of $(dH_{c2}/dT)_{T_c}$, because $H_{c2} \rightarrow 0$ for $T \rightarrow T_c$ (see below). In a finite external field we must take into account the influence of the magnetic field upon localization, which is

expressed by the violation of (5). This problem is far from being solved. However, if we neglect this influence, we can calculate the full dependence of the orbital upper critical field $H_{c2}(T)$. This is determined by the equation²⁶

$$\ln \frac{T}{T_c} = \pi T \sum_{\varepsilon_n} \left\{ \frac{1}{|\varepsilon_n| + \tilde{D}(2|\varepsilon_n|) \pi H / \phi_0} - \frac{1}{|\varepsilon_n|} \right\} \quad (23)$$

where $\tilde{D}(2\varepsilon_n)$ is determined from Eq. (8). Introducing the parameter

$$a = 1.23 \frac{\sigma}{\sigma^*} \left[1 + \frac{\sigma}{\sigma^*} (k_F \xi_0)^{-1/3} \right]^{-1} \quad (24a)$$

and calculating b_n , x , and S via the equations

$$2n+1 = b_n(b_n - a)^2; \quad b_n > a; \quad S = \sum_{n=0}^{\infty} b_n(2n+1)^{-2} \quad (24b)$$

$$\left[1 + \frac{x}{2(1+x)} \right] \ln x + \frac{\pi}{2} \frac{\sqrt{x}}{1+x} + \ln 3.56a^3 = 0$$

we obtain the characteristic parameters:

$$r(a) = -\frac{H_{c2}(0)}{T_c(dH_{c2}/dT)_{T_c}} = 2a^2xS \quad (25)$$

$$k(a) = -\frac{\pi^2\sigma}{8N(E_F)e^2\phi_0} \left(\frac{dH_{c2}}{dT} \right)_{T_c} = \frac{\pi^2 a}{8S}$$

These dependences are represented in Fig. 3. As we approach the mobility edge, $r(a)$ grows from the standard value of 0.69 typical for "dirty" superconductors²⁶ to the value 1.24 in the localization region, i.e., for $\sigma \ll \sigma^*$. This growth of $r(a)$ transforms the positive curvature in the dependence of

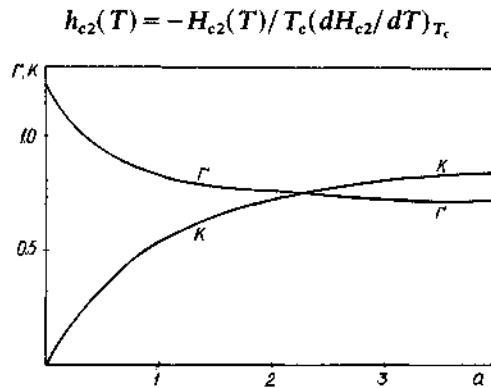


Fig. 3. Calculated dependences of r and k of Eqs. (25) on the effective disorder parameter a [Eq. (24a)].

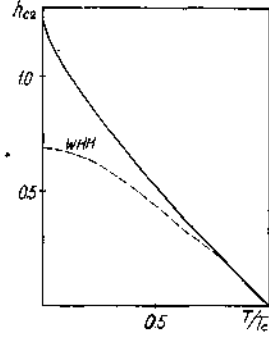


Fig. 4. Calculated dependence of $h_{c2}(T) = -H_{c2}(T)/T_c(dH_{c2}/dT)_{T_c}$ on temperature T in the localization region, $\sigma \ll \sigma^*$ (solid curve), and standard WHH dependence²⁶ for dirty superconductors (dashed curve).

on T observed for $\sigma \gg \sigma^*$ into a negative one in the region of $\sigma \leq \sigma^*$. Figure 4 shows $h_{c2}(T)$ in the localization region, i.e., for $E_F = E_c$.

Now we discuss the conditions when it is possible to neglect the magnetic field dependence of the diffusion coefficient $\tilde{D}(\omega_m)$. It is well known that a magnetic field diminishes the localization corrections due to the "maximally crossed diagrams"²⁷ and breaks the validity of Eq. (5).¹⁹ The relative change of $\tilde{D}(\omega_m)$ and the difference between ϕ and ψ is apparently proportional to $\tilde{D}(\omega_m)H/\omega_m\phi_0$, and near T_c when $\omega_m \sim T_c$ the change of $\tilde{D}(\omega_m)$ is small over the parameter $H\tilde{D}(T_c)/\phi_0T_c$. Thus, near T_c we can neglect the influence of magnetic field H_{c2} on diffusion due to $|(T_c - T)/T_c| \ll 1$, and our method of calculation correctly determines the values of $k(a)$. However, possible magnetic field corrections to $r(a)$ may be important. For $T \rightarrow 0$ the critical field H_{c2} grows, suppressing the localization corrections, and $\tilde{D}(\omega_m)$ grows, thus diminishing H_{c2} . However, according to Coffey *et al.*,¹³ this growth of $\tilde{D}(\omega_m)$ leads to the partial cancellation of the Coulomb contribution to the effective pairing constant g (see below). This effect was studied by the authors of Ref. 13 for the metallic region and $\sigma > \sigma^*$. However, they did not take into account the ω dependence of the effective diffusion coefficient, which becomes important for $\sigma \sim \sigma^*$. Our results show that the appropriate changes of H_{c2} are not small, so that taking account of changes in g , as in Ref. 13, is not sufficient for the correct determination of $H_{c2}(0)$. Thus, the final value of the correction to our estimate of $r(a)$ is not clear at present, and the difference between experimental values and our value of $r(a)$ can give an estimate of the magnetic field influence on the diffusion coefficient $\tilde{D}(\omega_m)$, i.e., upon localization.*

*Experimentally, dependences of $h_{c2}(T)$ similar to that shown in Fig. 4 were observed by Tenhover *et al.*²⁸ for amorphous MoRe. However their data for k do not differ from the standard value 0.69 [in calculating k , they use the experimental values of σ , $(dH_{c2}/dT)_{T_c}$, and of the coefficient γ in the temperature dependence of the electronic specific heat].

3. COULOMB INTERACTION FOR STRONGLY DISORDERED SUPERCONDUCTORS

3.1. Coulomb Kernel for the Gap Equation

In the BCS model discussed above we have assumed the existence of an effective pairing interaction g in the energy region of the order of $2\omega_D$ around the Fermi level. However, in real systems the pairing interaction is determined by the interplay between the attraction due to electron-phonon coupling and Coulomb repulsion.¹⁶ Clearly, for a strongly disordered system in the vicinity of the Anderson transition both interactions can change appreciably in comparison with a "pure" system.

It is well known that the Coulomb contribution to the effective pairing interaction is significantly weakened in comparison with the phonon contribution, due to the retarded nature of the electron-electron interaction via the exchange of virtual phonons. For the electron-phonon interaction the characteristic time is ω_D^{-1} , while for the Coulomb interaction in a "pure" system it is of the order of E_F^{-1} because this is the time during which the electrons pass each other in the Cooper pair. Both interactions are practically pointlike due to screening. With the growth of disorder an electron leaves the given region in space more slowly and this leads to an effective growth of Coulomb repulsion in the Cooper pair and to the corresponding lowering of T_c . This mechanism for the degradation of T_c with disorder was studied by Anderson *et al.*¹² using the scaling hypothesis. Below we shall consider this suppression of T_c within the self-consistent theory. In the metallic region our estimates are in qualitative agreement with Ref. 12, although quantitatively they are different. However, our analysis of T_c leads to the conclusion that superconductivity can survive in the localized phase if rather rigid conditions are satisfied.

In a strongly disordered system we must consider the matrix element of the screened Coulomb interaction $v(\mathbf{r}-\mathbf{r}')$ over exact eigenfunctions $\varphi_\nu(\mathbf{r})$ associated with exact eigenenergies ε_ν of an electron in the random field of this system:

$$\langle \mu\nu | v(\mathbf{r}-\mathbf{r}') | \nu\mu \rangle = \int d\mathbf{r} \int d\mathbf{r}' v(\mathbf{r}-\mathbf{r}') \varphi_\mu^*(\mathbf{r}') \varphi_\nu^*(\mathbf{r}) \varphi_\mu(\mathbf{r}) \varphi_\nu(\mathbf{r}') \quad (26)$$

Averaging this matrix element over two isoenergetic surfaces E_F and $E_F + \omega$ and over the disorder, we obtain the Coulomb kernel for the superconducting gap equation in the following form:

$$\begin{aligned} K_C(\omega) &= \frac{1}{N(E_F)} \left\langle \sum_{\mu\nu} \langle \mu\nu | v(\mathbf{r}-\mathbf{r}') | \nu\mu \rangle \delta(E_F - \varepsilon_\nu) \delta(E_F + \omega - \varepsilon_\mu) \right\rangle \\ &= \int d\mathbf{r} \int d\mathbf{r}' v(\mathbf{r}-\mathbf{r}') \langle \langle \rho_{E_F}(\mathbf{r}) \rho_{E_F+\omega}(\mathbf{r}') \rangle \rangle \end{aligned} \quad (27)$$

Here we have introduced Berezinskii-Gorkov spectral density²⁹:

$$\begin{aligned} \langle\langle \rho_{E_F}(\mathbf{r}) \rho_{E_F+\omega}(\mathbf{r}') \rangle\rangle &= \frac{1}{N(E_F)} \left\langle \sum_{\mu\nu} \varphi_\nu^*(\mathbf{r}) \varphi_\mu(\mathbf{r}) \varphi_\mu^*(\mathbf{r}') \varphi_\nu(\mathbf{r}') \right. \\ &\quad \left. \times \delta(E_F - \varepsilon_\nu) \delta(E_F + \omega - \varepsilon_\mu) \right\rangle \end{aligned} \quad (28)$$

which gives the complete information on the nature of the electronic states. In particular, in the localization region, i.e., for $E_F < E_c$, this spectral density contains a singular $\delta(\omega)$ contribution²⁹:

$$\langle\langle \rho_{E_F}(\mathbf{r}) \rho_{E_F+\omega}(\mathbf{r}') \rangle\rangle = P(\mathbf{r}-\mathbf{r}') \delta(\omega) + \dots \quad (29)$$

where

$$P(\mathbf{r}-\mathbf{r}') = \frac{1}{N(E_F)} \left\langle \sum_\nu \delta(E_F - \varepsilon_\nu) |\varphi_\nu(\mathbf{r})|^2 |\varphi_\nu(\mathbf{r}')|^2 \right\rangle \quad (30)$$

is the generalized inverse participation ratio connected with a finite probability of an electron returning to the initial point in an infinite time.³⁰

Fourier transforming (27), we get

$$K_C(\omega) = \int \frac{d^3\mathbf{q}}{(2\pi)^3} v(\mathbf{q}) \langle\langle \rho_{E_F} \rho_{E_F+\omega} \rangle\rangle_{\mathbf{q}} \quad (31)$$

Below we shall assume a pointlike interaction $v(\mathbf{q}) = v_0$. For $\omega \ll \tau^{-1}$ and $q \ll l^{-1}$ the Berezinskii-Gorkov spectral density possesses a diffusion contribution³⁰:

$$\langle\langle \rho_{E_F} \rho_{E_F+\omega} \rangle\rangle_{\mathbf{q}}^d = \frac{1}{\pi N(E_F)} \text{Im} \phi^{\text{RA}}(\mathbf{q}\omega) \quad (32)$$

Within the self-consistent theory of localization¹⁷⁻²¹ $\phi^{\text{RA}}(\mathbf{q}\omega)$ is determined by an analytic continuation $i\omega_m \rightarrow \omega + i\delta$ in (6). For the metallic region we have

$$\phi^{\text{RA}}(\mathbf{q}\omega) = -\frac{N(E_F)}{\omega + i\tilde{D}(\omega)q^2} \quad (33)$$

where

$$\tilde{D}(\omega) \approx \begin{cases} D; & |\omega| \ll \omega_c = \frac{1}{\tau} \left(\frac{\sigma}{\sigma_0} \right)^3 \\ D_0(-i\omega\tau)^{1/3}; & |\omega| \gg \omega_c \end{cases} \quad (34)$$

Without disorder ($\tau^{-1} = 0$) the diffusion contribution vanishes and the kernel $K_C(\omega)$ must reduce to the ordinary Coulomb potential $\mu = N(E_F)v_0$. Thus

we use the approximate relation

$$K_C(\omega) \approx \mu + K_C^d(\omega)$$

$$K_C^d(\omega) = v_0 \int \frac{d^3 \mathbf{q}}{(2\pi)^3} \langle \langle \rho_{E_F} \rho_{E_F+\omega} \rangle \rangle_{\mathbf{q}}^d \quad (35)$$

reproducing the main difference between pure and disordered metals by the value $K_C^d(\omega)$. Using the above relations, we shall find $K_C(\omega)$ and solve the linearized gap equation for the order parameter $\Delta(\omega)$ to determine T_c and the conditions for the existence of superconductivity.

3.2. Metallic Region

From (32)-(34) we obtain*

$$K_C^d(\omega) = v_0 \int \frac{d^3 \mathbf{q}}{(2\pi)^3} \langle \langle \rho_{E_F} \rho_{E_F+\omega} \rangle \rangle_{\mathbf{q}}^d \approx \frac{v_0}{2\pi^3} \left\{ \frac{1}{|\bar{D}(\omega)|l} - \frac{|\omega|^{1/2}}{|\bar{D}(\omega)|^{3/2}} \right\}$$

$$\approx \frac{v_0}{2\pi^3} \begin{cases} \frac{1}{Dl} - \frac{|\omega|^{1/2}}{D^{3/2}}; & |\omega| \ll \omega_c \\ \frac{1}{D_0 l (\omega\tau)^{1/3}}; & |\omega| \gg \omega_c \end{cases} \quad (36)$$

Here we have introduced the upper cutoff at q of the order of l^{-1} .^{31,32} Then we obtain the following approximate expression for the Coulomb kernel in the metallic region and near the mobility edge (see Figs. 5a and 5b):

$$K_C(\omega) = \mu \theta(E_F - |\omega|)$$

$$+ \frac{\mu}{k_F l} \begin{cases} \frac{\sigma_c}{\sigma}; & |\omega| < \omega_c \\ \frac{1}{(|\omega|\tau)^{-1/3}}; & \omega_c < |\omega| < \tau^{-1} \sim E_F \end{cases} \quad (37a)$$

$$(37b)$$

From (37) it can be readily seen that in the vicinity of the Anderson transition we obtain a considerable growth of the Coulomb repulsion due to diffusion renormalization, which was first considered by Altshuler and Aronov.³²

The situation with regard to the electron-phonon contribution to the pairing interaction is different. Diffusion renormalization of the electron-phonon vertex does not appear,^{33,34} because the appropriate corrections are

*These expressions actually define the Fock correction to the electronic density of states $-\delta N(E)/N(E_F)$ due to electron-electron interaction.³¹ In the region of "high" frequencies $|\omega| \gg \omega_c$ they slightly modify the expressions of Ref. 31, where the ω dependence of $\bar{D}(\omega) \sim \omega^{1/3}$ was neglected.

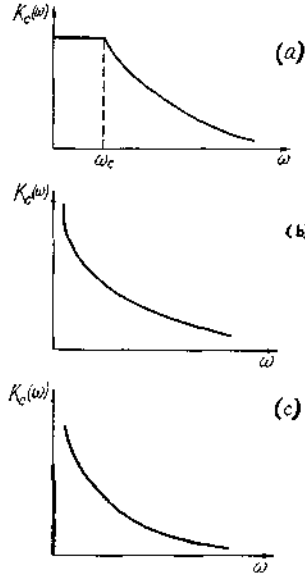


Fig. 5. Coulomb kernel (a) in the metallic region, (b) at the mobility edge, (c) and in the insulator.

cancelled when we take account of impurity vibrations. Of course, the value of the pairing interaction due to the electron-phonon interaction in a disordered system does change in comparison with the pure case. However, this change is relatively unimportant.^{12,33} Thus, following Ref. 12, we can assume that this interaction is described by some dimensionless parameter λ , which is nonzero for the energies in an interval of the order of $2\omega_D$ around the Fermi level, and is weakly dependent on disorder.

The transition temperature T_c is determined by the linearized gap equation, which we can take in the weak coupling form:

$$\begin{aligned} \Delta(\omega) = & \lambda \theta(\omega_D - \omega) \int_0^{\omega_D} \frac{d\omega'}{\omega'} \Delta(\omega') \operatorname{th} \frac{\omega'}{2T_c} \\ & - \theta(E_F - \omega) \int_0^{E_F} \frac{d\omega'}{\omega'} K_C(\omega - \omega') \Delta(\omega') \operatorname{th} \frac{\omega'}{2T_c} \end{aligned} \quad (38)$$

Consider first the metallic region and $\omega_c \gg \omega_D$, which according to the estimate of ω_c in (34) corresponds roughly to $\sigma \gg \sigma_c$ for typical values of $E_F/\omega_D \approx 10^2$, i.e., the system is not very close to the Anderson transition. We calculate the change in T_c due to a diffusion contribution in the Coulomb

kernel (37), using perturbation theory with respect to $K_C^d(\omega)$:

$$\frac{\delta T_c}{T_{c0}} = \left\{ \int_0^\infty \frac{d\omega}{\omega} \int_0^\infty \frac{d\omega'}{\omega'} \Delta_0(\omega) \operatorname{th} \frac{\omega}{2T_{c0}} K_C(\omega - \omega') \Delta_0(\omega') \operatorname{th} \frac{\omega'}{2T_{c0}} \right\} \\ \times \left\{ \frac{1}{2T_{c0}} \int_0^\infty d\omega [\Delta_0(\omega)]^2 \left(\operatorname{ch} \frac{\omega}{2T_{c0}} \right)^{-2} \right\}^{-1} \quad (39)$$

where $\Delta_0(\omega)$ is the zeroth-order solution (the usual two-step solution¹⁶) of (38) for the ordinary Coulomb kernel $K_C(\omega) = \mu \theta(E_F - \omega)$. Using (37a), we obtain

$$\frac{\delta T_c}{T_{c0}} \approx - \frac{\mu}{(\lambda - \mu_0^*)^2} \frac{1}{k_F l} \frac{\sigma_c}{\sigma} \quad (40)$$

where

$$T_{c0} = 1.13 \omega_D \exp \left(- \frac{1}{\lambda - \mu_0^*} \right), \quad \mu_0^* = \frac{\mu}{1 + \mu \ln(E_F / \omega_D)} \quad (41)$$

are the usual expressions for the critical temperature of the pure system and the standard Coulomb pseudopotential.¹⁶ Actually the change of T_c given by (40) is equivalent to the change of μ_0^* by the value

$$\delta \mu^* \approx \mu \sigma_c^2 / \sigma (\sigma + \sigma_c) \quad (42)$$

where we have used (14) and $\sigma_0 \approx \sigma_c (k_F l)$ to exclude the factor of $(k_F l)^{-1}$ in (40). According to (42), the Coulomb pseudopotential μ^* grows as σ drops and this dependence on σ here is stronger than in the similar expression of Ref. 12. This is due to our use of the expressions from the self-consistent theory of localization. The results of Ref. 12 can be obtained using another form of the generalized diffusion coefficient, equivalent to a scaling hypothesis on the q dependence introduced by Lee³⁵: $\tilde{D}(\omega \rightarrow 0, q) \approx (D_0 l) q$ for $q R_l \gg 1$. The self-consistent theory gives another limit: $\tilde{D}(\omega, q \rightarrow 0) \approx (D_0 l)^{2/3} (-i\omega)^{1/3}$ at the mobility edge. Our expression for μ^* allows a noticeable change of μ^* for the conductivity region $\sigma \approx 10^3 \Omega^{-1} \text{ cm}^{-1}$. Such a dependence can explain the typical drop of T_c in irradiated superconductors as their resistivity in the normal state grows^{24,25} in the Ioffe-Regel region. The expression for μ^* of Ref. 12 can explain the experimental data only by assuming that the values of the conductivity scale an order of magnitude larger than the typical Ioffe-Regel value, for which there seems to be no valid theoretical foundation.

Consider now the situation at the mobility edge itself, when $\sigma = 0$ and $\omega_c = 0$, and $K_C(\omega)$ is determined by the second expression in (37) for all frequencies below $\tau^{-1} \sim E_F$ (see Fig. 5b). In this case, as is shown in

Appendix B, the Coulomb effect on T_c can again be represented by the effective Coulomb pseudopotential μ^* . However, now we have ($\alpha = \text{const} \approx 1$)

$$\mu^* \approx \alpha \mu (\omega_D \tau)^{-1/3} \quad (43)$$

The value of T_c can remain finite at the mobility edge under rather rigid conditions: the parameters $E_F \sim \tau^{-1}$ and μ must be sufficiently small, while λ must be close to unity. As a crude estimate we take $\lambda \approx 1$, $\mu \leq 0.2$, and $E_F \leq 10^3 T_{c0}$. Apparently such a situation can be realized in some Chevrel phase superconductors³⁶ (see below).

Using (42) and (43), we can write down a simple interpolation formula for the dependence of μ^* on σ :

$$\mu^*(\sigma) = \mu_0^* + \frac{\alpha \mu (\omega_D \tau)^{-1/3} - \mu_0^*}{1 + (\omega_D \tau)^{-1/3} \sigma (\sigma + \sigma_c) / \sigma_c^2} \quad (44)$$

$$\omega_D \tau = \frac{\omega_D}{2E_F} \left(1 + \frac{\sigma}{\sigma_c} \right)$$

This expression describes the smooth crossover from the region where there is a weak effect of localization on T_c [Eq. (42)] to the vicinity of the Anderson transition [Eq. (43)] at $\omega_c \approx \omega_D$.

In Fig. 6 we compare the theoretical predictions of Eq. (44) with the experimental data for T_c obtained in Ref. 24 for SnMo_3S_6 . We have calculated the dependence of T_c on σ using the standard McMillan formula for T_c ¹² with $\mu^*(\sigma)$ given by (44). Following Ref. 24, we take the preexponential factor in the McMillan formula to be equal to 125 K, $\mu_0^* = 0.1$, and $\lambda = 1.06$. Then, for $E_F / \omega_D \approx 5$, we get $\mu \approx 0.13$. The theoretical curves in Fig. 6 are given for $\sigma_c \approx 1500 \Omega^{-1} \text{cm}^{-1}$ and $\alpha \approx 1.5$ and 2.0 in (44). Taking into account the crudeness of our theory, the agreement is quite satisfactory. Further discussion will be given in Section 4.

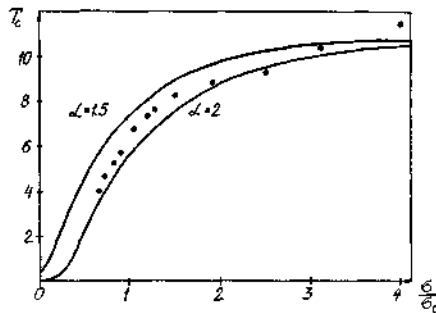


Fig. 6. Transition temperature versus conductivity. Comparison of theoretical curves with experimental data of Ref. 24. See text for details.

3.3. Localization Region

Consider now the region of $E_F < E_c$ i.e., an Anderson insulator. According to (27) and (29), in this case the Coulomb kernel has a $\delta(\omega)$ contribution connected to electron repulsion in one quantum state [see (30) and Ref. 31; see also Fig. 5c]:

$$K_C^1(\omega) = v_0 P \delta(\omega); \quad P = P(\mathbf{r} - \mathbf{r}')|_{\mathbf{r}=\mathbf{r}'} \sim R_l^{-3} \quad (45)$$

This mechanism acts in addition to those considered above. Using (45) as a full Coulomb kernel, we can solve (38) exactly (Appendix B). Then we obtain an equation for T_c in the approximate form

$$\ln \frac{T^*}{T_c} \approx \psi\left(\frac{1}{2} + \frac{\mu P}{4T_c N(E_F)}\right) - \psi\left(\frac{1}{2}\right) \quad (46)$$

where T^* is taken as the critical temperature at the mobility edge, i.e., determined by (41) with μ_0^* replaced by (43). In this way we actually overestimate the influence of Coulomb repulsion in the localization region. We see that this extra repulsion acts upon the superconducting T_c as magnetic impurities¹⁶ with an effective spin-flip time:

$$1/\tau_{sf} = \pi\mu P/N(E_F) \sim \mu/N(E_F)R_l^3 \quad (47)$$

Superconductivity survives for $\tau_{sf}^{-1} < 0.57T^*$, i.e., for

$$R_l > [\mu/N(E_F)T_c^*]^{1/3} \sim (\xi_0 k_F^2)^{1/3} \sim (\xi_0 l^2)^{1/3} \quad (48)$$

where the last estimates are roughly valid for typical parameters and correspond to the condition (18). Thus the Coulomb repulsion of electrons in the one-quantum state, important in the localization region,³¹ leads to a rapid destruction of superconductivity. The size of a possible coexistence region is roughly determined by (18) and (48).

The Coulomb gap effects³⁷ are unimportant here. The width of the Coulomb gap, according to Efros and Shklovskii,³⁷ is given by the estimate

$$\Delta_C \approx (e^2/\kappa^{3/2})[N(E_F)]^{1/2} \quad (49)$$

where κ is the dielectric function in the insulator region. Near the mobility edge, in the self-consistent theory we have³¹

$$\kappa \approx 4\pi e^2 N(E_F) R_l^2 \quad (50)$$

Thus $\Delta_C \sim [N(E_F)R_l^3]^{-1}$ and $\Delta_C \ll T_c$ if the condition (18) is satisfied. So the Coulomb gap can be safely neglected in the "coexistence" region.

This treatment again assumes that the electron-electron interaction is weak ($\mu \ll 1$) and can be described by the lowest order of perturbation theory. The influence of this interaction upon the metal-insulator transition,

i.e., on the spectral density (28), is neglected.³¹ However, one has to keep in mind the possible importance of Coulomb interactions in a real system, although, as we have mentioned, a complete theory of the metal-insulator transition in disordered systems is still lacking.

4. CONCLUSION

An experimental investigation of the effects discussed in this paper seems possible by the study of "high-temperature" superconductors disordered by irradiation with fast neutrons. Among the numerous experiments of this kind, the most interesting appear to be some results on irradiated molybdenum sulfides (Chevrel phase superconductors). For these compounds high values of initial $T_{c0} \approx 15$ K are typical, as well as rather narrow energy bands. According to band-structure calculations,³⁶ the Fermi level in these compounds is very close to the upper edge of the conduction band, and characteristic values of E_F are of the order of 10^3 K. These values seem to be ideal from the point of view of the above criteria.

We remark upon the results of studies of irradiated SnMo_5S_6 (Ref. 24) and $\text{Pb}_{1-x}\text{U}_x\text{Mo}_6\text{S}_8$.²⁵ Strong disordering of these compounds leads to a lowering of T_c to values of the order of 1 K, with the corresponding growth of the residual resistance up to values of several units of $10^{-3} \Omega\text{-cm}$, in agreement with the estimates of minimal metallic conductivity due to Mott and Davis.²³ The temperature coefficient of resistance becomes negative at all temperatures and of quite a significant value. The observed resistance is greater than the values typical for most "dirty" alloys from the Ioffe-Regal-Mooij region.³⁸ From the point of view of empirical criteria for localization,²³ these results seem very attractive. We have already noted that the investigated behavior of $(dH_{c2}/dT)_{T_c}$ in these systems is also in qualitative agreement with theoretical predictions.

Interestingly, the situation with regard to σ_c also seems satisfying (see Fig. 6). The value of $\sigma_c \approx 10^3 \Omega^{-1} \text{cm}^{-1}$, although different from the estimates of minimal metallic conductivity, are more appropriate than the values of this parameter determined from similar fits in Ref. 12. It has already been noted³⁹ that the "critical region" in σ during the metal-insulator transition in impurity bands is rather large experimentally. Accordingly, the values of σ_c determined from these experiments are an order of magnitude larger than the Mott estimates for σ_c . This seems to be in accordance with our values of σ_c determined from the T_c dependence on σ . In any event, one should not have expected good agreement between such a crude theory and experiment, and these data allow us to claim with some confidence that these compounds, irradiated with a sufficiently large fluence of fast neutrons, are really in the vicinity of the Anderson transition, while conserving

superconductivity. Of course, on the basis of existing data we cannot claim that either of these systems is actually in the state of an Anderson insulator. In these respects the accurate measurement of resistivity for very low temperatures in the normal state [i.e., for external magnetic fields greater than $H_{c2}(0)$] may be very important.

Finally, we note that the strong anisotropy of electron motion and relatively narrow energy bands in recently discovered organic superconductors⁴⁰ can lead to the possibility of Anderson localization in these systems for a weak disorder, i.e., for $\tau^{-1} \ll E_F$, so that the criteria for the coexistence of superconductivity and localization may greatly improve.

APPENDIX A

Here we give some details of the derivation of the expressions (15) and (16) for the GL coefficients. Using (3), (5), and (6), we obtain

$$A = \frac{1}{g} - 2N(E_F) \sum_{n \geq 0} \frac{1}{2n+1} = \frac{1}{g} - N(E_F) \ln 1.13 \frac{\omega_D}{T} = N(E_F) \ln \frac{T}{T_c} \quad (\text{A1})$$

where $n^* = \omega_D/2\pi T$ has been introduced to cut off the logarithmic divergence, taking into account that electron attraction exists in the energy region of $2\omega_D$ around the Fermi level. The generalized diffusion coefficient $\tilde{D}(\omega_m)$ does not contribute [due to $q=0$ in (3)]. This is a reflection of the Anderson theorem¹⁴: disorder influences T_c only through changes in the density of states $N(E_F)$.

We shall calculate the coefficient B , neglecting the weak dependence on q . Then it is seen from Fig. 7 that the contribution of the diagrams in Figs. 7a and 7b is small in comparison with that of Fig. 7c. The "triangular" vertex can be found in the self-consistent theory of localization as described in Ref. 31. We have

$$\gamma(\mathbf{q}=0, \omega_m = 2\varepsilon_n) \approx 1 + 1/(2\tau|\varepsilon_n|) \quad (\text{A2})$$

where the first term takes account of "high" frequencies, while the next is

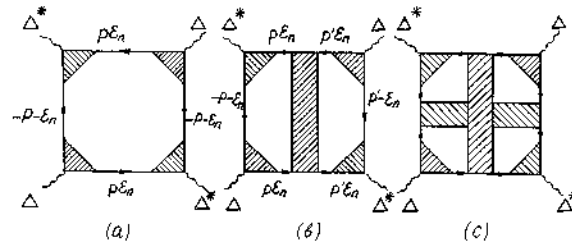


Fig. 7. Diagrams for calculating the coefficient B .

a diffusion contribution. Then, from Fig. 7a we get

$$\begin{aligned} B &\approx N(E_F)T \sum_{\varepsilon_n} \int_{-\infty}^{\infty} d\xi_p \gamma^4(\mathbf{q}=0, \omega_m = 2\varepsilon_n) G^2(\varepsilon_n \xi_p) G^2(-\varepsilon_n \xi_p) \\ &= N(E_F)T \frac{\pi}{2} \sum_{n \neq 0} \frac{1}{\varepsilon_n^3} = \frac{7\zeta(3)}{8\pi^2 T} N(E_F) \end{aligned} \quad (\text{A3})$$

where

$$G(\varepsilon_n \xi_p) = \left(i\varepsilon_n - \xi_p + \frac{i}{2\tau} \frac{\varepsilon_n}{|\varepsilon_n|} \right)^{-1} \quad (\text{A4})$$

is the usual approximation for the one-particle Green's function used in the self-consistent theory.¹⁸⁻²¹ Consider now calculations for C . Using (4)-(6), we find for the metallic region ($E_F > E_c$), not very close to the mobility edge, when $\tilde{D}(\omega_m) = D$,

$$\begin{aligned} C &= -i\pi TN(E_F) \sum_{\varepsilon_n} \frac{\partial^2}{\partial q^2} \frac{1}{2i|\varepsilon_n| + iDq^2} \Big|_{q=0} \\ &= \pi TN(E_F)D \sum_{\varepsilon_n} \frac{1}{2\varepsilon_n^2} = \frac{N(E_F)D}{\pi T} \sum_{n \neq 0} \frac{1}{(2n+1)^2} = \frac{\pi}{8T} N(E_F)D \end{aligned} \quad (\text{A5})$$

Analogously, for an insulator ($E_F < E_c$), but also not so close to the mobility edge, when

$$\tilde{D}(\omega_m) = D \frac{\omega_m}{\omega_m + 3D\omega_0^2/v_F^2}$$

[see (8)], we obtain

$$\begin{aligned} C &= \frac{\pi}{2} TN(E_F) \sum_{\varepsilon_n} \frac{1}{\varepsilon_n^2} \tilde{D}(2|\varepsilon_n|) \\ &= \pi TN(E_F)D \sum_{\varepsilon_n} \frac{1}{(2n+1)^2 + (2n+1)3D\omega_0^2/2\pi T v_F^2} \\ &= \frac{N(E_F)v_F^2}{3\omega_0^2} \left[\psi\left(\frac{1}{2} + \frac{3D\omega_0^2}{4\pi T v_F^2}\right) - \psi\left(\frac{1}{2}\right) \right] \\ &= N(E_F)R_i^2 \left[\psi\left(\frac{1}{2} + \frac{D}{4\pi TR_i^2}\right) - \psi\left(\frac{1}{2}\right) \right] \approx N(E_F)R_i^2 \ln \frac{1.78D}{\pi TR_i^2} \end{aligned} \quad (\text{A6})$$

where the approximate expression is valid for $DR_i^{-2} \gg 4\pi T$.

In the vicinity of the mobility edge, both for a metal and an insulator, we have^{18,21}

$$\tilde{D}(\omega_m) \approx (\pi/2)^{2/3} D_0 (\omega_m \tau)^{1/3} = (\pi/2\sqrt{3})^{2/3} (D_0 l)^{2/3} \omega_m^{1/3}$$

so that

$$\begin{aligned}
C &= \frac{\pi}{2} TN(E_F) \sum_{\epsilon_n} \frac{1}{\epsilon_n^2} D(2|\epsilon_n|) = \frac{\pi}{2} \left(\frac{\pi}{\sqrt{6}} \right)^{2/3} (D_0 l)^{2/3} TN(E_F) \sum_{\epsilon_n} \frac{1}{|\epsilon_n|^{5/3}} \\
&= \frac{1}{6^{1/3}} \left(\frac{D_0 l}{T} \right)^{2/3} N(E_F) \sum_{n \geq 0} \frac{1}{(2n+1)^{5/3}} \\
&= \frac{1}{6^{1/3}} \left(1 - \frac{1}{2^{5/3}} \right) \zeta \left(\frac{5}{3} \right) N(E_F) \left(\frac{D_0 l}{T} \right)^{2/3} \quad (A7)
\end{aligned}$$

Expression (A7) dominates over (A5) for

$$D/T_c \approx D_0 l / R_l T_c \ll D_0^{2/3} (l/T_c)^{2/3}$$

which defines the limits of applicability given in (16).

APPENDIX B

At the mobility edge $\omega_c = 0$ and the Coulomb kernel in (38) is determined mainly by the second term in (37b). Here we try to find a solution of (38) in the form

$$\Delta(\omega) = \Delta_1 \theta(\omega_D - |\omega|) + f(\omega) \quad (B1)$$

Then we get an integral equation for $f(\omega)$,

$$f(x) = \tilde{\mu} \Delta_1 F(x) - \tilde{\mu} \int_0^{\epsilon_F/\omega_D} dx' g(x-x') f(x') \frac{1}{x'} \text{th} \frac{\omega_D}{2T_c} x' \quad (B2)$$

where

$$\begin{aligned}
F(x) &= \int_0^1 dx' g(x-x') \frac{1}{x'} \text{th} \frac{\omega_D}{2T_c} x' \\
g(x) &= x^{-1/3}; \quad x = \omega/\omega_D; \quad \tilde{\mu} = \mu(\omega_D \tau)^{-1/3} \quad (B3)
\end{aligned}$$

Here $F(x)/\ln(\omega_D/T_c)$ changes from 4.2 to 1 for x changing from 0 to 1, and for $x \gg 1$ we get the asymptotic behavior $F(x) = x^{-1/3} \ln(\omega_D/T_c)$. Using the small difference between $(\omega_D/T_c)^{1/3}$ and $\ln(\omega_D/T_c)$ for any reasonable values of ω_D and T_c and the weak dependence of $F(x)$ on x for $0 < x < 1$, we come to the conclusion that the unknown function $f(x)$ from (B2) is weakly x dependent for $x < 1$ and $f(x) \sim x^{-1/3}$ for $x > 1$. Taking all this into account, we get the following equation for T_c :

$$1 = \lambda \ln \frac{\omega_D}{T_c} \left[1 - \frac{(\beta_1 \tilde{\mu} - m) \ln(\omega_D/T_c)}{1 + (\beta_2 \tilde{\mu} - m) \ln(\omega_D/T_c)} \right] \quad (B4)$$

where

$$\beta_1 = \left(\ln \frac{\omega_D}{T_c} \right)^{-2} \int_0^1 dx \int_0^1 dx' \frac{1}{xx'|x-x'|^{1/3}} \operatorname{th} \frac{\omega_D}{2T_c} x \operatorname{th} \frac{\omega_D}{2T_c} x' \approx 1$$

$$m = \frac{3}{2} \tilde{\mu}^2 / (1 + \beta_3 \tilde{\mu}); \quad 1 < \beta_2 < 4.2; \quad \frac{3}{2} < \beta_3 < 3 \quad (\text{B5})$$

For $\tilde{\mu} \gg 1$ we have $\beta_2 \approx 1$ and $\beta_3 \approx 3$. Thus from (B4) we obtain an estimate $\mu^* \approx \beta \tilde{\mu}$ with $0.5 < \beta < 3$; actually $\beta \approx 1$ for large values of $\tilde{\mu}$. This is the result given as (43).

Below the mobility edge ($E_F < E_c$) we can solve (38) with the Coulomb kernel given in (45) exactly. The additional Coulomb effects considered above, connected with "regular" contributions to the spectral density (28),³¹ can be taken into account with a simple substitution $\lambda \rightarrow \lambda^* = \lambda - \mu^*$, where μ^* is given by (43). Actually, we can convince ourselves that such a procedure overestimates the Coulomb repulsion in the localization region. It is easily seen that the solution of (38) in this case can be written as

$$\Delta(\omega) = \frac{\theta(\omega_D - |\omega|) \Delta_1}{1 + [\mu P / 2N(E_F) \omega] \operatorname{th}(\omega / 2T_c)} \quad (\text{B6})$$

where

$$\Delta_1 = \lambda^* \int_0^{\omega_D} d\omega \Delta(\omega) \frac{1}{\omega} \operatorname{th} \frac{\omega}{2T_c} \quad (\text{B7})$$

giving the equation for T_c of the following form:

$$1 = \lambda^* \int_0^{\omega_D} d\omega \frac{\operatorname{th}(\omega / 2T_c)}{\omega + [\mu P / 2N(E_F)] \operatorname{th}(\omega / 2T_c)} \quad (\text{B8})$$

which reduces to (46) with rather good accuracy.

ACKNOWLEDGMENTS

The authors appreciate discussions on different theoretical aspects of the problem with O. V. Dolgov, E. G. Maksimov, V. N. Fleurov, D. E. Khmel'nitskii, and D. I. Khomskii, as well as information on experimental investigations of irradiated superconductors and discussions with N. E. Alekseevskii, V. E. Arkhipov, and B. N. Goschitskii. They thank Prof. V. L. Ginzburg for his interest in this work. One of the authors (MVS) is grateful for the hospitality extended to him during his stay at the I. E. Tamm Department of Theoretical Physics of the P. N. Lebedev Physical Institute, where this work was performed.

REFERENCES

1. M. V. Sadovskii, *Usp. Fiz. Nauk* **133**, 223 (1981) [*Sov. Phys. Uspekhi* **24**, 96 (1981)].
2. Y. Nagaoka and H. Fukuyama, eds., *Anderson Localization* (Springer, Berlin, 1982).
3. P. W. Anderson, *Phys. Rev.* **189**, 1492 (1958).
4. J. Bardeen, L. N. Cooper, and J. R. Schrieffer, *Phys. Rev.* **106**, 162 (1957).
5. Y. Imry and M. Strongin, *Phys. Rev. B* **24**, 6353 (1981).
6. S. Maekawa and H. Fukuyama, *J. Phys. Soc. Japan* **51**, 1380 (1981).
7. S. Maekawa, in *Anderson Localization*, Y. Nagaoka and H. Fukuyama, eds. (Springer, Berlin, 1982), p. 103.
8. H. Takagi and Y. Kuroda, *Solid State Commun.* **41**, 643 (1982).
9. H. Takagi, R. Souda, and Y. Kuroda, *Prog. Theor. Phys.* **68**, 426 (1982).
10. H. Takagi and Y. Kuroda, *Prog. Theor. Phys.* **69**, 1677 (1983).
11. R. Oppermann, *J. Phys. Soc. Japan* **52**, 3554 (1983).
12. P. W. Anderson, K. A. Muttalib, and T. V. Ramakrishnan, *Phys. Rev. B* **28**, 117 (1983).
13. L. Coffey, K. A. Muttalib, and K. Levin, *Phys. Rev. Lett.* **52**, 783 (1984).
14. P. W. Anderson, *J. Phys. Chem. Solids* **11**, 26 (1959).
15. L. P. Gorkov, *Zh. Eksp. Teor. Fiz.* **37**, 1407 (1959).
16. P. G. de Gennes, *Superconductivity of Metals and Alloys* (W. A. Benjamin, New York, 1966).
17. W. Götze, *J. Phys. C* **12**, 1279 (1979); *Philos. Mag.* **43**, 219 (1981).
18. D. Vollhardt and P. Wölfle, *Phys. Rev. B* **22**, 4666 (1980); *Phys. Rev. Lett.* **48**, 699 (1982); in *Anderson Localizations*, Y. Nagaoka and H. Fukuyama, eds. (Springer, Berlin, 1982), p. 26.
19. D. Yoshioka, Y. Ono, and H. Fukuyama, *J. Phys. Soc. Japan* **50**, 3419 (1981).
20. A. V. Myasnikov and M. V. Sadovskii, *Fiz. Tverd. Tela* **24**, 3569 (1982).
21. B. Shapiro, *Phys. Rev. B* **25**, 4266 (1982).
22. A. F. Ioffe and A. R. Regel, *Prog. Semicond.* **4**, 237 (1960).
23. N. F. Mott and E. A. Davis, *Electron Processes in Non-Crystalline Materials* (Clarendon Press, Oxford, 1979).
24. S. A. Davydov, V. E. Arkhipov, V. I. Voronin, and B. N. Goschitskii, *Fiz. Metallov. Metalloved.* **55**, 931 (1983).
25. N. E. Alekseevskii, A. V. Mitin, V. N. Samosyuck, and V. I. Firsov, *Zh. Eksp. Teor. Fiz.* **85**, 1092 (1983).
26. N. R. Wethamer, E. Helfand, and P. C. Hohenberg, *Phys. Rev.* **147**, 295 (1966).
27. B. L. Altshuler, D. E. Khmel'nitskii, A. I. Larkin, and P. A. Lee, *Phys. Rev. B* **22**, 5142 (1980).
28. M. Tenhover, W. L. Johnson, and C. C. Tsuei, *Solid State Commun.* **38**, 53 (1981).
29. V. L. Berezinskii and L. P. Gorkov, *Zh. Eksp. Teor. Fiz.* **77**, 2498 (1979).
30. M. V. Sadovskii, *Zh. Eksp. Teor. Fiz.* **83**, 1418 (1982).
31. M. I. Katsnelson and M. V. Sadovskii, *Fiz. Tverd. Tela* **25**, 3372 (1983); *Zh. Eksp. Teor. Fiz.* **87**, 523 (1984).
32. B. L. Altshuler and A. G. Aronov, *Zh. Eksp. Teor. Fiz.* **77**, 2028 (1979).
33. B. Keck and A. Schmid, *J. Low Temp. Phys.* **24**, 611 (1976).
34. V. N. Fleurov, P. S. Kondratenko, and A. N. Kozlov, *J. Phys. F* **10**, 1953 (1980).
35. P. A. Lee, *Phys. Rev. B* **26**, 5882 (1982).
36. A. J. Freeman and T. Jarlborg, in *Superconductivity in Ternary Compounds II. Superconductivity and Magnetism*, M. B. Maple and F. Fischer, eds. (Springer Verlag, Berlin, 1982), p. 167.
37. A. L. Efros and B. I. Shklovskii, *J. Phys. C* **8**, L49 (1975).
38. J. H. Mooij, *Phys. Stat. Sol. (a)* **17**, 521 (1973).
39. T. F. Rosenbaum, K. Andres, G. A. Thomas and R. N. Bhatt, *Phys. Rev. Lett.* **45**, 1723 (1980); G. A. Thomas, M. A. Paalanen, and T. F. Rosenbaum, *Phys. Rev. B* **27**, 3897 (1983).
40. D. Jerome and H. J. Schulz, *Adv. Phys.* **31**, 299 (1982); J. Friedel and D. Jerome, *Contemp. Phys.* **23**, 583 (1982).

Increase of spatial fluctuations in superconductors near the Anderson transition

L. N. Bulaevskii and M. V. Sadovskii

P. N. Lebedev Physics Institute, Academy of Sciences of the USSR

(Submitted 20 November 1985)

Pis'ma Zh. Eksp. Teor. Fiz. **43**, No. 2, 76–78 (25 January 1986)

The superconducting order parameter has been found to exhibit strong, impurity-induced spatial fluctuations over a certain temperature interval near T_c . Far from the Anderson localization threshold, this interval is very narrow in comparison with the interval of strong thermodynamic fluctuations, and the superconducting order parameter is a self-averaging quantity. Because of the disorder, the fluctuations near the localization threshold are appreciable over the entire region of manifestation of the superconductivity.

In the work of Bulaevskii and Sadovskii¹ and Kapitulnik and Kotliar² the theory formulated by Abrikosov and Gor'kov and by Anderson for dirty three-dimensional superconductors with $k_F l \gg 1$ was extended to compounds with a very high level of disorder which are near the Anderson metal-insulator transition (in these compounds

the mean free path of an electron ($l \approx k_F^{-1}$). These authors^{1,2} have shown that the l dependence of the superconducting correlation length $\xi \equiv \xi(T=0) \approx (\xi_0 l)^{1/2}$ for $k_F l \gg 1$ gives way at the localization threshold to the dependence $\xi \approx (\xi_0 l^2)^{1/3}$ where $\xi_0 = 0.18 v_F/T_c$. A change of this sort accounts for the fact that at the localization threshold the interval of strong thermodynamic fluctuations near T_c , which is defined by the Ginzburg parameter $t_G = E_F^2/T_c^2 k_F^6 l^6$, is on the order of unity² (here $t = |T - T_c|/T_c$).

The results obtained by Bulaevskii and Sadovskii¹ and Kapitunik and Kotliar,² and all the preceding results for dirty superconductors were obtained under the assumption that the superconducting order parameter is self-averaged. In other words, it was assumed that the order parameter, averaged over the impurity configurations, adequately describes the behavior of the system. In order for this assumption to be true, the impurity-induced fluctuations of the order parameter in the sample must be small. We will find below a temperature interval t_D near T_c where this condition is not satisfied. We will show that $t_D \approx t_G^2 \ll t_G$ for $k_F l \gg 1$ and that the assumption that the order parameter is self-averaged far from the localization threshold is correct. At the localization threshold, however, $t_D \approx t_G \approx 1$ because of strong fluctuations of the electronic characteristics near the Anderson transition. Here the equations for the average order parameter cannot be used to describe superconductivity.

To estimate the fluctuation region t_D we use the functional for the unaveraged order parameter $\Delta(\mathbf{r})$

$$F_\xi(\Delta) = \int d\mathbf{r} [g^{-1} |\Delta(\mathbf{r})|^2 - \int d\mathbf{r}' K(\mathbf{r}, \mathbf{r}') \Delta(\mathbf{r}) \Delta(\mathbf{r}') + \frac{1}{2} BN(E_F) |\Delta(\mathbf{r})|^4],$$

$$K(\mathbf{r}, \mathbf{r}') = T \sum_{\mu, \nu, n} \varphi_\mu(\mathbf{r}) \varphi_\mu^*(\mathbf{r}') \varphi_\nu(\mathbf{r}) \varphi_\nu^*(\mathbf{r}') / (i\epsilon_n - \epsilon_\mu)(-i\epsilon_n - \epsilon_\nu), \quad (1)$$

$$\epsilon_n = \pi T(2n + 1),$$

where $\varphi_\mu(\mathbf{r})$ and ϵ_μ are exact intrinsic wave functions and energies of electrons for a given impurity configuration, and $N(E_F)$ is the average density of the electronic states at the Fermi level. The quantities $\varphi_\nu(\mathbf{r})$ and ϵ_ν are random values, so that the kernel $K(\mathbf{r}, \mathbf{r}')$, which depends on the arrangement of the impurities, fluctuates in space, causing corresponding fluctuations of the order parameter $\Delta(\mathbf{r})$. We ignore the fluctuations of the effective electron-attraction parameter g and also the coefficient $B(B = 7\zeta(3)/8\pi^2 T^2)$.

Assuming that the fluctuations of the kernel are small, we find from (1) the Ginzburg-Landau equation which describes the slow variations of the order parameter $\Delta(\mathbf{r})$ (the fluctuations of the kernel on the scale lower than ξ average out and lead to



FIG. 1.

only a shift of the transition temperature). The Ginzburg-Landau equation is

$$\left[\frac{T_{c0} - T}{T} + A(\mathbf{r}) - B |\Delta(\mathbf{r})|^2 + C \frac{\partial^2}{\partial r^2} \right] \Delta(\mathbf{r}) = 0,$$

$$C = \frac{1}{6} \int K_0(\mathbf{r}) r^2 d\mathbf{r}, \quad K_0(\mathbf{r} - \mathbf{r}') = \langle K(\mathbf{r}, \mathbf{r}') \rangle,$$

$$A(\mathbf{r}) = \int_0^{\omega_D} \frac{dE}{E} \tanh \frac{E}{2T_{c0}} \left[\frac{N(\mathbf{r}, E)}{N(E_F)} - 1 \right], \quad N(\mathbf{r}, E) = \sum_{\nu} |\varphi_{\nu}(\mathbf{r})|^2 \delta(E - \epsilon_{\nu}),$$
(2)

where $\langle \dots \rangle$ denotes averaging over the impurities, $C = \xi^2$, and $N(\mathbf{r}, E)$ is the local density of the electronic states. In (2) we have ignored the fluctuations of the coefficient C , and replaced $\int K_1(\mathbf{r}, \mathbf{r}') \Delta(\mathbf{r}') d\mathbf{r}'$ by $\Delta(\mathbf{r}) \int K_1(\mathbf{r}, \mathbf{r}') d\mathbf{r}' = A(\mathbf{r}) \Delta(\mathbf{r})$, where $K_1(\mathbf{r}, \mathbf{r}') = K(\mathbf{r}, \mathbf{r}') - K_0(\mathbf{r} - \mathbf{r}')$. The parameter T_{c0} in (2) is the transition temperature in which the long-wave fluctuations of the kernel are ignored.

We see from (2) that in the model under consideration the fluctuations $\Delta(\mathbf{r})$ depend on the distribution of the random $N(\mathbf{r}, E)$. For a further analysis we must find the correlation function of this quantity, $S(\mathbf{r}, \omega)$, which can be determined in terms of the leading and retarded Green's functions of the electron, $G_{L,R}(\mathbf{r}, \mathbf{r}')$, by means of the relation

$$S(\mathbf{r}, \omega) = [N(E_F)]^{-2} \langle N(\mathbf{r}, E_F + \omega) N(0, E_F) \rangle - 1$$

$$= [N(E_F)]^{-2} \text{Re} [\langle G_L(\mathbf{r}, \mathbf{r}, E_F + \omega) G_R(0, 0, E_F) - G_L(\mathbf{r}, \mathbf{r}, E_F + \omega) G_L(0, 0, E_F) \rangle] - 1.$$
(3)

Equation (2) with an arbitrary correlation function of $A(\mathbf{r})$ was considered previously^{3,4} in a study of the effect of structural inhomogeneities of samples on their superconducting properties. The analysis below is carried out in a similar manner. It follows from Refs. 3 and 4 that the superconducting properties of the system considered depend essentially on the behavior of the correlation function $S(q, \omega)$ at small values of q and ω .

Far from the localization threshold, the function $S(q, \omega)$ for $q \ll l^{-1}$ and $\omega \ll \tau^{-1} = v_F/l$ was found in Ref. 5 for a model of many orbitals at a lattice site. For $k_F l \gg 1$ the same result can be obtained by using a standard procedure of summing a perturbation-theory series over the scattering by impurities for (3). At small values of q and ω , the dominant contribution comes from the diagram in Fig. 1, where the wavy line corresponds to a diffusion, and also from a similar diagram with a cooperon. The function $S(q, \omega)$ is a singular function for small q and ω

$$S(q, \omega) \approx \frac{1}{[N(E_F)]^2 D_0^{3/2}} \text{Re} \frac{1}{(-i\omega + D_0 q^2)^{1/2}},$$
(4)

where $D_0 = lv_F/3$. The scaling function $S(q, \omega)$ is known at the localization thresh-

old⁶:

$$S(q, \omega) \approx L_\omega^3 F(qL_\omega), \quad L_\omega = [\omega N(E_F)]^{-1/3}. \quad (5)$$

This function can also be found from (4) if D_0 is replaced by the effective diffusion coefficient $D(q, \omega) = L_\omega^{-1} f(qL_\omega)$. A further analysis shows that upon integration over q and ω the dominant contribution will come from the region $q < \omega$. In the limit $q/\omega \rightarrow 0$ we have $f \approx 1$ and $F(x) \approx (1 + x^4)^{-1/4}$.

Using (2), (4), and (5) and carrying out some calculations similar to those in Ref. 3, we find that fluctuations of $N(\mathbf{r}, E)$ cause a shift in the transition temperature from T_∞ to T_c and $T_c > T_\infty$. Furthermore, the impurities cause the spatial fluctuations of the order parameter to increase as $T \rightarrow T_c$. Below T_c the fluctuational contribution due to disorder in the region $k_F l \gg 1$ at $t \ll 1$ is given by

$$\frac{\langle \Delta^2 \rangle - \langle \Delta \rangle^2}{\langle \Delta \rangle^2} = \left(\frac{t_D}{t} \right)^{1/2}, \quad \langle \Delta \rangle^2 = \frac{t}{B} \left[1 - 7 \left(\frac{t_D}{t} \right)^{1/2} \right], \quad (6)$$

where $t_D \approx t_G^2 \approx T_c^2 / E_F^2 k_F^2 l^6$. The contribution of thermodynamic fluctuations, Δ , to the dispersion is $(t_G/t)^{1/2}$. In a three-dimensional system with $k_F l \gg 1$, the disorder-induced fluctuations are thus considerably weaker than thermodynamic fluctuations.

At the localization threshold below T_c for $t \ll 1$ the quantity $(t_D/t)^{1/2}$ on the right sides of expressions (6) should be replaced by $|\ln t|/\sqrt{t}$. In this region the contribution of thermodynamic fluctuations is on the order of $1/\sqrt{t}$ and, in order of magnitude, $t_D \approx t_G \approx 1$, although there is reason to assume that disorder-induced fluctuations are slightly stronger than thermodynamic fluctuations. In the dielectric region the term $[N(E_F)]^{-1} \delta(\omega)$ should be added to the function $S(q, \omega)$ for small values of $q \ll R_l^{-1}$. Here t_D and t_G have a component which increases approximately as $[N(E_F) T_c R_l^3]^{-2}$ as the localization length, R_l , is decreased. The weak spatial fluctuations ($t_D \ll t_G$) become strong fluctuations, $t_D \approx t_G \approx 1$, when the conductivity is $\sigma \approx \sigma^* \approx \sigma_c (k_F \xi_0)^{-1/3}$, where $\sigma_c \approx e^2 k_F / \pi^3$ is on the order of $(2-5) \times 10^2 \Omega^{-1} \cdot \text{cm}^{-1}$.

We see that the impurities cause not only the superconducting correlation length, ξ , to decrease but also account for the spatial fluctuations of the order parameter of the sample, which increase as the Anderson transition is approached. Because of strong spatial fluctuations of the order parameter of the sample over the entire temperature range, a percolation mechanism for the screening and superconducting current flow is typical for a superconductor near the localization threshold.⁴ The quasi-particle spectrum in them is apparently gap-free.

We wish to thank B. I. Al'tshuler and D. E. Khmel'mitskiĭ for a useful discussion.

¹L. N. Bulaevskiĭ and M. V. Sadovskii, Pis'ma Zh. Eksp. Teor. Fiz. 39, 524 (1984) [JETP Lett. 39, 640 (1984); J. Low Temp. Phys. 59, 89 (1985)].

²A. Kapitulnik and G. Kotliar, Phys. Rev. Lett. 54, 473 (1985); Preprint, 1985.

³A. I. Larkin and Yu. N. Ovchinnikov, Zh. Eksp. Teor. Fiz. 61, 1221 (1971) [Sov. Phys. JETP 34, 651 (1972)].

- ⁴L. B. Ioffe and A. I. Larkin, *Zh. Eksp. Teor. Fiz.* **81**, 707 (1981) [*Sov. Phys. JETP* **54**, 378 (1981)].
- ⁵R. Oppermann and F. J. Wegner, *Z. Phys.* **B34**, 327 (1979).
- ⁶F. J. Wegner, in: *Anderson Localization*, eds. Y. Nagaoka and H. Fukuyama, Springer-Verlag, Springer Series in Solid State Sciences **39**, 8 (1982).

Translated by S. J. Amoretty

Inhomogeneous superconductivity in disordered metals

L. N. Bulaevskii, S. V. Panyukov, and M. V. Sadovskii

P. N. Lebedev Physics Institute, USSR Academy of Sciences

(Submitted 21 July 1986)

Zh. Eksp. Teor. Fiz. **92**, 672–688 (February 1987)

A parameter τ_D is introduced to describe the temperature region near T_c , in which the statistical spatial fluctuations of the order parameter are strong. It is shown on the basis of the Ginzburg–Landau functional, with the aid of the replica method, that two temperature superconductivity regimes are realized, depending on the degree of the disorder. At $\tau_D > \tau_D^* = 2.49\tau_G$, where τ_G is the Ginzburg parameter that characterizes the size of the region of strong thermodynamic fluctuations, the superconductivity is produced in spatially inhomogeneous fashion with droplike seeds. The drop density and their contribution to the free energy and to the diamagnetic susceptibility are obtained in a model of non-interacting drops. If $\tau_D < \tau_D^*$, superconductivity sets in below T_c simultaneously in the entire volume, i.e., the usual second-order transition is realized.

INTRODUCTION

The theory of dirty superconductors, developed by Abrikosov and Gor'kov^{1,2} and by Anderson,³ is the basis of the quantitative description of the superconducting properties of a large number of disordered alloys. As the theory of strongly disordered system progressed, however, it became clear that the main results of Refs. 1–3 must be modified to fit mean free paths l of the order of the Fermi wave number k_F^{-1} (of the order of the interatomic distance). A growth of disorder in three-dimensional systems causes the electron diffusion to stop at mean free path l shorter than a certain value $l_c \approx k_F^{-1}$, the electron diffusion ceases, the electronic states near the Fermi level become localized, and the system goes over into the state of an Anderson dielectric.^{4,5} This metal-insulator transition manifests itself in a continuous vanishing of the metallic conductivity (at $T = 0$) as l/l_c . At $l \gg l_c$ the conductivity is determined by the standard Drude formula and $\sigma \sim l$, whereas at $l \gtrsim l_c$ it decreases like $\sigma \sim (l - l_c)^\nu$, where ν is a certain critical exponent. The transition from diffusion to localization takes place at conductivities σ on the other of the so-called minimal metallic conductivity $\sigma_c \approx (e^2 k_F / \pi^3 \hbar) \approx (2-5) \cdot 10^2 \Omega^{-1} \cdot \text{cm}^{-1}$. The theory of dirty superconductors does not take localization effects into account and is valid for conductivities in the interval $(E_F/T_c)\sigma_c \gg \sigma \gg \sigma_c$.

The data known so far on the behavior of superconductors near the localization threshold are the following.

1. Assuming the density of states $N(E_F)$ to be independent of the Fermi level and the dimensionless electron-photon interaction parameter $\lambda_{e,ph}$ to be independent of l , it can be shown that T_c decreases with decrease of l , owing to the corresponding growth of the Coulomb pseudopotential μ^* . This effect is due to the increase of the delay of the Coulomb repulsion in the Cooper pair as the diffusion coefficient decreases on approaching the Anderson transition. The decrease of the superconducting transition temperature T_c begins in the region $\sigma \gg \sigma_c$ and becomes rapid at $\sigma \lesssim \sigma_c$ (Refs. 6–8). Belitz⁹ calculated the decrease of T_c due to the decrease of the effective density of the electronic states on the Fermi level under the influence of the Coulomb repulsion in the presence of impurities (the Al'tshuler-Aronov effect).

The enhancement of the spin fluctuations with increase of disorder, and the appearance of localized magnetic moments near the localization threshold, due to the electron repulsion,¹⁰ can also cause a decrease of T_c in ultradirty superconductors,^{11,12} but there is still no consistent quantitative theory of this effect. We note that the decrease of T_c due to the mutual influence of the disorder and of the Coulomb effect was first considered by Ovchinnikov¹³ and by Maekawa and Fukuyama (see Refs. 4 and 13) within the framework of the BCS model with allowance for the lowest localized corrections.

2. Bulaevskii and Sadovskii⁷ and later Kapitulnik and Kotliar¹⁴ found the superconducting coherence length ξ (at $T = 0$) in the region $\sigma < \sigma_c$, and also in the localization region ($l < l_c$). At the mobility threshold itself, where $l = l_c \approx k_F^{-1}$ and $\sigma = 0$, we have

$$\xi \approx (\xi_0 k_F^{-2})^{1/3}, \quad \xi_0 = 0.18 \hbar v_F / T_c.$$

In contrast to the standard theory of dirty superconductors with $l \gg l_c$ (Refs. 1 and 2), in which $\xi^2 \approx \xi_0 l$ is proportional to σ , as $l \rightarrow l_c$ we have $\sigma \rightarrow 0$ whereas ξ^2 remains different from zero both at the mobility threshold ($l = l_c$) and in the localization region, i.e., in an Anderson dielectric. The same result was obtained recently by Ma and Li¹⁵ who used another method. Obviously, these results are valid only if T_c does not vanish all the way to the Anderson transition, a situation possible only if rather stringent conditions imposed by the effects noted in Sec. 1 are met. The fact that ξ^2 differs from zero when σ vanishes at $l < l_c$ means conservation of the superconducting response in the phase of an Anderson dielectric.

3. As the disorder increases, the region of thermodynamic fluctuations near T_c increases. The width of this region is defined as $\tau_G T_c$, where the characteristic Ginzburg parameter for dirty superconductors is equal to $\tau_G = [\pi^2 T_c N(E_F) \xi^3]^{-2}$. Kapitulnik and Kotliar¹⁴ noted that near the mobility threshold, where $\xi \approx (\xi_0 k_F^{-2})^{1/3}$, the parameter τ_G does not contain a small quantity such as T_c / E_F (is not excluded, of course, that τ_G remains small because of a small numerical factor). Therefore a superconducting transition near the location threshold can in princi-

ple not become an analog of a λ transition in He⁴. Allowance for the fluctuations would lead in fact to a change of the critical exponents in the temperature dependence of the thermodynamic quantities near T_c compared with the corresponding exponents of the molecular-field theory.

All the cited theoretical analysis of the influence of disorder on superconductivity were made under the assumption that the superconducting order parameter is self-averaging. This remarks pertains both the the classical papers on dirty superconductors¹⁻³ and to all recent studies of superconductivity near and in the Anderson localization state.⁶⁻¹⁶ It is assumed here that the spatial fluctuations of the superconducting order parameter $\Delta(\mathbf{r})$ are small, and the use of the parameter $\langle \Delta(\mathbf{r}) \rangle$ is justified. It seems natural for such a procedure to be valid at $\sigma \gg \sigma_c$, but there are no grounds for believing it to be correct near the localization threshold.¹¹ In such a system the electronic characteristics fluctuate strongly, and we shall in Sec. I below that these fluctuations actually lead to substantial spatial fluctuations of the parameter $\Delta(\mathbf{r})$ (a brief summary of this section is given in Ref. 17).

In Sec. II we consider superconductors with spatial fluctuation of the local "temperature" of the superconducting transition. We shall show that if the amplitude of such statistical fluctuations exceeds a critical value, the superconductivity manifests itself with decrease of temperature in a spatially inhomogeneous manner, in the form of superconducting drops. We shall find the density of these drops as a function of temperature. In the model of noninteracting drops, we shall obtain also their contribution to the free energy of the system, and the diamagnetic susceptibility.

I. ESTIMATE OF THE REGION OF STRONG STATISTICAL FLUCTUATIONS OF THE SUPERCONDUCTING ORDER PARAMETER.

As a starting point, we consider the usual BCS Hamiltonian

$$\begin{aligned} \mathcal{H} &= \mathcal{H}_0 + \mathcal{H}_{int} + \mathcal{H}_M, \quad \mathcal{H}_M = \int d\mathbf{r} B^2(\mathbf{r})/8\pi, \\ \mathcal{H}_0 &= \int d\mathbf{r} \psi^\dagger(\mathbf{r}) \left[\frac{1}{2m} \left(i\hbar \nabla - \frac{e}{c} \mathbf{A}(\mathbf{r}) \right)^2 + U(\mathbf{r}) \right] \psi(\mathbf{r}), \quad (1) \\ \mathcal{H}_{int} &= \frac{1}{N(E_F)} \int d\mathbf{r} \lambda_{e,ph}(\mathbf{r}) \psi^\dagger(\mathbf{r}) \psi^\dagger(\mathbf{r}) \psi(\mathbf{r}) \psi(\mathbf{r}), \end{aligned}$$

where $\mathbf{B} = \text{curl } \mathbf{A}$ and $u(\mathbf{r})$ is a random potential in the disordered system. The pairing interaction can also fluctuate in space, but we assume hereafter that this interaction is weak, $\lambda_{e,ph}(\mathbf{r}) \ll 1$.

Let us write down Ginzburg-Landau functional for the non-averaged order parameter $\Delta(\mathbf{r})$. We introduce to this end the exact energy eigenvalues ϵ_μ and the exact eigenfunctions $\varphi_\mu(\mathbf{r})$ of the electrons, corresponding to the Hamiltonian \mathcal{H}_0 . We obtain with their aid a superconducting functional in the form¹⁸

$$\begin{aligned} \mathcal{F}_s\{\mathbf{A}(\mathbf{r}), \Delta(\mathbf{r})\} &= \int d\mathbf{r} \left\{ \frac{B^2(\mathbf{r})}{8\pi} + N(E_F) \int d\mathbf{r}' \right. \\ &\times \left. \left[\frac{\delta(\mathbf{r}-\mathbf{r}')}{\lambda_{e,ph}(\mathbf{r})} - K(\mathbf{r}, \mathbf{r}') \right] \Delta(\mathbf{r}) \Delta^*(\mathbf{r}') + \frac{1}{2} \lambda N(E_F) |\Delta(\mathbf{r})|^4 \right\}, \\ K(\mathbf{r}, \mathbf{r}') &= \frac{T}{N(E_F)} \sum_{\epsilon_n, \epsilon_\mu} \frac{\varphi_n^*(\mathbf{r}) \varphi_n(\mathbf{r}') \varphi_\mu^*(\mathbf{r}') \varphi_\mu(\mathbf{r})}{(i\epsilon_n - \epsilon_\mu)(-i\epsilon_n - \epsilon_\mu)}, \quad (2) \end{aligned}$$

$$\epsilon_n = \pi T(2n+1), \quad \lambda = 7\zeta(3)/8\pi^2 T^2.$$

The statistical fluctuations of $\lambda_{e,ph}(\mathbf{r})$ and of the kernel $K(\mathbf{r}, \mathbf{r}')$, (in view of the random character of the values of $\varphi_\nu(\mathbf{r})$ and ϵ_ν) cause spatial fluctuations of the superconducting order parameter $\Delta(\mathbf{r})$. We have neglected in (2) the fluctuations of the parameter λ ; it will be seen from the analysis that follows that they are less substantial than the fluctuations of the kernel $K(\mathbf{r}, \mathbf{r}')$. Assuming the fluctuations of the kernel $K(\mathbf{r}, \mathbf{r}')$ and of the parameter $\Delta(\mathbf{r})$ to be small, we estimate the temperature region in which this assumption turns out to be incorrect and where a description with the aid of the averaged order parameter is inadequate. It will be shown below that the variance is determined mainly by the long-wave variation of $\Delta(\mathbf{r})$. We can herefore transform from (2) to the GL functional for the order parameter:

$$\begin{aligned} \mathcal{F}_{GL}\{\mathbf{A}(\mathbf{r}), \Delta(\mathbf{r})\} &= \int d\mathbf{r} \left\{ \frac{B^2(\mathbf{r})}{8\pi} + N(E_F) \left[(\tau + t(\mathbf{r})) |\Delta(\mathbf{r})|^2 \right. \right. \\ &\quad \left. \left. + \xi^2 \left| \left(\nabla - \frac{2ie}{\hbar c} \mathbf{A}(\mathbf{r}) \right) \Delta(\mathbf{r}) \right|^2 + \frac{1}{2} \lambda |\Delta(\mathbf{r})|^4 \right] \right\}, \quad (3a) \end{aligned}$$

$$\xi^2 = \frac{1}{6} \int K_0(\mathbf{r}) r^2 d\mathbf{r}, \quad K_0(\mathbf{r}-\mathbf{r}') = \langle K(\mathbf{r}, \mathbf{r}') \rangle,$$

$$\tau = \frac{T}{T_{co}} - 1, \quad (3b)$$

where T_{co} is the transition temperature determined by the averaged kernel $K_0(\mathbf{r}-\mathbf{r}')$ with allowance for the short-wave fluctuations of the kernel $K(\mathbf{r}, \mathbf{r}')$. In the derivation of (3) we neglected the fluctuations of the coefficient ξ^2 . The function $t(\mathbf{r})$ plays here the role of the fluctuation local critical "temperature." It takes into account the fluctuations of the pairing interaction, for which $t(\mathbf{r}) = \lambda_{e,ph}^{-1}(\mathbf{r}) - \langle \lambda_{e,ph}^{-1}(\mathbf{r}) \rangle$, and also the fluctuations of the dipole density of the electronic states $N(\mathbf{r}, E_F)$:

$$t(\mathbf{r}) = \int_0^{\omega_D} \frac{dE}{E} \text{th} \frac{E}{2T_{co}} \left[\frac{N(\mathbf{r}, E)}{N(E_F)} - 1 \right],$$

$$N(\mathbf{r}, E) = \sum_{\nu} |\varphi_\nu(\mathbf{r})|^2 \delta(E - \epsilon_\nu), \quad N(E_F) = \langle N(\mathbf{r}, E_F) \rangle. \quad (4)$$

The functional for the fluctuations of the pairing interaction was investigated by Larkin and Ovchinnikov¹⁹ in connection with a study of the influence of structure inhomogeneities of the samples on their superconducting properties; the analysis that follows will be similar. Within the framework of perturbation theory in the fluctuation $\Delta(\mathbf{r})$ we obtain from (3) the renormalized temperature T_c and the variance of $\Delta(\mathbf{r})$:

$$\frac{T_c - T_{co}}{T_{co}} = \frac{1}{(2\pi)^2} \int \frac{\gamma(\mathbf{q}) d\mathbf{q}}{\xi^2 q^2}, \quad \gamma(\mathbf{q}) = \int d\mathbf{r} e^{i\mathbf{q}\cdot\mathbf{r}} \langle t(\mathbf{r}) t(0) \rangle, \quad (5a)$$

$$\frac{\langle \Delta^2 \rangle - \langle \Delta \rangle^2}{\langle \Delta \rangle^2} = \frac{1}{(2\pi)^2} \int \frac{\gamma(\mathbf{q}) d\mathbf{q}}{(\xi^2 q^2 + 2|\tau|)^2}. \quad (5b)$$

It follows from (5a) that the fluctuation-induced shift of T_c is positive and the contribution made to it by the short-wave fluctuations is generally speaking not small. According to (5b), the fluctuations of $\Delta(\mathbf{r})$ are determined mainly by the behavior of the correlation function $\gamma(\mathbf{q})$ at small q .

The value of $\gamma(\mathbf{q})$ neglecting the fluctuations of the pairing interactions, was obtained in Ref. 17. In dirty super-

conductors with $\sigma \gg \sigma_c$ (i.e., $l \gg k_F^{-1}$) we have $\gamma(0) \approx \xi N^{-2} (E_F) D_0^{-2}$, where $D_0 = v_F l / 3$ is the classical diffusion coefficient. We then obtain from (5)

$$\langle \Delta^2 \rangle / \langle \Delta \rangle^2 - 1 \approx (\tau_D / \tau)^{1/2}, \quad \tau_D = \gamma^2(0) \xi^{-6}, \quad (6)$$

where $\xi \approx (\xi_0 l)^{1/2}$. The parameter τ_D introduced by us defines the region in which statistical (spatial) fluctuations of the order parameter are significant.¹¹ It can be seen from (6) that $\tau_D \approx \tau_G^2 \ll \tau_G \ll 1$, in dirty superconductors, i.e., the statistical fluctuations are unimportant even in region where thermodynamic fluctuations are noticeable enough.

The situation changes radically in the vicinity of the mobility threshold, where³¹ $\gamma(\mathbf{q}) \approx \xi^3 \ln(1/\xi q)$. From (5) we obtain for the variance of $\Delta(\mathbf{r})$ the expression

$$\frac{\langle \Delta^2 \rangle}{\langle \Delta \rangle^2} - 1 \approx \frac{1}{(|\tau|)^{1/2}} \ln \frac{1}{|\tau|}. \quad (7)$$

According to (7), the statistical fluctuations near the mobility threshold turn out to be most substantial, and are stronger here than the thermodynamic fluctuations in view of the logarithmic factor in $\gamma(\mathbf{q})$. Thus, near the localization threshold we have $\tau_D \approx \tau_G \approx 1$. The transition from the regime of weak statistical fluctuations ($\tau_D \ll \tau_G$) to the regime of strong ones ($\tau_D \approx \tau_G$) takes place at the values $\sigma \approx \sigma^* \approx \sigma_c (k_F \xi_0)^{-1/3}$ of the conductivity, the physical meaning of which was discussed in Ref. 7. At this conductivity, a transition takes place from the usual theory of dirty superconductors to the relations typical of the vicinity of the localization threshold.

Below the localization threshold. The region of strong $\Delta(\mathbf{r})$ fluctuations expands even more. This is due to the appearance of an additional delta-function singularity in the correlator of the local density of states.²¹ We obtain accordingly in $\gamma(\mathbf{q})$ an additional term $[N(E_F) T_c (1 + R_l^2 q^2)]^{-1}$, where R_l is the localization radius of the electronic states on the Fermi level. The variance of $\Delta(\mathbf{r})$ acquires according to (5) at $R_l > \xi(T)$ another term in addition to (7)

$$\langle \Delta^2 \rangle / \langle \Delta \rangle^2 - 1 \approx [N(E_F) T_c R_l^2 \tau^2]^{-1},$$

which increases rapidly with decrease of the localization radius R_l ($R_l = \infty$ at the localization threshold). It is shown in Ref. 7 that if T_c remains different from zero at the localization threshold, the Cooper pairing survives with further increase of the disorder and with decrease of R_l only to values $R_l \gg [N(E_F) T_c]^{-1/3}$. This inequality means that the energy interval T_c spans many discrete levels whose centers are located inside a region with radius R_l (see also Ref. 15). In addition, it guarantees that the localization radius exceeds substantially the characteristic dimension of the Cooper pairs. We see now that under the same condition the relative variance of $\Delta(\mathbf{r})$ remains at a level on the order of unity in the entire temporal interval in which superconductivity exists in the dielectric phase.

If the statistical fluctuations of $t(\mathbf{r})$ are caused by randomly disposed regions with dimensions a , where $k_F^{-1} \ll a \ll \xi$, and with increased values of the electron-photon interaction parameter $\lambda_{e,ph} + \delta\lambda_{e,ph}$ (in view of the change of the structure of the dislocations, twinning planes, etc), we have for such a model

$$\gamma(0) = c(1-c)a^3(\delta\lambda_{e,ph}/\lambda_{e,ph})^2, \quad \tau_D = \gamma^2(0) \xi^{-6}, \quad (8)$$

where c is the relative total volume of the regions with altered parameter $\lambda_{e,ph}$. In this case, at $c \approx 1$ and $\delta\lambda_{e,ph}/\lambda_{e,ph} \approx 1$, the regime of strong statistical fluctuations $\tau_D \approx \tau_G$ is realized at $a \gg k_F^{-1} (E_F/T_c)^{1/3}$. This condition is compatible with the restriction $a \ll \xi$ assumed above. Note that at $a \gg \xi$ the appearance of inhomogeneous superconductivity is not surprising: on cooling it is formed initially only in regions with increased transition "temperature" corresponding to the parameter $\lambda_{e,ph} + \delta\lambda_{e,ph}$. A much less trivial factor is that at $a \ll \xi$ there is likewise no averaging of the superconducting properties if the level of the fluctuations of $t(\mathbf{r})$ [due to the fluctuations of $N(\mathbf{r}, E_F)$ or of $\lambda_{e,ph}(\mathbf{r})$] is high enough.

II. SUPERCONDUCTING TRANSITION IN SYSTEMS WITH STRONG DISORDER

1. Formulation of problem

We consider now superconductivity in systems with strong spatial statistical Gaussian fluctuations of the local transition "temperature" $T_c(\mathbf{r})$. We shall show that in this model, depending on the degree of disorder, i.e., on the ratio τ_D/τ_G , two types of superconducting transition are possible. At $\tau_D < \tau_D^* = 2.49\tau_G$ the superconductivity is a second-order phase transition at the point T_c . The superconducting order parameter is in this case equal to zero at $T > T_c$ and is spatially homogeneous over scales exceeding the correlation length $\xi(T)$ below T_c . Statistical fluctuations lead only to a change of the critical exponents in the temperature dependence of the basic characteristics of the system $\xi(T)$, $\lambda_L(t)$, and others.^{22,23}

At $\tau_D > \tau_D^*$ the superconducting state appears in inhomogeneous fashion even if the correlation radius a of the disorder-induced fluctuations of the temperature $T_c(\mathbf{r})$ is small compared with the superconducting correlation length ξ (we refer to disorder of this type, with $a \ll \xi$, as microscopic). The first to deduce the possibility of an inhomogeneous superconducting transition for microscopic disorder were Ioffe and Larkin.²⁴ Investigating the case of extremely strong disorder (in fact $\tau_D \gg (\tau_G \tau)^{1/2}$), they have shown that as the temperature is lowered the normal phase acquires localized superconducting regions (drops) with characteristic dimension $\xi(T)$. Far from T_c their density is low, but with further cooling the density and dimensions of the drops increase and they begin to overlap. The superconducting transition becomes percolative in this case.

The Ioffe-Larkin transition, valid in the limit of very strong disorder, did not take thermodynamic fluctuations into account and provided no criterion for the transition from the homogeneous superconductivity to the inhomogeneous ones. The corresponding criterion $\tau_D > \tau_D^* \approx 2.49\tau_G$ will be obtained below for a model with Gaussian fluctuations of $T_c(\mathbf{r})$.

According to the estimates given in Sec. I, if the impurities influence only the local density of states $N(\mathbf{r}, E_F)$ in the system, the parameter τ_D/τ_G increases from a very small value to values greater than unity as the disorder increases and a transition takes place from the $l \gg k_F^{-1}$ regime to the electron localization regime ($l \approx k_F^{-1}$). An onset of an inhomogeneous superconducting regime is therefore to be expected as the localization threshold is approached. In a system that contain regions with increased value of the

parameter $\lambda_{e,ph}$ under conditions $l \gg k_F^{-1}$, this regime can be realized also at parameter values $\tau_D \ll 1$, since $\tau_G \ll 1$ in such a system.

Our treatment of superconductors with large disorder will be based on the GL functional (3a) with a Gaussian distribution of the temperature $t(\mathbf{r})$. Given the distribution $t(\mathbf{r})$, the free energy of the system and the order-parameter correlator are equal to

$$F_s\{t(\mathbf{r})\} = -T \ln Z, \quad Z = \int D\{\mathbf{A}, \Delta\} \exp[-\mathcal{F}_{GL}\{\mathbf{A}, \Delta\}/T], \quad (9a)$$

$$\langle \Delta(\mathbf{r}) \Delta(\mathbf{r}') \rangle = Z^{-1} \int D\{\mathbf{A}, \Delta\} \Delta(\mathbf{r}) \Delta(\mathbf{r}') \exp[-\mathcal{F}_{GL}\{\mathbf{A}, \Delta\}/T], \quad (9b)$$

and they must be averaged, assuming that the correlator

$$\langle t(\mathbf{r}) t(\mathbf{r}') \rangle = \gamma \delta(\mathbf{r} - \mathbf{r}'), \quad \gamma = \tau_D^{-3} \xi^3, \quad (10)$$

is known. For Gaussian fluctuations with a correlator (10), the probability of a configuration with a given $t(\mathbf{r})$ distribution is

$$P\{t(\mathbf{r})\} = \exp\left[-\frac{1}{2\gamma} \int d\mathbf{r} t^2(\mathbf{r})\right]. \quad (11)$$

The problem reduces thus to calculation of the functions $F_s\{t(\mathbf{r})\}$ and $\langle \Delta(\mathbf{r}) \Delta(\mathbf{r}') \rangle$ (9b) and their subsequent averaging with the aid of (11).

We confine ourselves in this article to consideration of noninteracting drops. We can then disregard the presence of vortices in the sample, and in each drop the phase of the order parameter $\Delta(\mathbf{r})$ can be regarded as nonsingular.⁴⁾ Following the gauge transformation

$$\begin{aligned} \mathbf{A}(\mathbf{r}) &\rightarrow \mathbf{A}(\mathbf{r}) + (c\hbar/2e) \nabla \varphi(\mathbf{r}), \\ \Delta(\mathbf{r}) &\rightarrow \Delta(\mathbf{r}) \exp[-i\varphi(\mathbf{r})], \end{aligned}$$

where $\varphi(\mathbf{r})$ is the phase of the order parameter, the quantity $\Delta(\mathbf{r})$ in (9b) is real and the GL functional becomes

$$\begin{aligned} \mathcal{F}_{GL}\{\mathbf{A}(\mathbf{r}), \Delta(\mathbf{r})\} = \int d\mathbf{r} \left\{ \frac{B^2(\mathbf{r})}{8\pi} + N(E_F) \left[(\tau + t(\mathbf{r})) \Delta^2(\mathbf{r}) \right. \right. \\ \left. \left. + \frac{4e^2 \xi^2}{c^2 \hbar^2} A^2(\mathbf{r}) \Delta^2(\mathbf{r}) + \xi^2 (\nabla \Delta(\mathbf{r}))^2 + \frac{\lambda \Delta^4(\mathbf{r})}{2} \right] \right\}. \quad (12) \end{aligned}$$

Integration over the phase in (9) adds to the partition function an inessential constant factor which we shall disregard hereafter. To calculate the free energy of a system of noninteracting drops we shall use an approach similar to the fluctuation theory of nucleation of a new phase in first-order transitions, and also the replica method.

2. Fluctuation theory of drops

Superconducting drops can appear in a specified $t(\mathbf{r})$ configuration only in regions with locally higher superconducting-transition temperatures. We shall number these regions by the subscript i . The order parameter in each region is determined by a nontrivial localized solution $\Delta_d^{(i)}(\mathbf{r}) \neq 0$ of the GL equation, and the contribution of such a drop to the partition function of the system is

$$\begin{aligned} N^{(i)}\{t(\mathbf{r})\} \exp\left(-\frac{E_d^{(i)}\{t(\mathbf{r})\}}{T}\right), \\ E_d^{(i)}\{t(\mathbf{r})\} = \mathcal{F}_{GL}\{0, \Delta_d^{(i)}(\mathbf{r})\}, \end{aligned}$$

where $E_d^{(i)}$ is the drop energy, and the factor $N^{(i)}$ is determined by the contribution of the $\Delta(\mathbf{r})$ configurations that are close to the classical solution $\Delta_d^{(i)}(\mathbf{r})$. Summing the contribution of configurations containing an arbitrary number of drops and neglecting their interaction with one another, we obtain the partition function (9a) of the system,

$$\begin{aligned} Z = Z_0 \left[1 + \sum_i N^{(i)} \exp\left(-\frac{E_d^{(i)}}{T}\right) \right. \\ \left. + \frac{1}{2!} \sum_{i,j} N^{(i)} N^{(j)} \exp\left(-\frac{E_d^{(i)} + E_d^{(j)}}{T}\right) + \dots \right] \\ = Z_0 \exp\left[\sum_i N^{(i)} \exp\left(-\frac{E_d^{(i)}}{T}\right)\right]. \quad (13) \end{aligned}$$

Here Z_0 is the partition function of the system in the absence of drops. Substituting (13) in (9a) and averaging the free energy of the system over the $t(\mathbf{r})$ configurations, we get

$$F_s = -\frac{T}{N} \int D\{t(\mathbf{r})\} \sum_i N^{(i)}\{t(\mathbf{r})\} \exp\left(-\frac{\mathcal{F}_d^{(i)}\{t(\mathbf{r})\}}{T}\right), \quad (14)$$

where N is a normalization factor and \mathcal{F}_d assumes the role of the free energy of the drop:

$$\mathcal{F}_d\{t(\mathbf{r})\} = E_d\{t(\mathbf{r})\} - T \ln P\{t(\mathbf{r})\}. \quad (15)$$

The main contribution to the functional integral (14) is made by the configurations $t_0(\mathbf{r})$ that realize an extremum of the functional (15):

$$t_0(\mathbf{r}) = -\tilde{\gamma} \Delta_d^2(\mathbf{r}), \quad \tilde{\gamma} = \gamma N(E_F)/T_c. \quad (16)$$

Note that $t_0(\mathbf{r})$ is negative, since the drops appear in regions of higher superconducting-transition temperatures. Substitution of (16) in the GL equation that corresponds to the functional (3a) leads to a nonlinear equation for the order parameter $\Delta(\mathbf{r})$ in the superconducting drop. In dimensionless variables, this equation is

$$\Delta_d(r) = \left(\frac{\tau}{\tilde{\gamma} - \lambda}\right)^{1/2} \chi\left[\frac{r}{\xi(T)}\right], \quad \xi(T) = \frac{\xi}{\tau^{1/2}}, \quad (17)$$

$$\frac{1}{x} \frac{d^2}{dx^2} (x\chi(x)) - \chi(x) + \chi^3(x) = 0, \quad \chi(x \rightarrow \infty) = 0. \quad (18)$$

The asymptote of the function $\chi(x)$ at $x \gg 1$ is determined from the linearized form of Eq. (18), and $\chi(x) \sim x^{-1} e^{-x}$. The superconducting nuclei are thus localized over a scale of the order of the correlation radius $\xi(T)$. The quantity \mathcal{F}_{min} is obtained by substituting (16) and (17) in (15):

$$S_n(\tau) = \frac{\mathcal{F}_{min}}{T} = \frac{A \xi^3 \tau^{3/2}}{\gamma - \lambda T/N(E_F)} = \frac{A (\tau/\tau_D)^{3/2}}{1 - (\tau_0/\tau_D)^{3/2}}, \quad \lambda < \tilde{\gamma}. \quad (19a)$$

It determines, with exponential accuracy, the free energy (14) of the drops. The constant A in (19a) is equal to²⁵

$$A = \int_0^\infty dx x^2 \left[\chi^2(x) + \left(\frac{d\chi}{dx}\right)^2 - \frac{1}{2} \chi^4(x) \right] = 37.8. \quad (19b)$$

Note that the energy $E_d\{t_0(\mathbf{r})\}$ of superconducting drops is negative, and their production is energywise favored compared with the case of the spatially homogeneous solution

$\Delta(\mathbf{r}) = 0$. According to (19a), superconducting drops can exist only in the presence of sufficiently strong statistical fluctuations $\tau_D > \tau_G$; a rigorous restriction will be obtained below.

To determine the pre-exponential factor in (14) one must turn to the solution of the complete problem (11), (13). Neglecting its thermodynamic fluctuations, the order parameter can be obtained within the framework of the Ioffe-Larkin method.²⁴ We obtain for the free energy of the system and for the drop density ρ_s , the expressions

$$F_s(\tau) \approx -T\xi^{-3}(T) (\tau_D/\tau_G)^{3/2} \exp[-S_0(\tau)], \quad (20a)$$

$$\rho_s(\tau) \approx \xi^{-3}(T) S_0(\tau) \exp[-S_0(\tau)]. \quad (20b)$$

The exponent $S_0(\tau)$ is defined here by Eq. (19a) with $\lambda = 0$. Note that the pre-exponential factor in (20a) differs from that obtained in Ref. 24, which contains an inaccurate expression for the free energy of one drop. It is seen from (19a) that at $\lambda \ll \tilde{\gamma} S_0^{-1}(\tau)$ we obtain for $S_0(\tau)$ the result of the Ioffe-Larkin theory of weak thermodynamic fluctuations. This means that their approach is valid if the inequality $\tau_D \ll \tau \ll \tau_D^2/\tau_G$ holds, and this is possible only if $\tau_D \gg \tau_G$. It follows from (20) that in the region where these expressions are valid the average energy F_s/ρ_s of each drop is large compared with the temperature, and the two become comparable at $\lambda \approx \tilde{\gamma} S_0^{-1}(\tau)$. We confine ourselves hereafter to the region $\lambda \gg \tilde{\gamma} S_0^{-1}(\tau)$ i.e., $\tau \gg \tau_D^2/\tau_G$, where the contribution of the thermal fluctuations becomes substantial. It will be shown below that it is precisely in this limit that the fluctuations of the order parameter are small relative to the most probable configuration (17). This enables us to use standard field-theoretical methods to find the free energy of the system and the order-parameter correlator in the region of strong thermodynamic fluctuations.

3. Replica method and instantons

To average the logarithm of the partition function (9a) over $t(\mathbf{r})$ with weight (11) we use the replica method, which permits the averaging to be carried out in explicit form.²⁶

We express the average free energy (9a) of the system in the form

$$F = -T \lim_{n \rightarrow 0} \frac{1}{n} [\langle Z^n \rangle - 1]. \quad (21)$$

To calculate $\langle Z^n \rangle$ in accordance with the idea of the replica method, we assume first n to be an arbitrary integer. Expressing Z^n in terms of an n -fold functional integral over the fields of the replicas $\mathbf{A}_\alpha(\mathbf{r})$, $\Delta_\alpha(\mathbf{r})$, $\alpha = 1, \dots, n$ and carrying out exact Gaussian averaging over $t(\mathbf{r})$, we get

$$\begin{aligned} \langle Z^n \rangle &= \int D\{\mathbf{A}_\alpha, \Delta_\alpha\} \exp[-S_n\{\mathbf{A}_\alpha, \Delta_\alpha\}], \\ S_n\{\mathbf{A}_\alpha, \Delta_\alpha\} &= \int d\mathbf{r} \left\{ \sum_{\alpha=1}^n \frac{B_\alpha^2(\mathbf{r})}{8\pi} + \frac{N(E_F)}{T} \sum_{\alpha=1}^n \left[\tau \Delta_\alpha^2(\mathbf{r}) \right. \right. \\ &\quad \left. \left. + \frac{4e^2 \xi^2}{c^2 \hbar^2} \mathbf{A}_\alpha^2(\mathbf{r}) \Delta_\alpha^2(\mathbf{r}) + \xi^2 (\nabla \Delta_\alpha(\mathbf{r}))^2 + \frac{1}{2} \lambda \Delta_\alpha^4(\mathbf{r}) \right] \right. \\ &\quad \left. - \frac{1}{2} N(E_F) T^{-1} \tilde{\gamma} \left[\sum_{\alpha=1}^n \Delta_\alpha^2(\mathbf{r}) \right]^2 \right\}. \end{aligned} \quad (22)$$

Note that the random quantities $t(\mathbf{r})$ have already dropped out of these expressions, and that the action $S_n\{\mathbf{A}_\alpha, \Delta_\alpha\}$ is

translationally invariant. For the mean value of the order-parameter correlator (9b) we get

$$\begin{aligned} \langle \Delta(\mathbf{r}) \Delta(\mathbf{r}') \rangle \\ = \lim_{n \rightarrow 0} \frac{1}{n} \int D\{\mathbf{A}_\alpha, \Delta_\alpha\} \exp[-S_n\{\mathbf{A}_\alpha, \Delta_\alpha\}] \sum_{\alpha=1}^n \Delta_\alpha(\mathbf{r}) \Delta_\alpha(\mathbf{r}'), \end{aligned} \quad (23)$$

where we have symmetrized over the replica indices.

Far from the region of strong fluctuations of the order parameter $|\tau| \gg \tau_D, \tau_G$ the functional integrals (22) and (23) can be calculated by the saddle-point method. The external trajectories are classical solutions for the action (22), and when calculating the functional integrals account must be taken of the Gaussian fluctuations about them. The extremal trajectories are defined by

$$\left[\tau - \xi^2 \nabla^2 + \lambda \Delta_\alpha^2(\mathbf{r}) - \tilde{\gamma} \sum_{\beta=1}^n \Delta_\beta^2(\mathbf{r}) \right] \Delta_\alpha(\mathbf{r}) = 0, \quad \mathbf{A}_\alpha(\mathbf{r}) = 0. \quad (24)$$

These equations for $\Delta_\alpha(\mathbf{r})$ have a spatially homogeneous solution and localized (instanton) solutions. The latter correspond at $\tau > 0$ to superconducting drops. We confine ourselves in this article to considerations of non-interacting drops and consider only instanton solutions above T_c (at $\tau > 0$). We shall be interested hereafter only in those solutions that admit analytic continuation as $n \rightarrow 0$. We designate them $\Delta_\alpha^{(i)}(\mathbf{r})$, where the superscript i labels the type of solution. To find their contribution we must expand the action (22) accurate to terms quadratic in the deviations $\varphi_\alpha(\mathbf{r}) = \Delta_\alpha(\mathbf{r}) - \Delta_\alpha^{(i)}(\mathbf{r})$. It is shown in the Appendix that the fluctuations of the fields $\mathbf{A}_\alpha(\mathbf{r})$ can be neglected when isolated seeds are considered. The action (22) takes then the form

$$S_n\{\Delta_\alpha\} = S_n\{\Delta_\alpha^{(i)}\} + \frac{1}{2} \int d\mathbf{r} \sum_{\alpha, \beta} (\varphi_\alpha \hat{M}_{\alpha\beta}^{(i)} \varphi_\beta). \quad (25)$$

To calculate the functional integral over the fields φ_α we expand them in terms of the normalized eigenfunctions of the operator $\hat{M}^{(i)}$:

$$\varphi_\alpha(\mathbf{r}) = \sum_k c_k \varphi_{k\alpha}(\mathbf{r}), \quad \sum_\beta \hat{M}_{\alpha\beta}^{(i)} \varphi_{k\beta} = \epsilon_k \varphi_{k\alpha}. \quad (26)$$

Substitution of (26) in (25) yields for the action the expression

$$S_n\{\Delta_\alpha\} = S_n\{\Delta_\alpha^{(i)}\} + \frac{1}{2} \sum_k c_k^2 \epsilon_k. \quad (27)$$

The Gaussian functional integral in (22) is calculated by replacing the integration variables

$$\int D\{\varphi_\alpha\} \dots = \prod_k \int \frac{dc_k}{(2\pi)^{1/2}} \dots, \quad (28)$$

and its value is determined by the eigenvalue spectrum of the operator $\hat{M}^{(i)}$.

At $\lambda = 0$ Eqs. (24) are symmetric with respect to rotations in replica space, and admit of solutions of the form^{5,27}

$$\Delta_\alpha^{(i)}(\mathbf{r}) = \Delta_i(\mathbf{r}) e_\alpha, \quad \Delta_i(\mathbf{r}) = \left(\frac{\tau}{\tilde{\gamma}} \right)^{1/2} \chi \left[\frac{\mathbf{r}}{\xi(T)} \right],$$

$$\sum_{\alpha=1}^n e_{\alpha}^2 = 1, \quad (29)$$

where e_{α} is an arbitrary unit vector in replica space, and the function $\chi(x)$ was defined earlier. Such instantons corresponds to the already considered limiting case of weak thermodynamic fluctuations, and the action on them is given by $S_0(\tau)$ from (19a) at $\lambda = 0$.

At $\lambda \neq 0$ this symmetry of the action (22) is violated by the term $\lambda \Delta_{\alpha}^4$ (it plays the role of cubic anisotropy in replica space), and there are n types of instanton solutions of Eqs. (24):

$$\Delta_{\alpha}^{(i)}(r) = \Delta_d(r) \delta_{\alpha i}, \quad i=1, \dots, n. \quad (30)$$

The function $\Delta_d(r)$ is defined in (17) and the index i characterizes the direction, in replica space, along which spontaneous symmetry breaking takes place.⁵⁾ A number of important relations between the integrals of the function $\chi(x)$ can be found by noting that Eq. (18) can be obtained from the condition that the functional $A\{\chi(x)\}$ (19b) have an extremum with respect to $\chi(x)$. To this end, we replace $\chi(x)$ in it by $\alpha\chi(\beta x)$. The minimum of the function $A(\alpha, \beta)$ with respect to α and β should be reached at $\alpha = \beta = 1$, so that

$$\int_0^{\infty} dx x^2 \chi^2(x) = \frac{1}{3} \int_0^{\infty} dx x^2 \left(\frac{d\chi}{dx} \right)^2 = \frac{1}{4} \int_0^{\infty} dx x^2 \chi^4(x) = \frac{A}{8\pi}. \quad (31)$$

The action (22) on the instanton solution (30) is equal to the value of $S_0(\tau)$ given in (19a). It follows from (22) that the instanton contribution to $\langle Z^n \rangle$ is proportional to $n \exp[-S_0(\tau)]$, where the factor n is the result of summation of contributions of all n types of solutions (30). Substituting this expression in (21), we get for the free energy of the seeds the result (14) and (19) of the fluctuation theory. Allowance for the fluctuations of the replica fields in the vicinity of the classical solution enables us to find the pre-exponential factor in (14).

4. Pre-exponential factor in the case of strong thermodynamic fluctuations

The pre-exponential factor in F_s is determined by the replica-field configurations (26) near the external solution (30). The operator $\hat{M}^{(i)}$ on the solutions (30) is equal to

$$\begin{aligned} \hat{M}_{\alpha\beta}^{(i)} &= [\hat{M}_L \delta_{\alpha i} + \hat{M}_T (1 - \delta_{\alpha i})] \delta_{\alpha\beta}, \\ \hat{M}_{L,T} &= \frac{2N(E_F)}{T} [-\xi^2 \nabla^2 + \tau U_{L,T}(r)], \\ U_L(r) &= 1 - 3\chi^2[r/\xi(T)], \end{aligned} \quad (32)$$

$$U_T(r) = 1 - (1 - \lambda/\bar{\gamma})^{-1} \chi^2[r/\xi(T)].$$

Its eigenfunctions are

$$\varphi_{k,\alpha}^L(r) = \varphi_k^L(r) \delta_{\alpha i}, \quad \varphi_{k,\alpha}^T(r) = \varphi_k^T(r) \delta_{\alpha\beta}, \quad \beta \neq i, \quad (33)$$

where the functions $\varphi_k^{L,T}(r)$ are the solutions of the eigenvalue equations for the operators $\hat{M}_{L,T}$:

$$\hat{M}_{L,T} \varphi_k^{L,T}(r) = \varepsilon_k^{L,T} \varphi_k^{L,T}(r). \quad (34)$$

These equations have the form of Schrödinger equations

with the potential $U_{L,T}(r)$ shown schematically in Fig. 1. Let us examine the spectrum of these equations. The potential $U_L(r)$ always have a discrete level with zero eigenvalue $\varepsilon_1^L = 0$. Its presence is connected with the translational symmetry of Eq. (22). A solution of (24), other than (30) and having the same action, is the function $\Delta_{\alpha}^{(i)}(r + r_0)$ with a shift of the localization center by an arbitrary vector r_0 . The corresponding deviation $\varphi_{\alpha}(r)$ following a translation by an infinitely small vector δr_0 takes the form

$$\varphi_{\alpha}(r) = [\Delta_{\alpha}(r + \delta r_0) - \Delta_{\alpha}(r)] \delta_{\alpha i} = (J_L^{-1} \delta r_0) \varphi_i^L(r) \delta_{\alpha i}, \quad (35)$$

$$\varphi_i^L(r) = J_L^{-1} \frac{\partial \Delta_d(r)}{\partial r} \frac{r}{r},$$

$$J_L = \frac{1}{3} \int d\mathbf{r} \left(\frac{\partial \Delta_d}{\partial r} \right)^2 = \frac{S_0(\tau) T}{2\xi^2 N(E_F)}. \quad (36)$$

It can be verified by directly substituting (36) in (33) that the functions $\varphi_{i,x,y,z}^L(r)$ are eigenfunctions of the operator \hat{M}_L with zero eigenvalues. In (36) we have expressed with the aid of (17) and (31), in terms of the action (22), the integral that determines J_L . Comparison of (35) with the general expression (26) yields the differential of the coefficient c_i^L of the expansion (26): $dc_i^L = J_L^{-1/2} dr_0$. Since the eigenvalue is threefold degenerate, $J_L^{3/2}$ is the Jacobian of the transition from the coefficients c_i^L to the collective variables r_0 that determine the position of the superconducting drop. The integral with respect to r_0 yields the volume of the system V . By calculating the remaining Gaussian integrals with respect to c_k in (27) and (28), we obtain the contribution of the instanton configurations (30) to $\langle Z^n \rangle$ (22):

$$nV (J_L/2\pi)^{3n} [\det' \hat{M}_L]^{-n} [\det \hat{M}_T]^{(1-n)/2} \exp[-S_0(\tau)]. \quad (37)$$

the determinant of the operator is equal to the product of all its eigenvalues, and the prime denotes exclusion of the zero eigenvalues from this product. Substituting (37) in (21), we obtain the contribution of the superconducting drops to the free energy of the system:

$$F_s = -\theta_s(\tau) T,$$

$$\theta_s(\tau) = \left[\frac{TS_0(\tau)}{4\pi N(E_F)} \right]^n \left[\frac{\det \hat{M}_T}{\det' \hat{M}_L} \right]^{3n} \xi^{-3} \exp[-S_0(\tau)]. \quad (38)$$

To determine θ_s we must find the remaining eigenvalues of the operators \hat{M}_L and \hat{M}_T (32).

We consider first the operator \hat{M}_L . The angular dependence of the eigenfunction (36) obtained above corresponds to p -type state with orbital momentum $l = 1$. The min-

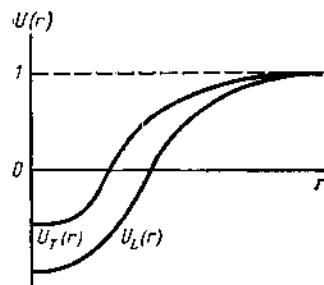


FIG. 1.

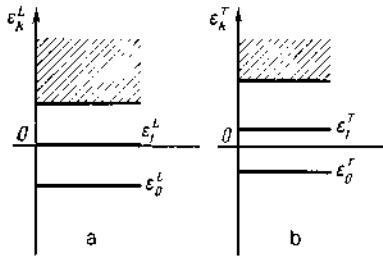


FIG. 2.

imum eigenvalue ϵ_0^L should correspond to a nondegenerate state with $l=0$. The operator \hat{M}_L should have thus at least one negative eigenvalue $\epsilon_0^L < \epsilon_1^L = 0$. A more rigorous analysis (Ref. 28) shows that such an eigenvalue is unique. The remaining eigenvalues ϵ_k^L with $k > 1$ are positive. The described eigenvalue spectrum of the operator \hat{M}_L is shown in Fig. 2 (the continuous section of the spectrum is shaded).

We consider now the eigenvalue spectrum of the operator \hat{M}_T . The quantity ρ_s in (38) is positive only if the operator \hat{M}_T has a single negative eigenvalue. We shall show below that this situation is realized if the condition $0 < \lambda < \lambda^* = 2\tilde{\gamma}/3$, is met, a condition that defines in fact that region of existence of superconducting drops. The spectrum of the eigenvalues of the operator \hat{M}_T is shown in Fig. 2.

In the case $\lambda \ll \lambda^*$ the minimum eigenvalue $\epsilon_0^T < 0$ can be obtained by perturbation theory in the small parameter λ / λ^* . At $\lambda = 0$ the operator \hat{M}_T (32) has a single zero eigenvalue $\epsilon_0^T = 0$. The corresponding Goldstone mode is connected with the isotropy of Eqs. (24) in replica space, and corresponds to rotation of the unit vector e_a (29) in replica space

$$\varphi_a(\mathbf{r}) = \Delta_a(\mathbf{r}) \delta e_a = (J_T^{-1/2} \delta e_a) \varphi_0^T(\mathbf{r}), \quad (39)$$

where the normalization component J_T and the function φ_0^T are equal to

$$\varphi_0^T(\mathbf{r}) = J_T^{-1/2} \Delta_d(\mathbf{r}), \quad J_T = \int d\mathbf{r} \Delta_d^2(\mathbf{r}) = S_0(\tau) T / 2\tau N(E_F). \quad (40)$$

It is easy to verify that the function (40) at $\lambda = 0$ is indeed a solution of Eq. (34) with zero eigenvalue $\epsilon_0^T = 0$. Comparing (39) with (26) we obtain the relation

$$c_{0\alpha}^T = J_T^{-1/2} \delta e_a. \quad (41)$$

At small $\lambda \ll \lambda^*$ we can neglect the change of the eigenfunction (40) of the operator \hat{M}_T . Its minimum eigenvalue ϵ_0^T is obtained by multiplying both halves of Eq. (34) for ϵ_0^T and by integrating with respect to the coordinate \mathbf{r} :

$$\epsilon_0^T = - \frac{2\lambda N(E_F)}{T} \int d\mathbf{r} \Delta_d^4(\mathbf{r}) / \int d\mathbf{r} \Delta_d^2(\mathbf{r}) = - \frac{8\lambda\tau}{\gamma}, \quad (42)$$

where we have used relations (17) and (30). The condition for the validity of the approach based on the instanton solutions (30) can be formulated in the form $\langle (\delta e_a)^2 \rangle \ll 1$. Since, as follows from (27), the characteristic values $(c_0^T)^2$ are proportional to $|\epsilon_0^T|^{-1}$, this condition takes the form $\lambda \gg \tilde{\gamma} S_0^{-1}(\tau)$. The opposite case of small λ was considered above using the Ioffe-Larkin approach. If $\tilde{\gamma} S_0^{-1}(\tau) \ll \lambda \ll \lambda^* = 2\tilde{\gamma}/3$, all the eigenvalues of the operator \hat{M}_T except ϵ_0^T can be calculated under the assumption

that $\lambda = 0$, and the eigenvalue ϵ_0^T is given by Eq. (42). It is easily seen that in this case all the eigenvalues of the operators \hat{M}_T and \hat{M}_L except ϵ_0^T and ϵ_1^L are proportional to $\tau N(E_F)/T$ and are independent of $\tilde{\gamma}$ and λ . A dimensional estimate of the ratio of their determinants yields therefore

$$|\det' \hat{M}_T / \det' \hat{M}_L| = [N(E_F) \tau / T]^2. \quad (43)$$

Substituting (42) and (43) in (38) we get

$$\begin{aligned} \theta_s(\tau) &\approx \frac{1}{\xi^3(T)} \left(\frac{\lambda}{\tilde{\gamma}} \right)^{1/2} S_0^{1/2}(\tau) \exp[-S_0(\tau)] \\ &\approx \xi^{-3}(T) \frac{\tau_0^{1/2} \tau_0^{1/2}}{\tau} \exp[-S_0(\tau)]. \end{aligned} \quad (44)$$

When calculating the order-parameter correlator (23) it suffices to take into account in the pre-exponential factor only the fluctuations due to the translational mode with zero eigenvalue:

$$\Delta_a(\mathbf{r}) = \Delta_d(\mathbf{r}) \delta_{a_i} + c_{i1}^T \varphi_{i,a}^L(\mathbf{r}) = \Delta_d(\mathbf{r} + \mathbf{r}_0) \delta_{a_i}. \quad (45)$$

We obtain as a result

$$\langle \Delta(\mathbf{r}) \Delta(\mathbf{r}') \rangle = \theta_s(\tau) \int d\mathbf{r}_0 \Delta_d(\mathbf{r} + \mathbf{r}_0) \Delta_d(\mathbf{r}' + \mathbf{r}_0). \quad (46)$$

The integration with respect to the coordinate \mathbf{r}_0 in (46) means in fact averaging over different drop-localization positions. After averaging, the correlator (46) depends only on the coordinate difference. Note that in view of the possible scatter of the drop amplitudes the parameter does not determine their density. To find the latter we must obtain the distribution of the drop amplitudes. At $\lambda \approx \tilde{\gamma} S_0^{-1}(\tau)$ expressions (38) and (44) are transformed into (20a) and (20b).

At $\lambda = \lambda^* = 2\tilde{\gamma}/3$ the operators \hat{M}_T and \hat{M}_L coincide. Accordingly, all their eigenvalues are equal and the operator \hat{M}_T has a single negative eigenvalue $\epsilon_0^T = 0$. At small $\lambda^* - \lambda \ll \lambda^*$ we obtain the eigenvalue ϵ_1^T by perturbation theory with the aid of the corresponding function (36):

$$\begin{aligned} \epsilon_1^T &= \frac{6N(E_F)}{T} (\lambda^* - \lambda) \int d\mathbf{r} \Delta_d^2(\mathbf{r}) \left(\frac{\partial \Delta_d}{\partial \mathbf{r}} \right)^2 / \int d\mathbf{r} \left(\frac{\partial \Delta_d}{\partial \mathbf{r}} \right)^2 \\ &\approx \frac{N(E_F) \tau}{T} \left(\frac{\lambda^*}{\lambda} - 1 \right). \end{aligned} \quad (47)$$

The remaining eigenvalues of the operator \hat{M}_T are positive at $\lambda < \lambda^*$. Using the result (47) for ϵ_1^T and setting the remaining $\epsilon_k^T = \epsilon_k^L$ for $k \neq 0$, we obtain at $\lambda^* - \lambda \ll \lambda^*$

$$\begin{aligned} \theta_s(\tau) &\approx \frac{1}{\xi^3(T)} \left(\frac{\lambda^*}{\lambda} - 1 \right)^{1/2} S_0^{1/2}(\tau) \exp[-S_0(\tau)], \\ \frac{\lambda^*}{\lambda} &= 0.64 \left(\frac{\tau_D}{\tau_a} \right)^{1/2}. \end{aligned} \quad (48)$$

As $\lambda \rightarrow \lambda^*$ the eigenvalue $\epsilon_1^T \rightarrow 0$ and account must be taken of the non-Gaussian character of the field fluctuations $\varphi_a(\mathbf{r})$. These fluctuations can lead to a change of relation (48) in the region of small $\lambda^* - \lambda \lesssim \tilde{\gamma} S_0^{-1}(\tau)$. Thus, superconducting drops exist only if $\tau_D > \tau_D^*$, and their density vanishes as $\lambda \rightarrow \lambda^*$ because the superconductivity is destroyed in the drops by thermodynamic fluctuations.

In the calculation of the order-parameter correlator it is necessary, in the case $\lambda^* - \lambda \ll \lambda^*$, to take into account in (23), besides the zeroth translational mode, also the contri-

bution of $n - 1$ modes of the operator \hat{M}_T , with eigenvalues ε_1^T that tend to zero as $\lambda \rightarrow \lambda^*$. Neglecting the contribution of the remaining mode, we can, in analogy with the derivation of (45), replace in (23) the quantity

$$\sum_{\alpha=1}^n \Delta_{\alpha}(\mathbf{r}) \Delta_{\alpha}(\mathbf{r}')$$

by

$$n \Delta_d \left(\mathbf{r} + J_L^{1/2} \sum_{\alpha=1}^n \mathbf{c}_{1,\alpha} \right) \Delta_d \left(\mathbf{r}' + J_L^{1/2} \sum_{\alpha=1}^n \mathbf{c}_{1,\alpha} \right). \quad (49)$$

Integrating over all the coefficients c_k in (28) and (23), we obtain for the order parameter the results (46), where the factor $\theta_s(\tau)$ is defined in (38). Note that over large scales the function (43) decreases like $\exp[-|\mathbf{r} - \mathbf{r}'|/\xi(T)]$ and does not contain the Ornstein-Zernike factor $|\mathbf{r}' - \mathbf{r}|^{-1}$.

CONCLUSION

We have shown here that in the case of sufficiently strong statistical fluctuations of the order parameter $\tau_D > \tau_D^*$ superconductivity is produced in the form of isolated seeds-superconducting drops. We found the free energy of such an inhomogeneous superconducting state and the correlator of the order parameter in the temperature region $\tau \gg \tau_D$, where the function θ_s defined in (38) is exponentially small: $\theta_s \sim \exp[-A(\tau/\tau_D)^{1/2}]$. The drops can be regarded here as noninteracting. They make an exponentially small contribution to the heat capacity of the system, to the conductivity, and to the diamagnetic susceptibility. To calculate the latter, we find the changes induced in the exponents of (19), (15), and (20) by a change of the external field H :

$$\Delta S_0(\tau, H) = \frac{4e^2 \xi^2 N(E_F)}{3c^2 \hbar^2 T} H^2 \int d\mathbf{r} r^2 \Delta_d^2(\mathbf{r}). \quad (50)$$

Differentiating the free energy $F_s(\tau, H)$ with respect to H , we get

$$\chi_s = -F_s(\tau) S_0(\tau) \xi^2(T) / \Phi_0^2, \quad (51)$$

where Φ_0 is the flux quantum.

The order parameter is locally small inside the drop in the region $\xi(T) = \xi \tau^{-1/2}$ only to the extent that $\tau^{1/2}$ is small, and local measurements (for example, with the aid of a tunnel-effect microscope) can reveal the appearance of the drops.

The theory predicts thus a strong enhancement of the thermodynamic and statistical fluctuations of the superconducting order parameter near the localization threshold. The thermodynamic fluctuations by themselves leave the system spatially homogeneous and therefore do not lead to a qualitatively new behavior. Statistical fluctuations alter the superconducting transition radically—it becomes percolative.²⁴ Although, there is as yet no quantitative theory of such a transition in the temperature region where the drop density is large, a number of qualitative conclusions that lend themselves to experimental verification can be drawn.

A transition in an inhomogeneous superconductivity regime should be strongly smeared in temperature, and the degree of smearing should depend on the current flow in the

measurements of R and on the field in the measurements of the magnetic susceptibility χ_s . In view of the strong fluctuations of $\Delta(\mathbf{r})$ there may be no BCS singularity in the density of states of the quasiparticles, and at $\tau_D \gg 1$ it will have a zero-gap character down to zero temperature (the same result is produced also by an increase of the frequency of the electron inelastic collisions near the localization threshold, owing to the enhancement of the Coulomb repulsion of the electrons²⁹). Finally, the inhomogeneous character of the superconductivity (of the drop) can be observed with the aid of local measurements, e.g., by tunnel-effect microscopy.

A substantial broadening of the superconducting transition and a smearing of the singularity in the density of states of the quasiparticles was indeed observed in granulated aluminum as the conductivity was lowered below $1000 \Omega^{-1} \cdot \text{cm}^{-1}$ (Ref. 29). These facts offer evidence of the increasing role of the fluctuations, although the only assumption made to interpret the zero-gap character of the spectrum at $\sigma = 10 \Omega^{-1} \cdot \text{cm}^{-1}$ was that the frequency of the electron inelastic collisions increases near the localization threshold.

Similar peculiarities of the superconducting behavior should occur also in systems with strong statistical fluctuations of the pairing interaction, independently of their proximity to the localization threshold. Naturally, far from the Anderson transition, there are in this case no grounds whatever for enhancement of the inelastic scattering of the electron, and the zero gap in the quasiparticle spectrum can be due only to statistical fluctuations of the superconducting order parameter.

The authors are grateful to B. L. Al'tshuler, S. L. Ginzburg, L. P. Gor'kov, I. A. Korenblit, A. I. Larkin, D. E. Khmel'nitskiĭ, and E. F. Shender for a helpful discussion of the questions touched upon in the paper.

APPENDIX

Let us show that thermodynamic fluctuations of the magnetic field in superconducting drops, which we have neglected above, have no effect in dirty superconductors.

We expand the action (22) in the vicinity of the instanton solution (30) in the deviations of $A_{\mu\alpha}$ and φ_{α} accurate to quadratic terms ($A_{\mu\alpha}$ are the components of the vector \mathbf{A}_{α} , and $\mu = 1, 2, 3$). The action (25) acquires then an additional term that describes the fluctuations of the magnetic field:

$$\frac{1}{2} \sum_{\mu, \nu, \alpha, \beta} \int d\mathbf{r} (A_{\mu\alpha} \hat{K}_{\mu\alpha, \nu\beta} A_{\nu\beta}), \quad (A.1)$$

where the quadratic-form operator \hat{K} is equal to

$$\hat{K}_{\mu\alpha, \nu\beta}^{(i)} = \hat{K}_{L\mu\nu} \delta_{\alpha\beta} \delta_{\alpha i} + \hat{K}_{T\mu\nu} \delta_{\alpha\beta} (1 - \delta_{\alpha i}), \quad (A.2)$$

$$K_{T\mu\nu}(\mathbf{r} - \mathbf{r}') = \frac{1}{T} D_{\mu\nu}^{-1}(\mathbf{r} - \mathbf{r}'), \quad (A.3)$$

$$K_{L\mu\nu}(\mathbf{r}, \mathbf{r}') = \frac{1}{T} D_{\mu\nu}^{-1}(\mathbf{r} - \mathbf{r}') + \frac{8e^2 N(E_F) \xi^2}{c^2 T} \Delta_d^2(\mathbf{r}) \delta_{\mu\nu}. \quad (A.4)$$

Here $D_{\mu\nu}(\mathbf{r})$ is the photon Green's function and is equal to $\delta_{\mu\nu}/r$ in the Coulomb gauge. Calculating the Gaussian integrals with respect to φ_{α} and $A_{\mu\alpha}$, we find that the magnetic-field fluctuations lead to the appearance of an additional multiplier Θ in the pre-exponential factor in (38). Regarding in (A.4) the term containing Δ_d^2 as a perturbation, we obtain for the factor Θ the expression

$$\Theta = \exp \left[\frac{8e^2 N(E_F) \xi^3}{c^2 T} \sum_{\mu} D_{\mu}(0) \int d\mathbf{r} \Delta_d^2(\mathbf{r}) + \frac{32e^4 N^2(E_F) \xi^4}{c^4 T} \times \sum_{\mu, \nu} \int d\mathbf{r} \int d\mathbf{r}' \Delta_d^2(\mathbf{r}) \Delta_d^2(\mathbf{r}') D_{\mu\nu}^2(\mathbf{r}-\mathbf{r}') + \dots \right]. \quad (\text{A.5})$$

The first term in the exponential of (A.5) gives the renormalization of the superconducting-transition temperature. It is the same for both the spatially homogeneous state and for drops, and can hereafter be regarded as carried out. The second term in the exponential of (A.5) describes the influence of the screening of the fluctuating magnetic field on the form of superconducting seed. Substituting in (A.5) the instanton solutions for $\Delta_d(\mathbf{r})$ and integrating with respect to \mathbf{r} and \mathbf{r}' , we obtain the condition under which this term in (A.4) is small and the influence of the magnetic field on the drop is negligible, in the form

$$\lambda_L \ll \lambda_c' (\lambda_L^2 \xi_0^2 / \xi^4(T)). \quad (\text{A.6})$$

This condition is certainly met in type-II superconductors with $\lambda_L \gtrsim \xi_0$. In type-I superconductors it restricts the value of the critical disorder at which the magnetic-field thermodynamic fluctuations influence the properties of the seeds.

¹The question of the size of the statistical fluctuations in dirty superconductors was first raised in Ref. 16.

²The parameter $\tau_G^{-1/2} \approx T_c N(E_F) \xi^3 = \langle \nu \rangle$, where N is the number of levels in the system in the energy interval T_c in a volume ξ^3 . The a condition that the fluctuation region be narrow is $\langle \nu \rangle \gg 1$. The parameter $\tau_G^{-1/2} \approx (\langle \nu \rangle - \langle \nu \rangle^2) / \langle \nu \rangle^2$, and determines the fluctuations of the relative number of levels.

³This result was obtained using the scaling dependence of the correlation function $\langle N(r, E_F + \omega) N(0, E_F) \rangle$ near the mobility threshold.²⁰

⁴When the drop interaction is evaluated, it is necessary to take into account the vortices in the region between the drops; the vortices destroy the phase coherence of the different seeds. A similar situation is encountered in granulated superconductors.

⁵At integer $n \geq 2$, Eqs. (24) have besides the solution (30) also solutions

with spontaneously broken symmetry along two and more coordinate axes in replica space. Such solutions, however, do not admit analytic continuation $n \rightarrow 0$ and will not be considered further.

¹A. A. Abrikosov and L. P. Gor'kov, Zh. Eksp. Teor. Fiz. **35**, 1158 (1958); **36**, 319 (1959) [Sov. Phys. JETP **8**, [sic] (1959); **9**, 220 (1959)].

²L. P. Gor'kov, *ibid.* **37**, 1407 (1959) [**10**, (1960)].

³P. W. Anderson, Phys. Chem. Solids **11**, 26 (1959).

⁴Anderson Localization, Y. Nagaoka and H. Fukuyama, eds., Springer, 1982.

⁵M. V. Sadovskii, Usp. Fiz. Nauk **133**, 223 (1981) [Sov. Phys. Usp. **24**, 96 (1981)]. Sov. Scient. Rev. Phys. Rev., I. M. Khaltnikov, ed., Vol. 7, Harwood Publ., 1986, p. 3.

⁶P. W. Anderson, K. A. Muttalib, and T. V. Ramakrishnan, Phys. Rev. **B28**, 117 (1983).

⁷L. N. Bulaeviskii and M. V. Sadovskii, Pis'ma Zh. Eksp. Teor. Fiz. **39**, 524 (1984) [JETP Lett. **39**, 640 (1984)]; J. Low Temp. Phys. **59**, 89 (1985).

⁸E. Kolley and W. Kolley, Z. Phys. **B57**, 185 (1984).

⁹D. Belitz, J. Phys. **F15**, 189 (1984).

¹⁰E. Kolley and W. Kolley, Z. Phys. **B56**, 2315 (1984).

¹¹H. Ebisawa, H. Fukuyama, and S. Maekawa, Preprint, 1985. H. Fukuyama, J. Phys. Soc. Jpn. **54**, 2393 (1984).

¹²Yu. I. Ovchinnikov, Zh. Eksp. Teor. Fiz. **64**, 719 (1973) [Sov. Phys. JETP **37**, 366 (1973)]; H. Fukuyama, H. Ebisawa, and S. Maekawa, J. Phys. Soc. Jpn. **53**, 3560 (1984).

¹³A. Kapitulnik and G. Kotliar, Phys. Rev. Lett. **54**, 473 (1985); Phys. Rev. **B33**, 3146 (1986).

¹⁴M. Ma and P. A. Lee, Phys. Rev. **B32**, 5658 (1985).

¹⁵C. Caroli, P. G. De Gennes, and J. Matricon, J. Phys. Rad. **23**, 707 (1962).

¹⁶L. N. Bulaeviskii and M. V. Sadovskii, Pis'ma Zh. Eksp. Teor. Fiz. **43**, 76 (1986) [JETP Lett. **43**, 99 (1986)].

¹⁷P. De Gennes, *Superconductivity of Metals and Alloys*, Benjamin, 1966.

¹⁸A. I. Larkin and Yu. N. Ovchinnikov, Zh. Eksp. Teor. Fiz. **61**, 1221 (1971) [Sov. Phys. JETP **34**, 651 (1972)].

¹⁹R. Oppermann and F. Wegner, J. Phys. **B34**, 327 (1979).

²⁰V. L. Berezinskii and L. P. Gor'kov, Zh. Eksp. Teor. Fiz. **77**, 2498 (1979) [Sov. Phys. JETP **50**, 1209 (1979)].

²¹D. E. Khmel'nitskii, *ibid.* **68**, 1960 (1975) [**41**, 981 (1975)].

²²T. C. Lubensky, Phys. Rev. **B11**, 3573 (1975).

²³L. B. Ioffe and A. I. Larkin, Zh. Eksp. Teor. Fiz. **81**, 707 (1981) [Sov. Phys. JETP **54**, 378 (1981)].

²⁴J. M. Lifshitz, S. A. Gredeskul, and L. A. Pastur, Introduction to the Theory of Disordered Systems, Nauka, 1982, p. 204.

²⁵G. Grinstein and A. Luther, Phys. Rev. **B13**, 1329 (1976).

²⁶J. L. Cardy, J. Phys. C11, L321 (1978). V. M. Sadovskii, Fiz. Tverd. Tela (Leningrad) **21**, 743 (1979) [Sov. Phys. Solid State **21**, 435 (1979)].

²⁷J. Zinn-Justin, Phys. Reports **70**, 109 (1981).

²⁸R. C. Dynes, J. P. Garno, G. Hertel, and T. P. Orlando, Phys. Rev. Lett. **53**, 2473 (1984).

Translated by J. G. Adashko

The two-particle Green function in a model of a one-dimensional disordered system: An exact solution?

M V Sadovskii and A A Timofeev

Institute of Electrophysics, Ural Branch of the USSR Academy of Sciences,
Komsomol'skaya ul. 34, 620219 Sverdlovsk, USSR

Received 4 July 1991

Abstract. The paper suggests an effective procedure for summing all Feynman diagrams for the two-particle Green function in a one-dimensional model with a Gaussian random field whose correlator is Lorentzian (in the momentum space) with its maximum at $Q = 2p_F$, with p_F the Fermi momentum. This model can be considered a Gaussian model of the Peierls transition (charge density and spin density waves) in a fluctuation region with a well-developed short-range order. The authors formulate a recurrence procedure for calculating the vertex part, which describes the response of the system to an external electromagnetic field, and obtain a general picture of the evolution of the frequency dependence of conductivity as a function of the short-range order correlation length, which describes absorption through a pseudogap and localization.

1. Introduction

There is only a limited number of models of the electronic properties of one-dimensional disordered systems that allow an exact solution [1, 2]. The interest in such models is due to the general problem of studying the electronic states in disordered systems and to specific problems of the physics of quasi-one-dimensional systems. Attention has especially focused on the manifestation of Anderson localization in the one-dimensional case for arbitrarily weak disorder [3–5]. Resolving this problem has proved extremely difficult since localization is determined by the properties of the two-particle Green function, about which very few exact statements are known.

The majority of exact results in the theory of one-dimensional disordered systems have been obtained by employing sophisticated mathematical techniques specially designed to describe one-dimensional problems and unsuitable for generalization to the multidimensional case. Only in a few cases have exact solutions been obtained via standard methods of the quantum theory of multiparticle systems [6]. Such models are of special interest primarily from the stand-point of checking the effectiveness of standard approximation methods. They could also lead to instructive results easily generalized to the multidimensional case.

A model of this kind was suggested some time ago by one of the present authors [7–9]. Within its framework it was established that the scattering of an electron on short-range order Gaussian fluctuations with a characteristic period determined by the wavevector $Q \propto 2p_F$ (p_F is the Fermi momentum) leads to the formation of a 'pseudogap' in the neighbourhood of the Fermi level that evolves

with variations in the short-range order correlation radius [9]. In the approximation of large correlation radii there has also been obtained an exact analytical solution for the two-particle Green function describing, among other things, the absorption of electromagnetic radiation through the pseudogap [7, 8]. For the particular case of commensurate fluctuations a similar model was considered in Wonneberger and Lautenschlager [10]. The results obtained in these papers have been used to interpret the optical properties of quasi-one-dimensional systems undergoing a Peierls transition [8, 11] and in some other problems (e.g., see [12]). Lately a model of the same kind has been suggested for interpreting a number of properties of high-temperature superconductors [13–15]. The authors of [15] suggest a general recurrence procedure for calculating the two-particle Green function that is valid for arbitrary short-range correlation radii and allows for all the respective perturbation-theory diagrams.

The present paper is devoted to a thorough study of the solution used in [15], an analysis of its special features from the viewpoint of the theory of one-dimensional disordered systems, and a comparison of the 'exact' results with those obtained within the framework of standard approximation methods.

2. The model

We consider an electron placed in a Gaussian random field $\Delta(x)$ with a correlation function

$$\langle \Delta(x)\Delta(x') \rangle = \Delta^2 \exp\{-|x-x'|\xi^{-1}\} \cos [2p_F(x-x')] \quad (1)$$

where Δ^2 is the mean square of a field fluctuation, and ξ the short-range order correlation radius. Such a correlator appears, for instance, in fluctuations of the order parameter in the Ginzburg–Landau model for a Peierls transition [16]. In what follows Δ and ξ are considered parameters of the theory. The Fourier transform of (1) is

$$\begin{aligned} \langle \Delta_Q \Delta_{-Q} \rangle &\equiv \Delta^2 S(Q) \\ &= 2\Delta^2 \left(\frac{\kappa}{(Q-2p_F)^2 + \kappa^2} + \frac{\kappa}{(Q+2p_F)^2 + \kappa^2} \right) \end{aligned} \quad (2)$$

with $\kappa = \xi^{-1}$. The simplest self-energy part of the one-electron Green function has the form (figure 1)

$$\begin{aligned} \Sigma(\varepsilon, p) &= \Delta^2 \int \frac{dQ}{2\pi} \frac{S(Q)}{\varepsilon - \xi_{p-Q} - i\delta \operatorname{sgn} \xi_{p-Q}} \\ &\cong \frac{\Delta^2}{\varepsilon + \xi_p + iv_F \kappa \operatorname{sgn} \xi_p} \\ &\equiv \Delta^2 G_0(\varepsilon; -\xi_p - iv_F \operatorname{sgn} \xi_p) \quad (p \propto p_F) \end{aligned} \quad (3)$$

where $\varepsilon_p \cong v_F(|p| - p_F)$, v_F is the Fermi velocity, and we have allowed for the fact that $\xi_{p-2p_F} = -\xi_p$.

We also consider the case of commensurate fluctuations [10], when $\xi_p = -W \cos(pa)$, with a the lattice constant, and $2p_F = \pi/a$ (half-filled bands, period

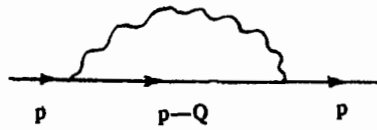


Figure 1. The simplest contribution to the self-energy part.

doubling). The diagram in figure 1 and the result of the (3) type were basic to the analysis conducted in [16]. In [7, 8] all Feynman diagrams for the one- and two-particle Green functions were summed for the asymptotic limit $\kappa \rightarrow 0$. An effective summation of all the diagrams for the one-particle Green function was carried out in [9] for arbitrary values of κ . In the n th order of the perturbation expansions in Δ^2 there are $n!$ diagrams in the case of incommensurate fluctuations and $(2n - 1)!! = (2n - 1)!/2^{n-1}(n - 1)!$ in the case of commensurate fluctuations (period doubling) [9]. Figure 2 shows all the important diagrams of the third order in Δ^2 for the one-electron Green function in the incommensurate case. The rules for calculating the contributions of arbitrary diagrams have been thoroughly discussed in [9]. Generally, the contribution of any diagram is determined by the position of the 'initial' and 'final' vertexes for the interaction lines. Here to each one-electron line following the 'initial' vertex there is assigned (see equation (3)) an expression of the free-particle propagator type in which $iv_F\kappa \operatorname{sgn} \xi_p$ is added to the denominator, while in a similar line following the 'final' vertex this term is subtracted from the denominator. The integers in figure 2 stand for the number of such contributions in each of the corresponding denominators. The reader can easily see that the contribution of any diagram with crossed interaction lines can be uniquely represented by a respective diagram without crossed interaction lines, since their contributions are equal (e.g., in figure 2 diagram (d) provides the same contribution as diagram (e)). The general procedure for such assigning is given in [9], in accordance with the method first suggested by Elyutin [17]. Each vertex is assigned an integer equal to the number of terms $iv_F\kappa$ in the denominator of the electron line following the given vertex. The initial vertex is assigned the integer $N_n = N_{n-1} + 1$, where N_{n-1} is the integer assigned to the closest vertex on the left. The final vertex is assigned the integer $N_{n-1} - 1$, where $N_0 = 0$ and n is the ordinal number of the vertex.

We introduce

$$v(k) = \begin{cases} (k + 1)/2 & \text{if } k = 2m + 1 \\ k/2 & \text{if } k = 2m \end{cases} \quad (4)$$

for the case of incommensurate fluctuations and

$$v(k) = k \quad (5)$$

for the case of commensurate fluctuations. It can easily be verified that the number of irreducible diagrams for the self-energy part that are equal to the given diagram without crossed interaction lines is given by the product of the factors $v(N_n)$ for all the initial vertexes of a given diagram. Hence, further analysis can be carried out in terms of diagrams without crossings, assigning to all initial vertexes the additional factors $v(N_n)$ [9, 17].

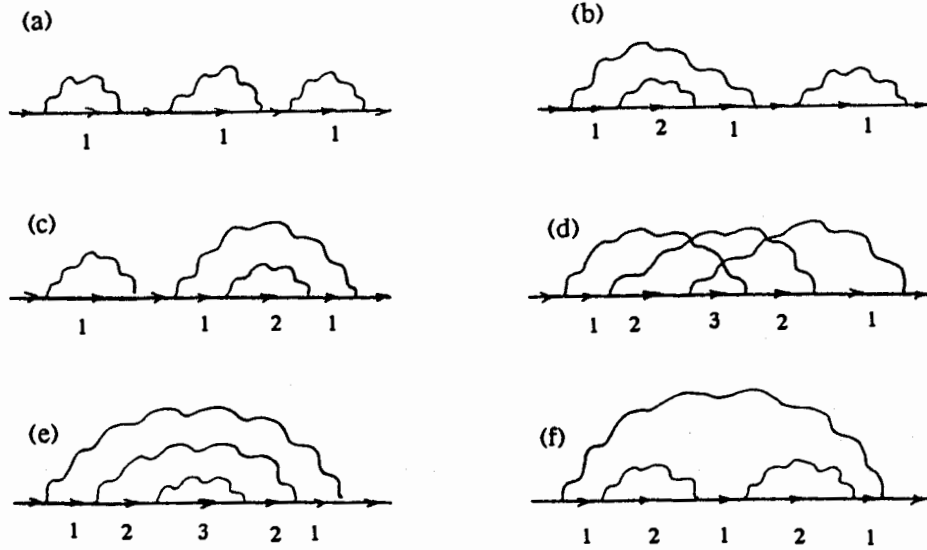


Figure 2. Δ^6 -order diagrams for the Green function (the incommensurate case).

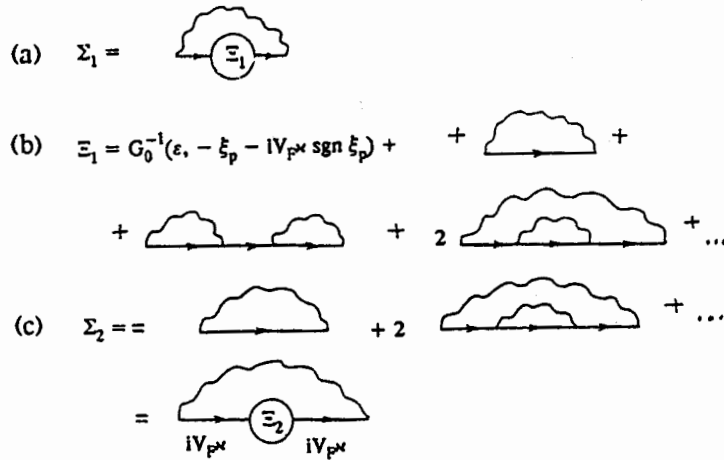


Figure 3. The diagrammatic structure of the recurrence procedure for the self-energy part.

Applying Elyutin's method makes it possible to build an exact representation for the one-electron Green function in the form of a continued fraction [9]. The structure of this solution is based on the ordinary Dyson equation

$$G^{-1}(\epsilon, \xi_p) = G_0^{-1}(\epsilon, \xi_p) - \Sigma_1(\epsilon, \xi_p) \tag{6}$$

where for the self-energy part we have (figure 3(a))

$$\begin{aligned}\Sigma_1(\varepsilon, \xi_p) &= \Delta^2 \Xi_1(\varepsilon, \xi_p) \frac{v(1)}{(\varepsilon + \xi_p + i v_F \kappa \operatorname{sgn} \xi_p)^2} \\ &= \Delta^2 v(1) G_0^2(\varepsilon, -\xi_p - i v_F \kappa \operatorname{sgn} \xi_p) \Xi_1(\varepsilon, \xi_p)\end{aligned}\quad (7)$$

and for $\Xi_1(\varepsilon, \xi_p)$ we have the expansion depicted in figure 3(b), where there are no diagrams with crossed interaction lines but where the k th vertex (counting from the left) with an 'outgoing' line is assigned a combinatorial factor $v(k)$ (4) or (5), which allows taking into account the contributions of all the diagrams with crossed interaction lines. Respectively, $\Xi_1(\varepsilon, \xi_p)$ can be written as

$$\Xi_1(\varepsilon, \xi_p) = G_0^{-2}(\varepsilon, -\xi_p - i v_F \kappa \operatorname{sgn} \xi_p) \frac{1}{G_0^{-1}(\varepsilon, -\xi_p - i v_F \kappa \operatorname{sgn} \xi_p) - \Sigma_2(\varepsilon, \xi_p)} \quad (8)$$

where $\Sigma_2(\varepsilon, \xi_p)$ is expressed by the sum of irreducible diagrams shown in figure 3(c):

$$\Sigma_2(\varepsilon, \xi_p) = \Delta^2 v(2) G_0^2(\varepsilon, \xi_p + 2i v_F \kappa \operatorname{sgn} \xi_p) \Xi_2(\varepsilon, \xi_p) \quad (9)$$

$$\Xi_2(\varepsilon, \xi_p) = G_0^{-2}(\varepsilon, \xi_p + 2i v_F \kappa \operatorname{sgn} \xi_p) \frac{1}{G_0^{-1}(\varepsilon, \xi_p + 2i v_F \kappa \operatorname{sgn} \xi_p) - \Sigma_3(\varepsilon, \xi_p)} \quad (10)$$

etc. The final result is

$$\Sigma_k(\varepsilon, \xi_p) = \Delta^2 G_0^2(\varepsilon, (-1)^k(\xi_p + i k v_F \kappa \operatorname{sgn} \xi_p)) v(k) \Xi_k(\varepsilon, \xi_p) \quad (11)$$

$$\begin{aligned}\Xi_k(\varepsilon, \xi_p) &= G_0^{-2}(\varepsilon, (-1)^k(\xi_p + i k v_F \kappa \operatorname{sgn} \xi_p)) \\ &\times \frac{1}{G_0^{-1}(\varepsilon, (-1)^k(\xi_p + i k v_F \kappa \operatorname{sgn} \xi_p)) - \Sigma_{k+1}(\varepsilon, \xi_p)}\end{aligned}\quad (12)$$

$$\begin{aligned}\Sigma_k(\varepsilon, \xi_p) &= \Delta^2 v(k) \frac{1}{G_0^{-1}(\varepsilon, (-1)^k(\xi_p + i k v_F \kappa \operatorname{sgn} \xi_p)) - \Sigma_{k+1}(\varepsilon, \xi_p)} \\ &\equiv \Delta^2 v(k) G_k(\varepsilon, \xi_p)\end{aligned}\quad (13)$$

$$G_k(\varepsilon, \xi_p) = [\varepsilon - (-1)^k(\xi_p + i k v_F \kappa \operatorname{sgn} \xi_p) - \Delta^2 v(k+1) G_{k+1}(\varepsilon, \xi_p)]^{-1} \quad (14)$$

with $G_{k=0}(\varepsilon, \xi_p) = G(\varepsilon, \xi_p)$. These recurrence relations yield an exact representation of the one-electron Green function in the form of a continued fraction. The results of numerical calculations of the corresponding electronic state density for different values of the short-range order correlation radius $\xi = \kappa^{-1}$ are given in [9]. The results exhibit, among other things, the formation of a pseudogap approximately 2Δ wide in

the vicinity of the Fermi level [7–11, 16] that gradually fills up (degrades) as ξ gets smaller.

Figures 4 and 5 illustrate the results of numerical calculations of the spectral density

$$A(\varepsilon, \xi_p) = \frac{1}{\pi} \text{Im } G^R(\varepsilon, \xi_p) \quad (15)$$

of the respective Green function (14) for different values of the parameter $W = v_F \kappa / \Delta$ (i.e., virtually the reciprocal correlation length). The energy scale is given in units of Δ (i.e., $E = \varepsilon / \Delta$ and $x = \xi_p / \Delta$).

In the case of well-defined quasiparticles the spectral density is simply $\delta(\varepsilon - \xi_p)$. The results depicted in figures 4 and 5 suggest that at small values of the parameter W (large correlation lengths $\xi \gg v_F / \Delta$) our solution contains no contributions of the quasiparticle type. This fact was noted in [7, 8], where it was demonstrated explicitly that there are no pole contributions to $G(\varepsilon, \xi_p)$ in the approximation of large correlation lengths. At the same time, figures 4 and 5 show that at fairly large values of W (small correlation lengths) the spectral density is represented by a fairly sharp peak at $\varepsilon \propto \xi_p$ corresponding to weakly damped one-electron excitations. The physical meaning of this result is simple. In the limit of $\xi = \kappa^{-1} \rightarrow 0$ the random field correlator (1) becomes short-ranged but is not reduced to the common [3, 5] ‘white noise’ limit. Although in this case all momenta in the integral with respect to Q become important, the scattering amplitude

$$\langle \Delta_Q \Delta_{-Q} \rangle \propto \frac{\Delta^2}{\kappa} \quad (16)$$

so that the effective scattering rate

$$\begin{aligned} \frac{1}{\tau} &\propto 2\pi N_0(\varepsilon_F) \frac{\Delta^2}{\kappa} = \frac{\Delta^2}{v_F \kappa} \\ &= \frac{\Delta}{W} \rightarrow 0 \quad \text{as} \quad \kappa \rightarrow \infty \end{aligned} \quad (17)$$

with $N_0(\varepsilon) = 1/2\pi v_F$ the one-electron density of states of free electrons. Correspondingly, in the limit of $\kappa \rightarrow \infty$ the freedom of the electrons becomes ever greater. This fact is important for the interpretation of the results that are given below. Similar behaviour (as figure 4 shows) appears as ξ_p grows, that is, as one moves away from the Fermi surface.

3. The two-particle Green function and the electromagnetic response

Let us now analyse the two-particle Green function (the vertex part), which determines the frequency dependence of conductivity and the dielectric constant of the system.

We begin by studying the response to a variation of the external scalar potential, $\delta\varphi_{q,\omega}$:

$$\delta G(\varepsilon, \xi_p) = G(\varepsilon, \xi_p) J(\varepsilon, \xi_p; \varepsilon + \omega, \xi_{p+q}) G(\varepsilon + \omega, \xi_{p+q}) \delta\varphi_{q,\omega} \quad (18)$$

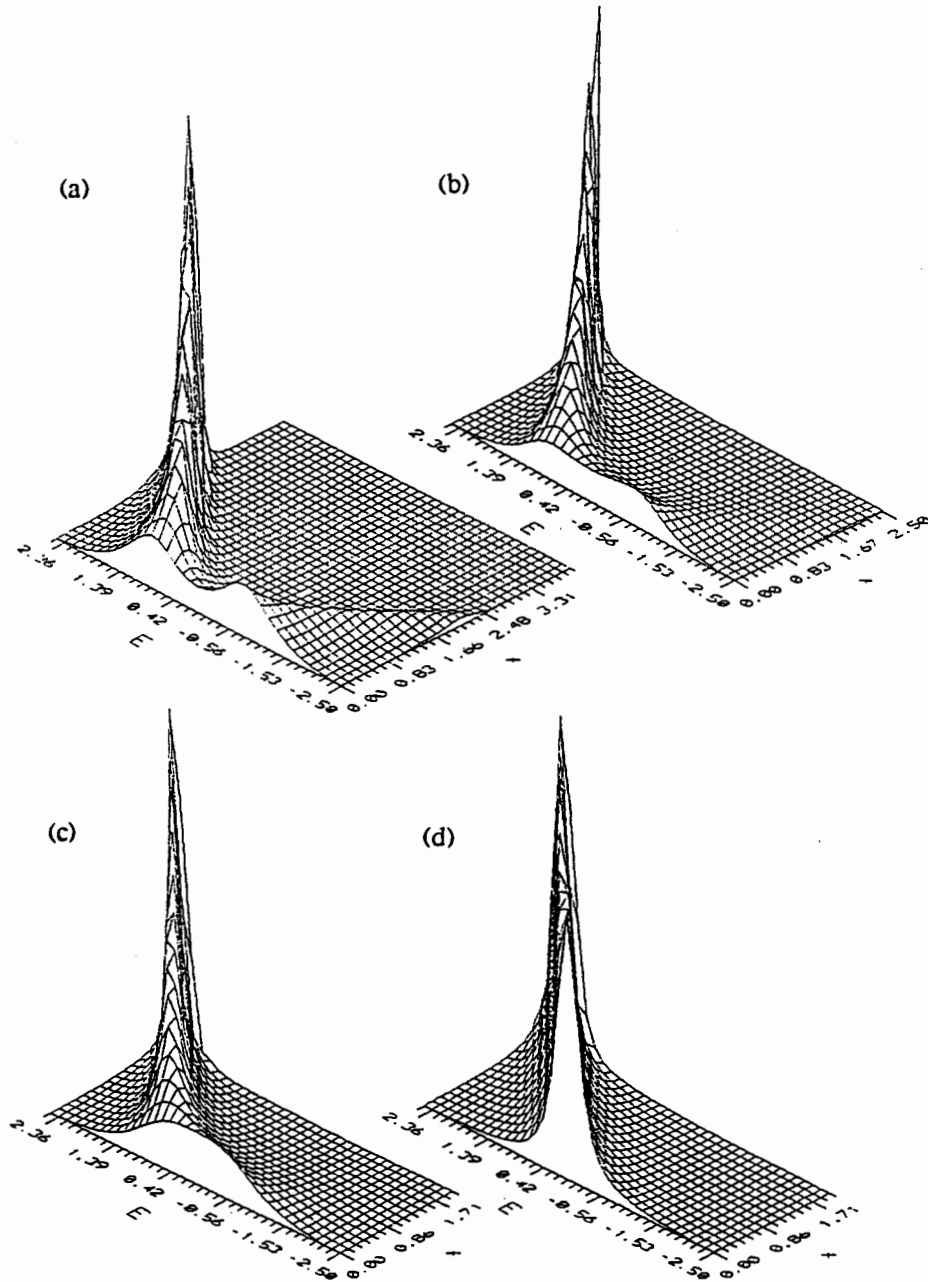


Figure 4. The surfaces of constant spectral density $A(E, x)$: $E = \epsilon/\Delta$, $x = \xi_p/\Delta$, and $W = v_F\kappa/\Delta$. (a) $W = 0.1$, (b) $W = 0.5$, (c) $W = 1.0$, and (d) $W = 5.0$.

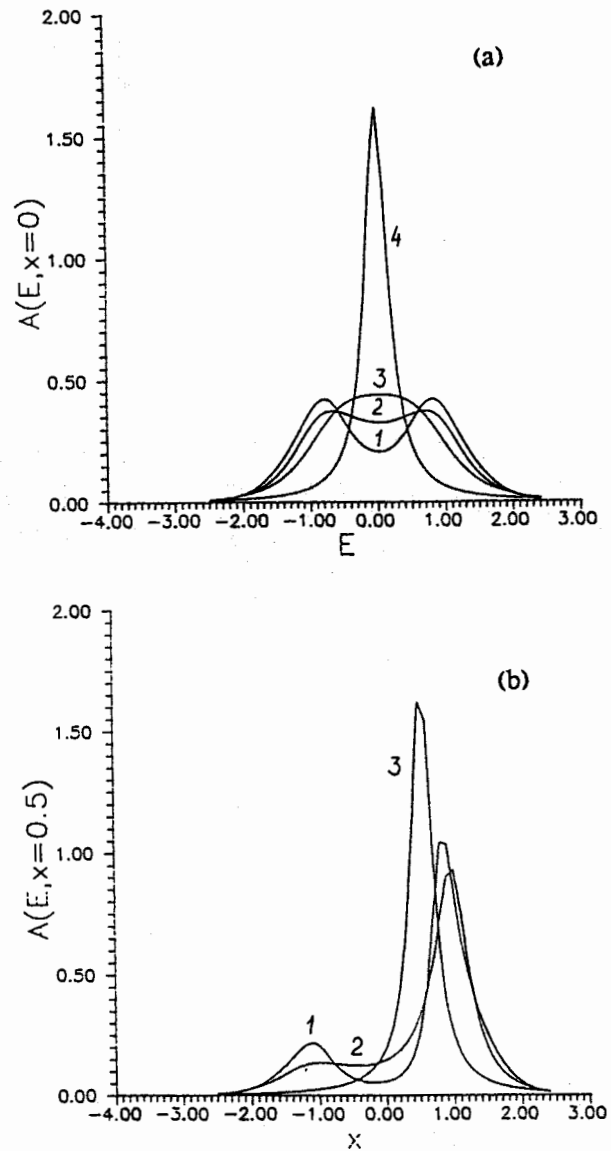


Figure 5. Characteristic cross sections of the surfaces of constant spectral density $A(E, x)$: (a) $x = 0$ at $W = 0.1$ (1), $W = 0.5$ (2), $W = 1.0$ (3), and $W = 5.0$ (4); (b) $x = 0.5$ at $W = 0.1$ (1), $W = 0.5$ (2), and $W = 5.0$ (3).

where the vertex part

$$J(\varepsilon, \xi_p; \varepsilon + \omega, \xi_{p+q}) = -\frac{\delta G^{-1}(\varepsilon, \xi_p)}{\delta \varphi_{q, \omega}} \quad (19)$$

for free particles (the free-particle Green function) is determined solely by the charge e .

Equation (6) yields

$$\begin{aligned} J(\varepsilon, \xi_p; \varepsilon + \omega, \xi_{p+q}) &= e + \frac{\delta \Sigma_1(\varepsilon, \xi_p)}{\delta \varphi_{q,\omega}} \\ &\equiv e + \mathcal{J}_1(\varepsilon, \xi_p; \varepsilon + \omega, \xi_{p+q}). \end{aligned} \quad (20)$$

The problem reduces to calculating the variational derivatives of diagrams of the type depicted in figure 3; the graphs with crossed lines may be ignored because they are taken into account by the respective combinatorial factors at the 'initial' vertexes.

Combining (13) and (14), we introduce the following hierarchy of vertex parts:

$$\begin{aligned} J_1(\varepsilon, \xi_p; \varepsilon + \omega, \xi_{p+q}) &= -\frac{\delta G_1^{-1}(\varepsilon, \xi_p)}{\delta \varphi_{q,\omega}} \\ &= e + \frac{\delta \Sigma_2(\varepsilon, \xi_p)}{\delta \varphi_{q,\omega}} \\ &\equiv e + \mathcal{J}_2(\varepsilon, \xi_p; \varepsilon + \omega, \xi_{p+q}) \\ J_{k-1}(\varepsilon, \xi_p; \varepsilon + \omega, \xi_{p+q}) &= -\frac{\delta G_{k-1}^{-1}(\varepsilon, \xi_p)}{\delta \varphi_{q,\omega}} \\ &= e + \frac{\delta \Sigma_k(\varepsilon, \xi_p)}{\delta \varphi_{q,\omega}} \\ &\equiv e + \mathcal{J}_k(\varepsilon, \xi_p; \varepsilon + \omega, \xi_{p+q}) \dots \end{aligned} \quad (21)$$

with $J_{k=0} \equiv J(\varepsilon, \xi_p; \varepsilon + \omega, \xi_{p+q})$. An important assumption is present here, namely, that the variational derivatives of the free-particle Green functions (with contributions $iv_F \kappa$ in the denominators) are still determined by the 'bare' charge e .

In what follows we will be mainly interested in the vertex of the RA type, with the incoming line of the A (advanced) type and the outgoing of the R (retarded) type. We can try to calculate the corresponding contributions to the variational derivatives $\delta \Sigma_k(\varepsilon, \xi_p)/\delta \varphi_{q,\omega}$ explicitly. Let us consider the simplest diagram for the first-order correction in Δ^2 to the vertex part (figure 6(a)). For the corresponding contribution we easily find that

$$\begin{aligned} \mathcal{J}_1^{(1)RA}(\varepsilon, \xi_p; \varepsilon + \omega, \xi_{p+q}) &= \Delta^2 \int \frac{dQ}{2\pi} S(Q) G_0^A(\varepsilon, \xi_{p-Q}) G_0^R(\varepsilon + \omega, \xi_{p-Q+q}) \\ &= \Delta^2 [G_0^A(\varepsilon, -\xi_p + iv_F \kappa) - G_0^R(\varepsilon + \omega, -\xi_{p+q} - iv_F \kappa)] \frac{1}{\omega + v_F q} \\ &= \Delta^2 G_0^A(\varepsilon, -\xi_p + iv_F \kappa) G_0^R(\varepsilon + \omega, -\xi_{p+q} - iv_F \kappa) \left(1 + \frac{2iv_F \kappa}{\omega + v_F q} \right) \end{aligned} \quad (22)$$

where we have used the identity

$$G_0^A(\varepsilon, \xi_p) G_0^R(\varepsilon + \omega, \xi_{p+q}) \equiv [G_0^A(\varepsilon, \xi_p) - G_0^R(\varepsilon + \omega, \xi_{p+q})] \frac{1}{\omega - v_F q}.$$

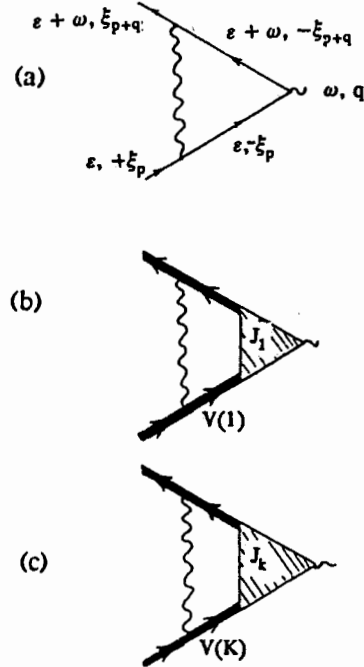


Figure 6. The simplest diagrams for the vertex part.

'Dressing' all the internal electron lines and employing the identity

$$G^A(\epsilon, \xi_p) G^R(\epsilon + \omega, \xi_{p+q}) \equiv [G^A(\epsilon, \xi_p) - G^R(\epsilon + \omega, \xi_{p+q})] \times \frac{1}{\omega - v_F q - \Sigma_1^R(\epsilon + \omega, \xi_{p+q}) + \Sigma_1^A(\epsilon, \xi_p)} \quad (23)$$

we obtain the contribution of the diagram in figure 6(b) in the following form:

$$\begin{aligned} \mathcal{J}_1^{RA}(\epsilon, \xi_p; \epsilon + \omega, \xi_{p+q}) &= \Delta^2 G_1^A(\epsilon, \xi_p) G_1^R(\epsilon + \omega, \xi_{p+q}) \\ &\times \left(1 + \frac{2iv_F \kappa}{\omega + v_F q - \Sigma_2^R(\epsilon + \omega, \xi_{p+q}) + \Sigma_2^A(\epsilon, \xi_p)} \right) \\ &\times J_1^{RA}(\epsilon, \xi_p; \epsilon + \omega, \xi_{p+q}) \end{aligned} \quad (24)$$

where we have assumed that an extra interaction line simply transforms the respective self-energy parts $\Sigma_1^{R,A}$ into $\Sigma_2^{R,A}$ in the spirit of the procedure discussed in section 2. A straightforward generalization for the contribution of the diagram depicted in

figure 6(c), with the lines dressed according to the rules suggested above, has the form

$$\begin{aligned}
 J_k^{RA}(\epsilon, \xi_p; \epsilon + \omega, \xi_{p+q}) &= \Delta^2 v(k) G_k^A(\epsilon, \xi_p) G_k^R(\epsilon + \omega, \xi_{p+q}) \\
 &\times \left\{ 1 + \frac{2iv_F \kappa k}{\omega - (-1)^k v_F q - \Sigma_{k+1}^R(\epsilon + \omega, \xi_{p+q}) + \Sigma_{k+1}^A(\epsilon, \xi_p)} \right\} \\
 &\times J_k^{RA}(\epsilon, \xi_p; \epsilon + \omega, \xi_{p+q}). \quad (25)
 \end{aligned}$$

The main feature here is the absence of terms of the $iv_F \kappa$ type in the denominator in the second term within the braces, which in the summation procedure discussed in section 1 were "shifted" from the proper self-energy parts to the corresponding free-particle Green functions.

In addition to the above assumptions concerning the properties of variational derivatives of the free-particle Green functions, this procedure forms the basis of the suggested method. This procedure does indeed take into account all the Feynman diagrams emerging in the problem, but it is based on important assumptions concerning the structure of separate terms in the series. Below we suggest additional arguments in favour of the validity of these assumptions.

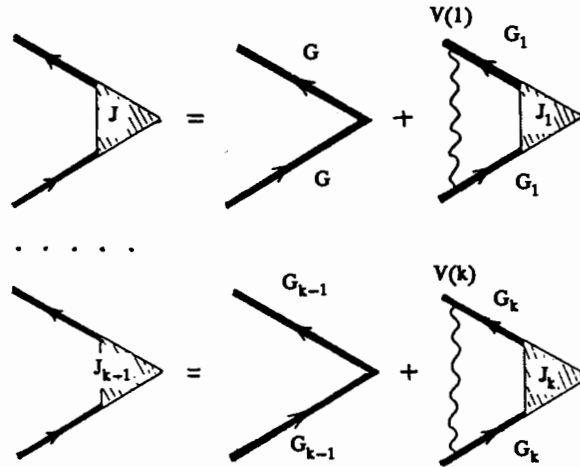


Figure 7. Diagrammatic representation of the equations for the vertex hierarchy.

As a result we arrive at the following fundamental recurrence relations for the vertex part:

$$\begin{aligned}
 J_{k-1}^{RA}(\epsilon, \xi_p; \epsilon + \omega, \xi_{p+q}) &= e + \Delta^2 v(k) G_k^A(\epsilon, \xi_p) G_k^R(\epsilon + \omega, \xi_{p+q}) J_k^{RA}(\epsilon, \xi_p; \epsilon + \omega, \xi_{p+q}) \\
 &\times \left\{ 1 + \frac{2iv_F \kappa k}{\omega - (-1)^k v_F q + v(k+1) \Delta^2 [G_{k+1}^A(\epsilon, \xi_p) - G_{k+1}^R(\epsilon + \omega, \xi_{p+q})]} \right\}. \quad (26)
 \end{aligned}$$

Diagrammatically these relations are depicted in figure 7

Further analysis can easily be done numerically: we truncate the continuous fraction for the G -function at a distant 'storey' assuming that the corresponding Σ_k is zero and that $J_k = \epsilon$ and then 'raise' to the physical limit of $k = 0$. One can easily verify that on the limit of $\kappa \rightarrow 0$ the suggested procedure leads to the series that was summed analytically in [7, 8].

To find the frequency dependence of the conductivity we can use the general relations discussed in [18, 19]. The conductivity is expressed in terms of the density-density retarded response function (the polarization operator) $\chi^R(q, \omega)$ as follows:

$$\sigma(\omega) = e^2 \lim_{q \rightarrow 0} \left(-\frac{i\omega}{q^2} \right) \chi^R(q, \omega). \quad (27)$$

The dielectric constant can also be easily found:

$$\text{Re } \epsilon(\omega) - 1 = -\frac{4\pi}{\omega} \text{Im } \sigma(\omega) \quad \text{Im } \epsilon(\omega) = \frac{4\pi}{\omega} \text{Re } \sigma(\omega).$$

The general expression for $\chi^R(q, \omega)$ has the following form [18, 19]:

$$\begin{aligned} \chi^R(q, \omega) = & \int d\epsilon \{ [f(\epsilon + \omega) - f(\epsilon)] \Phi^{\text{RA}}(\epsilon, q, \omega) \} \\ & + \int d\epsilon [f(\epsilon) \Phi^{\text{RR}}(\epsilon, q, \omega) - f(\epsilon + \omega) \Phi^{\text{AA}}(\epsilon, q, \omega)] \end{aligned} \quad (28)$$

where $f(\epsilon)$ is the Fermi distribution function, and the two-particle Green functions Φ^{RA} , Φ^{RR} , and Φ^{AA} are represented by loop diagrams of the type depicted in figure 8.

$$\Phi^{\text{RA}}(\epsilon, q, \omega) = \frac{1}{2\pi i} \sum_p \text{Diagram}$$

Figure 8. Diagrammatic representation of $\Phi^{\text{RA}}(\epsilon, q, \omega)$.

For $T = 0$ and $\omega \ll \epsilon_F$ we have [19]

$$\chi^R(q, \omega) = \omega [\Phi^{\text{RA}}(0, q, \omega) - \Phi^{\text{RA}}(0, 0, \omega)]. \quad (29)$$

We note the existence of an important relation of the Ward identity type [18, 19] that reflects the law of conservation of the number of particles (and is valid for $\omega \ll \epsilon_F$):

$$\Phi^{\text{RA}}(0, 0, \omega) = -\frac{N(\epsilon_F)}{\omega} \quad (30)$$

with $N(\epsilon_F)$ the exact (renormalized) density of states at the Fermi level. This equation was employed in deriving (29) and can be used to directly monitor the suggested recurrence procedure of calculating the two-particle Green function.

4. Results and discussion

As noted in [9], the recurrence procedure for finding the one-particle Green function (the density of states) converges very rapidly; a typical calculation time for the density of states at a given energy (with a high accuracy) amounts to less than one minute when a standard IBM PC/AT is used (if one starts from the 'storey' with $k = 50-100$). The situation is more complicated when conductivity and the dielectric constant are calculated and the procedure is more sensitive to the choice of parameters of interest to us. In the main section of the frequency interval, $0.5\Delta < \omega < 3\Delta$, and for intermediate values of $\xi = \kappa^{-1}$ ($0.2\Delta < v_F \kappa < 2\Delta$), satisfactory convergence is achieved for $k < (2-5) \times 10^2$ and the calculation time for conductivity at a fixed frequency amounts to several minutes. Outside the specified intervals the convergence grows markedly worse and becomes especially poor in the limit of very low frequencies and in the case of extremely large correlation lengths (note that in the latter case the exact analytical solution can be used [7, 8]).

The reliability of the suggested recurrence procedure can be verified by directly checking the validity of the exact formula (30). In doing so, one finds that calculating $N(\epsilon_F)$ in terms of the two-particle Green function $\Phi^{RA}(0, \omega)$ yields (at least for $\omega \ll \Delta$) a result agreeing perfectly with that of $N(\epsilon_F)$ calculated in terms of the one-electron Green function for various values of parameter κ . This can, apparently, serve as a strong indication that the employed method is correct, which makes it possible to speak of an 'exact' solution.

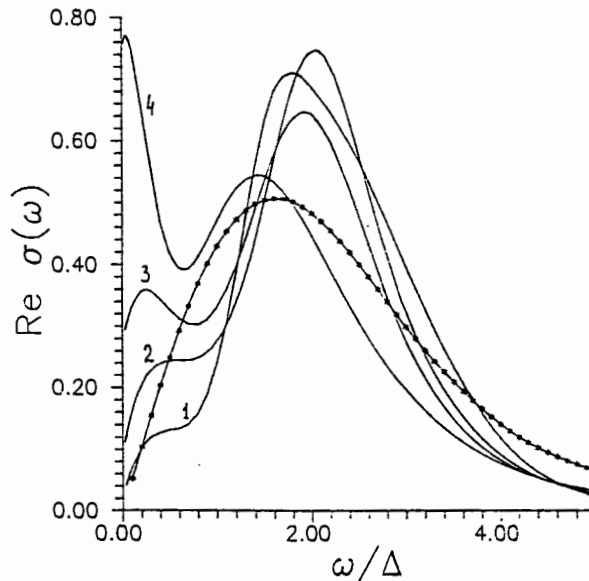


Figure 9. The frequency dependence of the real part of conductivity in the case of incommensurate fluctuations: $W = 0.1$ (1), $W = 0.5$ (2), $W = 1.0$ (3), and $W = 2.0$ (4); the * stand for the exact solution at $W = 0$ [7, 8].

In figure 9 we give the results of calculating the frequency dependence of

conductivity for the case of incommensurate short-range order fluctuations. The conductivity is given everywhere in units of $\omega_p^2/4\pi\Delta$ (there is an error in [15] concerning this scale—the presence of an extra factor of 2 in the denominator), with ω_p the plasma frequency, and the correlation length is determined by parameter $W = v_F\kappa/\Delta$. For the sake of comparison we also give the results of an exact analytical solution in the limit of $W \rightarrow 0$ [7, 8]. One can clearly see the successive degradation of the intensity of absorption through the pseudogap as ξ decreases (or W grows). For small W (or large ξ), the localized behaviour of $\text{Re}\sigma(\omega)$ in the low-frequency region, $\text{Re}\sigma(\omega \rightarrow 0) \rightarrow 0$, manifests itself in a way that is qualitatively similar to the behaviour discovered in another model [5]. There appears a characteristic additional maximum in the conductivity similar to the maximum obtained in the problem of conductivity in a system of δ -correlated impurities ('white noise') [5]. As W grows, the apparent localized behaviour disappears, changing to the Drude-like behaviour characteristic of free electrons. Thus, our model demonstrates an 'effective' Anderson transition, notwithstanding its one-dimensional nature.

Though this may seem to be paradoxical behaviour, it has a simple qualitative explanation based on the decrease of the effective scattering amplitude in the limit of large κ , a property discussed in section 2. Naturally, the frequency region where localization effects manifest themselves is drastically narrowed in the process and for all practical purposes disappears as the electrons' freedom increases. It is in this sense that we can speak of an effective Anderson transition.

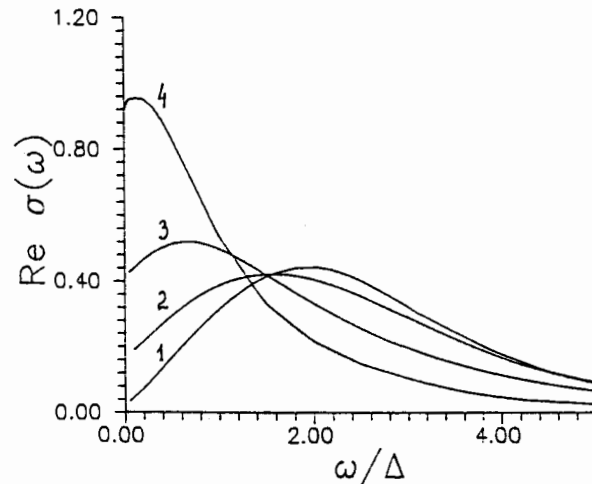


Figure 10. The frequency dependence of the real part of conductivity in the case of commensurate fluctuations: $W = 0.5$ (1), $W = 2.0$ (2), $W = 4.0$ (3), and $W = 8.0$ (4).

Figure 10 demonstrates the results of calculating $\text{Re}\sigma(\omega)$ for the case of commensurate short-range order fluctuations. Qualitatively, the picture noticeably differs from the incommensurate case: there is no additional maximum in the low-frequency region for small W . At the same time, the effective Anderson transition from the localized behaviour to the Drude-like becomes even more evident.

The suggested method can also be used to establish the frequency behaviour of the dielectric constant $\text{Re}\epsilon(\omega)$. The corresponding results are given in [15].

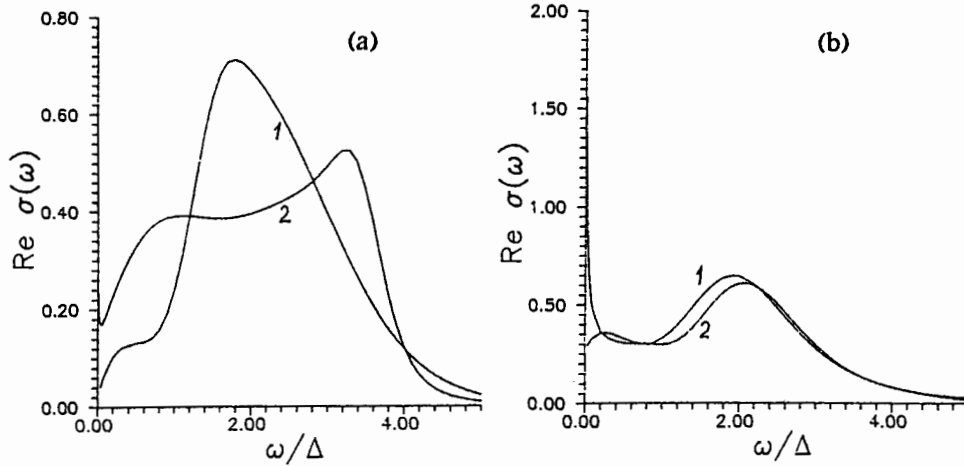


Figure 11. Comparison of the results of an 'exact' analysis with those obtained in the 'ladder' approximation: (a) $W = 0.1$ (1) the 'exact' solution and (2) the 'ladder' approximation; (b) $W = 1.0$ (1) the 'exact' solution and (2) the 'ladder' approximation.

It is interesting to compare the results of an 'exact' analysis with those of calculations carried out in the standard 'ladder' approximation, that is, an approximation that does not allow for diagrams with crossed interaction lines. In our method the transition to the 'ladder' approximation is very simple: one needs only to set all combinatorial factors $v(k)$ equal to unity (in both the incommensurate and the commensurate case). Figure 11 depicts the most characteristic curves for $\text{Re}\sigma$ plotted against ω for the incommensurate case. The reader can clearly see that for small W (figure 11(a)) the 'ladder' approximation gives a behaviour that drastically differs from 'exact'. Localized behaviour is distinctly absent from the low-frequency region, which is natural since localization is determined by diagrams with crossed interaction lines [18]. At the same time, for fairly large W (figure 11(b)) in the main frequency region the 'ladder' approximation yields results that are close to 'exact'. However, for low frequencies here, too, distinct discrepancies emerge: all tendency to localization vanishes. The same behaviour is observed in the commensurate case.

Note that the suggested method can also be easily used to analyse the one-dimensional model with a Gaussian random field correlator in the form of a simple Lorentzian centred at zero momentum transfer, $Q \approx 0$. Naturally, this model generates a density of states with a characteristic 'tail' at the band's edge. However, calculating the two-particle Green function yields trivial free behaviour in this model. For instance, it can easily be verified that $\text{Re}\epsilon(\omega) = 1 - \omega_p^2/\omega^2$. This result is an obvious corollary of the absence (in the one-dimensional case) of dissipation in scattering with low momentum transfer, $Q \ll 2p_F$. The electrons simply re-scatter near $\pm p_F$, the endpoints of the 'Fermi line'. Current dissipation requires scattering by $Q \sim 2p_F$,

which makes the electrons hop from one endpoint of the Fermi line to the other.

5. Conclusion

We have proposed an effective recurrence procedure for calculating the two-particle Green function in a one-dimensional model with a Gaussian random field of a special type that can describe short-range order fluctuations in systems of the Peierls type [8, 9] and, possibly, in high- T_c systems [15]. The procedure allows for all the Feynman diagrams that appear in the given problem and in this sense is 'exact', although it is based on certain assumptions concerning the structure of the terms in the perturbation series. The reliability of these assumptions is verified by the meaningfulness of the limiting cases of $\kappa \rightarrow 0$ and $\kappa \rightarrow \infty$ and by the fact that the exact 'Ward' identity holds for all values of κ .

The general pattern of the evolution of the frequency dependence of conductivity for various values of the short-range order correlation length describes absorption through a pseudogap and localized behaviour in the region of low ω and W . As W grows (or the correlation length decreases) an 'effective' Anderson transition occurs in the system, and this would seem to explain the drop in the scattering amplitude and the gradual transition to 'free' particles as W grows. From the practical viewpoint the frequency range where localization manifests itself narrows drastically and disappears. Such behaviour may lead to interesting consequences in real quasi-one-dimensional systems.

References

- [1] Halperin B I 1968 *Adv. Chem. Phys.* **13** 123
- [2] Erdős P and Herndon R C 1978 *Adv. Phys.* **31** 65
- [3] Berezinskii V L 1974 *Sov. Phys.-JETP* **38** 620
- [4] Abrikosov A A and Ryzhkin I A 1978 *Adv. Phys.* **27** 147
- [5] Gogolin A A 1982 *Phys. Rep.* **86** 1
Gogolin A A 1988 *Phys. Rep.* **166** 269
- [6] Abrikosov A A, Gor'kov L P and Dzyaloshinskii I E 1963 *Methods of Quantum Field Theory in Statistical Physics* (New York: Prentice-Hall)
- [7] Sadovskii M V 1974 *Sov. Phys.-JETP* **39** 845
- [8] Sadovskii M V 1975 *Sov. Phys. Solid State* **16** 1632
- [9] Sadovskii M V 1979 *Sov. Phys.-JETP* **50** 989
- [10] Wonneberger W and Lautenschlager R 1976 *J. Phys. C: Solid State Phys.* **9** 2865
- [11] Wonneberger W 1977 *J. Phys. C: Solid State Phys.* **10** 1073
- [12] Munz K M and Wonneberger W 1990 *Z. Phys.* **79** 15
- [13] Kampf A and Schrieffer J R 1990 *Phys. Rev. B* **41** 6399
- [14] Kampf A and Schrieffer J R 1990 *Phys. Rev. B* **42** 7967
- [15] Sadovskii M V and Timofeev A A 1991 *Superconductivity: Physics, Chemistry, Technology* **4** 11
- [16] Lee P A, Rice T M and Anderson P W 1973 *Phys. Rev. Lett.* **31** 462
- [17] Elyutin P V 1977 *Opt. Spectrosc. (USSR)* **43** 318
- [18] Maleev S V and Toperverg B P 1975 *Sov. Phys.-JETP* **42** 734
- [19] Vollhardt D and Wolfe P 1980 *Phys. Rev. B* **22** 4666

Self-consistent localization theory in the two-band model

M A Érkabaev and M V Sadovskii

Institute of Electrophysics, Ural Branch of the Russian Academy of Sciences,
Komsomol'skaya ul. 34a, 620219 Ekaterinburg, Russia

Received 30 June 1992

Abstract. This paper deals with calculations within the self-consistent localization theory of the conductivity, critical disorder, and the localization radius for the two-band model with Gaussian disorder. It demonstrates that at the Fermi level the localized states corresponding to the narrow band cannot coexist with the delocalized states in the wide band. Hybridization of the states of the narrow and wide bands leads to the delocalization of the system. The critical disorder corresponding to localization exceeds the values characteristic of an unhybridized wide band. Within a certain range of parameters of the system the behaviour of the conductivity may be nonmonotonic; for instance, it can increase with disorder owing to the evolution of the hybridization pseudogap in the density of states.

We study the Anderson localization of electrons in the two-band model with hybridization. Such a statement of the problem is of interest both from the viewpoint of possible applications to real disordered systems, such as alloys and compounds of transition metals and systems with heavy fermions, and for solving some questions of principal importance. Of greatest interest here, obviously, is the case of a relatively narrow (d) band that is near the Fermi level and inside a broad (s) band. This situation is not at all exotic from the experimenter's viewpoint, while from the theoretician's viewpoint it is interesting because for unhybridized bands the critical disorder corresponding to the localization of electronic states varies considerably—it is easier to localize a narrow band [1]. At times, especially when discussing experiments, some researchers assume that at the Fermi level the localized states, corresponding to the narrow band, 'coexist' with the delocalized states. The fact that this is impossible in principle has generally been known for a long time: hybridization with states of the broad band is certain to transform the localized states of the narrow band into delocalized states [2, 3].

At the same time the question of localization and the specific properties of localization in the two-band model have not, to our knowledge, received special attention. Below we consider this problem within the framework of the self-consistent localization theory [5–8], which makes it possible to carry out all calculations to the final result. We show that localization in the two-band model does indeed possess a number of features that can manifest themselves in experiments. For one thing, no 'coexistence' of localized and delocalized states is possible in the above sense, and the Anderson transition may occur only when a value of critical disorder exceeding that corresponding to localization of the electronic states of the unhybridized broad band is reached.

Our approach is based on the generalized Anderson model [1] with diagonal disorder, whose Hamiltonian in the momentum representation has the following form:

$$H = \sum_{\mathbf{k}, \mathbf{q}} h_{\mathbf{k}+\mathbf{q}, \mathbf{k}}^{\mu\nu} a_{\mathbf{k}+\mathbf{q}}^{\dagger\mu} a_{\mathbf{k}}^{\nu} \quad h_{\mathbf{k}+\mathbf{q}, \mathbf{k}}^{\mu\nu} = [\varepsilon_{\mathbf{k}}^{\mu} \delta^{\mu\nu} + \gamma(1 - \delta^{\mu\nu})] \delta_{\mathbf{q}, 0} + V_{\mathbf{q}}^{\mu} \delta^{\mu\nu} \quad (1)$$

with μ and ν the band indices. Here and in what follows we assume (if the opposite is not obvious) the summation convention over repeated indices valid, $a_{\mathbf{k}}^{\dagger\mu}$ and $a_{\mathbf{k}}^{\mu}$ are operators of creation and annihilation of a ' μ '-electron with momentum \mathbf{k} , $\varepsilon_{\mathbf{k}}^{\mu}$ is the spectrum of the ' μ '-electron in the tight binding approximation, and γ is the hybridization constant. The scattering potentials $V_{\mathbf{q}}^{\mu}$ are assumed distributed according to the Gaussian delta-correlated law

$$\langle V_{\mathbf{q}}^{\mu} V_{\mathbf{q}'}^{\nu} \rangle = \delta^{\mu\nu} \delta_{\mathbf{q}, -\mathbf{q}'} W^2 \quad (2)$$

with W the width of the disorder. Here we have ignored the off-diagonal correlations in the scattering potential, which simplifies calculations considerably.

We define the one-particle Green function averaged over the realizations of the random potential,

$$\mathcal{G}_{\mathbf{k}}^{\mu\alpha}(\mathcal{E}^{\pm}) \delta_{\mathbf{k}, \mathbf{k}'} = \langle G^{\mu\alpha}(\mathbf{k}, \mathbf{k}', \mathcal{E}^{\pm}) \rangle \quad (3)$$

with $\mathcal{E}^{\pm} = \mathcal{E} \pm i\delta$, as the solution of the equation

$$[(\mathcal{E}^{\pm} - \varepsilon_{\mathbf{k}}^{\mu}) \delta^{\mu\sigma} - \gamma(1 - \delta^{\mu\sigma}) - \Sigma_{\mathbf{k}}^{\mu\sigma}(\mathcal{E}^{\pm})] \mathcal{G}_{\mathbf{k}}^{\sigma\alpha}(\mathcal{E}^{\pm}) = \delta^{\mu\alpha} \quad (4)$$

where we have introduced $\Sigma_{\mathbf{k}}^{\mu\alpha}(\mathcal{E}^{\pm})$, the self-energy part. The contributions of the s- and d-states to the density of states of the system, $\rho(\mathcal{E}) = \rho^s(\mathcal{E}) + \rho^d(\mathcal{E})$, have the following form:

$$\rho^{s(d)}(\mathcal{E}) = -\frac{1}{\pi} \text{Im} \sum_{\mathbf{k}} \mathcal{G}_{\mathbf{k}}^{ss(dd)}(\mathcal{E}^+). \quad (5)$$

The dynamical conductivity of the system is [4, 8]

$$\sigma_{\mathcal{E}_F}(\omega) = \frac{2e^2}{\hbar\Omega^0} \lim_{q \rightarrow 0} \left(-\frac{i\omega}{q^2} \right) \chi_{\rho\rho}^{\mathcal{E}_F}(q; \omega)$$

where $\chi_{\rho\rho}^{\mathcal{E}_F}(q; \omega)$ is the density response function, and Ω^0 is the volume per lattice site.

For q and ω small we have

$$\chi_{\rho\rho}^{\mathcal{E}_F}(q; \omega) \simeq \omega \Phi_{\rho\rho}(q; \mathcal{E}_F^+ + \omega, \mathcal{E}_F^-) + \rho(\mathcal{E}_F) + O(\omega, q^2) \quad (6)$$

where

$$\begin{aligned} \Phi_{\rho\rho}(q; \mathcal{E}_F^+ + \omega, \mathcal{E}_F^-) &= \delta^{\mu\nu} \delta^{\alpha\beta} \sum_{\mathbf{k}, \mathbf{k}'} \Psi_{\mathbf{k}\mathbf{k}'}^{\mu\nu\alpha\beta}(q; \mathcal{E}_F^+ + \omega, \mathcal{E}_F^-) \\ \Psi_{\mathbf{k}\mathbf{k}'}^{\mu\nu\alpha\beta}(q; \mathcal{E}_F^+ + \omega, \mathcal{E}_F^-) &= -\frac{1}{2\pi i} \langle G^{\mu\alpha}(\mathbf{k}+, \mathbf{k}'+; \mathcal{E}_F^+ + \omega) G^{\nu\beta}(\mathbf{k}'-, \mathbf{k}-; \mathcal{E}_F^-) \rangle \end{aligned} \quad (7)$$

is the two-particle Green function averaged over the realizations of the random potential and satisfies the Bethe-Salpeter equation

$$\begin{aligned} \Psi_{\mathbf{k}\mathbf{k}'}^{\mu\nu\alpha\beta}(q; \mathcal{E}_F^+ + \omega, \mathcal{E}_F^-) &= \mathcal{G}_{\mathbf{k}^+}^{\mu\sigma}(\mathcal{E}_F^+ + \omega) \mathcal{G}_{\mathbf{k}^-}^{\nu\delta}(\mathcal{E}_F^-) \left[-\frac{1}{2\pi i} \delta_{\mathbf{k}\mathbf{k}'} \delta^{\sigma\alpha} \delta^{\delta\beta} \right. \\ &\quad \left. + \sum_{\mathbf{k}''} U_{\mathbf{k}\mathbf{k}''}^{\sigma\delta\eta\lambda}(q; \mathcal{E}_F^+ + \omega, \mathcal{E}_F^-) \Psi_{\mathbf{k}''\mathbf{k}'}^{\eta\lambda\alpha\beta}(q; \mathcal{E}_F^+ + \omega, \mathcal{E}_F^-) \right] \end{aligned} \quad (8)$$

with $U_{\mathbf{k}\mathbf{k}'}^{\mu\nu\alpha\beta}(q; \mathcal{E}_F^+ + \omega, \mathcal{E}_F^-)$ the irreducible vertex part. Here $\mathbf{k}\pm = \mathbf{k} \pm \mathbf{q}/2$.

In the self-consistent Born approximation with q and ω small

$$\begin{aligned} \Sigma_{\mathbf{k}}^{\mu\alpha}(\mathcal{E}_F^{\pm}) &\simeq \mp i \Delta_{\mathcal{E}_F}^{\mu} \delta^{\mu\alpha} & \Delta_{\mathcal{E}_F}^{s(d)} &= \pi \rho^{s(d)}(\mathcal{E}_F) W^2 \\ U_{\mathbf{k}\mathbf{k}'}^{\mu\nu\alpha\beta} \alpha\beta(q; \mathcal{E}_F^+ + \omega, \mathcal{E}_F^-) &\simeq \delta^{\mu\nu} \delta^{\mu\alpha} \delta^{\nu\beta} U_{\mathcal{E}_F}^{\nu} & U_{\mathcal{E}_F}^{s(d)} &= \frac{\Delta_{\mathcal{E}_F}^{s(d)}}{\pi \rho^{s(d)}(\mathcal{E}_F)} \\ \Phi_{\rho\rho}(q; \mathcal{E}_F^+ + \omega, \mathcal{E}_F^-) &\simeq \rho(\mathcal{E}_F) \frac{i}{-i\omega + D_{\mathcal{E}_F} q^2} \end{aligned} \quad (9)$$

with $D_{\mathcal{E}_F}$ the Born diffusion coefficient of the system,

$$\begin{aligned} \rho(\mathcal{E}_F) D_{\mathcal{E}_F} &= \rho^s(\mathcal{E}_F) D_{\mathcal{E}_F}^s + \rho^d(\mathcal{E}_F) D_{\mathcal{E}_F}^d \\ D_{\mathcal{E}_F}^s &= \frac{1}{d\pi\rho^s(\mathcal{E}_F)} \sum_{\mathbf{k}} \{ [\text{Im} \mathcal{G}^{ss}(\mathcal{E}_F^+)] (\nabla_{\mathbf{k}} \varepsilon_{\mathbf{k}}^s)^2 + [\text{Im} \mathcal{G}^{sd}(\mathcal{E}_F^+)]^2 (\nabla_{\mathbf{k}} \varepsilon_{\mathbf{k}}^s \nabla_{\mathbf{k}} \varepsilon_{\mathbf{k}}^d) \}. \end{aligned} \quad (10)$$

Here d is the dimensionality of the space, and $D_{\mathcal{E}_F}^d$ is obtained from $D_{\mathcal{E}_F}^s$ by interchanging the band indices s and d .

Combining the calculation of the two-particle Green function with the self-consistent approach to localization theory in the spirit of [5–10] yields

$$\Phi_{\rho\rho}(q; \mathcal{E}_F^+ + \omega, \mathcal{E}_F^-) \simeq \rho(\mathcal{E}_F) \frac{i}{-i\omega + D_{\mathcal{E}_F}(\omega) q^2} \quad (11)$$

where we have introduced $D_{\mathcal{E}_F}(\omega)$, the generalized diffusion coefficient of the system, which can be found by solving the following self-consistent system of equations:

$$\rho(\mathcal{E}_F) D_{\mathcal{E}_F}(\omega) = \rho^s(\mathcal{E}_F) D_{\mathcal{E}_F}^s(\omega) + \rho^d(\mathcal{E}_F) D_{\mathcal{E}_F}^d(\omega) \quad (12)$$

$$\begin{aligned} \rho^s(\mathcal{E}_F) D_{\mathcal{E}_F}^s(\omega) &= \rho^s(\mathcal{E}_F) D_{\mathcal{E}_F}^s - \frac{\Theta_{\mathcal{E}_F}^{ss}}{\pi\rho(\mathcal{E}_F)} \sum_{\mathbf{q}} \frac{\rho^s(\mathcal{E}_F) D_{\mathcal{E}_F}^s(\omega)}{-i\omega + D_{\mathcal{E}_F}(\omega) q^2} \\ &\quad - \frac{\Theta_{\mathcal{E}_F}^{sd}}{\pi\rho(\mathcal{E}_F)} \sum_{\mathbf{q}} \frac{\rho^d(\mathcal{E}_F) D_{\mathcal{E}_F}^d(\omega)}{-i\omega + D_{\mathcal{E}_F}(\omega) q^2} \end{aligned} \quad (13)$$

$$\begin{aligned} \rho^d(\mathcal{E}_F) D_{\mathcal{E}_F}^d(\omega) &= \rho^d(\mathcal{E}_F) D_{\mathcal{E}_F}^d - \frac{\Theta_{\mathcal{E}_F}^{dd}}{\pi\rho(\mathcal{E}_F)} \sum_{\mathbf{q}} \frac{\rho^d(\mathcal{E}_F) D_{\mathcal{E}_F}^d(\omega)}{-i\omega + D_{\mathcal{E}_F}(\omega) q^2} \\ &\quad - \frac{\Theta_{\mathcal{E}_F}^{ds}}{\pi\rho(\mathcal{E}_F)} \sum_{\mathbf{q}} \frac{\rho^s(\mathcal{E}_F) D_{\mathcal{E}_F}^s(\omega)}{-i\omega + D_{\mathcal{E}_F}(\omega) q^2} \end{aligned}$$

where

$$\Theta_{\mathcal{E}_F}^{\text{ss}} = \frac{2\Delta_{\mathcal{E}_F}^{\text{s}}}{d\pi\rho^{\text{s}}(\mathcal{E}_F)D_{\mathcal{E}_F}^{\text{s}}} \sum_{\mathbf{k}} \{ \Delta_{\mathcal{E}_F}^{\text{s}} \mathcal{G}_{\mathbf{k}}^{\text{ss}}(\mathcal{E}_F^+) \mathcal{G}_{\mathbf{k}}^{\text{ss}}(\mathcal{E}_F^-) \} \\ \times \{ [\text{Im} \mathcal{G}_{\mathbf{k}}^{\text{ss}}(\mathcal{E}_F^+)]^2 (\nabla_{\mathbf{k}} \varepsilon_{\mathbf{k}}^{\text{s}})^2 + \text{Im} \mathcal{G}_{\mathbf{k}}^{\text{sd}}(\mathcal{E}_F^+)]^2 (\nabla_{\mathbf{k}} \varepsilon_{\mathbf{k}}^{\text{s}} \nabla_{\mathbf{k}} \varepsilon_{\mathbf{k}}^{\text{d}}) \} \quad (14)$$

$$\Theta_{\mathcal{E}_F}^{\text{sd}} = \frac{2\Delta_{\mathcal{E}_F}^{\text{d}}}{d\pi\rho^{\text{d}}(\mathcal{E}_F)D_{\mathcal{E}_F}^{\text{d}}} \sum_{\mathbf{k}} \{ \Delta_{\mathcal{E}_F}^{\text{d}} \mathcal{G}_{\mathbf{k}}^{\text{sd}}(\mathcal{E}_F^+) \mathcal{G}_{\mathbf{k}}^{\text{sd}}(\mathcal{E}_F^-) \} \\ \times \{ [\text{Im} \mathcal{G}_{\mathbf{k}}^{\text{dd}}(\mathcal{E}_F^+)]^2 (\nabla_{\mathbf{k}} \varepsilon_{\mathbf{k}}^{\text{d}})^2 + \text{Im} \mathcal{G}_{\mathbf{k}}^{\text{ds}}(\mathcal{E}_F^+)]^2 (\nabla_{\mathbf{k}} \varepsilon_{\mathbf{k}}^{\text{d}} \nabla_{\mathbf{k}} \varepsilon_{\mathbf{k}}^{\text{s}}) \}.$$

The coefficients $\Theta_{\mathcal{E}_F}^{\text{ds}}$ and $\Theta_{\mathcal{E}_F}^{\text{dd}}$ can be obtained from the corresponding relations by interchanging s and d.

Equation (11)–(14) formulate of the self-consistent localization theory for the two-band model with hybridization. If in the first equation in (13) we put $\rho^{\text{d}}(\mathcal{E}) \equiv 0$ and in the second $\rho^{\text{s}}(\mathcal{E}) \equiv 0$, the two transform, as $\gamma \rightarrow 0$, into the appropriate equations for the unhybridized s- and d-bands.

In the metallic region, equations (6) and (11)–(13) yield the following expression for the DC conductivity: $\sigma = \sigma_{\text{Born}} - \sigma_{\text{corr}}$, where $\sigma_{\text{Born}} = \sigma_{\text{B}}^{\text{s}} + \sigma_{\text{B}}^{\text{d}}$, and

$$\sigma_{\text{corr}} = \frac{1}{2} \left[(\sigma_{\text{B}}^{\text{s}} + \vartheta^{\text{ss}}) + (\sigma_{\text{B}}^{\text{d}} + \vartheta^{\text{dd}}) \right. \\ \left. - \{ [(\sigma_{\text{B}}^{\text{s}} - \vartheta^{\text{ss}}) + (\sigma_{\text{B}}^{\text{d}} - \vartheta^{\text{dd}})]^2 \right. \\ \left. + 4[\sigma_{\text{B}}^{\text{s}}(\vartheta^{\text{dd}} - \vartheta^{\text{ds}}) + \sigma_{\text{B}}^{\text{d}}(\vartheta^{\text{ss}} - \vartheta^{\text{sd}}) - (\vartheta^{\text{ss}}\vartheta^{\text{dd}} - \vartheta^{\text{ss}}\vartheta^{\text{dd}})] \}^{1/2} \right]. \quad (15)$$

Here

$$\sigma_{\text{B}}^{\text{s(d)}} = \frac{2e^2}{\hbar\Omega^0} \rho^{\text{s(d)}}(\mathcal{E}_F) D_{\mathcal{E}_F}^{\text{s(d)}} \quad \vartheta^{\mu\nu} = \frac{2e^2}{\pi\hbar\vartheta^0} I\Theta_{\mathcal{E}_F}^{\mu\nu} \\ I_{\mathcal{E}_F}(\omega) = \int_{|\mathbf{q}| < k_0} \frac{\delta^d \mathbf{q}}{(2\pi)^d} \frac{1}{-i\omega/D_{\mathcal{E}_F}(\omega) + q^2} \quad (16)$$

with k_0 the cut-off momentum. In the metallic region, as $\omega \rightarrow 0$, we have $-i\omega/D_{\mathcal{E}_F}(\omega) \rightarrow 0$ and

$$I \equiv I_{\mathcal{E}_F}(\omega)|_{\omega \rightarrow 0} \simeq \frac{\pi^{d/2} k_0^{d-2} \Gamma(d/2 - 1)}{(2\pi)^d \Gamma(d/2)} \quad \text{for } d > 2.$$

We define the critical disorder W_c corresponding to the localization of the electronic states of the system for \mathcal{E}_F fixed by the condition $\sigma_{\mathcal{E}_F}[W_c] = 0$, which yields

$$\frac{\sigma_{\text{B}}^{\text{s}}(\vartheta^{\text{dd}} - \vartheta^{\text{ds}}) + \sigma_{\text{B}}^{\text{d}}(\vartheta^{\text{ss}} - \vartheta^{\text{sd}})}{\vartheta^{\text{ss}}\vartheta^{\text{dd}} - \vartheta^{\text{ds}}\vartheta^{\text{sd}}} = 1. \quad (17)$$

For γ small,

$$\left(\frac{\sigma^s}{\vartheta^{ss}}\right)_{\gamma \equiv 0} + \left(\frac{\sigma^d}{\vartheta^{dd}}\right)_{\gamma \equiv 0} + O(\gamma^2) = 1$$

which shows that the critical disorder W_c is greater than $\max\{W_c^s, W_c^d\}$ and increases with γ .

In the region of localized states, $\sigma_{\text{Born}} < \sigma_{\text{corr}}$, we define the localization radius ξ by the following relation [6, 7]:

$$\lim_{\omega \rightarrow 0} \left(-\frac{i\omega}{D_{\mathcal{E}_F}(\omega)} \right) = \frac{1}{\xi^2}. \quad (18)$$

At $d = 3$, combining equations (12) and (13), we arrive at an equation determining the localization radius for different sets of the system parameters:

$$\frac{1}{\xi k_0} \tanh^{-1}(\xi k_0) = 1 - \frac{\sigma_B^s (\vartheta^{dd} - \vartheta^{ds}) + \sigma_B^d (\vartheta^{ss} - \vartheta^{sd})}{\vartheta^{ss}\vartheta^{dd} - \vartheta^{ds}\vartheta^{sd}}. \quad (19)$$

Numerical calculations are done for a simple cubic lattice with a half-filled band. We introduce the following model density of states [11]:

$$\begin{aligned} \rho_0(\mathcal{E}) &= \sum_{\mathbf{k}} \delta(\mathcal{E} - \varepsilon_{\mathbf{k}}) \\ &= \frac{2}{\pi w} \left[1 - \left(\frac{\mathcal{E}}{w} \right)^2 \right]^{1/2} \theta(w - |\mathcal{E}|) \\ \sum_{\mathbf{k}} \delta(\mathcal{E} - \varepsilon_{\mathbf{k}}) (\nabla_{\mathbf{k}} \varepsilon_{\mathbf{k}})^2 &= \frac{2V_{\text{max}}^2}{\pi w} \left[1 - \left(\frac{\mathcal{E}}{w} \right)^2 \right]^{3/2} \theta(w - |\mathcal{E}|) \end{aligned} \quad (20)$$

where w is the band halfwidth, $-w < \varepsilon_{\mathbf{k}} < w$, $V_{\text{max}} = aw/\sqrt{3}$ is the maximum velocity in the semielliptical band, and a the lattice parameter. We also assume that for unperturbed bands $\varepsilon_{\mathbf{k}}^s \equiv \varepsilon_{\mathbf{k}}$ and $\varepsilon_{\mathbf{k}}^d \equiv \alpha\varepsilon_{\mathbf{k}}$, $0 < \alpha < 1$, with α the scaling parameter.

For a fixed set of system parameters $\{\alpha, \gamma, W, \mathcal{E}\}$ we calculate the 'Born damping' $\Delta_{\mathcal{E}}^{\mu}$ as the solution of the self-consistent system of equations (9) with the initial approximation

$$\rho^s(\mathcal{E}) = \rho_0(\mathcal{E}) \quad \rho^d(\mathcal{E}) = \frac{\rho_0(\mathcal{E}/\alpha)}{\alpha}.$$

Equations (16), (14) and (10) can now be used to calculate the contributions to the Born conductivity σ_B^{μ} and the coefficients $\vartheta^{\mu\nu}$. For the cut-off momentum one usually takes $k_0 = \kappa\pi/a$, with $\kappa \simeq 1, \dots, 2$ a parameter. In our calculations $\kappa = \pi^2/9$.

The results of numerical calculations with $\alpha = 0.1$ are presented in figures 1-5, where $\rho(\mathcal{E})$ is given in units of $(\pi w)^{-1}$; \mathcal{E} , γ , and W are in units of w ; σ in units of $\sigma_0 \equiv e^2/9\pi\hbar a$; and ξ in units of a .

Figure 1 demonstrates the behaviour of the density of states $\rho(\mathcal{E})$ for various values of the hybridization constant γ . When hybridization occurs, the curve of ρ plotted

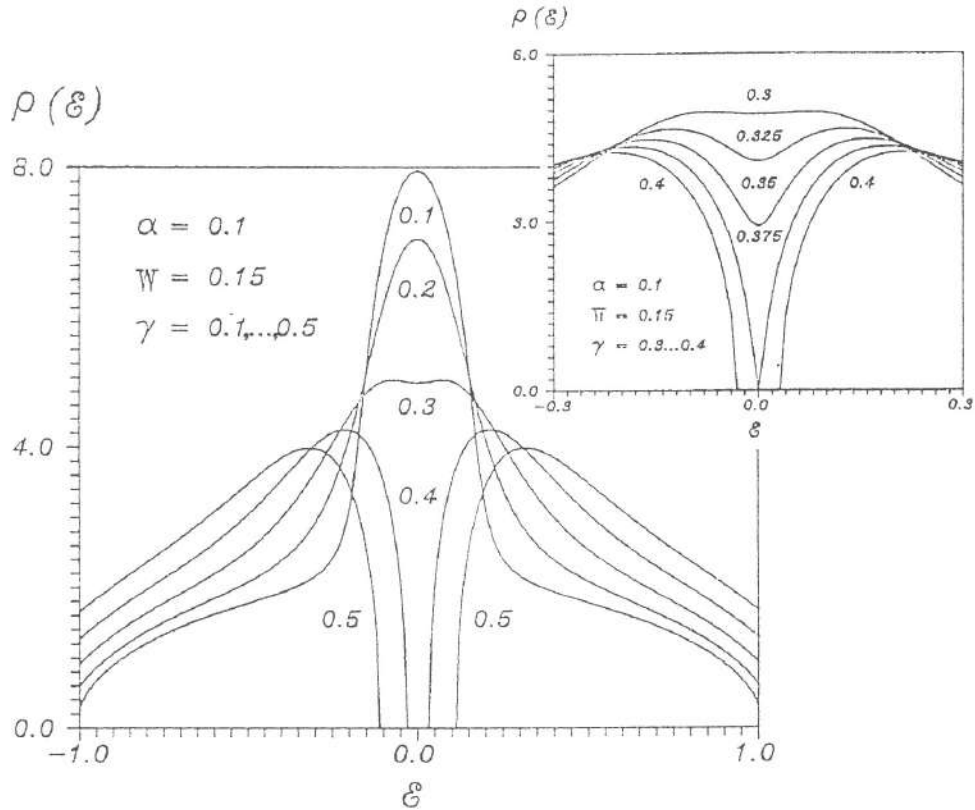


Figure 1. Density of states $\rho(\mathcal{E})$ for various values of the hybridization constant γ .

against \mathcal{E} acquires what is known as a pseudogap, whose depth increases with γ for W fixed. For $\gamma \geq \alpha^{1/2}w$, in the limit of $W \rightarrow 0$, the density of states $\rho(\mathcal{E})$ at the middle of the band vanishes and a hybridization gap forms. A further increase in γ causes the hybridization gap to broaden. As W grows with γ fixed, the hybridization gap closes and the depth of the pseudogap decreases owing to the increase in $\rho(\mathcal{E})$.

Figure 2 depicts the curves for the system's DC conductivity σ plotted against the disorder width W for different values of the hybridization constant γ . For $\gamma < \alpha^{1/2}w$, the conductivity decreases as W grows and vanishes at $W = W_c(\gamma)$, which corresponds to an Anderson transition. The nonmonotonicity of σ for small values of W , due to the hybridization pseudogap, increases with γ , and for $\gamma \geq \alpha^{1/2}w$ a metal-insulator transition caused by the formation of a hybridization gap may occur. In this event in the region of small values of W a rather exotic increase in σ with W is observed at a fixed value of γ , an increase is due to the evolution of the hybridization pseudogap in the density of states. A further increase in W at a fixed γ brings about an increase in the localization correction. This leads to growth saturation and a rapid decrease in σ , with σ vanishing at $W = W_c(\gamma)$.

The dependence of the critical disorder W_c on the hybridization constant γ is depicted in figure 3. We see that W_c increases with γ .

Figure 4 depicts the curves for σ , DC conductivity, plotted against the hybridization constant γ for different values of the disorder width W .

The system is in the localized states region, for $W > W_c^0$, where $W_c^0 \gtrsim W_c^s$, with

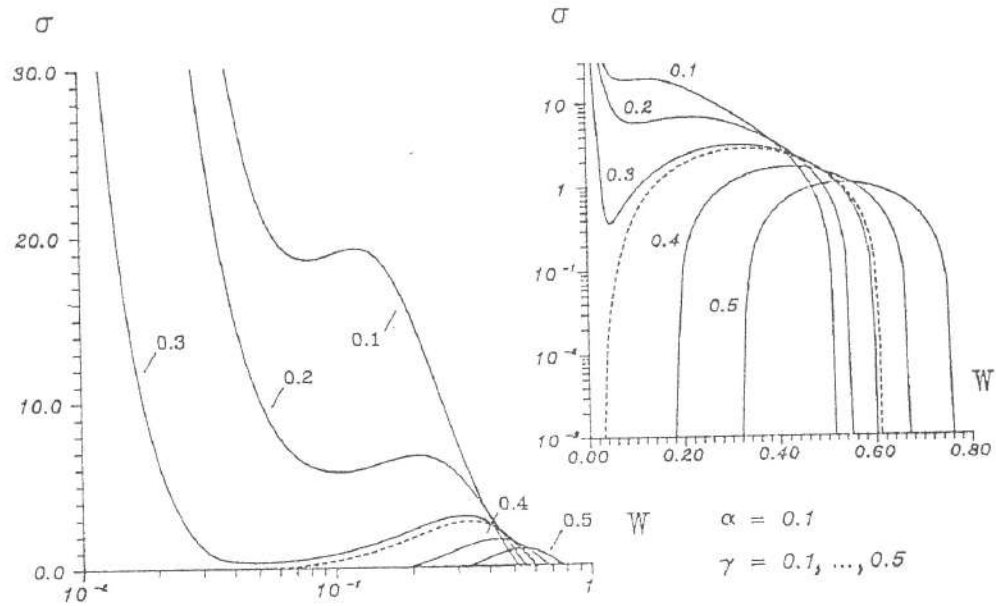


Figure 2. DC conductivity σ of the system as the function of the disorder width W for different values of the hybridization constant γ . The broken curves correspond to $\gamma = \alpha^{1/2} w$.

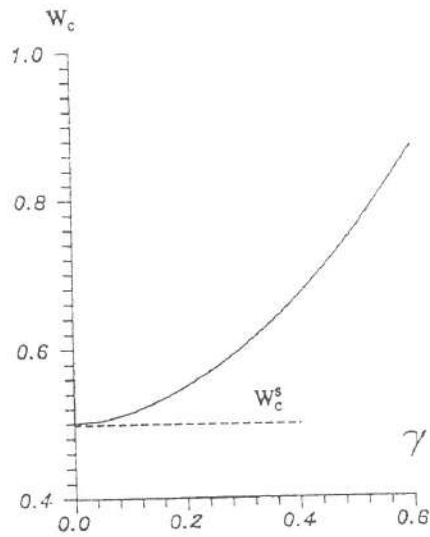


Figure 3. Critical disorder W_c as a function of the hybridization constant γ . The broken horizontal line depicts W_c^s , the critical disorder of the unhybridized s-band.

W_c^0 the critical disorder of the system as $\gamma \rightarrow 0$, and for $\gamma < \gamma_c$, where γ_c is determined from the condition $W_c(\gamma_c) = W$. As γ increases at a fixed W , the system may become

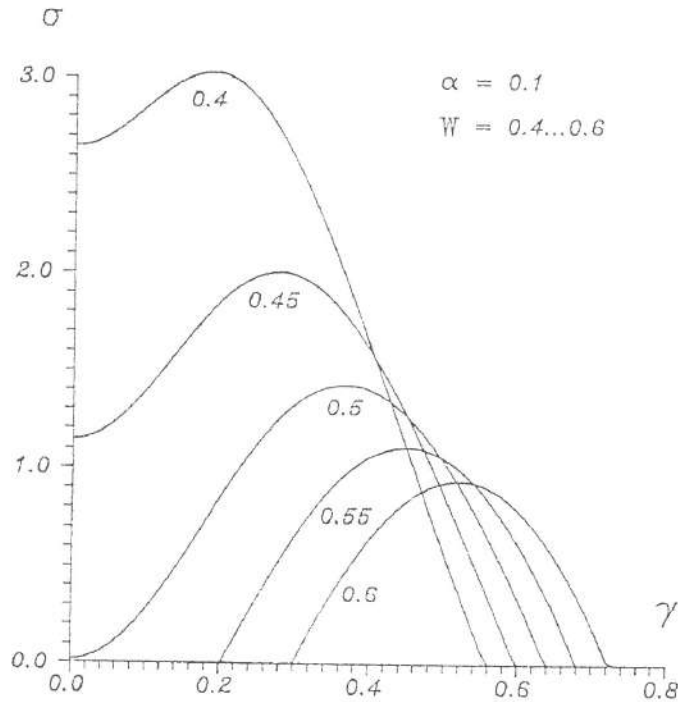


Figure 4. The DC conductivity of the system, σ , as a function of the hybridization constant γ for different values of the disorder width W .

delocalized for $\gamma \geq \gamma_c$. A further increase in γ at a fixed W leads to an increase in σ owing, apparently, to the contribution of band-to-band transitions. The value of σ rapidly becomes saturated and, later, decreases because of the widening of the hybridization pseudogap in the density of states.

For $W < W_c^0$, an increase in γ in the region of small values of γ also leads to an increase in σ owing to the contribution of band-to-band transitions, and again the value of σ becomes rapidly saturated and then falls off owing to the evolution of the hybridization pseudogap in the density of states.

The curves in figure 5 for the localization radius ξ as the function of the disorder width W at different values of the hybridization constant γ demonstrate the divergence of ξ as $W \rightarrow W_c$, with the critical disorder W_c obviously depending on γ .

Our results show that an Anderson transition in the two-band model possesses a number of features setting it apart from the standard case. Hybridization of states of the narrow and wide bands leads to delocalization in the system, and the critical disorder corresponding to localization exceeds the value characteristic of an unhybridized wide band. This indicates that at the Fermi level the localized states corresponding to the narrow band cannot coexist with the delocalized states corresponding to the wide band. From the experimenter's viewpoint, the most interesting is the nonmonotonic behaviour of conductivity (for one thing, the increase in conductivity with disorder).

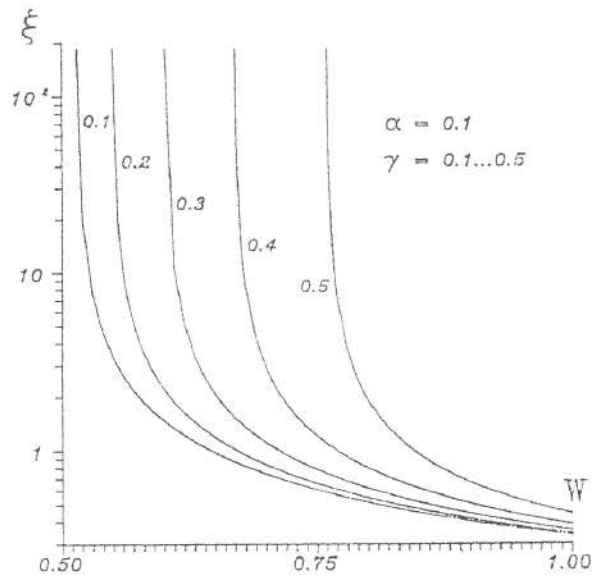


Figure 5. The localization radius ξ of the system plotted against the disorder width W for different values of the hybridization constant γ .

Acknowledgment

We are grateful to É Z Kuchinskiĭ for his interest in our work and for numerous constructive discussions.

References

- [1] Anderson P W 1958 *Phys. Rev.* **109** 1492
- [2] Mott N F 1974 *Metal-Insulator Transitions* (London: Taylor & Francis)
- [3] Economou E N and Cohen M H 1972 *Phys. Rev. B* **5** 2931
- [4] Maleev S V and Toperverg B P 1975 *Zh. Eksp. Teor. Fiz.* **69** 1440
- [5] Vollhardt D and Wölfle P 1980 *Phys. Rev. B* **22** 4666
- [6] Vollhardt D and Wölfle P 1982 *Phys. Rev. Lett.* **48** 699
- [7] Wölfle P and Vollhardt D 1982 *Anderson Localization* ed Y Nagaoka and H Fukuyama (Berlin: Springer) p 26
- [8] Sadovskii M V 1985 *Soviet Scientific Reviews-Physics Reviews* ed I M Khalatnikov (New York: Harwood Academic) p 1
- [9] Myasnikov A V and Sadovskii M V 1982 *Fiz. Tverd. Tela (Leningrad)* **24** 3569
- [10] Kotov E A and Sadovskii M V 1983 *Z. Phys. B* **51** 17
- [11] Velicky B 1969 *Phys. Rev.* **184** 614

Suppression of superconductivity close to the metal–insulator transition in strongly disordered systems

É. Z. Kuchinskiĭ, M. V. Sadovskii, and M. A. Érkabaev

Electrophysics Institute Ural Branch, Russian Academy of Sciences, 620049 Ekaterinburg, Russia
(Submitted 24 October 1996)

Zh. Éksp. Teor. Fiz. **112**, 192–199 (July 1997)

By means of the self-consistent theory proposed earlier for a metal–insulator transition in strongly disordered systems, which takes into account interelectron interaction effects, the effects of the suppression of the superconducting–transition temperature T_c , caused by the formation of a Coulomb pseudo-gap in the density of states, are studied in a wide interval of disorder values—from a weakly disordered metal to an Anderson insulator. It is shown that the proposed theory gives a satisfactory description of the experimental data for a number of systems that have been studied. © 1997 American Institute of Physics. [S1063-7761(97)01607-7]

1. INTRODUCTION

The problem of the degradation of the superconducting–transition temperature under conditions of strong disordering has attracted the attention of theoreticians for a rather long time.¹ It is closely associated with the question of the breakdown of the superconducting state close to the metal–insulator transition caused by disordering.² A number of mechanisms for the suppression of T_c have been proposed, such as an increase of the Coulomb pseudopotential,^{3,4} the effect of Coulomb corrections to the density of states,⁵ etc. Most of these papers discussed only small corrections to T_c because of these mechanisms.

The theory of the metal–insulator transition proposed in Refs. 6 and 7, which generalizes the self-consistent localization theory^{8,9} in the direction of taking into account electron–electron interaction effects, made it possible to study the behavior of a generalized diffusion coefficient over a wide range of variation of the system parameters both in the metallic and in the insulator regions. The substantial influence of electron–electron interaction on the generalized diffusion coefficient was treated. These results were used to study the behavior of the single-particle density of states of the system, taking into account the influence of electron–electron interaction effects.

The results of the corresponding calculations demonstrate the formation and evolution of a Coulomb pseudo-gap in the density of states of a system close to the Fermi level. In the metallic region, the behavior of the density of states close to the Coulomb pseudo-gap corresponds to the ordinary Al'tshuler–Aronov root correction.¹⁰ When one approaches the metal–insulator transition as the disorder parameter increases, the depth of the pseudo-gap increases and the effective width of the region of the root behavior decreases; at the metal–insulator transition point, the density of states at the Fermi level goes to zero, i.e., a Coulomb gap forms. In the insulator region, for the case of a band of finite width in the region of the Coulomb gap, a quadratic dependence of the density of states is obtained. The effective width of the corresponding region increases with increasing disorder parameter. This recalls the well-known behavior of the Efros–Shklovskii Coulomb gap¹¹ in the insulator region far

from the metal–insulator transition point. Such behavior of the density of states gives good qualitative agreement with experiments in a number of disordered systems close to the metal–insulator transition,¹ from amorphous alloys^{12–16} to disordered single-crystal metal oxides, including high-temperature superconductors.¹⁷

In this paper, the results of calculations of the density of states of a system for the case of a band of finite width are used to numerically study how Coulomb pseudo-gap effects in the density of states affect the suppression of superconductivity close to the metal–insulator transition.

Superconductivity in strongly disordered systems will be treated in terms of a simple BCS model. In the weak-binding approximation, the linearized equation for the gap has the following form:²

$$\Delta(\xi) = - \int_{-\infty}^{\infty} d\xi' V(\xi, \xi') N(\xi') \frac{1}{2\xi'} \tanh\left(\frac{\xi'}{2T_c}\right) \Delta(\xi'). \quad (1)$$

Here $N(\xi)$ is the density of states of the disordered system averaged over the implementations of the disorder, allowing for electron–electron interaction effects, and $V(\xi, \xi')$ is the effective interaction potential. The only difference from the standard approach is that the nontrivial dependence of $N(\xi)$ on electron energy ξ measured from the Fermi level E_F is taken into account here.

It is assumed in BCS theory that an effective electron–electron attraction exists, which is determined by a certain balance between pairing due to electron–phonon interaction and Coulomb repulsion. The following will be regarded as the effective interaction potential:

$$V(\xi, \xi') = V_c(\xi, \xi') + V_{\text{ph}}(\xi, \xi'), \quad (2)$$

where $V_c(\xi, \xi') = V_c \theta(E_F - |\xi|) \theta(E_F - |\xi'|)$ and $V_{\text{ph}}(\xi, \xi') = -V_{\text{ph}} \theta(\omega_D - |\xi|) \theta(\omega_D - |\xi'|)$ are the electron–electron and electron–phonon interaction potentials, respectively, and ω_D is the Debye frequency. The constants $V_c > 0$ and $V_{\text{ph}} > 0$ correspond to repulsion and attraction, acting in substantially different energy intervals: $E_F \gg \omega_D$.

After substituting this expression into Eq. (1) and transforming, using the parity of the slit function $\Delta(\xi)$, we get

$$\begin{aligned} \Delta(\xi) = & [V_{\text{ph}}\theta(\omega_D - \xi) - V_c\theta(E_F - \xi)] \\ & \times \int_0^{\omega_D} d\xi' N(\xi') \frac{1}{\xi'} \tanh\left(\frac{\xi'}{2T_c}\right) \Delta(\xi') - V_c\theta(E_F \\ & - \xi) \int_{\omega_D}^{E_F} d\xi' N(\xi') \frac{1}{\xi'} \tanh\left(\frac{\xi'}{2T_c}\right) \Delta(\xi'). \quad (3) \end{aligned}$$

As usual, we shall seek the solution of this equation in a two-step form:¹⁸

$$\Delta(\xi) = \begin{cases} \Delta_{\text{ph}}, & |\xi| < \omega_D, \\ \Delta_c, & \omega_D < |\xi| < E_F, \end{cases} \quad (4)$$

where Δ_{ph} and Δ_c are certain constants that can be determined, after substituting Eq. (4) into Eq. (3), from a system of homogeneous equations of the following form:

$$\begin{aligned} & \left\{ 1 - (V_{\text{ph}} - V_c)N_0(0)K\left(\frac{\omega_D}{2T_c}\right) \right\} \Delta_{\text{ph}} + V_cN_0(0) \left[K\left(\frac{E_F}{2T_c}\right) \right. \\ & \left. - K\left(\frac{\omega_D}{2T_c}\right) \right] \Delta_c = 0, \quad (5) \\ & V_cN_0(0)K\left(\frac{\omega_D}{2T_c}\right) \Delta_{\text{ph}} + \left\{ 1 + V_cN_0(0) \left[K\left(\frac{E_F}{2T_c}\right) \right. \right. \\ & \left. \left. - K\left(\frac{\omega_D}{2T_c}\right) \right] \right\} \Delta_c = 0. \end{aligned}$$

Here $N_0(0)$ is the single-particle density of states of noninteracting electrons at the Fermi level, and we have introduced the notation

$$K(\xi) = \int_0^{\xi} d\xi' \frac{1}{\xi'} \tanh \xi' \left[\frac{N(2T_c\xi')}{N_0(0)} \right]. \quad (6)$$

The condition for this homogeneous system of equations to be solvable is the equation for determining T_c :

$$\begin{aligned} (\lambda - \mu^*)K\left(\frac{\omega_D}{2T_c}\right) &= 1, \\ \mu^* &= \mu \left\{ 1 + \mu \left[K\left(\frac{E_F}{2T_c}\right) - K\left(\frac{\omega_D}{2T_c}\right) \right] \right\}^{-1}, \quad (7) \end{aligned}$$

where μ^* is the Coulomb pseudopotential, $\mu = V_cN_0(0)$ is the Coulomb repulsion constant, and $\lambda = V_{\text{ph}}N_0(0)$ is the pairing constant due to the electron-phonon interaction. In the pure limit, when the density of states at the Fermi level can be regarded as constant, the usual equation of BCS theory follows from this.

Equation (7) for determining T_c has been studied numerically over a wide region of variation of the system parameters in both the metal and the insulating states. The density of states of the system was computed using the lower-order corrections in the interelectron interaction.^{6,7}

$$N(\xi) = -\frac{1}{\pi} \text{Im} \int \frac{d^3\mathbf{p}}{(2\pi)^3} G^R(\mathbf{p}, \xi), \quad (8)$$

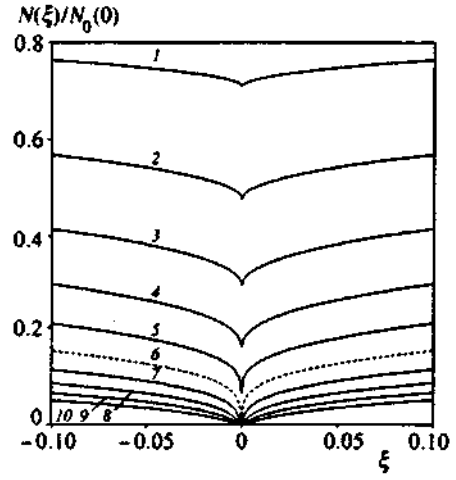


FIG. 1. Density of states of a system in the case of a band of finite width $2E_F$ when $(8/3\pi)\mu = 1.0$, for various values of the disorder parameter $(p_F l)^{-1}$: 1—0.1..., 5—0.5 in the metallic region, 7—0.7..., 10—1.0 in the insulator region. The dashed curve 6 corresponds to the metal-insulator transition point. Energy ε is in units of $D_0k_0^2$ in the graph.

where $G^{R(A)}(\mathbf{p}, \xi) = [\xi - \xi_p \pm i\gamma - \Sigma_{ee}^{R(A)}(\mathbf{p}, \xi)]^{-1}$ is the retarded (advanced) single-particle Green's function, and $\Sigma_{ee}^{R(A)}(\mathbf{p}, \xi)$ is the Fock contribution to the eigenenergy part:^{6,10}

$$\begin{aligned} \Sigma_{ee}^{R(A)}(\mathbf{p}, \xi) &\approx 4i\gamma^2\mu N_0^{-1}(0)G_0^{R(A)}(\mathbf{p}, \xi) \\ &\times \int_{\xi}^{\infty} \frac{d\omega}{2\pi} \int_{|\mathbf{q}| < k_0} \frac{d^3\mathbf{q}}{(2\pi)^3} \\ &\times \frac{1}{[-i\omega + D(\omega)q^2]^2}. \quad (9) \end{aligned}$$

Here $D(\omega)$ is a generalized diffusion coefficient, which satisfies the following self-consistent nonlinear integral equation:^{6,7}

$$\begin{aligned} \frac{D(\omega)}{D_0} &= 1 - \frac{1}{\pi N_0(0)} \frac{D(\omega)}{D_0} \int_{|\mathbf{q}| < k_0} \frac{d^3\mathbf{q}}{(2\pi)^3} \\ &\times \frac{1}{-i\omega + D(\omega)q^2} \\ &+ \frac{8i}{3\pi} \frac{\mu D_0}{\pi N_0(0)} \int_{\omega}^{\infty} d\Omega \int_{|\mathbf{q}| < k_0} \frac{d^3\mathbf{q}}{(2\pi)^3} \\ &\times \frac{q^2}{(-i(\Omega + \omega) + D(\Omega + \omega)q^2)(-i\Omega + D(\Omega)q^2)^2}, \quad (10) \end{aligned}$$

where $D_0 = E_F/3m\gamma$ is the classical diffusion coefficient, $\gamma = 1/2\tau$ is the Born damping, τ is the free path time, $k_0 = \min\{p_F, l^{-1}\}$ is the cutoff momentum, p_F is the Fermi momentum, and l is the free path length. The values shown below for static conductivity were also obtained by numerically solving Eq. (10).^{6,7}

Figure 1 shows the behavior of the density of states of the system close to the Fermi level, demonstrating the evo-

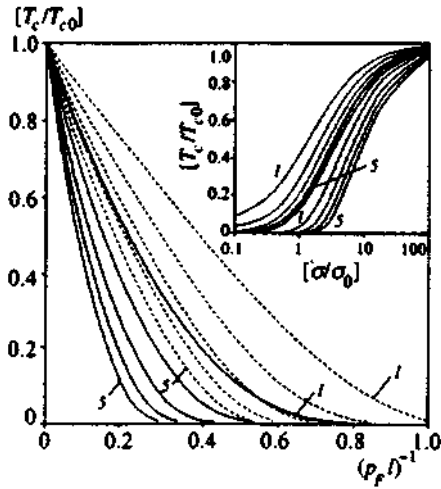


FIG. 2. Degradation of T_c as a function of the disorder parameter $(p_F l)^{-1}$ for a fixed pairing constant λ ($\lambda=0.5$ —continuous curves, $\lambda=1.0$ —dashed curves) for various values of the Coulomb repulsion constant $(8/3\pi)\mu$: 1—0.2, ..., 5—1.0. The inset shows the dependence of T_c on the static conductivity σ of the system for the corresponding values of the pairing constant λ and Coulomb repulsion constant μ .

lution of the Coulomb pseudo-gap as the disorder parameter increases. It is this behavior that results in suppression of the superconducting transition temperature.

The graphs in Fig. 2 demonstrate the suppression of T_c with increasing disorder parameter $(p_F l)^{-1}$ for various values of the Coulomb repulsion constant μ with fixed pairing constant λ . For large μ , as disorder $(p_F l)^{-1}$ increases, T_c rapidly decreases and goes to zero in the metallic region far from the metal–insulator transition. When μ is reduced, the falloff of T_c with increasing disorder $(p_F l)^{-1}$ slows down, and, for small μ and large λ (dashed curves in figure), superconductivity can occur in the insulating region.² The latter is clearly demonstrated by the graphs in the inset of Fig. 2, which shows the dependence of T_c on the static conductivity σ of the system for corresponding values of the pairing constant λ and the Coulomb repulsion constant μ . For large μ , T_c rapidly decreases as conductivity σ decreases, and superconductivity is suppressed in the metallic region rather far from the metal–insulator transition. When μ is reduced, the falloff of T_c slows down with decreasing conductivity σ , and, for small μ and rather large λ (dashed curves in inset), T_c remains finite in the limit $\sigma \rightarrow 0$.

The graphs in Fig. 3 demonstrate the degradation of T_c as the disorder parameter $(p_F l)^{-1}$ increases for various values of the pairing constant λ with fixed Coulomb repulsion constant μ . For small λ , as the disorder $(p_F l)^{-1}$ increases, T_c rapidly decreases and goes to zero in the metallic region far from the metal–insulator transition. When λ is increased, the decrease of T_c with increasing disorder $(p_F l)^{-1}$ slows down, and, for sufficiently large λ , the superconductivity is suppressed only in the insulating region. The dependence of the Coulomb pseudopotential μ^* on the disorder parameter $(p_F l)^{-1}$ shown in the inset of Fig. 3 for corresponding values of the pairing constant λ and the Coulomb repulsion constant μ demonstrates an insignificant increase of the Coulomb pseudopotential μ^* with increasing disorder $(p_F l)^{-1}$

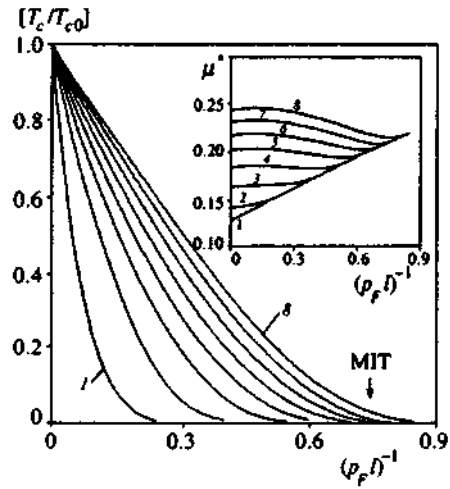


FIG. 3. Degradation of T_c as a function of the disorder parameter $(p_F l)^{-1}$ for fixed Coulomb repulsion constant $(8/3\pi)\mu=0.4$ for various values of the pairing constant λ : 1—0.3, 2—0.4, ..., 8—1.0. The inset shows the dependence of the Coulomb pseudopotential μ^* on the disorder parameter $(p_F l)^{-1}$ for the corresponding values of the pairing constant λ and the Coulomb repulsion constant μ . The arrow shows the position of the metal–insulator transition point μ .

close to the superconductivity-suppression point. This is apparently fairly natural, since the different processes that renormalize the matrix element of the Coulomb interaction in Eq. (2) because of Anderson localization effects and electron–electron interaction and that substantially increase the Coulomb pseudopotential close to the metal–insulator transition² are not considered in this case.

Similar behavior of T_c as a function of static conductivity σ and of the disorder parameter was experimentally observed in a number of disordered systems that remain superconducting close to the metal–insulator transition caused by disordering.^{1,2,12–17,19–21} The results of our numerical calculations agree well with experiments in the amorphous alloys InO_x ,¹⁴ $\text{Nb}_x\text{Si}_{1-x}$,^{15,16} and $\text{Au}_x\text{Si}_{1-x}$.^{19–21}

Reference 14 presented the results of measurements of the disorder parameter $(p_F l)^{-1}$ for the amorphous alloy InO_x , as well as data for T_c and static conductivity close to the metal–insulator transition.

According to Refs. 6 and 7, the static conductivity of the system close to the metal–insulator transition has the following form:

$$\sigma = \sigma_0 [(p_F l) W_c(\mu) - 1]. \quad (11)$$

Here σ_0 is some characteristic conductivity scale close to the metal–insulator transition, and $W_c(\mu)$ is the disorder parameter corresponding to the metal–insulator transition, which depends on the Coulomb repulsion constant.

Approximating the experiment for the static conductivity of the amorphous alloy InO_x by Eq. (11) makes it possible to estimate the characteristic conductivity scale σ_0 and, from the value of W_c , the Coulomb repulsion constant μ . Satisfactory correlations (see inset in Fig. 3) are obtained for the following values of the parameters: $\sigma_0 \approx 324.95$ $(\Omega \cdot \text{cm})^{-1}$, $W_c \approx 0.606$, and $\mu \approx 1.0$.

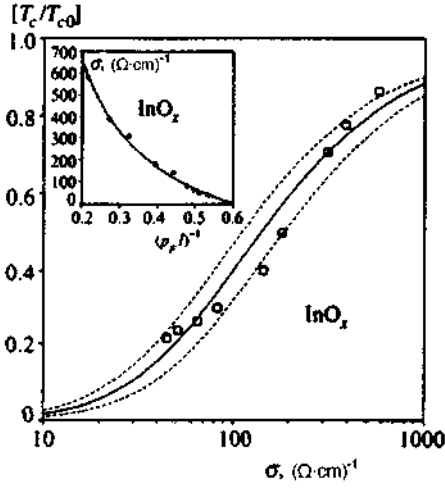


FIG. 4. Behavior of T_c as a function of static conductivity σ for the amorphous alloy InO_x . The inset shows the results of an approximation of the data for the static conductivity σ as a function of the disorder parameter $(pFl)^{-1}$.

Figure 4 shows a comparison of our results with the experimental data for T_c as a function of the static conductivity σ of the amorphous alloy InO_x , using $T_{c0}=3.41$ K, $\omega_D=112$ K, and $E_F=9.98 \times 10^4$ K, $[\omega_D/E_F] \approx 1.1 \times 10^{-3}$ for pure In and the resulting values of σ_0 and μ , which makes it possible to estimate the pairing constant λ . Satisfactory correlation is obtained for $\lambda \approx 0.45$. The dashed curves correspond to the values $\lambda \approx 0.4$ and 0.5 .

Let us consider the results of studies of the dependence of T_c and the static conductivity on the Si concentration in the amorphous alloys $\text{Nb}_x\text{Si}_{1-x}$ (Refs. 15, 16) and $\text{Au}_x\text{Si}_{1-x}$ (Refs. 19–21) close to the metal–insulator transition. Assuming a disorder parameter proportional to the Si concentration for these systems, so that $(pFl)^{-1} \sim 1-x$, we transform Eq. (11) for the static conductivity close to the metal–insulator transition to the form

$$\sigma = \sigma_0 \frac{x - x_c}{1 - x}, \quad (12)$$

where x_c is the critical concentration (corresponding to Nb or Au) at the metal–insulator transition point.

Approximating the experiment for the static conductivity of the amorphous alloys $\text{Nb}_x\text{Si}_{1-x}$ and $\text{Au}_x\text{Si}_{1-x}$ by Eq. (12) makes it possible to estimate the characteristic conductivity scale σ_0 and the critical concentration x_c . Satisfactory correlations (see the inset in Figs. 5 and 6) are obtained for the following values of the parameters:

$$\text{Nb}_x\text{Si}_{1-x}: \quad \sigma_0 \approx 1963.9 (\Omega \cdot \text{cm})^{-1}, \quad x_c \approx 0.115;$$

$$\text{Au}_x\text{Si}_{1-x}: \quad \sigma_0 \approx 2782.13 (\Omega \cdot \text{cm})^{-1}, \quad x_c \approx 0.14.$$

The graphs in Figs. 5 and 6 demonstrate the comparison of our results with the experimental data for T_c as a function of static conductivity σ in the amorphous alloys $\text{Nb}_x\text{Si}_{1-x}$ and $\text{Au}_x\text{Si}_{1-x}$, using the values of σ_0 shown above and the following parameters: $T_{c0}=9.26$ K, $\omega_D=276$ K, and $E_F=6.18 \times 10^4$ K, $[\omega_D/E_F] \approx 3.0 \times 10^{-3}$ for pure Nb; $T_{c0}=T_{c\text{max}} \approx 0.86$ K, $\omega_D=170$ K, and $E_F=6.42 \times 10^4$ K,

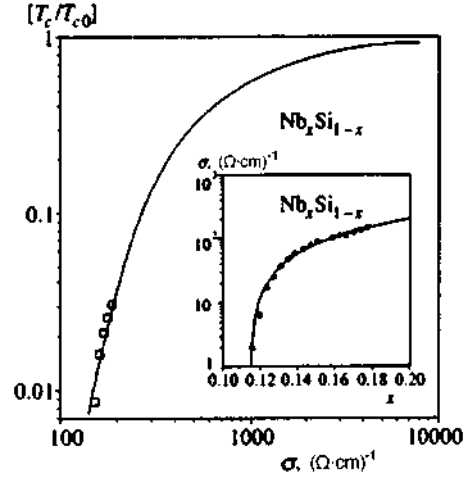


FIG. 5. Behavior of T_c as a function of static conductivity σ for the amorphous alloy $\text{Nb}_x\text{Si}_{1-x}$. The inset shows the results of an approximation of the data for the static conductivity σ as a function of the Nb concentration.

$[\omega_D/E_F] \approx 0.9 \times 10^{-3}$ for $\text{Au}_x\text{Si}_{1-x}$. This comparison makes it possible to estimate the pairing constant λ . Assuming a Coulomb repulsion constant of $\mu \approx 1$ for these systems, satisfactory correlation can be obtained with $\lambda \approx 0.54$ for $\text{Nb}_x\text{Si}_{1-x}$ and with $\lambda \approx 0.62$ for $\text{Au}_x\text{Si}_{1-x}$.

Of course, these computations, which are based on the BCS model, are oversimplified. A consistent approach to the problem of computing the superconducting transition temperature must be based on a solution of the Eliashberg equations and must use realistic models of the electron–electron interaction.¹⁸ This is especially true of the results given above for large values of the pairing constant λ , which demonstrate that superconductivity can exist in the insulating region. At the same time, we have not questioned the genesis of the initial T_{c0} in a pure system in this paper, but have been occupied only with the question of how T_c depends on the disorder. In this sense, the results can be qualitatively applied in the strong bonding region. We should point out that it is still necessary to more consistently take into account disorder

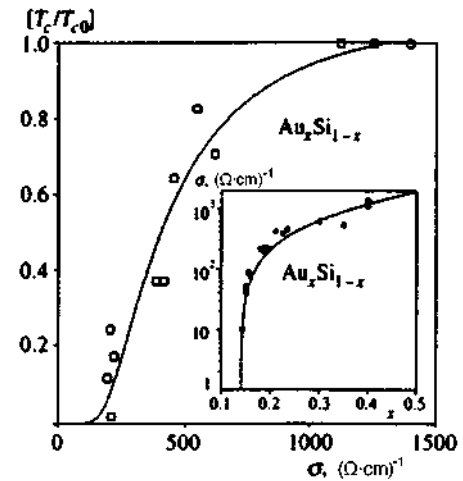


FIG. 6. Behavior of T_c as a function of static conductivity σ for the amorphous alloy $\text{Au}_x\text{Si}_{1-x}$. The inset shows the results of an approximation of the data for the static conductivity σ as a function of the Au concentration.

der effects in the Coulomb-interaction matrix element, which is associated with an additional T_c -degradation mechanism.²⁻⁴ As was pointed out above, this paper has taken into account only the effects of the formation of a Coulomb pseudo-gap in the density of states. It is possible that the satisfactory agreement with experiment obtained above indicates that the effects of the variation of the density of states play a dominant role in the T_c -degradation mechanism, as was noted earlier (at the level of small corrections) in Ref. 5.

This work was carried out with the partial financial support of the Russian Fund for Fundamental Research (Grant 96-02-16065) and also as part of Project IX.1 of the Statistical Physics Program of the State Committee for Science and Technology of Russia.

¹D. Belitz and T. R. Kirkpatrick, *Rev. Mod. Phys.* **66**, 261 (1994).

²M. V. Sadovskii, *Sverkhprovodnost' (KIAE)* **8**, 337 (1995) submitted to *Phys. Rep.* (1996).

³P. W. Anderson, K. A. Muttalib, and T. V. Ramakrishnan, *Phys. Rev. B* **28**, 117 (1983).

⁴L. N. Bulaevskii and M. V. Sadovskii, *J. Low Temp. Phys.* **59**, 89 (1985).

⁵D. Belitz *et al.*, *Phys. Rev. B* **40**, 111 (1989).

⁶É. Z. Kuchinskiĭ, M. V. Sadovskii, V. G. Suvarov, and M. A. Érkabaev, *Zh. Éksp. Teor. Fiz.* **107**, 2027 (1995) [*JETP* **80**, 1122 (1995)].

⁷É. Z. Kuchinskiĭ and M. A. Érkabaev, *Fiz. Tverd. Tela* **39**, 412 (1997) [*Phys. Solid State* **39**, 357 (1997)].

⁸D. Volthardt and P. Wölfle, in *Electronic Phase Transitions*, ed. W. Hanke and Yu. Kopaev (North-Holland, Amsterdam, 1992), p. 1.

⁹M. V. Sadovskii, *Sci. Rev. Phys. A* **7**, 1 (1986).

¹⁰B. L. Al'tshuler and A. G. Aronov, *Zh. Éksp. Teor. Fiz.* **77**, 2028 (1979) [*Sov. Phys. JETP* **50**, 968 (1979)].

¹¹A. L. Efros and B. I. Shklovskii, in *Electron-Electron Interaction in Disordered Systems*, ed. M. Pollak and A. L. Efros (North-Holland, Amsterdam, 1984), p. 409.

¹²W. L. McMillan and J. Mochele, *Phys. Rev. Lett.* **46**, 556 (1981).

¹³Y. Imry and Z. Ovadyahu, *Phys. Rev. Lett.* **49**, 841 (1982).

¹⁴A. T. Fiory and A. F. Hebard, *Phys. Rev. Lett.* **52**, 2057 (1984).

¹⁵G. Hertel, D. J. Bishop, E. G. Spencer, J. M. Rowel, and R. C. Dynes, *Phys. Rev. Lett.* **50**, 743 (1983).

¹⁶D. J. Bishop, E. G. Spencer, and R. C. Dynes, *Solid-State Electron.* **28**, 73 (1985).

¹⁷H. Srikanth, K. P. Rajeev, G. V. Shivashankar, and A. K. Raychaudhuri, *Physica C* **195**, 87 (1992).

¹⁸S. V. Vonsovskii, Yu. A. Izyumov, and É. Z. Kurmaev, *Superconductivity of the Transition Metals, Their Alloys and Compounds* (Nauka, Moscow, 1997).

¹⁹N. Nishida, M. Yamaguchi, T. Furubayashi, M. Morigaki, H. Ishimoto, and K. Ono, *Solid State Commun.* **44**, 305 (1982).

²⁰T. Furubayashi, N. Nishida, M. Yamaguchi, M. Morigaki, and H. Ishimoto, *Solid State Commun.* **55**, 513 (1985).

²¹N. Nishida, T. Furubayashi, M. Yamaguchi, M. Morigaki, and H. Ishimoto, *Solid-State Electron.* **28**, 81 (1985).

Translated by W. J. Manthey

The Ginzburg–Landau expansion and the slope of the upper critical field in superconductors with anisotropic normal-impurity scattering

A. I. Posazhennikova and M. V. Sadovskii*)

Institute of Electrophysics, Ural Branch of the Russian Academy of Sciences, 620049 Ekaterinburg, Russia
(Submitted 16 May 1997)

Zh. Éksp. Teor. Fiz. **112**, 2124–2133 (December 1997)

We carry out the Ginzburg–Landau expansion for superconductors with anisotropic s and d pairing in the presence of anisotropic normal-impurity scattering, which enhances the stability of d pairing with respect to disordering. We find that the slope of the curve of the upper critical field, $|dH_{c2}/dT|_{T_c}$, in superconductors with d pairing behaves nonlinearly as disorder grows: at low scattering anisotropy the slope rapidly decreases with increasing impurity concentration, then gradually but nonlinearly increases with concentration, reaches its maximum, and then rapidly decreases, vanishing at the critical impurity concentration. In superconductors with anisotropic s pairing, $|dH_{c2}/dT|_{T_c}$ always increases with impurity concentration, finally reaching the familiar asymptotic value characteristic of the isotropic case, irrespective of whether there is anisotropic impurity scattering. © 1997 American Institute of Physics. [S1063-7761(97)01412-1]

1. INTRODUCTION

The problem of determining the type of Cooper pairing is still occupying center stage in high- T_c superconductivity studies. Most experiments and a number of theoretical models¹ indicate that the majority of high- T_c oxides have $d_{x^2-y^2}$ -anisotropic pairing with the zeros of the gap function lying on the Fermi surface. Other variants of anisotropic pairing have also been proposed, e.g., the so-called anisotropic s pairing,^{2,3} which also gives rise to zeros in the gap function (but without a change in sign in the order parameter) or to minima in the gap function at the Fermi surface in the same directions in the Brillouin zone as in the case of d pairing (here, too, there are experimental indications that verify this fact). Borkovski and Hirschfeld⁴ and Fehrenbacher and Norman⁵ pointed out that controlled injection of normal impurities (disordering) can serve as an effective method of experimentally distinguishing the above types of anisotropic pairing, since it would lead to a markedly different behavior of the density of states in these types of superconductor. In our previous paper (see Ref. 6) we found that measuring the evolution of the slope of the curve of the upper critical field, $|dH_{c2}/dT|_{T_c}$, as the degree of disorder changes, at least in principle, serve the same purpose: in superconductors with d pairing the magnitude of this slope rapidly decreases with increasing disorder, while in the case of anisotropic s pairing the slope of the field increases with disorder, which is similar to the behavior in the isotropic case.

Recently, Harañ and Nagi⁷ examined an interesting model with anisotropic impurity scattering. They found that when the d -type scattering anisotropy is strong, the breaking of d -type Cooper pairs decreases substantially because of normal-impurity scattering, which in the isotropic case is described by the well-known Abrikosov–Gor’kov formula for magnetic impurities in a isotropic superconductor.^{4–6} Thus, by allowing for anisotropic impurity scattering we can, at least in principle, resolve one of the main problems of high- T_c superconductor physics: the contradiction between the

clear indications that d pairing exists in high- T_c superconductors and the relative stability of such superconductors with respect to disordering.⁸ This explanation of the remarkable stability of high- T_c superconducting cuprates with respect to disordering, if there is indeed d pairing in such cuprates, is not the only one (see, e.g., the explanation given in Ref. 9), but the simplicity of the model of Ref. 7 is appealing and stimulates calculations of other characteristics of superconductors with “exotic” types of pairing, with allowance for the possible role of anisotropic normal-impurity scattering. The present paper is a direct generalization of Ref. 6 to this case. It will be shown that allowance for anisotropic impurity scattering leads (in the case of d pairing) to striking anomalies in the behavior of the slope of the curve of the upper critical field as a function of the degree of disorder (impurity concentration). As in Ref. 6, we base our reasoning on a microscopic derivation of the Ginzburg–Landau expansion in the impurity system.

2. THE GINZBURG–LANDAU EXPANSION

Let us consider a two-dimensional electron system with an isotropic Fermi surface and a separable Cooper-pairing potential of the form^{4,5}

$$V(\mathbf{p}, \mathbf{p}') \equiv V(\phi, \phi') = -Ve(\phi)e(\phi'), \quad (1)$$

where ϕ is the polar angle determining the direction of the electron momentum \mathbf{p} in the highly conducting plane, and for $e(\phi)$ we adopt the simplest model:

$$e(\phi) = \begin{cases} \sqrt{2} \cos(2\phi) & (d \text{ pairing}), \\ \sqrt{2} |\cos(2\phi)| & (\text{anisotropic } s \text{ pairing}). \end{cases} \quad (2)$$

We assume, as usual, that the attraction constant V is finite in a layer of thickness $2\omega_c$ in the vicinity of the Fermi level (ω_c is the characteristic frequency of the photons that ensure the attraction of the electrons). In this case the superconducting gap (the order parameter) has the form

$$\Delta(\mathbf{p}) \equiv \Delta(\phi) = \Delta e(\phi), \quad (3)$$

where the positions of the zeros of the gap function at the Fermi surface for the s and d cases coincide.

We take a superconductor containing ‘‘normal’’ (non-magnetic) impurities that are distributed at random in space with a concentration ρ . Following Harań and Nagi,⁷ we assume that the square of the impurity scattering amplitude can be written as

$$|V_{\text{imp}}(\mathbf{p}, \mathbf{p}')|^2 \equiv |V_{\text{imp}}(\phi, \phi')|^2 = |V_0|^2 + |V_1|^2 f(\phi) f(\phi'), \quad (4)$$

where V_0 is the amplitude of isotropic point scattering, V_1 is the amplitude of anisotropic scattering, and the model function $f(\phi)$ (depending on the same polar angle that defines the direction of the electron momentum) determines the nature of the anisotropic impurity scattering. We assume that the scattering is ‘‘essentially’’ isotropic and introduce the following constraints:⁷

$$|V_1|^2 \leq |V_0|^2, \quad \langle f \rangle = 0, \quad \langle f^2 \rangle = 1, \quad (5)$$

where the angle brackets stand for averaging over the directions of momentum at the Fermi surface (the angle ϕ). Accordingly, the second term in (4) describes the deviations from isotropic scattering.

The normal and anomalous Green’s functions in such a superconductor are¹⁰

$$G(\omega, \mathbf{p}) = -\frac{i\tilde{\omega} + \xi_{\mathbf{p}}}{\tilde{\omega}^2 + \xi_{\mathbf{p}}^2 + |\tilde{\Delta}(\mathbf{p})|^2},$$

$$F(\omega, \mathbf{p}) = \frac{\tilde{\Delta}^*(\mathbf{p})}{\tilde{\omega}^2 + \xi_{\mathbf{p}}^2 + |\tilde{\Delta}(\mathbf{p})|^2}, \quad (6)$$

where $\omega = (2n+1)\pi T$,

$$\tilde{\omega}(\mathbf{p}) = \omega + i\rho \int \frac{d\mathbf{p}'}{(2\pi)^2} |V_{\text{imp}}(\mathbf{p}-\mathbf{p}')|^2 G(\omega, \mathbf{p}'),$$

$$\tilde{\Delta}(\mathbf{p}) = \Delta(\mathbf{p}) + \rho \int \frac{d\mathbf{p}'}{(2\pi)^2} |V_{\text{imp}}(\mathbf{p}-\mathbf{p}')|^2 F(\omega, \mathbf{p}'), \quad (7)$$

and ξ is the electron energy measured from the Fermi level.

To find the transition, or critical, temperature T_c we can restrict ourselves to the linear approximation in Δ in Eqs. (7):

$$\tilde{\omega} = \omega + i\rho \frac{N(0)}{2\pi} \times \int d\xi \int_0^{2\pi} d\phi \{ |V_0|^2 + |V_1|^2 f(\phi) f(\phi') \} \frac{\tilde{\omega}}{\tilde{\omega}^2 + \xi^2},$$

$$\tilde{\Delta} = \Delta + \rho \frac{N(0)}{2\pi} \times \int d\xi \int_0^{2\pi} d\phi \{ |V_0|^2 + |V_1|^2 f(\phi) f(\phi') \} \frac{\tilde{\Delta}}{\tilde{\omega}^2 + \xi^2}. \quad (8)$$

The linearized equation for the gap function, which determines the transition temperature T_c , is

$$\Delta(\mathbf{p}) = -T_c \sum_{\omega} \int \frac{d\mathbf{p}'}{(2\pi)^2} V(\mathbf{p}, \mathbf{p}') \frac{\tilde{\Delta}(\mathbf{p}')}{\tilde{\omega}^2 + \xi_{\mathbf{p}}'^2}. \quad (9)$$

Applying standard methods to Eq. (9) and the renormalization equations (8), we arrive at an equation for the transition temperature T_c in general form:

$$\ln \frac{T_c}{T_{c0}} = (\langle e \rangle^2 + \langle ef \rangle^2 - 1) \left[\Psi\left(\frac{1}{2} + \frac{\gamma_0}{2\pi T_c}\right) - \Psi\left(\frac{1}{2}\right) \right] + \langle ef \rangle^2 \left[\Psi\left(\frac{1}{2}\right) - \Psi\left(\frac{1}{2} + \frac{\gamma_0}{2\pi T_c} \left(1 - \frac{\gamma_1}{\gamma_0}\right)\right) \right], \quad (10)$$

where T_{c0} is the transition temperature in the absence of impurities, $\Psi(x)$ is the logarithmic derivative of the gamma function, $\gamma_0 = \pi\rho V_0^2 N(0)$ and $\gamma_1 = \pi\rho V_1^2 N(0)$ are, respectively, the isotropic and anisotropic scattering frequencies, and $\langle ef \rangle^2$ determines the overlap of the functions $e(\mathbf{p})$ and $f(\mathbf{p})$.

For simplicity we select the function $f(\mathbf{p})$ in a form similar to (2):

$$f(\mathbf{p}) \equiv f(\phi) = \sqrt{2} \cos(2\phi), \quad (11)$$

which ensures a maximum overlap in the d case. A more general approach can be found in Ref. 7. We can now write the renormalization equations (8) as follows:

$$\tilde{\omega} = \omega + i \frac{\gamma_0}{\pi} \int d\xi \frac{\tilde{\omega}}{\tilde{\omega}^2 + \xi^2} + i \frac{\gamma_1}{\pi^2} \cos(2\phi) \int d\xi \int d\phi' \cos(2\phi') \frac{\tilde{\omega}}{\tilde{\omega}^2 + \xi^2},$$

$$\tilde{\Delta} = \Delta + i \frac{\gamma_0}{\pi} \int d\xi \frac{\tilde{\Delta}}{\tilde{\omega}^2 + \xi^2} + i \frac{\gamma_1}{\pi^2} \cos(2\phi) \int d\xi \int d\phi' \cos(2\phi') \frac{\tilde{\Delta}}{\tilde{\omega}^2 + \xi^2}. \quad (12)$$

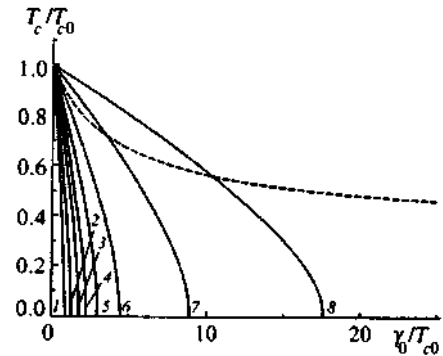


FIG. 1. T_c as a function of the disorder parameter γ_0/T_{c0} . The dashed curve corresponds to the case of s pairing and the solid curves, to the case of anisotropic d pairing for the following values of γ_1/γ_0 : curve 1, 0.0; curve 2, 0.3; curve 3, 0.5; curve 4, 0.6; curve 5, 0.7; curve 6, 0.8; curve 7, 0.9; and curve 8, 0.95.

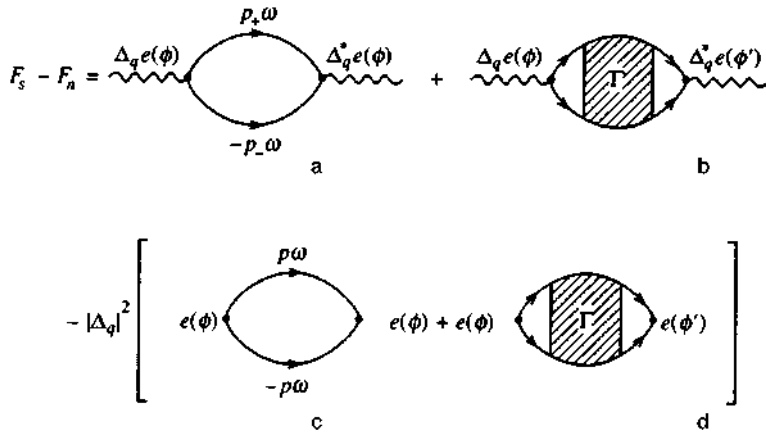


FIG. 2. The diagrammatic representation of the Ginzburg-Landau expansion. The electron lines are “dressed” by impurity scattering; Γ is the vertex part of the impurity scattering calculated in the ladder approximation. The diagrams (c) and (d) are calculated for $q=0$ and $T=T_c$, and $p_{\pm}=p \pm q/2$.

This yields the well-known expression for the renormalized frequency in both cases of interest:

$$\tilde{\omega} = \omega + \gamma_0 \operatorname{sgn} \omega. \quad (13)$$

In the case of d pairing the symmetry of the gap function in the presence of impurities does not change:

$$\tilde{\Delta} = \Delta \frac{|\tilde{\omega}|}{|\tilde{\omega}| - \gamma_1}. \quad (14)$$

When there is s pairing, the gap is renormalized by a constant independent of the angle ϕ and the frequency γ_1 :

$$\tilde{\Delta} = \Delta + \Delta_0 \frac{2\sqrt{2}\gamma_0}{\pi|\omega|}. \quad (15)$$

As a result, the equation for T_c in a superconducting with d pairing becomes

$$\ln \frac{T_c}{T_{c0}} = \Psi\left(\frac{1}{2}\right) - \Psi\left(\frac{1}{2} + \left(1 - \frac{\gamma_1}{\gamma_0}\right) \frac{\gamma_0}{2\pi T_c}\right). \quad (16)$$

For a superconductor with anisotropic s pairing we have

$$\ln \frac{T_c}{T_{c0}} = \left(1 - \frac{8}{\pi^2}\right) \left[\Psi\left(\frac{1}{2} + \frac{\gamma_0}{2\pi T_c}\right) - \Psi\left(\frac{1}{2}\right) \right]. \quad (17)$$

Note that in Eq. (17) there is no dependence on the anisotropic scattering rate.

Figure 1 plots T_c vs. γ_0/T_{c0} for the case of d pairing for different values of γ_1/γ_0 . For an s -type superconductor the transition temperature T_c becomes weakly suppressed as γ_0/T_{c0} increases. For a d -type superconductor the transition temperature T_c at small values of γ_1 becomes suppressed very rapidly, but as γ_1/γ_0 increases, the critical value γ_{0c}/T_{c0} at which superconductivity disappears rapidly increases.

As usual, for the order parameter in which the free energy is expanded we take the gap function. Here we assume that the amplitude $\Delta(T)$ is a slowly varying function of position. In momentum space we have the following Fourier transfer of the order parameter:

$$\Delta(\phi, q) = \Delta_q(T) e(\phi). \quad (18)$$

The Ginzburg-Landau expansion for the difference of free energies of the superconducting and normal states has the following form (accurate to within terms quadratic in Δ in the region of small values of q):

$$F_s - F_n = A|\Delta_q|^2 + q^2 C|\Delta_q|^2; \quad (19)$$

it is determined by the diagrams (see Fig. 2) of the loop expansion for the electron free energy in the order-parameter

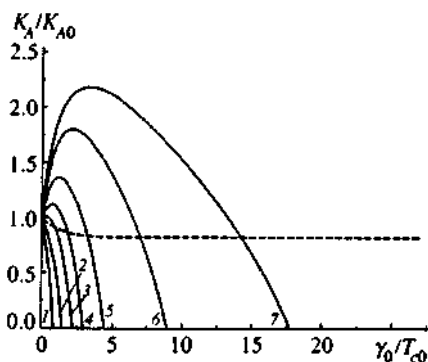


FIG. 3. The dimensionless coefficient K_A/K_{A0} as a function of the disorder parameter γ_0/T_{c0} . The dashed curve corresponds to the case of s pairing and the solid curves to the case of anisotropic d pairing, for the following values of γ_1/γ_0 : curve 1, 0.0; curve 2, 0.4; curve 3, 0.6; curve 4, 0.7; curve 5, 0.8; curve 6, 0.9; and curve 7, 0.95.

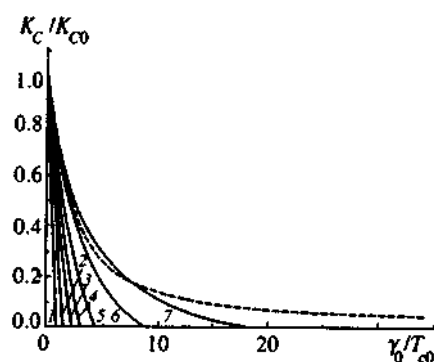


FIG. 4. The dimensionless coefficient K_C/K_{C0} as a function of the disorder parameter γ_0/T_{c0} . The dashed curve corresponds to the case of s pairing and the solid curves to the case of anisotropic d pairing, for the following values of γ_1/γ_0 : curve 1, 0.0; curve 2, 0.4; curve 3, 0.6; curve 4, 0.7; curve 5, 0.8; curve 6, 0.9; and curve 7, 0.95.

fluctuation field with a small wave vector \mathbf{q} . Subtraction of the diagrams (c) and (d) guarantees that the coefficient A vanishes at the transition point $T=T_c$. In Appendices A and B we give the details of calculations of, respectively, the vertex part Γ_{pp} and the Ginzburg–Landau coefficients for a d -type superconductor. Note that for d -type superconductors the “diffusion” renormalization due to the diagrams of type (b) and (d) is zero to within terms quadratic in q , provided that the anisotropy of impurity scattering is ignored. For an s -type superconductor the calculations are similar, but here there is no dependence on the anisotropic component of the scattering.

As a result, the Ginzburg–Landau coefficients can be written as

$$A=A_0K_A, \quad C=C_0K_C, \quad (20)$$

where A_0 and C_0 are the usual expressions for isotropic s pairing:¹¹

$$A_0=N(0)\frac{T-T_c}{T_c}, \quad C_0=N(0)\frac{7\zeta(3)}{48\pi^2}\frac{v_F^2}{T_c^2}; \quad (21)$$

here v_F and $N(0)$ are the electron velocity and the density of states at the Fermi surface. All properties of the models are contained in the dimensionless coefficients K_A and K_C . In the absence of impurities we have $K_A^0=1$ and $K_C^0=3/2$ in both models. For a system with impurities we have the following.

(A) d pairing:

$$K_A=\frac{\gamma_0}{4\pi T_c}\int_{-\omega_c}^{\omega_c}\frac{d\xi}{\xi} \times \int_{-\infty}^{\infty}d\omega\frac{\omega+\xi}{(\omega^2+\gamma_0^2)\cosh^2\left(\frac{\omega+\xi}{2T_c}\right)}+\frac{\gamma_1(2\gamma_0+\gamma_1)}{4T_c} \times \int_{-\infty}^{\infty}d\omega\frac{\omega^2}{(\omega^2+\gamma_0^2)(\omega^2+(\gamma_0-\gamma_1)^2)\cosh^2\left(\frac{\omega}{2T_c}\right)}, \quad (22)$$

$$K_C=\frac{3\pi T_c}{7\zeta(3)\gamma_1}\left\{\frac{2\pi T_c}{\gamma_1}\left[\Psi\left(\frac{1}{2}+\frac{\gamma_0-\gamma_1}{2\pi T_c}\right)-\Psi\left(\frac{1}{2}+\frac{\gamma_0}{2\pi T_c}\right)\right]+\Psi'\left(\frac{1}{2}+\frac{\gamma_0-\gamma_1}{2\pi T_c}\right)\right\}; \quad (23)$$

(B) anisotropic s pairing:

$$K_A=\frac{\gamma_0}{\pi T_c}\left\{\frac{1}{4}\int_{-\omega_c}^{\omega_c}\frac{d\xi}{\xi} \times \int_{-\infty}^{\infty}d\omega\frac{\omega+\xi}{(\omega^2+\gamma_0^2)\cosh^2\left(\frac{\omega+\xi}{2T_c}\right)}+\frac{2\gamma_0}{\pi}\right\}$$

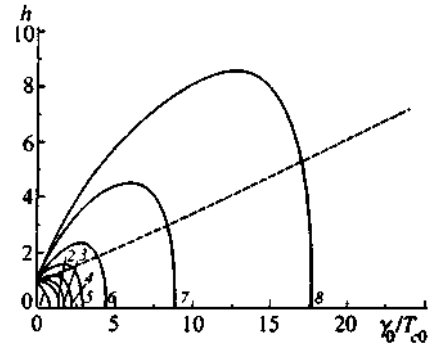


FIG. 5. The normalized slope of the curve of the upper critical field, $h=|dH_{c2}/dT|_{T_c}/|dH_{c2}/dT|_{T_{c0}}$, as a function of the disorder parameter γ_0/T_{c0} . The dashed curve corresponds to the case of s pairing and the solid curves to the case of anisotropic d pairing for the following values of γ_1/γ_0 : curve 1, 0.0; curve 2, 0.4; curve 3, 0.5; curve 4, 0.6; curve 5, 0.7; curve 6, 0.8; curve 7, 0.9; and curve 8, 0.95.

$$\times \int_{-\infty}^{\infty}d\omega\frac{1}{(\omega^2+\gamma_0^2)\cosh^2\left(\frac{\omega}{2T_c}\right)}, \quad (24)$$

$$K_C=-\frac{3(\pi^2-8)}{28\pi^2\zeta(3)}\Psi''\left(\frac{1}{2}+\frac{\gamma_0}{2\pi T_c}\right) + \frac{24\pi^2}{7\zeta(3)\gamma_0^2}\frac{T_c^2}{(\pi^2-8)\gamma^2}\ln\frac{T_c}{T_{c0}}+\frac{6\pi}{7\zeta(3)}\frac{T_c}{\gamma_0}. \quad (25)$$

The results of numerical calculations of the dimensionless coefficients as functions of the parameter γ_0/T_{c0} in the case of d pairing for different values of γ_1/γ_0 are depicted in Figs. 3 and 4.

3. THE UPPER CRITICAL FIELD

As is well known,¹¹ the behavior of the Ginzburg–Landau coefficients A and C determines the temperature dependence of the upper critical magnetic field near T_c :

$$H_{c2}=\frac{\phi_0}{2\pi\xi^2(T)}=-\frac{\phi_0}{2\pi}\frac{A}{C}, \quad (26)$$

where $\phi_0=c\pi/e$ is the magnetic flux quantum, and $\xi(T)$ is the temperature-dependent coherence length. From this we can easily find the slope of the curve representing the temperature dependence of H_{c2} near T_c , i.e., the temperature derivative of the field:

$$\left|\frac{dH_{c2}}{dT}\right|_{T_c}=\frac{24\pi\phi_0}{7\zeta(3)v_F^2}T_c\frac{K_A}{K_C}. \quad (27)$$

For an s -type superconductor the slope of the curve of the upper critical field is independent of the anisotropic scattering. Figure 5 depicts the dependence of the dimensionless parameter $h=|dH_{c2}/dT|_{T_c}/|dH_{c2}/dT|_{T_{c0}}$ on the disorder parameter γ_0/T_{c0} in the case of d pairing for different values of γ_1/γ_0 . In the case of anisotropic s pairing, the slope of the curve of the upper critical field increases with disorder

as usual,⁶ and in the strong scattering limit, $\gamma_0 \gg T_c$, the dependence of h on γ_0 becomes linear and the slope is given by the well-known Gor'kov formula¹²

$$\frac{\sigma}{N(0)} \left| \frac{dH_{c2}}{dT} \right|_{T_c} = \frac{8e^2}{\pi^2} \phi_0, \quad (28)$$

where $\sigma = N(0)e^2 v_F^2 / 3 \gamma_0$ is the electron conductivity in the normal phase with isotropic s pairing, characteristic of ordinary dirty superconductors. Hence strong disorder suppresses the anisotropy of the gap, and we pass to the usual limit of a dirty superconductor.

In the case of d pairing, the slope of the curve of the field H_{c2} for small values of γ_1 / γ_0 rapidly drops to zero on the scale $\gamma_0 \sim T_{c0}$. In the interval $0.5 \leq \gamma_1 / \gamma_0 \leq 0.6$ the behavior of the slope changes dramatically: first h increases slowly but nonlinearly with γ_0 / T_{c0} , then it passes through a maximum, and then rapidly drops. The length of the section where the slope grows rapidly increases as $\gamma_1 \rightarrow \gamma_0$. We believe that such strong anomalies in the way the slope of the curve of the upper critical field depends on the disorder parameter can be used to determine the pairing type and the possible role of anisotropic scattering in unusual superconductors. Unfortunately, in the case of high- T_c superconducting systems the situation is complicated by the well-known nonlinearity of the temperature dependence of H_{c2} , a feature observed in a broad temperature range starting at T_c , and by a certain indeterminacy in the experimental methods used to determine H_{c2} .

The present work was partially supported by the Russian Fund for Fundamental Research (Project 96-02-16065), by the Statistical Physics State Program (Project IX.1), and by the High- T_c Superconductivity State Program of the Russian Ministry of Science (Project 96-051).

APPENDIX A: CALCULATION OF THE VERTEX PART $\Gamma_{\mathbf{p}\mathbf{p}'}$ IN THE LADDER APPROXIMATION

The Bethe–Salpeter equation for the vertex part is

$$\Gamma_{\mathbf{p}\mathbf{p}'} = U(\mathbf{p}, \mathbf{p}') + \sum_{\mathbf{p}''} U(\mathbf{p}, \mathbf{p}'') G^R(\mathbf{p}'') G^A(\mathbf{p}'') \Gamma_{\mathbf{p}''\mathbf{p}'}, \quad (A1)$$

where $U(\mathbf{p}, \mathbf{p}')$ is the irreducible vertex part. We take $U(\mathbf{p}, \mathbf{p}')$ in the form (the ladder approximation)

$$U(\mathbf{p}, \mathbf{p}') = \rho V_0^2 + \rho V_1^2 f(\mathbf{p}) f(\mathbf{p}'). \quad (A2)$$

Then Eq. (A1) can be written as follows:

$$\Gamma_{\mathbf{p}\mathbf{p}'} = \rho V_0^2 + \rho V_1^2 f(\mathbf{p}) f(\mathbf{p}') + \rho V_0^2 \Psi(\mathbf{p}') + \rho V_1^2 f(\mathbf{p}) \Phi(\mathbf{p}'), \quad (A3)$$

where

$$\Psi(\mathbf{p}') = \sum_{\mathbf{p}''} G^R(\mathbf{p}'') G^A(\mathbf{p}'') \Gamma_{\mathbf{p}''\mathbf{p}'},$$

$$\Phi(\mathbf{p}') = \sum_{\mathbf{p}''} f(\mathbf{p}'') G^R(\mathbf{p}'') G^A(\mathbf{p}'') \Gamma_{\mathbf{p}''\mathbf{p}'}. \quad (A4)$$

From (A3) we can obtain a self-consistent system of equation for the functions $\Psi(\mathbf{p}')$ and $\Phi(\mathbf{p}')$:

$$\begin{cases} \Psi(\mathbf{p}') = \rho V_0^2 I_1 + \rho V_1^2 f(\mathbf{p}') I_2 + \rho V_0^2 I_1 \Psi(\mathbf{p}') + \rho V_1^2 I_2 \Phi(\mathbf{p}'), \\ \Phi(\mathbf{p}') = \rho V_0^2 I_2 + \rho V_1^2 f(\mathbf{p}') I_3 + \rho V_0^2 I_2 \Psi(\mathbf{p}') + \rho V_1^2 I_3 \Phi(\mathbf{p}'), \end{cases} \quad (A5)$$

where

$$I_1 = \sum_{\mathbf{p}} G^R(\mathbf{p}) G^A(\mathbf{p}),$$

$$I_2 = \sum_{\mathbf{p}} f(\mathbf{p}) G^R(\mathbf{p}) G^A(\mathbf{p}),$$

$$I_3 = \sum_{\mathbf{p}} f^2(\mathbf{p}) G^R(\mathbf{p}) G^A(\mathbf{p}). \quad (A6)$$

Solving the system of equations (A5), we arrive at expressions for $\Psi(\mathbf{p}')$ and $\Phi(\mathbf{p}')$ and hence for the vertex part:

$$\Gamma_{\mathbf{p}\mathbf{p}'} = \frac{\rho V_0^2 (1 - \rho V_1^2 I_3 + \rho V_1^2 f(\mathbf{p}') I_2) + \rho V_1^2 (f(\mathbf{p}) f(\mathbf{p}') (1 - \rho V_0^2 I_1) + \rho V_0^2 f(\mathbf{p}) I_2)}{(1 - \rho V_0^2 I_1)(1 - \rho V_1^2 I_3) - \rho V_0^2 \rho V_1^2 I_2^2}. \quad (A7)$$

APPENDIX B: THE GINZBURG–LANDAU COEFFICIENTS

The diagram (a) in Fig. 2 corresponds to

$$-\frac{T}{(2\pi)^2} \Delta_q^2 \sum_{\omega} \int d\mathbf{p}_2 \cos^2(2\phi) G_{\omega}(\mathbf{p}_+) G_{-\omega}(\mathbf{p}_-) =$$

$$-\Delta_q^2 T N(0) \sum_{\omega} \int \frac{d\xi}{\bar{\omega}^2 + \xi^2}$$

$$+ \Delta_q^2 q^2 \frac{N(0) \pi v_F^2 T_c}{8} \sum_{\omega} \frac{1}{|\bar{\omega}|^3}. \quad (B1)$$

The diagram (c) in Fig. 2 corresponds to

$$-\frac{T}{(2\pi)^2} \Delta_q^2 \sum_{\omega} \int d\mathbf{p}_2 \cos^2(2\phi) G_{\omega}(\mathbf{p}) G_{-\omega}(\mathbf{p}) =$$

$$-\Delta_q^2 T_c N(0) \sum_{\omega} \int \frac{d\xi}{\tilde{\omega}^2 + \xi^2}. \quad (\text{B2})$$

The diagram with a ‘‘diffuson’’ (Fig. 2b) yields

$$-T \sum_{\omega} \sum_{\mathbf{p}\mathbf{p}'} \sqrt{2} \cos(2\phi) G^R(\mathbf{p}_+) G^A(\mathbf{p}_-) \Gamma_{\mathbf{p}\mathbf{p}'} \\ \times \sqrt{2} \cos(2\phi') G^R(\mathbf{p}'_+) G^A(\mathbf{p}'_-). \quad (\text{B3})$$

If we take (A6) and (A7) into account, Eq. (B3) becomes

$$-TN(0) \pi \gamma_1 \sum_{\omega} \left[\frac{1}{|\tilde{\omega}|(|\tilde{\omega}| - \gamma_1)} - \frac{v_F^2 (2|\tilde{\omega}| - \gamma_1) q^2}{8|\tilde{\omega}|^3 (|\tilde{\omega}| - \gamma_1)^2} \right]. \quad (\text{B4})$$

Note that when there is no anisotropic scattering component, for d -type superconductors the diffusion renormalization due to the diagrams of the type depicted in Fig. 2c is zero to within terms quadratic in q .

Reasoning along similar lines, we arrive at an expression corresponding to the diagram (d) in Fig. 2:

$$-TN(0) \pi \gamma_1 \sum_{\omega} \frac{1}{|\tilde{\omega}|(|\tilde{\omega}| - \gamma_1)}. \quad (\text{B5})$$

Writing the expression for $F_s - F_n$ and separating out the coefficients of q raised to the zeroth power and of q^2 , we can obtain the expressions for the corresponding Ginzburg–Landau coefficients.

^{*}E-mail: sadovski@ief.intec.ru

¹D. Pines, *Physica C* **235–240**, 113 (1994).

²S. Chakravarty, A. Subdó, P. W. Anderson, and S. Strong, *Science* **261**, 337 (1993).

³A. I. Liechtenstein, I. I. Mazin, and O. K. Andersen, *Phys. Rev. Lett.* **74**, 2303 (1995).

⁴L. S. Borkovski and P. J. Hirschfeld, *Phys. Rev. B* **49**, 15 404 (1994).

⁵R. Fehrenbacher and M. R. Norman, *Phys. Rev. B* **50**, 3495 (1994).

⁶A. I. Posazhennikova and M. V. Sadovskii, *JETP Lett.* **63**, 358 (1996).

⁷G. Harañ and A. D. S. Nagi, *Phys. Rev. B* **54**, 15 463 (1996).

⁸M. V. Sadovskii, ‘Sverkhprovodimost’: *Fiz. Khim. Tekhnol.* **8**, 337 (1995); submitted to *Phys. Rep.* (1997).

⁹M. V. Sadovskii and A. I. Posazhennikova, *JETP Lett.* **65**, 270 (1997).

¹⁰A. A. Abrikosov, L. P. Gor’kov, and I. Ye. Dzyaloshinski, *Quantum Field Theoretical Methods in Statistical Physics*, Pergamon Press, New York (1965).

¹¹P. G. de Gennes, *Superconductivity of Metals and Alloys*, W. A. Benjamin, New York (1966).

¹²L. P. Gor’kov, *Zh. Éksp. Teor. Fiz.* **37**, 1407 (1959) [*Sov. Phys. JETP* **10**, 998 (1960)].

Translated by Eugene Yankovsky

Combinatorial analysis of Feynman diagrams in problems with a Gaussian random field

É. Z. Kuchinskiĭ and M. V. Sadovskĭĭ

Institute of Electrophysics, Ural Division, Russian Academy of Sciences, 620049 Ekaterinburg, Russia
(Submitted 16 May 1997)

Zh. Éksp. Teor. Fiz. **113**, 664–678 (February 1998)

We construct an algorithm for calculating the generating function for the number of skeleton graphs of the irreducible self-energy and vertex parts in the diagram technique for problems with a Gaussian random field. The exact recursion relation, defining the number of graphs in any order of perturbation theory, and the asymptotics in the high-order limit are found. The results obtained are applied to an analysis of the problem of an electron in a Gaussian random field with a white-noise correlator. A closed integral equation for the one-electron Green’s function, the kernel of which is determined by the generating function, can be constructed in the approximation of equal skeleton graphs for the self-energy part in a given order of perturbation theory. An analysis shows that the approximation considered gives a qualitatively correct description of the tail of the state density in the region of negative energies and, probably, is fully applicable in the most interesting region of strong scattering near the edge of the original band where the asymptotics of the Green’s function and the state density can be determined in the limit of infinitely strong scattering. © 1998 American Institute of Physics. [S1063-7761(98)02102-7]

1. INTRODUCTION

Methods of summing Feynman diagrams are widely used in the consideration of a broad class of problems in theoretical physics in which the propagation of elementary perturbations (or quasiparticles) in statistically random fields created by an inhomogeneity is investigated. The simplest example of such a system is an electron propagating in a system of impurity atoms. It was precisely for this problem that the diagram technique to be considered in this paper was first formulated.^{1,2} A similar technique is used in considering problems of statistical radiophysics and optics associated with the propagation of electromagnetic waves in disordered media.³ The equivalent mathematical approach is applicable for a number of problems in the theory of critical phenomena in disordered systems,⁴ in the problem of a polymer chain with an excluded volume and other problems in the physics of polymer systems.⁵ Exactly the same diagram technique describes the regular model of critical phenomena with a zero-component order parameter.⁴

Information about the combinatorial analysis of graphs, i.e., about the number of diagrams of a given type in a given order of perturbation theory, is extremely useful in considering problems associated with the summation of Feynman diagrams. In this paper we will investigate in detail the question of the combinatorial analysis of diagrams in the above-mentioned class of problems.

2. GENERATING FUNCTION OF SKELETON DIAGRAMS: RECURSION RELATION

To be specific we will discuss the problem of an electron with energy E and momentum \mathbf{p} , propagating in a Gaussian random field (a system of random impurities).^{1,2} The average

one-particle Green’s function is defined by the diagram series shown in Fig. 1a. This expansion is reduced in the usual fashion to the Dyson form:

$$G(E, p) = \frac{1}{E - \varepsilon_p - \Sigma(E, p)}, \tag{1}$$

where $\varepsilon_p = p^2/2m$ is the spectrum of a free electron, and the eigen-energy part $\Sigma(E, p)$ is determined by the skeleton graphs of Fig. 1b, in which the interior electron line represents the total (or dressed) Green’s function $G(E, p)$.

The total number of graphs in the N th order of perturbation theory in the expansion of Fig. 1a, as it is easy to see, is equal to

$$G_N = (2N - 1)!! = \frac{(2N - 1)!}{2^{N-1}(N - 1)!}, \tag{2}$$

this is determined simply by the number of methods of connecting $2N$ vertices by N impurity lines. The problem of determining the analogous number of graphs Σ_N in the expansion of Fig. 1b is much more complicated, and as far as we know there is no exact answer in the literature. The simple inequality

$$(2N - 1)!! > \Sigma_N > (2N - 3)!!, \tag{3}$$

was found in Ref. 6, which only gives a fairly rough estimate of the quantity Σ_N . As we will see, the problem can be solved exactly. This follows directly from the exact solution of the problem of an electron in a random potential $V(\mathbf{r}) = V$, where the quantity V does not depend on the spatial coordinate r but has a Gaussian distribution with width $\langle V^2 \rangle = W^2$. It is natural that in this case the diagram technique has the standard form of Fig. 1, and each line of impurity interaction transfers zero momentum, i.e., it corre-

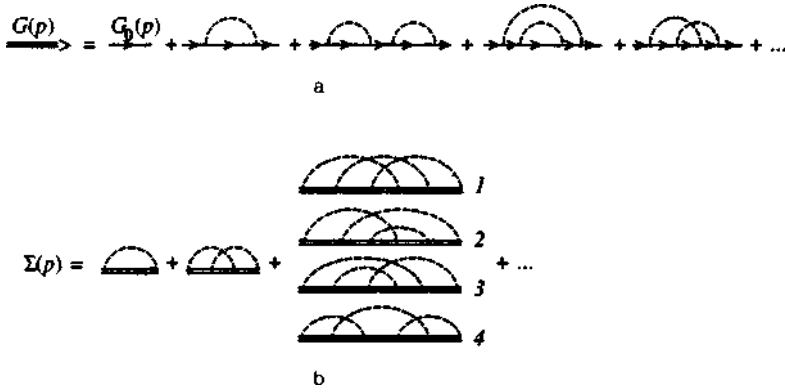


FIG. 1. Diagram series for average one-electron Green's function (a) and self-energy part (b). Dashed line corresponds to mean-square correlator of random field, G_0 is the free Green's function.

sponds (in the momentum representation) to the correlator $(2\pi)^d W^2 \delta(\mathbf{q})$ (d is the dimensionality of space).^{7,8} All contributions of the same order in the expansion of Fig. 1a turn out to be the same, and the series for the Green's function is represented in the form⁷

$$G(E, p) = G_0(E, p) \left\{ 1 + \sum_{N=1}^{\infty} (2N-1)!! G_0^{2N}(E, p) W^{2N} \right\}. \quad (4)$$

Then through the use of the representation

$$(2N-1)!! = \frac{1}{\sqrt{2\pi}} \int_{-\infty}^{\infty} dt t^{2N-2} e^{-t^2/2} \quad (5)$$

the series (4) is easily summed and we obtain¹⁾

$$G(E, p) = \frac{1}{W} \Psi \left(\frac{1}{WG_0(E, p)} \right), \quad (6)$$

where the function

$$\Psi(z) = -\frac{1}{\sqrt{2\pi}} \int_{-\infty}^{\infty} dt e^{-t^2/2} \frac{1}{t-z}, \quad (7)$$

has been introduced.

Let us consider the self-energy part, corresponding to the Green's function (6). Since the addition of an impurity line leads in this problem simply to the additional multiplier $W^2 G^2$, the self-energy part defined by the expansion of Fig. 1b can be written in the form

$$\Sigma = Q(W^2 G^2) W^2 G, \quad (8)$$

where $Q(x)$ is some function. We will see that this function is the generating function of the number of skeleton graphs for the self-energy part, i.e., its Taylor series expansion coefficients give the desired numbers Σ_N .

Let us write the Dyson equation for the problem being considered:

$$G = G_0 + G_0 \Sigma G = G_0 (1 + Q(W^2 G^2) W^2 G^2). \quad (9)$$

Introducing $z = (WG_0)^{-1}$ and $y = W^2 G^2$, we obtain the following parametric representation of $Q(y)$ from Eqs. (6) and (9):

$$\begin{aligned} 1 + yQ(y) &= z\Psi(z) = z\sqrt{y}, \\ y &= \Psi^2(z). \end{aligned} \quad (10)$$

This representation of the function Q is rather inconvenient. Let us show that a differential equation can be obtained for it. It is easy to prove that the function $\Psi(z)$ satisfies the usual dispersion relation²⁾

$$\begin{aligned} \text{Re } \Psi(z) &= \frac{1}{\pi} \int_{-\infty}^{\infty} dt \frac{\text{Im } \Psi(t)}{t-z}, \\ \frac{1}{\pi} \text{Im } \Psi(t) &= \mp \frac{1}{\sqrt{2\pi}} e^{-t^2/2}, \end{aligned} \quad (11)$$

from which it follows immediately that $\Psi(z)$ satisfies the differential equation

$$\frac{d\Psi}{dz} = 1 - z\Psi \quad (12)$$

with the initial condition

$$\Psi(z = \pm i0) = \mp i\sqrt{\pi/2}. \quad (13)$$

Differentiating the first equation in (10) with respect to y , we obtain

$$\frac{dz}{dy} = \frac{1}{2} y^{-3/2} \left\{ 2y^2 \frac{dQ(y)}{dy} + yQ(y) - 1 \right\}. \quad (14)$$

Differentiating the second equation in (10) with respect to z and using Eq. (12), we have

$$\begin{aligned} \frac{dy}{dz} &= 2\Psi(z) \frac{d\Psi(z)}{dz} = 2\Psi(z)(1 - z\Psi(z)) \\ &= -2y^{3/2} Q(y). \end{aligned} \quad (15)$$

By equating Eqs. (14) and (15), we obtain a nonlinear differential equation for $Q(y)$:

$$\frac{dQ(y)}{dy} = \frac{1}{2y^2} \{ 1 - Q^{-1}(y) + y(Q)(y) \}. \quad (16)$$

Using Eqs. (10) and (13), we obtain $y = \Psi^2(z)|_{z=\pm i0} = -\pi/2$, so that

$$Q \left(-\frac{\pi}{2} \right) = \frac{z\Psi(z) - 1}{7} \Big|_{z=\pm i0} = \frac{2}{\pi}, \quad (17)$$

TABLE I.

N	$\Gamma_N = a_N$	$b_N = a_N / (2N + 1)!!$	$\Sigma_N = a_{N-1}$	$U_N = (2N - 1)a_{N-1}$
1	1	0.3333	1	1
2	4	0.2667	1	3
3	27	0.2571	4	20
4	248	0.2624	27	189
5	2830	0.2722	248	2232
6	38232	0.2829	2830	3120
7	593859	0.2930	38232	497016
8	10401712	0.3019	593859	8907885
9	202601898	0.3158	10401712	176829104
10	4342263000	0.3211	202601898	3849436062
$N \gg 1$	$\frac{1}{e} \left[1 - \frac{5}{4N} \right] (2N + 1)!!$	$\frac{1}{e} \left[1 - \frac{5}{4N} \right]$	$\frac{1}{e} \left[1 - \frac{5}{4N} \right] (2N - 1)!!$	$\frac{1}{e} \left[1 - \frac{9}{4N} \right] (2N + 1)!!$

which is the initial condition for Eq. (16). Note that the point $Q(0) = 1$, with an obviousness that follows from the diagram representation for Σ , is a singular point for Eq. (16) and cannot serve as the initial condition.

Equation (16) can be rewritten in a form that is more convenient for further analysis

$$Q(y) = 1 + y \frac{d}{dy} y Q^2(y). \tag{18}$$

We are interested in the Taylor series expansion of $Q(y)$:

$$Q(y) = \sum_{n=0}^{\infty} a_n y^n. \tag{19}$$

Since the number of skeleton diagrams of N th order for the self-energy part is simply the coefficient for W^{2N} in the series expansion of Σ in powers of W^2 , it is easy to see that Eq. (8) gives the desired Σ_N in the form

$$\Sigma_N = a_{N-1}. \tag{20}$$

This also means that the function $Q(y)$ is the generating function for the combinatorial factors Σ_N of interest to us.

The substitution of Eq. (19) into (18) leads to the following recursion relation for the coefficients a_n :

$$a_n = n \sum_{m=0}^{n-1} a_m a_{n-1-m}, \tag{21}$$

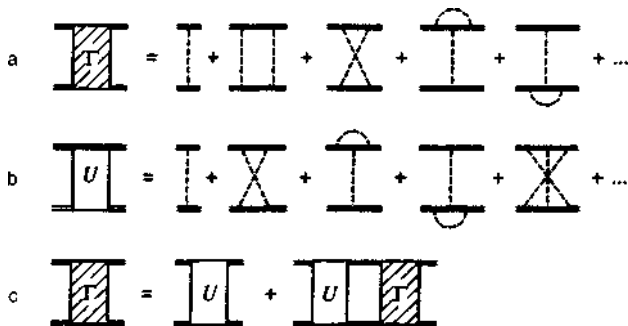


FIG. 2. Diagram series for the total vertex part Γ (a), for the irreducible vertex U (b), and the Bethe-Salpeter equation interrelating Γ and U (c).

where $a_0 = 1$. It follows directly from $a_0 = 1$ that $Q(0) = 1$. It is precisely in this sense that this point is singular—the relation $Q(0) = 1$ is satisfied for any initial conditions for which Eq. (18) has a solution.

From Eq. (21) it is easy to find the a_n values for small n ; the corresponding results are listed in Table I.

By knowing the combinatorial analysis of the diagrams for the self-energy part, we can easily reproduce the combinatorial analysis for the two-particle Green's function—both for the total vertex part Γ and for the irreducible vertex U , the diagram expansion for which is given in Fig. 2. Actually, the self-energy part Σ is related to the total vertex Γ by the equation represented graphically in Fig. 3. For a problem with zero transferred momentum^{7,8} this equation has the form

$$\Sigma = W^2 G (1 + G^2 \Gamma). \tag{22}$$

Therefore, for the number of N th-order diagrams in the total vertex Γ_N we obtain immediately

$$\Gamma_N = \Sigma_{N+1} = a_N. \tag{23}$$

Thus, the function $Q(y)$ is also the generating function for the number of diagrams of the total vertex part.

The number of N th-order diagrams for the irreducible vertex U_N can easily be obtained if it is noted that a break of any of the $2N - 1$ interior Green's lines in the diagram for the N th-order self-energy part generates the corresponding diagram for the N th-order contribution to the irreducible vertex U (Fig. 4). Therefore,

$$U_N = (2N - 1) \Sigma_N = (2N - 1) a_{N-1}. \tag{24}$$

In the Appendix we rederive the differential equation (18) for the generating function $Q(y)$ using only the Bethe-



FIG. 3. Equations relating the eigen-energy part to the total vertex.

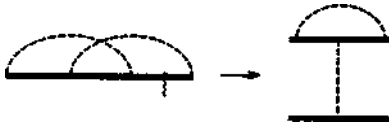


FIG. 4. Breaking of any of $2N - 1$ interior lines of the Green's function in N th-order skeleton diagram for self-energy part produces corresponding diagram for U .

Salpeter equation, which relates U to Γ , and the Ward identity, without using the explicit form of the Green's function (6).

3. ASYMPTOTICS FOR THE NUMBER OF DIAGRAMS FOR LARGE N

In the high-order limit $N \gg 1$ it becomes inconvenient to use the recursion relation (21) in view of the factorial increase in the number of diagrams.⁶ At the same time the very fact of factorial growth can be used for a considerable simplification of the problem. We rewrite Eq. (21) in the form

$$a_n = na_0a_{n-1} + na_1a_{n-2} + na_2a_{n-3} + \dots, \tag{25}$$

where $a_0 = 1, a_1 = 1, a_2 = 4$. It is natural to assume that in the limit of large n we have $a_n \approx (2n + \beta)a_{n-1}$; then $a_{n-2} \approx a_{n-1}/(2n - 2 + \beta)$, etc. The substitution of these expressions into Eq. (25) immediately gives $\beta = 1$ and

$$a_n = \left(2n + 1 + O\left(\frac{1}{n}\right)\right)a_{n-1}. \tag{26}$$

This means that in the limit of large n we have $a_n \sim (2n + 1)!!$. We define b_n as

$$b_n = \frac{a_n}{(2n + 1)!!}. \tag{27}$$

Substituting Eq. (27) into (21), we obtain a recursion relation for b_n :

$$b_n = n \sum_{m=0}^{n-1} \frac{(2m + 1)!!(2n - 2m - 1)!!}{(2n + 1)!!} b_m b_{n-1-m}, \tag{28}$$

and $b_0 = 1$. In the limit of large n and taking into account $b_1 = 1/3, b_2 = 4/15$, which limits the accuracy to the order of b/n^2 (where $b \sim b_n \sim b_{n-1} \sim b_{n-2} \sim b_{n-3}$), we obtain

$$\Delta b_n = b_n - b_{n-1} = \frac{5}{4} \frac{b_{n-1}}{n^2} + O\left(\frac{b}{n^3}\right). \tag{29}$$

Thus, in the limit of large n we can write the following differential equation for b_n :

$$\frac{db_n}{dn} = \frac{5}{4} \frac{b_n}{n^2} + O\left(\frac{b}{n^3}\right), \tag{30}$$

from which it immediately follows that

$$b_n = b \exp\left(-\frac{5}{4} \frac{1}{n} + O\left(\frac{1}{n^2}\right)\right) = b \left\{1 - \frac{5}{4} \frac{1}{n} + O\left(\frac{1}{n^2}\right)\right\}. \tag{31}$$

Of course, on the basis of such an analysis it is impossible to determine the constant $b = \lim b_n$ as $n \rightarrow \infty$. A numerical

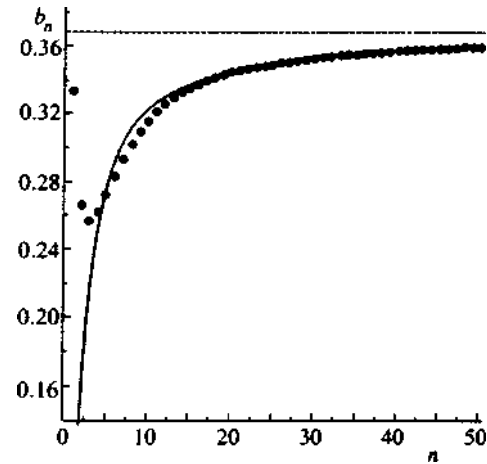


FIG. 5. Behavior of b_n with increase in n . Points correspond to b_n values obtained from recursion relation (28), the curve corresponds to the asymptotic dependence $e^{-1}(1 - 5/4n)$, the dashed line corresponds to the asymptotic function $1/e$.

analysis of the behavior of b_n using the recursion relation (28) completely corroborates the relationship (31) (see Fig. 5) and gives $b = 1/e = 0.36787944\dots$ (Calculations were carried out up to $n = 5000$, which ensures the stated accuracy.) We know of no analytical method for obtaining this curious result.

Finally, the asymptotics of the number of diagrams of different types for large N have the form³⁾

$$\begin{aligned} \Sigma_N = a_{N-1} &= b_{N-1}(2N - 1)!! \\ &= \frac{1}{e} \left\{1 - \frac{5}{4} \frac{1}{N} + O\left(\frac{1}{N^2}\right)\right\} (2N - 1)!! \\ &= \frac{1}{\sqrt{\pi e}} \left\{1 - \frac{5}{4} \frac{1}{N} + O\left(\frac{1}{N^2}\right)\right\} 2^N \Gamma\left(N + \frac{1}{2}\right), \end{aligned} \tag{32}$$

$$\begin{aligned} \Gamma_N = a_N &= \frac{1}{e} \left\{1 - \frac{5}{4} \frac{1}{N} + O\left(\frac{1}{N^2}\right)\right\} (2N + 1)!! \\ &= \frac{1}{\sqrt{\pi e}} \left\{1 - \frac{5}{4} \frac{1}{N} + O\left(\frac{1}{N^2}\right)\right\} 2^{N+1} \Gamma\left(N + \frac{3}{2}\right), \end{aligned} \tag{33}$$

$$\begin{aligned} U_N = (2N - 1)a_{N-1} &= \frac{1}{e} \left\{1 - \frac{5}{4} \frac{1}{N} + O\left(\frac{1}{N^2}\right)\right\} (2N - 1) \\ &\quad \times (2N - 1)!! = \frac{1}{e} \left\{1 - \frac{9}{4} \frac{1}{N} + O\left(\frac{1}{N^2}\right)\right\} (2N + 1)!! \\ &= \frac{1}{\sqrt{\pi e}} \left\{1 - \frac{9}{4} \frac{1}{N} + O\left(\frac{1}{N^2}\right)\right\} 2^{N+1} \Gamma\left(N + \frac{3}{2}\right). \end{aligned} \tag{34}$$

It is interesting to note that

$$\frac{\Sigma_N}{G_N} = b_{N-1} = \frac{1}{e} \left\{1 - \frac{5}{4} \frac{1}{N} + O\left(\frac{1}{N^2}\right)\right\} \rightarrow \frac{1}{e}, \tag{35}$$

$$\frac{U_N}{\Gamma_N} = 1 - \frac{1}{N} + O\left(\frac{1}{N^2}\right) \rightarrow 1. \tag{36}$$

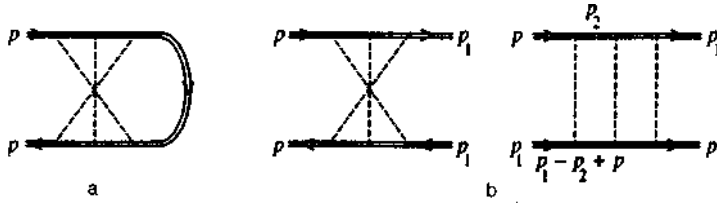


FIG. 6. (a)—base graph used in constructing approximation for eigen-energy part, (b)—expanded sequence of maximally intersecting graphs gives ladder in the case of system invariance with respect to time reversal operation.

Table I summarizes the principal results for the number of graphs of different types.

4. ELECTRON IN GAUSSIAN RANDOM FIELD WITH WHITE-NOISE CORRELATOR

As an example of the practical use of the results obtained above let us consider the problem of an electron in a Gaussian random field with a white-noise correlator when the impurity interaction line corresponds to the expression^{1,2,9}

$$\omega(\mathbf{p}_1, \mathbf{p}_2, \mathbf{p}_3, \mathbf{p}_4) = W^2 \delta(\mathbf{p}_1 - \mathbf{p}_2 + \mathbf{p}_3 - \mathbf{p}_4), \quad (37)$$

where $W^2 = \rho V^2$, ρ is the density of impurity atoms, and V is the Born amplitude of scattering at a point impurity. It is well-known that the principal difficulties in this problem arise at energies defined by the condition⁹

$$|E| \lesssim \gamma(E) \quad \text{or} \quad |E| \lesssim E_{sc}, \quad (38)$$

where $\gamma(E) = \pi \rho V^2 N(E)$ is the Born damping ($N(E)$ is the state density, corresponding to the energy E), $E_{sc} \sim m^{d/(4-d)} (\rho V^2)^{2/(4-d)}$ is the characteristic size of the critical region near the band edge, where strong scattering arises. These difficulties are associated primarily with the impossibility of selecting a particular dominant sequence of Feynman diagrams similarly to what is done in the weak scattering region⁴ $E \gg \gamma(E)$, $E \gg E_{sc}$.^{1,2} Actually, all diagrams for the self-energy part are of the same order in the $|E| \lesssim E_{sc}$ region and must be taken into account.

The perturbation theory series for the self-energy part is shown in Fig. 1b in terms of skeleton graphs. By means of simple variable replacements one can show that all third-order graphs in this expansion are equal to one another (diagrams of Fig. 1b (1–4)). Although this equality breaks down in even the next order, it is reasonable to formulate an approximation in which it is assumed that all graphs of this type are equal in each order of perturbation theory. Such an approximation should give satisfactory results primarily in the critical region $|E| \lesssim E_{sc}$, where all contributions have at least the same order of magnitude. We choose as the base graph in each order the maximally intersecting type shown in Fig. 6a. The sequence of interaction lines entering into it for systems that are invariant with respect to time reversal can be transformed into a ladder, as shown in Fig. 6b. Then the complete series for the self-energy part in our approximation is represented in the form

$$\Sigma(p) = \sum_{n=1}^{\infty} W^2 \sum_{\mathbf{p}_1} \sum_{\mathbf{p}_2} [W^2 G(\mathbf{p}_1 + \mathbf{p}_2 + \mathbf{p}) G \times (-\mathbf{p}_2)]^{n-1} G(\mathbf{p}_1)$$

$$= \sum_{\mathbf{p}_1} W^2 Q \left[W^2 \sum_{\mathbf{p}_2} G(\mathbf{p}_1 - \mathbf{p}_2 + \mathbf{p}) G(\mathbf{p}_2) \right] G(\mathbf{p}_1), \quad (39)$$

where the definitions (19) and (20) were used, as well as the property $G(\mathbf{p}) = G(-\mathbf{p})$ in an isotropic system. Correspondingly, we obtain the closed equation for the average one-particle Green's function in the form

$$G^{-1}(p) = G_0^{-1}(p) - W^2 \sum_{\mathbf{q}} Q \left[W^2 \sum_{\mathbf{p}_1} G(\mathbf{p}_1 - \mathbf{q}) \times G(\mathbf{p}_1) \right] G(\mathbf{p} + \mathbf{q}), \quad (40)$$

where $G_0^{-1}(p) = E - p^2/2m$. The entire nontrivial part of the problem being considered is now expressed by means of the generating function $Q(y)$, which determines the kernel of the complex nonlinear integral equation (40). Restricting consideration to the first term of the expansion (19) gives $Q = 1$, and Eq. (40) reduces to the standard problem of summing nonintersecting graphs.^{1,2} An obvious advantage of the result (40) compared with the standard approach,^{1,2} based on identifying the dominant sequence of diagrams (for example, taking account of only the first graph in Fig. 1b), is that it formally accounts for all diagrams, which is done, however, in the approximation that all skeleton graphs for the self-energy part are equal in a given order of perturbation theory.

Equation (40) is an extremely complicated nonlinear integral equation and cannot be solved in general form, and what is more we do not know the general form of the function $Q(y)$ (which, moreover, enters into Eq. (40) as a function of a complex argument). We will restrict ourselves below to some qualitative analysis of the consequences arising from Eq. (40). We write Eq. (40) in compact form as

$$G^{-1}(p) = G_0^{-1}(p) - W^2 Q [W^2 G \otimes G] \otimes G, \quad (41)$$

where the generalized product (or convolution) of functions

$$F \otimes \Phi = \sum_{\mathbf{p}} F(\mathbf{p} - \mathbf{q}) \Phi(\mathbf{p}), \quad (42)$$

has been introduced, and we return to the system of Eqs. (10) which define the function Q parametrically. The second equation in (10) is now written as

$$G \otimes G = \frac{1}{W^2} \Psi^2(z). \quad (43)$$

We saw above that $z = W^{-1} G_0^{-1}$ holds in the problem with zero transferred momentum. Let us examine the limit $W \rightarrow 0$ in Eq. (43). Then the left side of Eq. (43) is reduced to

$G_0 \otimes G_0$, and on the right side one can assume, by analogy with the problem with zero transferred momentum, $z \sim W^{-1}$ and can use the asymptotic form $\Psi(z) \approx 1/z$ for $|z| \gg 1$. There is some error here since the exact form of $\Psi(z)$ is

$$\Psi(z) = R(z) + i \sqrt{\frac{\pi}{2}} e^{-z^2/2}, \tag{44}$$

where an asymptotic expansion of the form

$$R(z) = e^{-z^2/2} \int_0^z e^{t^2/2} dt = \frac{1}{z} + \frac{1}{z^3} + \frac{3}{z^5} + \dots \left(-\frac{\pi}{4} < \arg z < \frac{\pi}{4} \right). \tag{45}$$

exists for $R(z)$. We use the asymptotic form $\Psi(z) \approx 1/z$, which is not completely true, but the results obtained by using this approximation are corroborated in a more rigorous but much more lengthy analysis. Thus, in the limit $W \rightarrow 0$ Eq. (43) reduces to

$$G_0 \otimes G_0 = \frac{1}{W^2 z^2} \quad \text{or} \quad z = \frac{1 + O(W^2)}{W \sqrt{G_0 \otimes G_0}}. \tag{46}$$

Correspondingly, in the limit $W \rightarrow 0$ we can write

$$G \otimes G = \frac{1}{W^2} \Psi^2 \left(\frac{1}{W \sqrt{G_0 \otimes G_0}} \right). \tag{47}$$

in place of (43). Let us consider the energy region $E < 0$, where the fluctuational tail of the state density arises.^{9,10} In this case we have $z \in \text{Re}$ from Eq. (46). By means of Eqs. (44) and (46) we obtain

$$G \otimes G \approx G_0 \otimes G_0 - i \frac{2}{W} \sqrt{\frac{\pi}{2}} \sqrt{G_0 \otimes G_0} \times \exp \left\{ -\frac{1}{2W^2 G_0 \otimes G_0} \right\}, \tag{48}$$

from (47), where, as we now see, the second term also produces a fluctuational tail of the state density. Using

$$\sum_{\mathbf{q}} G \otimes G = \sum_{\mathbf{p}} \sum_{\mathbf{q}} G(\mathbf{p} - \mathbf{q}) G(\mathbf{p}) = \left(\sum_{\mathbf{p}} G(\mathbf{p}) \right)^2.$$

we obtain immediately from Eq. (48) the state density in the form

$$N(E) = -\frac{1}{\pi} \sum_{\mathbf{p}} \text{Im} G^R(E, \mathbf{p}) = \frac{1}{\sqrt{2\pi}W} \frac{\sum_{\mathbf{q}} \sqrt{G_0 \otimes G_0} \exp\{-1/(2W^2 G_0 \otimes G_0)\}}{|\sum_{\mathbf{p}} G_0(E, \mathbf{p})|}. \tag{49}$$

Thereafter everything is determined by the specific form of $G_0 \otimes G_0$ in spaces of different dimension.

In the one-dimensional ($d=1$) case all of the integrals entering into Eq. (49) are calculated exactly. After rather involved but fairly elementary calculations we obtain

$$N(E) = \frac{1}{2\pi} \sqrt{\frac{2m}{|E|}} \exp \left\{ -\sqrt{2} \frac{|E|^{3/2}}{m^{1/2}W^2} \right\}. \tag{50}$$

The argument of the exponential in Eq. (50) differs from the known exact result of Halperin¹¹ (see also Chapter 11 in Ref. 10) by the absence of a 4/3 multiplier. The pre-exponential function in Eq. (50) also differs from the exact, which is $\sim |E|/W^2$.¹¹ Nevertheless, the behavior of the state density tail is reproduced quite satisfactorily in a qualitative sense in our approximation. In this regard let us recall the widespread notion that the state density tail cannot be obtained at all from perturbation theory.

Analogous (but still approximate) calculations of the state density using Eq. (49) for $d=3$ yield

$$N(E) \sim \exp \left\{ -\sqrt{2} \frac{|E|^{1/2}}{m^{3/2}W^2} \right\}. \tag{51}$$

Here the exponential once more coincides with the known result of the nonperturbative instanton approach within the accuracy of a constant.^{9,12-14} The pre-exponential multiplier, omitted in Eq. (51), following from Eq. (49), does not coincide with any of the known versions obtained in the cited papers. Nevertheless, the result (51) for the dominant exponent is also quite satisfactory despite the approximate character of Eq. (51).

An analysis of the consequences of Eq. (40) in the strong-coupling region,⁹ defined by condition (38), i.e., in the vicinity of the edge of the initial band where a transition from spatial to localized states occurs, is of special interest. There is every basis for assuming that in this region the approximation of equal contributions to the self-energy part in a given order of perturbation theory can turn out to be good simply because of the known fact that they are equal in order of magnitude. A strong condition of the type (38), obviously, is equivalent to passing to the limit $W \rightarrow \infty$. In this limit in the zeroth approximation one can ignore in Eq. (41) the first term on the right side compared with the second and can write

$$G^{-1}(\mathbf{p}) = -W^2 Q[W^2 G \otimes G] \otimes G. \tag{52}$$

We see that this corresponds to the limit $z = \pm i0$ in Eq. (43) for $y = -\pi/2$ in Eq. (10). In this case Eq. (43) is reduced to

$$W^2 G \otimes G = \Psi(z = \pm i0) = -\pi/2, \tag{53}$$

and we have from Eq. (17)

$$Q[W^2 G \otimes G] = 2/\pi. \tag{54}$$

The formal solution of Eq. (53) has the form

$$G = \pm i \sqrt{\frac{\pi}{2}} \frac{1}{W \sqrt{\mathcal{N}}}, \tag{55}$$

where $\mathcal{N} = \sum_{\mathbf{p}} 1$ is the number of states in the band. It is easy to see that this equation is satisfied by the direct substitution of Eqs. (55) and (54) into (52). Thus, in a first approximation in the limit $W \rightarrow \infty$ one can write the Green's function in the form

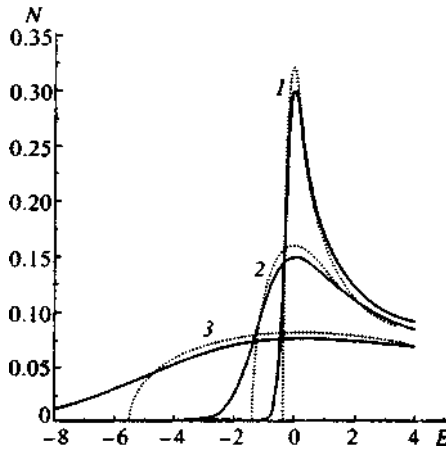


FIG. 7. State density in one-dimensional system for different values of the mean square of random field $W^2(2m)^{1/2}/E_0^{3/2}$: 1—0.25, 2—2, 3—16. Solid curves represent exact solution, dotted curves represent self-consistent Born approximation (56). Energy is given in units of E_0 and the state density in units of $\sqrt{2m/E_0}$, where E_0 is arbitrary.

$$G(p) = \frac{1}{G_0^{-1}(p) - (2/\pi)W^2 \Sigma_p G(p)}, \quad (56)$$

which agrees surprisingly well with the result of the self-consistent Born approximation (the first diagram in Fig. 1b or Fig. 3)^{1,2} to within the redundant multiplier $2/\pi$. Equation (56) leads in an obvious manner to the state density of the Born approximation $N_0(E)$, which practically coincides for $d=3$ with the state density of the free electron model (with a one-loop displacement of the band edge taken into account). Figure 7 shows a comparison of the results following from Eq. (56) for the state density in a one-dimensional ($d=1$) system with the exact Halperin result,¹¹ demonstrating satisfactory agreement of these results in the strong-coupling region $|E| < E_{sc} \sim m^{1/3}W^{4/3}$, the width of which increases with an increase in W . It must be pointed out that although the tail of the state density is suppressed with an increase in W (see Eq. (50)), the intermediate region where $|E| \sim E_{sc}$ increases.

It is possible that a result of the form (56) makes it possible to justify qualitatively using the simplest Born approximation for the one-electron Green's function in approaches such as the self-consistent localization theory^{9,15}—the mobility threshold occurs in the strong-coupling region $|E| \leq E_{sc}$ (38), where the approximation (56) turns out to be quite satisfactory and the Green's function actually has the simple Born form.

This work was partially supported by the Russian Fund for Fundamental Research (Project 96-02-16065) and was also carried out within the framework of Project IX.I of the Statistical Physics Government Program of the Russian Ministry of Science. The authors are grateful to A. I. Posazhenikova for assisting with the numerical calculations.

APPENDIX

Let us derive Eq. (18) for the generating function $Q(y)$ without using the explicit form of the one-particle Green's

function (6). In problems with zero momentum transfer momentum the Bethe–Salpeter equation of Fig. 2c has the form

$$\Gamma = U + UG^2\Gamma, \quad (A1)$$

so that

$$\Gamma = \frac{U}{1 - UG^2}. \quad (A2)$$

Using Eqs. (A2) and (22), we obtain an equation relating the self-energy part to the irreducible vertex U :

$$\Sigma = \frac{W^2G}{1 - UG^2}. \quad (A3)$$

We use the Ward identity

$$W^2 \frac{\partial}{\partial W} \Big|_G \frac{\Sigma}{W} = UG, \quad (A4)$$

the validity of which is easy to see by means of Eqs. (8) and (24), and Eq. (A2) in order to write

$$W^2 \frac{\partial}{\partial W} \Big|_G \frac{\Sigma}{W} = UG = \frac{1}{G} \left\{ 1 - W^2 \frac{G}{\Sigma} \right\}$$

or

$$\Sigma = W^2G + W^2G \Sigma \frac{\partial}{\partial W} \Big|_G \frac{\Sigma}{W}. \quad (A5)$$

Using Eq. (8), we obtain the desired differential equation for Q :

$$\begin{aligned} Q(W^2G^2) &= 1 + W^2GQ(W^2G^2) \frac{\partial}{\partial W} \Big|_G W G Q(W^2G^2) \\ &= 1 + W^2G^2 \frac{d}{d(W^2G^2)} W^2G^2 Q^2(W^2G^2), \end{aligned}$$

which is rewritten as

$$Q(y) = 1 + y \frac{d}{dy} y Q^2(y). \quad (A6)$$

Note, however, that from these arguments it is impossible to find the correct boundary condition (17), which is closely related to the relation (11), reflecting the causality principle.

¹From a mathematical viewpoint this means Borel summation.
²The sign of the imaginary part corresponds to treating the retarded or advanced Green's functions.
³An asymptotic limit of the form (32), $\Sigma_N \approx c \cdot 2^N \Gamma(N + \beta)$, was obtained in Ref. 6 by the Lipatov method; however, the coefficients c and β were not found.
⁴In this case the nonintersecting diagrams dominate, so that one can take account of only the first diagram in Fig. 1b.
⁵For $d > 4$ knowledge of the asymptotic form (32) and the statistical analysis of Ref. 6 make it possible to determine the correct exponent of W^{-1} in the pre-exponential function of the state density. In this case our approximation is equivalent to the hypothesis, used in Ref. 6, that the high-order contributions are stationary, which is valid for $d > 4$.

¹S. F. Edwards, *Philos. Mag.* **3**, 1020 (1958).
²A. A. Abrikosov, L. P. Gor'kov, and I. E. Dzyaloshinskiĭ, *Methods of Quantum Field Theory in Statistical Physics* (Fizmatgiz, Moscow, 1962; Prentice-Hall, Englewood Cliffs, NJ, 1963), Chap 7.

- ³S. N. Rytov, Yu. A. Kravtsov, and V. N. Tatarskiĭ, *Principles of Statistical Radiophysics* (Nauka, Moscow, 1978, Springer, New York, 1987), Pt. II, Chap. VIII.
- ⁴S. Ma, *Modern Theory of Critical Phenomena* (Benjamin, Reading, Massachusetts, 1976; Mir, Moscow, 1980), Chap. 10.
- ⁵A. Yu. Grosberg and A. R. Khokhlov, *Statistical Physics of Macromolecules* (Nauka, Moscow, 1989; AIP, New York, 1994), Chap. 2.
- ⁶I. M. Syslov, Zh. Éksp. Teor. Fiz. **102**, 1951 (1992) [Sov. Phys. JETP **75**, 1049 (1992)].
- ⁷L. V. Keldysh, Dissertation...doctor phys. math. sciences (FIAN, Moscow, 1965).
- ⁸A. L. Efros and B. I. Shklovskii, *Electronic Properties of Doped Semiconductors* (Springer, New York, 1984), Chap. 11.
- ⁹M. V. Sadovskii, Sov. Sci. Rev. A—Phys. Rev. **7**, 1 (1986).
- ¹⁰I. M. Lifshits, S. A. Gredeskul, and L. A. Pastur, *Introduction to the Theory of Disordered Systems* (Wiley, New York, 1988), Chap. IV.
- ¹¹B. I. Halperin, Phys. Rev. **139**, A104 (1965).
- ¹²J. Cardy, J. Phys. C **11**, L321 (1978).
- ¹³M. V. Sadovskii, Fiz. Tverd. Tela **21**, 743 (1979) [Sov. Phys. Solid State **21**, 435 (1979)].
- ¹⁴I. M. Suslov, Zh. Éksp. Teor. Fiz. **111**, 1896 (1997) [JETP **84**, 1036 (1997)].
- ¹⁵D. Vollhardt and P. Wölfle, in *Electronic Phase Transition*, ed. by W. Hanke and Yu. V. Kopayev (North-Holland, Amsterdam, 1992), p. 1.

Translated by Eugene R. Heath

The Ginzburg–Landau expansion in the simple model of a superconductor with a pseudogap

A. I. Posazhennikova^{*}) and M. V. Sadovskii[†])

Institute of Electrophysics, Ural Branch of the Russian Academy of Sciences, 620049 Ekaterinburg, Russia

(Submitted 16 June 1998)

Zh. Éksp. Teor. Fiz. **115**, 632–648 (February 1999)

We propose a simple model of the electron spectrum of a two-dimensional system with hot sections on the Fermi surface that significantly transforms the spectral density (pseudogap) in these sections. Using this model, we set up a Ginzburg–Landau expansion for *s* and *d* type Cooper pairing and analyze the effect of the pseudogap in the electron spectrum on the main properties of a superconductor. © 1999 American Institute of Physics.
[S1063-7761(99)01802-8]

1. INTRODUCTION

Among the various anomalies in the properties of high- T_c superconductors, the existence of a pseudogap in the electron spectrum of such materials at carrier concentrations below the optimum value has drawn much attention.^{1,2} The most striking proof of the existence of this remarkable state has been obtained in measurements of photoemission spectra with angular resolution in the BSCCO system,^{3,4} which demonstrated that the normal phase ($T > T_c$) exhibits essentially anisotropic variations in the spectral density of the current carriers. In particular, in these experiments the maximum pseudogap value was observed near the point $(\pi, 0)$ in the Brillouin zone, while no pseudogap was observed along the diagonal. Correspondingly, the Fermi surface disintegrates near the point $(\pi, 0)$, while along the diagonal the surface remains intact. In this sense it is common to speak of a *d* type pseudogap symmetry, which coincides with the symmetry of a superconducting gap in such systems. These anomalies exist up to temperatures $T \approx T^*$ much higher than T_c .

There are many theoretical approaches that attempt to give an explanation of such anomalies. Two main groups of these approaches can be singled out: the pattern of formation of Cooper pairs above T_c (see Ref. 1, 5 and 6), and an alternation scheme based on the assumption that fluctuations of antiferromagnetic short-range order play the key role.^{7–11}

Most papers on the subject deal mainly with the study of the pseudogap state of a high- T_c system in the normal phase ($T > T_c$). Our goal was to investigate the qualitative effects of the influence of a pseudogap in the electron spectrum on the main superconducting properties. We use the ideas developed in Refs. 7–11 but propose a very simple model of the pseudogap state in the normal phase, a model that allows a complete analytical investigation. On the basis of this model we do a microscopic derivation of the Ginzburg–Landau expansion for systems with *s* and *d* pairings and study the qualitative effects of the influence of a pseudogap (the disintegration of sections of the Fermi surface) on the main properties of the superconducting state.

2. ELEMENTARY MODEL OF A PSEUDOGAP STATE OF A TWO-DIMENSIONAL ELECTRON SYSTEM

As noted earlier, we adopt the simplest possible model of a pseudogap state, a model based on the picture of well-developed fluctuations of short-range antiferromagnetic order and close the model of ‘‘hot points’’ on the Fermi surface.^{10,11} Let us assume that the Fermi surface of the two-dimensional electron system has the shape depicted in Fig. 1. A similar Fermi surface was proposed by Zheleznyak *et al.*,¹² who remarked that this Fermi surface resembles very closely the one observed by Dessau *et al.*^{13,14} for some high- T_c systems. We assume that the short-range order fluctuations are static and Gaussian and define their correlation function as follows (cf. Ref. 7):

$$S(\mathbf{q}) = \frac{1}{\pi^2} \frac{\xi^{-1}}{(q_x - Q_x)^2 + \xi^{-2}} \frac{\xi^{-1}}{(q_y - Q_y)^2 + \xi^{-2}} \quad (1)$$

for $-p_x^0 \leq q_x \leq p_x^0$ and $-p_y^0 \leq q_y \leq p_y^0$, where ξ is the correlation length of the fluctuations, and $Q_x = Q_y = 2p_F$. For values of q_x and q_y that lie outside the specified ranges we assume that $S(\mathbf{q}) = 0$. The effective interaction between electrons and these fluctuations will be described by the quantity $(2\pi)^2 W^2 S(\mathbf{q})$, where the parameter W with the dimensions of energy defines the energy scale (width) of the pseudogap. Thus, we assume that only electrons belonging to the ‘‘hot’’ sections of the Fermi surface are scattered by the short-range fluctuations, with the scattering being actually one-dimensional.

The choice of the scattering vector $\mathbf{Q} = (2p_F, 2p_F)$ presupposes a pattern of incommensurate fluctuations. Below we will consider the case of commensurate scattering with $\mathbf{Q} = (\pi/a, \pi/a)$, where a is the lattice constant. In the limit $\xi \rightarrow \infty$, such a model allows an exact solution by the methods proposed by Sadovskii,^{15,16} while for finite ξ one can employ the method developed by Sadovskii and Timofeev^{17,18} (with certain reservations; see Refs. 10, 11, and 19). Below we examine the simple case with $\xi \rightarrow \infty$, where the effective interaction with fluctuations (1) takes the simplest form

$$(2\pi)^2 W^2 \delta(q_x - 2p_F) \delta(q_y - 2p_F) \quad (2)$$

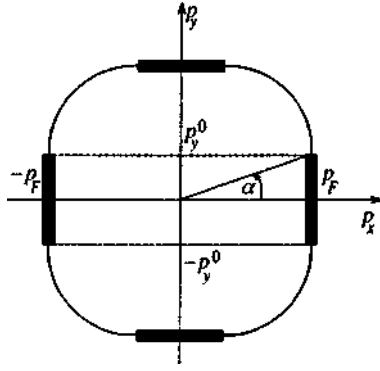


FIG. 1. The Fermi surface of a two-dimensional system. The hot sections are depicted by thick straight lines, whose width is of order $\sim \xi^{-1}$.

for $-p_x^0 \leq q_x \leq p_x^0$ and $-p_y^0 \leq q_y \leq p_y^0$. Here we can easily sum the entire perturbation series for an electron scattered by such fluctuations^{15,16} and obtain the one-electron Green's function in the form

$$G(\epsilon_n, p) = \int_0^\infty d\zeta \exp(-\zeta) \frac{i\epsilon_n + \xi_p}{(i\epsilon_n)^2 - \xi_p^2 - \zeta W^2(\phi)}, \quad (3)$$

where $\xi_p = v_F(|\mathbf{p}| - p_F)$, with v_F the velocity at the Fermi surface, $\epsilon_n = (2n + 1)\pi T$, and $W(\phi)$ is defined for $0 \leq \phi \leq \pi/2$ as follows:

$$W(\phi) = \begin{cases} W, & 0 \leq \phi \leq \alpha, & \frac{\pi}{2} - \alpha \leq \phi \leq \frac{\pi}{2}, \\ 0, & \alpha \leq \phi \leq \frac{\pi}{2} - \alpha. \end{cases} \quad (4)$$

Here $\alpha = \tan^{-1}(p_y^0/p_x^0)$, and ϕ is the polar angle, which specifies the director of the vector \mathbf{p} in the (p_x, p_y) plane. For other values of ϕ , the parameter $W(\phi)$ is determined quite similarly to (4) by symmetry considerations. Clearly, by varying α within the range $0 \leq \alpha \leq \pi/4$, we actually change the size of the hot sections on the Fermi surface, in which sections the nesting condition $\xi_{p-Q} = -\xi_p$ is satisfied. In particular, $\alpha = \pi/4$ corresponds to a square Fermi surface on which the nesting condition is satisfied everywhere. Outside the hot sections [the second inequality in (4)] the Green's function (3) simply coincides with the free-electron Green's function.

The spectral density corresponding to the Green's function (3), is

$$\rho(\epsilon, \xi_p) = -\frac{1}{\pi} \operatorname{sgn} \epsilon \operatorname{Im} G(\epsilon, \xi_p) \quad (5)$$

$$= \begin{cases} \frac{1}{W^2} (|\epsilon| + \xi_p \operatorname{sgn} \epsilon) \theta(\epsilon^2 - \xi_p^2) \exp \frac{\epsilon^2 - \xi_p^2}{W^2}, & \\ \text{if } 0 \leq \phi \leq \alpha, & \frac{\pi}{2} - \alpha \leq \phi \leq \frac{\pi}{2}, \\ \delta(\epsilon - \xi_p), & \\ \text{if } \alpha \leq \phi \leq \frac{\pi}{2} - \alpha, & \end{cases} \quad (6)$$

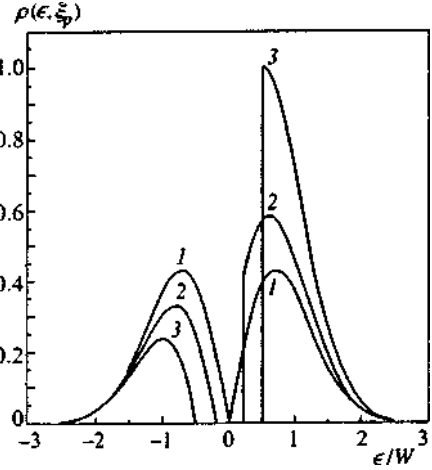


FIG. 2. Spectral density of the Green's function in a hot section of the Fermi surface: curve 1, $\xi_p = 0$; curve 2, $\xi_p = 0.1W$; and curve 3, $\xi_p = 0.5W$.

and has a similar form in the other quadrants of the Brillouin zone. Equation (6) demonstrates the non-Fermi-liquid (pseudogap) behavior with a d -type symmetry in the vicinity of the hot sections of the Fermi surface and the free behavior in the cold sections. The behavior of the spectral density in a hot section of the Fermi surface is depicted schematically in Fig. 2. Allowing for the fact that the integral with respect to the polar angle ϕ of an arbitrary function $f[W(\phi)]$, with $W(\phi)$ defined in (4), is obviously

$$\int_0^{2\pi} d\phi f[W(\phi)] = 8\alpha f[W(\phi)] + (2\pi - 8\alpha)f(0), \quad (7)$$

we can use (6) to easily find the density of states:

$$\begin{aligned} \frac{N(E)}{N_0(0)} &= -\frac{1}{\pi} \int_0^{2\pi} \frac{d\phi}{2\pi} \int_{-\infty}^\infty d\xi_p \operatorname{Im} G^R(\epsilon, \xi_p) \\ &= \frac{4}{\pi} \alpha N_W(\epsilon) + \left(\pi - \frac{4}{\pi} \alpha \right) N_0(0), \end{aligned} \quad (8)$$

where $N_0(0)$ is the density of free-electron states at the Fermi level, and $N_W(\epsilon)$ is the density of states in the one-dimensional problem (a square Fermi surface) found in Refs. 15 and 16:

$$\begin{aligned} \frac{N_W(\epsilon)}{N_0(\epsilon)} &= \left| \frac{\epsilon}{W} \right| \int_0^{\epsilon^2/W^2} d\zeta \frac{\exp(-\zeta)}{\sqrt{\epsilon^2/W^2 - \zeta}} \\ &= 2 \left| \frac{\epsilon}{W} \right| \exp\left(-\frac{\epsilon^2}{W^2}\right) \operatorname{Erfi} \frac{\epsilon}{W}, \end{aligned} \quad (9)$$

where $\operatorname{Erfi} x$ is the probability integral (error function) of imaginary argument.

Figure 3 depicts the density-of-state curves in our model for different values of the parameter α , i.e., for hot sections of different size. We see that the pseudogap in the density of states becomes obscured rather quickly as the area of the hot sections decreases and generally is not very distinct. In a certain sense the effect of a decreasing α is similar to the effect of a decreasing correlation length ξ of the fluctuations,^{17,18} so that in this sense the above approxima-

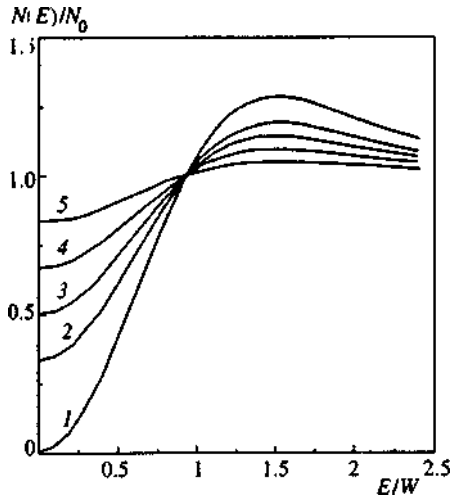


FIG. 3. Density of electron states for hot sections of different size: curve 1, $\alpha = \pi/4$; curve 2, $\alpha = \pi/6$; curve 3, $\alpha = \pi/8$; curve 4, $\alpha = \pi/12$; and curve 5, $\alpha = \pi/24$.

tion $\xi \rightarrow \infty$ may not be a stringent restriction on the applicability of the model. One advantage of this approximation is the possibility of obtaining all the results in analytical form.

Concluding Sec. 2, we examine briefly the case of commensurate fluctuations, $\mathbf{Q} = (\pi/a, \pi/a)$. Figure 4 depicts the model of the Fermi surface used in this problem. The hot sections touch the boundaries of a new Brillouin zone that appears after long-range order (e.g., antiferromagnetic) has set in, and the strong scattering by fluctuations occurs at $\mathbf{Q} = (\pi/a, \pi/a)$. In this geometry the pseudogap opens in the direction of the diagonals of the Brillouin zone, which does not correspond to experiments involving high- T_c superconductors but is of certain theoretical interest. The problem is solved in the same way as in the previous case and generalizes the solution of the one-dimensional model first found by Wonneberger and Lautenschlager.¹⁹ The one-electron Green's function is similar to (3), and $W(\phi)$ is again a function with a period $\pi/2$, but "turned" with respect to the

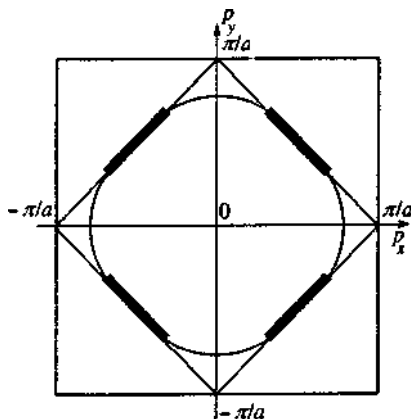


FIG. 4. The Fermi surface in the Brillouin zone of a two-dimensional system in the hot-section model for the case of short-range order fluctuations corresponding to period doubling. Also shown are the boundaries of the new Brillouin zone, which arises after long-range order sets in (e.g., due to an antiferromagnetic transition).

previous model through an angle of $\pi/4$ for $-\pi/4 + \alpha \leq \phi \leq \pi/4 + \alpha$:

$$W(\phi) = \begin{cases} W, & \pi/4 - \alpha \leq \phi \leq \pi/4 + \alpha, \\ 0, & -\pi/4 + \alpha \leq \phi \leq \pi/4 - \alpha, \end{cases} \quad (10)$$

where $0 \leq \alpha \leq \pi/4$. Moreover, in the present case we must allow for a different combination of the Feynman diagrams, which must correspond to electron scattering by commensurate fluctuations.¹⁹ As a result, in (3) we must replace

$$\int_0^\infty d\xi \exp(-\xi) \quad (11)$$

with

$$\int_0^\infty \frac{d\xi}{2\sqrt{\pi\xi}} \exp\left(-\frac{\xi}{4}\right). \quad (12)$$

3. THE EQUATION FOR T_c

Let us now investigate the problem of superconductivity in the adopted model. We assume that the potential for Cooper pairing has the usual separable form²⁰

$$V(\mathbf{p}, \mathbf{p}') = V(\phi, \phi') = -Ve(\phi)e(\phi'), \quad (13)$$

where as before ϕ is the angle specifying the direction of electron momentum \mathbf{p} in the plane, and $e(\phi)$ obeys the following model:

$$e(\phi) = \begin{cases} 1 & (s \text{ pairing}), \\ \sqrt{2} \cos 2\phi & (d \text{ pairing}). \end{cases} \quad (14)$$

As usual, the attractive constant V is assumed finite in a certain strip of width $2\omega_c$ in the vicinity of the Fermi level (ω_c is the characteristic frequency of the photons ensuring the attraction of electrons). In this case the superconducting gap (the order parameter) has the form

$$\Delta(\mathbf{p}) \equiv \Delta(\phi) = \Delta e(\phi). \quad (15)$$

The equation for the transition temperature T_c can be obtained from the ordinary equation for Cooper instability,

$$1 - \chi(0,0) = 0, \quad (16)$$

where the generalized Cooper susceptibility $\chi(0,0)$ can be calculated by exact summation of the entire series of diagrams that allow for scattering by the short-range order fluctuations (2), in the same way the polarization operator was calculated by Sadovskii.^{15,16} As a result the equation for T_c becomes

$$\begin{aligned} \frac{1}{V} = & - \int_0^\infty d\xi \exp(-\xi) T_c \sum_n \int_0^\infty \frac{d^2p}{(2\pi)^2} e^2(\phi) \{ G_{\xi W^2} \\ & \times (\epsilon_n; \mathbf{p}, \mathbf{p}) G_{\xi W^2}(-\epsilon_n; -\mathbf{p}, -\mathbf{p}) + F_{\xi W^2} \\ & \times (\epsilon_n; \mathbf{p}, \mathbf{p} - \mathbf{Q}) F_{\xi W^2}(-\epsilon_n; -\mathbf{p}, -\mathbf{p} + \mathbf{Q}) \}, \end{aligned} \quad (17)$$

where

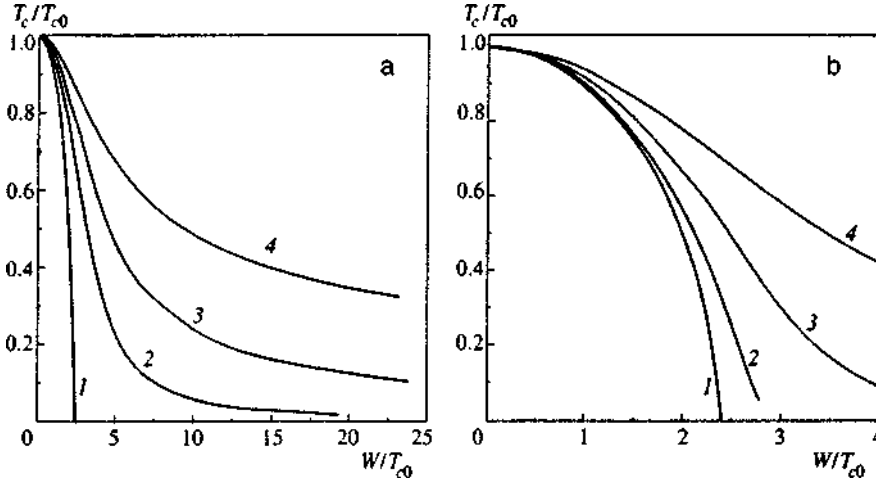


FIG. 5. T_c/T_{c0} as a function of the effective pseudogap width W/T_{c0} for hot sections of different size in the incommensurate fluctuation model for (a) s pairing (curve 1, $\alpha = \pi/4$; curve 2, $\alpha = \pi/6$; curve 3, $\alpha = \pi/8$; and curve 4, $\alpha = \pi/12$), and (b) d pairing (curve 1, $\alpha = \pi/4$; curve 2, $\alpha = \pi/6$; curve 3, $\alpha = \pi/8$; and curve 4, $\alpha = \pi/12$).

$$G_{\zeta W^2}(\epsilon_n; \mathbf{p}, \mathbf{p}) = \frac{i\epsilon_n + \xi_p}{(i\epsilon_n)^2 - \xi_p^2 - \zeta W^2(\phi)},$$

$$F_{\zeta W^2}(\epsilon_n; \mathbf{p}, \mathbf{p} - \mathbf{Q}) = \frac{\sqrt{\zeta} W(\phi)}{(i\epsilon_n)^2 - \xi_p^2 - \zeta W^2(\phi)} \quad (18)$$

are, respectively, the normal and anomalous Green's functions of a system with a dielectric gap.^{15,16}

Applying standard transformations to (17), we get

$$\frac{1}{V} = \int_0^\infty d\zeta$$

$$\times \exp(-\zeta) T_c \sum_n \int_0^\infty \frac{d^2 p}{(2\pi)^2} \frac{e^2(\phi)}{\epsilon_n^2 + \xi_p^2 + \zeta W^2(\phi)}. \quad (19)$$

Summing over the frequencies yields

$$\frac{1}{V} = \frac{N(0)}{2\pi} \int_0^\infty d\zeta \exp(-\zeta) \int_{-\infty}^\infty d\xi$$

$$\times \int_0^{2\pi} \frac{d\phi e^2(\phi)}{2\sqrt{\xi^2 + \zeta W^2(\phi)}} \tanh \frac{\sqrt{\xi^2 + \zeta W^2(\phi)}}{2T_c}. \quad (20)$$

If we now integrate with respect to ϕ as we did in (7), we arrive at the following formulas:

$$\frac{1}{g} = \frac{4\alpha}{\pi} \int_0^\infty d\zeta \exp(-\zeta) \int_0^{\omega_c} \frac{d\xi}{\sqrt{\xi^2 + \zeta W^2}} \tanh \frac{\sqrt{\xi^2 + \zeta W^2}}{2T_c}$$

$$+ \left(1 - \frac{4\alpha}{\pi}\right) \int_0^{\omega_c} \frac{d\xi}{\xi} \tanh \frac{\xi}{2T_c} \quad (21)$$

for s pairing, and

$$\frac{1}{g} = \frac{4\alpha + \sin 4\alpha}{2\pi} \int_0^\infty d\zeta \exp(-\zeta) \int_0^{\omega_c} \frac{d\xi}{\sqrt{\xi^2 + \zeta W^2}}$$

$$\times \tanh \frac{\sqrt{\xi^2 + \zeta W^2}}{2T_c} + \frac{\pi - 4\alpha - \sin 4\alpha}{2\pi} \int_0^{\omega_c} \frac{d\xi}{\xi} \tanh \frac{\xi}{2T_c} \quad (22)$$

for d pairing. Here $g = N(0)V$ is the dimensionless Cooper-pairing constant. Figure 5 depicts curves representing the dependence of T_c/T_{c0} on the parameter W/T_{c0} , which specifies the effective pseudogap width, for different values of α (here T_{c0} is the transition temperature of an ideal system without a pseudogap). We see that for both types of pairing the occurrence of a pseudogap in the hot sections of the Fermi surface causes significant suppression of T_c , and the larger these hot sections are the stronger the suppression. Naturally, the suppression of T_c is stronger in the case of d pairing than in the case of s pairing, since the dielectrization of the spectrum (pseudogap) is in antiphase with the pairing interaction.

For commensurate fluctuations (Fig. 4) and d -type pairing, the equation for T_c becomes

$$\frac{1}{g} = \frac{4\alpha - \sin 4\alpha}{2\pi} \int_0^\infty d\zeta \exp(-\zeta/4) \int_0^{\omega_c} \frac{d\xi}{\sqrt{\xi^2 + \zeta W^2}}$$

$$\times \tanh \frac{\sqrt{\xi^2 + \zeta W^2}}{2T_c} + \frac{\pi - 4\alpha + \sin 4\alpha}{2\pi} \int_0^{\omega_c} \frac{d\xi}{\xi} \tanh \frac{\xi}{2T_c}. \quad (23)$$

Curves presenting the dependence of T_c/T_{c0} on the parameter W/T_{c0} for different values of α in this case are depicted in Fig. 6. Here the suppression of T_c by the pseudogap is less noticeable, since the superconducting gap reaches its maximum on the cold sections of the Fermi surface, where there is no pseudogap.

4. THE GINZBURG-LANDAU EXPANSION

The standard Ginzburg-Landau expansion for the difference in the free-energy densities of the superconducting and normal states is

$$F_s - F_n = A|\Delta_q|^2 + q^2 C|\Delta_q|^2 + \frac{B}{2}|\Delta_q|^4, \quad (24)$$

where Δ_q is the Fourier transform of the order parameter:

$$\Delta(\phi, q) = \Delta_q e(\phi). \quad (25)$$

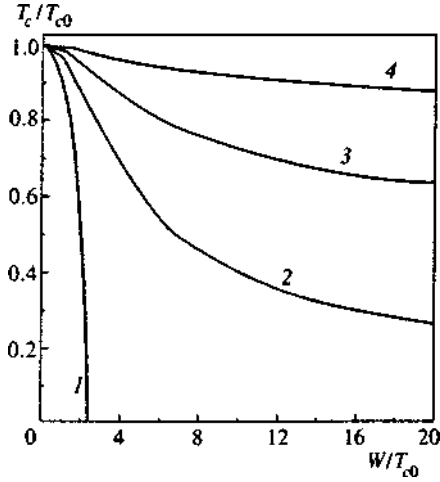


FIG. 6. T_c/T_{c0} as a function of the effective pseudogap width W/T_{c0} for hot sections of different size in the commensurate fluctuation model for the case of d pairing: curve 1, $\alpha = \pi/4$; curve 2, $\alpha = \pi/6$; curve 3, $\alpha = \pi/8$; and curve 4, $\alpha = \pi/12$.

Expansion (24) can be represented by the diagrams of the loop expansion for the free energy in the field of the order parameter fluctuations with a small wave vector \mathbf{q} . These diagrams are depicted in Fig. 7, where all processes of scattering by short-range order fluctuations (2) are summed exactly in all loops (this can easily be done if we use the method developed in Refs. 15 and 16). In all other respects the method of calculation is similar to that used Ref. 20.¹⁾ As in Ref. 20, subtraction of the second diagram in Fig. 7 ensures the vanishing of the coefficient A at the transition point $T = T_c$. As a result, the Ginzburg–Landau coefficients can be written

$$A = A_0 K_A, \quad C = C_0 K_C, \quad B = B_0 K_B, \quad (26)$$

where by A_0 , C_0 , and B_0 we denote the expressions for the case of a two-dimensional isotropic s superconductor in the absence of a pseudogap ($\alpha = 0$),

$$A_0 = N(0) \frac{T - T_c}{T_c}, \quad C_0 = N(0) \frac{7\zeta(3)}{32\pi^2} \frac{v_F^2}{T_c^2},$$

$$B_0 = N(0) \frac{7\zeta(3)}{8\pi^2 T_c^2}, \quad (27)$$

and all the features of the models are reflected in the dimensionless coefficients K_A , K_C , and K_B . In the absence of a pseudogap, all these coefficients are equal to unity, while in the case of d pairing only K_B differs from unity, or $K_B = 3/2$.

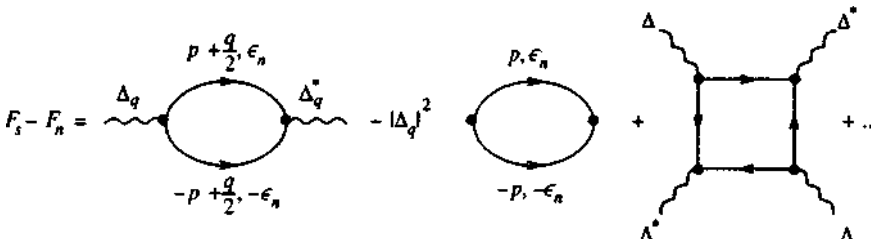


FIG. 7. The diagrammatic representation of the Ginzburg–Landau expansion in the field of short-range order fluctuations. The electron lines represent Nambu matrices composed of normal and anomalous Green's functions (18), and the loops are averaged over the parameter ζ with a distribution (11) or (12). The second loop is calculated for $q = 0$ and $T = T_c$.

In particular, straightforward calculations yield

$$A = N(0) \frac{T - T_c}{2T_c^2} \frac{1}{2\pi} \int_0^\infty d\zeta \exp(-\zeta) \int_0^{\omega_c} d\xi$$

$$\times \int_0^{2\pi} \frac{d\phi e^2(\phi)}{\cosh^2(\sqrt{\xi^2 + \zeta W^2(\phi)}/2T_c)}, \quad (28)$$

so that after integrating with respect to ϕ we get

$$K_A = \frac{1}{2T_c} \beta_a \int_0^\infty d\zeta \exp(-\zeta)$$

$$\times \int_0^{\omega_c} \frac{d\xi}{\cosh^2(\sqrt{\xi^2 + \zeta W^2(\phi)}/2T_c)} + 1 - \beta_a, \quad (29)$$

where

$$\beta_a = \begin{cases} \frac{4\alpha}{\pi} & (s \text{ pairing}), \\ \frac{4\alpha + \sin 4\alpha}{\pi} & (d \text{ pairing}). \end{cases} \quad (30)$$

Figure 8 depicts curves representing the dependence of K_A on the effective pseudogap width W/T_{c0} for different values of α . Here we show only the curves for the case of s pairing. Qualitatively the corresponding curves for d pairing are similar, but all variations are on essentially smaller scales of W/T_{c0} , as in Fig. 5.

To calculate C , we must perform an expansion in a Taylor series in powers of \mathbf{q} in the expression

$$- \int_0^\infty d\zeta \exp(-\zeta) T_c \sum_n \int_0^\infty \frac{d^2 p}{(2\pi)^2} e^2(\phi) \{ G_{\zeta W^2(\phi)}$$

$$\times (\epsilon_n; \mathbf{p}_+, \mathbf{p}_+) G_{\zeta W^2(\phi)}(-\epsilon_n; -\mathbf{p}_-, -\mathbf{p}_-) + F_{\zeta W^2(\phi)}$$

$$\times (\epsilon_n; \mathbf{p}_+, \mathbf{p}_+ - \mathbf{Q}) F_{\zeta W^2(\phi)}(-\epsilon_n; -\mathbf{p}_-, -\mathbf{p}_+ + \mathbf{Q}) \}, \quad (31)$$

where $\mathbf{p}_\pm = \mathbf{p} \pm \mathbf{q}/2$, and select the terms with \mathbf{q}^2 . To simplify presentation, from now on we will use the notation

$$G_{\zeta W^2(\phi)}(\epsilon_n; \mathbf{p}, \mathbf{p}) \equiv G_{pp},$$

$$F_{\zeta W^2(\phi)}(\epsilon_n; \mathbf{p}, \mathbf{p} - \mathbf{Q}) \equiv F_{pp-Q}.$$

After lengthy calculations we arrive at an expression for the coefficient C :

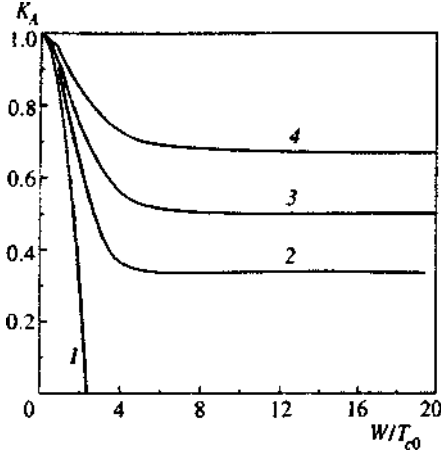


FIG. 8. The coefficient K_A as a function of the effective pseudogap width W/T_{c0} for hot sections of different size in the incommensurate fluctuation model for the case of s pairing: curve 1, $\alpha = \pi/4$; curve 2, $\alpha = \pi/6$; curve 3, $\alpha = \pi/8$; and curve 4, $\alpha = \pi/12$.

$$C = -T_c \frac{N(0)}{2\pi} v_F^2 \sum_n \int_0^\infty d\xi \exp(-\xi) \int d\xi \times \int_0^{2\pi} d\phi \frac{e^2(\phi)(\xi^2 - 3\epsilon_n^2 - 3\xi W^2(\phi)) \cos^2 \phi}{2(\epsilon_n^2 + \xi^2 + \xi W^2(\phi))^3}. \quad (32)$$

Accordingly, after integrating over ξ and the angle ϕ , we arrive at an expression for the dimensionless coefficient K_C :

$$K_C = \beta_c \frac{4\pi^3 T_c^3}{7\xi(3)} \int_0^\infty d\xi \exp(-\xi) \sum_n \frac{1}{(\sqrt{\epsilon_n^2 + \xi W^2})^3} + 1 - \beta_c, \quad (33)$$

where $\beta_c = \beta_a$ [see Eq. (30)]. The respective relations between K_C and the parameter W/T_{c0} for the case of s pairing are depicted in Fig. 9. The pattern is similar for d pairing, but all variations are on essentially smaller scales of W/T_{c0} .

Examining the fourth-order term in the Ginzburg–Landau expansion is even more difficult technically. To obtain an expression for the coefficient B , we must find the trace of the product of four Green's functions $\hat{\mathbf{G}}_{\mathbf{p}}$, each of which is a Nambu matrix composed of normal and anomalous Green's functions (18):

$$\hat{\mathbf{G}}_{\mathbf{p}} = \begin{pmatrix} G_{p,p} & F_{p,p-Q} \\ F_{p-Q,p} & G_{p-Q,p-Q} \end{pmatrix}.$$

After we find the trace of the matrix $\hat{\mathbf{G}}_{\mathbf{p}} \hat{\mathbf{G}}_{-\mathbf{p}} \hat{\mathbf{G}}_{\mathbf{p}} \hat{\mathbf{G}}_{-\mathbf{p}}$, we can write an expression for B :

$$B = N(0) T_c \sum_{\epsilon_n} \int_0^\infty d\xi \exp(-\xi) \int_0^{2\pi} \frac{d^2 p e^4(\phi)}{(2\pi)^2} \times \{ (G_{p,p} G_{-p,-p} + F_{p,p-Q} F_{-p,-p+Q})^2 + G_{p,p} G_{-p,-p} F_{-p+Q,p} F_{p-Q,p} + G_{-p+Q,-p+Q} G_{-p,-p} F_{p,p-Q} F_{p-Q,p} + G_{p,p} G_{p-Q,p-Q} F_{-p+Q,-p} F_{-p,-p+Q} \}.$$

$$+ G_{p-Q,p-Q} G_{-p+Q,-p+Q} F_{p,p-Q} F_{-p,-p+Q}. \quad (34)$$

Here we can directly verify that the sum of the last two terms in (34) yields a zero contribution, so that

$$B = N(0) T_c \sum_{\epsilon_n} \int_0^\infty d\xi \exp(-\xi) \int_0^{2\pi} \frac{d^2 p e^4(\phi)}{(2\pi)^2} \times (G_{p,p} G_{-p,-p} + F_{p,p-Q} F_{-p,-p+Q})^2. \quad (35)$$

This implies that

$$B = \frac{N(0) T_c}{2\pi} \sum_n \int_0^\infty d\xi \exp(-\xi) \times \int_{-\infty}^\infty d\xi \int_0^{2\pi} \frac{d\phi e^4(\phi)}{(\epsilon_n^2 + \xi^2 + \xi W^2(\phi))^2}, \quad (36)$$

and after integrating with respect to ξ and ϕ we arrive at an expression for K_B similar to (33):

$$K_B = \beta_b \frac{4\pi^3 T_c^3}{7\xi(3)} \int_0^\infty d\xi \exp(-\xi) \sum_n \frac{1}{(\sqrt{\epsilon_n^2 + \xi W^2})^3} + 1 - \beta_b, \quad (37)$$

where

$$\beta_b = \begin{cases} \frac{4\alpha}{\pi}, & (s \text{ pairing}), \\ \frac{4\alpha}{\pi} + \frac{4 \sin 4\alpha}{3\pi} + \frac{\sin 8\alpha}{6\pi}, & (d \text{ pairing}). \end{cases} \quad (38)$$

Thus, for s pairing the coefficients K_B and K_C simply coincide.

To conclude Sec. 4 we give the explicit expressions for the dimensionless Ginzburg–Landau coefficients for the case of d pairing in the model of commensurate short-range order fluctuations:

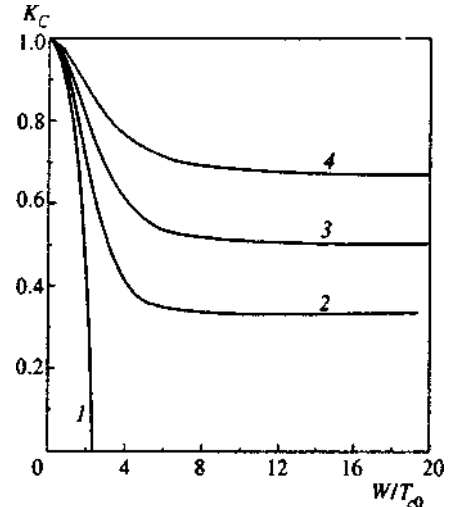


FIG. 9. The coefficient K_C as a function of the effective pseudogap width W/T_{c0} for hot sections of different size in the incommensurate fluctuation model for the case of s pairing: curve 1, $\alpha = \pi/4$; curve 2, $\alpha = \pi/6$; curve 3, $\alpha = \pi/8$; and curve 4, $\alpha = \pi/12$.

$$K_A = \beta_a \frac{1}{2T_c} \int_0^\infty \frac{d\xi \exp(-\xi/4)}{2\sqrt{\pi\xi}} \times \int_0^{\omega_c} \frac{d\xi}{\cosh^2(\sqrt{\xi^2 + \zeta W^2}/2T_c)} + 1 - \beta_a, \quad (39)$$

$$K_{C,B} = \beta_{c,b} \frac{4\pi^3 T_c^3}{7\zeta(3)} \int_0^\infty \frac{d\xi \exp(-\xi/4)}{2\sqrt{\pi\xi}} \times \sum_n \frac{1}{(\sqrt{\epsilon_n^2 + \zeta W^2})^3} + 1 - \beta_{c,b}, \quad (40)$$

where

$$\beta_a = \beta_c = \frac{4\alpha - \sin 4\alpha}{\pi},$$

$$\beta_b = \frac{4\alpha}{\pi} - \frac{\sin 4\alpha}{6\pi} (5 + \cos 4\alpha). \quad (41)$$

It is also easy to write the formulas reflecting the dependence of these coefficients on W/T_{c0} and different values of α . Qualitatively these expressions are similar to those in the incommensurate case, and the main difference are due to a different scale along the W/T_{c0} axis (cf. Fig. 6).

5. PHYSICAL CHARACTERISTICS OF SUPERCONDUCTORS WITH A PSEUDOGAP

As is known, the Ginzburg–Landau equations determine two characteristic lengths, the coherence length and the penetration depth for the magnetic field.

The coherence length at a given temperature, $\xi(T)$, is the characteristic scale of inhomogeneity in the order parameter Δ , which means it is actually the size of the Cooper pair:

$$\xi^2(T) = -\frac{C}{A}. \quad (42)$$

In ordinary superconductors (in the absence of a pseudogap),

$$\xi_{BCS}^2(T) = -\frac{C_0}{A_0}, \quad (43)$$

$$\xi_{BCS}(T) \approx 0.74 \frac{\xi_0}{\sqrt{1 - T/T_c}}, \quad (44)$$

where $\xi_0 = 0.18v_F/T_c$. For our case we have

$$\frac{\xi^2(T)}{\xi_{BCS}^2(T)} = \frac{K_C}{K_A}. \quad (45)$$

The corresponding dependence of $\xi^2(T)/\xi_{BCS}^2(T)$ on the parameter W/T_{c0} for the case of d pairing and incommensurate short-range order fluctuations is depicted in Fig. 10.

The penetration depth for the magnetic field in an ordinary superconductors is given by the formula

$$\lambda_{BCS}(T) = \frac{1}{\sqrt{2}} \frac{\lambda_0}{\sqrt{1 - T/T_c}}, \quad (46)$$

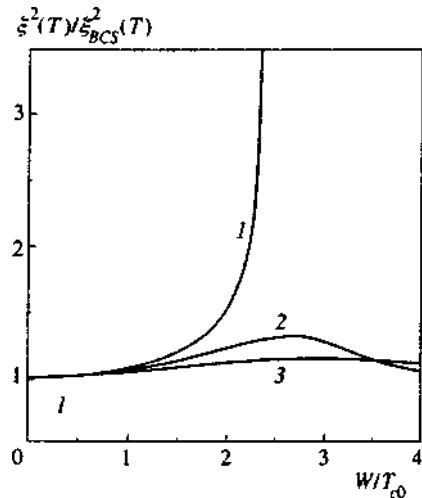


FIG. 10. The coherence length $\xi^2(T)/\xi_{BCS}^2(T)$ as a function of the effective pseudogap width W/T_{c0} in the model of d pairing: curve 1, $\alpha = \pi/4$; curve 2, $\alpha = \pi/8$; and curve 3, $\alpha = \pi/12$.

where $\lambda_0^2 = mc^2/4\pi ne^2$ determines the penetration depth at $T=0$. For the general case we have an expression for the penetration depth in terms of the Ginzburg–Landau coefficients:

$$\lambda^2(T) = -\frac{c^2}{32\pi e^2} \frac{B}{AC}. \quad (47)$$

Then in the adopted model we have

$$\frac{\lambda(T)}{\lambda_{BCS}(T)} = \left(\frac{K_B}{K_A K_C} \right)^{1/2}. \quad (48)$$

Curves representing the dependence of this parameter on the effective pseudogap width for the case of d pairing are depicted in Fig. 11.

Now let us calculate the Ginzburg–Landau parameter

$$\kappa = \frac{\lambda(T)}{\xi(T)} = \frac{c}{4eC} \sqrt{\frac{B}{2\pi}}. \quad (49)$$

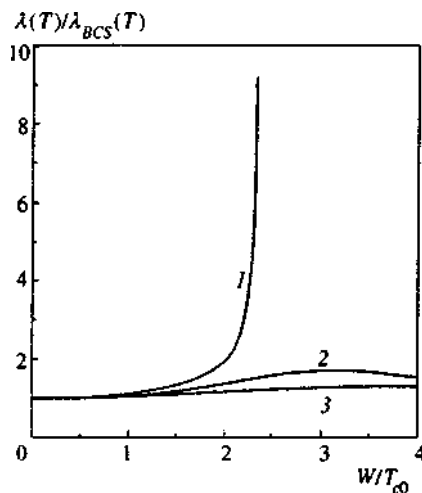


FIG. 11. The penetration depth $\lambda(T)/\lambda_{BCS}(T)$ as a function of the effective pseudogap width W/T_{c0} in the model of d pairing: curve 1, $\alpha = \pi/4$; curve 2, $\alpha = \pi/8$; and curve 3, $\alpha = \pi/12$.

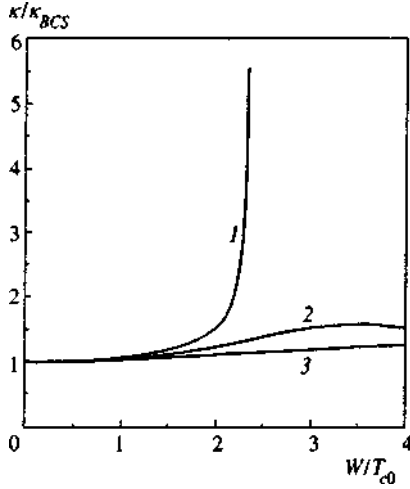


FIG. 12. The Ginzburg–Landau parameter $\kappa/\kappa_{\text{BCS}}$ as a function of the effective pseudogap width W/T_{c0} in the model of d pairing: curve 1, $\alpha = \pi/4$; curve 2, $\alpha = \pi/8$; and curve 3, $\alpha = \pi/12$.

In this model of a superconductor,

$$\frac{\kappa}{\kappa_{\text{BCS}}} = \frac{\sqrt{K_B}}{K_C}, \tag{50}$$

where

$$\kappa_{\text{BCS}} = \frac{3c}{\sqrt{7\zeta(3)}} \frac{T_c}{e v_F^2 \sqrt{N(0)}} \tag{51}$$

is the Ginzburg–Landau parameter for the ordinary case. Curves representing the dependence of $\kappa/\kappa_{\text{BCS}}$ on W/T_{c0} for the case of d pairing are depicted in Fig. 12.

Near T_c the upper critical field H_{c2} is expressed in terms of Ginzburg–Landau coefficients:

$$H_{c2} = -\frac{\phi_0}{2\pi} \frac{A}{C}, \tag{52}$$

where $\phi_0 = c\pi/e$ is the quantum of magnetic flux. Then the slope of the curve for the upper critical field near T_c is

$$\left| \frac{dH_{c2}}{dT} \right|_{T_c} = \frac{24\pi\phi_0}{7\zeta(3)v_F^2} T_c \frac{K_A}{K_C}. \tag{53}$$

Curves representing the dependence of the slope of the curves for the field, $|dH_{c2}/dT|_{T_c}$, normalized to the slope of the curves for the field at T_{c0} , on the effective pseudogap width W/T_{c0} for the case of d pairing are depicted in Fig. 13. We see that the slope rapidly decreases with increasing pseudogap width.

We can also calculate the size of the heat-capacity discontinuity at the transition point, which is generally calculated by the formula

$$\frac{C_s - C_n}{\Omega} = \frac{T_c}{B} \left(\frac{A}{T - T_c} \right)^2, \tag{54}$$

where C_s and C_n are the heat capacities of the superconducting and normal states, respectively, and Ω is the volume. This readily yields a formula for the size of the heat-capacity discontinuity at T_{c0} ($W=0$):

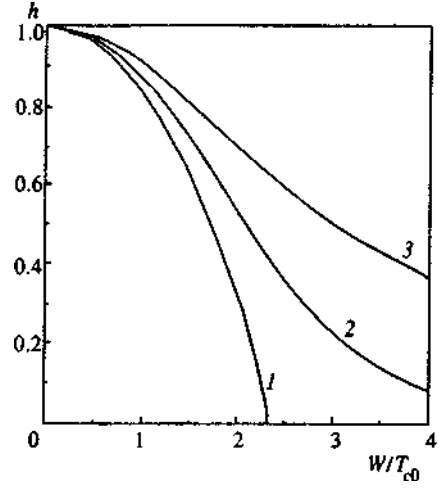


FIG. 13. The normalized slope of the curves for the upper critical field as a function of the effective pseudogap width W/T_{c0} in the model of d pairing: curve 1, $\alpha = \pi/4$; curve 2, $\alpha = \pi/8$; and curve 3, $\alpha = \pi/12$.

$$\left(\frac{C_s - C_n}{\Omega} \right)_{T_{c0}} = N(0) \frac{8\pi^2 T_{c0}}{7\zeta(3)}. \tag{55}$$

Then the size of the heat-capacity discontinuity in our model can be expressed in terms of the dimensionless coefficients K_A and K_B as follows:

$$\frac{(C_s - C_n)_{T_c}}{(C_s - C_n)_{T_{c0}}} = \frac{T_c}{T_{c0}} \frac{K_A^2}{K_B}. \tag{56}$$

Curves representing the dependence of the size of the heat-capacity discontinuity on the effective pseudogap width for the case of d pairing are depicted in Fig. 14. We see that the discontinuity diminishes as the pseudogap widens.

Curves representing the dependence of the above quantities for the case of s pairing and for the model of commensurate fluctuations are more or less (qualitatively) similar to

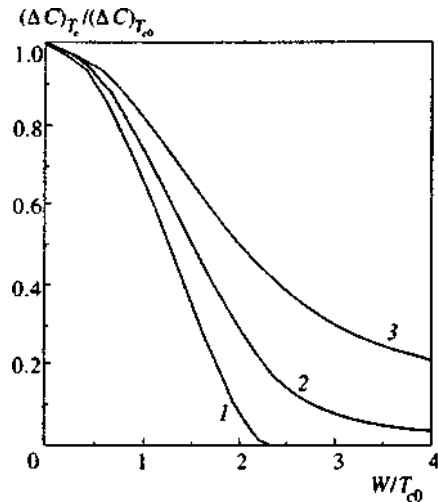


FIG. 14. The normalized size of the heat-capacity discontinuity as a function of the effective pseudogap width W/T_{c0} in the model of d pairing: curve 1, $\alpha = \pi/4$; curve 2, $\alpha = \pi/8$; and curve 3, $\alpha = \pi/12$.

those depicted in Figs. 10–14, differing in the scale along the W/T_{c0} axis, in accordance with Figs. 5 and 6.

6. CONCLUSION

We have studied a very simple model of a pseudogap in a two-dimensional electron model, which nevertheless qualitatively explains a number of observed features of the electron structure of underdoped high- T_c superconducting systems. In particular, with this model one can easily obtain the d symmetry of the pseudogap state, a symmetry that is due to the pattern of the hot sections on the Fermi surface caused by strong scattering by fluctuations of short-range (antiferromagnetic) order. Naturally, the model can be directly generalized to the case of a large number of hot sections, and it can reformulated in a way that is closer to the model of hot points (Refs. 10 and 11); other generalizations can also be made fairly easily.

The main simplifying assumption (and the main drawback) of the model is that we use the $\xi \rightarrow \infty$ limit for the fluctuation correlation length, due to which the main results can be written as formulas. In reality ξ is not very large and depends on the temperature and the degree of doping, so that it is an important parameter that controls the physical picture of all phenomena. Our model allows, at least in principle, a generalization to finite ξ in the sense of Refs. 17 and 18, but all calculations becomes extremely involved. At the same time it is clear that the effect of a finite ξ reduces mainly to a situation in which the pseudogap becomes closed,^{17,18} so that in this sense (as noted earlier) it simulates a decrease in the size of the hot sections in our model. This is true for effects basically controlled by the density of states (an example of a corresponding quantity is the transition temperature T_c). At the same time, this is not true of “kinetic” quantities (determined by the two-particle Green’s function), such as the coefficient C of the gradient term in the Ginzburg–Landau expansion.

Another radical simplification of our model is the assumption that short-range order fluctuations are static and Gaussian. The validity of this assumption can be justified in the high-temperature limit $T \gg \omega_{sf}$, where ω_{sf} is the characteristic frequency of spin fluctuations.^{9–11} Accordingly, the validity of the assumption that the fluctuations are static is questionable at temperatures near T_c . Nevertheless, our investigation shows that the Ginzburg–Landau expansion provides a good description of the influence of the main effect of “disintegration” of certain sections of the Fermi surface on the main characteristics of a superconductor with a pseudogap, and demonstrates the important role of pseudo-

gap anomalies in the formation of a superconducting state in the region of the phase diagram of high- T_c systems where these effects manifest themselves already in the normal phase. More realistic models will be analyzed later.

The authors are grateful to É. Z. Kuchinskii for useful discussions. The present work was partially supported by the Russian Fund for Fundamental Research (Project 96-02-16065), by the Statistical Physics State Program (Project IX.1), and by the High- T_c Superconductivity State Program of the Russian Ministry of Science (Project 96-0.51).

*E-mail: posazhen@ief.uran.ru

†E-mail: sadovski@ief.uran.ru

¹A similar treatment of the Ginzburg–Landau expansion in a model of the Peierls transition was carried out by McKenzie.²¹

¹M. Randeria, Varenna Lectures 1997, E-prints archive cond-mat/9710223.

²M. Randeria and J. C. Campuzano, Varenna Lectures 1997, E-prints archive cond-mat/9709107.

³H. Ding, T. Yokoya, J. C. Campuzano, T. Takahashi, M. Randeria, M. R. Norman, T. Mochiku, K. Kadowaki, and J. Giapintzakis, *Nature (London)* **382**, 51 (1996).

⁴H. Ding, M. R. Norman, T. Yokoya, T. Takeuchi, M. Randeria, J. C. Campuzano, T. Takahashi, T. Mochiki, and K. Kadowaki, *Phys. Rev. Lett.* **78**, 2628 (1997).

⁵V. B. Geshkenbein, L. B. Ioffe, and A. I. Larkin, *Phys. Rev. B* **55**, 3173 (1997).

⁶V. Emery, S. A. Kivelson, and O. Zachar, *Phys. Rev. B* **56**, 6120 (1997).

⁷A. P. Kampf and J. R. Schrieffer, *Phys. Rev. B* **41**, 6399 (1990); **42**, 7967 (1990).

⁸V. Barzykin and D. Pines, *Phys. Rev. B* **52**, 13 585 (1995).

⁹D. Pines, *Tr. J. of Physics* **20**, 535 (1996).

¹⁰J. Schmalian, D. Pines, and Stojkovic, *Phys. Rev. Lett.* **80**, 3839 (1998).

¹¹J. Schmalian, D. Pines, and Stojkovic, E-prints archive cond-mat/9804129.

¹²A. T. Zheleznyak, V. M. Yakovenko, and I. E. Dzyaloshinskii, *Phys. Rev. B* **55**, 3200 (1997).

¹³D. S. Dessau, Z.-X. Shen, D. M. King, D. S. Marshall, L. W. Lombardo, P. H. Dickinson, A. G. Loeser, J. DiCarlo, C.-H. Park, A. Kapitulnik, and W. E. Spicer, *Phys. Rev. Lett.* **71**, 2781 (1993).

¹⁴Z.-X. Shen and D. S. Dessau, *Phys. Rep.* **253**, 1 (1995).

¹⁵M. V. Sadovskii, *Zh. Éksp. Teor. Fiz.* **66**, 1720 (1974) [*Sov. Phys. JETP* **39**, 845 (1974)].

¹⁶M. V. Sadovskii, *Fiz. Tverd. Tela (Leningrad)* **16**, 2504 (1974) [*Sov. Phys. Solid State* **16**, 1632 (1975)].

¹⁷M. V. Sadovskii, *Zh. Éksp. Teor. Fiz.* **77**, 2070 (1979) [*Sov. Phys. JETP* **50**, 989 (1979)].

¹⁸M. V. Sadovskii and A. A. Timofeev, *Sverkhprovodimost’: Fiz., Khim., Tekhnol.* **4**, 11 (1991) [*Supercond., Phys. Chem. Technol.* **4**, 9 (1991)]; *J. Mosc. Phys. Soc.* **1**, 391 (1991).

¹⁹W. Wonneberger and R. Lautenschlager, *J. Phys. C: Solid State Phys.* **9**, 2865 (1976).

²⁰A. I. Posazhennikova and M. V. Sadovskii, *Zh. Éksp. Teor. Fiz.* **112**, 2124 (1997) [*JETP* **85**, 1162 (1997)].

²¹R. H. McKenzie, *Phys. Rev. B* **52**, 16 428 (1995).

Models of the pseudogap state of two-dimensional systems

É. Z. Kuchinskii^{*}) and M. V. Sadovskii[†])

Institute of Electrophysics, Ural Branch of the Russian Academy of Sciences, 620049 Ekaterinburg, Russia
(Submitted 9 September 1998)

Zh. Éksp. Teor. Fiz. **115**, 1765–1785 (May 1999)

We analyze several almost exactly solvable models of the electronic spectrum of two-dimensional systems with well-developed short-range-order dielectric (e.g., antiferromagnetic) or superconducting fluctuations that give rise to an anisotropic pseudogap state in certain segments of the Fermi surface. We develop a recurrence procedure for calculating the one-electron Green's function that is equivalent to summing all Feynman diagrams. The procedure is based on an approximate ansatz for higher order terms in the perturbation series. We do detailed calculations of the spectral densities and the one-electron density of states. Finally, we analyze the limits of the adopted approximations and some important points concerning the substantiation of these approximations. © 1999 American Institute of Physics.
[S1063-7761(99)01805-3]

1. INTRODUCTION

In recent years there has been an upsurge of interest in observations of the pseudogap in the spectrum of elementary excitations of high- T_c superconductors in the range of current carrier concentrations below the optimum.^{1,2} The corresponding anomalies were observed in a number of experiments, such as measurements of optical conductivity, NMR, inelastic neutron scattering, and angle-resolved photoemission (ARPES; see the review cited in Ref. 1). Probably the most striking evidence that such an unusual state exists was obtained in ARPES experiments,^{3,4} which demonstrated the presence of essentially anisotropic changes in the current-carrier spectral density within a broad temperature range in the normal (nonsuperconducting) phase of these systems (see the review in Ref. 2). A remarkable feature observed in these experiments was the presence of a maximum of the corresponding anomalies close to the point $(\pi, 0)$ in the Brillouin zone, while no such anomalies were observed in the direction of the zone diagonal [the point (π, π)], which actually means that near the point $(\pi, 0)$ the Fermi surface is destroyed, while the Fermi-liquid behavior in the direction of the zone diagonal is retained. In this sense it is usually said that the pseudogap symmetry is of the d -wave type, which coincides with the symmetry of the superconducting energy gap in these compounds.^{1,2} At the same time, the very fact that these anomalies exist at temperatures much higher than the superconducting transition temperature and at nonoptimal carrier concentrations could point to a different nature of these anomalies, not related directly to Cooper pairing.

There are many theoretical papers in which the authors attempt to explain the observed anomalies. Two main areas of such research can be identified. One is based on the idea that Cooper pairs form at temperatures higher than the superconducting transition temperature.^{1,5–7} In the other it is assumed that pseudogap phenomena are due primarily to antiferromagnetic (AFM) short-range-order fluctuations.^{8–12}

Some time ago one of the authors of the present paper

(M.V.S.) proposed an exactly solvable model of pseudogap formation in a one-dimensional system due to well-developed short-range-order charge density wave (CDW) or spin density wave (SDW) fluctuations (see Refs. 13–17). Recently this model has attracted the attention of researchers in connection with attempts to explain the pseudogap state of high- T_c cuprates.^{11,12,18–20} In particular, Schmalian *et al.*^{11,12} made an important generalization of this model to the case of a two-dimensional system of electrons that is in the random field of well-developed spin fluctuations (short-range-order AFM fluctuations). In the model of hot spots on the Fermi surface developed in Refs. 11 and 12, the researchers obtained, via the formal scheme developed in Refs. 15–17, a detailed description of pseudogap anomalies at high temperatures (the weak-pseudogap region). Tchernyshyov¹⁹ and Ren²⁰ used a simplified variant of the model developed in Refs. 13 and 14, which corresponds to the limit of very large correlation lengths of short-range-order fluctuations, to describe the pseudogap state determined by well-developed fluctuations of superconducting (SC) short range order. In a recent paper,²¹ this simplified model was used to analyze the Ginzburg–Landau expansion (for different types of Cooper pairing) in a system with strong CDW (SDW, AFM) fluctuations using the model of hot patches on the Fermi surface proposed in the paper. At the same time, Tchernyshyov²² reviewed in detail the model developed in Refs. 13–17 and found an error in the earlier papers^{15–17} in the analysis of the case of finite correlation lengths of short-range-order fluctuations. In Ref. 12 it was suggested that this error is insignificant, especially in analyzing the two-dimensional hot-spot model, which is of the main interest to the physics of high- T_c systems.

The aim of the present paper is to analyze a number of important aspects of the almost exactly solvable model, mainly in the two-dimensional case. To this end we consider both the case of short-range-order CDW (SDW, AFM) fluctuations in the hot-spot model^{11,12} and the possibility of using the model within the framework of fluctuation Cooper

pairing^{7,19,20} (SC short-range-order fluctuations), in particular, in the most interesting case of d -wave pairing. In addition to a general analysis of the reliability of the formal scheme used in Refs. 11–17, we do detailed calculations of the spectral density and the one-electron density of states for the hot-spot model^{11,12} and in the scenario of fluctuation Cooper pairing.

2. THE HOT-SPOT MODEL

2.1. Description of model and an “almost exact” solution for the Green’s function

The model of a nearly ferromagnetic Fermi liquid^{23,24} is based on the picture of well-developed fluctuations of AFM short-range-order fluctuations within a wide region of the phase diagram of high- T_c systems. This model introduces the effective interaction of electrons and spin fluctuations that is described by the dynamic spin susceptibility $\chi_q(\omega)$, which is determined mainly from the fit to the data of NMR experiments:²⁴

$$V_{\text{eff}}(\omega, \mathbf{q}) = g^2 \chi_q(\omega) \approx \frac{g^2 \xi^2}{1 + \xi^2 (\mathbf{q} - \mathbf{Q})^2 - i\omega/\omega_{\text{sf}}}, \quad (1)$$

where g is the coupling constant, ξ is the correlation length of the spin fluctuations, $\mathbf{Q} = (\pi/a, \pi/a)$ is the vector of antiferromagnetic ordering in the insulator phase, ω_{sf} is the characteristic frequency of spin fluctuations, and a is the lattice constant (of a square lattice).

Since the dynamic spin susceptibility $\chi_q(\omega)$ has peaks at wave vectors that are in the vicinity of $(\pi/a, \pi/a)$, two types of quasiparticle arise in the system: “hot” quasiparticles with momenta in the vicinity of hot spots on the Fermi surface, and “cold” quasiparticles with momenta in the parts of the Fermi surface surrounding the diagonals of the Brillouin zone, $|p_x| = |p_y|$ (see Refs. 11 and 12). Such terminology is related to the fact that quasiparticles from the vicinity of hot spots are strongly scattered through a vector of order \mathbf{Q} by spin fluctuations (1), while for particles with momenta far from hot spots this interaction is relatively weak.

In what follows we consider the case of high temperatures, $\pi T \gg \omega_{\text{sf}}$, which corresponds to the “weak pseudogap” region in the phase diagram.^{11,12} In this case spin dynamics is irrelevant and we can limit ourselves to the static approximation:

$$V_{\text{eff}}(\mathbf{q}) = \tilde{\Delta}^2 \frac{\xi^2}{1 + \xi^2 (\mathbf{q} - \mathbf{Q})^2}, \quad (2)$$

where $\tilde{\Delta}$ is an effective parameter with the dimensions of energy, which in the model of AFM fluctuations can be written¹²

$$\tilde{\Delta}^2 = g^2 T \sum_{m\mathbf{q}} \chi_q(i\omega_m) = g^2 \langle \mathbf{S}_i^2 \rangle / 3, \quad (3)$$

with \mathbf{S}_i the spin at a lattice site (Cu ions in the CuO_2 plane for high- T_c cuprates). Below we consider $\tilde{\Delta}$ (as well as ξ) a phenomenological parameter that determines the effective width of the pseudogap.

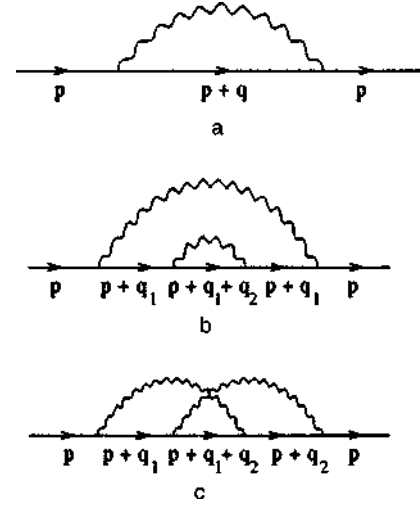


FIG. 1. First- and second-order self-energy diagrams for an electron interacting with short-range-order fluctuations.

Calculations can be simplified significantly if we replace (2) with a model interaction of the form (cf. a similar model in Ref. 8)

$$V_{\text{eff}}(\mathbf{q}) = \Delta^2 \frac{2\xi^{-1}}{\xi^{-2} + (q_x - Q_x)^2} \frac{2\xi^{-1}}{\xi^{-2} + (q_y - Q_y)^2}, \quad (4)$$

where $\Delta^2 = \tilde{\Delta}^2/4$. Actually, Eq. (4) is quite similar to (2) and differs quantitatively very little in the most important region $|\mathbf{q} - \mathbf{Q}| < \xi^{-1}$.

Consider the first-order correction in V_{eff} to the electron self-energy, represented by the diagram in Fig. 1a:

$$\Sigma(\varepsilon_n, \mathbf{p}) = \sum_{\mathbf{q}} V_{\text{eff}}(\mathbf{q}) \frac{1}{i\varepsilon_n - \xi_{\mathbf{p}+\mathbf{q}}}. \quad (5)$$

The main contribution to the sum over \mathbf{q} is provided by the region close to $\mathbf{Q} = (\pi/a, \pi/a)$. Then, writing

$$\xi_{\mathbf{p}+\mathbf{q}} = \xi_{\mathbf{p}+\mathbf{Q}+\mathbf{k}} \approx \xi_{\mathbf{p}+\mathbf{Q}} + \mathbf{v}_{\mathbf{p}+\mathbf{Q}} \cdot \mathbf{k}, \quad (6)$$

where $v_{\mathbf{p}+\mathbf{Q}}^\alpha = \partial \xi_{\mathbf{p}+\mathbf{Q}} / \partial p_\alpha$, and integrating over \mathbf{k} , we obtain¹⁾

$$\Sigma(\varepsilon_n, \mathbf{p}) = \frac{\Delta^2}{i\varepsilon_n - \xi_{\mathbf{p}+\mathbf{Q}} + (|v_{\mathbf{p}+\mathbf{Q}}^x| + |v_{\mathbf{p}+\mathbf{Q}}^y|) \kappa \text{sign } \varepsilon_n}, \quad (7)$$

with $\kappa = \xi^{-1}$.

The spectrum of bare (free) quasiparticles can be taken from Refs. 11 and 12:

$$\xi_{\mathbf{p}} = -2t(\cos p_x a + \cos p_y a) - 4t' \cos p_x a \cos p_y a, \quad (8)$$

where t is the nearest-neighbor-hopping integral, t' is the next-nearest-neighbor-hopping integral for a square lattice, and μ is the chemical potential. When real high- T_c systems were analyzed in Refs. 11 and 12, it was assumed, e.g., for $\text{YBa}_2\text{Cu}_3\text{O}_{6+\delta}$, that $t = 0.25$ eV and $t' = -0.45t$, and μ was fixed by hole concentration. Below we show that the analysis of the situation for different relationships between t and t' produces interesting results.

We now turn to second-order corrections to self-energy, which are depicted in Figs. 1b and 1c. Using (4) we obtain

$$\begin{aligned} \Sigma(b) = & \Delta^4 \int \frac{d\mathbf{k}_1}{\pi^2} \int \frac{d\mathbf{k}_2}{\pi^2} \frac{\kappa}{\kappa^2 + k_{1x}^2} \frac{\kappa}{\kappa^2 + k_{1y}^2} \frac{\kappa}{\kappa^2 + k_{2x}^2} \\ & \times \frac{\kappa}{\kappa^2 + k_{2y}^2} \frac{1}{i\varepsilon_n - \xi_{\mathbf{p}+\mathbf{Q}} - v_{\mathbf{p}+\mathbf{Q}}^x k_{1x} - v_{\mathbf{p}+\mathbf{Q}}^y k_{1y}} \\ & \times \frac{1}{i\varepsilon_n - \xi_{\mathbf{p}} - v_{\mathbf{p}}^x(k_{1x} + k_{2x}) - v_{\mathbf{p}}^y(k_{1y} + k_{2y})} \\ & \times \frac{1}{i\varepsilon_n - \xi_{\mathbf{p}+\mathbf{Q}} - v_{\mathbf{p}+\mathbf{Q}}^x k_{1x} - v_{\mathbf{p}+\mathbf{Q}}^y k_{1y}}, \end{aligned} \quad (9)$$

$$\begin{aligned} \Sigma(c) = & \Delta^4 \int \frac{d\mathbf{k}_1}{\pi^2} \int \frac{d\mathbf{k}_2}{\pi^2} \frac{\kappa}{\kappa^2 + k_{1x}^2} \frac{\kappa}{\kappa^2 + k_{1y}^2} \frac{\kappa}{\kappa^2 + k_{2x}^2} \\ & \times \frac{\kappa}{\kappa^2 + k_{2y}^2} \frac{1}{i\varepsilon_n - \xi_{\mathbf{p}+\mathbf{Q}} - v_{\mathbf{p}+\mathbf{Q}}^x k_{1x} - v_{\mathbf{p}+\mathbf{Q}}^y k_{1y}} \\ & \times \frac{1}{i\varepsilon_n - \xi_{\mathbf{p}} - v_{\mathbf{p}}^x(k_{1x} + k_{2x}) - v_{\mathbf{p}}^y(k_{1y} + k_{2y})} \\ & \times \frac{1}{i\varepsilon_n - \xi_{\mathbf{p}+\mathbf{Q}} - v_{\mathbf{p}+\mathbf{Q}}^x k_{2x} - v_{\mathbf{p}+\mathbf{Q}}^y k_{2y}}, \end{aligned} \quad (10)$$

where we have employed the spectrum (8), from which, in particular, it follows that $\xi_{\mathbf{p}+2\mathbf{Q}} = \xi_{\mathbf{p}}$ and $\mathbf{v}_{\mathbf{p}+2\mathbf{Q}} = \mathbf{v}_{\mathbf{p}}$ at $\mathbf{Q} = (\pi/a, \pi/a)$. If $v_{\mathbf{p}}^x$ and $v_{\mathbf{p}+\mathbf{Q}}^y$ are of the same sign, the integrals in (9) and (10) are determined solely by the poles of the Lorentzians determining the interaction with short-range-order fluctuations. Doing an elementary contour integration, we get²⁾

$$\begin{aligned} \Sigma(b) = & \Sigma(c) \\ = & \Delta^4 \frac{1}{[i\varepsilon_n - \xi_{\mathbf{p}+\mathbf{Q}} + i(|v_{\mathbf{p}+\mathbf{Q}}^x| + |v_{\mathbf{p}+\mathbf{Q}}^y|)\kappa]^2} \\ & \times \frac{1}{i\varepsilon_n - \xi_{\mathbf{p}} + i2(|v_{\mathbf{p}}^x| + |v_{\mathbf{p}}^y|)\kappa}. \end{aligned} \quad (11)$$

Here and below we assume, for the sake of definiteness, that ε_n is positive. Clearly, when the velocity projections are of the same sign, we can use this approach to calculate the contributions of any higher-order diagrams. Accordingly, the contribution of an N th-order diagram to the self-energy part in the interaction (4) is

$$\Sigma^{(N)}(\varepsilon_n, \mathbf{p}) = \Delta^{2N} \prod_{j=1}^{2N-1} \frac{1}{i\varepsilon_n - \xi_j + in_j v_j \kappa}, \quad (12)$$

where $\xi_j = \xi_{\mathbf{p}+\mathbf{Q}}$ and $v_j = |v_{\mathbf{p}+\mathbf{Q}}^x| + |v_{\mathbf{p}+\mathbf{Q}}^y|$ for odd j , and $\xi_j = \xi_{\mathbf{p}}$ and $v_j = |v_{\mathbf{p}}^x| + |v_{\mathbf{p}}^y|$ for even j . Here n_j is the number of interaction lines surrounding the j th Green's function in a given diagram.

In this case any diagram with crossing interaction lines is equal to a diagram of the same order with noncrossing

interaction lines. Hence actually we may consider only diagrams with noncrossing interaction lines, taking into account the diagrams with crossing lines by introducing additional combinatorial factors into the interaction vertices. This method was first introduced (in another problem) by Elyutin²⁵ and was used in Refs. 15–17 for a one-dimension model of the pseudogap state.

As a result we arrive at the following expression for the one-electron Green's function in the form of a recurrence relation (the continued fraction representation; see Refs. 15–17):

$$G^{-1}(\varepsilon_n, \xi_{\mathbf{p}}) = G_0^{-1}(\varepsilon_n, \xi_{\mathbf{p}}) - \Sigma_1(\varepsilon_n, \xi_{\mathbf{p}}), \quad (13)$$

$$\Sigma_k(\varepsilon_n, \xi_{\mathbf{p}}) = \Delta^2 \frac{v(k)}{i\varepsilon_n - \xi_k + ikv_k \kappa - \Sigma_{k+1}(\varepsilon_n, \xi_{\mathbf{p}})}, \quad (14)$$

where $\xi_k = \xi_{\mathbf{p}+\mathbf{Q}}$ and $v_k = |v_{\mathbf{p}+\mathbf{Q}}^x| + |v_{\mathbf{p}+\mathbf{Q}}^y|$ for odd k , and $\xi_k = \xi_{\mathbf{p}}$ and $v_k = |v_{\mathbf{p}}^x| + |v_{\mathbf{p}}^y|$ for even k . The combinatorial factor

$$v(k) = k \quad (15)$$

corresponds to our case of commensurate fluctuations with $\mathbf{Q} = (\pi/a, \pi/a)$ (see Ref. 15). Clearly, one can easily analyze the case of incommensurate fluctuations, where \mathbf{Q} is not locked to the period of the reciprocal lattice. In this case, diagrams with interaction lines surrounding an odd number of vertices are significantly smaller than diagrams with interaction lines surrounding an even number of vertices. Hence only the latter diagrams should be taken into account.^{13–17} As a result, the recurrence relation (14) is retained, but the combinations of the diagrams and hence the combinatorial factor change:¹⁵

$$v(k) = \begin{cases} \frac{k+1}{2} & \text{for } k \text{ odd,} \\ \frac{k}{2} & \text{for } k \text{ even.} \end{cases} \quad (16)$$

In Refs. 11 and 12, the spin structure of the interaction in the ‘‘almost antiferromagnetic’’ Fermi-liquid model (the spin-fermion model of Ref. 12) was taken into account. This leads to more complicated combinations in the commensurate case with $\mathbf{Q} = (\pi/a, \pi/a)$. More precisely, spin-conserving scattering yields formally commensurate combinations, while spin-flip scattering is described by diagrams of the incommensurate type (a ‘‘charged’’ random field, to use the terminology of Ref. 12). As result, the recurrence relation for the Green's function is still of the form (14), but the combinatorial factor $v(k)$ is now^{11,12}

$$v(k) = \begin{cases} \frac{k+2}{3} & \text{for } k \text{ odd,} \\ \frac{k}{3} & \text{for } k \text{ even.} \end{cases} \quad (17)$$

As noted earlier, the solution (14) can be obtained only if the signs of the velocity projections $v_{\mathbf{p}+\mathbf{Q}}^x(v_{\mathbf{p}+\mathbf{Q}}^y)$ and $v_{\mathbf{p}}^x(v_{\mathbf{p}}^y)$ are the same. Below we analyze the situation when this is really the case. When the signs are different, the integrals of the form (9) and (10), corresponding to higher-order corrections, cannot be calculated in such a simple form as

above because contributions from the poles of the electron Green's functions become important. Here instead of simple expressions of the form (11) we have much more complicated expressions and (even more importantly) the very fact that broad classes of diagrams with crossing and noncrossing interaction lines are equal is not true any more [the reader will recall that it was this fact that made it possible to classify higher-order contributions and to obtain the "exact" solution (14)]. This problem is important only for the case of finite correlation lengths $\xi = \kappa^{-1}$ of fluctuations, while in the limit $\xi \rightarrow \infty$ ($\kappa \rightarrow 0$) the exact solution for the Green's function is independent of the velocities $\mathbf{v}_{\mathbf{p}}$ and $\mathbf{v}_{\mathbf{p}+\mathbf{Q}}$ and can easily be obtained in analytic form by the methods developed in Refs. 13 and 14 (see also Ref. 12). In the one-dimensional model considered in Refs. 13–17, the signs of the corresponding velocity projections are always different (they correspond to electrons travelling "right" and "left"). This fact was stressed in a recent paper by Tchernyshyov.²² In the Appendix we analyze these difficulties in detail for the one-dimensional case and show that the ansatz of the form (12) used in Refs. 15–17 for the contributions of higher-order diagrams and the solution (14) yield a very good approximation even when the velocity projections have opposite signs. Obviously, this solution is exact in the limits $\xi \rightarrow \infty$ ($\kappa \rightarrow 0$) and $\xi \rightarrow 0$ ($\kappa \rightarrow \infty$) and provides a fairly good (quantitative) description in the region of finite correlation lengths.

2.2. Analysis of the spectrum

For the energy spectrum (8) we can easily specify the conditions (the relationships between t , t' , and μ) for the solution (14) to be exact. First, let us define the region of the parameters t , t' , and μ where there are hot spots on the Fermi surface, i.e., the conditions for the existence of points connected by the vector $\mathbf{Q} = (\pi/a, \pi/a)$. If $\mathbf{p} = (p_x, p_y)$ specifies the position of a hot spot on the Fermi surface, the point $\mathbf{p} + \mathbf{q} = (p_x + \pi/a, p_y + \pi/a)$ must also belong to the Fermi surface, so that for the spectrum (8) we have

$$-2t(\cos p_x a + \cos p_y a) - 4t' \cos p_x a \cos p_y a - \mu = 0, \quad (18)$$

$$2t(\cos p_x a + \cos p_y a) - 4t' \cos p_x a \cos p_y a - \mu = 0.$$

This yields the conditions needed for hot spots to exist:

$$\cos p_y a = -\cos p_x a, \quad \cos^2 p_x a = \mu/4t'. \quad (19)$$

Thus, hot spots on the Fermi surface exist if

$$0 \leq \mu/4t' \leq 1. \quad (20)$$

We now define the region of the parameters t , t' , and μ where the solution (14) is exact by requiring that the products $v_{\mathbf{p}}^x v_{\mathbf{p}+\mathbf{Q}}^x$ and $v_{\mathbf{p}}^y v_{\mathbf{p}+\mathbf{Q}}^y$ be positive. We have

$$v_{\mathbf{p}}^x = \frac{\partial \xi_{\mathbf{p}}}{\partial p_x} = 2ta \sin p_x a + 4t'a \sin p_x a \cos p_y a,$$

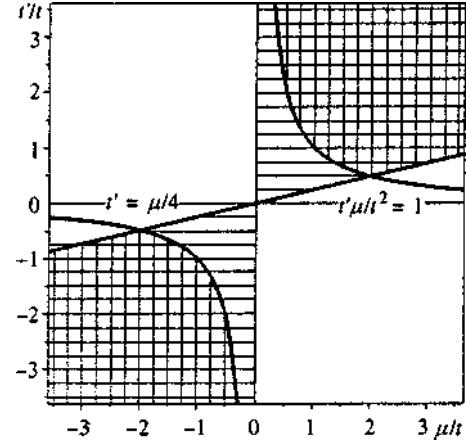


FIG. 2. The region of parameters where hot spots exist (hatched) and the region where such spots exist and the velocity projections have the same sign (doubly hatched).

$$v_{\mathbf{p}}^y = \frac{\partial \xi_{\mathbf{p}}}{\partial p_y} = 2ta \sin p_y a + 4t'a \sin p_y a \cos p_x a,$$

$$v_{\mathbf{p}}^x v_{\mathbf{p}+\mathbf{Q}}^x = 16t'^2 a^2 \sin^2 p_x a \left[\cos^2 p_y a - \left(\frac{t}{2t'} \right)^2 \right],$$

$$v_{\mathbf{p}}^y v_{\mathbf{p}+\mathbf{Q}}^y = 16t'^2 a^2 \sin^2 p_y a \left[\cos^2 p_x a - \left(\frac{t}{2t'} \right)^2 \right]. \quad (21)$$

Clearly, for the Fermi surface to have points where the projections of velocities have the same sign, $|t'/t|$ must be greater than 1/2. Here we are chiefly interested in the region surrounding the hot spots, where on account of (19) we have

$$v_{\mathbf{p}}^x v_{\mathbf{p}+\mathbf{Q}}^x = v_{\mathbf{p}}^y v_{\mathbf{p}+\mathbf{Q}}^y = 4t^2 a^2 \left(1 - \frac{\mu}{4t'} \right) \left(\frac{\mu t'}{t^2} - 1 \right). \quad (22)$$

Thus, the projections of velocities at hot spots have the same sign if

$$\mu t' / t^2 > 1. \quad (23)$$

Obviously, the same condition ensures that $\mathbf{v}_{\mathbf{p}} \mathbf{v}_{\mathbf{p}+\mathbf{Q}}$ is positive (this is needed for the solution (14) to be valid in the model described in Refs. 11 and 12).

Figure 2 depicts the region of parameters where hot spots exist (the hatched area), or $0 \leq \mu/4t' \leq 1$, and the region where such spots exist and the velocity projections have the same sign ($\mu t' > 1$). Figure 3 depicts, for different values of the chemical potential μ (band filling), the Fermi surfaces specified by the spectrum (8) for which these conditions are either met or not met.

2.3. Spectral density and density of states

Let us examine the spectral density

$$A(E, \mathbf{p}) = -\frac{1}{\pi} \text{Im } G^R(E, \mathbf{p}), \quad (24)$$

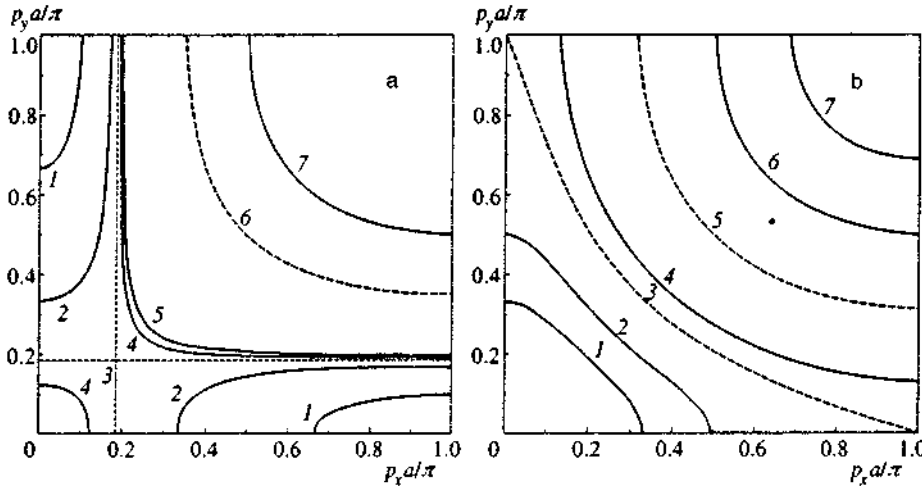


FIG. 3. Fermi surfaces defined by the spectrum (8) for different values of the chemical potential μ (band filling) and the parameter t'/t . (a) The case where $t'/t = -0.6$ and μ/t has the following values: curve 1, -2.2 ; curve 2, -1.8 ; curve 3, -1.666 ; curve 4, -1.63 ; curve 5, -1.6 ; curve 6, 0; and curve 7, 2; the solution (14) is exact in the vicinity of hot spots (the velocity projections are of the same sign) for $\mu/t < -1.666 \dots$, and hot spots exist if μ/t is negative. (b) The case where $t'/t = -0.4$ (which is characteristic of high- T_c cuprates) and μ/t has the following values: curve 1, -2.2 ; curve 2, -2 ; curve 3, -1.6 ; curve 4, -1.3 ; curve 5, 0; curve 6, 2; and curve 7, 4; hot spots exist if $-1.6 < \mu/t < 0$.

where $G^R(E, \mathbf{p})$ is the retarded Green's function obtained by ordinary analytic continuation of (13) into the real energy axis E . Figure 4 depicts the energy dependence of $A(E, \mathbf{p})$ obtained from (13) and (14) for different variants of the combinatorial factors (15) and (16). Since the energy dependence of the spectral density in the case of the combinations (17) for the spin-fermion model is qualitatively (and even quantitatively) very close to that obtained in the incommensurate case, Eq. (16), we have not displayed it in Fig. 4a so as to save space. For $t'/t = -0.6$ and $\mu/t = -1.8 < t'/t = 1.666$, the projections of the velocities at the hot spots have the same sign and the solution (14) defines the Green's function exactly. We see that in the incommensurate case (16) (Fig. 4a) as well as for the combinations (17) of the spin-fermion model, the spectral density at a hot spot clearly exhibits non-Fermi-liquid behavior (for large values of the correlation length ξ of the fluctuations). In the case of commensurate combinations, Eq. (15) (Fig. 4b), it is precisely at a hot spot that the spectral density has a single peak and, in this sense, is similar to the spectral density of an ordinary Fermi liquid even when ξ is large. However, even in the vicinity of a hot spot the spectral density acquires two non-Fermi-liquid peaks (the "shadow" band) for large values of ξ (see the inset in Fig. 4b).

Far from hot spots, the velocity projections have, in general, opposite signs, even if condition (23) is met. Accordingly, the recurrence relation (14) for the Green's function is not exact. At the same time, as ξ increases, the region with the hot spot in the momentum space narrows and the accuracy of our approximation grows. However, from a discussion in the Appendix it becomes clear that our ansatz (12) and the solution (14) only slightly overestimate the role of the finiteness of the correlation length ξ . There we also propose a slightly different variant of the solution, Eq. (A11), which somewhat underestimates this role. The insets in Fig. 4 depict the energy dependence of the spectral density far from a hot spot for different combinations, (15) and (16).

Figure 5 depicts the energy dependence of the spectral density for the combinations (15) and (16) at a hot spot with $t'/t = -0.4$, which, according to Schmalian *et al.*,^{11,12} corresponds to the $\text{YBa}_2\text{Cu}_3\text{O}_{6+\delta}$ system. The spectral density in the case of the combinations (17) of the spin-fermion model is very close to that obtained in the incommensurate case (16). For such a value of t'/t , even at hot spots the velocity projections have opposite signs. However, the spectral density (in the incommensurate case) obtained from the solution with "alternating" κ , Eq. (A11) (the dashed curve in Fig. 5a) is seen to be very close to that obtained from (14). This

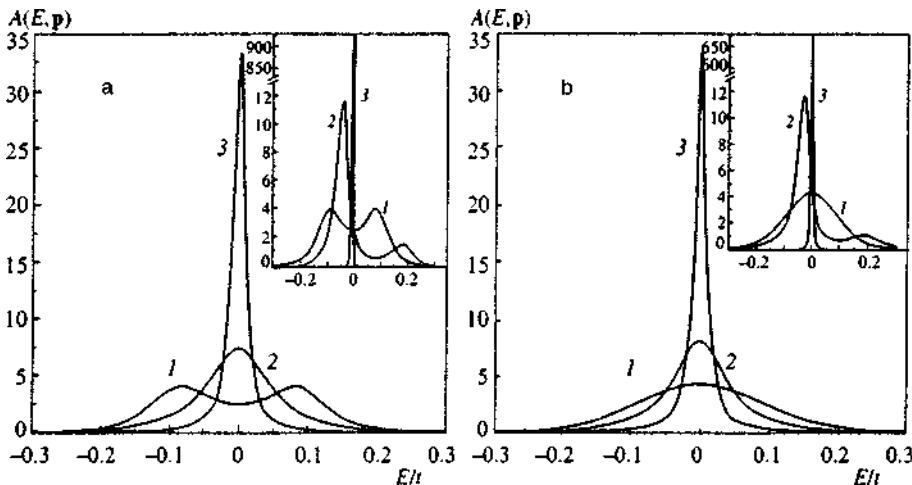


FIG. 4. Energy dependence of the spectral density at a hot spot ($p_x a/\pi = 0.1666$ and $p_y a/\pi = 0.8333$) for different diagram combinations at $t'/t = -0.6$ and $\mu/t = -1.8$, when the solution (14) is exact: (a) the incommensurate case, and (b) the commensurate case. The correlation length corresponds to the following values of κa : curve 1, 0.01; curve 2, 0.1; and curve 3, 0.5; $\Delta = 0.1t$. The insets depict the energy dependence of the spectral density for the corresponding diagram combinations at $\kappa a = 0.01$: curve 1, at the hot spot $p_x a/\pi = 0.1666$ and $p_y a/\pi = 0.8333$; curve 2, near the hot spot $p_x a/\pi = 0.1663$ and $p_y a/\pi = 0.8155$; and curve 3, far from the hot spot $p_x a/\pi = 0.0$ and $p_y a/\pi = 0.333$.

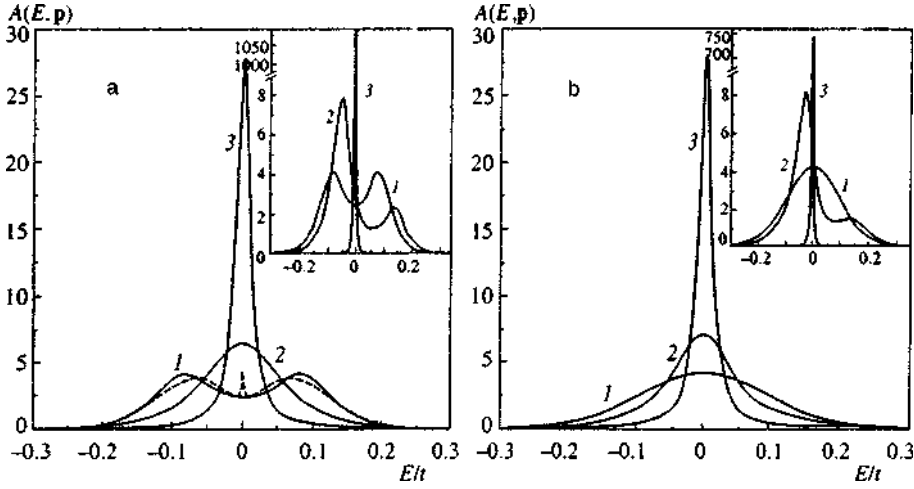


FIG. 5. Energy dependence of the spectral density at a hot spot ($p_x a/\pi=0.142$ and $p_y a/\pi=0.857$) for different diagram combinations at $t'/t=-0.4$ and $\mu/t=-1.3$, which approximately corresponds to high- T_c cuprates: (a) the incommensurate case [the dashed curve represents the spectral density for the incommensurate case obtained by (A11)], and (b) the commensurate case. The correlation length corresponds to the following values of κa : curve 1, 0.01; curve 2, 0.1; and curve 3, 0.5; $\Delta=0.1t$. The insets depict the energy dependence of the spectral density for the corresponding diagram combinations at $\kappa a=0.01$: curve 1, at the hot spot $p_x a/\pi=0.142$ and $p_y a/\pi=0.857$; curve 2, near the hot spot $p_x a/\pi=0.145$ and $p_y a/\pi=0.843$; and curve 3, far from the hot spot $p_x a/\pi=p_y a/\pi=0.375$.

suggests that the ansatz (12) and solution (14) quantitatively are close to an exact solution. We stress once more that the solution (14) is exact in the limits $\xi \rightarrow \infty$ and $\xi \rightarrow 0$, while for finite ξ it provides a good interpolation between the two limits.

Now consider the one-electron density of states,

$$N(E) = \sum_{\mathbf{p}} A(E, \mathbf{p}) = -\frac{1}{\pi} \sum_{\mathbf{p}} \text{Im} G^R(E, \mathbf{p}), \quad (25)$$

determined by the integral of the spectral density $A(E, \mathbf{p})$ over the entire Brillouin zone. Earlier we have seen that although for some topologies of the initial Fermi surface (band fillings) we can guarantee that near hot spots the signs of the velocity projections are the same, far from hot spots the signs are usually different, and the solution (14) based on the ansatz (12) is only an approximation. Correspondingly, using the solution (14) to calculate the density of states also yields an approximation, according to (25). Figure 6 depicts the densities of states obtained from (13), (15), and (25) with allowance for the spectrum (8), for different diagram combinations, Eqs. (15), (16), and (17), at $t'/t=-0.4$ (Fig. 6a) and $t'/t=-0.6$ (Fig. 6b). We see that at $t'/t=-0.4$ the density of states vs. energy curves acquire a dip (pseudogap). This decrease in the density of states is weakly dependent on the

correlation length ξ (see the inset in Fig. 6a). If the band filling is such that the Fermi level μ lands in this energy interval, there are hot spots on the Fermi surface. At $t'/t=-0.6$, the region where the hot spots exist is rather wide, but nevertheless the pseudogap in the density of states is essentially unobservable. What can be seen is a smearing of the Van Hove singularity, a singularity that exists when there is no scattering by fluctuations.

3. MODEL OF "SUPERCONDUCTING" FLUCTUATIONS

3.1. Description of model and the solution for the Green's function

As noted earlier, pseudogap phenomena can probably be explained by employing the idea of fluctuation Cooper pairing at temperatures above the superconducting transition temperature T_c (see Refs. 1, 5–7). Consider the simplest possible model approach to this problem. Figure 7a depicts the self-energy diagram of first order in the fluctuation propagator of Cooper pairs for $T > T_c$. Bearing in mind that we wish to consider both ordinary s -wave pairing and d -wave pairing, which is a characteristic feature of high- T_c systems, we introduce the pairing interaction of the simplest (separable) form

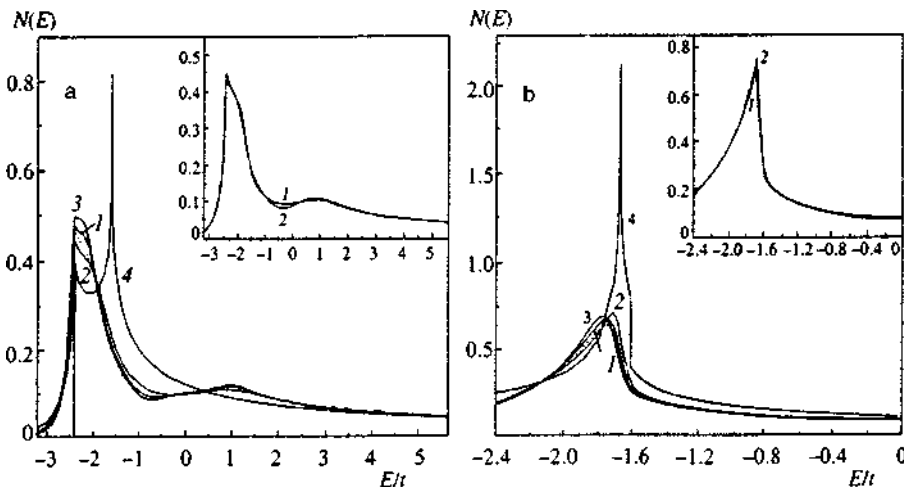


FIG. 6. One-electron density of states for different diagram combinations: (a) the case where $t'/t=-0.4$ and $\mu/t=-1.3$, and (b) the case where $t'/t=-0.6$ and $\mu/t=-1.8$. Curves 1 correspond to the incommensurate case, curves 2 to the commensurate case, curves 3 to the combinations of the spin-fermion model, and curves 4 to the case where there is no AFM fluctuations. The dotted curves represent the spectral density for the incommensurate case obtained by (A11), $\Delta/t=1$, and the correlation length corresponds to $\kappa a=0.1$. The insets depict the one-electron densities of states energy for the corresponding diagram combinations at $\kappa a=0.1$ (curves 1) and $\kappa a=0.01$ (curves 2).

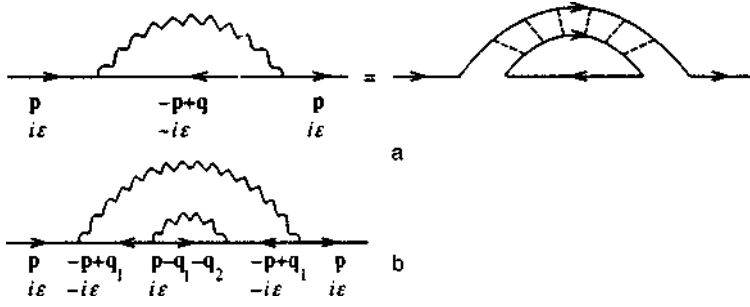


FIG. 7. Self-energy diagrams in the model of SC fluctuations: (a) the first-order diagram with an “explanation” of the meaning of the wave line, the fluctuation operator of Cooper pairs (the dashed lines correspond to pairing interaction), and (b) the second-order diagram.

$$V(\mathbf{p}, \mathbf{p}') = -Ve(\phi)e(\phi'), \quad (26)$$

where ϕ is the polar angle specifying the direction of the electron momentum \mathbf{p} in the plane, and for $e(\phi)$ we use the model dependence adopted in Refs. 26 and 27:

$$e(\phi) = \begin{cases} 1 & \text{for } s\text{-wave pairing,} \\ \sqrt{2} \cos 2\phi & \text{for } d\text{-wave pairing.} \end{cases} \quad (27)$$

As usual, the coupling constant V is assumed finite for electrons within an energy layer near the Fermi surface. Then the self-energy part corresponding to Fig. 7a takes the form

$$\Sigma(\varepsilon_n, \mathbf{p}) = \sum_{mp} V_{\text{eff}}(i\omega_m, \mathbf{q}) G(i\omega_m - i\varepsilon_n, -\mathbf{p} + \mathbf{q}), \quad (28)$$

where the effective interaction with SC fluctuations is given by the expression

$$V_{\text{eff}}(i\omega_m, \mathbf{q}) = - \frac{Ve^2(\phi)}{1 - VT \sum_{np} G_0(i\varepsilon_n, \mathbf{p}) G_0(i\omega_m - i\varepsilon_n, -\mathbf{p} + \mathbf{q}) e^2(\phi)} \quad (29)$$

Below we assume that the SC fluctuations are static, so that in (33) we can limit ourselves to the term with $\omega_m = 0$. Here the static approximation is valid for $\pi T \gg \omega_{\text{SC}} = 8(T - T_c)/\pi$, which is formally similar to the condition $\pi T \gg \omega_{\text{sf}}$ used in the hot-spot model. The closer the system is to the superconducting transition point, the better the condition is met. Then the effective interaction can be written

$$V_{\text{eff}}(\mathbf{q}) \approx - \frac{\tilde{\Delta}^2 e^2(\phi)}{\xi^{-2}(T) + \mathbf{q}^2}, \quad (30)$$

where

$$\xi(T) = \frac{\xi_0}{\sqrt{(T - T_c)/T_c}}, \quad \xi_0 \approx 0.18v_F/T_c, \quad (31)$$

with ξ_0 the ordinary coherence length of the superconductor, and $\tilde{\Delta}^2 = 1/N(E_F)\xi_0^2$ (here $N(E_F)$ is the density of states at the Fermi level E_F). Of course, within the elementary BCS model considered here,

$$\tilde{\Delta} \approx 2\pi^2 T_c \frac{T_c}{E_F} \sim \Delta_0 \frac{\Delta_0}{E_F} \ll \Delta_0$$

(where Δ_0 is the energy gap of the superconductor at $T = 0$), and so the obvious problem of explaining the scale of

the anomalies observed in the experiments arises. However, below we again assume that ξ and $\tilde{\Delta}$ are phenomenological parameters of the theory, bearing in mind that in high- T_c systems these parameters should be found from experiments rather than from a simple BCS-type theory, which does not apply to this case anyway.

Reasoning in the same way as we did in passing from (2) to (4), instead of (30) we introduce the model interaction

$$V_{\text{eff}}(\mathbf{q}) = -\Delta^2 e^2(\phi) \frac{2\xi^{-1}}{\xi^{-2} + q_x^2} \frac{2\xi^{-1}}{\xi^{-2} + q_y^2}, \quad (32)$$

where $\Delta^2 = \tilde{\Delta}^2/4$. Quantitatively this is very close to Eq. (30) and simplifies calculations significantly by making it possible to classify the contributions of higher-order diagrams. In this case the first-order contribution of the diagram in Fig. 7a has the form

$$\Sigma^{(1)}(\varepsilon_n, \mathbf{p}) = \frac{\Delta^2 e^2(\phi)}{i\varepsilon_n + \xi_{\mathbf{p}} + i(|v_x| + |v_y|)\kappa \text{sign } \varepsilon_n}, \quad (33)$$

where $v_x = v_F \cos \phi$, $v_y = v_F \sin \phi$, and $\kappa = \xi^{-1}$. The contribution of the second-order diagram in Fig. 7b is

$$\begin{aligned} \Sigma^{(2)}(\varepsilon_n, \mathbf{p}) &= (\Delta^2 e^2(\phi))^2 \\ &\times \int \frac{dq_{1x}}{\pi} \frac{\kappa}{\kappa^2 + q_{1x}^2} \int \frac{dq_{1y}}{\pi} \frac{\kappa}{\kappa^2 + q_{1y}^2} \\ &\times \int \frac{dq_{1x}}{\pi} \frac{\kappa}{\kappa^2 + q_{2x}^2} \int \frac{dq_{1y}}{\pi} \frac{\kappa}{\kappa^2 + q_{2y}^2} \\ &\times \frac{1}{(i\varepsilon_n + \xi_{\mathbf{p}} - \mathbf{v}_1 \cdot \mathbf{q}_1)^2} \frac{1}{i\varepsilon_n - \xi_{\mathbf{p}} - \mathbf{v}_2 \cdot \mathbf{q}_1 - \mathbf{v}_2 \cdot \mathbf{q}_2}, \end{aligned} \quad (34)$$

where $\mathbf{v}_1 = -\mathbf{v}_2 = \mathbf{v}_F$. We can easily see that in the given problem we have essentially the same rules of the diagrammatic technique as in the hot-spot model with combinations corresponding to the incommensurate case. This becomes especially obvious if we study the topology of the interaction line (the fluctuation propagator of Cooper pairs) in the diagram of Fig. 7a: we see that in higher orders the only diagrams that exist are those in which the interaction line surrounds an even number of vertices. Equation (34) is similar to (9), but the signs of the velocity projections in the denominators of the Green's functions are always different, $\mathbf{v}_1 = -\mathbf{v}_2$. Hence contributions to the integrals over momentum

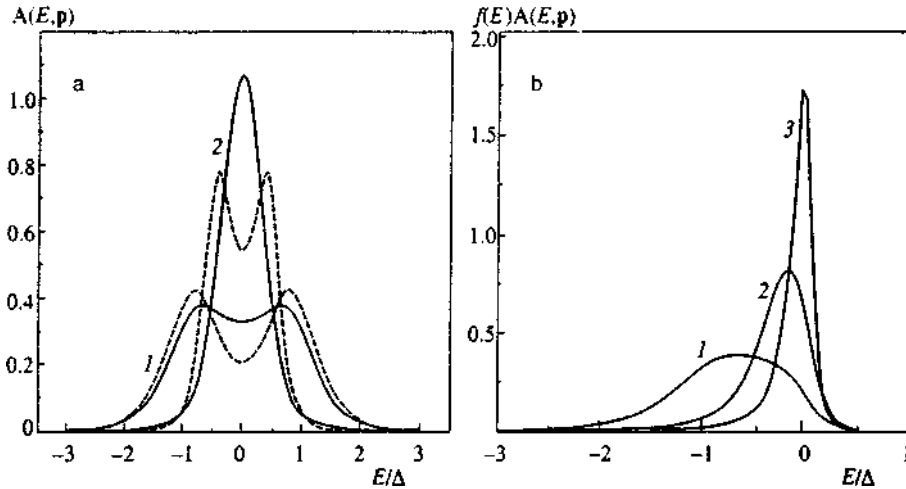


FIG. 8. (a) Energy dependence of the spectral density $A(E, \mathbf{p})$ for the case of d -wave fluctuation pairing at different values of the polar angle ϕ , which defines the direction of electron momentum in the plane: curve 1, $\phi=0$; and curve 2, $\phi=\pi/6$. The correlation length corresponds to $v_F\kappa/\Delta=0.5$ (solid curves). (b) Energy dependence of the product $f(E)A(E, \mathbf{p})$ ($f(E)$ is the Fermi function): curve 1, $\phi=0$; curve 2, $\phi=\pi/6$; curve 3, $\phi=\pi/4.83$. The temperature (in the Fermi function) is $T=0.1\Delta$, and $v_F\kappa/\Delta=0.5$.

transfer in higher-order diagrams are provided not only by the poles of Lorentzians but also by the poles of the Green's functions. Nevertheless (bearing in mind the discussion in the Appendix) we can estimate the contribution of higher-order diagrams by using the ansatz (12), i.e., we calculate all the integrals in, say, (34) as if the velocity projections were of the same sign, and then in the answer we put $\mathbf{v}_1 = -\mathbf{v}_2 = \mathbf{v}_F$. We again arrive at a recurrence relation for the Green's function of the form (14):

$$\Sigma_k(\varepsilon_n, \xi_p) = \frac{\Delta^2 e^2(\phi) v(k)}{i\varepsilon_n - (-1)^k \xi_p + ikv_F\kappa(|\cos\phi| + |\sin\phi|) - \Sigma_{k+1}(\varepsilon_n, \xi_p)}, \quad (35)$$

where $v(k)$ has been defined in (16). Of course, Eq. (35) is an approximation, but it gives the exact result in the limits $\kappa \rightarrow 0$ ($\xi \rightarrow \infty$) and $\kappa \rightarrow \infty$ ($\xi \rightarrow 0$) and provides a fairly good (quantitative) interpolation between these two limits for finite correlation lengths.

3.2. Spectral density and density of states

Figure 8a depicts the energy dependence of the spectral density $A(E, \mathbf{p})$ [Eq. (24)] of the one-particle Green's func-

tion calculated by (35) for different values of the polar angle ϕ determining the direction of electron momentum in the plane (here we assume that $|\mathbf{p}| = p_F$) for the case of d -wave fluctuation pairing. Clearly, in the vicinity of the point $(\pi/a, 0)$ of the Brillouin zone, the spectral density exhibits non-Fermi-liquid (pseudogap) behavior. As the vector \mathbf{p} rotates in the direction of the zone diagonal, the double-peak structure disappears and the spectral density becomes a typical Fermi-liquid spectral density with a single peak, and the closer the value of ϕ is to $\pi/4$ the narrower the peak. The spectral density undergoes a similar transformation as the correlation length ξ becomes smaller.

Figure 8b depicts the evolution of $f(E)A(E, \mathbf{p})$ (here $f(E)$ is the Fermi distribution), which is actually the parameter measured in ARPES experiments.² Note that the curves in Fig. 8b closely resemble the curves obtained in Refs. 11 and 12 in the hot-spot model. The picture of destruction of the Fermi surface suggested by these calculations is very similar to the one that follows from the experimental data obtained by Norman *et al.*²⁸ for $\text{Bi}_2\text{Sr}_2\text{CaCu}_2\text{O}_{8+\delta}$.

In the case of s -wave fluctuation pairing, the pseudogap appears isotropically on the entire Fermi surface, and the spectral density is of the non-Fermi-liquid type everywhere for large fluctuation lengths ξ of SC fluctuations.

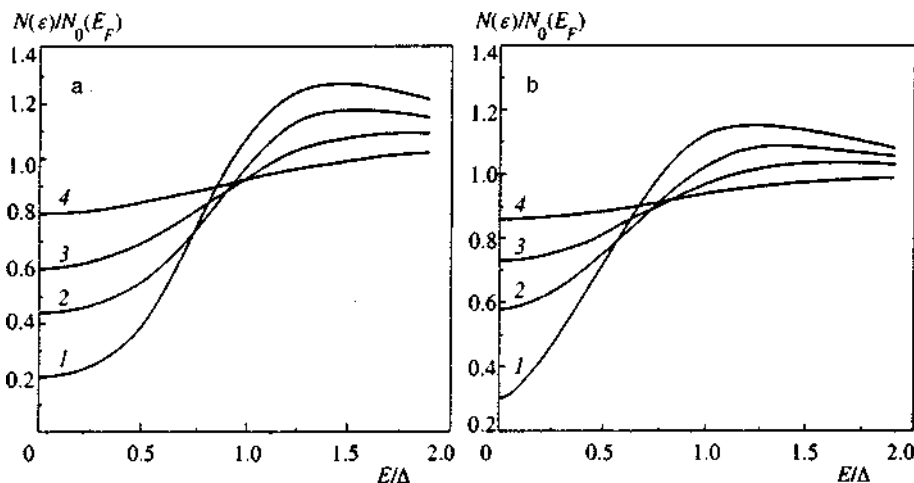


FIG. 9. One-electron density of states in the model of SC fluctuations: (a) in the case of s -wave pairing, and (b) in the case of d -wave pairing. The curves are built for the following values of the parameter $v_F\kappa/\Delta$, which determines the correlation lengths of short-range order fluctuations: 0.1 (curve 1), 0.5 (curve 2), 1.0 (curve 3), and 2.0 (curve 4).

In Fig. 9 we present the results of calculations of the one-electron density of states using (35) for the case of s -wave pairing (Fig. 9a) and in the case of d -wave pairing (Fig. 9b) for different correlation lengths of the SC fluctuations. We see that for d -wave pairing the pseudogap in the density of states is not so pronounced as for s -wave pairing, even for large correlation lengths of the fluctuations. At the same, Fig. 9 clearly shows that in the model of SC fluctuations the pseudogap is more pronounced than the hot-spot model discussed earlier.

4. CONCLUSION

We have examined almost exactly solvable models of the pseudogap state of the electronic spectrum of two-dimensional systems. These models are based on alternative scenarios of the origin of these anomalies: the picture of “dielectric” (AFM, SDW, CDW) fluctuations, which gives rise to the hot-spot model, and the picture of fluctuational formation of Cooper pairs above T_c (SC fluctuations). The term “almost exactly solvable” means that in this approach it is possible to sum the entire series of Feynman diagrams for the one-electron Green’s function (and actually also for the two-electron Green’s function^{16,17}), using for the higher-order diagrams the approximate ansatz (12). As shown in the Appendix and also by the numerical examples in the main body of the text, the ansatz guarantees a rather good approximation (speaking quantitatively) to the exact solution in the region of finite correlation lengths ξ of short-range-order fluctuations, while in the limits $\xi \rightarrow \infty$ and $\xi \rightarrow 0$ our solution is exact.

Our calculations of spectral densities have shown that in both scenarios we can obtain a rather appealing picture (from the standpoint of possible comparison with the experimental data in high- T_c cuprates) of destruction of the Fermi-liquid state in specific (hot) parts of the Fermi surface, with the Fermi-liquid state retained in the remaining (cold) part of the Fermi surface. Such non-Fermi-liquid behavior is due to the strong scattering of electrons by short-range-order fluctuations, and the larger the correlation length ξ the more pronounced the behavior. At the same time, there are certain differences between these two scenarios, which can, in principle, be utilized in the analysis of the situation in real systems. In particular, in the hot-spot model (AFM fluctuations), the pseudogap in the density of states is relatively small (see Fig. 6). In the model of SC fluctuations the pseudogap in the density of states is much more visible (see Fig. 9). At the same time, the model of dielectric AFM fluctuations appears to be more attractive even from a simple consideration of the phase diagram of a high- T_c system: pseudogap anomalies are observed in the underdoped region, and the closer the system is to a dielectric AFM state the more pronounced are the anomalies. It is in this region that we can expect the short-range-order dielectric (AFM) fluctuations to play a more important role, the correlation length ξ to increase, etc. It is rather difficult to understand why in this region of the phase diagram the fluctuational formation of Cooper pairs (SC fluctuations) may become more important. On the contrary, it would seem that such formation should manifest itself in

the region close to optimal doping (corresponding to the maximum superconducting transition temperature). Moreover, an obvious problem inherent in this scenario is that of explaining the characteristic scales of the anomalies (in temperature and in energy). The problem cannot be resolved by using simple approaches based on the BCS theory—the solution requires new microscopic approaches.^{5,7} The models considered in the present paper are useful in analyzing the pseudogap formation in both scenarios, since they are actually based on a fairly general (semiphenomenological) form of the correlation function of short-range-order fluctuations.

The authors would like to express their gratitude to Oleg Tchernyshyov for supplying the preliminary information on his analysis of the one-dimensional model. This was partially supported by the Russian Fund for Fundamental Research (Project 96-02-16065) and Project No. IX.1 of the Statistical Physics State Program and Project No. 96-051 of the High- T_c Superconductors State Program of the Russian Ministry of Science.

APPENDIX: ANALYSIS OF THE ONE-DIMENSIONAL MODEL

Let us examine in greater detail the use of the ansatz (12) in estimating the contributions of higher-order diagrams. We limit ourselves to the analysis of the one-dimensional model,^{15–17} since in one dimension the problem is most serious.²² We are interested in the vicinity of the Fermi points $+p_F$ and $-p_F$, with electrons scattered by Gaussian short-range-order fluctuations scattering by a momentum $Q \sim \pm -2p_F$, shifting them from one end of the Fermi line to the other with an accuracy of order $\xi^{-1} = \kappa$ (Refs. 13–17). We examine the electronic spectrum in the linearized approximation, $\xi_{p \pm p_F} = \pm -v_F p$, and assume, for the sake of brevity, that $v_F = 1$. Here the system consists of two types of electron: those electrons that move to the left, and those that move to the right. It is convenient to do our analysis in a representation²² in which the equation of motion for the electrons in the given model takes the form^{18,22}

$$\left(i\hat{1} \frac{\partial}{\partial t} - i\hat{\sigma}_3 \frac{\partial}{\partial x} \right) \hat{\Psi}(t, x) = \begin{pmatrix} 0 & \Delta(x) \\ \Delta^*(x) & 0 \end{pmatrix} \hat{\Psi}(t, x). \quad (\text{A1})$$

We limit ourselves to incommensurate fluctuations, i.e., $\Delta^*(x) \neq \Delta(x)$. The spinor $\hat{\Psi} = \begin{pmatrix} \psi_+ \\ \psi_- \end{pmatrix}$ describes “right” and “left” electrons. The fluctuations $\Delta(x)$ are assumed Gaussian with $\langle \Delta(x) \rangle = 0$ and $\langle \Delta^*(x) \Delta(x') \rangle = |\Delta|^2 \exp(-\kappa|x-x'|)$. The free propagator in the frequency–coordinate representation is

$$G_0(\varepsilon x) = i\theta(\varepsilon \sigma_3 x) \text{sign}(\varepsilon) \exp(i\varepsilon \sigma_3 x), \quad (\text{A2})$$

with $\sigma_3 = +1$ for right particles and $\sigma_3 = -1$ for left particles. A particle traversing a path of length l produces a phase factor $e^{i\varepsilon l}$. When calculating specific diagrams, it is convenient to change the integration variables from the coordinates x_k of interaction vertices to the lengths l_k of paths traversed by particles from one scattering act to another.²² Here it is important to account for the fact that these path lengths are not independent, since for a given diagram the

total particle displacement $x-x'$ is always fixed. The rules of the diagrammatic technique for calculating $G(\varepsilon, x-x')$ that result are as follows:²²

1. A solid line of length l_k yields a factor $-ie^{il_k(\varepsilon-(-1)^k p)}$.
2. A wavy (interaction) line connecting vertices m and n gives a factor

$$|\Delta|^2 \exp(-\kappa|x_m-x_n|) = |\Delta|^2 \exp\left(-\kappa\left|\sum_{k=m}^{n-1} (-1)^k l_k\right|\right).$$

3. Integration over all l_k is done from 0 to ∞ .
4. Integration over p is done with a weighting factor $e^{ip(x-x')}/2\pi$.

In calculating $G(\varepsilon, p)$ the last rule can simply be dropped. These rules show that allowing for the finiteness of the correlation length $\xi = \kappa^{-1}$ leads in each diagram to a damping of the corresponding transition amplitude with the displacement of the particle. Taking this effect into account exactly constitutes a complicated problem, but lower and upper bounds on this effect can be found. On the one hand, we have the obvious inequality

$$\exp\left(-\kappa\left|\sum_{k=m}^{n-1} (-1)^k l_k\right|\right) > \exp\left(-\kappa\sum_{k=m}^{n-1} l_k\right). \quad (A3)$$

By using the right-hand side of (A3) as the interaction line we overestimate the transition amplitude damping (i.e., effectively overestimate κ). We can easily see that the use of this approximation in calculating the Green's function in the momentum representation amounts to adding $i\kappa$ to the denominator in each Green's function surrounded by the interaction line and yields an expression for any higher-order correction of the form (12) (cf. Ref. 22). For instance, the following expression corresponds to the diagram in Fig. 1b (we assume that $\varepsilon > 0$ and $\delta = 0^+$):

$$\Delta G(\varepsilon, p) = \Delta^4 \frac{1}{\varepsilon - p + i\delta} \left(\frac{1}{\varepsilon + p + i\kappa} \times \frac{1}{\varepsilon - p + 2i\kappa} \frac{1}{\varepsilon + p + i\kappa} \right) \frac{1}{\varepsilon - p + i\delta}, \quad (A4)$$

which is similar to (9) and (11). On the other hand, we can employ the inequality

$$\exp\left(-\kappa\left|\sum_{k=m}^{n-1} (-1)^k l_k\right|\right) < \exp\left(-\kappa\sum_{k=m}^{n-1} (-1)^{k-m} l_k\right). \quad (A5)$$

By using the right-hand side of (A5) for the interaction line we underestimate the transition amplitude damping (i.e., effectively underestimate κ). It may seem that this choice of the expression for the interaction line can even increase the transition amplitude over its value at $\kappa = 0$, but this is not so. Since we are considering the incommensurate case, where the interaction line surrounds only an even number of vertices (i.e., an odd number of l_k), the choice of a specific sign in the exponent after the absolute-value sign has been removed is determined by what number of l_k is greater, the odd or the even. This leads to a situation in which the effec-

tive transition amplitude of any higher-order diagram can only decrease. For the diagram in Fig. 1b in the coordinate representation the contribution of the interaction lines is

$$e^{-\kappa l_2} e^{-\kappa|l_1-l_2-l_3|} \rightarrow e^{-\kappa l_2} e^{-\kappa(l_1-l_2+l_3)} = e^{-\kappa(l_1+l_3)}. \quad (A6)$$

In the momentum representation this yields

$$\Delta G(\varepsilon, p) = \Delta^4 \frac{1}{\varepsilon - p + i\delta} \left(\frac{1}{\varepsilon + p + i\kappa} \frac{1}{\varepsilon - p + i\delta} \frac{1}{\varepsilon + p + i\kappa} \right) \times \frac{1}{\varepsilon - p + i\delta}, \quad (A7)$$

An analysis of any higher-order diagram shows that in this case the contributions of all N -order diagrams are equal and in the momentum representation have the form (the alternating- κ ansatz)

$$G_N(\varepsilon, p) = |\Delta|^{2N} \frac{1}{(\varepsilon - p + i\delta)^{N+1}} \frac{1}{(\varepsilon + p + i\kappa)^N}. \quad (A8)$$

Then the entire series can easily be summed, much like the case with $\kappa = 0$ (Refs. 13 and 14), and for the Green's function we obtain

$$G^R(\varepsilon, p) = \sum_{N=0}^{\infty} N! G_N(\varepsilon, p) = \int_0^{\infty} d\zeta e^{-\zeta} \frac{\varepsilon + p + i\kappa}{(\varepsilon - p + i\delta)(\varepsilon + p + i\kappa) - \zeta|\Delta|^2}. \quad (A9)$$

This expression can easily be used to calculate the corresponding spectral density or the one-particle density of states:

$$\frac{N(\varepsilon)}{N(E_F)} = \frac{v_F \kappa}{\pi} \int_{-\infty}^{\infty} d\xi_p \int_0^{\infty} d\zeta \times e^{-\zeta} \frac{\zeta|\Delta|^2}{(\varepsilon^2 - \xi_p^2 - \zeta|\Delta|^2)^2 + (v_F \kappa)^2 (\varepsilon - \xi_p)^2}, \quad (A10)$$

where we have restored v_F . In Fig. 10 we compare the densities of states for different values of κ (or correlation length) that we calculated by the alternating- κ ansatz and a recurrence relation of the form (12) in the one-dimensional model.¹⁵⁻¹⁷ We see that the results are quantitatively close for almost all values of κ . Since, as noted earlier, our main ansatz (12) and (A4) somewhat overestimates the role of the finiteness of κ , while the alternating- κ ansatz (A7) underestimates it, we can easily see that the exact value of the density of states differs little from these two approximations to the contributions of higher-order diagrams. The situation with the spectral densities is similar. Actually this means that the results for the main physical quantities determined by the one-electron Green's function are not strongly dependent on the way in which a finite κ enters the expressions for higher-order diagrams. What is important is that we must take into account (at least approximately) all perturbation-theory diagrams with allowance for their different combinations. This

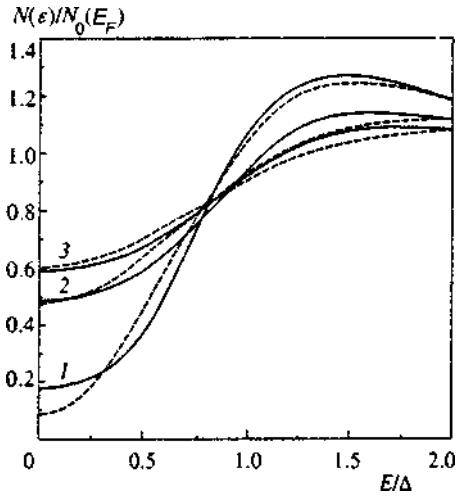


FIG. 10. One-electron density of states in the one-dimensional model for different values of the parameter $v_F \kappa/\Delta$: 0.1 (curve 1), 0.8 (curve 2), and 1.2 (curve 3). The solid curves represent the results of calculations by formulas of the form (12) and (14) (Ref. 15), and the dashed curves represent the results of calculations by (A10).

should not come as a big surprise, since the main effect of pseudogap formation is due primarily to backward scattering by a vector $Q \sim 2p_F$, which is accounted for exactly in the limit $\xi \rightarrow 0$, while the effect of a finite κ reduces to an additional weak modulation of the random field, which leads to damping of the field's correlator and smearing of the pseudogap.

Naturally, the alternating- κ ansatz can also be written in the form of a recurrence relation of the form (14) for two-dimensional models, which were discussed in the main body of the text. For instance, if the hot-spot model we have

$$\Sigma_k(\varepsilon_n, \xi_{\mathbf{p}}) = \Delta^2 \frac{v(k)}{i\varepsilon_n - \xi_k + i\alpha_k v_k \kappa - \Sigma_{k+1}(\varepsilon_n, \xi_{\mathbf{p}})}, \quad (\text{A11})$$

where $\alpha_k = 1$ for odd k , and $\alpha_k = 0$ for even k . The other notation is explained in the main body of the text. The data on the density of states obtained via (A11) are depicted in Fig. 6 and corroborate our conclusions. For the model of SC fluctuations an expression similar to (A11) can also easily be written.

Note that the alternating- κ ansatz is formal and is used here only to show that this more or less arbitrary approximation (which underestimates the role of the finiteness of κ in higher-order diagrams) leads to results that are quantitatively very close to those obtained by the building-up- κ ansatz (12) and (A4) (which generally overestimates this role). The latter approximation was used in Refs. 15–18 and in the main part of the present paper and has a much deeper meaning. As noted earlier, this approximation is exact in the vicinity of hot spots for values of the parameters of the bare spectrum, t , t' , and μ (topologies of the Fermi surface), that guarantee equal signs for the velocity projections at the hot spots connected by the vector \mathbf{Q} . Reasoning along similar lines, in the one-dimensional model we can obtain an expression of the form (12) or (A4) for the higher-order contributions if we consider a model for the correlator of short-range-order fluc-

tuations with its maximum at an arbitrary scattering vector \mathbf{Q} much shorter than p_F . In this case, for large correlation lengths ξ , the electrons are scattered by fluctuations, staying always on one branch (right or left) of the spectrum. Here expressions of the form (A4) remain exact. After this is done, in the final expressions for the contributions of higher-order diagrams we perform a continuation to the region $Q \sim 2p_F$ of interest to us, since the only dependence on Q is already present via the bare electron spectrum. A similar result can be achieved by varying the chemical potential μ (band filling).

^{*})E-mail: kuchinsk@ief.uran.ru

[†])E-mail: sadovski@ief.uran.ru

¹)A model similar in meaning to the one used here but differing somewhat from (4) was employed by Schmalian *et al.*:^{11,12}

$$V_{\text{eff}}(\mathbf{k}) = \Delta^2 \frac{2\xi^{-1}}{\xi^{-2} + k_{\parallel}^2} \frac{2\xi^{-1}}{\xi^{-2} + k_{\perp}^2},$$

where k_{\parallel} and k_{\perp} are the projections of the vector \mathbf{k} parallel and perpendicular to $v_{\mathbf{p}+\mathbf{Q}}$, so that a result similar to (7) is obtained:

$$\Sigma(\varepsilon_n, \mathbf{p}) = \frac{\Delta^2}{i\varepsilon_n - \xi_{\mathbf{p}+\mathbf{Q}} + i|v_{\mathbf{p}+\mathbf{Q}}|k \text{ sign } \varepsilon_n}.$$

²)In the model of V_{eff} employed by Schmalian *et al.*:^{11,12} for the case $v_{\mathbf{p}} \cdot v_{\mathbf{p}+\mathbf{Q}} > 0$ the following expression can be derived in a similar way:

$$\Sigma(\text{b}) = \Sigma(\text{c}) = \Delta^4 \frac{1}{[i\varepsilon_n - \xi_{\mathbf{p}+\mathbf{Q}} + i|v_{\mathbf{p}+\mathbf{Q}}|\kappa]^2} \times \frac{1}{i\varepsilon_n - \xi_{\mathbf{p}+\mathbf{Q}} + i2|v_{\mathbf{p}}|(|\cos\phi| + |\sin\phi|)\kappa},$$

where ϕ is the angle between $v_{\mathbf{p}}$ and $v_{\mathbf{p}+\mathbf{Q}}$.

¹M. Randeria, Varenna Lectures 1997, E-prints archive cond-mat/9710223.

²M. Randeria and J. C. Campuzano, Varenna Lectures 1997, E-prints archive cond-mat/9709107.

³H. Ding, T. Yokoya, J. C. Campuzano, T. Takahashi, M. Randeria, M. R. Norman, T. Mochiku, K. Kadowaki, and J. Giapintzakis, *Nature (London)* **382**, 51 (1996).

⁴H. Ding, M. R. Norman, T. Yokoya, T. Takeuchi, M. Randeria, J. C. Campuzano, T. Takahashi, T. Mochiki, and K. Kadowaki, *Phys. Rev. Lett.* **78**, 2628 (1997).

⁵V. B. Geshkenbein, L. B. Ioffe, and A. I. Larkin, *Phys. Rev. B* **55**, 3173 (1997).

⁶V. J. Emery, S. A. Kivelson, and O. Zachar, *Phys. Rev. B* **56**, 6120 (1997).

⁷J. Maly, B. Janko, and K. Levin, E-printsarchive cond-mat/9710187 (1997); cond-mat/9805018 (1998).

⁸A. P. Kampf and J. R. Schrieffer, *Phys. Rev. B* **41**, 6399 (1990); **42**, 7967 (1990).

⁹V. Barzykin and D. Pines, *Phys. Rev. B* **52**, 13 585 (1995).

¹⁰D. Pines, *Tr. J. of Physics* **20**, 535 (1996).

¹¹J. Schmalian, D. Pines, and B. Stojković, *Phys. Rev. Lett.* **80**, 3839 (1998).

¹²J. Schmalian, D. Pines, and B. Stojković, E-prints archive cond-mat/9804129 (1998).

¹³M. V. Sadovskii, *Zh. Éksp. Teor. Fiz.* **66**, 1720 (1974) [*Sov. Phys. JETP* **39**, 845 (1974)].

¹⁴M. V. Sadovskii, *Fiz. Tverd. Tela (Leningrad)* **16**, 2504 (1974) [*Sov. Phys. Solid State* **16**, 1632 (1974)].

¹⁵M. V. Sadovskii, *Zh. Éksp. Teor. Fiz.* **77**, 2070 (1979) [*Sov. Phys. JETP* **50**, 989 (1979)].

¹⁶M. V. Sadovskii and A. A. Timofeev, *Sverkhprovodimost': Fiz., Khim., Tekhnol.* **4**, 11 (1991) [*Supercond., Phys. Chem. Technol.* **4**, 9 (1991)].

¹⁷M. V. Sadovskii and A. A. Timofeev, *J. Mosc. Phys. Soc.* **1**, 391 (1991).

¹⁸R. H. McKenzie and D. Scarratt, *Phys. Rev. B* **54**, R12 709 (1996).

¹⁹O. Tchernyshyov, *Phys. Rev. B* **56**, 3372 (1997).

²⁰H. C. Ren, E-prints archive cond-mat/9612184 (1996).

²¹A. I. Posazhennikova and M. V. Sadovskii, E-prints archive cond-mat/9806199 (1998).

- ²²O. Tchernyshyov, E-prints archive cond-mat/9804318 (1998).
- ²³P. Monthoux, A. V. Balatsky, and D. Pines, Phys. Rev. B **46**, 14 803 (1992).
- ²⁴P. Monthoux and D. Pines, Phys. Rev. B **47**, 6069 (1993); **48**, 4261 (1994).
- ²⁵P. V. Elyutin, Opt. Spektrosk. **43**, 542 (1977) [Opt. Spectrosc. **43**, 318 (1977)].
- ²⁶L. S. Borkowski and P. J. Hirschfeld, Phys. Rev. B **49**, 15 404 (1994).
- ²⁷R. Fehrenbacher and M. R. Norman, Phys. Rev. B **50**, 3495 (1994).
- ²⁸M. R. Norman, H. Ding, M. Randeria, J. C. Campuzano, T. Yokoya, T. Takeuchi, T. Takahashi, T. Mochiki, K. Kadowaki, P. Guptasarma, and D. G. Hinks, E-prints archive cond-mat/9710163 (1997).

Translated by Eugene Yankovsky

SOLIDS
Electron Properties

Superconductivity in a Simple Model of the Pseudogap State

E. Z. Kuchinski * and M. V. Sadovski **

Institute of Electrophysics, Ural Division, Russian Academy of Sciences, Yekaterinburg, 620049 Russia

*e-mail: kuchinsk@ief.uran.ru

**e-mail: sadovski@ief.uran.ru

Received September 20, 1999

Abstract—An analysis is made of characteristics of the superconducting state (*s*- and *d*-pairing) using a simple, exactly solvable model of the pseudogap state produced by fluctuations of the short-range order (such as antiferromagnetic) based on a Fermi surface model with “hot” sections. It is shown that the superconducting gap averaged over these fluctuations is nonzero at temperatures higher than the mean-field superconducting transition temperature T_c over the entire sample. At temperatures $T > T_c$ superconductivity evidently exists in isolated sections (“drops”). Studies are made of the spectral density and the density of states in which superconducting characteristics exist in the range $T > T_c$ however, in this sense the temperature $T = T_c$ itself is no different in any way. These anomalies show qualitative agreement with various experiments using underdoped high-temperature superconducting cuprates. © 2000 MAIK “Nauka/Interperiodica”.

1. INTRODUCTION

Among the numerous anomalies in the electronic properties of high-temperature superconductors particular interest is being directed toward the pseudogap state observed mainly at below-optimum carrier concentrations [1, 2]. These anomalies appear in many experiments such as optical conductivity measurements, NMR, inelastic neutron scattering, angle-resolved photoemission spectroscopy (ARPES), and so on (see the review [1]). Particularly clear evidence of the existence of this state is observed in ARPES experiments [1, 3] which demonstrate essentially anisotropic changes in the spectral density of the carriers over a wide range of temperature in the normal and superconducting phases of these systems. The maximum of these anomalies is observed near the point $(\pi, 0)$ in the Brillouin zone, while they are almost completely absent in the direction of the zone diagonal [near the point (π, π)]. Qualitatively these anomalies can be considered as the complete “destruction” of the Fermi surface near the point $(\pi, 0)$, with Fermi-liquid behavior conserved in the direction of the diagonal. In this sense it is usual to talk of the “*d*-symmetry” of the pseudogap matching the symmetry of the superconducting gap in these compounds [1–3]. However, the fact that pseudogap anomalies are observed up to temperatures $T \sim T^*$, appreciably higher than T_c , may indicate that the nature of these anomalies is completely different and is not directly related to superconducting pairing. This conclusion is also supported by the fact that the pseudogap state is mainly observed for nonoptimum compositions close to the antiferromagnetic phase of high-temperature superconducting cuprates.

In the theoretical context, attempts to construct models of the pseudogap state of high-temperature

superconductors follow two main approaches. One is based on the very popular model of the formation of Cooper pairs above the superconducting transition temperature [2, 4–7]. The other assumes that the pseudogap state is caused by fluctuations of the antiferromagnetic short-range order (see, for example, [8–12]).

Most theoretical studies have been made of the pseudogap state in the normal phase $T > T_c$. In a recent study [13] Posazhennikova and Sadovskii proposed a very simple, exactly solvable model of the pseudogap state, based on the concept that the Fermi surface has “hot” (planar) sections, and this model was used to construct a Ginzburg–Landau expansion for various types of Cooper pairing and to study the qualitative effects of the pseudogap (caused by fluctuations of the antiferromagnetic short-range order) on the fundamental properties of superconductors near T_c . The present paper is devoted to the further development of this simplified model and analyzes the characteristic features of the superconducting state over the entire temperature range $T < T_c$.

2. MODEL OF THE PSEUDOGAP STATE

We shall analyze an extremely simplified model of the pseudogap state [13] based on a pattern of well-developed fluctuations of the short-range antiferromagnetic order, similar to the model of “hot spots” on the Fermi surface [11].¹ We shall assume that the Fermi surface of a two-dimensional electron system has the form shown in Fig. 1. This type of Fermi surface has in fact been observed in ARPES experiments on high-

¹ We note that our analysis can essentially also be applied to the case of short-range order fluctuations of the charge density wave type and other similar models.

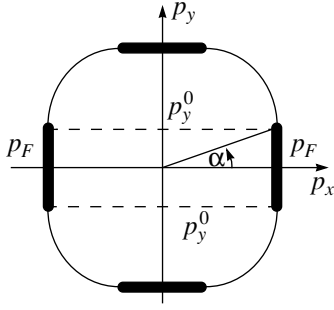


Fig. 1. Fermi surface of a two-dimensional system. The hot sections, of width $\sim \xi^{-1}$, are shown by the heavy lines.

temperature superconducting cuprates (see, for example, the very recent studies [14, 15]). We shall assume that the fluctuations of the short-range order are static and Gaussian, determining their correlation function in the following form (see [8]):

$$S(\mathbf{q}) = \frac{1}{\pi^2} \frac{\xi^{-1}}{(q_x - Q_x)^2 + \xi^{-2}} \frac{\xi^{-1}}{(q_y - Q_y)^2 + \xi^{-2}}, \quad (1)$$

where ξ is the correlation length of the fluctuations and the scattering vector is taken in the form $Q_x = \pm 2k_F$, $Q_y = 0$ or $Q_y = \pm 2k_F$, $Q_x = 0$. We postulate that only electrons from the planar (“hot”) parts of the Fermi surface shown in Fig. 1 interact with these fluctuations and this scattering is in fact one-dimensional. The effective electron interaction with these fluctuations will be described by $(2\pi)^2 W^2 S(\mathbf{q})$ where the parameter W has the dimensions of energy and determines the energy scale (width) of the pseudogap.² The choice of scattering vector $\mathbf{Q} = (\pm 2k_F, 0)$ or $\mathbf{Q} = (0, \pm 2k_F)$ implies a pattern of incommensurate fluctuations (it is possible to generalize to the commensurate case [13] but we do not consider this here). In the limit $\xi \rightarrow \infty$, this model can have an exact solution using methods proposed for the one-dimensional case in [16]. For finite ξ we can construct an “almost” exact solution [11, 12] using a generalization of the one-dimensional approach developed in [17, 18]. In the present study we only consider the simplest variant of the model with $\xi \rightarrow \infty$, when the effective interaction with the fluctuations (1) has the very simple form:³

$$(2\pi)^2 W^2 \{ \delta(q_x \pm 2p_F) \delta(q_y) + \delta(q_y \pm 2p_F) \delta(q_x) \}. \quad (2)$$

In this case we can easily sum all the perturbation theory series for an electron scattered at these fluctuations

² We can say that we are introducing the effective interaction “constant” with fluctuations of the type $W_{\mathbf{p}} = W[\theta(p_x^0 - p_x)\theta(p_x^0 + p_x) + \theta(p_y^0 - p_y)\theta(p_y^0 + p_y)]$.

³ We stress that because of the Gaussian nature of the fluctuations the limit $\xi \rightarrow 0$ does not imply the establishment of any long-range order.

[16] and for the single-electron Green’s function we obtain [13]

$$G(\epsilon_n, p) = \int_0^\infty dD \mathcal{P}(D) \frac{i\epsilon_n + \xi_p}{(i\epsilon_n)^2 - \xi_p^2 - D(\phi)^2}, \quad (3)$$

where $\xi_p = v_F(|\mathbf{p}| - p_F)$ (v_F is the velocity at the Fermi surface), $\epsilon_n = (2n + 1)\pi T$, and the fluctuating dielectric gap $D(\phi)$ is only nonzero in the hot sections:

$$D(\phi) = \begin{cases} D, & 0 \leq \phi \leq \alpha, \quad \frac{\pi}{2} - \alpha \leq \phi \leq \frac{\pi}{2}, \\ 0, & \alpha \leq \phi \leq \frac{\pi}{2} - \alpha, \end{cases} \quad (4)$$

where $\alpha = \arctan(p_y^0/p_F)$ and ϕ is the polar angle determining the direction of the vector \mathbf{p} in the plane $p_x p_y$. For other values of ϕ the value of $D(\phi)$ is obviously determined by analogy with (4) from symmetry concepts.

The amplitude of the dielectric gap D is random and obeys a Rayleigh distribution [17] (its phase is then also random and uniformly distributed on the interval $(0, 2\pi)$):

$$\mathcal{P}(D) = \frac{2D}{W^2} \exp\left(-\frac{D^2}{W^2}\right). \quad (5)$$

Thus, at the hot sections the Green’s function has the form of a “normal” Gor’kov Green’s function averaged over the fluctuations of the dielectric gap D distributed in accordance with (5). The “anomalous” Gor’kov functions at these “dielectrified” sections are zero (because of the random phases of the dielectric gap D), which corresponds to the absence of any long-range order but their pair averages are nonzero and make some contribution to the two-particle Green’s function [13, 16]. By varying the parameter α in (4) in the range $0 \leq \alpha \leq \pi/4$, we can change the size of the hot sections on the Fermi surface for which the nesting conditions $\xi_{p-Q} = -\xi_p$ is satisfied. In particular $\alpha = \pi/4$ corresponds to a square Fermi surface. Outside the hot sections [the second inequality in (4)] the Green’s function (3) is simply the same as the Green’s function of the free electrons.

Results of calculations of the electron density of states and the spectral density corresponding to (3) are presented in [13] and demonstrate the formation of a pseudogap (having the characteristic width $\sim 2W$) and non-Fermi-liquid behavior at the hot sections. In the model having a finite correlation length ξ the Green’s function for these sections is represented as a continuous fraction [19] (see similar results in [11, 12, 17, 18]). In this case, the spectral density demonstrates increasingly smeared behavior (compared with the case $\xi \rightarrow \infty$) with decreasing ξ , which was described in detail in [11, 12, 18]. In [19] this model was used to calculate the optical conductivity of a two-dimensional system in the pseudogap state.

3. SUPERCONDUCTIVITY IN THE PSEUDOGAP STATE

We shall now analyze superconductivity using this model. We shall assume that superconducting pairing is caused by an attractive potential which has the following very simple form [13]:

$$V(\mathbf{p}, \mathbf{p}') = V(\phi, \phi') = -Ve(\phi)e(\phi'). \quad (6)$$

Here ϕ is the angle which, as before, determines the direction of the electron momentum \mathbf{p} in the plane and for $e(\phi)$ we take the simplest model dependence:

$$e(\phi) = \begin{cases} 1 & (s\text{-pairing}), \\ \sqrt{2}\cos(2\phi) & (d\text{-pairing}). \end{cases} \quad (7)$$

The attraction constant V is usually assumed to be non-zero in a certain layer of width $2\omega_c$ near the Fermi level (ω_c is the characteristic quantum frequency responsible for the attraction of electrons). In this case, the superconducting gap has the form

$$\Delta(\mathbf{p}) \equiv \Delta(\phi) = \Delta e(\phi). \quad (8)$$

We shall first consider superconductivity in a system in which there is a fixed dielectric gap D at the “hot” sections of the Fermi surface. The problem of superconductivity in a system with a partially dielectrified spectrum at various parts of the Fermi surface has been addressed in various studies (see, for example [20, 21]) and was analyzed by Bilbro and McMillan [22] using a model very close to our case, from which we can use some of the results directly or simply generalize them.

In particular, for s -pairing the equation for the superconducting gap Δ in this model has the form

$$1 = \lambda \int_0^{\omega_c} d\xi \left\{ \tilde{\alpha} \frac{\tanh \frac{\sqrt{\xi^2 + D^2 + \Delta^2(D)}}{2T}}{\sqrt{\xi^2 + D^2 + \Delta^2(D)}} + (1 - \tilde{\alpha}) \frac{\tanh \frac{\sqrt{\xi^2 + \Delta^2(D)}}{2T}}{\sqrt{\xi^2 + \Delta^2(D)}} \right\}, \quad (9)$$

where $\lambda = VN_0(0)$ is the dimensionless pair-interaction constant [$N_0(0)$ is the density of states of free electrons at the Fermi level] and the parameter $\tilde{\alpha} = 4\alpha/\pi$ determines the fraction of hot (planar) sections on the Fermi surface.

In equation (9) the first term on the right-hand side corresponds to the contribution of hot (dielectrified) sections for which the electron spectrum has the form

[22] $E_p = \sqrt{\xi_p^2 + D^2 + \Delta^2}$ and the second term gives the contribution of the “cold” (metal) sections where the

spectrum has the usual form in BCS theory: $E_p = \sqrt{\xi_p^2 + \Delta^2}$. Equation (9) determines the superconducting gap $\Delta(D)$ for a fixed dielectric gap D which is non-zero at the “hot” sections.

For d -pairing the similar equation has the form

$$1 = \lambda \frac{4}{\pi} \int_0^{\omega_c} d\xi \times \left\{ \int_0^{\alpha} d\phi e^2(\phi) \frac{\tanh \frac{\sqrt{\xi^2 + D^2 + \Delta^2(D)}e^2(\phi)}{2T}}{\sqrt{\xi^2 + D^2 + \Delta^2(D)}e^2(\phi)} + \int_{\alpha}^{\pi/4} d\phi e^2(\phi) \frac{\tanh \frac{\sqrt{\xi^2 + \Delta^2(D)}e^2(\phi)}{2T}}{\sqrt{\xi^2 + \Delta^2(D)}e^2(\phi)} \right\}. \quad (10)$$

It can be seen from these equations that $\Delta(D)$ decreases with increasing D and $\Delta(0)$ is the same as the usual gap Δ_0 in the absence of any dielectrification at the planar sections which appears at the temperature $T = T_{c0}$ determined by

$$1 = \lambda \int_0^{\omega_c} \frac{d\xi}{\xi} \tanh \frac{\xi}{2T_{c0}} \quad (11)$$

both for s - and d -pairing.

For $D \rightarrow \infty$ the first terms in (9) and (10) vanish since the corresponding equations for $\Delta_{\infty} = \Delta(D \rightarrow \infty)$ have the form

$$1 = \lambda \int_0^{\omega_c} \frac{d\xi(1 - \tilde{\alpha})}{\sqrt{\xi^2 + \Delta_{\infty}^2}} \tanh \frac{\sqrt{\xi^2 + \Delta_{\infty}^2}}{2T} \quad (12)$$

(s -pairing),

$$1 = \lambda \frac{4}{\pi} \int_0^{\omega_c} d\xi \int_{\alpha}^{\pi/4} \frac{d\phi e^2(\phi)}{\sqrt{\xi^2 + \Delta_{\infty}^2}e^2(\phi)} \tanh \frac{\sqrt{\xi^2 + \Delta_{\infty}^2}e^2(\phi)}{2T} \quad (13)$$

(d -pairing).

Equation (12) agrees with the equation for the gap $D = 0$ with the renormalized coupling constant $\tilde{\lambda} = \lambda(1 - \tilde{\alpha})$ so that for s -pairing

$$\Delta_{\infty} = \Delta_0 \quad (\tilde{\lambda} = \lambda(1 - \tilde{\alpha})) \quad (14)$$

and thus a nonzero gap for $D \rightarrow \infty$ appears when $T < T_{c\infty}$,

$$T_{c\infty} = T_{c0} \quad (\tilde{\lambda} = \lambda(1 - \tilde{\alpha})). \quad (15)$$

For the case of d -pairing we obtain from equation (13)

$$T_{c\infty} = T_{c0} (\tilde{\lambda} = \lambda(1 - \alpha_d)), \tag{16}$$

where

$$\alpha_d = \tilde{\alpha} + \frac{\sin(\pi\tilde{\alpha})}{\pi} \tag{17}$$

is the effective fraction of planar sections for d -pairing. Hence, for $T < T_{c\infty}$ the gap is nonzero for any values of D and decreases from Δ_0 to Δ_∞ with increasing D . When $T_{c\infty} < T < T_{c0}$, the gap is only nonzero when $D < D_{\max}$. The corresponding dependences of Δ on D are easily obtained by solving equations (9) and (10) numerically.

In our model of the pseudogap state the dielectric gap D is not fixed but is a random quantity with a distribution given by (5). The equations obtained above must be averaged over all these fluctuations. Then we can directly calculate the exact superconducting gap $\langle \Delta \rangle$ averaged over the fluctuations of D :

$$\begin{aligned} \langle \Delta \rangle &= \int_0^\infty dD \mathcal{P}(D) \Delta(D) \\ &= \frac{2}{W^2} \int_0^\infty dD D \exp\left(-\frac{D^2}{W^2}\right) \Delta(D). \end{aligned} \tag{18}$$

The dependences $\Delta(D)$ described above have the result that the average gap (18) is nonzero as far as $T = T_{c0}$, i.e., as far as the superconducting transition temperature in the absence of pseudogap anomalies. However, the superconducting transition temperature T_c in a superconductor with a pseudogap is clearly lower than T_{c0} [13]. This paradoxical behavior of $\langle \Delta \rangle$ evidently implies that local regions with $\Delta \neq 0$ (superconducting drops) induced by fluctuations of D appear over the entire temperature range $T_c < T < T_{c0}$ and a superconducting state coherent over the entire sample is only established in the region $T < T_c$. Quite clearly, this qualitative picture can only be completely substantiated by analyzing a more realistic model where the fluctuations of the antiferromagnetic short-range order have a finite length ξ .⁴ However, the simplicity of the $\xi \rightarrow \infty$ model considered here means that an exact solution can be obtained immediately for $\langle \Delta \rangle$.

In order to determine the superconducting transition temperature T_c in the entire sample we shall use the standard procedure of the mean-field approximation (see, for example, a similar procedure applied to a superconductor with impurities [24]) which is under the assumption of self-averaging of the superconducting gap over the fluctuations of D (i.e., Δ is independent

of the fluctuations of D). The equations for the mean-field gap Δ_{mf} then have the form

$$\begin{aligned} 1 &= \lambda \int_0^{\omega_c} d\xi \left\{ \tilde{\alpha} \frac{2}{W^2} \int_0^\infty dD D \exp\left(-\frac{D^2}{W^2}\right) \right. \\ &\times \left. \frac{\tanh \frac{\sqrt{\xi^2 + D^2 + \Delta_{mf}^2}}{2T}}{\sqrt{\xi^2 + D^2 + \Delta_{mf}^2}} + (1 - \tilde{\alpha}) \frac{\tanh \frac{\sqrt{\xi^2 + \Delta_{mf}^2}}{2T}}{\sqrt{\xi^2 + \Delta_{mf}^2}} \right\} \end{aligned} \tag{19}$$

for s -pairing and

$$\begin{aligned} 1 &= \lambda \frac{4}{\pi} \int_0^{\omega_c} d\xi \left\{ \int_0^\infty dD D \exp\left(-\frac{D^2}{W^2}\right) \right. \\ &\times \int_0^\alpha d\phi e^2(\phi) \frac{\tanh \frac{\sqrt{\xi^2 + D^2 + \Delta_{mf}^2} e^2(\phi)}{2T}}{\sqrt{\xi^2 + D^2 + \Delta_{mf}^2} e^2(\phi)} \\ &\left. + \int_\alpha^{\pi/4} d\phi e^2(\phi) \frac{\tanh \frac{\sqrt{\xi^2 + \Delta_{mf}^2} e^2(\phi)}{2T}}{\sqrt{\xi^2 + \Delta_{mf}^2} e^2(\phi)} \right\} \end{aligned} \tag{20}$$

for d -pairing.

From equations (19) and (20) we can easily derive the corresponding equations for T_c . For example, for s -pairing we have

$$\begin{aligned} 1 &= \lambda \left\{ \tilde{\alpha} \frac{2}{W^2} \int_0^\infty dD D \exp\left(-\frac{D^2}{W^2}\right) \right. \\ &\times \left. \int_0^{\omega_c} \frac{d\xi}{\sqrt{\xi^2 + D^2}} \tanh \frac{\sqrt{\xi^2 + D^2}}{2T_c} + (1 - \tilde{\alpha}) \int_0^{\omega_c} \frac{d\xi}{\xi} \tanh \frac{\xi}{2T_c} \right\}. \end{aligned} \tag{21}$$

For d -pairing $\tilde{\alpha}$ in (21) must be replaced by α_d from (17). These equations for T_c are the same as those obtained in the microscopic derivation of the Ginzburg–Landau expansion using this model in [13] where they were studied in detail. In general we always have $T_{c\infty} < T_c < T_{c0}$.

⁴ The qualitative situation here resembles the formation of an inhomogeneous superconducting state induced by strong fluctuations of the local density of states near the Anderson metal–insulator transition [23, 24].

The temperature dependences of the average gap $\langle\Delta\rangle$ and the mean-field gap Δ_{mf} obtained by means of a numerical solution of the equations from our model for the case of s -pairing are plotted in Fig. 2.⁵ The gap Δ_{mf} vanishes when $T = T_c < T_{c0}$, while $\langle\Delta\rangle$ is nonzero as far as $T = T_{c0}$, and the corresponding “tails” in the temperature dependence of $\langle\Delta\rangle$ in the range $T_c < T < T_{c0}$ are, in our view, consistent with the existence of superconducting “drops” in this region in the absence of superconductivity over the entire sample, as was described above. We note that the temperature dependences $\langle\Delta(T)\rangle$ presented in Fig. 2 are similar to those for the gap in underdoped high-temperature superconducting cuprates extracted from ARPES experiments [3, 25] and from measurements of the specific heat [26] assuming that the observed temperature T_c in these samples corresponds to our mean-field T_c whereas drops with $\langle\Delta\rangle \neq 0$ exist in the range $T > T_c$ as far as T_{c0} which is substantially higher than T_c . This interpretation of the data would imply that in the absence of a pseudogap the underdoped cuprates would have a significantly higher superconducting transition temperature.

Although, in our opinion, superconductivity is not present over the entire sample when $T_c < T < T_{c0}$, the existence of a nonzero average gap $\langle\Delta\rangle$ in this region leads to the appearance of various anomalies in the observable quantities, such as the tunneling density of states and the spectral density measured in ARPES experiments, as we shall see subsequently.

4. SPECTRAL DENSITY AND DENSITY OF STATES

The delayed electron Green’s function near the hot section of the Fermi surface in the superconducting state has the form

$$G^R(E, \xi_p) = \int_0^\infty dD \mathcal{P}(D) \times \frac{E + \xi_p}{(E + i0)^2 - \xi_p^2 - D^2 - \Delta^2(D)e^2(\phi)}. \quad (22)$$

The corresponding spectral density is:

$$A(E, \xi_p) = -\frac{1}{\pi} \text{Im} G^R(E, \xi_p) = \frac{2}{W^2} \int_0^\infty dD D \exp\left(-\frac{D^2}{W^2}\right) (E + \xi_p) \times \delta(\xi_p^2 + D^2 + \Delta^2(D)e^2(\phi) - E^2). \quad (23)$$

⁵ For d -pairing the temperature dependences of $\langle\Delta\rangle$ and Δ_{mf} are qualitatively similar to the corresponding dependences for s -pairing.

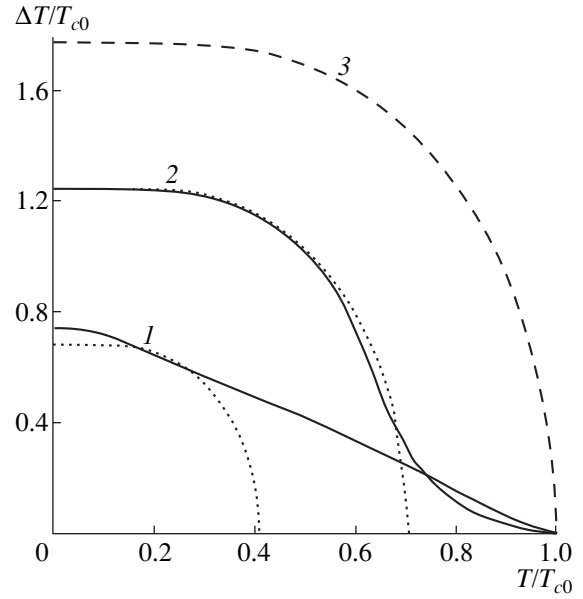


Fig. 2. Temperature dependences of the superconducting gaps Δ_{mf} (dotted curves), $\langle\Delta\rangle$ (solid curves), and Δ_0 (dashed curve) for s -pairing: (1) $\lambda = 0.4$, $\tilde{\alpha} = 2/3$, $\omega_c/W = 3$ ($T_c/T_{c0} = 0.42$), (2) $\lambda = 0.4$, $\tilde{\alpha} = 0.2$, $\omega_c/W = 1$ ($T_c/T_{c0} = 0.71$).

Using the mean-field procedure, in which we assume that $\Delta = \Delta_{mf}$ does not depend on D , we obtain

$$A_{mf}(E, \xi_p) = \frac{|E| + \xi_p \text{sgn} E}{W^2} \times \exp\left(\frac{\xi_p^2 + \Delta_{mf}^2 e^2(\phi) - E^2}{W^2}\right) \times \theta(E^2 - \xi_p^2 - \Delta_{mf}^2 e^2(\phi)). \quad (24)$$

In this approximation a gap appears in the spectral density at the Fermi surface ($\xi_p = 0$) when $|E| < \Delta_{mf}$, and disappears when $T \rightarrow T_c$ ($\Delta_{mf} \rightarrow 0$). In fact we have seen that the gap Δ depends strongly on the dielectric gap D [see (9) and (10)] so that from (23) we have

$$A(E, \xi_p) = \sum_i \frac{|E| + \xi_p \text{sgn} E}{W^2} \exp\left(-\frac{D_i^2}{W^2}\right) \times \left|1 + \frac{d\Delta^2(D)}{dD^2}\bigg|_{D=D_i} e^2(\phi)\right|^{-1}, \quad (25)$$

where D_i are the positive roots of the equation $D^2 + \xi_p^2 + \Delta^2(D)e^2(\phi) - E^2 = 0$. The energy dependences of the spectral density for $\xi_p = 0$, i.e., for the electron momentum at the Fermi surface (we shall subsequently confine our analysis to this case) are plotted in Figs. 3 and 4 for s - and d -pairing respectively.

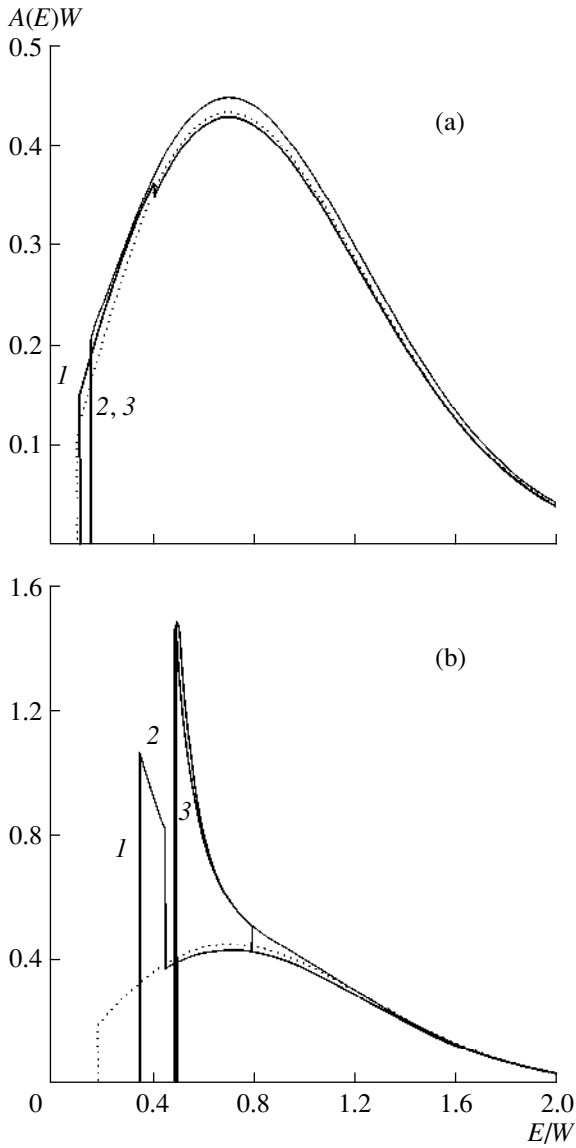


Fig. 3. Spectral density at the Fermi surface for *s*-pairing and $T/T_{c0} = (1)$ 0.8, (2) 0.4, (3) 0.1: (a) $\lambda = 0.4$, $\tilde{\alpha} = 0.2$, $\omega_c/W = 1$ ($T_c/T_{c0} = 0.71$, $T/T_{c0} = 0.54$); dotted curve—mean-field spectral density $A_{mf}(E)$ for $T/T_{c0} = 0.4$; (b) $\lambda = 0.4$, $\tilde{\alpha} = 2/3$, $\omega_c/W = 3$ ($T_c/T_{c0} = 0.42$, $T_{c\infty}/T_{c0} = 7 \times 10^{-3}$); the dotted curve gives the mean-field spectral density $A_{mf}(E)$ for $T/T_{c0} = 0.1$.

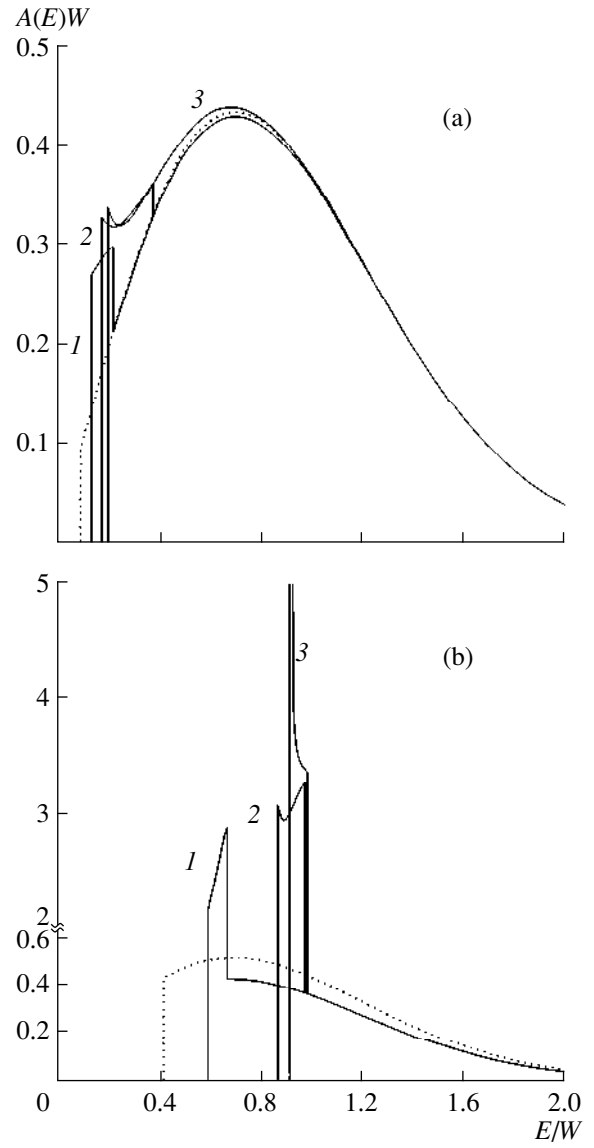


Fig. 4. Spectral density at the Fermi surface in the direction $\phi = 0$ for *d*-pairing when $T/T_{c0} = (1)$ 0.8, (2) 0.6, (3) 0.1: (a) $\lambda = 0.4$, $\tilde{\alpha} = 0.2$, $\omega_c/W = 1$ ($T_c/T_{c0} = 0.42$, $T_{c\infty}/T_{c0} = 0.2$); (b) $\lambda = 0.4$, $\tilde{\alpha} = 2/3$, $\omega_c/W = 5$ ($T_c/T_{c0} = 0.48$, $T_{c\infty}/T_{c0} \sim 10^{-18}$). The dotted curves give the mean-field spectral density $A_{mf}(E)$ for $T/T_{c0} = 0.1$.

For $T_{c\infty} < T < T_{c0}$ a discontinuity is observed in the spectral density at $E = D_{\max}$ caused by a discontinuity in the derivative $d\Delta^2(D)/dD^2$ at $D = D_{\max}$ (i.e., the maximum value of D at which the gap $\Delta(D)$ is nonzero). Effects involving the finite correlation length ξ of the fluctuations inevitably smooth this discontinuity, although the characteristic dip after the principal spectral density peak is conserved. A similar dip was observed in the ARPES experiments [1, 3] although this has not yet been fully interpreted.

For the case of *s*-pairing the value of $D^2 + \Delta^2(D)$ increases with increasing D so that the equation $D^2 + \Delta^2(D) - E^2 = 0$ only has roots for $|E| > \Delta_0$. Thus, the gap in the spectral density is observed when $|E| < \Delta_0$ so that the width of this gap is determined by the value of Δ_0 and not Δ_{mf} . In addition, the gap in the spectral density appears when $T = T_{c0}$ and the behavior of the spectral density at the point $T = T_c$ does not exhibit qualitative changes.

For d -pairing when the pseudogap width W is fairly small and the fraction of planar sections α_d is small, the value of $D^2 + \Delta^2(D)e^2(\phi)$ also increases with increasing D and the width of the gap in the spectral density becomes equal to $\Delta_0 e(\phi)$ as in the case of s -pairing. However, as the pseudogap width W and the fraction of planar sections increase, $D^2 + \Delta^2(D)e^2(\phi)$ decreases with increasing D for fairly small D with the result that the width of the gap in the spectral density becomes smaller than Δ_0 and for $E = \Delta_0$ a discontinuity appears in the spectral density (the discontinuity at $E = D_{\max}$ is also retained).

We shall now analyze the tunneling density of states $N(E)$. For s -pairing we have

$$\begin{aligned} \frac{N(E)}{N_0(0)} &= \frac{2}{W^2} \int_0^\infty dDD \exp\left(-\frac{D^2}{W^2}\right) \\ &\times \left\{ \tilde{\alpha} \frac{|E|}{\sqrt{E^2 - D^2 - \Delta^2(D)}} \theta(E^2 - D^2 - \Delta^2(D)) \right. \\ &\left. + (1 - \tilde{\alpha}) \frac{|E|}{\sqrt{E^2 - \Delta^2(D)}} \theta(E^2 - \Delta^2(D)) \right\}. \end{aligned} \quad (26)$$

Under the assumption of self-averaging the gap Δ is equal to Δ_{mf} and does not depend on the fluctuations of D , and then

$$\begin{aligned} \frac{N_{mf}(E)}{N_0(0)} &= \left\{ \tilde{\alpha} \frac{2}{W^2} \int_0^{\sqrt{E^2 - \Delta_{mf}^2}} dDD \exp\left(-\frac{D^2}{W^2}\right) \right. \\ &\times \frac{|E|}{\sqrt{E^2 - D^2 - \Delta_{mf}^2}} + (1 - \tilde{\alpha}) \frac{|E|}{\sqrt{E^2 - \Delta_{mf}^2}} \left. \right\} \\ &\times \theta(E^2 - \Delta_{mf}^2). \end{aligned} \quad (27)$$

In this approximation when $|E| < \Delta_{mf}$ a gap appears in the density of states and disappears when $T \rightarrow T_c$ ($\Delta_{mf} \rightarrow 0$) but in this case a singularity remains (as discussed in [13]) in the form of a pseudogap caused by the antiferromagnetic fluctuations:

$$\begin{aligned} \frac{N(E)}{N_0(0)} &= \tilde{\alpha} \frac{2}{W^2} \int_0^E dDD \exp\left(-\frac{D^2}{W^2}\right) \\ &\times \frac{|E|}{\sqrt{E^2 - D^2}} + (1 - \tilde{\alpha}). \end{aligned} \quad (28)$$

In fact $\Delta(D)$ in (26) depends strongly on D in accordance with (9). It can be seen from (26) and the corresponding dependence $\Delta(D)$ that when $T < T_{c\infty}$ a gap is observed in the density of states for $E < \Delta_\infty$ but when

$T > T_{c\infty}$, no gap is observed but some contribution to the pseudogap associated with the superconducting pairing still remains. For $T_c < T < T_{c0}$ the gap function $\Delta(D)$ is nonzero when $D < D_{\max}$ so that differences from the pseudogap behavior caused only by antiferromagnetic fluctuations are observed in the density of states when $T_c < T < T_{c0}$ and the antiferromagnetic pseudogap (28) is only retained when $T > T_{c0}$.

Figure 5 shows the behavior of the density of states in the s -case at various temperatures. A kink on the density of states is observed at $|E| = \Delta_0$ and when $T > T_{c\infty}$ a second kink is observed for $|E| = \Delta_{\max} > \Delta_0$ although this kink is only appreciable at high temperatures $T \sim T_{c0}$. The density of states only undergoes qualitative changes at $T = T_{c0}$, and there are no particular features at the mean-field temperature T_c .

For d -pairing the expression for the density of states has the form

$$\begin{aligned} \frac{N(E)}{N_0(0)} &= \frac{4}{\pi} \frac{2}{W^2} \int_0^\infty dDD \exp\left(-\frac{D^2}{W^2}\right) \\ &\times \left\{ \int_0^\alpha d\phi \frac{|E|}{\sqrt{E^2 - D^2 - \Delta^2(D)e^2(\phi)}} \right. \\ &\times \theta(E^2 - \Delta^2(D)e^2(\phi) - D^2) \\ &\left. + \int_\alpha^{\pi/4} d\phi \frac{|E|}{\sqrt{E^2 - \Delta^2(D)e^2(\phi)}} \theta(E^2 - \Delta^2(D)e^2(\phi)) \right\}. \end{aligned} \quad (29)$$

Under the assumption of self-averaging the gap Δ is equal to Δ_{mf} and does not depend on D . The width of the superconducting pseudogap in the density of states is then of the order Δ_{mf} , the corresponding contribution disappears when $T \rightarrow T_c$, and only the pseudogap associated with the antiferromagnetic fluctuations (28) remains. In reality in (29) Δ depends on D and is determined by equation (10).

The behavior of the density of states in the d case is shown in Fig. 6. As in the case of s -pairing a substantial difference is observed between the exact density of states and that obtained in the mean-field approximation as a result of fluctuations of the superconducting gap (superconducting drops) caused by antiferromagnetic fluctuations of the short-range order. The exact density of states does not in fact sense the superconducting transition in the entire system which takes place at $T = T_c$. In this case, the characteristic width of the superconducting gap (pseudogap) in the density of states is of the order Δ_0 and not Δ_{mf} as follows from the mean-field approximation. The corresponding contributions become observable at $T = T_{c0} > T_c$.

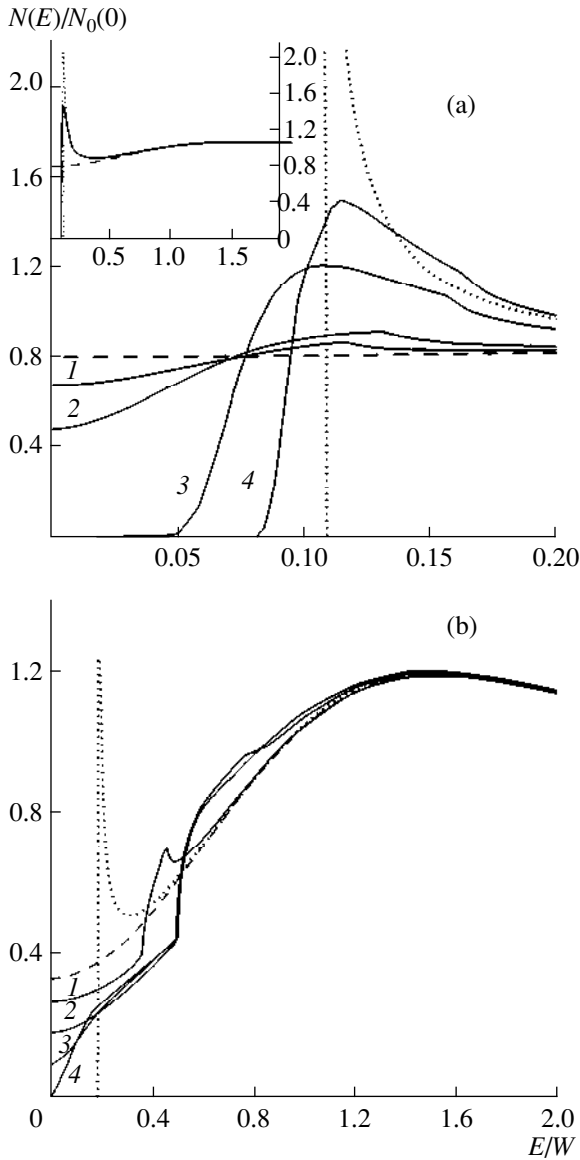


Fig. 5. Spectral density for *s*-pairing: (a) $\lambda = 0.4$, $\tilde{\alpha} = 0.2$, $\omega_c/W = 1$ ($T_c/T_{c0} = 0.71$, $T_c/T_{c0} = 0.54$), $T/T_{c0} = 0.8$ (1), 0.71 (2), 0.54 (3), 0.4 (4); dotted curve is mean-field density of states $N_{mf}(E)$ for $T_c/T_{c0} = 0.4$; inset shows density of states for $T_c/T_{c0} = 0.4$; (b) $\lambda = 0.4$, $\tilde{\alpha} = 2/3$, $\omega_c/W = 3$ ($T_c/T_{c0} = 0.42$, $T_{c\infty}/T_{c0} = 7 \times 10^{-3}$), $T/T_{c0} = 0.8$ (1), 0.42 (2), 0.2 (3), 0.05 (4); dotted curve is mean-field density of states $N_{mf}(E)$ for $T_c/T_{c0} = 0.2$, dashed curve displays pseudogap behavior of density of states for $T > T_{c0}$.

5. CONCLUSIONS

In this study we have continued our investigation of characteristic features of the superconducting state using a highly simplified model of the pseudogap in a two-dimensional electron system which can have an exact solution [13]. The main simplifying assumption of our model (in addition to the condition of static fluctuations) involves using the limit $\xi \rightarrow \infty$ for the corre-

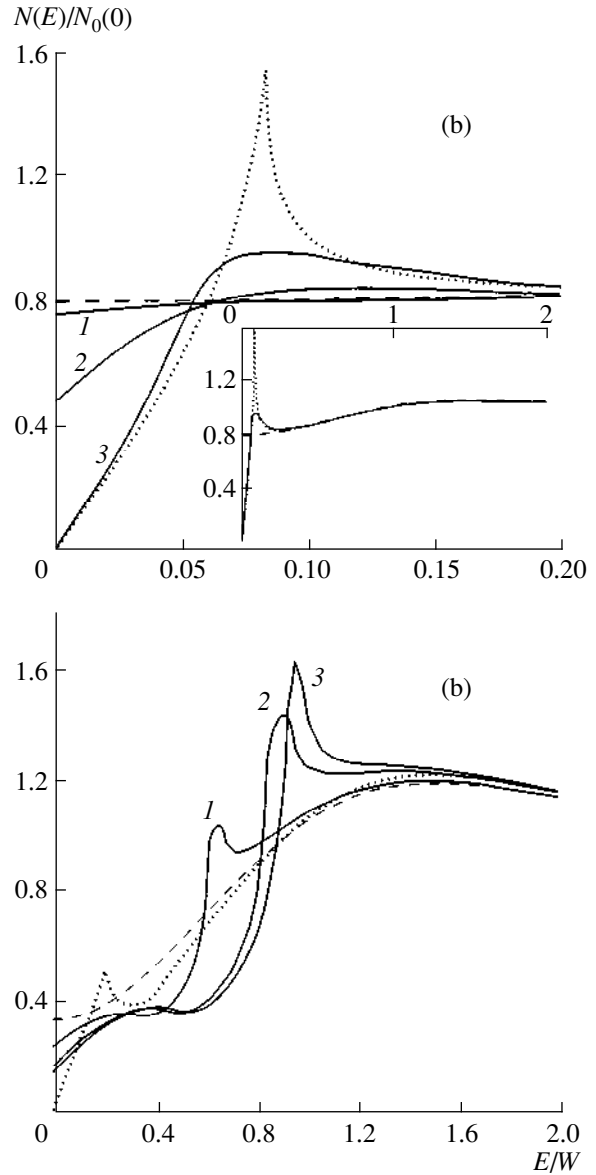


Fig. 6. Spectral density for *d*-pairing: (a) $\lambda = 0.4$, $\tilde{\alpha} = 0.2$, $\omega_c/W = 1$ ($T_c/T_{c0} = 0.42$, $T_c/T_{c0} = 0.2$), $T/T_{c0} = 0.8$ (1), 0.42 (2), 0.2 (3); dotted curve is mean-field density of states $N_{mf}(E)$ for $T_c/T_{c0} = 0.2$; inset shows density of states for $T_c/T_{c0} = 0.2$; (b) $\lambda = 0.4$, $\tilde{\alpha} = 2/3$, $\omega_c/W = 5$ ($T_c/T_{c0} = 0.48$, $T_{c\infty}/T_{c0} \sim 10^{-18}$), $T/T_{c0} = 0.8$ (1), 0.48 (2), 0.1 (3); dotted curve is mean-field density of states $N_{mf}(E)$ for $T_c/T_{c0} = 0.1$, dashed curve displays pseudogap behavior of density of states for $T > T_{c0}$.

lation length of the antiferromagnetic fluctuations of the short-range order, which allows us to obtain fundamental equations in a fairly clear form. In particular, in this limit we can easily find an exact expression for the average superconducting gap (18). In principle, this model of a pseudogap state can be generalized to finite correlation lengths [11, 12, 19] although it is unclear how far an analysis of superconductivity outside the

scope of the mean-field approach can be carried out as part of this generalization, as we did above for the case $\xi \rightarrow \infty$. It is qualitatively clear that finite ξ leads to some smearing of characteristics such as kinks and discontinuities, which were obtained in the $\xi \rightarrow \infty$ model in the dependences of T_c and other characteristics of the superconducting state on ξ .

The results obtained above indicate that the pseudogap state induced by antiferromagnetic fluctuations of the short-range order (or similar fluctuations of charge density waves) not only leads to important characteristics of the normal state [11, 12, 19] but also gives fairly unusual properties of the superconducting state caused by the partial dielectrification of the electron spectrum (non-Fermi-liquid behavior) at the hot sections of the Fermi surface. These characteristics correlate with various anomalies observed in the superconducting state of underdoped high-temperature superconducting cuprates. Naturally a more serious comparison with the experiment can only be made using a more realistic approach which particularly allows for the effects of finite correlation length ξ which in real systems are relatively small. At low temperatures it is also important to allow for the fluctuation dynamics.

ACKNOWLEDGMENTS

This work was partly supported by the Russian Foundation for Basic Research (project no. 99-02-16285) and also by the State Programs "Statistical Physics" (project no. 020) and High-Temperature Superconductivity of the Russian Ministry of Science and Education (project no. 96-051).

REFERENCES

1. T. Timusk and B. Statt, Rep. Prog. Phys. **62**, 61 (1999).
2. M. Randeria, E-print archive, cond-mat/9710223 (1997).
3. M. Randeria and J. C. Campuzano, E-print archive, cond-mat/9709107 (1997).
4. V. B. Geshkenbein, L. B. Ioffe, and A. I. Larkin, Phys. Rev. B **55**, 3173 (1997).
5. V. Emery, S. A. Kivelson, and O. Zachar, Phys. Rev. B **56**, 6120 (1997).
6. J. Maly, B. Janko, and K. Levin, E-print archive, cond-mat/9710187 (1997); cond-mat/9805018 (1997).
7. V. P. Gusynin, V. M. Loktev, and S. G. Sharapov, Zh. Éksp. Teor. Fiz. **115**, 1243 (1999) [JETP **88**, 685 (1999)].
8. J. R. Kampf and A. P. Schrieffer, Phys. Rev. B **41**, 6399 (1990); **42**, 7967 (1990).
9. M. Langer, J. Schmalian, S. Grabowski, and K. H. Bennemann, Phys. Rev. Lett. **75**, 4508 (1995).
10. J. J. Deisz, D. W. Hess, and J. W. Serene, Phys. Rev. Lett. **76**, 1312 (1996).
11. J. Schmalian, D. Pines, and B. Stojkovic, Phys. Rev. Lett. **80**, 3839 (1998); Phys. Rev. B **60**, 667 (1999).
12. E. Z. Kuchinski and M. V. Sadovskii, Zh. Éksp. Teor. Fiz. **115**, 1765 (1999) [JETP **88**, 968 (1999)]; E-print archive, cond-mat/9808321 (1998).
13. A. I. Posazhennikova and M. V. Sadovskii, Zh. Éksp. Teor. Fiz. **115**, 632 (1999) [JETP **88**, 347 (1999)]; E-print archive, cond-mat/9806199 (1998).
14. R. Gatt, S. Christensen, B. Frazer, *et al.*, E-print archive, cond-mat/9906070 (1999).
15. D. L. Feng, W. J. Zheng, K. M. Shen, *et al.*, E-print archive, cond-mat/9908056 (1999).
16. M. V. Sadovskii, Zh. Éksp. Teor. Fiz. **66**, 1720 (1974) [Sov. Phys. JETP **39**, 845 (1974)]; Fiz. Tverd. Tela (Leningrad) **16**, 2504 (1974) [Sov. Phys. Solid State **16**, 1632 (1974)].
17. M. V. Sadovskii, Zh. Éksp. Teor. Fiz. **77**, 2070 (1979) [Sov. Phys. JETP **50**, 989 (1979)].
18. M. V. Sadovskii and A. A. Timofeev, Sverkhprovodimost': Fiz., Khim., Tekh. **4**, 11 (1991); J. Mosc. Phys. Soc. **1**, 391 (1991).
19. M. V. Sadovskii, Pis'ma Zh. Éksp. Teor. Fiz. **69**, 447 (1999) [JETP Lett. **69**, 483 (1999)]; E-print archive, cond-mat/9902192 (1999).
20. Yu. V. Kopaev, Tr. Fiz. Inst. Akad. Nauk SSSR **86**, 3 (1975).
21. *Problems of High-Temperature Superconductivity*, Ed. by V. L. Ginzburg and D. A. Kirzhnits (Nauka, Moscow, 1977), Chap. 5.
22. G. Bilbro and W. L. McMillan, Phys. Rev. B **14**, 1887 (1976).
23. L. N. Bulaevskii, S. V. Panyukov, and M. V. Sadovskii, Zh. Éksp. Teor. Fiz. **92**, 672 (1987) [Sov. Phys. JETP **65**, 380 (1987)].
24. M. V. Sadovskii, Sverkhprovodimost': Fiz., Khim., Tekh. **8**, 337 (1995); M. V. Sadovskii, Phys. Rep. **282**, 225 (1997).
25. H. Ding, M. R. Norman, T. Yokoya, *et al.*, Phys. Rev. Lett. **78**, 2628 (1997).

Translation was provided by AIP

Superconductivity in the Pseudogap State Induced by Short-Order Fluctuations

É. Z. Kuchinski * and M. V. Sadovski **

Institute of Electrophysics, Ural Division, Russian Academy of Sciences,
ul. Komsomol'skaya 34, Yekaterinburg, 620016 Russia

*e-mail: kuchinsk@iep.uran.ru

**e-mail: sadovski@iep.uran.ru

Received September 5, 2000

Abstract—Peculiarities of the superconducting state (s and d pairing) are considered in a simple model of the pseudogap state caused by short-range fluctuations (e.g., of the antiferromagnetic type), which is based on the model of a Fermi surface with “hot” regions. A system of Gor'kov recurrence equations is constructed taking into account all diagrams in perturbation theory in the electron interaction with short-range fluctuations. The superconducting transition temperature is determined, and the temperature variation of the energy gap depending on the pseudogap width and the correlation length of short-range fluctuations is analyzed. In a similar approximation, a microscopic derivation of the Ginzburg–Landau expansion is carried out, and the behavior of the main physical parameters of the superconductor near the transition temperature is studied depending on the pseudogap width as well as the correlation length of the fluctuations. The obtained results are in qualitative agreement with a number of experiments with underdoped HTSC cuprates. © 2001 MAIK “Nauka/Interperiodica”.

1. INTRODUCTION

The pseudogap state observed in a wide region on the phase diagram for HTSC cuprates leads to numerous anomalies in their properties in the normal as well as superconducting states [1]. These anomalies can be explained using two basic theoretical scenarios. The first is based on the model of the formation of Cooper pairs even above the superconducting transition temperature [2–4], followed by the stabilization of their phase coherence at $T < T_c$. The second assumes that the origin of the pseudogap state is associated with fluctuations of the antiferromagnetic (AFM) short-range order existing in the region of underdoped compositions on the phase diagram [5–7]. A number of recent experimental results convincingly demonstrate the validity of the second scenario [8, 9].

Most of theoretical publications are devoted to an analysis of the models of the pseudogap state in the normal phase at $T > T_c$. We proposed [10, 11] a very simple exactly solvable model of the pseudogap, which is based on the concept of “hot” (planar) regions existing on the Fermi surface. In the framework of this model, the Ginzburg–Landau expansion was constructed for various types of Cooper pairing [10] and the peculiarities of the superconducting state in the range of $T < T_c$ [11], caused by short-range fluctuations of the AFM type, were analyzed. We used an extremely simplified model of Gaussian short-range fluctuations with an infinitely large correlation length, which allowed us to obtain the exact solution for the pseudogap state. In real

systems, the correlation length of AFM fluctuations is finite and comparatively small [6]. The present work is mainly devoted to the generalization of the main results obtained by us earlier [10, 11] to the case of finite correlation lengths of the short-range AFM fluctuations and to the analysis of the main parameters of the superconducting state as functions of this correlation length and the effective width of the pseudogap.

2. MODEL OF THE PSEUDOGAP STATE

The simplified model of the pseudogap state [10, 11] under investigation is based on the pattern of well-developed fluctuations of the antiferromagnetic short-range order and is close to the model of “hot points” on the Fermi surface [6]. We assume that the Fermi surface of a 2D electronic system has the form depicted in Fig. 1. Such a Fermi surface was observed in a number of ARPES experiments on HTSC cuprates [12, 13]. It should be noted that the assumption concerning the existence of plane regions is not of fundamental importance for our model. However, it considerably simplified the calculations which could also be in principle made in a more realistic model of hot points. Such a model of the Fermi surface was applied long ago to HTSC cuprates by many authors [14–16] who thoroughly analyzed, among other things, the microscopic criteria for the existence of the antiferromagnetic and superconducting phases. We will be using a purely phenomenological model presuming the existence in a system of static Gaussian fluctuations of a short-range

order with a correlation function (structural factor) of the form [5]

$$S(\mathbf{q}) = \frac{1}{\pi^2} \frac{\xi^{-1}}{(q_x - Q_x)^2 + \xi^{-2}} \frac{\xi^{-1}}{(q_y - Q_y)^2 + \xi^{-2}}, \quad (1)$$

where ξ is the correlation length of the fluctuations, and the scattering vector is taken in the form $Q_x = \pm 2k_F$, $Q_y = 0$, or $Q_y = \pm 2k_F$, $Q_x = 0$, which envisages the presence of incommensurate fluctuations. The factorized form of correlator (1) introduced in [5] considerably simplifies the calculations and is virtually identical quantitatively to the conventional isotropic Lorentzian in the range $|\mathbf{q} - \mathbf{Q}| < \xi^{-1}$, which is the most important for our analysis [7].

The least physically justified assumption concerns the static form of fluctuations and can be used only at high temperatures [6, 7]. At low temperatures, including those corresponding to the superconducting phase, the spin dynamics may naturally turn out to be quite significant. This also applies to the microscopic theory of Cooper pairing in the model of a “nearly antiferromagnetic” Fermi liquid [17, 18]. However, we assume that the static approximation used here is sufficient for an analysis of the qualitative effect of pseudogap formation on the superconductivity, which will be described by using a purely phenomenological approach of the BCS theory.

We present the effective interaction of electrons with AFM fluctuations in the form

$$V_{\text{eff}} = (2\pi)^2 W^2 S(\mathbf{q}), \quad (2)$$

where parameter W determines the energy scale (width) of the pseudogap. We assume that only the electrons belonging to planar (hot) regions on the Fermi surface interact with fluctuations, so that the value of W effectively differs from zero only for these electrons [10, 11]. We completely disregard the spin structure of the interaction, which could be easily taken into account [6], but this would make our calculations more cumbersome. In this sense, our analysis can be applied literally to a description of the interaction between short-range fluctuations and charge density waves rather than spin density waves. We also assume that this simplifying assumption is insignificant for an analysis of the qualitative effects of the pseudogap state on superconductivity that we are interested in.

The factorized form of correlator (1), and hence of the effective interaction (2), makes the scattering from fluctuations one-dimensional. In the limit of an infinitely large correlation length ($\xi \rightarrow \infty$), the model of scattering from such fluctuations has an exact solution [10, 11, 19]. For a finite ξ , we can construct an “almost exact” solution [7] generalizing the one-dimensional approach proposed in [20]. In this case, the sum of the

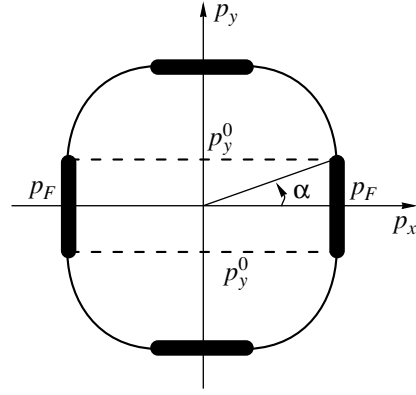


Fig. 1. Fermi surface of a two-dimensional system. Hot regions are shown by bold lines of thickness $\sim \xi^{-1}$.

entire diagrammatic series for the one-particle Green’s function for electrons from the planar regions on the Fermi surface (where the nesting condition $\xi_{\mathbf{p} \pm \mathbf{Q}} = -\xi_{\mathbf{p}}$ for the electron spectrum is satisfied) can be (approximately) determined.

For the contribution of an arbitrary diagram, we can write the following ansatz for the N -order eigenenergy component in the interaction (2) [7, 20]:

$$\Sigma^{(N)}(\varepsilon_n, \mathbf{p}) = W^{2N} \prod_{j=1}^{2N-1} G_{0k_j}(\varepsilon, \mathbf{p}), \quad (3)$$

$$G_{0k_j}(\varepsilon_n, \mathbf{p}) = \frac{1}{i\varepsilon_n - (-1)^j \xi_{\mathbf{p}} + ik_j \kappa},$$

where $\kappa = v_F \xi^{-1}$ (v_F is the Fermi velocity), k_j is the number of interaction curves embracing the j th electron line in the diagram (starting from the origin), and $\varepsilon_n = 2\pi T(n + 1/2)$ (we assume for definiteness that $\varepsilon_n > 0$). Thus, the contribution of any diagram is actually determined only by the set of integers k_j . Any diagram with the intersection of the lines of interaction is identical to a certain diagram of the same order without intersection of interaction lines, and the contribution of all diagrams with intersections can be taken into account through the combinatorial factors $v(k_j)$ ascribed to interaction lines on diagrams without intersections [20, 7, 6]. In the model of incommensurate fluctuations under investigation, we have

$$v(k) = \begin{cases} \frac{k+1}{2} & \text{for odd } k, \\ \frac{k}{2} & \text{for even } k. \end{cases} \quad (4)$$

As a result, we arrive at the following recurrence procedure (presentation in the form of a chain fraction) for

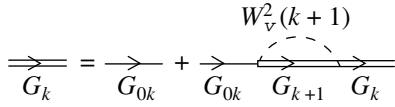


Fig. 2. Diagrammatic representation of the recurrence relation for a one-particle Green's function.

the one-particle Green's function $G(\varepsilon_n, \mathbf{p})$ for electrons from hot regions [20, 7, 6]:

$$G_k(\varepsilon_n, \mathbf{p}) = \frac{1}{i\varepsilon_n - (-1)^k \xi_{\mathbf{p}} + ik\kappa - W^2 v(k+1)G_{k+1}(\varepsilon_n, \mathbf{p})}, \quad (5)$$

$$G(\varepsilon_n, \mathbf{p}) \equiv G_0(\varepsilon_n, \mathbf{p}).$$

The diagrammatic representation of this procedure is illustrated in Fig. 2.

Ansatz (3) for the contribution of an arbitrary N -order diagram is usually not exact [7, 21]. However, in the 2D case, we can indicate the topologies of the Fermi surface for which representation (3) is exact [7]. In the remaining cases, it can be proved [7] that this representation exaggerates (in a certain sense) the role of the finiteness of the correlation length ξ in the given order of perturbation theory. In the 1D case, when this problem is especially vital [7, 21], it turns out that the calculations of the density of states on the basis of approximation (3) for incommensurate fluctuations give a nearly perfect quantitative coincidence [22] with the results of the exact numerical simulation of this problem, which was carried out in [23, 24].¹ In the limit $\xi \rightarrow \infty$, ansatz (3) can be reduced to the exact solution [19], while in the limit $\xi \rightarrow 0$, it leads to a physically correct limit of free electrons for a fixed value of W .

Outside hot regions, electrons do not interact with fluctuations altogether in our model, and the Green's function remains free:

$$G(\varepsilon_n, \mathbf{p}) = G_{00}(\varepsilon_n, \mathbf{p}) = \frac{1}{i\varepsilon_n - \xi_{\mathbf{p}}}. \quad (6)$$

The model considered above leads to a non-Fermi-liquid (two-hump) behavior of the spectral density in hot regions on the Fermi surface and to a blurred pseudogap in the density of states (cf. similar results in the model of hot points [6, 7]). In cold regions of the Fermi surface, we observe the conventional Fermi-liquid behavior (free electrons).

¹ In the case of a one-dimensional problem with commensurate fluctuations, ansatz (3) fails to describe only a weak Dyson singularity in the density of states near the center of the pseudogap [23, 24], also providing a quantitatively good approximation to the exact results beyond the pseudogap. Note that in the 2D case, the Dyson singularity in the density of states is just absent in all probability.

3. GOR'KOV EQUATIONS FOR A SUPERCONDUCTOR WITH A PSEUDOGAP

In our previous publications [10, 11], we analyzed the peculiarities of the superconducting state in the exactly solvable model of the pseudogap state induced by short-range AFM fluctuations with an infinitely large correlation length ($\xi \rightarrow \infty$). Among other things, it was proved [11] that AFM fluctuations may lead to strong fluctuations of the semiconducting order parameter (energy gap Δ), which violate the standard assumption concerning the self-averaging of the gap [25–27]. This assumption makes it possible to average (over the configurations of the random field of static short-range fluctuations) the order parameter Δ and various combinations of the electron Green's functions appearing in the basic equations of the theory. The conventional arguments in favor of such an independent averaging are usually formulated as follows [25, 27]. The value of Δ varies over characteristic scales of length of the order of the coherence length $\xi_0 \sim v_F/\Delta_0$ in the BCS theory, while Green's functions vary rapidly over much smaller scales of the order of atomic spacings. Naturally, the latter assumption becomes incorrect when a new characteristic length $\xi \rightarrow \infty$ appears for the electronic subsystem. At the same time, if the antiferromagnetic correlation length $\xi \ll \xi_0$ (i.e., if AFM correlations correlate over distances smaller than the characteristic size of Cooper pairs), the assumption concerning the self-averaging of Δ must be preserved, being violated only in the region where $\xi > \xi_0$. For this reason, the subsequent analysis will be carried out assuming self-averaging of the energy gap of a superconductor over AFM fluctuations. This allows us to use the standard approach of the theory of disordered superconductors (mean-field approximation in the language of [11]). In this case, the interesting question concerning superconductivity in the absence of self-averaging of the order parameter is not considered. It should be noted that for real HTSC cuprates, we apparently always have $\xi \sim \xi_0$, so that these materials fall in the most complicated range of parameters of the theory.

Following [10, 11], we assume that the superconducting pairing is governed by the attraction potential of the following simplest form:

$$V(\mathbf{p}, \mathbf{p}') = V(\phi, \phi') = -Ve(\phi)e(\phi'), \quad (7)$$

where ϕ is the polar angle determining the direction of the electron momentum \mathbf{p} in a plane, and for $e(\phi)$ we assume the following simplest model dependence:

$$e(\phi) = \begin{cases} 1 & (s\text{-pairing}), \\ \sqrt{2} \cos(2\phi) & (d\text{-pairing}). \end{cases} \quad (8)$$

As usual, the constant of attraction V is assumed to be other than zero in a certain layer of width $2\omega_c$ in the vicinity of the Fermi level (ω_c is the characteristic fre-

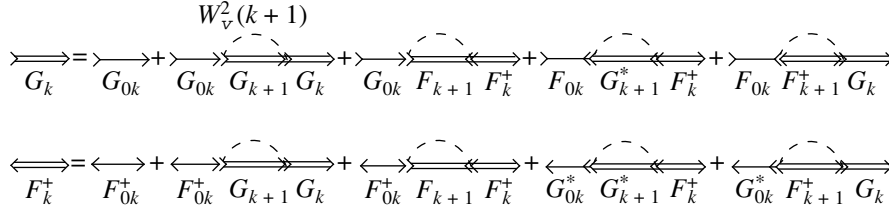


Fig. 3. Diagrammatic representation of the recurrence relation for Gor'kov's equations.

quency of quanta ensuring the attraction of electrons). In this case, the superconducting gap has the form

$$\Delta(\mathbf{p}) \equiv \Delta(\phi) = \Delta e(\phi). \quad (9)$$

In order to simplify the notation, we will henceforth assume that the gap Δ just stands for $\Delta(\phi)$ and will write explicitly the angular dependence only when required.

The perturbation theory in the interaction with AFM fluctuations (1) for the superconducting state must be constructed on “free” normal and anomalous Green's functions for the superconductor:

$$G_{00}(\varepsilon_n, \mathbf{p}) = -\frac{i\varepsilon_n + \xi_{\mathbf{p}}}{\varepsilon_n^2 + \xi_{\mathbf{p}}^2 + |\Delta|^2}, \quad (10)$$

$$F_{00}^+(\varepsilon_n, \mathbf{p}) = \frac{\Delta^*}{\varepsilon_n^2 + \xi_{\mathbf{p}}^2 + |\Delta|^2}.$$

In the adopted model with planar regions on the Fermi surface, the electron spectrum in the regions orthogonal to the p_x axis has the form $\xi_{\mathbf{p}} = v_F(|p_x| - p_F)$ since the electron velocity \mathbf{v} is perpendicular of the p_y axis (a symmetric situation is also observed in the regions orthogonal to p_y). Consequently, in the case of s -pairing, when the value of Δ is independent of the direction of the momentum, the problem becomes completely one-dimensional in the model with an interaction of form (1) and (2). In the case of d -pairing, the situation is more complicated since the value of $\Delta(\phi)$ depends on p_y even in the planar regions orthogonal to p_x (and, symmetrically, on the regions orthogonal to p_y). For this reason, it is convenient to analyze d -pairing by using instead of Eq. (1) the correlator of fluctuations in the form

$$S(\mathbf{q}) = \frac{1}{\pi} \left\{ \frac{\xi^{-1}}{(q_x \mp 2p_F)^2 + \xi^{-2}} \delta(q_y) + \frac{\xi^{-1}}{(q_y \mp 2p_F)^2 + \xi^{-2}} \delta(q_x) \right\}. \quad (11)$$

In this case, the interaction does not affect p_y and p_x in the planar regions orthogonal, respectively, to p_x and p_y , and the problem becomes completely one-dimensional again.

We can now formulate an analogue of approximation (3) for the superconducting state also. The details of the substantiation of the relations presented below are given in Appendix A. The contribution of an arbitrary N -order diagram in interaction (2) to the total normal or anomalous Green's function has the form of a product of $N + 1$ “free” normal G_{0k_j} and anomalous ($F_{0k_j}^+$) Green's functions with frequencies and gaps renormalized in a certain way (see below). Here k_j is the number of the interaction curves embracing the given j th electron line (starting from the origin of the diagram). As in the normal phase, the contribution of any diagram is determined by the set of integers k_j , and each diagram with the intersection of interaction curves is equivalent to a certain diagram of the same order without intersection of these curves. Consequently, we can again consider only diagrams without intersections of interaction curves, taking into account the contribution of the remaining diagrams through the same combinatorial factors $v(k)$ ascribed to the interaction curves as in the normal phase. As a result, we obtain a diagrammatic analogue of the Gor'kov equations [28] presented in Fig. 3. Accordingly, we have two coupled recurrence equations for the normal and anomalous Green's functions:

$$G_k = G_{0k} + G_{0k} \tilde{G} G_k - G_{0k} \tilde{F} F_k^+ - F_{0k} \tilde{G}^* F_k^+ - F_{0k} \tilde{F}^+ G_k, \quad (12)$$

$$F_k^+ = F_{0k}^+ + F_{0k}^+ \tilde{G} G_k + -F_{0k}^+ \tilde{F} F_k^+ + G_{0k}^* \tilde{G}^* F_k^+ + G_{0k}^* \tilde{F}^+ G_k,$$

where

$$\tilde{G} = W^2 v(k+1) G_{k+1}, \quad \tilde{F}^+ = W^2 v(k+1) F_{k+1}^+, \quad (13)$$

$$G_{0k}(\varepsilon_n, \mathbf{p}) = -\frac{i\varepsilon_n + (-1)^k \xi_{\mathbf{p}}}{\tilde{\varepsilon}_n^2 + \xi_{\mathbf{p}}^2 + |\tilde{\Delta}|^2}, \quad (14)$$

$$F_{0k}^+(\varepsilon_n, \mathbf{p}) = \frac{\tilde{\Delta}^*}{\tilde{\varepsilon}_n^2 + \xi_{\mathbf{p}}^2 + |\tilde{\Delta}|^2}.$$

and the renormalized frequency $\tilde{\varepsilon}$ and gap $\tilde{\Delta}$

$$\tilde{\varepsilon}_n = \eta_k \varepsilon_n, \quad \tilde{\Delta} = \eta_k \Delta, \quad \eta_k = 1 + \frac{k\kappa}{\sqrt{\varepsilon_n^2 + |\Delta|^2}} \quad (15)$$

have been introduced in analogy with the case of superconductors with impurities [28].

Equations (12)–(15) can easily be used to derive a system of recurrence relations directly for the real and imaginary components of the normal Green's function and for the anomalous Green's function:

$$\begin{aligned} \text{Im}G_k &= \frac{\tilde{\varepsilon} - \text{Im}\tilde{G}}{(\tilde{\varepsilon} - \text{Im}\tilde{G})^2 + ((-1)^k \xi_{\mathbf{p}} + \text{Re}\tilde{G})^2 + |\tilde{\Delta} + \tilde{F}|^2}, \\ \text{Re}G_k &= \frac{(-1)^k \xi_{\mathbf{p}} + \text{Re}\tilde{G}}{(\tilde{\varepsilon} - \text{Im}\tilde{G})^2 + ((-1)^k \xi_{\mathbf{p}} + \text{Re}\tilde{G})^2 + |\tilde{\Delta} + \tilde{F}|^2}, \\ F_k^+ &= \frac{\tilde{\Delta}^* + \tilde{F}^+}{(\tilde{\varepsilon} - \text{Im}\tilde{G})^2 + ((-1)^k \xi_{\mathbf{p}} + \text{Re}\tilde{G})^2 + |\tilde{\Delta} + \tilde{F}|^2}. \end{aligned} \quad (16)$$

Let us introduce the following notation:

$$\text{Im}G_k = -\varepsilon_n J_k, \quad \text{Re}G_k = -(-1)^k \xi_{\mathbf{p}} R_k, \quad F_k^+ = \Delta^* f_k. \quad (17)$$

It turns out that the recurrence relations for J_k and f_k are completely identical in this case so that $J_k = f_k$. Finally, we arrive at the following system of recurrence relations for J_k and R_k :

$$\begin{aligned} J_k &= [\eta_k + W^2 \nu(k+1)J_{k+1}] \\ &\times [(\varepsilon_n^2 + \Delta^2)^{1/2} (\eta_k + W^2 \nu(k+1)J_{k+1})^2 \\ &+ \xi_{\mathbf{p}}^2 (1 + W^2 \nu(k+1)R_{k+1})^2]^{-1}, \\ R_k &= [1 + W^2 \nu(k+1)R_{k+1}] \\ &\times [(\varepsilon_n^2 + \Delta^2)^{1/2} (\eta_k + W^2 \nu(k+1)J_{k+1})^2 \\ &+ \xi_{\mathbf{p}}^2 (1 + W^2 \nu(k+1)R_{k+1})^2]^{-1}. \end{aligned} \quad (18)$$

The normal and anomalous Green's functions for the superconductor we are interested in can be defined in terms of R_0 and J_0 ,

$$\text{Im}G = -\varepsilon_n J_0, \quad \text{Re}G = -\xi_{\mathbf{p}} R_0, \quad F^+ = \Delta^* J_0, \quad (19)$$

and have the form of a totally summed series in the perturbation theory in the interaction of an electron with short-range antiferromagnetic fluctuations in the semiconductor.

4. SUPERCONDUCTING TRANSITION TEMPERATURE AND THE TEMPERATURE DEPENDENCE OF THE GAP

The energy gap in a superconductor is defined by the equation

$$\Delta(\mathbf{p}) = -T \sum_{\mathbf{p}'} \sum_{\varepsilon_n} V_{sc}(\mathbf{p}, \mathbf{p}') F(\varepsilon_n, \mathbf{p}'). \quad (20)$$

The anomalous Green's function on planar regions of the Fermi surface can be determined from Eqs. (19) by using the recurrence procedure (18). In our model, the scattering from AFM fluctuations on the remaining (cold) part of the Fermi surface is absent, and the anomalous Green's function has the same form as in Eqs. (10). As a result, Eq. (20) for s -pairing taking into account dependence (8) assumes the form

$$\begin{aligned} 1 &= \lambda \left\{ \tilde{\alpha} T \sum_{\varepsilon_n} \int_{-\omega_c}^{\omega_c} d\xi J_0(\varepsilon_n \xi) \right. \\ &\left. + (1 - \tilde{\alpha}) \int_0^{\omega_c} d\xi \frac{\tanh \frac{\sqrt{\xi^2 + \Delta^2}}{2T}}{\sqrt{\xi^2 + \Delta^2}} \right\}, \end{aligned} \quad (21)$$

where $\lambda = VN_0(0)$ is the dimensionless constant of the pairing interaction ($N_0(0)$ is the density of states for free electrons at the Fermi level) and $\tilde{\alpha} = 4\alpha/\pi$, where α is the angular dimension of a planar region on the Fermi surface (see Fig. 1). In our further numerical calculations, we will assume (quite arbitrarily) that $\tilde{\alpha} = 2/3$, i.e., $\alpha = \pi/6$, which is close, for example, to the results obtained in [12].

In the case of d -pairing, we must take into account the angular dependence of gap (9), and Eq. (20) assumes the form

$$\begin{aligned} 1 &= \lambda \frac{4}{\pi} \left\{ T \int_0^{\alpha} d\phi e^2(\phi) \sum_{\varepsilon_n} \int_{-\omega_c}^{\omega_c} d\xi J_0(\varepsilon_n \xi) \right. \\ &\left. + \int_{\alpha}^{\pi/4} d\phi e^2(\phi) \int_0^{\omega_c} d\xi \frac{\tanh \frac{\sqrt{\xi^2 + \Delta^2 e^2(\phi)}}{2T}}{\sqrt{\xi^2 + \Delta^2 e^2(\phi)}} \right\}. \end{aligned} \quad (22)$$

Figure 4 shows the temperature dependences of the gap width calculated from Eq. (21) in the case of s -pairing for various values of correlation length (parameter $\kappa = \nu_F \xi^{-1}$) of the fluctuations. In the case of d -pairing, the corresponding qualitative dependences are quite similar.

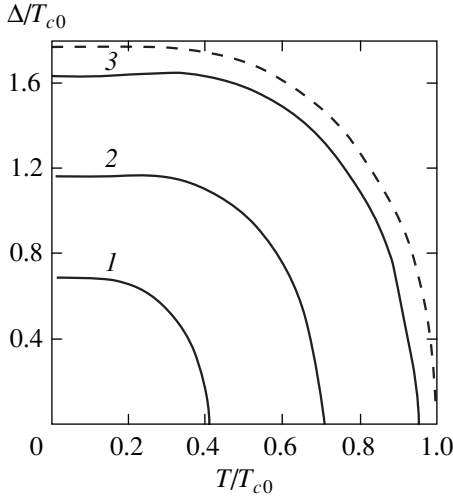


Fig. 4. Temperature dependence of the superconducting gap width in the case of s -pairing for various values of correlation length (parameter $\kappa = v_F \xi^{-1}$) for AFM fluctuations, calculated for $\lambda = 0.4$, $\omega_c/W = 3$, $\kappa/W = 0$ (1), 1.0 (2), and 10.0 (3). The dashed curve describes $\Delta(T)$ in the absence of a pseudogap.

The equation for the superconducting transition temperature T_c follows directly from Eqs. (21) and (22) for $\Delta \rightarrow 0$. In this case, $J_0(\Delta \rightarrow 0)$ is independent of ϕ and is the same for s - and d -pairing. Accordingly, the equation for T_c has the form

$$1 = \lambda \left\{ \alpha_{\text{eff}} T_c \sum_{\epsilon_n = -\omega_c}^{\omega_c} \int d\xi J_0(\epsilon_n \xi; \Delta \rightarrow 0) + (1 - \alpha_{\text{eff}}) \int_0^{\omega_c} d\xi \frac{\tanh \xi / (2T_c)}{\xi} \right\}, \quad (23)$$

where the “effective” fraction of planar regions on the Fermi surface is defined as

$$\alpha_{\text{eff}} = \begin{cases} \tilde{\alpha} & (s\text{-pairing}), \\ \tilde{\alpha} + \frac{1}{\pi} \sin(\pi \tilde{\alpha}) & (d\text{-pairing}). \end{cases} \quad (24)$$

The theoretical dependence of T_c on the pseudogap width W and correlation length (parameter $\kappa = v_F \xi^{-1}$) are shown in Fig. 5 (T_{c0} is the superconducting transition temperature in the absence of a pseudogap).

The general qualitative conclusion is the same as in [10, 11]: the pseudogap suppresses superconductivity due to a partial “dielectrization” of the electron spectrum in hot regions on the Fermi surface. The suppression effect is the strongest for $\kappa = 0$ (infinitely large cor-

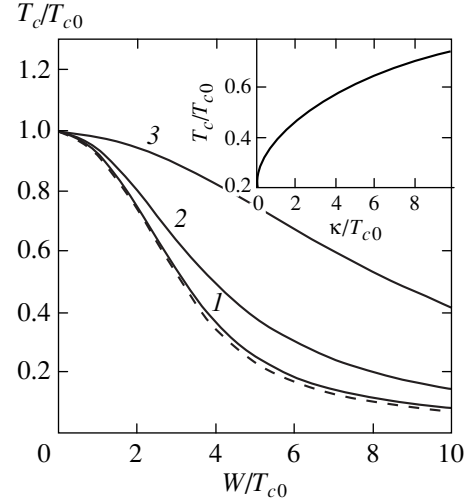


Fig. 5. Dependence of the superconducting transition temperature on the pseudogap width W and the correlation length (parameter $\kappa = v_F \xi^{-1}$) for AFM fluctuations: $\kappa/W = 0.1$ (1), 1.0 (2), and 10.0 (3). The dashed curve corresponds to $\kappa = 0$ [10]. The inset shows the dependence of T_c on κ for $W/T_{c0} = 5$.

relation length of AFM fluctuations) [10, 11] and decreases with the correlation length, which is quite in accordance with the experimental phase diagram of HTSC systems.

It should be emphasized once again that all the results described above are valid under the assumption of the self-averaging of the superconducting order parameter (gap) in AFM fluctuations (mean-field approximation [11]), which holds for not very large values of the correlation length $\xi < \xi_0$, where ξ_0 is the coherence length for the superconductor (the size of Cooper pairs at $T = 0$). For $\xi \gg \xi_0$, considerable non-self-averaging effects appear, which are manifested in the emergence of characteristic “tails” on the temperature dependence of the averaged gap in the temperature range $T_c < T < T_{c0}$ [11].

5. COOPER INSTABILITY. RECURRENCE PROCEDURE FOR THE VERTEX PART

It is well known that the superconducting transition temperature can also be determined in a different way, namely, from the equation for the Cooper instability of the normal phase:

$$1 - V\chi(0, 0) = 0, \quad (25)$$

where the generalized Cooper susceptibility is described by the graph in Fig. 6. In this case, we are dealing with the problem of calculation of the “triangular” vertex component taking into account the interaction with AFM fluctuations. For the one-dimensional analogue of our problem (and for real frequencies, $T = 0$), the corresponding recurrence procedure was formulated in [29]. For the 2D model considered by us

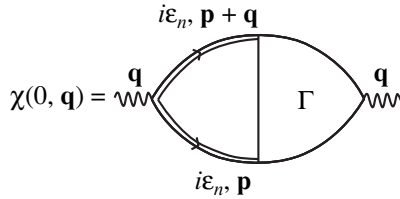


Fig. 6. Diagram for the generalized Cooper susceptibility.

here, this procedure was used for calculating the optical conductivity [30]. The procedure can easily be generalized to the case of Matsubara frequencies. Henceforth, we will assume for definiteness that $\epsilon_n > 0$. This gives

$$\Gamma_{k-1}(\epsilon_n, -\epsilon_n, \mathbf{q}) = 1 + W^2 v(k) G_k \bar{G}_k \times \left\{ 1 + \frac{2ik\kappa}{2i\epsilon_n - (-1)^k v_F q - W^2 v(k+1)(G_{k+1} - \bar{G}_{k+1})} \right\} \times \Gamma_k(\epsilon_n, -\epsilon_n, \mathbf{q}), \quad (26)$$

$$\Gamma(\epsilon_n, -\epsilon_n, \mathbf{q}) \equiv \Gamma_0(\epsilon_n, -\epsilon_n, \mathbf{q}),$$

where $G_k = G_k(\epsilon_n, \mathbf{p} + \mathbf{q})$ and $\bar{G}_k = G_k(-\epsilon_n, \mathbf{p})$ are calculated in accordance with relations (5).

In order to find T_c , we consider the vortex where $\mathbf{q} = 0$. In this case, $\bar{G}_k = G_k^*$, and the vertices Γ_k become real-valued, which considerably simplifies procedure (26). Using a notation similar to (17), we obtain from relations (5) and (26)

$$\Gamma_{k-1} = 1 + W^2 v(k) \frac{J_k}{1 + W^2 v(k+1) J_{k+1}} \Gamma_k, \quad (27)$$

while for R_k and J_k we have recurrence relations coinciding with Eqs. (18) for $\Delta = 0$.

The following exact relation (which will be proved below) of the type of the Word identity holds:

$$G(\epsilon_n, \mathbf{p}) G(-\epsilon_n, \mathbf{p}) \Gamma(\epsilon_n, -\epsilon_n, 0) = (\xi_p^2 R_0^2(\epsilon_n, \xi_p) + \epsilon_n^2 J_0(\epsilon_n, \xi_p)) \times \Gamma_0(\epsilon_n, -\epsilon_n, 0) \equiv J_0(\epsilon_n, \xi_p) = -\frac{1}{\epsilon_n}(\epsilon_n, \mathbf{p}). \quad (28)$$

A numerical analysis completely confirms the validity of this relation, demonstrating complete matching between the recurrence procedures for the one-particle Green's function and for the vertex component.² Since $J_0(\Delta \rightarrow 0)$ coincides with J_0 in the normal phase, relation (28) just leads to the coincidence of the equation for T_c obtained from the Cooper instability condition (25),

² Note that an analytic proof of this relation through a direct comparison of the recurrence procedures themselves for the Green's function and the vertex component is not at all obvious.

$$1 = \lambda \left\{ \alpha_{\text{eff}} T_c \sum_{\epsilon_n = -\omega_c}^{\omega_c} \int d\xi (\xi_p^2 R_0^2(\epsilon_n, \xi_p) + \epsilon_n^2 J_0(\epsilon_n, \xi_p)) \times \Gamma_0(\epsilon_n, -\epsilon_n, 0) + (1 - \alpha_{\text{eff}}) \int_0^{\omega_c} d\xi \frac{\tanh(\xi/2T_c)}{\xi} \right\} \quad (29)$$

and Eq. (23) obtained as a result of the linearization of the equation for the gap in spite of the apparently different recurrence procedures used for their derivation and taking into account AFM fluctuations.

6. THE GINZBURG-LANDAU EXPANSION

The Ginzburg-Landau expansion in the exactly solvable model of a pseudogap with an infinitely large correlation length of AFM fluctuations was constructed in [10]. Here, we will generalize these results to the case of finite correlation lengths.

We write the Ginzburg-Landau expansion for the difference in the free energy densities of the superconducting and normal states in the standard form

$$F_s - F_n = A|\Delta_q|^2 + q^2 C|\Delta_q|^2 + \frac{B}{2}|\Delta_q|^4, \quad (30)$$

where Δ_q is the amplitude of the Fourier component of the order parameter:

$$\Delta(\phi, \mathbf{q}) = \Delta_q e(i\phi). \quad (31)$$

Expansion (30) is determined by the graphs of the loop-type expansion for the free energy in the field of order parameter fluctuations with a small wave vector \mathbf{q} [10].

We present the Ginzburg-Landau coefficients in the form

$$A = A_0 K_A, \quad C = C_0 K_C, \quad B = B_0 K_B, \quad (32)$$

where A_0 , C_0 , and B_0 denote the standard expressions for these coefficients in the case of an isotropic s -pairing:

$$A_0 = N_0(0) \frac{T - T_c}{T_c}, \quad C_0 = N_0(0) \frac{7\zeta(3) v_F^2}{32\pi^2 T_c^2}, \quad (33)$$

$$B_0 = N_0(0) \frac{7\zeta(3)}{8\pi^2 T_c^2}.$$

In this case, all the peculiarities of the model under investigation, which are associated with the emergence of a pseudogap, are contained in the dimensionless coefficients K_A , K_C , and K_B . In the absence of a pseudogap, all these coefficients are equal to unity ($K_B = 3/2$ only in the case of d -pairing). For this reason, we will normalize coefficient K_B for d -pairing to this value, presenting the numerical results for $\tilde{K}_B = (2/3)K_B$.

Let us consider the generalized Cooper susceptibility (Fig. 6)

$$\chi(\mathbf{q}, 0; T) = -T \sum_{\varepsilon_n} \sum_{\mathbf{p}} G(\varepsilon_n, \mathbf{p} + \mathbf{q}) \times G(-\varepsilon_n, \mathbf{p}) e^2(\phi) \Gamma(\varepsilon_n, -\varepsilon_n, \mathbf{q}). \quad (34)$$

Using relations (28), we can easily write coefficients K_A and K_C in the form

$$K_A = \frac{\chi(\mathbf{q}, 0; T) - \chi(0, 0; T_c)}{A_0} = \alpha_{\text{eff}} \frac{T_c}{T - T_c} \times \left\{ T \sum_{\varepsilon_n = \pi T(2n+1) - \omega_c}^{\omega_c} \int d\xi J_0(\varepsilon_n, \xi) - T_c \sum_{\varepsilon = \pi T_c(2n+1) - \omega_c}^{\omega_c} \int d\xi J_0(\varepsilon, \xi) \right\} + 1 - \alpha_{\text{eff}}, \quad (35)$$

$$K_C = \lim_{q \rightarrow 0} \frac{\chi(\mathbf{q}, 0; T) - \chi(0, 0; T_c)}{q^2 C_0} = \frac{32\pi^2 T_c^3}{7\zeta(3) v_F q^2} = \alpha_{\text{eff}} \left\{ \sum_{\varepsilon_n = \pi T(2n+1) - \omega_c}^{\omega_c} \int d\xi J_0(\varepsilon_n, \xi) - \sum_{\varepsilon = \pi T_c(2n+1) - \omega_c}^{\omega_c} \int d\xi G\left(\varepsilon_n, \xi + \frac{1}{2} v_F q\right) \times \Gamma(\varepsilon_n, -\varepsilon_n, q) G\left(-\varepsilon_n, \xi - \frac{1}{2} v_F q\right) \right\} + 1 - \alpha_{\text{eff}}. \quad (36)$$

The situation with coefficient B in the general case is much more complicated. Considerable simplifications can be made by confining the analysis to the case of $q = 0$ in the order $|\Delta_q|^4$, as is usually done in actual practice. Then coefficient B can be determined directly from the anomalous Green's function F for which we already have the recurrence procedure (18) and (19). Indeed, let us consider the diagrammatic series for the anomalous Green's function presented in Fig. 7a. It can easily be seen that

$$\lim_{\Delta \rightarrow 0} \frac{F(\varepsilon_n, \mathbf{p})}{\Delta} = G(\varepsilon_n, \mathbf{p}) G(-\varepsilon_n, \mathbf{p}) + \dots = G(\varepsilon_n, \mathbf{p}) G(-\varepsilon_n, \mathbf{p}) \Gamma(\varepsilon_n, -\varepsilon_n, 0), \quad (37)$$

which, by the way, immediately proves relation (28) taking into account Eqs. (19). Consequently, for the

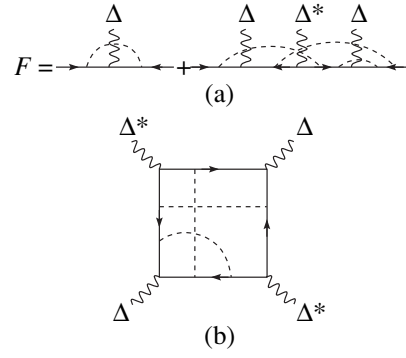


Fig. 7. (a) Diagrammatic series for the anomalous Green's function; dashed curves correspond to AFM fluctuations; (b) diagram defining coefficient K_B .

bipartite loop $\chi(0, 0)$, we have

$$\chi(0, 0) = T \sum_{\mathbf{p}} \sum_{\varepsilon_n} \lim_{\Delta \rightarrow 0} \frac{F(\varepsilon_n, \mathbf{p})}{\Delta} = T \sum_{\mathbf{p}} \sum_{\varepsilon_n} J_0(\Delta = 0). \quad (38)$$

For the “four-tail” diagram in Fig. 7b defining coefficient B , we similarly obtain

$$-T \sum_{\mathbf{p}} \sum_{\varepsilon_n} \lim_{\Delta \rightarrow 0} \frac{F(\varepsilon_n, \mathbf{p})/\Delta - \lim_{\Delta \rightarrow 0} F(\varepsilon_n, \mathbf{p})/\Delta}{|\Delta|^2} = -T \sum_{\mathbf{p}} \sum_{\varepsilon_n} \lim_{\Delta \rightarrow 0} \frac{J_0(\Delta) - J_0(\Delta = 0)}{|\Delta|^2}, \quad (39)$$

where $J_0(\Delta)$ is determined through the recurrence procedure (18). As a result, for the dimensionless coefficient K_B , we have

$$K_B = \alpha_B \frac{8\pi^2 T_c^3}{7\zeta(3)} \times \sum_{-\omega_c}^{\omega_c} d\xi \lim_{\Delta \rightarrow 0} \frac{J_0(\Delta = 0) - J_0(\Delta)}{|\Delta|^2} + 1 - \alpha_B, \quad (40)$$

where

$$\alpha_B = \begin{cases} \tilde{\alpha} & (s\text{-pairing}), \\ \tilde{\alpha} + \frac{4}{3\pi} \sin \pi \tilde{\alpha} + \frac{1}{6\pi} \sin 2\pi \tilde{\alpha} & (d\text{-pairing}). \end{cases} \quad (41)$$

The obtained relations allow us to carry out direct numerical calculations of the coefficients K_A , K_C , and K_B . Figure 8 shows, by way of an example, the calculated dependence of K_C on the pseudogap width W and on the correlation length of AFM fluctuations (parameter $\kappa = v_F \xi^{-1}$). The corresponding dependences for K_A and K_B are qualitatively similar. In particular, for $\kappa = 0$, we just have $K_B = K_C$ [10].

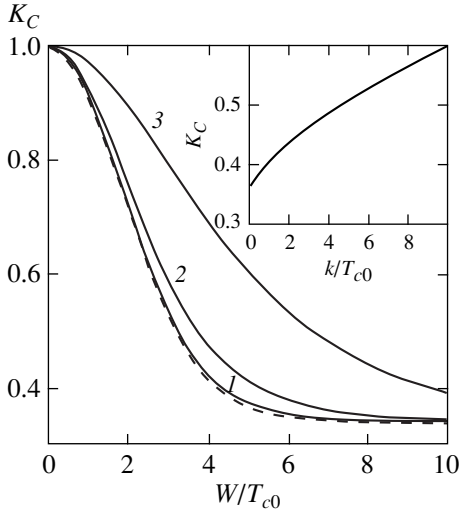


Fig. 8. Dependence of coefficient K_C on the pseudogap width W and the correlation length (parameter $\kappa = v_F \xi^{-1}$) for AFM fluctuations: $\kappa/W = 0.1$ (1), 1.0 (2), and 10.0 (3). The dashed curve corresponds to $\kappa = 0$ [10]. The inset shows the dependence of K_C on κ for $W/T_{c0} = 5$.

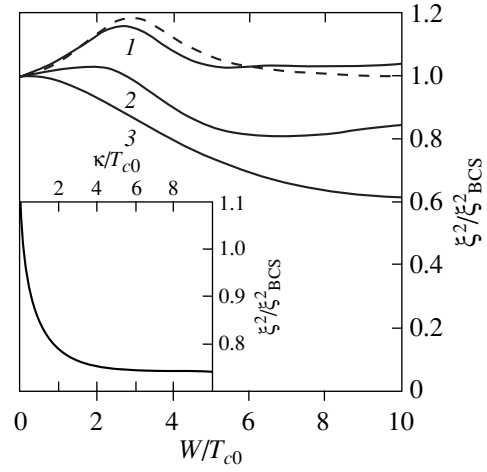


Fig. 9. Dependence of the coherence length on the pseudogap width W and the correlation length (parameter $\kappa = v_F \xi^{-1}$) for AFM fluctuations: $\kappa/W = 0.1$ (1), 1.0 (2), and 10.0 (3). The dashed curve corresponds to $\kappa = 0$ [10]. The inset shows the dependence of the coherence length on κ for $W/T_{c0} = 5$.

7. PHYSICAL PARAMETERS OF SUPERCONDUCTORS WITH A PSEUDOGAP

The Ginzburg–Landau equations define two characteristic lengths for superconductors: the coherence length and the magnetic field penetration depth.

The coherence length $\xi(T)$ at a given temperature determines the characteristic scale of inhomogeneities in the order parameter Δ :

$$\xi^2(T) = -C/A. \tag{42}$$

In the absence of a pseudogap, we have

$$\xi_{BCS}^2(T) = -C_0/A_0, \tag{43}$$

$$\xi_{BCS}(T) \approx 0.74 \xi_0 / \sqrt{1 - T/T_c}, \tag{44}$$

where $\xi_0 = 0.18 v_F / T_c$. In the model under investigation, we can write

$$\xi^2(T) / \xi_{BCS}^2(T) = K_C / K_A. \tag{45}$$

The corresponding dependences of $\xi^2(T) / \xi_{BCS}^2(T)$ on the pseudogap width W and on the correlation length of fluctuations (parameter κ) in the case of d -pairing are presented in Fig. 9. Note that the coherence length varies insignificantly.

For the magnetic field penetration depth in a superconductor without a pseudogap, we have

$$\lambda_{BCS}(T) = \frac{1}{\sqrt{2}} \frac{\lambda_0}{\sqrt{1 - T/T_c}}, \tag{46}$$

where $\lambda_0^2 = mc^2 / 4\pi ne^2$ defines the penetration depth at $T = 0$. In the general case, we have

$$\lambda^2(T) = -\frac{c^2}{32\pi e^2} \frac{B}{AC}. \tag{47}$$

Then, in the model under investigation, we can write

$$\frac{\lambda(T)}{\lambda_{BCS}(T)} = \left(\frac{K_B}{K_A K_C} \right)^{1/2}. \tag{48}$$

The dependences of these quantity in the case of d -pairing are presented graphically in Fig. 10.

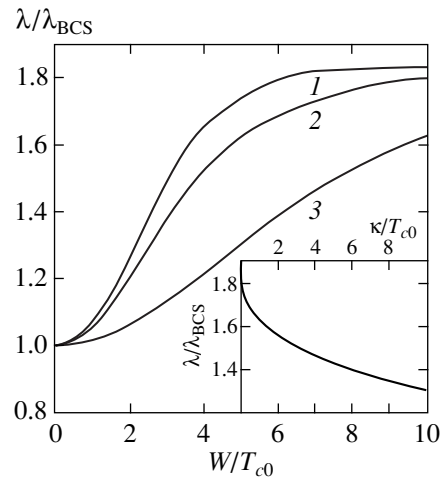


Fig. 10. Dependence of the penetration depth on the pseudogap width W and the correlation length (parameter $\kappa = v_F \xi^{-1}$) for AFM fluctuations: $\kappa/W = 0.1$ (1), 1.0 (2), and 10.0 (3). The inset shows the dependence of the penetration depth on κ for $W/T_{c0} = 5$.

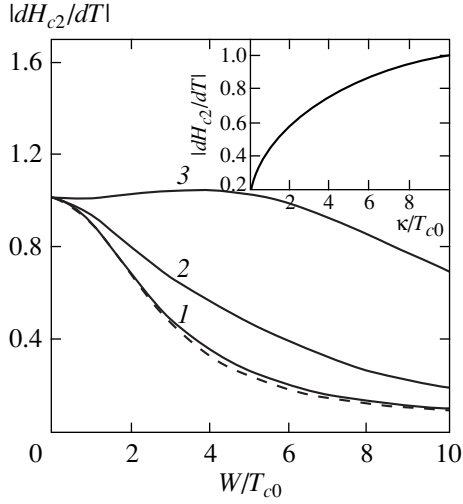


Fig. 11. Dependence of the slope of the upper critical field on the pseudogap width and on the correlation length (parameter $\kappa = v_F \xi^{-1}$) for AFM fluctuations: $\kappa/W = 0.1$ (1), 1.0 (2), and 10.0 (3). The dashed curve corresponds to $\kappa = 0$ [10]. The inset shows the dependence of the slope of H_{c2} on κ for $W/T_{c0} = 5$.

In the vicinity of T_c , the upper critical field H_{c2} can be expressed in terms of the Landau–Ginzburg coefficients:

$$H_{c2} = \frac{\phi_0}{2\pi\xi^2(T)} = -\frac{\phi_0 A}{2\pi C}, \quad (49)$$

where $\phi_0 = c\pi/e$ is the magnetic flux quantum. In this case, the slope of the curve describing the upper critical field in the vicinity of T_c is given by

$$\left| \frac{dH_{c2}}{dT} \right|_{T_c} = \frac{24\pi\phi_0}{7\zeta(3)v_F^2} T_c \frac{K_A}{K_C}. \quad (50)$$

Figure 11 shows graphically the derivative $|dH_{c2}/dT|_{T_c}$ normalized to the derivative at temperature T_{c0} as a function of the effective width W of the pseudogap and the correlation parameter κ in the case of d -pairing. It can be seen that for large correlation lengths, the derivative of the field decreases rapidly with increasing pseudogap width. However, for small correlation lengths, this parameter can slightly increase for small values of the pseudogap width. For a fixed pseudogap width, the function dH_{c2}/dT increases noticeably for a decreasing correlation length of fluctuations.

Finally, let us consider the heat capacity jump at the transition point:

$$\frac{C_s - C_n}{\Omega} = \frac{T_c}{B} \left(\frac{A}{T - T_c} \right)^2, \quad (51)$$

where C_s and C_n are the heat capacities of the superconducting and normal states and Ω is the sample volume.

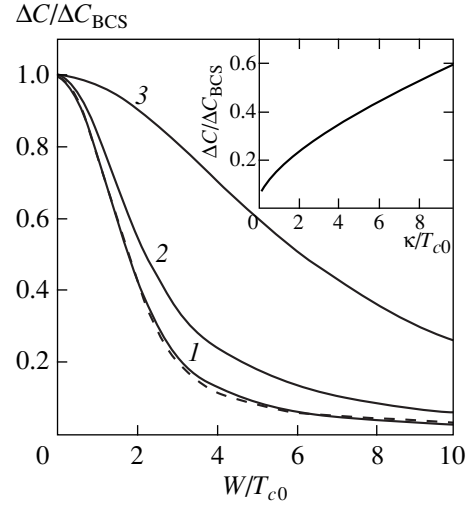


Fig. 12. Dependence of the heat capacity on the pseudogap width and jump on the correlation length (parameter $\kappa = v_F \xi^{-1}$) for AFM fluctuations: $\kappa/W = 0.1$ (1), 1.0 (2), and 10.0 (3). The dashed curve corresponds to $\kappa = 0$ [10]. The inset shows the dependence of the heat capacity jump on κ for $W/T_{c0} = 5$.

At temperature T_{c0} (in the absence of a pseudogap, $W = 0$), we have

$$\left(\frac{C_s - C_n}{\Omega} \right)_{T_{c0}} = N(0) \frac{8\pi^2 T_{c0}}{7\zeta(3)}. \quad (52)$$

The relative jump in the heat capacity in the model under investigation can be written as

$$\frac{(C_s - C_n)_{T_c}}{(C_s - C_n)_{T_{c0}}} = \frac{T_c K_A^2}{T_{c0} K_B}. \quad (53)$$

The corresponding dependences on the effective pseudogap width W and the correlation length parameter κ in the case of d -pairing are presented in Fig. 12. It can be seen that the heat capacity jump decreases rapidly with increasing pseudogap width and, on the contrary, increases upon a decrease in the correlation length of AFM fluctuations.

For superconductors with s -pairing, the dependences of the physical quantities considered above are basically quite similar. The only difference is a larger scale of W for which the corresponding changes take place. This corresponds to a higher stability of isotropic superconductors to a partial dielectrization of the electron spectrum due to the formation of a pseudogap in hot regions on the Fermi surface [10, 11].

From the physical parameters of a superconductor, detailed experimental data have been obtained for heat capacity jump [8]. In complete qualitative agreement with our conclusions, the heat capacity jump for the Bi-2212 system decreases rapidly upon a transition to the range of underdoped compositions for which the pseudogap width increases. According to the results

obtained by Tallon and Loram [8], the pseudogap width (parameter $2W$ in our case) varies from a value of the order of 700 K for the hole concentration $p = 0.05$ to a value of the order of $T_c \sim 100$ K in the vicinity of the optimal concentration $p = 0.16$, vanishing for $p = 0.19$. In this case, a clearly manifested correlation between the decrease in the heat capacity jump and the increase in the effective pseudogap width is observed. Unfortunately, we are not aware of detailed results on the concentration dependence of correlation length of fluctuations and, accordingly, of the corresponding dependences of physical parameters of a superconductor. Qualitatively, the correlation length increases as we go over to the range of underdoped compositions, so that the effect of a decrease in the heat capacity jump is quite justified from this point of view.

8. CONCLUSION

In this work, we continue our study of the peculiarities of the superconducting state on the basis of a rather rough model of the pseudogap state of a two-dimensional electronic system [10, 11], which nevertheless is in qualitative agreement with a number of observed singularities in the electronic structure of underdoped HTSC cuprates. In our earlier publications [10, 11], we considered a nonrealistic limit of an infinitely large correlation length of fluctuations with the short-range antiferromagnetic order, which, however, allowed us to find the exact analytic solution of the problem. Here, we have carried out a generalization to the realistic case of finite correlation lengths, which takes into account all the diagrams of perturbation theory in the interaction of electrons with short-range fluctuations in the same way as in [10, 11]. The analysis was carried out using the standard (mean-field in terms of [11]) approach based on the assumption of the self-averaging of the superconducting order parameter in the fluctuations of the random field induced by AFM fluctuations. It was proved in [11] that this assumption is not substantiated in the limit $\xi \rightarrow \infty$. At the same time, it is undoubtedly valid for $\xi \ll \xi_0$ (where ξ_0 is the coherence length of the superconductor at $T = 0$, i.e., the size of Cooper pairs). Thus, it remains for us to solve the extremely complicated problem of taking into account the non-self-averaging effects for $\xi > \xi_0$. It was mentioned above that in real HTSC systems, ξ is in all probability of the order of ξ_0 so that non-self-averaging effects for the superconducting gap of the type of those considered in [11] can be quite significant. These effects are manifested of the form of “tails” on the temperature dependence of the averaged gap at $T > T_c$ (the pattern of superconducting “drops” [11]).

Another significant simplification in our model is the assumption concerning the static (Gaussian) type of short-range fluctuations. This assumption is justified only in the limit of high temperatures $T \gg \omega_{sf}$ (where ω_{sf} is the characteristic frequency of spin fluctuations)

[6, 7]. For this reason, its application to the superconducting phase for $T < T_c$ is quite dubious. We believe, however, that the simplified analysis carried out above can be used for describing the most significant effects of variation of the electron spectrum (formation of a pseudogap in hot regions on the Fermi surface) on the superconductivity in such a system. If we took into account the dynamics of spin fluctuations, we would inevitably leave the limits of the simple phenomenology of the BCS model and would have to analyze in detail the microscopic aspects of the pairing interaction. Such a program can hardly be realized at present. Moreover, the problem of inclusion of all orders of perturbation theory in AFM fluctuations appears as completely futile on account of the dynamics of the spin subsystem.

ACKNOWLEDGMENTS

This research was partly supported by the Russian Foundation for Basic Research (project no. 99-02-16285) and CRDF (grant no. REC-005) as well as by the State program “Statistical Physics” (project no. 108-11(00-P)) and the State program on HTSC (project no. 96-051).

APPENDIX

Coordinate Representation: Normal and Anomalous Green's Functions

Let us consider some technical aspects of the derivation of the recurrence relation for Gor'kov's equations (12)–(15). We will confine our analysis to two regions on the Fermi surface, which are orthogonal to the p_x axis and coupled through the scattering vector $\mathbf{Q} = (\pm 2p_F, 0)$. In this case, the problem becomes purely one-dimensional since the velocity component $v_y = 0$ and the electron spectrum in the linearized form $\xi_{p_x \mp p_F} = \pm v_F p_x$ is completely independent of the y -component of the momentum. For the sake of brevity, we will henceforth assume that $v_F = 1$.

It is convenient to carry out the calculations in the coordinate representation [21], analyzing the motion of an electron in the field of Gaussian AFM fluctuations $W(x) \neq W^*(x)$ (incommensurate case) with the correlator

$$\langle W^*(x)W(x') \rangle = W^2 e^{-k|x-x'|}. \quad (\text{A.1})$$

In this case, the propagators corresponding to the normal and anomalous Green's functions (10) of the superconductor assume the form

$$G_{00}(x) = \int_{-\infty}^{\infty} \frac{dp_x}{2\pi} e^{ip_x x} G_{00}(p_x)$$

$$= -\frac{i}{2} \left(\frac{\varepsilon_n}{\sqrt{\varepsilon_n^2 + |\Delta|^2}} + \sigma_3 \operatorname{sgn} x \right) \exp(-\sqrt{\varepsilon_n^2 + |\Delta|^2} x), \quad (\text{A.2})$$

$$F_{00}(x) = \int_{-\infty}^{\infty} \frac{dp_x}{2\pi} e^{ip_x x} F_{00}^+(p_z)$$

$$= \frac{\Delta^*}{\sqrt{\varepsilon_n^2 + |\Delta|^2}} \exp(-\sqrt{\varepsilon_n^2 + |\Delta|^2} x),$$

where $\sigma_3 = 1$ for particles moving to the right and $\sigma_3 = -1$ for particles moving to the left. Scattering at fluctuations transforms “right” particles to “left” ones, and vice versa. It can be seen from expressions (A.2) that a particle traversing a distance of length l gives the factor $\exp(-\sqrt{\varepsilon_n^2 + |\Delta|^2} l)$.

For calculating specific diagrams, is it convenient [21] to go over from the integration with respect to coordinates x_k of interaction vertices to the integration over paths l_k traversed by a particle between individual scattering acts by fixing the total displacement $x - x'$. The interaction curve connecting vertices m and n on the electron line in this case corresponds to the factor

$$W^2 |\Delta|^2 \exp(-\kappa |x_m - x_n|)$$

$$= W^2 |\Delta|^2 \exp\left(-\kappa \left| \sum_{k=m}^{n-1} (-1)^k l_k \right| \right). \quad (\text{A.3})$$

The integration over all values of l_k is carried out from 0 to ∞ .

Thus, considering the finiteness of the correlation length of fluctuations leads to the emergence of a certain “damping” of the corresponding transition amplitude in each diagram with increasing distance traversed by an electron. It is very difficult to take into account this effect exactly. In [7], however, we used the obvious inequality

$$\exp\left(-\kappa \left| \sum_{k=m}^{n-1} (-1)^k l_k \right| \right) > \exp\left(-\kappa \sum_{k=m}^{n-1} l_k \right) \quad (\text{A.4})$$

and replaced the exponential in (A.3) by the exponential from the right-hand side of (A.4). This is equivalent to the replacement of the correlator (A.1) of random fields by an analogous expression in which the distance $|x - x'|$ in the exponent is replaced by the total distance traversed by a particle between the scattering acts at points x and x' . Therefore, in accordance with Eq. (A.4), we slightly overestimate the role of the damping factor κ in each diagram of the series in perturbation theory. As a result of such a substitution, the diagrams of all orders can be calculated easily and reproduce exactly ansatz (3) for the normal phase [21]. It was mentioned above that the results obtained in this way, for example,

for the density of states are in good agreement with the results of exact numerical simulation of the problem under investigation [23, 24]. This is an additional argument in favor of the approximation used, extending the qualitative estimates obtained in [7].

We will use the same approximation for analyzing the diagrams in perturbation theory in the superconducting phase, which are constructed on propagators (A.2). In this case, the role of interaction with fluctuations is reduced only to the addition of the factor $e^{-\kappa l_k}$ to each normal or anomalous Green's function (A.2), which is embraced by the given interaction curve or, which is the same, to the addition of κ to $\sqrt{\varepsilon_n^2 + |\Delta|^2}$ in the exponent of each such Green's function. Returning to the momentum representation, we can easily verify that the contribution of any higher-order diagram is determined by the product of the corresponding number of normal and anomalous Green's functions of the form

$$G_{0k}(p) = \frac{i\varepsilon_n \frac{\varepsilon_k}{\sqrt{\varepsilon_n^2 + |\Delta|^2}} + (-1)^k \xi_p}{\varepsilon_k^2 + \xi_p^2}, \quad (\text{A.5})$$

$$F_{0k}^+(p) = \frac{\Delta^* \frac{\varepsilon_k}{\sqrt{\varepsilon_n^2 + |\Delta|^2}}}{\varepsilon_k^2 + \xi_p^2},$$

where $\varepsilon_k = \sqrt{\varepsilon_n^2 + |\Delta|^2} + k\kappa$, k being the number of interaction curves embracing a given Green's function. The factor $(-1)^k$ appears due to the fact that the scattering transforms “right” particles into “left” ones, and vice versa. Introducing the renormalized frequency and gap width in accordance with relations (15), we see that relations (A.5) can be reduced to the standard form (14), which completes the justification of the recurrence procedure (12) and (15).

REFERENCES

1. T. Timusk and B. Statt, Rep. Prog. Phys. **62**, 61 (1999).
2. V. B. Geshkenbein, L. B. Ioffe, and A. I. Larkin, Phys. Rev. B **55**, 3173 (1997).
3. V. Emery, S. A. Kivelson, and O. Zachar, Phys. Rev. B **56**, 6120 (1997).
4. V. P. Gusynin, V. M. Loktev, and S. G. Sharapov, Zh. Éksp. Teor. Fiz. **115**, 1243 (1999) [JETP **88**, 685 (1999)].
5. A. P. Kampf and J. R. Schrieffer, Phys. Rev. B **41**, 6399 (1990); **42**, 7967 (1990).
6. J. Schmalian, D. Pines, and B. Stojkovic, Phys. Rev. Lett. **80**, 3839 (1998); Phys. Rev. B **60**, 667 (1999).
7. É. Z. Kuchinski and M. V. Sadovskii, Zh. Éksp. Teor. Fiz. **115**, 1765 (1999) [JETP **88**, 968 (1999)]; cond-mat/9808321 (1998).

8. J. L. Tallon and J. W. Loram, cond-mat/0005063 (2000); Physica C (Amsterdam) (2000) (in press).
9. V. M. Krasnov, A. Yurgens, D. Winkler, *et al.*, Phys. Rev. Lett. **84**, 5860 (2000); cond-mat/0006479 (2000).
10. A. I. Posazhennikova and M. V. SadoVski , Zh. Éksp. Teor. Fiz. **115**, 632 (1999) [JETP **88**, 347 (1999)]; cond-mat/9806199 (1998).
11. É. Z. Kuchinski and M. V. SadoVski , Zh. Éksp. Teor. Fiz. **117**, 613 (2000) [JETP **90**, 535 (2000)]; cond-mat/9910261 (1999).
12. R. Gatt, S. Christensen, B. Frazer, *et al.*, cond-mat/9906070 (1999).
13. D. L. Feng, W. J. Zheng, K. M. Shen, *et al.*, cond-mat/9908056 (1999).
14. A. Virosztek and J. Ruvalds, Phys. Rev. B **42**, 4064 (1990).
15. J. Ruvalds, C. T. Rieck, S. Tewari, *et al.*, Phys. Rev. B **51**, 3797 (1995).
16. A. T. Zheleznyak, V. M. Yakovenko, and I. E. Dzyaloshinskii, Phys. Rev. B **55**, 3200 (1997).
17. P. Monthoux, A. V. Balatsky, and D. Pines, Phys. Rev. B **46**, 14 803 (1992).
18. P. Monthoux and D. Pines, Phys. Rev. B **47**, 6069 (1993); **49**, 4261 (1994).
19. M. V. SadoVski , Zh. Éksp. Teor. Fiz. **66**, 1720 (1974) [Sov. Phys. JETP **39**, 845 (1974)]; Fiz. Tverd. Tela (Leningrad) **16**, 2504 (1974) [Sov. Phys. Solid State **16**, 1632 (1974)].
20. M. V. SadoVski , Zh. Éksp. Teor. Fiz. **77**, 2070 (1979) [Sov. Phys. JETP **50**, 989 (1979)].
21. O. Tchernyshyov, Phys. Rev. B **59**, 1358 (1999).
22. M. V. SadoVski , cond-mat/9912318 (1999); Physica C (Amsterdam) (2000) (in press).
23. L. Bartosch and P. Kopietz, Phys. Rev. B **60**, 15 488 (1999).
24. A. Millis and H. Monien, Phys. Rev. B **61**, 12 496 (2000).
25. L. P. Gor'kov, Zh. Éksp. Teor. Fiz. **37**, 1407 (1959) [Sov. Phys. JETP **10**, 998 (1960)].
26. P. G. de Gennes, *Superconductivity of Metals and Alloys* (Benjamin, New York, 1966; Mir, Moscow, 1968).
27. M. V. SadoVski , *Superconductivity and Localization* (World Scientific, Singapore, 2000); Phys. Rep. **282**, 225 (1997); Sverkhprovodimost': Fiz., Khim., Tekh. **8**, 337 (1995).
28. A. A. Abrikosov, L. P. Gor'kov, and I. E. Dzyaloshinski , *Methods of Quantum Field Theory in Statistical Physics* (Fizmatgiz, Moscow, 1963; Prentice-Hall, Englewood Cliffs, 1963).
29. M. V. SadoVski and A. A. Timofeev, Sverkhprovodimost': Fiz., Khim., Tekh. **4**, 11 (1991); J. Mosc. Phys. Soc. **1**, 391 (1991).
30. M. V. SadoVski , Pis'ma Zh. Éksp. Teor. Fiz. **69**, 447 (1999) [JETP Lett. **69**, 483 (1999)]; cond-mat/9902192 (1999).

Translated by N. Wadhwa

SOLIDS
Electronic Properties

Superconductivity in the Exactly Solvable Model of Pseudogap State: The Absence of Self-Averaging

É. Z. Kuchinski * and M. V. Sadovski **

*Institute of Electrophysics, Ural Division, Russian Academy of Sciences,
ul. Komsomol'skaya 34, Yekaterinburg, 620016 Russia*

*e-mail: kuchinski@iep.uran.ru

**e-mail: sadovski@iep.uran.ru

Received October 4, 2001

Abstract—The features of the superconducting state are studied in the simple exactly solvable model of the pseudogap state induced by fluctuations of the short-range “dielectric” order in the model of the Fermi surface with “hot” spots. The analysis is carried out for arbitrary short-range correlation lengths ξ_{corr} . It is shown that the superconducting gap averaged over such fluctuations differs from zero in a wide temperature range above the temperature T_c of the uniform superconducting transition in the entire sample, which is a consequence of non-self-averaging of the superconducting order parameter over the random fluctuation field. In the temperature range $T > T_c$, superconductivity apparently exists in individual regions (drops). These effects become weaker with decreasing correlation length ξ_{corr} ; in particular, the range of existence for drops becomes narrower and vanishes as $\xi_{\text{corr}} \rightarrow 0$, but for finite values of ξ_{corr} , complete self-averaging does not take place. © 2002 MAIK “Nauka/Interperiodica”.

1. INTRODUCTION

Among a large number of anomalies in the electronic properties observed in high-temperature superconductors (HTSC) based on copper oxides, the so-called pseudogap state [1, 2] existing in a broad region of their phase diagram has become an object of intense studies in recent years. There are two main trends in constructing the models of the pseudogap state of high- T_c superconductors. One of these trends is based on the popular model of formation of Cooper pairs above the superconducting transition temperature [3]. In the other trend, it is assumed that the pseudogap state is associated with fluctuations of the antiferromagnetic short-range order or with other similar fluctuations of the “dielectric” origin (e.g., fluctuations of charge density waves [2]).

In our opinion [2], the preferable scenario of the formation of the pseudogap state in HTSC is the pattern based on the existence (in the corresponding region of the phase diagram) of strong scattering of charge carriers from developed short-range fluctuations of the dielectric type (antiferromagnetic or charge density waves). This scattering leads to a considerable non-Fermi liquid rearrangement of the electron spectrum in certain regions of the momentum space in the vicinity of the Fermi surface around the so-called hot spots or near hot (flat) regions on this surface [2]. The preference of the dielectric and not superconducting scenario of the formation of a pseudogap [3] is confirmed by a series of experiments which are discussed, for example, in the review [2]. In the present work, we naturally

adhere to the same point of view. It should be emphasized, however, that the origin of the pseudogap state in HTSC remains unclear and can be determined only as a result of further experimental investigations.

Most of the available theoretical publications are devoted to an analysis of the effect of the pseudogap on the properties of a system in the normal state, and only an insignificant number of such publications deal with the features of superconductivity in this state [4–6]. For example, superconductivity in a simple exactly solvable model of the pseudogap state, which is based on the model of the Fermi surface of a 2D system with hot spots [4], was considered by us in [5]. In this work, we used the exact solution for the pseudogap, which was obtained earlier [7] for the one-dimensional case, in the limit of very large correlation lengths of dielectric short-range fluctuations. It was proved that the superconducting gap averaged over short-range fluctuations generally differs from zero in the temperature range exceeding the mean-field superconducting transition temperature T_c corresponding, according to [5], to the emergence of a homogeneous superconducting state in the entire sample. It was hence concluded in [5] that, in the temperature range $T > T_c$, superconducting drops are formed in the system and exist down to the superconducting transition temperature T_{c0} in the absence of a dielectric pseudogap. This effect was attributed in [5] to the absence of self-averaging in the superconducting order parameter (gap) under the conditions when the correlation length of short-range fluctuations exceeds the coherence length (the size of Cooper pairs) in the theory of superconductivity.

The effects of finiteness of the correlation length of short-range fluctuations was taken into account in [6] under the assumption of self-averaging of the superconducting gap over such fluctuations. In this publication, the effect of the pseudogap on T_c was analyzed, the behavior of the gap in the region $T < T_c$ was considered, and the microscopic derivation of the Ginzburg–Landau expansion was carried out for $T \sim T_c$. We used the approach based on the almost exact solution of the general model of the pseudogap state with Gaussian short-range fluctuations, which was proposed in [8, 9] for the 1D case and generalized for the 2D problem in [10, 11]. In this approach, it is difficult to go beyond the scope of the assumption concerning the self-averaging of the superconducting gap. It should be noted that the presence or absence of such a self-averaging has been studied insufficiently. In most cases, self-averaging is just assumed from physical considerations with a reference to essentially different scales of lengths over which the superconducting order parameter (coherence length ξ_0) and the basic parameters of the electron subsystem (atomic spacing or the reciprocal Fermi momentum in the impurity problem [12–14] or the short-range correlation length ξ_{corr} in the pseudogap model under investigation [2, 5, 6]) change noticeably. In particular, in our model of pseudogap, we should expect complete self-averaging of the superconducting gap for $\xi_{\text{corr}} \ll \xi_0$ [2, 6]. We are not aware of publications in which the problem of self-averaging of the gap is investigated in an exactly solvable model of disorder.

The present work mainly aims precisely at such an investigation in the framework of a very simple (although, perhaps, not very realistic) 1D model of the pseudogap state induced by dielectric short-range fluctuations with a finite correlation length, which was proposed in a recent publication by Bartosch and Kopietz [15]. The exact solution proposed in this work and close essentially to the models considered earlier [7–9] makes it possible to carry out a sufficiently comprehensive analysis of the self-averaging problem under investigation in the 2D model of hot spots [4, 6, 11]. In addition, we will analyze the temperature dependences of the superconducting gap in a superconductor with a dielectric pseudogap.

2. SIMPLIFIED MODEL OF THE PSEUDOGAP STATE

Let us consider the exactly solvable model of the pseudogap state, proposed in [15], using a slightly different approach. We assume that an electron performs a one-dimensional motion in a periodic field of the form

$$V(x) = 2D \cos(Qx + \phi). \quad (1)$$

We choose $Q = 2p_F - k$, where p_F is the Fermi momentum and $k \ll p_F$ is a certain detuning from the preferred

scattering vector $2p_F$.¹ We choose the electron spectrum in the following conventional form linearized near the Fermi level:

$$\begin{aligned} \xi_1 &\equiv \xi_p = v_F(|p| - p_F), \\ \xi_{p-2p_F} &= -\xi_p \quad (\text{nesting}), \\ \xi_2 &\equiv \xi_{p-Q} = -\xi_p - v_F k \equiv -\xi_p - \eta, \end{aligned} \quad (2)$$

where we have introduced the variable $\eta = v_F k$ (v_F is the Fermi velocity), which will be widely used in the subsequent analysis. Field (1) can be written in the form

$$\begin{aligned} V(x) &= D \exp(i2p_F x - ikx) \\ &+ D^* \exp(-i2p_F x + ikx), \end{aligned} \quad (3)$$

where the complex amplitude has been introduced as a result of the substitution $D \rightarrow D e^{i\phi}$.

Such a problem can be solved in an elementary way. In the two-wave approximation of the conventional band theory, the one-electron (normal) Green's function corresponding to the (diagonal) transition $p \rightarrow p$ in the Matzubara representation has the form

$$\begin{aligned} g_{11}(i\varepsilon_n p p) &= \frac{1}{i\varepsilon_n - \xi_1} + \frac{1}{i\varepsilon_n - \xi_1} \\ &\times D^* \frac{1}{i\varepsilon_n - \xi_2} D \frac{1}{i\varepsilon_n - \xi_1} + \dots \\ &= \frac{i_{\xi_n - \xi_2}}{(i\varepsilon_n - \xi_1)(i\varepsilon_n - \xi_2) - |D|^2} \\ &= \frac{i\varepsilon + \xi + \eta}{(i\varepsilon - \xi)(i\varepsilon + \xi + \eta) - |D|^2}, \end{aligned} \quad (4)$$

where we have introduced in the last equality the notation $\xi_p = \xi$ and $\varepsilon_n = \varepsilon$, which will be widely used below to simplify the form of the equations. We can also introduce the nondiagonal (anomalous) Green's function corresponding to the Umklapp process $p \rightarrow p - Q$:

$$\begin{aligned} g_{12}(i\varepsilon_n p p - Q) &= \frac{1}{i\varepsilon_n - \xi_1} D^* \frac{1}{i\varepsilon_n - \xi_2} + \dots \\ &= \frac{D^*}{(i\varepsilon_n - \xi_1)(i\varepsilon_n - \xi_2) - |D|^2} \\ &= \frac{D^*}{(i\varepsilon - \xi)(i\varepsilon + \xi + \eta) - |D|^2}. \end{aligned} \quad (5)$$

Let us now suppose that field (1) is random. Following [15], we consider a rather specific model of disorder, in which the detuning vector k is regarded as a ran-

¹ Such a choice of the vector for the antiferromagnetic superstructure or for a structure of the of charge density wave type implies incommensurate ordering and corresponding fluctuations.

dom quantity and its distribution function is written in the form of the Lorentzian²:

$$\mathcal{P}_k(k) = \frac{1}{\pi} \frac{\kappa}{k^2 + \kappa^2}, \quad (6)$$

where $\kappa \equiv \xi_{\text{corr}}^{-1}$ and ξ_{corr} is the short-range correlation length. Phase ϕ in expression (1) is also regarded as a random quantity distributed uniformly on the interval from 0 to 2π :

$$\mathcal{P}_\phi(\phi) = \begin{cases} \frac{1}{2\pi} & \text{for } 0 \leq \phi \leq 2\pi, \\ 0, & \text{for remaining values.} \end{cases} \quad (7)$$

The field correlation function $V(x)$ at various points can be calculated elementary and is given by

$$\langle V(x)V(x') \rangle = 2D^2 \cos[2p_F(x-x')] \times \exp[-\kappa|x-x'|], \quad (8)$$

where the angle brackets denote averaging over distributions (6) and (7). The random field with precisely this correlation function was considered in the well-known publication [16] as well as in [7–9], where it was assumed that the field is of the Gaussian type.³ The random field $V(x)$ considered here is not Gaussian in the general case [15]. The Fourier transform (8) has the form of a typical Lorentzian defining the effective interaction of an electron with short-range fluctuations [2]:

$$V_{\text{eff}}(q) = 2D^2 \times \left\{ \frac{\kappa}{(q-2p_F)^2 + \kappa^2} + \frac{\kappa}{(q+2p_F)^2 + \kappa^2} \right\}. \quad (9)$$

It is an interaction of this type that was considered in all publications on the “dielectric” pseudogap cited above.

Green’s functions averaged over an ensemble of random fields of type (1) with distributions (6) and (7) are calculated by elementary integration. The mean value of the anomalous Green’s function (5) is just equal to zero (after averaging over distribution (7)), which corresponds to the absence of a long-range dielectric order. The averaged Green’s function (4) can easily be obtained by term-by-term integration of series (4) with respect to (6) and is given by

$$\begin{aligned} G(i\varepsilon_n p) &= \frac{1}{i\varepsilon_n - \xi_p} + \frac{1}{i\varepsilon_n - \xi_p} \\ &\times D^* \frac{1}{i\varepsilon_n + \xi_p + i v_F \kappa} D \frac{1}{i\varepsilon_n - \xi_p} \\ &+ \frac{1}{i\varepsilon_n - \xi_p} D^* \frac{1}{i\varepsilon_n + \xi_p + i v_F \kappa} D \frac{1}{i\varepsilon_n - \xi_p} \\ &\times D^* \frac{1}{i\varepsilon_n + \xi_p + i v_F \kappa} D \frac{1}{i\varepsilon_n - \xi_p} + \dots \\ &= \frac{i\varepsilon_n + \xi_p + i v_F \kappa}{(i\varepsilon_n - \xi_p)(i\varepsilon_n + \xi_p + i v_F \kappa) - |D|^2}. \end{aligned} \quad (10)$$

This is the exact solution for the Green’s function that was proposed in [15].

In the subsequent analysis, we can assume that not only the phase of field (1) fluctuates, but also its amplitude D , and the corresponding Green’s function can be obtained by simple averaging of expression (10) with the corresponding distribution $\mathcal{P}_D(D)$. In particular, the amplitude distribution can be chosen in the form of the Rayleigh distribution [7, 8, 15]:

$$\mathcal{P}_D(D) = \frac{2D}{W^2} \exp\left(-\frac{D^2}{W^2}\right). \quad (11)$$

Averaging of correlators (8) and (9) in this case leads to the simple substitution $D \rightarrow W$. The average electron Green’s function now assumes the form

$$\begin{aligned} G(i\varepsilon_n p) &= \int_0^\infty dD \mathcal{P}_D(D) \\ &\times \frac{i\varepsilon_n + \xi_p + i v_F \kappa}{(i\varepsilon_n - \xi_p)(i\varepsilon_n + \xi_p + i v_F \kappa) - |D|^2} \\ &= \int_0^\infty d\zeta e^{-\zeta} \frac{i\varepsilon_n + \xi_p + i v_F \kappa}{(i\varepsilon_n - \xi_p)(i\varepsilon_n + \xi_p + i v_F \kappa) - \zeta W^2}, \end{aligned} \quad (12)$$

where W determines the energy width of the pseudogap. In the limit of large correlation lengths of fluctuations of field (1), i.e., for $\xi_{\text{corr}} \rightarrow \infty$ ($\kappa \rightarrow 0$), solution (12) coincides with that obtained in [7] for a Gaussian random field. For finite values of κ , it coincides with the solution proposed in [11] in the formal analysis of the accuracy of approximations used in [8, 9], where the general problem of an electron in a Gaussian random field with a paired correlator of type (8) was considered. In [11, 15], it was proved that the density of states corresponding to Green’s function (12) possesses a characteristic blurred pseudogap in the vicinity of the Fermi level, the values of the density of states being quite close quantitatively [11, 15, 17] (virtually for all energy values in the incommensurate case) to the values obtained in [8] as well as to the results of

² In fact, we are speaking here of a specific model of phase fluctuations of field (1).

³ For a Gaussian field, all higher order correlators of field $V(x)$ are factorized, according to Wick, through paired correlators (8).

exact numerical simulation of the problem with a Gaussian random field which was carried out in [18–20].⁴

If field (1) is created by fluctuations of a certain dielectric order parameter (e.g., antiferromagnetic order parameter or that of charge density waves), distribution (11) may correspond to its Gaussian fluctuations in the range of fairly high temperatures [10, 11]. As the temperature decreases below a certain characteristic value, the amplitude fluctuations become “frozen out” even before the emergence of the corresponding long-range order in the system (cf. [3, 21]) and we can simply set $D = W$, while the phase fluctuations are present down to very low temperatures. For this reason, we will use a solution of type (10), leading to a clearly manifested pseudogap for large correlation lengths ξ_{corr} [16], assuming the low-temperature mode of short-range fluctuations. Since we do not consider the microscopic aspects of dielectric fluctuations, all the parameters characterizing such fluctuations (like the correlation length $\xi_{\text{corr}} = \kappa^{-1}$ and amplitudes D and W , viz., the energy width of the pseudogap) are treated here as phenomenological parameters. The low- or high-temperature mode of short-range fluctuations can be realized in a similar way at temperatures differing, for example, from the superconducting transition temperature.

A generalization to the case of a 2D electron system typical of HTSC cuprates can be carried out on the basis of the model of hot spots on the Fermi surface which was considered in [4–6]. In this case, it is assumed that two independent systems of fluctuations of type⁵ (1), which are oriented along the orthogonal axes x and y and which interact only with electrons from flat regions of the 2D Fermi surface, are orthogonal to these axes. We assume that the 2D potential in which an electron is moving is factorized in these directions: $V(x, y) = V(x)V(y)$ [4–6]. The size of flat (hot) regions is defined by parameter α , the angular size of a flat region viewed from the center of the Brillouin zone being equal to 2α [2, 4–6]. In particular, the value of $\alpha = \pi/4$ corresponds to a square Fermi surface (complete nesting), when the entire Fermi surface is hot. For $\alpha < \pi/4$, the Fermi surface contains cold regions on which the scattering from fluctuations of the dielectric order parameter is assumed to be absent and the electrons are treated as free. In this model, various characteristics defined by the integrals over the Fermi surface consist of additive contributions from hot and cold regions. The pseudogap rearrangement of the electron spectrum takes place only in the hot regions (and in

their vicinity), while the Fermi liquid behavior is preserved in the cold regions [2].

This pattern is in qualitative agreement with the results of numerous ARPES experiments on underdoped HTSC cuprates [1, 2], which indicate that pseudogap anomalies appear in the vicinity of point $(0, \pi)$ in the Brillouin zone and vanish as we pass to its diagonal. The presence of flat regions on the Fermi surface for HTSC cuprates was also reliably observed in ARPES experiments made by several independent groups [2].

3. GOR'KOV EQUATIONS AND THEIR SOLUTION FOR THE PSEUDOGAP STATE

An analysis of superconductivity in a system with a pseudogap induced by short-range fluctuations of the dielectric type will be carried out under the simplest assumption concerning the existence of a pairing interaction of the BCS type, characterized by the attraction constant V , which, as usual, is assumed to have a non-zero value in a certain layer of width $2\omega_c$ in the vicinity of the Fermi level (ω_c is the characteristic frequency of quanta ensuring the attraction between electrons). The same approach was used by us in [4–6]. In the present work, we confine our analysis to the s -type pairing only. There are no principal difficulties for analyzing the d pairing typical of HTSC cuprates, but the presence of the angular dependence (anisotropy) of the superconducting gap in this case necessitates [4, 5] additional integration, which considerably increases the computing time. At the same time, it was proved in [4–6] that the effect of the pseudogap on superconductivity is virtually the same in the s and d cases, the only difference being in fact in the scales of the parameters leading to the corresponding changes in the main characteristics of the superconducting state (d pairing is less stable to the dielectrization of the electron spectrum than the s pairing).

Superconductivity in cold regions of the Fermi surface is described by the standard equations of the BCS theory. For this reason, we concentrate our attention on the derivation of the Gor'kov equations in the 1D model, which is equivalent to an analysis of hot regions in the 2D case [5, 6]. In fact, Green's functions (4), (5) for a 1D system in the periodic field (1) form the matrix

$$\begin{aligned} g_{11} &= \frac{i\varepsilon_n - \xi_2}{(i\varepsilon_n - \xi_1)(i\varepsilon_n - \xi_2) - |D|^2}, \\ g_{12} &= \frac{D^*}{(i\varepsilon_n - \xi_1)(i\varepsilon_n - \xi_2) - |D|^2}, \\ g_{21} &= \frac{D}{(i\varepsilon_n - \xi_1)(i\varepsilon_n - \xi_2) - |D|^2}, \\ g_{22} &= \frac{i\varepsilon_n - \xi_1}{(i\varepsilon_n - \xi_1)(i\varepsilon_n - \xi_2) - |D|^2}. \end{aligned} \quad (13)$$

⁴ Using the method developed in [7], it is also possible to calculate exactly the two-particle Green's function and the corresponding frequency dependences of conductivity [15] in the model under investigation. Unfortunately, the specific form of the disorder being considered leads to a nonphysical behavior at zero frequency, which corresponds to an ideal conductor.

⁵ It should be noted that this pattern is roughly similar to the concept of phase separation in HTSC cuprates (stripes) [22] if we treat the correlation length ξ_{corr} as a characteristic size (period) of stripe regions [2].

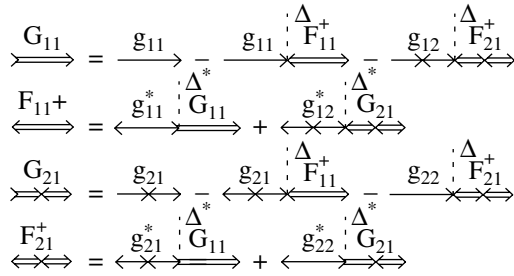


Fig. 1. Gor'kov equations in a 1D periodic field.

In the presence of Cooper pairing, the Gor'kov equations constructed on Green's functions of type (13) can be depicted by the graphs shown in Fig. 1. In analytic form, this system of equations can be written as

$$\begin{aligned} G_{11} &= g_{11} - g_{11} \Delta F_{11}^+ - g_{12} \Delta F_{21}^+, \\ F_{11}^+ &= g_{11}^* \Delta^* G_{11} + g_{12}^* \Delta^* G_{21}, \\ G_{21} &= g_{21} - g_{21} \Delta F_{11}^+ - g_{22} \Delta F_{21}^+, \\ F_{21}^+ &= g_{21}^* \Delta^* G_{11} + g_{22}^* \Delta^* G_{21}, \end{aligned} \tag{14}$$

where the superconducting gap is determined, as usual, from the relation

$$\begin{aligned} \Delta^* &= VT \sum_{n,p} F_{11}^+(\epsilon_n p) \\ &= \lambda T \sum_n \int_{-\infty}^{\infty} d\xi_p F_{11}^+(\epsilon_n \xi_p) \equiv \lambda T \sum_n \overline{F_{11}^+(\epsilon_n)}. \end{aligned} \tag{15}$$

Here, $\lambda = N_0(0)V$ is the dimensionless constant of pairing interaction, and $N_0(0)$ is the density of states of free electrons at the Fermi level.

The solution of the system of equations (14) gives

$$\begin{aligned} G_{11} &= -\frac{1}{\text{Det}} [(i\epsilon + \xi_1)(\epsilon^2 + \xi_2^2 + D^2 + \Delta) \\ &\quad - D^2(\xi_1 + \xi_2)] = -\frac{1}{\text{Det}} \{ (i\epsilon + \xi) [\epsilon^2 + (\xi + \eta)^2 \\ &\quad + D^2 + \Delta^2] + D^2 \eta \}, \\ F_{11}^+ &= -\frac{1}{\text{Det}} \Delta^* (\epsilon^2 + \xi_2^2 + D^2 + \Delta^2) \\ &= -\frac{1}{\text{Det}} \Delta^* [\epsilon^2 + (\xi + \eta)^2 + D^2 + \Delta^2], \end{aligned} \tag{16}$$

where

$$\begin{aligned} \text{Det} &= (\epsilon^2 + \xi_1^2 + D^2 + \Delta^2)(\epsilon^2 + \xi_2^2 + D^2 + \Delta^2) \\ &\quad - (\xi_1 + \xi_2)^2 D^2 = (\epsilon^2 + \xi^2 + D^2 + \Delta^2) \\ &\quad \times (\epsilon^2 + (\xi + \eta)^2 + D^2 + \Delta^2) - \eta^2 D^2, \end{aligned} \tag{17}$$

and D is the real amplitude of the fluctuation field (1). In accordance with relation (15), the Gor'kov Green's function F_{11}^+ determines the energy gap of the superconductor. Taking into account the random nature of the field of dielectric fluctuations, Eq. (15) must be averaged over the fluctuations of phase $\eta = v_F k$ and amplitude D using distributions (6) and (11) (for the high-temperature fluctuation mode).

The cumbersome but direct calculations of the integral in Eq. (15) by the residue method give

$$\begin{aligned} \overline{F_{11}^+(\epsilon)} &= \frac{\pi \Delta^*}{\sqrt{2}} \\ &\times \left\{ \sqrt{\left(\tilde{\epsilon}^2 + D^2 + \frac{\eta^2}{4} \right)^2 - \eta^2 D^2} + \tilde{\epsilon}^2 + D^2 - \frac{\eta^2}{4} \right\}^{-1/2} \\ &\times \left\{ 1 + \frac{\tilde{\epsilon}^2 + D^2 + \frac{\eta^2}{4}}{\sqrt{\left(\tilde{\epsilon}^2 + D^2 + \frac{\eta^2}{4} \right)^2 - \eta^2 D^2}} \right\} \\ &\equiv \pi \Delta^* \overline{\mathcal{F}}(\epsilon, \Delta, \eta, D), \end{aligned} \tag{18}$$

where

$$\tilde{\epsilon} = \sqrt{\epsilon^2 + \Delta^2}. \tag{19}$$

Using now Eq. (15), we immediately obtain the following equation for the superconducting gap in the 2D model of hot regions [4–6]:

$$1 = 2\pi\lambda T \sum_{n=0}^{\left[\frac{\omega_c}{2\pi T} \right]} \left\{ \tilde{\alpha} \overline{\mathcal{F}}(\epsilon, \Delta, \eta, D) + \frac{1 - \tilde{\alpha}}{\tilde{\epsilon}} \right\}, \tag{20}$$

where $\tilde{\alpha} = (4/\pi)\alpha$ is the relative fraction of hot regions on the Fermi surface. The second term in Eq. (20) gives the standard BCS contribution from cold regions constituting the fraction $(1 - \tilde{\alpha})$ on the Fermi surface. Summation over n in Eq. (20) is carried out up to the maximum value determined by the integral part of the ratio $\omega_c/2\pi T$.

Using Eq. (20) and numerical calculations, we can find the gap width $\Delta(\eta, D)$ for fixed values of η and D (i.e., for the given value of the random field of fluctuations (1)) for any temperature. Then, by averaging over distributions (6) and (11), we can find the temperature dependences of the averaged gap. In particular, for the low-temperature mode of dielectric fluctuations, it is

sufficient to carry out averaging over phase η only; the superconducting gap in this case is given by

$$\langle \Delta \rangle = \frac{1}{\pi} \int_{-\infty}^{\infty} d\eta \frac{v_F \kappa}{\eta^2 + v_F^2 \kappa^2} \Delta(\eta, D). \quad (21)$$

In the high-temperature approximation, averaging over amplitude D with distribution (11) must also be carried out:

$$\begin{aligned} \langle \Delta \rangle &= \frac{2}{W^2} \int_0^{\infty} dD D \exp\left(-\frac{D^2}{W^2}\right) \frac{1}{\pi} \\ &\times \int_{-\infty}^{\infty} d\eta \frac{v_F \kappa}{\eta^2 + v_F^2 \kappa^2} \Delta(\eta, D). \end{aligned} \quad (22)$$

As a result, we obtain the temperature dependences of the averaged superconducting gap $\langle \Delta \rangle$ without resorting to any statistical assumptions like that concerning the self-averaging of the order parameter. Similarly, we can

also calculate the temperature dependences of variance $\langle \Delta^2 \rangle - \langle \Delta \rangle^2$, from which we can judge the extent of randomness of Δ , i.e., on the presence or absence of self-averaging. The results of corresponding calculations will be discussed in the next section.

It was noted in the Introduction that, in most publications on superconductivity in disordered systems, an analysis is carried out under the assumption of self-averaging of the superconducting gap Δ . In this case, Δ is in fact regarded as a nonrandom quantity independent of the random characteristics of the field in which the electrons forming Cooper pairs propagate. In our case, these are the amplitude D and the phase η of field (1); accordingly, the self-averaging over these parameters can be analyzed separately.

Let Δ be a parameter self-averaging over fluctuations of η . In this case, we can assume that Δ in Eq. (16) is independent of η . Accordingly, the anomalous Gor'kov function averaged over fluctuations of η has the form

$$\langle F_{11}^+ \rangle = \frac{\Delta^*}{\pi} \int_{-\infty}^{\infty} d\eta \frac{v_F \kappa}{\eta^2 + v_F^2 \kappa^2} \frac{\varepsilon^2 + (\xi + \eta)^2 + D^2 + \Delta^2}{(\varepsilon^2 + \xi^2 + D^2 + \Delta^2)(\varepsilon^2 + (\xi + \eta)^2 + D^2 + \Delta^2) - \eta^2 D^2}. \quad (23)$$

This integral can be evaluated directly; after cumbersome calculations, we obtain

$$\begin{aligned} \langle F_{11}^+ \rangle &= \Delta^* \\ &\times \frac{\tilde{\varepsilon}^2 (1 + v_F \kappa / \tilde{\varepsilon})^2 + D^2 (1 + v_F \kappa / \tilde{\varepsilon}) + \xi^2}{[(1 + v_F \kappa / \tilde{\varepsilon}) \tilde{\varepsilon}^2 + \xi^2 + D^2]^2 + v_F^2 \kappa^2 \xi^2}. \end{aligned} \quad (24)$$

Accordingly, we can also evaluate the integral of expression (24) appearing in the equation for the pseudogap:

$$\overline{\langle F_{11}^+ \rangle} \equiv \int_{-\infty}^{\infty} d\xi \langle F_{11}^+ \rangle = \frac{\pi \Delta^* (1 + v_F \kappa / 2\tilde{\varepsilon})}{\sqrt{D^2 + \tilde{\varepsilon}^2 (1 + v_F \kappa / 2\tilde{\varepsilon})^2}}. \quad (25)$$

Thus, in spite of the cumbersome form of the anomalous Green's function (24), the inclusion of interaction with fluctuations in hot (flat) regions on the Fermi surface in the equation for the gap can be reduced to the standard renormalization,

$$\begin{aligned} \varepsilon &\longrightarrow \varepsilon \left(1 + \frac{v_F \kappa}{2\tilde{\varepsilon}}\right) = \varepsilon \left(1 + \frac{v_F \kappa}{2\sqrt{\varepsilon^2 + \Delta^2}}\right), \\ \Delta &\longrightarrow \Delta \left(1 + \frac{v_F \kappa}{2\tilde{\varepsilon}}\right) = \Delta \left(1 + \frac{v_F \kappa}{2\sqrt{\varepsilon^2 + \Delta^2}}\right), \end{aligned} \quad (26)$$

similar to that emerging in the problem taking into account the effect of impurities on superconductivity

[23] and already encountered in the context of the problem under investigation in [6]. The analogy with the impurity problem is almost complete since the quantity $v_F \kappa = v_F \xi_{\text{corr}}^{-1}$ is the characteristic reciprocal time of electron flight through a short-range region with a length on the order of ξ_{corr} . Naturally, the effect of the pseudogap is also associated with the emergence of the square of the dielectric gap D^2 in Eqs. (24) and (25).

Ultimately, the equation for the superconducting gap in the model of hot spots under the assumption of self-averaging over phase fluctuations assumes the form

$$1 = 2\pi\lambda T$$

$$\times \sum_{n=0}^{\left[\frac{\omega_c}{2\pi T}\right]} \left\{ \tilde{\alpha} \frac{1 + v_F \kappa / 2\tilde{\varepsilon}}{\sqrt{D^2 + \tilde{\varepsilon}^2 (1 + v_F \kappa / 2\tilde{\varepsilon})^2}} + \frac{1 - \tilde{\alpha}}{\tilde{\varepsilon}} \right\}. \quad (27)$$

This equation can obviously be solved more easily than Eq. (20) with subsequent averaging (21). In the absence of fluctuations of the dielectric field amplitude D , which is the case in the low-temperature region of short-range fluctuations, it is precisely Eq. (27) that determines the mean-field (in terms of [5]) behavior of $\Delta(T)$ relative to fluctuations of the random field (1).

In the high-temperature region of short-range fluctuations with distribution (11) for D , under the assumption of self-averaging over the fluctuations of D also,

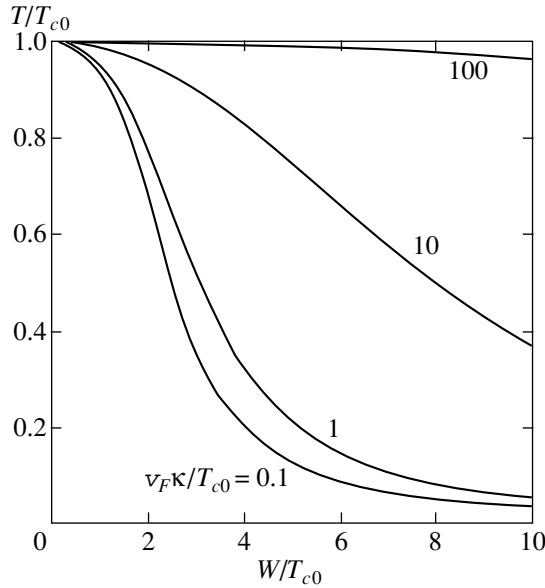


Fig. 2. Superconducting transition temperature in the low-temperature region of dielectric fluctuations as a function of the pseudogap width W for various values of the correlation length $v_F\kappa/T_{c0}$ of dielectric fluctuations.

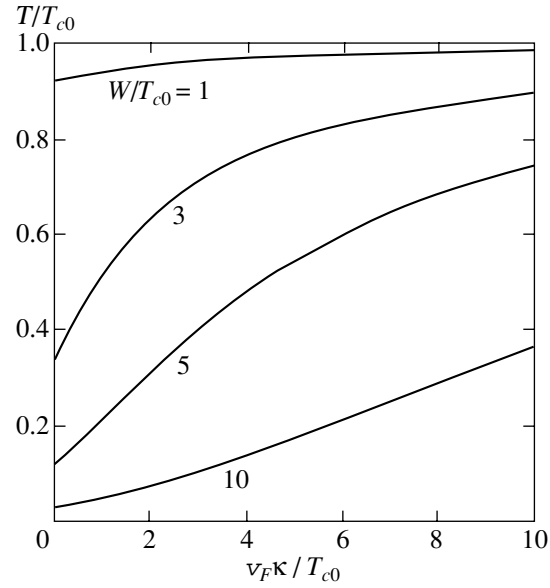


Fig. 3. Superconducting transition temperature in the low-temperature region of dielectric fluctuations as a function of the correlation length of these fluctuations for various values of the pseudogap width W/T_{c0} .

we obtain the following equation for the averaged superconducting gap:

$$1 = 2\pi\lambda T \sum_{n=0}^{\lfloor \frac{\omega_c}{2\pi T} \rfloor} \left\{ \frac{2\tilde{\alpha}}{W^2} \int_0^\infty dD D \exp\left(-\frac{D^2}{W^2}\right) \times \frac{1 + v_F\kappa/2\tilde{\epsilon}}{\sqrt{D^2 + \tilde{\epsilon}^2(1 + v_F\kappa/2\tilde{\epsilon})^2}} + \frac{1 - \tilde{\alpha}}{\tilde{\epsilon}} \right\}. \tag{28}$$

This equation describes a situation similar to that considered in detail in our earlier publication [6], where we included the effect produced on superconductivity by Gaussian dielectric short-range fluctuations using the approach proposed in [8, 9]. In this case, fluctuations of field (1) are taken into account exactly, but it is assumed that Δ is self-averaging. It will be demonstrated below that all the results following from Eq. (28) are quite close to those obtained in [6]. As $\kappa \rightarrow 0$ ($\xi_{\text{corr}} \rightarrow \infty$), Eq. (28) is transformed into a similar mean-field equation derived in [5]. The superconducting transition temperature obtained from Eq. (27) or (28) can apparently be identified with the temperature at which an infinitely narrow gap (superconductivity) emerges uniformly in the entire sample [5].

In the next section, we will consider the results of numerical solution of Eqs. (27) and (28) in comparison with the results of exact analysis based on Eqs. (20)–(22).

4. BASIC RESULTS AND DISCUSSION

Let us now consider the results of a numerical analysis of the equations given in the previous section.⁶

Figures 2 and 3 show the superconducting transition temperature T_c in the low-temperature range of dielectric fluctuations (the temperature at which the mean-field gap defined by Eq. (27) vanishes) as a function of the pseudogap width W (which coincides in the present case with the dielectric gap amplitude D) and of the correlation length, respectively. The results are in qualitative agreement with the corresponding results for the high-temperature range of dielectric fluctuations (where T_c is defined by Eq. (28)) as well as with the results obtained by us earlier [6] in a somewhat different model of short-range dielectric fluctuations with a finite correlation length. Upon an increase in the pseudogap width W , the mean-field temperature T_c is suppressed. A decrease in the correlation length blurs the pseudogap [2, 8, 15] and, accordingly, diminishes the suppression of T_c .

Solid curves in Fig. 4 present the temperature dependences of the superconducting gap $\langle \Delta \rangle$ averaged over both amplitude D and phase η (the high-temperature region of short-range fluctuations, where $\langle \Delta \rangle$ is described by formula (22)) for various values of $v_F\kappa$. The dashed curves describe the corresponding mean-field temperature dependences of the superconducting gap, which were obtained under the assumption of self-averaging of the superconducting order parameter over

⁶ In the numerical analysis, it was assumed that the fraction of flat regions on the Fermi surface is $\alpha = 2/3$.

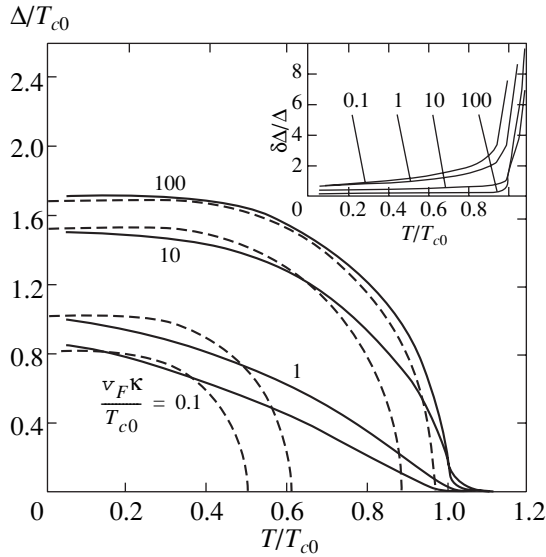


Fig. 4. Temperature dependence of the superconducting gap in the high-temperature region of dielectric fluctuations. Solid curves correspond to the superconducting gap $\langle \Delta \rangle$ averaged over amplitude D and phase η and described by expression (22). Dashed curves correspond to the mean-field superconducting gap defined by Eq. (28). The inset shows the temperature dependence of the relative root-mean-square fluctuation of the superconducting gap. The curves are plotted for $W/T_{c0} = 3$ and for various values of $v_F\kappa/T_{c0}$.

both the amplitude fluctuations and the phase fluctuations described by Eq. (28).

The superconducting gap averaged over fluctuations also differs from zero in a temperature range above the superconducting transition temperature T_c , which corresponds to vanishing of the mean-field superconducting gap (i.e., the gap which is homogeneous in the entire sample). Moreover, it can be seen that the superconducting gap averaged over fluctuations differs from zero in a narrow temperature region above the superconducting transition temperature T_{c0} in the absence of short-range fluctuations also. This is due to the fact that there exist fluctuations of phase η , for which the Fermi level falls to the region of the peaks of density of states, which are associated with the formation of the dielectric gap. Indeed, the density of states for a specific realization of phase η and of the dielectric gap amplitude D has the form

$$\frac{N(E)}{N_0(0)} = -\frac{1}{\pi N_0(0)} \text{Im} \sum_{\mathbf{p}} g_{11}^R(E, \mathbf{p}, \mathbf{p})$$

$$= \begin{cases} \frac{|E + \eta/2|}{\sqrt{(E + \eta/2)^2 - D^2}} & \text{for } |E + \eta/2| > D, \\ 0 & \text{for remaining values,} \end{cases} \quad (29)$$

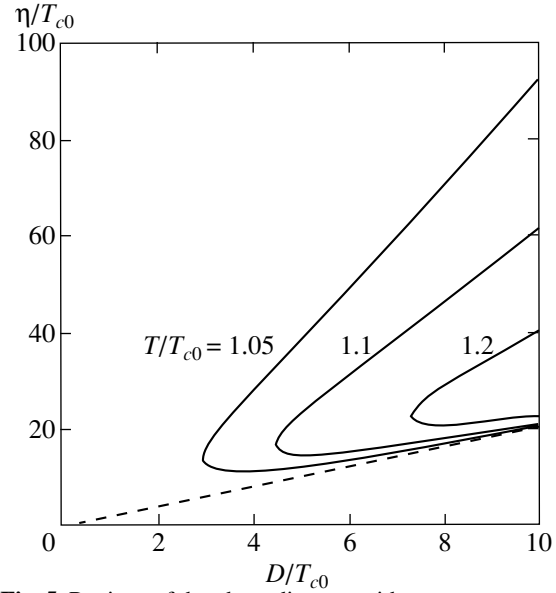


Fig. 5. Regions of the phase diagram with a nonzero superconducting gap for various temperatures above T_{c0} . The dashed line corresponds to $D = \eta/2$.

where $g_{11}^R(E, \mathbf{p}, \mathbf{p})$ is the retarded Green's function which can be obtained from Eq. (4) by the standard analytic continuation $i\varepsilon_n \rightarrow E + i0$ and $N_0(0)$ is the density of states at the Fermi level in the absence of short-range fluctuations. Consequently, for $\eta/2 \approx D$, the Fermi level corresponds to the peaks of the density of states, which leads to an increase in the superconducting gap $\Delta(\eta, D)$. Moreover, an increase in the dielectric gap amplitude D broadens the peaks in the density of states (29); consequently, if the condition $\eta/2 \approx D$ remains in force, the superconducting gap $\Delta(\eta, D)$ increases with D . As a result, at any temperature above T_{c0} and for large amplitudes of the dielectric gap $D > D^*(T)$, the phase diagram plotted in the η vs. D coordinates always contains a narrow region in the vicinity of the straight line $\eta/2 = D$, in which the superconducting gap $\Delta(\eta, D)$ differs from zero (see Fig. 5). This leads to the emergence of an exponentially small tail on the temperature dependence of the superconducting gap $\langle \Delta \rangle$ averaged over fluctuations in the temperature range above T_{c0} .⁷

The inset to Fig. 4 shows the temperature dependence of the relative root-mean-square fluctuation $\delta\Delta/\Delta = \sqrt{\langle \Delta^2 \rangle - \langle \Delta \rangle^2} / \langle \Delta \rangle$ of the superconducting gap for the high-temperature mode of dielectric fluctuations. In the case of large short-range correlation lengths ($\xi_0/\xi_{\text{corr}} \ll 1$), the superconducting order parameter fluctuations are very strong in the entire temperature range, indicating the obvious non-self-averaging of

⁷ In the model under investigation, this effect is obviously a consequence of the one-dimensional nature of the random field of fluctuations, leading to corresponding singularities in the density of states (29). For this reason, it may turn out to be not universal and inherent only in the given simplified model.

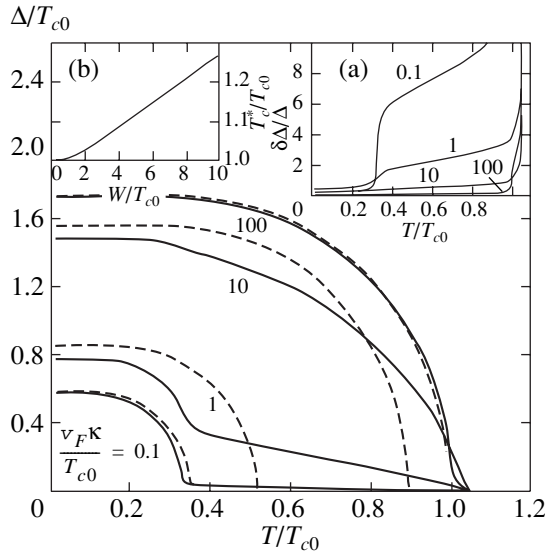


Fig. 6. Temperature dependence of the superconducting gap in the low-temperature region of dielectric fluctuations. Solid curves correspond to the superconducting gap $\langle \Delta \rangle$ averaged over phase η for a fixed amplitude $D = W$, described by expression (21). Dashed curves correspond to the mean-field superconducting gap defined by Eq. (27). Inset (a) shows the temperature dependence of the relative root-mean-square fluctuation of the superconducting gap. The curves are plotted for $W/T_{c0} = 3$ and for various values of $v_F\kappa/T_{c0}$. Inset (b) shows the dependence of the critical temperature T_c^* on the pseudogap width.

the superconducting order parameter. Surprisingly, the superconducting gap fluctuations are quite strong in the region of small correlation lengths also (at least in the temperature range $T > T_c$). In particular, the tail on the temperature dependence of $\langle \Delta \rangle$ for $T > T_c$ is noticeable even for $v_F\kappa/T_{c0} = 100$, when $\xi_0/\xi_{\text{corr}} \approx 30 \geq 1$.

Solid curves in Fig. 6 are the temperature dependences of the superconducting gap $\langle \Delta \rangle$ averaged over phase η (see Eq. (21)) in the low-temperature mode of dielectric fluctuations, when the amplitude fluctuations of the dielectric gap are frozen out and $D = W$. The dashed curves are the corresponding temperature dependences of the mean-field superconducting gap obtained under the assumption of self-averaging of the superconducting order parameter over the fluctuations of phase η , which are defined by Eq. (27). For large short-range correlation lengths, the averaged gap for $T < T_c$ is very close to the mean-field gap and has a relatively small tail in the range $T > T_c$. Such a behavior in the low-temperature mode of dielectric fluctuations is associated with the fact that, for $\xi_{\text{corr}} \rightarrow \infty$, the randomness of such a model disappears altogether ($\eta = 0$, $D = W$). Accordingly, the root-mean-square fluctuation of the gap, which is shown in the inset to Fig. 6 for a large correlation length, is quite small for $T < T_c$, but increases sharply for $T > T_c$. As the correlation length

decreases, the superconducting gap fluctuations $\delta\Delta$ for $T < T_c$ first increase just due to the increase in randomness (parameter $v_F\kappa$ determines the width of the distribution of phase η) and then decrease in the region $\xi_0/\xi_{\text{corr}} \gg 1$. In the tail region of the averaged superconducting gap ($T > T_c$), the superconducting gap fluctuations are very strong. Although they decrease with the short-range correlation length ξ_{corr} , they still remain significant even for small correlation lengths, i.e., in the region $\xi_0/\xi_{\text{corr}} \gg 1$.

As in the high-temperature mode of dielectric fluctuations, the tail on the temperature dependence of the average gap is observed for $T > T_{c0}$ also. This can be explained by the above-mentioned factors. However, the dielectric gap amplitude in the low-temperature mode is not random any longer, but is strictly fixed ($D = W$). For this reason, for $T_{c0} < T < T_c^*$, where T_c^* is determined by the condition $D^*(T_c^*) = W$, there exists a narrow region of phases near $\eta = 2W$ in which the superconducting gap $\Delta(\eta, W)$ differs from zero, but no such region is present for $T > T_c^*$ (see Fig. 5); T_c^* is the temperature to which the tail of the averaged gap extends, i.e., the critical temperature for the averaged gap $\langle \Delta \rangle$. It follows from the definition of T_c^* that it is obviously independent of the correlation length and depends only on W . Since the width of the peaks of the density of states (29) (and, hence, of $\Delta(\eta, D)$) also increases with D as long as the condition $\eta/2 \approx D$ is satisfied, the value of T_c^* increases with W . The dependence of T_c^* on W is shown on the corresponding inset to Fig. 6.

5. CONCLUSIONS

In the present work, we have studied the features of the superconducting state in the framework of the extremely simplified model of the pseudogap in a 2D electron system, which has an exact solution. The main result is the obvious absence of complete self-averaging of the superconducting order parameter (energy gap) over the random field of dielectric fluctuations leading to the formation of the pseudogap state. This fact is quite astonishing from the viewpoint of the standard model of superconductivity in disordered systems [12–14]. The absence of self-averaging, which is manifested in the emergence of strong fluctuations of the gap, can be seen most clearly in the range of temperatures exceeding the mean-field superconducting transition temperature T_c that can be obtained from the standard equations written under the assumption of self-averaging of the order parameter. This temperature is identified by us with the temperature of the emergence of a homogeneous superconducting state in the entire sample, while the superconducting state in a real disordered system is inhomogeneous. The superconducting

state can exist in the range $T > T_c$ in the form of individual regions (drops) formed as a result of random fluctuations of the local density of electron states. In contrast to our previous publication [5], in which this pattern was considered in the limit of very large short-range correlation lengths $\xi_{\text{corr}} \rightarrow \infty$, the application of the model [15] has made it possible to obtain the complete solution for arbitrary values of ξ_{corr} . This solution has demonstrated the absence of complete self-averaging of the superconducting gap even for $\xi_{\text{corr}} < \xi_0$, which contradicts the naive expectations following from the standard approach [2]. It was noted above that we are not aware of publications in which the self-averaging of Δ would be considered in the framework of exactly solvable models of disorder. In the present paper, such an analysis has been carried out. It is unclear, however, to what extent the obtained results will be preserved in more realistic models.

For further investigations associated with the given model, it would be interesting to analyze the behavior of the spectral density of the electron and tunnel densities of states as was done in our earlier work [5] in the limit $\xi_{\text{corr}} \rightarrow \infty$. In particular, it would be interesting to investigate the problem of self-averaging of the density of states, which is assumed in the theory of disordered system almost in all cases.

As regards the comparison with the experimental data on high-temperature superconductors, it should be noted that the existence of microscopic superconducting regions coexisting with predominant regions of the semiconductor type with a typical pseudogap in the electron spectrum of $\text{Bi}_2\text{Sr}_2\text{CaCu}_2\text{O}_{8+\delta}$ films was clearly demonstrated in [24, 25] using the method of scanning electron microscopy for measuring the local density of states. These observations are in qualitative agreement with the main conclusions drawn on the basis of the model under investigation.

ACKNOWLEDGMENTS

The work was partly financed by the Russian Foundation for Basic Research (project no. 99-02-16285), CRDF (grant no. REC-005), and the Program of Fundamental Studies "Quantum Macrophysics" of the Presidium of the Russian Academy of Sciences, as well as in the framework of state contracts of the Ministry of Industry and Science nos. 108-11(00)-P under the program "Statistical Physics" and 107-1(00)-P (contract no. 7/01) under the HTSC program.

REFERENCES

1. T. Timusk and B. Statt, Rep. Prog. Phys. **62**, 61 (1999).
2. M. V. Sadovskii, Usp. Fiz. Nauk **171**, 539 (2001).

3. V. M. Loktev, R. M. Quick, and S. G. Sharapov, submitted to Phys. Rep.; cond-mat/0012082.
4. A. I. Posazhennikova and M. V. Sadovskii, Zh. Éksp. Teor. Fiz. **115**, 632 (1999) [JETP **88**, 347 (1999)].
5. É. Z. Kuchinski and M. V. Sadovskii, Zh. Éksp. Teor. Fiz. **117**, 613 (2000) [JETP **90**, 535 (2000)]; Physica C (Amsterdam) **341-348**, 879 (2000).
6. É. Z. Kuchinski and M. V. Sadovskii, Zh. Éksp. Teor. Fiz. **119**, 553 (2001) [JETP **92**, 480 (2001)].
7. M. V. Sadovskii, Zh. Éksp. Teor. Fiz. **66**, 1720 (1974) [Sov. Phys. JETP **39**, 845 (1974)]; Fiz. Tverd. Tela (Leningrad) **16**, 2504 (1974) [Sov. Phys. Solid State **16**, 1632 (1974)].
8. M. V. Sadovskii, Zh. Éksp. Teor. Fiz. **77**, 2070 (1979) [Sov. Phys. JETP **50**, 989 (1979)].
9. M. V. Sadovskii and A. A. Timofeev, Sverkhprovodimost: Fiz., Khim., Tekh. **4**, 11 (1991); M. V. Sadovskii and A. A. Timofeev, J. Mosc. Phys. Soc. **1**, 391 (1991).
10. J. Schmalian, D. Pines, and B. Stojkovic, Phys. Rev. Lett. **80**, 3839 (1998); Phys. Rev. B **60**, 667 (1999).
11. É. Z. Kuchinski and M. V. Sadovskii, Zh. Éksp. Teor. Fiz. **115**, 1765 (1999) [JETP **88**, 968 (1999)].
12. L. P. Gor'kov, Zh. Éksp. Teor. Fiz. **37**, 1407 (1959) [Sov. Phys. JETP **10**, 998 (1959)].
13. P. G. de Gennes, *Superconductivity of Metals and Alloys* (Benjamin, New York, 1966; Mir, Moscow, 1968).
14. M. V. Sadovskii, *Superconductivity and Localization* (World Scientific, Singapore, 2000); Phys. Rep. **282**, 225 (1997); Sverkhprovodimost: Fiz., Khim., Tekh. **8**, 337 (1995).
15. L. Bartosch and P. Kopietz, Eur. Phys. J. B **17**, 555 (2000).
16. P. A. Lee, T. M. Rice, and P. W. Anderson, Phys. Rev. Lett. **31**, 462 (1973).
17. M. V. Sadovskii, Physica C (Amsterdam) **341-348**, 811 (2000).
18. L. Bartosch and P. Kopietz, Phys. Rev. B **60**, 15488 (1999).
19. L. Bartosch, submitted to Ann. Phys. (Leipzig); cond-mat/0102160.
20. A. J. Millis and H. Monien, Phys. Rev. B **61**, 12496 (2000).
21. S. A. Brazovskii and I. E. Dzyaloshinski, Zh. Éksp. Teor. Fiz. **71**, 2338 (1976) [Sov. Phys. JETP **44**, 1233 (1976)].
22. J. Tranquada, J. Phys. Chem. Solids **59**, 2150 (1998).
23. A. A. Abrikosov, L. P. Gor'kov, and I. E. Dzyaloshinskii, *Methods of Quantum Field Theory in Statistical Physics* (Fizmatgiz, Moscow, 1962; Prentice-Hall, Englewood Cliffs, 1963).
24. T. Cren, D. Roditchev, W. Sacks, *et al.*, Phys. Rev. Lett. **84**, 147 (2000).
25. T. Cren, D. Roditchev, W. Sacks, and J. Klein, submitted to Europhys. Lett.

Translated by N. Wadhwa

Graduated in 1971 the Physical Department of the Ural State University (Sverdlovsk).

Ph.D. - 1975, Dr.Sci. - 1986.

1971-1974 - Ph.D work - theoretical department of P.N. Lebedev Physical Institute, USSR Academy of Sciences, Moscow.

1974-1986 - researcher at the Institute for Metal Physics USSR Academy of Sciences, Ural Scientific Centre (Sverdlovsk).

In 1987-2017 head of theoretical physics laboratory of the Institute for Electrophysics, Russian Academy of Sciences, Ural Branch (Ekaterinburg), at present the chief researcher in this laboratory. During 1993-2002 - deputy director of the Institute. In 2011-2013 also headed the laboratory of quantum theory of condensed matter, Institute for Metal Physics, Russian Academy of Sciences, Ural Branch, in 2013-2018 chief researcher of this laboratory and scientific supervisor of the Department of Theoretical Physics of the Institute for Metal Physics.

Professor of the Ural State University (Theoretical Physics), 1991-2010.

Author of more than 150 papers on condensed matter theory. Main interests - electronic theory of disordered systems (Anderson localization, pseudogap), superconductivity (disordered superconductors, high-temperature superconductivity). Developed the field theory approach to Anderson localization, self-consistent theory of localization, theory of superconductors close to the Anderson transition. Formulated exactly solvable models of the pseudogap state, models of disorder effects in the theory of Peierls transition. Recent interests were connected with extensions of dynamical mean field theory approach to the theory of electrons in strongly correlated systems and theoretical studies of iron based superconductors.

Corresponding member of the Russian Academy of Sciences (1994), Full Member (2003), member of the Presidium of the Ural Branch of RAS, member of the Bureau of the Physics Division of RAS and the RAS Commission on pseudoscience, member of American Physical Society, Fellow of the Institute of Physics (UK) - 2002. Member of editorial boards of JETP and Physics Uspekhi. Member of the "July 1st Club" opposing 2013 governmental reform of the Russian Academy of Sciences.

A.G. Stoletov Prize in Physics of the Russian Academy of Sciences (2002)

V.L. Ginzburg Gold Medal of the Russian Academy of Sciences (2016)

M.N. Mikheev Silver Medal of the Institute for Metal Physics (2017)

S.V. Vonsovsky Gold Medal of the Ural Branch of the Russian Academy of Sciences (2018)

